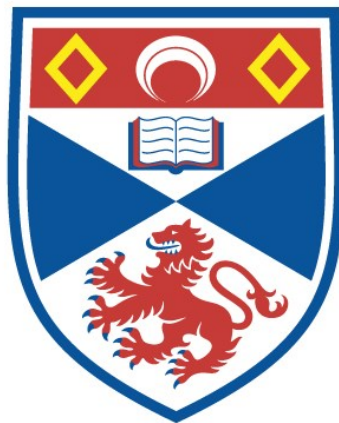


THE PETROLOGY AND MINERAL CHEMISTRY OF
THE SHIRA RING COMPLEX, NORTHERN NIGERIA

John N. Bennett

A Thesis Submitted for the Degree of PhD
at the
University of St Andrews



1980

Full metadata for this item is available in
St Andrews Research Repository
at:
<http://research-repository.st-andrews.ac.uk/>

Please use this identifier to cite or link to this item:
<http://hdl.handle.net/10023/16437>

This item is protected by original copyright

THE PETROLOGY AND MINERAL CHEMISTRY OF
THE SHIRA RING COMPLEX, NORTHERN NIGERIA

I certify that John N. Bennett has been engaged in research
for 3 years at the University of St. Andrews, that he has
fulfilled the conditions of Ordinance No. 12 (St. Andrews)
and the resolution of the University Court, 1967, No. 1, and
that he is qualified to submit this thesis for the degree
of Doctor of Philosophy.

John N. Bennett

I certify that the following thesis is based on the results
of research carried out by me, that it is my own composition,
and that it has not previously been presented for a higher
degree.

Thesis presented for the degree of
Doctor of Philosophy in the Faculty of Science
of the University of St. Andrews

THE PETROLOGY AND MINERAL CHEMISTRY OF
THE SHINA RING COMPLEX, NORTHERN ALBERTA

Th 9478

Thesis presented for the degree of
Doctor of Philosophy in the Faculty of Science
of the University of Alberta

CERTIFICATE

I certify that John N. Bennett has been engaged in research for 9 terms at the University of St. Andrews, that he has fulfilled the conditions of Ordinance No.12 (St. Andrews) and the Resolution of the University Court, 1967, No.1, and that he is qualified to submit this thesis for the degree of Doctor of Philosophy.

P. Bowden .

I certify that the following thesis is based on the results of research carried out by me, that it is my own composition, and that it has not previously been presented for a higher degree.

J.N. Bennett

"Mark what life the scholar's life recall,

Tell, sorry, want, To Anne from and the jail."

and

To my father, Geoffrey William Bennett,
who died the month this thesis began.

David Johnson

The Vanity of Human Wishes

ABSTRACT

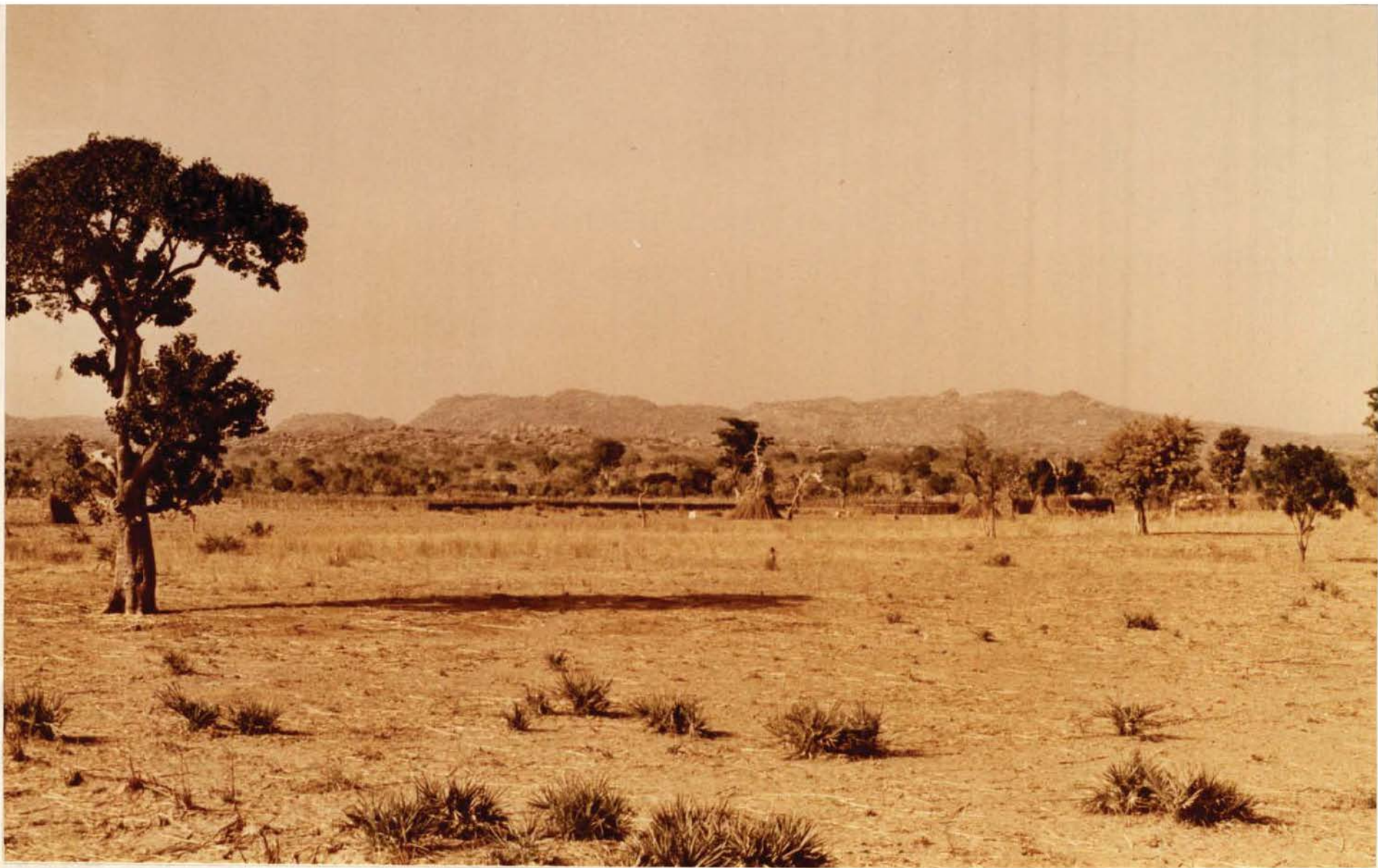
The Shira complex belongs to the anorogenic province of Niger and Nigeria. It is dominated by peralkaline syenites and granites and has an estimated area of 152 sq.km. Apart from a related intrusion of granite porphyry at Zigau to the southwest, the Shira complex can be divided into three centres. Centre 1 is dominated by the Shira quartz syenite and this has been intruded by a large cone sheet of Birji granite and by microgranite dykes. These peralkaline syenites and granites are believed to represent successive intrusions from a progressively differentiating magma chamber. The Birji granite has two facies distinguished by the habit of the arfvedsonite and both facies exhibit layering. Centre 2 is composed of the Andaburi granite and a small intrusion of Amdulayi syenite. Centre 3 consists of the very poorly exposed Eldewo aluminous biotite granite.

The Zigau granite porphyry contains phenocrysts of alkali feldspar, quartz, fayalite and ferrohedenbergite in a quartzofeldspathic groundmass. The Shira quartz syenite consists of microperthite, quartz, ferrichterite-arfvedsonite and aenigmatite. The Birji granite contains microperthite, quartz, arfvedsonite and a little aegirine, and the dykes related to it have a similar mineralogy but are more mafic-rich. The Andaburi granite consists of microperthite, quartz, ferrichterite-arfvedsonite and aegirine. The Amdulayi syenite has three facies which collectively contain microperthite, quartz, ferrowinchite-arfvedsonite, aenigmatite and aegirine. The Eldewo granite contains microperthite, quartz and biotite.

Several minerals have been discovered which are either new to the province or are recorded for the first time in Nigeria, namely, aegirine-hedenbergite, chevkinite and narsarsukite.

In the Zigau granite porphyry, fayalite has a composition of Fa93-100 and the pyroxene is ferrohedenbergite with sodic margins. Amphiboles from the Shira complex exhibit a compositional trend from ferrorichterite or ferrowinchite to arfvedsonite. In the syenitic rocks there are two periods of alkali pyroxene growth - early aegirine-hedenbergite and later aegirine, separated by a period of amphibole and aenigmatite crystallisation. Aenigmatite occurs in the syenitic rocks, which have the highest Ti contents, but it shows limited compositional range. Biotite composition in the aluminous granite is close to the theoretical annite end-member.

Whole rock geochemical data suggest that there is a progression from the syenites to the highly fractionated granites. With regard to the occurrence and characteristics of the peralkaline and aluminous granites in particular, it is concluded that the peralkaline syenites and granites from Shira are the result of fractional crystallisation from a basaltic parent, whereas the aluminous rocks are the result of partial melting in the continental crust.



The Shira ring complex from the south.

	<u>CONTENTS</u>	<u>page</u>
List of Figures		i
List of Plates		iii
List of Tables		vi
Chapter 1. THE YOUNGER GRANITES OF NIGERIA AND NIGER		1
1.1 Objectives		1
1.2 Introduction		1
1.3 Structure		2
1.4 Geochronology		4
1.5 Geochemistry		5
1.6 Mineralogy		6
1.7 Mineralisation		7
1.8 Petrogenesis		8
1.9 Peralkaline rocks		9
1.10 Syenitic rocks		19
1.11 Aluminous rocks		23
Chapter 2. FIELD GEOLOGY		29
2.1 General		29
2.2 Introduction		30
2.3 The Zigau granite porphyry		31
2.4 The Shira alkali feldspar quartz syenite		32
2.5 The Birji alkali feldspar granite		37
2.6 The Andaburi alkali feldspar granite		48
2.7 The Amdulayi alkali feldspar syenite / quartz syenite		52
2.8 The Eldewo biotite alkali feldspar granite		53
2.9 Miscellaneous rocks		54

	<u>page</u>
Chapter 3. PETROGRAPHIC DESCRIPTION	56
3.1 Zigau fayalite ferrohedenbergite granite porphyry	56
3.2 Shira aenigmatite ferrorichterite alkali feldspar quartz syenite	66
3.3 Birji aegirine arfvedsonite alkali feldspar granite	90
3.4 Andaburi ferrorichterite alkali feldspar granite	116
3.5 Amdulayi ferrowinchite/ferrorichterite alkali feldspar syenite / quartz syenite	126
3.6 Eldewo biotite alkali feldspar granite	139
3.7 Miscellaneous rocks	148
 Chapter 4. MINERAL CHEMISTRY	 151
4.1 Introduction	151
4.2 Amphibole	152
4.3 Pyroxene	175
4.4 Aenigmatite	189
4.5 Chevkinite	198
4.6 Narsarsukite	202
4.7 Biotite	205
4.8 Fayalite	211
4.9 Fe-Ti oxides	217
4.10 Feldspars	219
 Chapter 5. GEOCHEMISTRY	 231
5.1 Introduction	231
5.2 The Shira complex	231
5.3 The Niger-Nigeria province	240
5.4 Discussion	249
5.5 Conclusions	256

	<u>page</u>
Chapter 6. PETROGENESIS	258
6.1 Introduction	258
6.2 Geochronology and possible mantle plumes	259
6.3 Radiogenic and stable isotopes	264
6.4 Paucity of intermediate and basic rocks	268
6.5 Peralkaline granites and related rocks	271
6.6 Aluminous granites and mineralisation	276
6.7 Conclusions	280
References	281
Acknowledgements	305
Appendices	
(1) Modal analyses.	307
(2) Mineral separation, X-ray diffractometry and X.R.D. data.	314
(3) Mineral analysis and structural formulae.	318
(4) Whole rock analysis.	325
Maps	in pocket
13. Schematic diagram for the structure of an amphibole.	168
14. Temperature-xygen fugacity diagram for alkali amphiboles.	172
15. Di-Fe-Sr-Ye diagram for calcic pyroxenes from the Shira complex.	180
16. Na-Ti-(Fe ²⁺) diagram for all pyroxenes from the Shira complex.	181
17. Cartesian diagrams of selected elements in pyroxenes from the Shira complex.	182
18. Cartesian diagrams of selected elements in augenite from the Shira complex.	190
19. Cartesian diagrams of selected elements in xenogranite from the Shira complex and elsewhere.	194

LIST OF FIGURES

		<u>page</u>
1.	Location map of the Niger-Nigeria Younger Granite province.	facing 1
2.	Location map of anorogenic ring complexes in Nigeria.	facing 29
3.	Simplified outcrop and locality map of the Shira complex.	facing 30
4.	Schematic cross-section through the Birji granite.	facing 40
5.	Schematic view of the evolution of the magma chamber at centre 1.	facing 47
6.	Ca v alkalis diagram for amphiboles from the Zigau granite porphyry.	154
7.	Ca v alkalis diagram for amphiboles from the Shira quartz syenite.	156
8.	Ca v alkalis diagram for amphiboles from the Birji granite.	158
9.	Ca v alkalis diagram for amphiboles from the Andaburi granite.	160
10.	Ca v alkalis diagram for amphiboles from the Amdulayi syenite/quartz syenite.	162
11.	Ca v alkalis summary diagram for amphiboles from the Shira complex and elsewhere.	facing 164
12.	Cartesian diagrams of selected elements in amphiboles from the Shira complex and elsewhere in Nigeria.	164
13.	Schematic diagram for the structure of an amphibole.	168
14.	Temperature-oxygen fugacity diagram for alkali amphiboles.	172
15.	Di-Hd-En-Fs diagram for calcic pyroxenes from the Shira complex.	180
16.	Na-Mg-(Fe ²⁺ +Mn) diagram for all pyroxenes from the Shira complex.	facing 181
17.	Cartesian diagrams of selected elements in pyroxenes from the Shira complex.	182
18.	Cartesian diagrams of selected elements in aenigmatite from the Shira complex.	192
19.	Cartesian diagram of selected elements in aenigmatite from the Shira complex and elsewhere.	194

	<u>page</u>
20. Modified Foster diagram for trioctahedral micas from the Eldewo biotite granite.	facing 212
21. Al v 100Mg/(Mg+Fe) diagram for trioctahedral micas from the Shira complex and elsewhere.	facing 213
22. Al[6] v Fe ₂ diagram for trioctahedral micas from the Shira complex.	facing 214
23. TiO ₂ -FeO-Fe ₂ O ₃ diagram for oxide minerals from the Shira complex and elsewhere in Nigeria.	facing 218
24. An-Ab-Or diagram for plagioclase and alkali feldspars from the Shira complex.	221
25. Two theta 060 v $\bar{2}04$ diagram for alkali feldspars.	facing 222
26. Harker diagrams for averaged whole rock values, geochemical indices and trace elements from the Shira complex.	235
27. AFM diagram for the Shira complex.	facing 238
28. Normative Q-Ab-Or diagram for the Shira complex.	facing 239
29. Harker diagrams for selected oxides from the Niger-Nigeria province.	facing 245
30. Summary Harker diagrams of averaged values for the Niger-Nigeria province.	245
31. Summary Harker-type diagrams for trace elements from the Niger-Nigeria province.	facing 246
32. AFM and AFA diagrams for the Niger-Nigeria province.	246
33. AFM, iron-enrichment and total alkali variation diagrams for the Niger-Nigeria province.	247
34. Summary normative Q-Ab-Or diagram for the Niger-Nigeria province.	facing 248
35. I.U.G.S. classification diagrams for modal analyses from a) the Niger-Nigeria province and b) the Shira complex.	facing 276
36. Generalised evolutionary diagram for various igneous suites.	facing 277
37. X-ray diffractogram of micropertthite from the Shira quartz syenite.	317
38. Ca v alkalis diagram for wet analyses of amphiboles from Nigeria.	facing 324

LIST OF PLATES

	<u>page</u>
Frontispiece	
The Shira ring complex from the south.	
1. Large exfoliated surfaces and boulder piles of the Shira quartz syenite.	33
2. Two phases of dilatational microgranite dykes within the Shira quartz syenite.	33
3. View of the N edge of the Gora enclave.	36
4. Margin of the Gora enclave.	36
5. Distinctive geomorphology of the Birji granite.	38
6. Gradational contact between the acicular and poikilitic facies of the Birji granite.	38
7. Layering in the poikilitic facies of the Birji granite.	41
8. Layering in the poikilitic facies of the Birji granite.	41
9. Close-up view of arfvedsonite layers in the poikilitic facies of the Birji granite.	42
10. Sub-parallel orientation of arfvedsonite laths in the acicular facies of the Birji granite.	42
11. Multiple, elongate enclaves of Shira quartz syenite in the Birji granite.	45
12. Angular volcanic enclave enclosed and partly brecciated by the Birji granite.	45
13. The texture and variable turbidity of alkali feldspars in the Zigau granite porphyry.	58
14. Fayalite and ferrohedenbergite phenocrysts in the Zigau granite porphyry.	58
15. The texture and variable turbidity of alkali feldspars in the Shira quartz syenite.	68
16. Growth zoning in alkali feldspar from the Shira quartz syenite.	68
17. Zoned amphibole from the Shira quartz syenite.	70
18. Aegirine-hedenbergite enclosed by alkali feldspar in the Shira quartz syenite.	70

	<u>page</u>
19. Microenclave in the Shira quartz syenite.	73
20. Texture of metasomatically altered Shira quartz syenite adjacent to the Birji granite.	73
21. Quartz and albite replacement of growth zoned alkali feldspar in a metasomatically altered Shira quartz syenite.	77
22. Narsarsukite in a granitic (?)dyke in the Shira quartz syenite.	77
23. Aegirine and arfvedsonite needles replacing alkali feldspar in the Birji granite.	92
24. Fluid inclusions in potassic and sodic lamellae in microperthite of the Birji granite.	92
25. Domain structure in quartz.	94
26. Aegirine replacement of arfvedsonite.	94
27. Late crystallising zircon aggregate in Birji granite.	96
28. Zeolite filled miarolitic cavity in the Birji granite.	96
29. Texture of the poikilitic facies of the Birji granite.	97
30. Overgrowths of arfvedsonite replacing alkali feldspar in the Birji granite.	97
31. Aegirine preferentially replacing arfvedsonite around quartz crystals.	99
32. Layering in the Birji granite.	99
33. Texture of layered sample of the Birji granite used for modal analyses.	101
34. Texture of the Andaburi granite.	118
35. Localised astrophyllite replacement of arfvedsonite in the Andaburi granite.	118
36. Eddy patterns shown by arfvedsonite and aegirine crystals in the matrix of a porphyritic microgranite dyke in the Andaburi granite.	121
37. Stellate aegirine crystals in microgranite sheet in the Andaburi granite.	121

	<u>page</u>
38. Texture of the coarse grained Amdulayi syenite.	128
39. Intergrowth of ferrowinchite/ferro-richterite with ilmenite in the Amdulayi syenite.	128
40. Interstitial aenigmatite in the coarse grained Amdulayi syenite.	129
41. Intergrowth of aenigmatite and ferrowinchite/ferrorichterite in the coarse grained Amdulayi syenite.	129
42. Texture of the equigranular facies of the Amdulayi quartz syenite.	131
43. Interstitial aenigmatite in the porphyritic facies of the Amdulayi quartz syenite.	131
44. Partly resorbed plagioclase within an enclave in the porphyritic facies of the Amdulayi quartz syenite.	135
45. Ferroaugite crystal in the porphyritic facies of the Amdulayi quartz syenite, being replaced by biotite and richterite.	135
46. Texture of the Eldewo biotite granite.	140
47. Zinnwaldite overgrowth around brown annitic biotite, Eldewo biotite granite.	140
48. Texture of the medium grained facies of the Eldewo biotite granite.	144
49. Green, filamentous overgrowths to annitic biotite in the Eldewo biotite granite.	144
50. Fragmental texture to the Yana agglomerate.	149
51. Texture of the Chida porphyritic granophyre.	149
52. Electron microprobe analyses of pyroxenes from the Eldewo biotite and other rocks.	facing 179
53. Electron microprobe analyses of pyroxenes from the Amdulayi syenite/quartz syenite and the Amdulayi granite.	facing 180
54. Correlation matrix for microprobe analyses of pyroxenes from the Chida complex.	facing 182
55. Electron microprobe analyses of aenigmatite from the Chida complex.	facing 190
56. Means and standard deviations of aenigmatite from the Chida complex.	190

LIST OF TABLES

	<u>page</u>
1. Occurrence of plagioclase in the fayalite, pyroxene and hornblende bearing granites and granite porphyries of the Nigerian sub-province.	facing 26
2. Modal analyses of rocks from the Shira complex.	facing 57
3. Electron microprobe analyses of amphiboles from the Zigau granite porphyry.	facing 154
4. Electron microprobe analyses of amphiboles from the Shira quartz syenite.	facing 155/156
5. Electron microprobe analyses of amphiboles from the Birji granite.	facing 157/158
6. Electron microprobe analyses of amphiboles from the Andaburi granite.	facing 160
7. Electron microprobe analyses of amphiboles from the Amdulayi syenite.	facing 161
8. Electron microprobe analyses of amphiboles from the Amdulayi quartz syenite.	facing 162
9. Correlation matrix for microprobe analyses of amphiboles from the Shira complex.	facing 163
10. Electron microprobe analyses of amphiboles from Ailsa Craig, W Scotland.	facing 166
11. Electron microprobe analyses of pyroxenes from the Zigau granite porphyry.	facing 177
12. Electron microprobe analyses of pyroxenes from the Shira quartz syenite.	facing 178
13. Electron microprobe analyses of pyroxenes from the Birji granite and other rocks.	facing 179
14. Electron microprobe analyses of pyroxenes from the Amdulayi syenite/quartz syenite and the Andaburi granite.	facing 180
15. Correlation matrix for microprobe analyses of pyroxenes from the Shira complex.	facing 182
16. Electron microprobe analyses of aenigmatite from the Shira complex.	facing 190
17. Means and standard deviations of aenigmatite from the Shira complex.	190

	<u>page</u>
18. Correlation matrix for aenigmatite analyses from the Shira complex and elsewhere.	facing 193
19. Electron microprobe analyses of chevkinite from the Shira quartz syenite.	facing 199
20. Electron microprobe analyses of narsarsukite from the Shira complex.	facing 203
21. Electron microprobe analyses of fayalite and accompanying minerals.	facing 205
22. Electron microprobe analyses of trioctahedral micas from the Shira complex.	facing 211
23. Electron microprobe analyses of ilmenite and magnetite from the Shira complex.	facing 217
24. Electron microprobe analyses of plagioclase from the Zigau granite porphyry.	facing 220
25. Electron microprobe analyses of alkali feldspar from the Shira complex.	facing 221
26. Analyses of rocks from the Shira complex.	232/233
27. Mean values and standard deviations for major rock types, dykes and enclaves within the Shira complex.	facing 234
28. Mean values, standard deviations and ranges for whole rock analyses of the major rock types from the Niger-Nigeria province.	facing 240
29. Correlation matrix for major and trace elements in the Niger-Nigeria Younger Granite province.	facing 249
30. Modal analyses of rocks from the Niger-Nigeria province.	309-312
31. Summary of X.R.D. data from alkali feldspars.	facing 317
32. X.R.D. reflections of microperthite from the Shira ferrorichterite alkali feldspar quartz syenite.	facing 318
33. Analytical conditions for elements determined by W.D.S. on the electron microprobe.	320
34. Comparison of structural formulae of arfvedsonite.	facing 323
35. X.R.F. analytical conditions.	facing 326

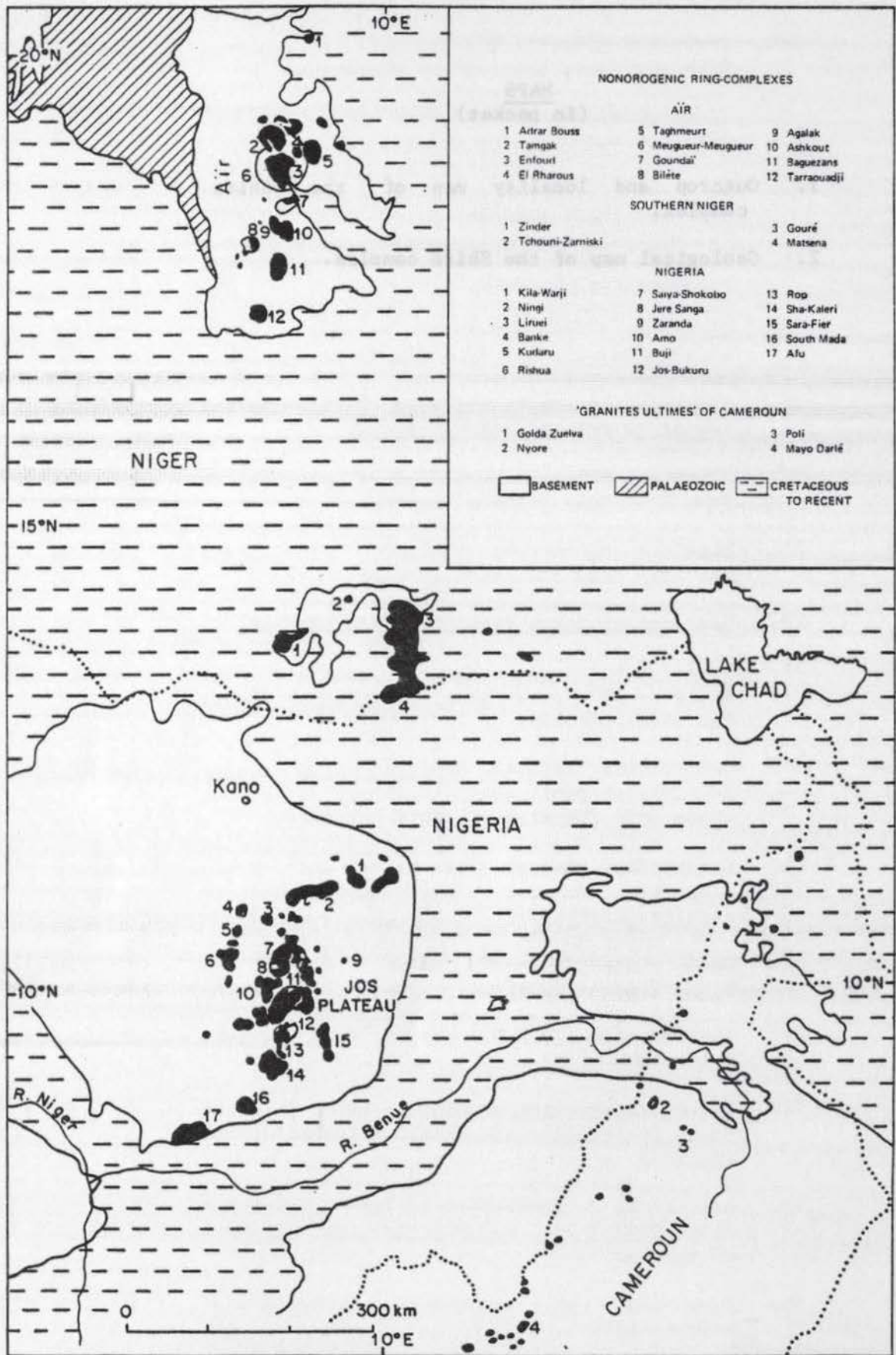


Figure 1. Location map of the Niger-Nigeria Younger Granite province (from Bowden & Turner, 1974).

CHAPTER 1THE YOUNGER GRANITES OF NIGERIA AND NIGER1.1 Objectives

The Younger Granites of Niger and Nigeria constitute an igneous province which is one of the best studied examples of mid-plate magmatism in the world, partly because the aluminous biotite granites are the source of economic columbite and alluvial cassiterite deposits. However, the peralkaline granites have received comparatively little attention. From a study of the dominantly peralkaline complex at Shira, it is hoped that a contribution can be made to a better understanding of the petrology, mineral chemistry and genesis of anorogenic, oversaturated igneous rocks. Before examining the Shira complex in detail though, it is worthwhile reviewing the character of the province in order to highlight areas where problems related to the nature and genesis of anorogenic, peralkaline rocks in particular, are still outstanding. In addition, this review offers an opportunity to describe the main features of rock types which are treated separately in Chapter 5.

1.2 Introduction.

The Younger Granites of Nigeria and Niger constitute a suite of high level, sub-volcanic, anorogenic intrusions exposed over a distance of about 1250 km between the 8th and 10th meridians (Figure 1). They have long been recognised as distinct from the 'Older' granites and granodiorites (Falconer, 1911), which were emplaced during the Pan-African orogeny of about 600 my ago (Grant, 1969, 1970; van Breemen et al., 1977). The Younger Granites are dominantly granitic but include minor associated syenites, gabbros and anorthosites. They form a ring

complex province (Bain, 1934; Jacobson et al., 1958; Macleod et al., 1971) which decreases in age from 487 my for the Adrar Bouss complex in N. Niger (Karche and Vachette, 1976) to 144 my in the Afu complex, central Nigeria (Bowden et al., 1976). The chief characteristics of the province may be conveniently summarised under the following headings.

1.3 Structure

Falconer (1910, 1911) recognised that the Younger Granite intrusions cut sharply across the structure of the country rocks, with little cataclasis, deformation or contact metamorphism. Knowledge of the structure and petrology of the Younger Granites was enhanced after the formation of the Geological Survey of Nigeria in 1919, through the publication of a series of Bulletins which represented the outcome of reconnaissance geological surveys (Falconer, 1921; Falconer and Raeburn, 1923; Falconer et al., 1926; Raeburn et al., 1927). Kudaru, the first Younger Granite intrusion to be studied in detail, was shown to have a ring form with a centripetal arrangement of successive major intrusions while minor intrusions had a conical structure (Bain, 1934). Although Bain viewed the intrusion as a cedar-tree laccolith, it was clear that his contemporaries regarded it as a ring complex (Bain, 1934, p.238). As a result of a study of the nearby Ririwai (1) complex (Jacobson, 1947) the concept of granitic ring complexes in the province became established (2).

The generalised evolution of a ring complex begins with the eruption of lavas, tuffs and agglomerates from central volcanoes or from vents localised along a ring fault, followed by the extrusion of more homogeneous (crystal-rich) rhyolitic volcanic rocks, with accompanying

(1) On older maps and publications this complex is spelt Liruei.

(2) A ring complex may be defined as an association of high level, subvolcanic ring shaped intrusions often associated with ring dykes, cone sheets and volcanic rocks.

surface cauldron subsidence forming a caldera, and cone sheet formation (Jacobson et al., 1958). The importance of caldera formation during the development of a ring complex has recently been emphasised (Turner and Bowden, 1979). Subsequently, granitic ring dykes were intruded, and these in particular constitute an important and characteristic structural feature of the province (Jacobson et al., op.cit.). Finally, sub-volcanic granites (and minor syenites, etc.) were intruded, often coming into contact with volcanic rocks which, however, rarely show any sign of up-doming. These intrusions commonly have an elliptical or semi-circular outline and often exhibit a centripetal arrangement of successive phases, an observation which can be readily explained by successive episodes of cauldron subsidence (Jacobson et al., op.cit.). However, these authors also noticed that the pattern formed by successive granites could alternatively be profoundly eccentric and reflect shifts in the centre of magmatic activity with time.

Such magmatic behaviour in the province has been emphasised by Turner (1962, 1963), who described a series of overlapping magmatic centres from the Sara-Fier complex. Since, in general, individual magmatic centres in the province tend to have similar diameters and activity at one centre ceased before a new centre was initiated, Turner (op.cit.) suggested that a discrete high level magma chamber directly underlay each magmatic centre.

In the Younger Granites of Niger, a generalised plutonic sequence begins with a syenitic ring dyke or an anorthositic intrusion, which is followed by ring dykes or stocks of syenite or peralkaline granite and ends with minor aluminous granites (Black et al., 1967). In this region, the Air (1) mountains, both the Younger Granites and the country rocks are much better exposed than in Nigeria, such that there

(1) The correct spelling is with an umlaut over the "i", and it is pronounced 'aye-eer'.

is "clear evidence that the form (of the intrusion) has been controlled by pre-existing wrench faults and jointing in the basement" (Black and Girod, 1970). The age progression and N-S alignment of Younger Granite intrusions has led to speculation that the emplacement of the ring complexes may be connected with a more fundamental structural control, that of the rifting of Gondwana and separation of S.America from Africa (eg. Turner, 1973, Black and Girod, 1970).

The sub-surface structure of some ring complexes has been investigated by gravity surveys (Ajakaiye, 1968, 1974; Ajakaiye and Sweeney, 1974). For the Ririwai, Banke and Dutsen Wai complexes a gravity deficiency, relative to the country rocks down to a maximum depth of 10km, was found; no basic rocks could therefore be detected. A regional gravity survey over much of Nigeria revealed that many individual complexes have discrete gravity contour closures centred on them, strongly suggesting that the observed negative gravity anomaly is due solely to the rocks of each particular complex (Ajakaiye, 1970). Not surprisingly therefore, the area of least gravitational force was found to coincide with the greatest concentration of Younger Granites, on the Jos Plateau, while the area with the smallest anomaly occurs close to the Kila-Warji and Zigau-Shira intrusions.

1.4 Geochronology

For about 50 years after the Younger Granites were first recognised, they were regarded as being of Precambrian age. However, with the advent of radiometric dating techniques, fergusonite - an accessory mineral from the Younger Granites and occurring in alluvial deposits on the Jos Plateau - was dated at about 160 my by the U/Pb and Th/Pb methods (Darnley et al., 1962). These authors also quoted unpublished K/Ar analyses of biotite (162 my) and a 206 Pb/U age (204 my) for pyrochlore as being compatible. A more comprehensive study also

indicated a Jurassic age for the central Nigerian complexes (Jacobson et al., 1963). In Niger, (apparent) stratigraphic evidence indicated a post-Devonian - pre-Cretaceous age for the Younger Granites (Black et al., 1967). However, radiometric age data invalidated the supposed Devonian age for the contact metamorphosed sedimentary rocks concerned, since the Adrar Bouss complex which intrudes them is Ordovician (Karche and Vachette, 1976, 1978). Other evidence also pointed to a Palaeozoic age for the Niger complexes, where a biotite from Elmeki gave a K/Ar age of 460 my (Brunnschweiler, 1974). In support of a pre-Jurassic age for these complexes, Brunnschweiler noted that rhyolite pebbles had been discovered near Taghouaji (1) in sedimentary rocks that were at least as old as L. Jurassic, and probably older.

Subsequently, a southerly decreasing age trend from Adrar Bouss, N. Niger (487 my) through Zarniski, S.Niger (289-330 my) to Afu, central Nigeria (144 my) has been confirmed by the Rb/Sr method (van Breemen and Bowden, 1973; Bowden et al., 1976; Karche and Vachette, 1976).

1.5 Geochemistry

Prior to 1958 there were few published analyses of Younger Granites, largely due to the tedious analytical methods then available. A geochemical characterisation of the province has listed such features as low MgO and CaO, and high total Fe, F, Li, Rb, Y, Nb, Hf, U and Th (Jacobson et al., 1958). Shortly afterwards, much additional trace element data was published (Bowden, 1964, 1966a, 1966b), some of which has been used in an attempt to define evolutionary trends (eg. Butler et al., 1962).

More recently, the rare earth elements have been determined

(1) Pre-1978 publications use the spelling Tarraouadji.

and like many of the trace elements mentioned, found to be relatively abundant, with the exception of Eu which may often be markedly depleted (Aleksiyev, 1970; Bowden and van Breemen, 1972; Bowden and Whitley, 1974). Other geochemical features of the province have been summarised in several publications (Macleod et al., 1971; Bowden and Turner, 1974; Bowden et al., 1976; Jacobson and Macleod, 1977).

1.6 Mineralogy

Petrographic descriptions of the Younger Granite minerals are numerous but the most complete are given in Buchanan et al. (1971) and Rocci (1960). From a chemical viewpoint, the mafic minerals are Fe-rich (eg. fayalite and hedenbergite) in keeping with the low MgO content of the rocks, and much mineral chemical data is now available (Jacobson et al., 1958; Fabries and Rocci, 1965; Borley, 1963a, 1963b, 1976b; Borley and Frost, 1963). The most comprehensive study of any mineral group is for the amphiboles, in which a range of composition from 'hastingsite' to 'riebeckitic arfvedsonite' has been described (Borley, 1963b). The amphiboles are also Fe-rich; the alkali amphiboles contain significant quantities of Li and F which substitute for Fe and OH respectively. No correlation between composition and optical properties was found, although systematic variations between composition and cell parameters were detected (Frost, 1963). An attempt to define the temperature of crystallisation of various minerals by using experimentally determined mineral stability data, has been made (Fabries and Rocci, 1965; Borley, 1976b).

Amphiboles and micas from the Taghouaji complex have been chemically studied; brown or red-brown biotites from coarse grained microperthite granites are close to the annite end member, while green or colourless micas from albitic granites are siderophyllites and are richer in Li and Al (Fabries and Rocci, 1965). Alkali feldspars from the

granites and syenites have a range in structural state from orthoclase to maximum microcline; this range has been interpreted to represent an increasing degree of post-magmatic alteration by aqueous fluid (Badejoko, 1977).

The province is also characterised by a wide range of accessory minerals in response to the abundance of many trace elements; these minerals include zircon, monazite, thorite, xenotime, apatite, fluorite, columbite, cryolite, allanite, thomsenolite and fergusonite (Jacobson et al., 1958), astrophyllite and amblygonite (Macleod et al., 1971), and narsarsukite (Jeremine and Christophe-Michel-Levy, 1961). It should be pointed out however, that some of these minerals may be secondary, and most of the identifications are optical only and little supporting chemical data is available. A summary of the chief mineral associations is given by Jacobson et al. (1958).

1.7 Mineralisation

The mineralisation associated with the Younger Granites has been the chief motivating force behind geological research in the province, ever since deposits of alluvial cassiterite were first discovered (Calvert, 1912).

There are two distinct periods of mineralisation in the Younger Granites: first a pre-joint metasomatic episode during which columbite, thorite and xenotime were introduced into the aluminous granites and cryolite and pyrochlore were introduced into the peralkaline granites. This episode was followed by a post-joint mineralisation period in the aluminous granites only, when cassiterite, wolframite and Fe, Cu, Zn, Sn and Pb sulphides were precipitated (e.g. Abaa, 1976; Bowden and Jones, 1974). Although the province is noted for cassiterite, the most abundant mineral in replacement veins may often be sphalerite, with the occasional concentration of other zinc or beryllium

minerals such as genthelvite or phenakite (Taylor, 1959; Bowden and Kinnaird, 1978). In Niger, similar mineralisation has been recognised, but occurs on a more limited scale owing to the paucity of biotite granites (Raulais, 1946, 1948, 1957; Black et al., 1967).

1.8 Petrogenesis

The close spatial relationship between the ring complexes and Cainozoic volcanism is possibly of some importance, as both may be related to events in the mantle associated with continental rifting (Black and Girod, 1970). The linear arrangement of the anorogenic complexes together with a southerly decreasing age trend towards the margin of the continent, lends support to this idea (Turner, 1973; van Breemen and Bowden, 1973). A possible connection between the systematic age variations for the Younger Granites and a 'hot-spot' in the mantle has been suggested (Karche and Vachette, 1976, 1978), but the data is not readily compatible with palaeomagnetic evidence, as pointed out by Bowden et al. (1976a).

For some rock types, namely coarse grained biotite granites, Rb/Sr isotopic data indicates that the most likely source is a partial melt of the lower crust, while other rock types apparently show more evidence for crustal contamination of a mantle or lower crustal partial melt (van Breemen et al., 1975). However for rocks with high Rb/Sr ratios, such 'contamination' may alternatively be due to a lengthy post-emplacement history involving selective transfer of Rb from deeper levels of a pluton to the apical region, which would ultimately lead to enrichment in radiogenic Sr without the need for 'contamination' from country rocks (Vidal et al., 1979).

A two-stage model whereby a basaltic liquid (being a partial melt from the mantle) collected at the base of the crust and underwent fractional crystallisation, and at the same time acted as a heat source

to cause melting in the crust, has been proposed (Bowden and Turner, 1974; Turner and Bowden, 1979). The possible petrogenetic significance of anorthosite bodies among the Niger complexes has been discussed by Black (1965). Black suggests that a tholeiitic parental liquid would crystallise plagioclase as the pressure decreased, in which case the residual melt would be syenitic. Continued differentiation of this syenitic melt could therefore lead to the formation of peralkaline granites - a rock type believed to be more abundant in Niger than Nigeria. In contrast, only small volumes of 'anorthosite' have been reported from Nigeria, and have been regarded as unrelated to Younger Granite genesis (Wright, 1975).

Melting experiments on a charnockitic rock known to occur in the basement of Nigeria, have shown that it is possible to produce a partial melt which could evolve towards a liquid of biotite granite composition. However, the same starting material could not produce a peralkaline derivative unless a peralkaline fluid was available at the time of melting (Brown and Bowden, 1973).

1.9 Peralkaline rocks

1.9.1 Introduction

As will be shown in Chapter 2, the Shira complex is dominated by hypersolvus peralkaline granites and syenites. It is therefore pertinent to review the present state of knowledge of these rocks within the Younger Granite province, and examine areas where problems of their character and genesis remain. In view of the relative paucity of detailed descriptions of peralkaline rocks from the Niger sub-province, the following review is biased towards occurrences in Nigeria.

A peralkaline rock may be defined as one in which the peralkalinity (or agpaitic) index, the mole proportion $[\text{Na}_2\text{O} + \text{K}_2\text{O}] /$

Al₂O₃, is greater than 1.0.

Obviously, not all peralkaline rocks in the Younger Granite literature have been analysed, but a peralkaline character may be inferred from their mineralogy, which invariably includes a sodic amphibole or pyroxene. In this review, unless otherwise stated, the nomenclature of the alkali amphibole has been changed from riebeckite to arfvedsonite. The term riebeckite has been used previously to describe blue or blue-green, highly pleochroic amphiboles in this province since their initial discovery (Lacroix, 1905), and has been applied with little discretion ever since. However, with chemical data, Borley (1963b) showed that the Nigerian alkali amphiboles were more sodic than riebeckite and lie along the riebeckite-arfvedsonite solid solution series. Borley (op.cit.) therefore called them riebeckitic arfvedsonites. More recently, Ike (1979) has suggested that even this term may be unnecessary and that the alkali amphiboles, in general, may simply be termed arfvedsonites. Moreover, in terms of ideal end-members, riebeckite contains only 2 out of 3 possible Na atoms (arfvedsonite) per half unit-cell, and so it is natural to expect that as the peralkalinity index of the rock increases, the amphibole would become more arfvedsonitic in response. In those rocks where an optically zoned amphibole has been described, clearly the term arfvedsonite may be slightly in error in that only the margin is likely to be arfvedsonitic.

Another potential source of error in published descriptions of peralkaline rocks in the province is that mineralogical interpretation has often been somewhat subjective. In particular, there is frequent reference to the habit of arfvedsonite and aegirine as being 'intergrown'. Intergrown and interpenetrating are not synonymous and it is unfortunate that most petrographic descriptions use the clearly generic term 'intergrown', instead of the purely descriptive term 'interpenetrating'. Of particular importance in this respect, is that

previous workers do not appear to acknowledge the possibility of replacement of alkali amphibole by aegirine.

For present purposes, it is convenient to divide the 'peralkaline' rocks into three groups on the basis of their texture and mineralogy : 1) hypersolvus granites in which perthitic (or antiperthitic) alkali feldspar is the sole or dominant feldspar; 2) albite-rich granites in which discrete albite laths occur scattered throughout the rock; and 3) 'riebeckite biotite' granites, which may or may not be strictly peralkaline, but which have much closer affinity to the truly peralkaline granites than to the aluminous biotite granites. The latter two rock types are included in this review, even though comparable facies do not occur in the Shira complex, because they share many of the same characteristics as type 1), and hence may have a similar origin.

1.9.2 Peralkaline alkali feldspar granites

These granites have perthitic (or anti-perthitic) alkali feldspar as the sole feldspar and may therefore be termed hypersolvus. They are widely distributed throughout the province, but decrease in abundance southwards, in central Nigeria, where aluminous biotite granites are dominant.

The following summary of principal characteristics of peralkaline rocks in the province is based largely on two Bulletins of the Geological Survey of Nigeria (Buchanan et al., 1971; Jacobson and Macleod, 1977), but additional information has been obtained from Black (1963), Black et al. (1967), Turner (1974a), Turner and Webb (1974) and Turner and Bowden (1979).

The main features of the peralkaline rocks therefore, are as follows (see Figures 1 and 2 for locations) :

1. Emplacement as ring dykes (Sara-Fier, Amo, Buji, Gamawa, Zuku,

Ningi) or as central intrusions (Kigom, Tongola, Jere-Sanga, Saiya-Shokobo, Kудару, Zuku).

2. As a result of (1), they may be either relatively early or late in the intrusive sequence, but are generally post-granite porphyry and pre-biotite granite.

3. Contacts may be relatively shallow dipping (Sara-Fier, Tongola, Saiya-Shokobo, Kудару) or steep (Sha-Kaleri, Jere-Sanga, Amo).

4. They may occasionally break through the confines of a ring fracture (Kудару).

5. They appear to be more abundant in the older sub-province of Niger than in Nigeria (according to existing maps).

6. There is a common association of syenites (> 10% plagioclase, I.U.G.S.) and alkali feldspar syenites (< 10% plagioclase) with peralkaline granites (Zuku, Gamawa, Dutse, Kila Warji, Ningi, Air).

7. The intrusions are sometimes associated with crushing and shearing in older rocks (Sha-Kaleri, Saiya-Shokobo).

8. Margins may be pegmatitic (Sha-Kaleri, Kigom, Tongola), porphyritic and/or chilled (Jere-Sanga), exhibit a poikilitic habit to the amphibole (Kigom, Shere), or have any combination of these features.

9. Some occurrences have gradational albitic zones (Kigom) or margins (Shere).

10. Angular xenoliths of older rocks may be locally abundant (Sha-Kaleri, Shere, Tongola), and these may undergo textural and mineralogical changes as a result of incorporation in the peralkaline granite (Shere).

11. Numerous small rounded syenitic xenoliths containing blue-green amphibole, biotite and large crystals of clear (?)alkali feldspar are described from one area (Sha-Kaleri) and are abundant at Shira (this study).

12. Intergranular albite and anti-perthitic texture is common, and

together with the ubiquitous occurrence of arfvedsonite and/or aegirine, indicates that peralkalinity is due to a relative abundance of Na rather than K.

13. Alkali feldspar commonly has blue amphibole or aegirine 'inclusions', while plagioclase appears to be entirely absent from these rocks.

14. Altered fayalite (chevkinite?) has been described from one peralkaline granite (Sha-Kaleri), apparently as residual cores to zoned amphibole. Otherwise, there is an absence of fayalite, calcic amphibole or pyroxene, and Fe-Ti oxides.

15. Amphibole may sometimes be optically zoned, in which case the term 'arfvedsonite' may be an oversimplification. However, in the original literature, it appears to be the very presence of optically zoned alkali amphibole (deep green or olive-green core and a blue-green rim, Sha-Kaleri) which led to the name arfvedsonite being used instead of riebeckite.

16. Arfvedsonite often occurs in intimate 'intergrowth' with aegirine.

17. Zircon is a very common accessory mineral.

18. Aenigmatite is rare but it may not have been recognised in the literature prior to the 1960's. It is possible that the 'altered fayalite' crystals found in the core of zoned amphiboles in the Sha-Kaleri complex may be a case of chevkinite or aenigmatite mistakenly reported.

Thus, some outstanding problems associated with the hypersolvus peralkaline granites are :

(a) the relationship, if any, between syenites (in general) and peralkaline granites,

(b) the nature and origin of small (< 10 cm) syenitic xenoliths,

(c) the origin and paragenesis of aenigmatite,

(d) the relationship between alkali amphibole and aegirine,

- (e) the nature of the optical zoning in alkali amphibole,
- (f) the reason for the absence of Fe-Ti oxides and plagioclase,
- (g) the relationship between the perthitic hypersolvus peralkaline granites and the albite rich varieties,
- (h) the nature and importance of rock-fluid interaction.

1.9.3 Albite arfvedsonite granites

These albite-rich rocks have so far been studied only (1) in the Nigerian sub-province where they occur as small bodies which are demonstrably intruded late in the magmatic sequence for any particular complex. Their margins are commonly highly pegmatitic but may instead exhibit a markedly poikilitic amphibole in contrast to the interior; they have a sugary white appearance in hand specimen and are easily weathered such that they always form areas of low relief. In thin section, they have a highly distinctive texture in which there are clear rounded quartz crystals, acicular but ragged arfvedsonite crystals and discrete euhedral laths of albite which pervade the rock and apparently replace the other minerals. There is a characteristic suite of accessory minerals including fluorite, cryolite, pyrochlore, and zircon, which probably reflects the concentration of trace elements. The abundance of Nb and U/Th in particular, led to economic interest in these rocks (Mackay and Beer, 1952). These unusual rocks have probably been thoroughly recrystallised by, or are the product of, late stage residual peralkaline fluid (Borley et al., 1976).

The following essential features of the albite arfvedsonite granites have been summarised from the work of several authors in Buchanan et al. (1971) and also from Jacobson and Macleod (1977) :

1. They are always present as small exposures - of the order of only a

(1) There is a brief mention of an 'albite-riebeckite-microcline' granite in the Aroyan complex, Niger (Black et al., 1967).

few sq.kms or less.

2. Where contact relations have been observed, they are late in the intrusive sequence.

3. Quartz, alkali feldspar, arfvedsonite pegmatite or quartz 'knots' are common towards the margins: the pegmatite may have a banded appearance due to alternating concentration of arfvedsonite and felsic minerals (Buji).

4. Within adjacent basement rocks, there may be a marginal zone of 'hydrothermal activity' (Dutsen Wai), and at Ririwai the adjacent biotite granite has joint surfaces coated with arfvedsonite.

5. Considerable textural variation across the exposure is common (well described at Ririwai).

6. Although aegirine has not apparently been found in marginal pegmatite, it is abundant in the body of the rock and is usually intensely 'intergrown' with arfvedsonite.

From these characteristics, some important discussion points emerge :

(a) The modifications to adjacent or included (Shere) older rocks, textural variability, trace element and accessory mineral content and association with marginal pegmatite, all clearly point to an abundant fluid phase.

(b) In the Shere and Kigom complexes, there are albitic (?) roof zones to an otherwise 'normal' peralkaline granite. This, together with the limited areal extent of the albite arfvedsonite granites, may imply that they are relatively limited in depth and grade into the more common alkali feldspar granite. If this supposition were true, the albite arfvedsonite granites would be relatively vulnerable to erosion and this might explain their greater rarity in the older complexes in Niger.

1.9.4 Riebeckite annite granites

These granites have, in the past, been referred to as riebeckite biotite granites. In contrast to the preceding sections, the original nomenclature of the amphibole is here retained; the reasons for this are that : (a) modern analytical data indicates that the amphibole composition lies between a low Ca ferrorichterite, riebeckite and arfvedsonite (Abernethy, in prep.) - therefore, no useful purpose would result from changing the name; (b) the unpublished analytical data referred to above indicates that some of the amphibole compositions fall closer to riebeckite than either ferrorichterite or arfvedsonite. These compositions, and also those that lie between low Ca ferrorichterite and riebeckite at least, are probably less sodic than would be expected from a 'normal' alkali feldspar peralkaline granite. Thus, the 'riebeckite' compositions may vary in sympathy with their host rock compositions which commonly have a peralkalinity index < 1.0 .

The name of the mica however, has been changed. The mica has previously been referred to as 'biotite', but it has a very distinctive pleochroism (X = bronze-red colour) and recent analyses have shown that it has an unusual composition. It lies along the annite-ferriannite solid solution series and has a particularly low Al content (Abernethy, in prep.).

In the past the mineralogy of the riebeckite biotite granites has, not unnaturally, led to speculation as to whether they represent a link between the peralkaline and aluminous (i.e. P.I. <1.0) granites within the province (e.g. Jacobson et al., 1958). In assessing whether this suggestion has any foundation, the following major features of the riebeckite annite granites may be significant (summarised from Buchanan et al., 1971) :

1. They may occur in ring dyke form (Rop, Amo) or as stock-like intrusions late in the intrusive sequence (Jere-Sanga). Basement

xenoliths are common in the ring dyke occurrences.

2. They may have sharp, vertical contacts against older rocks and exhibit considerable local development of marginal pegmatite (Jere-Sanga), or flow alignment of amphibole laths (Rop). Pegmatitic development as found at the Fiskam Mata outcrop (d8) of Jere-Sanga, would be most unusual for a 'normal' (ie. non-annite bearing) peralkaline granite and may reflect a higher volatile content.

3. Several occurrences apparently have gradational contacts with surrounding rocks (eg. Amo), although this may be largely due to poor exposure. In other areas, there is strong field evidence for the production of riebeckite annite granite by (metasomatic) reaction between a peralkaline granite and either an earlier 'hornblende pyroxene' granite (Shere) or a roof pendant of biotite granite (Kigom).

4. As a result of (3), individual occurrences sometimes show a modal variation across the exposure, typically from amphibole rich centres to annite rich margins (Jere-Sanga), or pronounced textural variation according to the width of the intrusion (Rop).

5. Aegirine and annite do not coexist (eg. Kigom).

6. Plagioclase is absent.

7. Annite has crystallised later than the amphibole (Amo).

8. Chemical analyses show that these granites commonly have a peralkalinity index < 1.0 .

These characteristics indicate to the writer that within the Younger Granite province there has not been a magma of 'riebeckite biotite' granite composition. Instead, it appears that this facies occurs solely by 'contamination' of or alkali loss from an original peralkaline granite. Such contamination has possibly resulted from the activity of a fluid phase with an adjacent or enclosed block of non-peralkaline (aluminous) granite. In this regard, it is significant to note that the 'biotite' composition, as its colour and distinctive

pleochroism would suggest, has a unique (low Al) composition.

Thus, there does not appear to be a case for this rock type being an intermediate in the generic sense, between the peralkaline and aluminous granites; rather, the riebeckite annite granite is a marginal zone of a peralkaline granite and as such, it will not be discussed further.

1.10 Syenitic rocks

1.10.1 Introduction

Within the Nigerian sub-province, basic and intermediate rocks occupy only about 5% of the surface area of the ring complexes, although this proportion is apparently higher in Niger (Black et al., 1967). The syenites usually precede the intrusion of granites and form topographically prominent hills. Among the mafic minerals 'hornblende' is the most common. Plagioclase often exhibits gradational or oscillatory zoning with a compositional range of An 20-40, while alkali feldspar has only poorly developed perthitic texture. "The high proportion of plagioclase to orthoclase in some facies indicates that they belong to the monzonite or dioritic families" (Jacobson et al., 1958).

As there is a paucity of information concerning the volcanic syenitic rocks (i.e. trachytes and related rocks), this discussion is concerned only with the sub-volcanic syenitic intrusions. From Figure 33c it may be seen that all analysed syenites in the province are quartz normative, except two samples which have neither quartz or nepheline in the norm. There are two mineralogically distinct types of 'syenite' within the province and their principal characteristics are summarised below, from information taken from Black (1963, 1965),

Buchanan et al. (1971), Jacobson and Macleod (1977), Turner (1963, 1971), Turner and Bowden (1979) and an unpublished manuscript on the Kila-Warji complex by D.C.Turner (1974b).

1.10.2 Alkali feldspar syenites

Included in this term are those syenitic rocks in which alkali feldspar is practically the only feldspar present and includes both alkali feldspar syenites and alkali feldspar quartz syenites (Streckeisen, 1976). Their essential characteristics may be summarised as follows:

1. Apparently steep sided, stock-like intrusions, sometimes with abundant pendants and xenoliths of basement rocks (Pankshin, Zuku).
2. In Nigeria at least, they do not occur in the same complex with plagioclase bearing syenites.
3. They may be closely associated with peralkaline granites (Tchouni-Zarniski, Gamawa) or themselves have close peralkaline affinities (Zuku, Gamawa, Guraka).
4. Commonly there is considerable textural variation across a single exposure (Zuku, Gamawa). Quartz rich margins may grade into a 'hornblende' granite (Zaranda). Texturally and mineralogically, several show close affinities to the (fayalite) 'hornblende' granites and porphyries.
5. Amphibole-alkali feldspar pegmatite may be locally abundant towards the margins.
6. Alkali feldspar usually has a lamellar perthitic texture, and/or has clear cores with a turbid outer zone, commonly with inclusions of fayalite, pyroxene, amphibole or a little biotite - the outer part being particularly rich in inclusions. There is little intergranular albite.
7. The mafic minerals include fayalite, pyroxene, amphibole, aenigmatite, and biotite. Accessory minerals include iron-ore, apatite,

allanite (?chevkinite), well formed zircon, and interstitial quartz. Clinopyroxene occurs as a colourless or pale brown variety (?ferroaugite) and also a pale brown-green or pale green type with dark green margins which may be (sodic) ferrohedenbergite. Amphibole is brown-green or dark green with bluish zones, may have a spongy habit and enclose pyroxene. In sympathy with the textural variations already noted, the proportions and type of the mafic mineral assemblage may vary across an exposure.

1.10.3 Two-feldspar syenites

These plagioclase bearing syenites may take the form of arcuate or ring dyke intrusions (Saiya-Shokobo, Jere-Sanga) or central intrusions (Kila-Warji). They are usually porphyritic and have phenocrysts of oligoclase-andesine rimmed and partly resorbed by alkali feldspar set in a matrix of microperthite, quartz and mafic minerals. At Ningi and Jere-Sanga, the proportion of plagioclase is high enough to warrant the term monzonite or 'syenomonzonite'.

'Hornblende' is the most common mafic mineral but it is usually accompanied by and may enclose, (ferro)augitic or (ferro)hedenbergitic pyroxene, minor fayalitic olivine, biotite, iron-ore, apatite, allanite and zircon.

In the Ningi, Kila Warji, Goure and many of the Air complexes, syenite is associated with peralkaline granites.

1.10.4 Discussion

From this brief summary, several important points are worthy of emphasis. There are peralkaline and aluminous varieties of syenite but no single Nigerian complex appears to exhibit both types. However, both can occur in association with peralkaline granites and so it is possible that the syenites themselves may have a fundamental connection

with these granites.

In an unpublished manuscript on the Kila Warji complex, Turner (1974b) discussed the possible importance of plagioclase, in which the following points are significant. In the Kila-Warji complex, a chilled margin to the porphyritic syenite contains plagioclase phenocrysts which are much smaller than in the main body of the rock. This implies that plagioclase grew in the magma (1) and is not a xenocrystal phase from the basement.

In addition, a 30 cm block of anorthosite has been discovered in the porphyritic syenite (D.C.Turner) which suggests that plagioclase could accumulate and that parts of the cumulate were subsequently brought to the surface. Since large anorthositic bodies are found in Niger, the possibility that they may be connected with the genesis of peralkaline rocks by removing Ca and Al from a parental magma, has been given serious consideration (Black, 1965). In fact, in the Kila-Warji complex, there is a steady increase in the size of the alkali feldspar phenocrysts and proportion of quartz, accompanying a decrease in the mafic mineral content from the porphyritic trachyte through the porphyritic syenite and Kila syenite, to the quartz syenite porphyry. This suggests that a simple crystal fractionation process has operated in these rocks.

Thus there are several clues suggesting a connection between the two-feldspar syenites, the alkali feldspar syenites and peralkaline granites, and one of the principal objects of this work is to investigate the association more fully, with particular reference to the Shira complex.

(1) However, it is a little difficult to reconcile this point with the fact that plagioclase shows good evidence for resorption and is mantled by alkali feldspar (Badejoko, 1977).

1.11 Aluminous rocks

1.11.1 Introduction

The immediate purpose of this short review is to summarise the literature with which the Zigau granite porphyry may be compared - that is, the fayalite, pyroxene and hornblende bearing granites and porphyries, exclusive of the biotite granites. The geochemistry of this group of rocks will be reviewed in Chapter 5. As in preceding sections, this section deals only with the sub-volcanic intrusions, although as will be shown in Chapter 5, there are close geochemical (and mineralogical) links between this rock group and the majority of volcanic rocks. 'Quartz porphyries' are here regarded as volcanic rocks. Since there are often several different intrusions of rocks belonging to this group, individual intrusions are suffixed by the code given by Buchanan et al. (1971).

Original mineral names as found in the literature are used. In some cases it would be preferable to replace the term 'hornblende' with hastingsite, where an analysis is available (see Borley and Frost, 1963); however, from the colour and zoning of the amphiboles described, it appears that the term hastingsite would be insufficient to cover the likely range of composition, so 'hornblende' is retained to describe a dominantly iron-rich, calcic amphibole.

In many descriptions fayalite and pyroxene are either altered or present only as very small grains. Probably for this reason, petrographers have been unspecific about the type of clinopyroxene present and therefore the original term 'pyroxene' has to be retained. The present review is based upon field and petrographic descriptions of 50 intrusions from 18 ring complexes in Nigeria, taken from Buchanan et al. (1971). Both porphyritic and equigranular rocks are included because (i) of their mineralogical and chemical similarity, (ii) there is sometimes a gradation between these facies, and (iii) both the

equigranular and porphyritic varieties may occur as true ring dykes.

1.11.2 Principal characteristics

The chief field and petrographic features are as follows:

1. Occurrence as ring dykes (Dagga-Allah, Sara-Fier S4) or stock-like intrusions (Jarawa, Sutumi); in both, contacts with the host rock are steep and sharp (where preserved as roof pendants however, the contact angle is shallow, e.g. Kwandonkaya).
2. The ring dyke occurrences are early in the magmatic history and tend to be obliterated by later intrusions (e.g. Sho, Rop complex).
3. Chilled margins in which there is a reduction in grain size and/or in the size and number of phenocrysts, are common. These margins generally have biotite as the only mafic mineral (Jos-Bukuru, m2; Rop, r11; Sha-Kaleri, u6).
4. Pegmatitic margins are rare (Sha-Kaleri, u3; Sara-Fier, s15).
5. Within one exposure there are several instances of gradational textural changes from one facies to another (Sara-Fier, s9, s'3, s'4).
6. Xenoliths of the basement may be common along the outer contact of a circular, stock-like intrusion (Kagoro) or along narrow portions of a granite porphyry dyke (Shere, m'7). The width of an intrusion can also control the texture, and narrow sections may be granophyric (Tongola, b4).
7. Some ring-dyke porphyry intrusions may represent a transition from a feeder dyke (quartz porphyry) for a fragmental surface eruption, to a 'normal' granite porphyry (Jos-Bukuru, m4).
8. Some granite porphyry ring dykes may have mylonitised (Jos-Bukuru, m2) or doleritic margins (Shere, m'7). They are able to (contact) metamorphose older volcanic rocks to an andalusite-cordierite hornfels (Jos-Bukuru, m2).
9. Both porphyries and granites are noted for their relative abundance

of small (1-10 cm) dark, rounded xenoliths (Ganawuri, ol; Shere, m'7; Jos-Bukuru, m'2; Rop, r3, r11; Sara-Fier, s11). These xenoliths are generally of quartz microsyenite with microperthite, large euhedral crystals of zoned plagioclase and composite crystals of perthite and plagioclase (oligoclase), and interstitial amphibole and quartz.

10. In many instances where fayalite appears in the name of a rock it has not actually been observed except as pseudomorphs of generally unidentified material (?iddingsite, ?bowlingite). Fayalite is however, still present in chilled margins (Jarawa, m'1).

11. By comparing petrographic descriptions with modal analyses, and the published descriptions with thin sections in this Department, it is apparent that insufficient attention has been paid to the plagioclase content of these rocks (see later).

12. Occasionally, quartz may constitute < 15% of the rock and using the I.U.G.S. classification system (Streckeisen, 1976) it would be regarded as a quartz syenite (Sha-Kaleri, ul3; Saiya-Shokobo, a4; Sara-Fier, s'5).

13. Feldspar is typically an alkali feldspar with a lamellar or patchily perthitic texture, often with a narrow dentate film of exsolved albite, which rims discrete plagioclase crystals, or in the case of the porphyries is aggregated into glomeroporphyritic masses. Commonly it is zoned with a clear, cryptoperthitic core to a cloudy microperthitic margin; in the porphyries the latter may enclose part of the matrix (Tongola, b3). Microcline twinning is very rare (Sutumi, g2).

14. Quartz in the porphyries is often of bipyramidal form and may therefore represent an alpha-pseudomorph after the high temperature beta-form. In the granites and the porphyries, quartz is usually found as chains and clusters of relatively early formation which are partly surrounded by alkali feldspar.

15. Pyroxene may be colourless, pale green or pale brown, and may exist

as phenocrysts and in the matrix of the porphyries (Tongola, b3). In the granites it is usually present as rounded grains enclosed by amphibole, but only in trace amounts.

16. Amphibole is anhedral to subhedral, usually brown or green and may be zoned or have margins that have a blue-green colour. Towards the margins, it may develop a sieve texture (Amo, h4). In some rocks, it has been analysed and shown to be hastingsite (Borley, 1963b) with an extinction angle $Z:c$ about 30 degrees. It is commonly rimmed by biotite or completely pseudomorphed by it (Sara-Fier).

17. Accessory minerals occur in the mafic aggregates and include fluorite, iron ore (often skeletal), apatite, fergusonite, and well formed and sometimes unusually large crystals of zircon and allanite.

1.11.3 Discussion

The main properties of the 'fayalite, pyroxene and hornblende' granites and granite porphyries, as summarised above, will be referred to in the remainder of this work as necessary. For the present therefore, the writer wishes to direct attention to one particular aspect of these rocks, namely the presence of plagioclase feldspar. The presence or absence of plagioclase is vitally important for classification purposes and as an indicator of petrologic association with other rock types in the province.

Table 1 lists the occurrences of fayalite, pyroxene and 'hornblende' bearing granites and porphyries in Nigeria, together with a list of those exposures that have a modal analysis and/or have a petrographic description which is sufficient for an estimation of the presence of plagioclase. In many descriptions alkali feldspar is, for example, described as the 'dominant' feldspar but only in a few cases is the remainder of the feldspathic component specified - usually as 'discrete albite' which is rimmed by alkali feldspar. By studying thin

sections of comparable rocks from Nigeria, it is apparent that such 'discrete albite' is in fact more calcic (of oligoclase-andesine composition) and it is usually present in these rocks. Thus, it would appear that in published petrographic descriptions, the presence of discrete crystals of plagioclase has not received sufficient attention, and consequently these granites and porphyries have been regarded as almost entirely hypersolvus (one-feldspar) rocks. To illustrate the previous point, in seven examples from Table 1, no plagioclase is reported in the petrographic description, yet (discrete) 'albite' appears in the modal analysis, while in another seven cases, plagioclase is either reported or can be inferred (by descriptions of 'discrete albite') to be present in the rock, and appears in the mode. Thus in half the examples where modal analyses are given, the presence of plagioclase appears to have been insufficiently emphasized or ignored. In fact, of the 50 occurrences of fayalite, pyroxene or 'hornblende' bearing rocks in Table 1 where there is a sufficiently good petrographic description, plagioclase is either reported or can be inferred to be present in 21 cases (ie. about half of the total). In many of these 21 instances albite-oligoclase or even oligoclase-andesine is reported, but in the remainder only 'discrete albite' is mentioned. The present author's view that such 'discrete albite' is of oligoclase-andesine composition (ie. $> \text{An } 10$) is supported by the fact that true albite laths ($< \text{An } 10$) are probably restricted to the so-called 'albitised' mica or amphibole granites, which in any case have a highly distinctive texture and mineralogy. Also, a close look at many plagioclase crystals in these rocks reveals zoning and rimming by alkali feldspar - features not shown by albite in 'albitised' rocks of the Province.

1.11.4 Biotite granites

In view of the minor importance of biotite granite in the Shira complex together with the fact that the biotite granites are presently the subject of a special study (Abernethy, in prep.), it is inappropriate to review these rocks as extensively as the others. However, the biotite granites are mentioned in Chapters 5 and 6 in connection with the geochemistry and petrogenesis of the province, in which case their relevant features are summarised where necessary. At this point therefore, it is sufficient to mention that they may bear appreciable quantities of plagioclase, exhibit dispersed (columbite) or vein controlled (Zn-Sn-W) types of mineralisation, are aluminous, occur in relatively greater proportions in Nigeria compared to Niger and usually dominate and end the magmatic cycle in any particular intrusive centre or complex (Mackay et al., 1971).

The Shira complex consists of a series of intrusions which are generally aligned north-south, but overall the topography is such that the plains to the south have an elevation of little over 1000 ft above sea level and belong to a physiographic region known as the Sahel. To the north, the area is more undulating and consists of the Shira Plateau (Gordon and Mackay, 1971). This plateau consists of a series of low hills which form an orientated elongate ridge, but the Gays Plains are covered by a more even carpet of scallan sand which blankets most of the plateau. The climate of the region is divided into a dry season from November to April and a wet season from May to October. Between 400 and 700 mm of rain occurs annually, although this falls in a period of only 50 days per year, mostly in August. During the dry season, the hot land wind (harmattan) blows from the Sahara, but during the wet season the wind is from the south and the temperature is higher.

Figure 2. Location map of anorogenic ring complex in Nigeria. The Shira Plateau complex lies in the north. Solid lines are ring dikes.

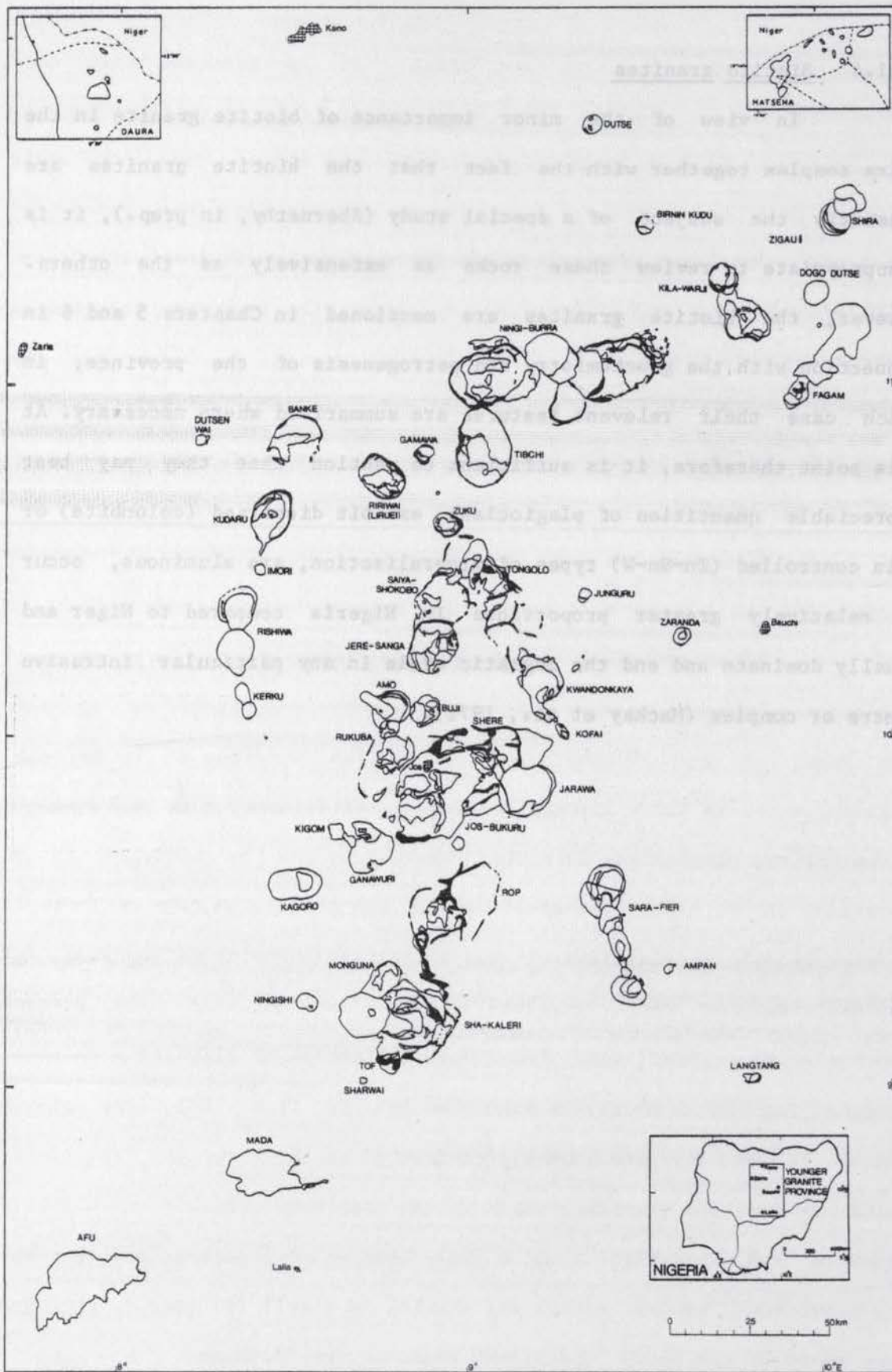


Figure 2. Location map of anorogenic ring complexes in Nigeria. The Shira ring complex lies in the NE. Bold lines are ring dykes.

CHAPTER 2FIELD GEOLOGY2.1 General

The town of Shira, after which the complex is named, is situated within the southern part of the complex 180 km ESE from Kano at 11°27'N, 10°03'E. The complex itself is shown in relation to other Nigerian complexes in Figure 2. It has maximum surface dimensions of 16x10 km, has its long axis orientated NNE and has a postulated area, above and beneath superficial deposits, of 152 sq.km. It is situated on either side of a hard surfaced, single track road from Yana to Azare and is close to the main Kano-Potiskum road (Figure 3). Access to the complex is therefore good. In the south rocks of the Shira complex reach a maximum height of about 200 m above the surrounding plains, but overall the topography is much more subdued. The plains to the south have an elevation of little over 400 m above sea level and belong to a physiographic region known as the Gaya plains. To the north, the area is more undulating and forms part of the Lantewa dunefield (Bawden and Jones, 1973). This dunefield consists of unconsolidated aeolian sands which form NE orientated elongate ridges, but the Gaya plains are covered by a more even veneer of aeolian sand which blankets most bedrock exposure. The climate of the region is divided into a dry season from November to April and a wet season from May to October. Between 800 and 900 mm of rainfall occur annually, although this falls on an average of only 60 days per year, mostly in August. During the dry season a dry, dust laden wind (harmattan) blows from the Ténéré region of the Sahara, but during March and April, the sun is overhead and both temperature and humidity rise. The mean maximum temperature in April is about 38 degrees C, but it commonly exceeds 45 degrees C (113 degrees F).

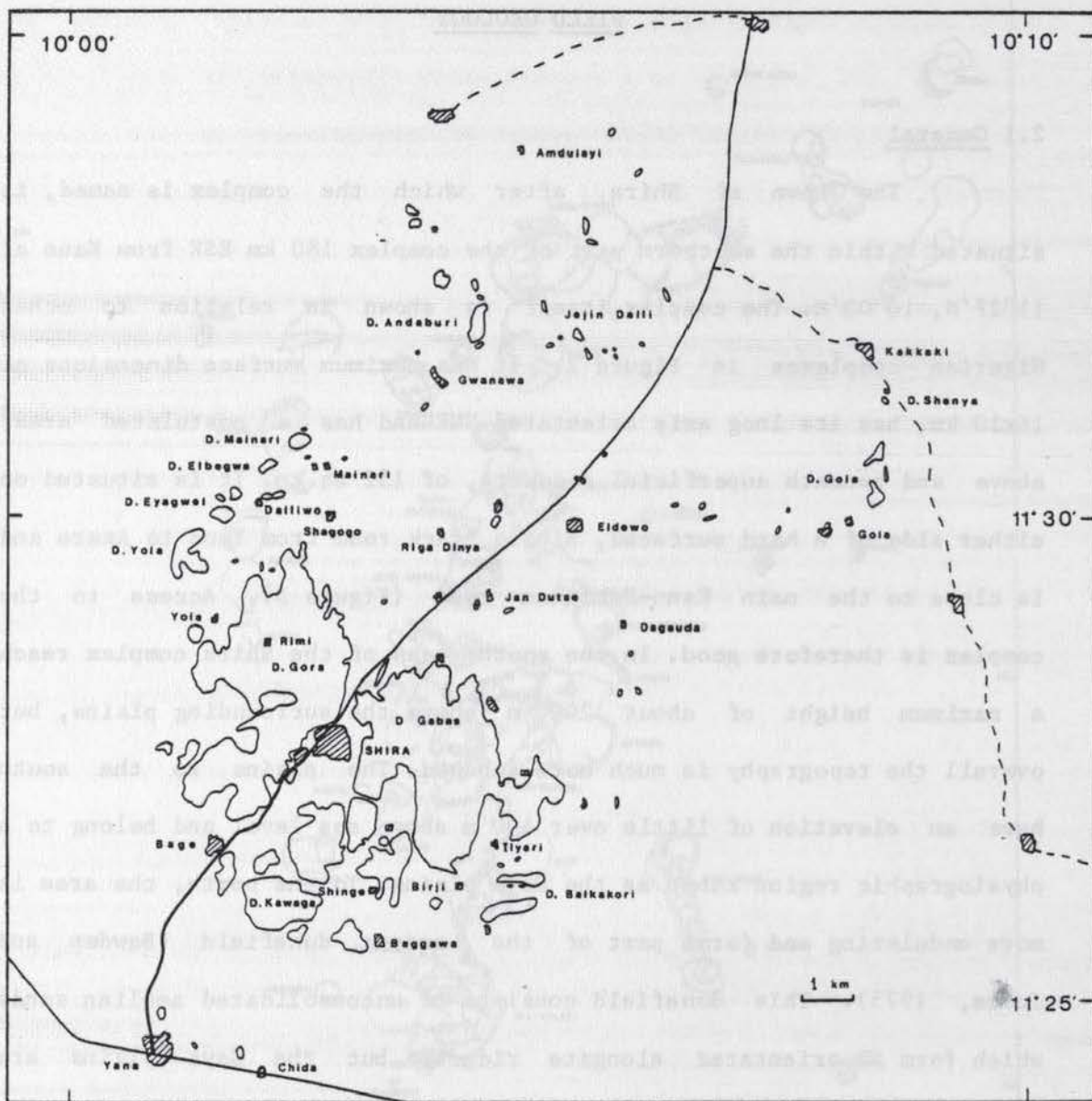


Figure 3. Simplified outcrop and locality map of the Shira complex. Rock exposure is enclosed by a solid line and prominent hills are prefixed by D, being the abbreviation for Dutsen meaning 'hill of' in Hausa. Villages are shown by diagonal lines.

Drainage from the Shira complex is radial, by short ephemeral streams that are quickly absorbed by the surrounding aeolian sand and they are not an obstacle to access. Immediately to the west of Zigau however, the virtually perennial Bunga river drains inland to Lake Chad from the Jos Plateau.

Apart from two brief sample collecting trips of a few days each in 1975-6, fieldwork for this study was carried out throughout the month of April, 1977. The complex was mapped using 1:40,000 scale aerial photographs (taken in November 1971). Field information was transferred from photograph overlays to 1:50,000 contoured topographic maps, using a radial line plotter, in order to make the maps which accompany this work. Both the aerial photographs and maps were supplied by the Directorate of Overseas Surveys.

2.2 Introduction

In what appears to be the only geological reference in the literature to the Shira complex, Falconer (1911, p.133) found that in the Shira granite, "...riebeckite builds elongate crystals more or less idiomorphic in the prism zone and frequently intergrown with aegirine". Presumably it is on the basis of this reference that the complex appears on 1:2 million scale geological maps of Nigeria (eg. Carter, 1964). Not surprisingly therefore, the size of the complex was found, during the course of this work, to be much larger than had hitherto been supposed, although the northern half is particularly poorly exposed.

The Shira complex may be described as having three centres (in addition to the isolated Zigau granite porphyry); these centres are dominated by or are composed of 1) the Shira quartz syenite, 2) the Andaburi granite, and 3) the Eldewo biotite granite. The complex consists dominantly of peralkaline rocks except for the Eldewo biotite granite and the small Zigau granite porphyry.

By reason of the poor exposure, age relations between some rock units cannot be accurately determined. For example, the relative age of the Zigau granite porphyry is not known, but by analogy with granite porphyries in other complexes, is presumed to be the earliest intrusion. The Shira quartz syenite is cut by the arcuate Birji granite but the time relations between these rock units and the northern Andaburi granite are not known with certainty. The Andaburi granite is however, intruded by the Eldewo biotite granite and from the pattern of exposures, the latter would also appear to be later than the Shira quartz syenite.

It is therefore possible that there has been a progressive northeastward shift in magmatic activity with time, until the central biotite granite ended the magmatic sequence, and the probable order of intrusion for the major rock units is as follows :

1. Zigau granite porphyry
2. Shira alkali feldspar quartz syenite
3. Birji alkali feldspar granite
4. Andaburi alkali feldspar granite
5. Amdulayi alkali feldspar syenite
6. Eldewo alkali feldspar (biotite) granite

Accordingly, this is the order in which the rock units will be discussed in the succeeding sections.

2.3 The Zigau granite porphyry

The small body of granite porphyry at Zigau is associated with the Shira complex by proximity rather than petrologic similarity. It extends for 3 km almost due N-S beside the Zigau-Foggo track. The northern end crosses the Kano-Potiskum road about 11 km from Shira town and the southern extremity terminates near the village of Gabati.

The intrusion is up to 500 m wide and rises up to 50 m above

the surrounding plain, but its exposed area is little more than 1 sq.km. It is cut by several joint controlled valleys and it forms a prominent headland against the Bunga river which flows northward along the western margin of the porphyry. No contact with the country rock has been observed but it is presumed to have a dyke-like form. The body contains numerous small, dark, rounded enclaves which may be sparsely porphyritic.

2.4 The Shira alkali feldspar quartz syenite

Virtually the entire topographic relief of the Shira complex is due to the coarse grained alkali feldspar quartz syenite (henceforth referred to simply as the quartz syenite), which rises to a maximum height of 632 m above sea level and up to 200 m above the surrounding plains (Frontispiece). The quartz syenite forms the majority of centre 1 and the town of Shira is situated in a valley in the centre of the outcrop (Figure 3). The postulated surface area beneath superficial deposits is 69.5 sq.km. Outcrops of quartz syenite consist of very large exfoliated slabs or, more commonly, occur as groups of very large boulders (Plate 1). Jointing is prominent on aerial photographs, particularly east of Shira, but is not obvious when viewed from the ground because of the boulder strewn outcrops. However, some joints have been selectively eroded to form linear depressions, the dominant directions being N-S and SW-NE.

Aeolian sand obscures the outer contact with the country rock, or 'basement' as it is more usually referred to. However, the curvature of exposures toward the centre of the complex suggests that the biotite granite to the north, is younger. In this case, the Shira quartz syenite would be the oldest major intrusion in the southern part of the complex. It is cut by the Birji granite and by several dykes or cone sheets which may be radial or tangential to the arcuate intrusion. Close to the Birji



Plate 1. Large exfoliated surfaces and boulder piles of the Shira quartz syenite, just N of Shira, looking NE across the Azare road.



Plate 2. Two phases of dilatational microgranite dykes within the Shirà quartz syenite at D.Eyagwel.

granite, the host quartz syenite has undergone some textural changes which are apparent in the field as a whiter, fresher appearance to the alkali feldspar. The petrographic changes accompanying this metasomatic effect are discussed in more detail in Chapter 3.

In the Shira complex as a whole, dykes and enclaves are not abundant ; however, probably both are best developed in the Shira quartz syenite. The dykes occur preferentially close to the arcuate granite, are commonly parallel (or sometimes radial) to that intrusion and have a mineralogy and bulk chemistry which suggests that they are closely related to it. The orientation of these peralkaline, medium or fine grained granitic dykes is shown on Map 2. Almost all the dykes are subparallel to the contacts of the Birji granite and occur preferentially on the southern or western side of the arc. Nevertheless, there does not appear to be a consistency of dip: some dykes dip towards the arcuate granite and others dip away from it. They may be up to 4 m wide but usually have a width of 10-30 cm. They are often traceable for the length of an exposure of quartz syenite, for example, 145 m at D.Elbegwa. Along its length however, a dyke may bifurcate into two or more narrower dykes for a short distance, or change direction by up to 15 degrees. Sometimes there is another, slightly narrower, dyke which runs parallel to the main dyke for its entire length; or alternatively an adjacent sinuous or discontinuous dyke which is not obviously dilatational, may have a heterogeneous appearance and marginal banding. The dykes are all melanocratic, dark blue or grey in colour and usually have a much fresher appearance than the quartz syenite, even though they commonly weather to shallow troughs. The majority have parallel sides, are dilatational and there may be more than one period of emplacement (Plate 2). Larger quartz or alkali feldspar crystals sometimes impart a slightly porphyritic texture, while shiny, elongate amphibole laths are commonly visible on the surface. They may be up to 4 m wide but usually

have a width of 10-30 cm.

Exceptions to these general observations occur at D.Mainari. On the S side of the hill there is a 10 cm wide pegmatite vein containing amphibole crystals up to 5 cm long, which is cut by a later dyke. Along the centre of the hill and forming a slight ridge, there is a dyke of melanocratic, medium grained granite which, at the E end, dips south at 36 degrees with a strike of 075 degrees. It is about 10 m wide and has a heterogeneous texture dominated by a sub-parallel arrangement of elongate amphibole crystals, interspersed with areas having no obvious amphibole orientation. The size and texture of this dyke is unlike the more usual melanocratic microgranite dykes, and it is probably structurally continuous with the Birji granite itself. On the N slopes of D.Mainari there is a localised vein system 20 cm wide, in which there are well developed, undulatory aegirine layers with intervening felsic zones. The veins have irregular margins and do not appear to be dilatational.

Enclaves occurring within the Shira quartz syenite are, with one exception, small, dark, rounded and syenitic. The major exception is a large body, perhaps 200 m wide, which is situated on the north side of, and adjacent to, Shira market, close to the centre of the exposed Shira quartz syenite. The body is known as the Gora enclave, which is a peralkaline microgranite with aegirine laths visible in hand specimen. It weathers to a lower profile with much smaller boulders than the host rock (Plate 3). The body is highly variable in colour and texture: the colour varies from cream to grey or blue, and the texture from a medium grained equigranular granite of varying mafic content, to a sparsely porphyritic rock with a patchy distribution of coarser and finer grained areas. Along the northern margin, on the edge of D.Gora overlooking the Azare road, the enclave has been fragmented considerably by the intrusion of the Shira quartz syenite (Plate 4). At this margin the



Plate 3. View of the N edge of the Gora enclave at the edge of D.Gora, close to the Azare road. The enclave weathers to smaller boulders than the Shira quartz syenite to the left. Looking S.



Plate 4. Margin of the Gora enclave which has been broken up into numerous small blocks by the Shira quartz syenite. Same locality as above.

xenolithic blocks are relatively large and angular compared to the other type of enclaves discussed below. In only one other locality has a similar enclave been found - in D.Kawaga towards the SW margin of the complex, but it is therefore possible that the original extent of this microgranite was greater. The presently exposed body is however, considered to be a roof pendant.

The other type of enclave occurs as small (1-10 cm) bodies which are scattered comparatively widely throughout the quartz syenite, although not abundantly. Their presence may often be noted on the sides of large boulders but they are rarely capable of being sampled. These small enclaves appear to be more abundant towards the margins of the exposed quartz syenite.

At a small hill close to Mainari, slightly porphyritic, melanocratic enclaves (1-10 cm) occur in relative abundance; they are syenitic and medium grained. Nearby, at the E end of D.Dalliwo, several larger (about 30 cm) syenitic enclaves occur, which are similarly medium grained and slightly porphyritic.

Towards the centre of the exposure W of Shira, one small syenitic enclave is unusual in having well oriented alkali feldspars, while an adjacent variety is highly porphyritic and the white alkali feldspar crystals are aggregated.

2.5 The Birji alkali feldspar granite

2.5.1 Introduction

The Birji alkali feldspar granite is an inclined intrusion within the Shira quartz syenite and it extends through an arc of 120 degrees for a distance of 13.5 km. It has a maximum width of about 1 km and a postulated surface area beneath superficial deposits, of about 10.9 sq.km. The granite has a distinctive appearance in the field, with significantly smaller, darker coloured boulders than the host quartz



Plate 5. Distinctive geomorphology of the Birji granite (left) compared to the Shira quartz syenite. S of Shira town, W of the Azare road.

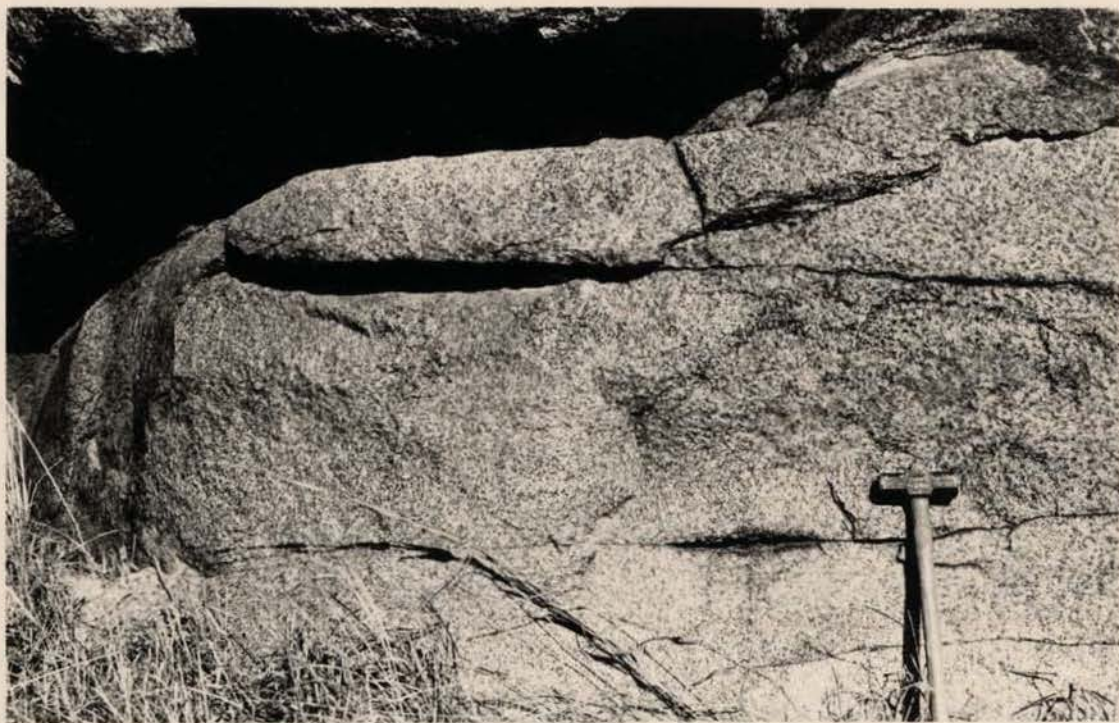


Plate 6. Gradational contact between the acicular (lower left) and poikilitic facies (upper right) of the Birji granite.

syenite (Plate 5). The boulders are rounded and usually fresh and comparatively easy to sample.

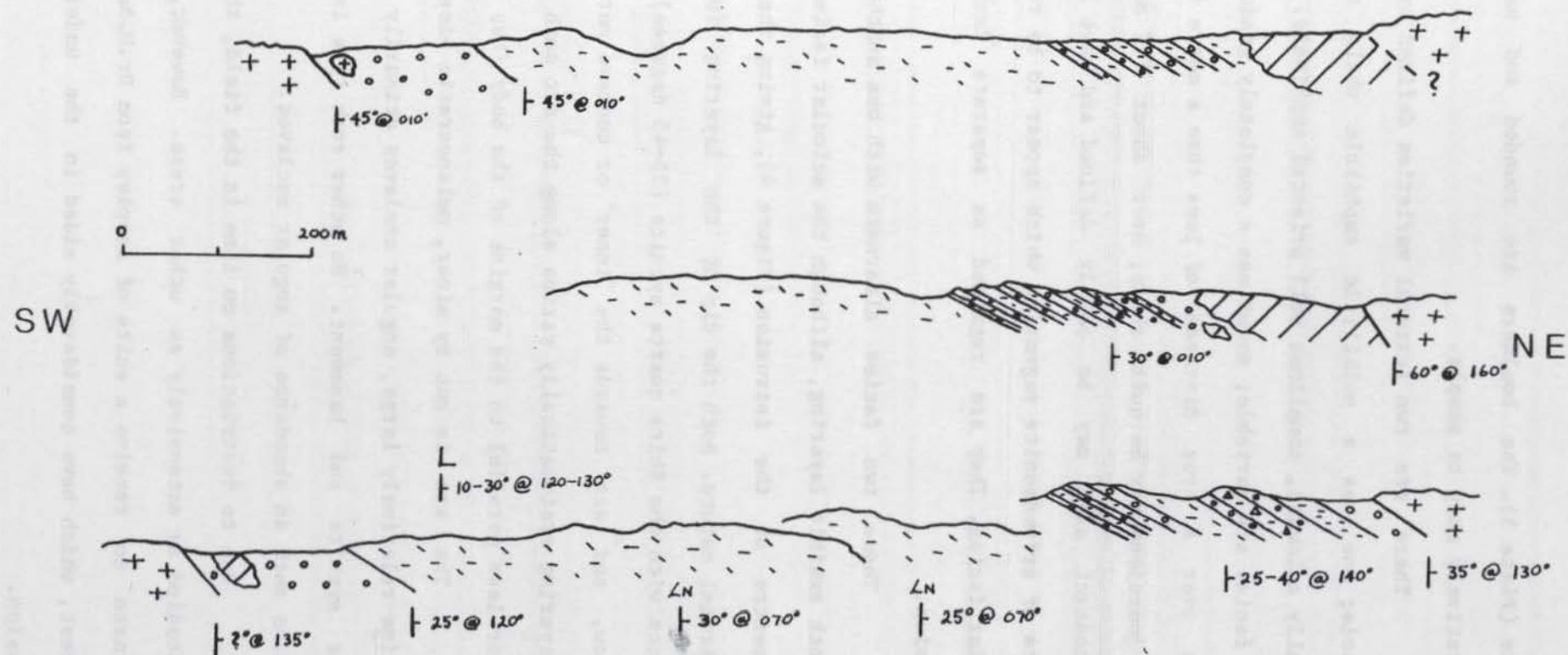
There are two textural varieties defined by the habit of the amphibole; one has a poikilitic amphibole while the other has a generally acicular, sometimes well oriented amphibole. Contacts between these facies are variable; sometimes a completely gradational transition occurs over a true distance of less than a metre (Plate 6), whereas other junctions may be quite sharp, over about 1-2 cm. Alternatively, the contact area may be poorly defined and have irregularly shaped pockets of arfvedsonite pegmatite which appear to be related more to the acicular facies. They are regarded as separate facies of the same intrusion.

These two facies alternate with one another across the zone and both exhibit layering, although the acicular facies is dominant in the centre of the intrusion (Figure 4), giving the granite a broadly symmetrical nature. Both the dip of the layering (0-45 degrees) and contacts with the Shira quartz syenite (25-45 degrees) are comparatively shallow, and are towards the 'inner' or concave margin. The strike of the layering systematically varies along the arc such that it remains more or less parallel to the margins of the body (Map 2).

The arc is cut by minor, melanocratic microgranite dykes and contains relatively large, angular enclaves primarily of volcanic rock, quartz syenite and basement. No other rock type in the Shira complex contains such an abundance of angular enclaves.

Due to restrictions on time in the field, the arcuate zone was not studied as extensively as other areas. However, the writer was fortunate to receive a suite of samples from Dr.M.Barriere, University of Brest, which have considerably aided in the understanding of this intrusion.

Figure 4. Schematic cross-section through the Birji granite, drawn from field information given by Prof.M.Barriere. Each part of the diagram represents a sampling traverse across an individual hill. Crosses = Shira quartz syenite. Diagonal lines = equigranular granite. Circles and dashes represent the poikilitic and acicular facies of the Birji granite respectively. Triangles = pegmatite. Ln = lamination. L = layering.



2.5.2 Structure

The loose boulder outcrops are often a considerable handicap to the location and measurement of the orientation of marginal contacts. However, near the mid-point of the intrusion, at two localities on the inner and one on the outer margin with the Shira quartz syenite, the contact dips at between 35 and 45 degrees. In addition, the 'dyke' in the centre of D.Mainari is probably a narrow continuation of the arc, albeit with a textural change, and it dips south-eastwards at 36 degrees. The contact is sharp in each case. The internal structure of the arc, as indicated by the orientation of enclaves and the layering, is concordant with the contacts, and the body can be regarded as a large cone sheet. Essential information regarding the form of the arc has been summarised in Figure 4.

Cone sheets are not very abundant in Nigeria and tend to occur as minor, often multiple intrusions of microgranite at Kudaru and Zuku, for example (Jacobson and Macleod, 1977). However, the nearest equivalent structure appears to be the aplitic granite (s6) which forms a border to centre 1 at Sara-Fier, described by Turner (in Buchanan et al., 1971, p.126). This Sara-Fier cone sheet is particularly notable in its abundance of basement xenoliths and also for some evidence which points to it being a composite (?layered) body.

2.5.3 Layering

Layering has not previously been described from granitic rocks in this province but occurs within the Birji granite as planar zones of arfvedsonite concentration, in both the poikilitic and acicular facies (Plates 7-10). Hence, reference to a single layer is taken to mean the mafic rich zone. In addition, the acicular facies often has a sub-parallel orientation of the amphibole laths (in non-layered areas) which gives rise to a noticeable lineation (Plate 10). For any one



Plate 7. Layering in the poikilitic facies of the Birji granite, W end of D.Dalliwo.

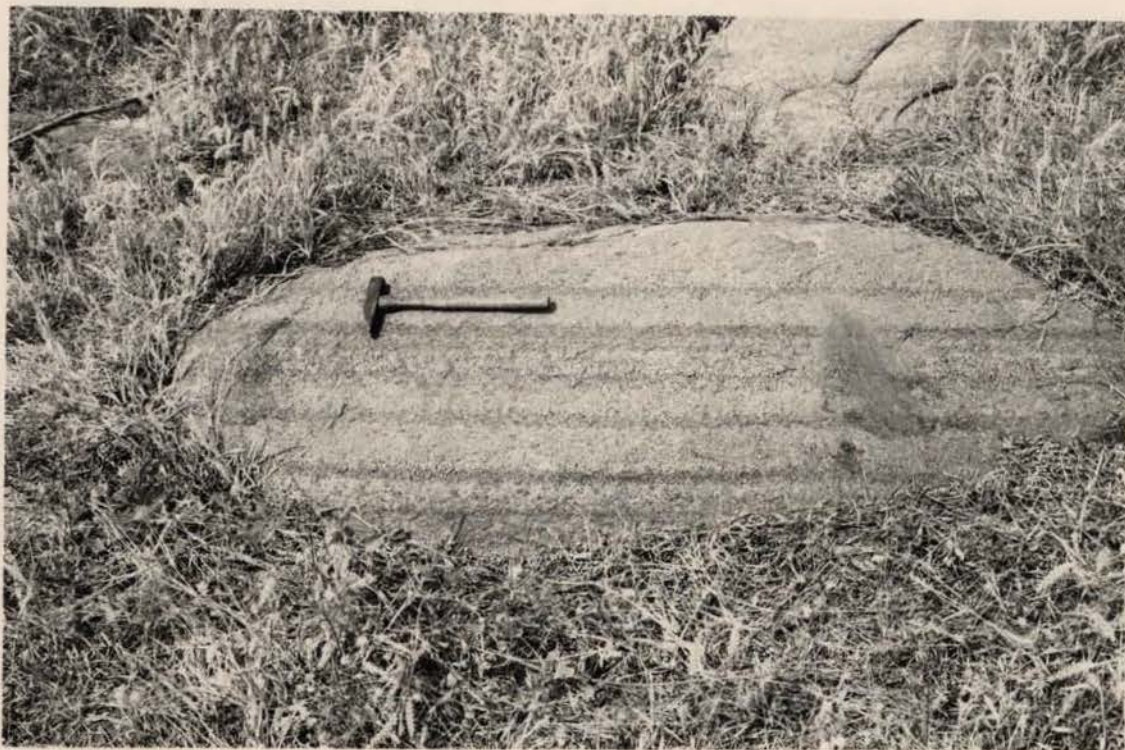


Plate 8. Layering in the poikilitic facies of the Birji granite. Loose boulder near Shinge.

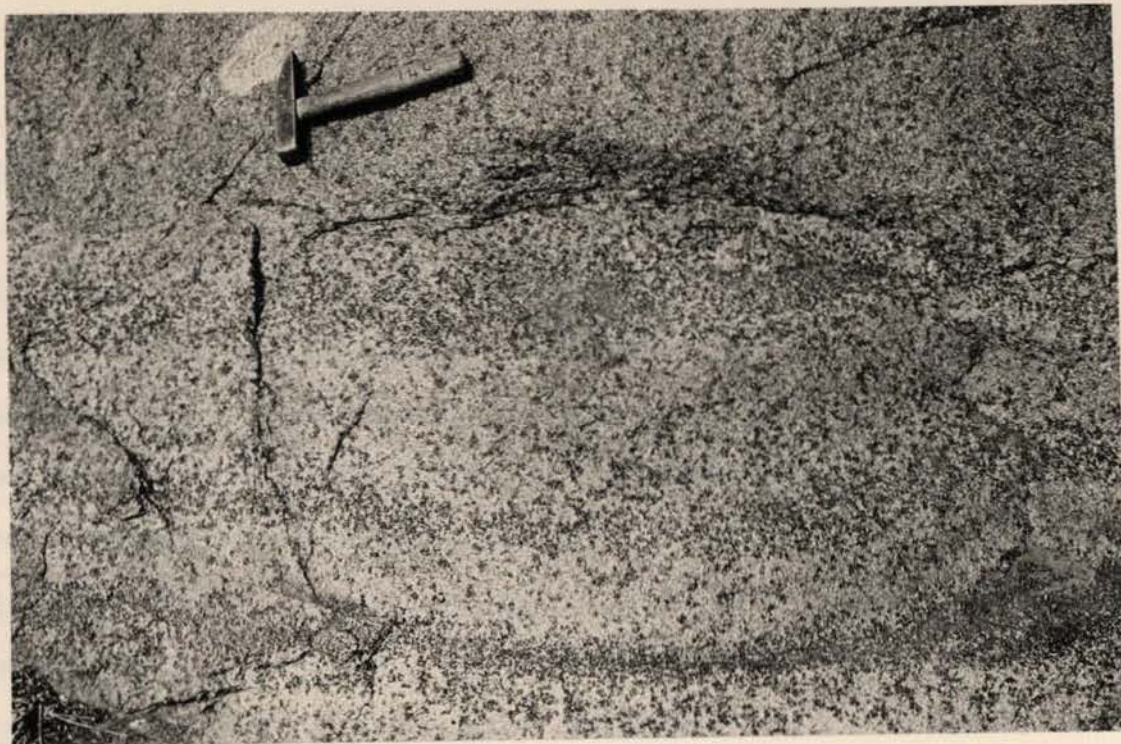


Plate 9. Close-up view of arfvedsonite layers in the poikilitic facies of the Birji granite. (Near locality SH101)

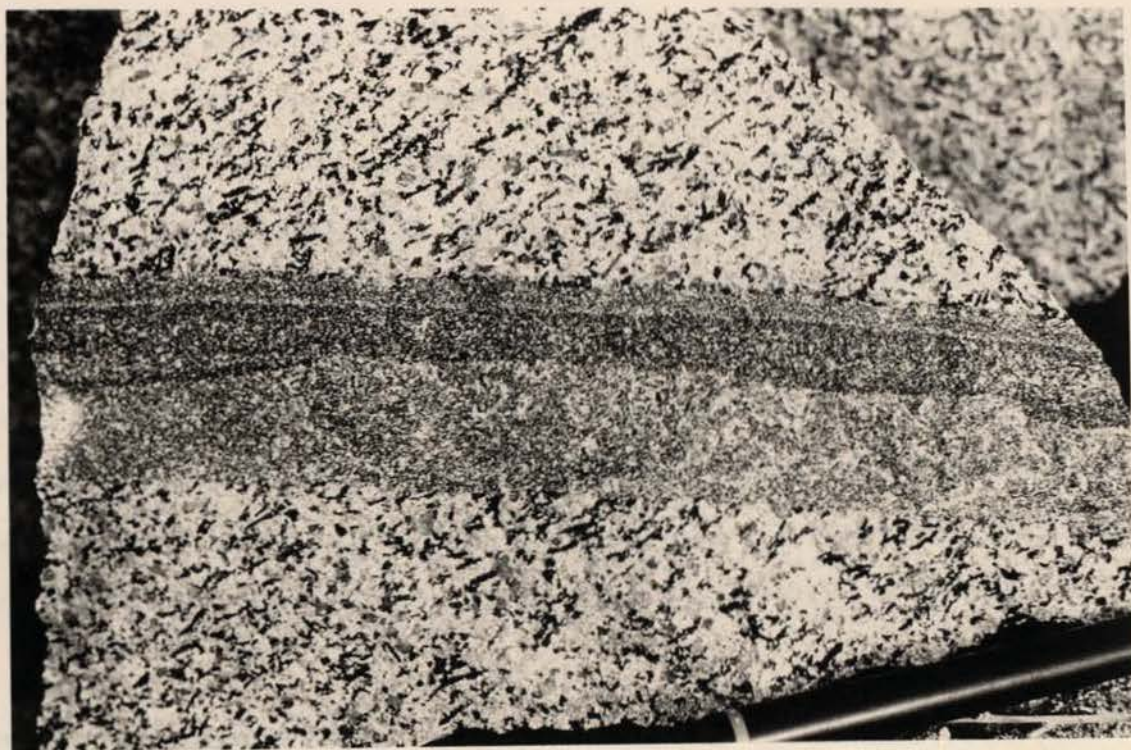


Plate 10. Sub-parallel orientation of arfvedsonite laths in the acicular facies of the Birji granite. Sample cut by melanocratic dyke (SH95).

layered zone, the individual layers may exhibit a constancy of dip and thickness which extends the length of available exposure (> 50 m). The layering in the poikilitic facies (Plates 7-8) is usually more regular than in the acicular facies where individual layers may be more sharply defined and yet exhibit slight irregularities and thickness variations. Some layers in the latter facies become thin and fade out altogether or are slightly saucer shaped, but both the upper and lower margins are equally diffuse or sharp as the case may be (Plate 9). Also, there appears to be a slight grain size reduction in some mafic layers within the acicular facies. A single layer may vary from 1-15 cm and may occasionally bifurcate such that a narrow felsic layer is sandwiched between two slightly wider mafic layers.

Close scrutiny of an intervening felsic area reveals some suggestion of preferred orientation of alkali feldspar, but this is not a dominant feature. However, other evidence to suggest that there may have been some movement in the still unconsolidated rock parallel to the layering is provided by enclaves or screens of quartz syenite. At one locality within the acicular facies the layers above an enclave are planar or gently undulating, whereas those in line with the enclave are slightly more disturbed. In general though, evidence for laminar flow is lacking and only very slight movement of a crystal-mush for example, would be sufficient to account for the features observed. Field evidence for preferred orientation of the often well-formed alkali feldspars is lacking and a model for the layering based upon gravitational settling of the (early formed) feldspar is not indicated.

2.5.4 Enclaves and dykes

There are abundant enclaves of the Shira quartz syenite within the arcuate granite and many of them are markedly elongate with dimensions of the order of 1-10 x 50-100 m, and are orientated parallel

to the strike of the zone, so that they may be regarded as screens of the older rock. They can be mistaken easily for dykes however, were it not for other occurrences which reveal their truly xenolithic nature.

The elongate nature of the enclaves presumably reflects the known jointed nature of the original quartz syenite, together with joints produced by the stress field associated with the emplacement of the Birji granite. This is particularly well shown on a 15 m high face a short way S of Shira town, on the W of the road; here there are numerous elongate enclaves of quartz syenite, of varying dimensions up to a maximum length of 0.4-5 m. They are parallel to one another and have an apparent NE dip of about 30 degrees (Plate 11). Some of them have a bleached margin or a zone with a micrographic intergrowth, suggesting slight modification as a result of incorporation in the arcuate granite.

Other quartz syenite enclaves however, are more equidimensional. In these cases the margins are usually cusped rather than planar. Orientation of amphibole laths in the acicular facies often appears to be truncated by these enclaves and sometimes there is a zone of amphibole concentration (approx. 5 cm wide) along the face which is at a high angle to the lineation direction. Some enclaves may be lozenge shaped with their long axes parallel to the amphibole lineation.

At two localities, towards the W margin and at another area close to the E contact, there are exposures of a medium grained granite with acicular amphibole crystals. This granite is also xenolithic and blocks of it are surrounded by the Birji granite. Since it is clearly distinct from the Shira quartz syenite, it would appear to be an earlier intrusive phase along this arcuate zone, which has subsequently been disrupted by the Birji granite.

With one exception which will be mentioned later, all occurrences of (probable) volcanic rocks in the complex are as enclaves within the Birji granite. They appear to be concentrated preferentially



Plate 11. Multiple, elongate enclaves of Shira quartz syenite in the Birji granite, W side of Azare road from SH5. (Rock surface is thickly dust covered.)



Plate 12. Angular volcanic enclave enclosed and partly brecciated by the Birji granite (SH80).

toward the inner margin, although this may reflect a bias due to exposure. They are not well exposed since the larger exposures are rubbly hollows whose contacts are largely obscured. At locality SH98, one such exposure may be traced for about 100 m and is elongated parallel to the nearby margin of the granite. Smaller (1-3 m) enclaves however, exhibit angular shape with sharp margins and are often partly brecciated by the granite (Plate 12). At localities SH96 and SH98, the enclaves consist of extremely fine grained, blue-grey flinty rocks having a weak foliated appearance on exposed surfaces, on which a thin white weathering crust has formed.

On the NW edge of D.Gora at locality SH29, there are several facies of volcanic rocks among a number of separate enclaves. The largest occurrence is an agglomerate or lithic rich tuff with clasts of aphyric and crystal rich volcanic material up to 3 cm in diameter. Nearby, an angular block is extremely crystal rich and has a texture reminiscent of the quartz porphyries found in other complexes, with aggregated feldspar up to 1 cm across.

Similarly, the only exposures of basement rocks in the complex are as enclaves (or inferred xenolithic bodies) within the Birji granite. At the SH29 locality, a 3 m angular enclave of Older Granite (SH29/3) is observed enclosed by the poikilitic facies. It is very coarse grained and has prominent white alkali feldspars and noticeable cloudy quartz grains. Two other basement (granite) outcrops occur - towards the E end of the arc. At the SH89 locality the outcrop is about 20 m wide; on the N side there is a sharp E-W contact which dips steeply northwards against the poikilitic facies while the S margin is hidden by overburden. The outcrop has several N-W trending narrow shear zones running through it. Locality SH91 is a different facies of basement; it is a deformed leucogranite with a foliation due to subparallel alignment of quartz and mafic minerals.

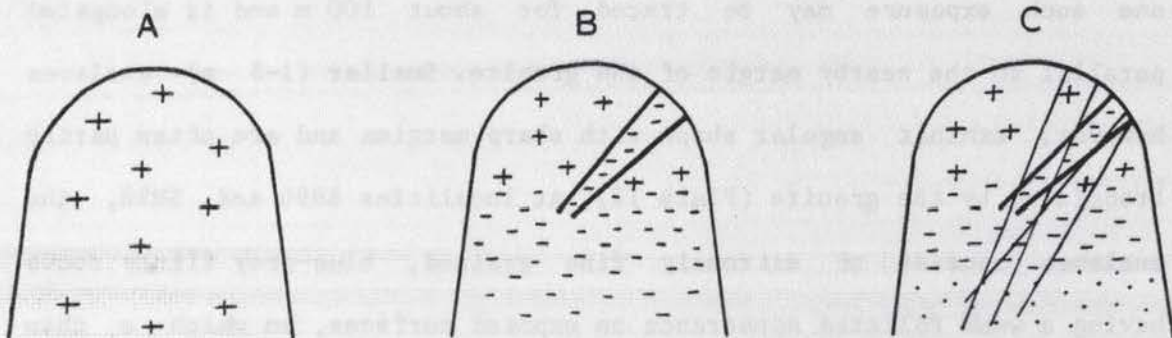


Figure 5. Schematic evolutionary diagram showing the possible relationship between the rock types at centre 1. An originally homogeneous peralkaline magma (A) undergoes in situ crystal fractionation to give an upper feldspar-rich zone (of Shira quartz syenite) and a lower mafic-rich zone which is intruded as a cone sheet (of Birji granite) - (B). Finally, the residual highly peralkaline and mafic-rich liquid is intruded as dilatational dykes which cut both the Shira quartz syenite and Birji granite.

The presence of basement enclaves in the Birji granite is not too surprising in view of their abundance in the cone sheet at Sara-Fier, but the latter case is admittedly the outermost intrusion, against the country rock. At Shira, there are also very fine grained, apparently volcanic enclaves as well, and their association with basement enclaves is puzzling. However, assuming the Shira complex had an early volcanic episode, then presumably enclaves of basement and volcanic rocks could have fallen into later magma chambers. Given the close field relationship between the Birji granite and the dykes, it will be shown in Chapter 5 that there is a progression in geochemical characteristics between the Shira quartz syenite, the Birji granite and the associated dykes. This has led to an evolutionary model relating these three rock types, which is shown schematically in Figure 5. This model postulates that these rock types are essentially connected by in-situ fractionation of a single magma and that the Birji granite and the dyke rocks are the product of progressive alkali feldspar fractionation and are trapped at deeper and deeper levels of the magma chamber. In this case, xenoliths falling into the magma at an early stage would probably not be able to descend through the lower, dense, Fe-rich layer and would therefore be available for transport up a conical fracture along with the Birji granite.

Several amphibole rich pegmatites of irregular shape occur, but they are often as loose boulders and their precise field relations are not known. At one locality though, a pegmatite clearly occurs in dyke-like form (SH83/3). In addition, the Birji granite is cut by a few narrow (5-30 cm) melanocratic fine or medium grained granitic dykes which may be equigranular or sparsely porphyritic.

The importance of these dykes (and those which cut the Shira quartz syenite) is that they are believed to represent the final stage of an in situ fractionation scheme (Figure 5). Essentially, the

evolutionary scheme envisaged for the southern part of the complex is as follows: intrusion of an originally (probably homogeneous) peralkaline granitic magma which underwent in situ fractionation to produce an upper zone rich in alkali feldspar and a lower (denser) zone rich in mafic components. After prolonged crystallisation, fracturing of the roof zone led to the intrusion of a large cone-sheet of magma derived from the still liquid lower zone, to give the Birji granite. At a later stage when the magma chamber had a comparatively small volume of silicate liquid remaining, further fracturing in the vicinity of the (Birji) cone sheet, led to the formation of relatively narrow, dilatational, highly peralkaline microgranite dykes.

The model depends upon the known (Chapter 3) paragenesis of the felsic and mafic minerals in the sense that alkali feldspar is one of the earliest minerals to crystallise whereas aenigmatite and amphibole form later. Therefore it is natural to expect that alkali feldspar, being less dense than the residual, more mafic rich liquid, would tend to form at the top of the magma chamber. In Chapter 5 it will be shown that there is a geochemical progression between these three rock types in the sense that there is an increase in peralkalinity index and mafic mineral components from the Shira quartz syenite to the dykes, compatible with progressive alkali feldspar fractionation.

2.6 Andaburi granite

The Andaburi peralkaline granite occurs in the north of the complex and is very poorly exposed. There are no contacts with country rock visible. Outcrops of Andaburi granite are scattered over a wide area such that the area beneath superficial sediments is estimated at about 42 sq.km. There are two main groups of exposures: the first is around Jejin Dalli in the north, while the second group stretches south from D.Shenya to Gola (Map 1). They are separated by a broad, low valley

in which there is no exposure and in which a river flows NE during the wet season. Another, scattered group of exposures occurs between Eldewo and Gola.

Exposures do not lie more than a few metres above the surrounding plains of aeolian sand and location of them from aerial photographs is difficult or impossible. In addition, the majority of exposure occurs within a forest reserve with difficult access and limited visibility.

A short way south of Kakkaki village there is a group of low exposures in the form of SW-NE trending parallel ridges, collectively called Dutsen Shenya, which show a number of important features. Here, the granite is slightly porphyritic, in contrast to the usual equigranular texture, and the alkali feldspars exhibit synneusis with aggregates up to 1 cm across; some exhibit clear or greenish cores with a white rim, or show white fractures traversing the clear cores. Quartz may also be aggregated but the groups are not as large (4-5 mm), while mafic minerals are restricted to the matrix. Within one small outcrop, several enclaves can be observed. A porphyritic microgranite enclave, up to 60 cm diameter, has phenocrysts of aggregated quartz or alkali feldspar set in a fine grained grey matrix which is spotted with darker mafic clots. Another, less abundant type is dark, very fine grained and about 10-20 cm in diameter.

A single porphyritic dyke about 30 cm wide contains fragments of the host granite. The margins are not as sharp as is usual for microgranite dykes and there are mafic stringers penetrating the host for 1-2 cm. The other interesting feature of these outcrops is the presence of multiple, narrow grey-blue cataclasis zones. They have extremely sharp margins with the slightly porphyritic Andaburi granite and contain numerous well defined lensoid fragments (2-5 mm wide) of the wallrock. These shear zones are about 1-5 cm wide and orientated N-S,

parallel to the inferred margin of the intrusion.

Three isolated exposures of Andaburi granite occur between Eldewo and Gola, and two more occur close to Gola itself. Of the former, two exposures have a slightly porphyritic texture, pink colour and a few pegmatitic pockets, while the other has the normal cream colour and equigranular texture. The most southerly of the three exposures (SH47) consists of an E-W ridge which is xenolithic and heterogeneous in colour and texture. The enclaves sometimes have unusual characteristics. One measures 1x0.5 m, has a 'spherulitic' appearance in which aegirine needles 1-1.5 cm long are abundant; and there is a sheaf of slightly larger amphibole crystals. Within the matrix, 'spherulitic' areas contain graphic quartz/feldspar intergrowths. Another enclave is 2 m long and has a colloform or botryoidal texture defined by alternations of grain size and mafic and felsic rich areas. At the E end of the ridge there is a low, flat exposure of pink medium grained biotite granite which has a near-horizontal contact with the Andaburi granite above. The latter is cut by numerous 1-3 cm wide greisen veins which cut both rock types. The area of biotite granite exposed is only of the order of 200 sq.m, but is sufficient to indicate the age relations between the two rock types.

Among the more extensive exposures of Andaburi granite within Jedin Dalli, several minor intrusions are found. In the outcrops close to the small intrusion of Amdulayi syenite a pair of blue microgranite dykes (2 and 10 cm wide respectively) occur. They have an extremely fresh appearance, are dilatational, have a strike of 040 degrees and dip NW at 70 degrees. There is a faint 'lineation' visible on the surface which is at an angle of about 20 degrees to the walls and which might indicate the direction of dilation. The 10 cm wide vein (SH49) is continuous over 80 m, and has occasional wall-rock fragments in it. Narrow microsyenite and pegmatitic veins cut the blue microgranite

dykes.

On the N edge of Jejin Dalli, there is a broad flat outcrop of granite which is cut by a 0.6 m wide, very fine grained, dark blue dilatational dyke (SH59/1) which has an exposed length of 18 m. Narrow (2-4 mm) pale coloured zones in the dyke resemble bands due to flow layering and there are contraction fractures normal to the walls which do not penetrate the host granite. As far as it is possible to determine in such a low outcrop, the dyke is vertical and has sharp margins with no sign of alteration in the granite. The dyke is flecked with small, sparse, cream coloured alkali feldspar phenocrysts.

Further south, in the centre of Jejin Dalli, the granite is cut by good examples of dilatational dykes (SH60). These dykes are 2-17 cm wide, dark blue-grey in colour, very fine grained and contain numerous angular fragments of the granite which, in many cases, can be shown to have moved very little. The dykes have a general strike direction of 140 degrees, the largest of which is traceable for 17 m. Adjacent outcrops are devoid of such dykes, but similar ones occur not far away at locality SH48.

In the exposures at Dutsen Andaburi itself, there are a number of dykes and enclaves. Along the S margin of the exposure there is a sheet-like intrusion (SH55/1) of microgranite which dips 26 degrees due N. It is about 25 cm wide and like the vertical dykes previously observed, has a weak banding within it which is at about 20 degrees to the walls. The margins are sharp. Close to this intrusion is a vertical pegmatitic vein (SH55/2) with a strike of 118 degrees and a width of 2-3 cm. It contains acicular aegirine crystals up to 8 mm long set in a coarse granitic matrix. In addition, nearby boulders contain isolated pegmatitic knots.

150 m N of locality SH55, large exfoliated boulders are cut by a series of up to 20 cm wide aegirine microgranite dykes which show a

range in alkali feldspar phenocryst content (SH56/1-3); these phenocrysts are commonly aggregated. In the same area, there is a subhorizontal pegmatitic sheet with a mineralogical foliation parallel to its margins. At one time it must have acted as a fault because a small vertical dyke is offset by about 5 cm.

Approximately halfway along the W side of D. Andaburi, the exposure is xenolithic and cut by several pegmatitic intrusions. One such enclave sampled is a fine grained, grey microsyenite (SH57/1). The pegmatitic sheets are crudely banded into mafic and felsic areas. Large acicular aegirine crystals may occur in radial habit and there are numerous red-brown areas within the matrix in which no crystal form can be seen.

2.7 The Amdulayi alkali feldspar syenite/quartz syenite

This rock is usually known as the Amdulayi syenite and occurs as a small intrusion in the NW corner of the Andaburi granite. It is exposed in three small hills about 2 km SW of Amdulayi village. In the northernmost of these, the syenite is exposed as a central hollow surrounded by Andaburi granite. The granite is cut by several blue microgranite dykes (SH49) which have a strike of 040 degrees; they do not occur in the syenite, and are themselves cut by thin (5-10 cm) medium grained dilatational syenite dykes with a strike of 086 degrees - this direction follows a joint direction in the granite. Near the margins, 30-50 cm wide enclaves of the granite can be found, but it is not possible to determine accurately the angle of the contact. Marginal areas are however, free of pegmatite or chilling. At this locality (SH50) the syenite is strictly an alkali feldspar quartz syenite and is medium to coarse grained with cream coloured feldspar.

About 100 m south are the central hills of the three mentioned; a medium grained, slightly porphyritic quartz syenite

(SH25/1) occurs on the E side. It contains several enclaves of Andaburi granite which are cut by a number of 2-10 cm wide syenitic veins (SH25/2) trending at 060 degrees. The syenite contains abundant, small (1-2 cm), dark, porphyritic enclaves which are fine grained and rounded. About 200 m ESE of this exposure there is an isolated hill composed entirely of boulders of a very coarse grained alkali feldspar syenite. There is an absence of enclaves, but a few narrow microsyenite veins are present.

All three exposures form a compact group and it is likely that despite the textural variation, they belong to the same intrusive body.

2.8 Eldewo biotite alkali feldspar granite

The Eldewo biotite granite occurs in the centre of the complex and is the most poorly exposed rock type of all, with only a few scattered boulders projecting above the flat aeolian landscape. Nevertheless, since these outcrops are widely scattered and a few occur relatively close to the peralkaline granites to the north and south, a reasonable estimate of the area of the granite beneath superficial deposits is approximately 29.5 sq.km. Due to their poor exposure all outcrops of biotite granite are assumed to be textural variants of the same intrusive body.

The central exposures near Eldewo and Riga Dinya, and near Jejin Dalli, have a coarse grained, equigranular texture and a deep cream or pink colour. These exposures consist of one or more boulders which do not exceed 3 m in height. At the SH63 and SH65 localities close to Jejin Dalli, the individual boulder outcrops of biotite granite are cut by amphibole bearing pegmatitic dykes. The close proximity of the peralkaline Andaburi granite together with these veins would suggest that the Eldewo biotite granite is older. However, at the SH63 locality the dyke is 15 cm wide and dips at only 30 degrees with a strike of

105 degrees; that is, it dips away from the Andaburi granite.

Towards the SE, among exposures of Andaburi granite between Eldewo and Gola, there is a small outcrop of pink medium to coarse grained biotite granite, which is distinctly less coarse grained than the type locality at Eldewo. This outcrop clearly underlies the Andaburi granite, and thin, dark greisen veins cut both rock types.

The southernmost exposure of 'biotite granite' occurs close to Jan Dutse (1). Here, in a small hill which is generally deep pink/red in colour, it is apparent that whatever the original rock was, it has been intensely altered. This rock has a texture equivalent to a coarse grained granite except that no feldspar remains; instead, it is apparently pseudomorphed by jasper. Aggregated quartz grains do not appear to have been affected. Other areas of the exposure are pale pink and the feldspar replacement process has apparently not gone so far, or has been of a different nature, since there is an abundance of a white clay mineral, probably kaolinite.

To the north and south of Gwanawa there are two other outcrops of biotite granite which are important in defining the approximate position of the margin of the body. Both are pink, medium to coarse grained, slightly porphyritic rocks. The northern of these two outcrops is the size of a single boulder only.

2.9 Miscellaneous rocks

2.9.1 Yana agglomerate

This agglomerate is found just to the E of Yana village where it occurs in the form of a low elongate ridge less than 100 m long which is aligned NW-SE. It is prominent on aerial photographs because it is much darker in appearance than other rocks in the complex. It is composed

(1) Hausa for red rock.

of rounded 3-10 cm diameter clasts which are very fine grained and appear to consist solely of a pre-existing volcanic rock. The matrix is more easily weathered than the clasts (which are prominent on exposed surfaces as a result), and consists of a tuffaceous material having a crude foliation which dips 40 degrees SW with a NW-SE strike, parallel to the length of the hill.

2.9.2 Chida porphyritic granophyre

The Chida porphyritic granophyre occurs close to Chida village on the Kano-Potiskum road, a short way E of the Yana agglomerate. The exposure consists of a group of large pink coloured boulders which have phenocrysts of quartz and alkali feldspar set in a granophyric matrix. Acicular amphibole crystals indicate that this granophyre has affinities with the peralkaline granites.

Microscopic description

The Chida porphyry consists essentially of phenocrysts of orthopyroxene, quartz, feldspar and feldspathic set in a matrix of quartz-feldspathic granophyre.

Among the phenocrysts, the ratio of alkali feldspar to quartz is about 1:1 or 2:1. In the matrix the ratio is approximately 1:1. Pyroxene and feldspathic also occur as phenocrysts but the total alkali feldspar content does not exceed 10% of the rock, as shown in the modal analysis in Table 2. The characteristic feature of the alkali feldspar is that it forms symplectic grains 3-10 cm across which are usually composed of 1 to 3 crystals. Small feldspathic or feldspar crystals are usually enclosed also. The junction between adjacent alkali feldspar crystals within a group, and occasional overgrowths are visible where a line of small feldspathic or amphibole inclusions

CHAPTER 3PETROGRAPHIC DESCRIPTION3.1 Zigau fayalite ferrohedenbergite granite porphyry

When fresh, the Zigau porphyry is a dark grey-green porphyritic rock carrying abundant phenocrysts of alkali feldspar and to a lesser extent, quartz. The alkali feldspar phenocrysts are glomeroporphyritic and may be colourless with white fractures, or slightly altered, pale yellow or yellow-brown in colour and have a more clearly defined appearance against the grey matrix. The alkali feldspar aggregates are up to 1 cm across and set in a fine grained matrix which is spotted with small, dark areas of mafic minerals generally up to 2 mm in diameter. Dark, fine grained enclaves can be seen on the rock surface.

3.1.1 Microscopic description

The Zigau porphyry consists essentially of phenocrysts of cryptoperthite, quartz, fayalite and ferrohedenbergite set in a turbid, quartzofeldspathic groundmass.

Among the phenocrysts, the ratio of alkali feldspar to quartz is about 3:1 or 4:1, whereas in the matrix the ratio is approximately 1:1. Fayalite and ferrohedenbergite also occur as phenocrysts but the total mafic mineral content does not exceed 10% of the rock, as shown in the modal analysis in Table 2. The characteristic feature of the alkali feldspar is that it forms synneusis groups 5-10 mm across which are usually composed of 3 to 5 crystals. Small ferrohedenbergite or fayalite crystals are commonly enclosed along the junction between adjacent alkali feldspar crystals within a group, and occasional overgrowths are visible where a line of small ferrohedenbergite or amphibole inclusions

Table 2. Modal analysis of rocks from the Shira complex

A. Zigau fay. ferrohed. gnt. porph.		B. Shira ferrichterite alkali feldspar quartz syenite and the Shira market xenolith					Shira mkt. xeno.	
		Shira quartz syenite						
Sample	202/w	Sample	SH4	SH105	Average	Sample	SH109/1	
Counts	3000	Counts	9005	11,655		Counts	3000	
	%		%	%	%		%	
Alk.feld.	64.22	Alk.feld.	71.22	79.31	75.26	Alk.feld.	55.93	
Quartz	25.34	Quartz	15.28	12.65	13.96	Quartz	33.30	
Amph.	2.72	Amph.	9.61	7.31	8.46	Amph.	6.47	
Ferrohed.	3.28	Aegirine	1.97	0.56	1.27	Aegirine	3.80	
Fayalite	1.30	Aenig.	1.92	0.18	1.05	Zircon	0.50	
Ilmenite	2.14							
Access.	1.00							

C. Birji arfvedsonite alkali feldspar granite									
Sample	15a	SH30	SH72/4	SH72/5	SH9	SH18	SH82	49a	
Counts	7743	3000	3000	3000	2503	2516	2504	11,556	
	Poikilitic facies		Poik. mafic layer	Adjacent felsic zone		Acicular facies		Average acicular facies	Pegmatite
	%	%	%	%	%	%	%	%	%
Alk.feld.	74.32	59.43	43.60	41.80	51.10	51.43	53.12	51.88	56.15
Quartz	19.73	28.90	29.70	35.33	26.33	21.90	24.88	24.37	22.08
Amph.	5.95	4.00	5.50	13.63	21.57	24.88	18.17	21.54	19.34
Aegirine		7.67	21.20	9.24	1.00	1.79	3.83	2.21	2.42

D. Layered samples from the acicular facies of the Birji granite								
Sample	38a	38a	38a	38a	38a	38a	39a	39a
Counts	1525	1626	Average	Mafic	Mafic	Average	Mafic	Pelsic
	Felsic zone A	Felsic zone C	felsic zone	zone B	zone D	mafic zone	zone	zone
	%	%	%	%	%	%	%	%
Alk.feld.	69.25	67.71	68.48	66.92	72.51	71.22	66.30	69.58
Quartz	21.18	24.23	22.71	11.40	7.66	9.53	14.48	23.64
Amph.	9.57	8.06	8.81	18.68	19.83	19.25	19.22	6.78

E. Andaburi ferrichterite alkali feldspar granite				F. Amdulayi ferrowinohite alkali feldspar syenite/quartz syenite				
Sample	SH22	SH44/2	Sample	SH59/1	Sample	SH25/5	SH50	SH51
Counts	5436	3000	Counts	3000	Counts	3000	3000	3000
		Marginal facies		Dyke		med.gr. xeno. facies	med.gr. equigr. facies	e.gr. facies
	%	%		%		%	%	%
Alk.feld.	62.69	64.03	Matrix	84.10	Alk.feld.	60.43	65.63	83.03
Quartz	27.04	19.03	Alk.feld.	5.73	Quartz	12.20	11.20	3.70
Amph.	7.50	12.27	Quartz	5.30	Amph.	1.40		10.37
Aegirine	2.77	2.77	Amph.	4.87	Aegirine	24.70	22.73	
Iron ore		1.90			Iron ore + zircon	1.27	0.44	1.37
					Aenig.			1.53

G. Eldewo biotite alkali feldspar granite				
Sample	SH21	SH21	SH106	SH47/6
Counts	2312	10,091	2700	3000
Alk.feld.	60.90	62.63	62.52	61.80
Quartz	32.18	33.01	33.04	33.67
Biotite	5.97	4.36	4.15	4.53
Access.	0.95		0.27	

occurs close to, and concentric with, the margin of an alkali feldspar.

Alkali feldspar shows varying degrees of turbidity between samples. Where the alkali feldspar is yellow-brown in colour, it is generally completely turbid, except for the largest crystals or aggregates which may have clear cores (Plate 13). In fresher specimens, turbidity occurs selectively around the margin and along fractures in the crystal in such a way that the width of the turbidity along a fracture frequently decreases towards the centre of a crystal. The resulting pattern is often irregular in detail, having a fern-leaf appearance. No perthitic texture is visible in the clear zones but the turbid areas do show a poorly developed perthitic texture under high power. A structural change is implied by a difference in extinction position between the two zones. X-ray diffraction of a bulk alkali feldspar separate (phenocrysts and matrix) indicates that the feldspar is an intermediate microcline crypto- or microperthite which appears in Figure 25 as the least ordered alkali feldspar in the complex.

Five microprobe analyses from separate alkali feldspar crystals (Table 25) indicate a range in composition from Or27 to Or46. This compositional range is from K-albite (anorthoclase) to Na-sanidine (Smith, 1974, Vol.1), and the analyses are plotted in Figure 24.

Rarely, euhedral or subhedral plagioclase crystals occur which are mantled by alkali feldspar; in one example the plagioclase has numerous embayments and inclusions of matrix. The embayments are filled by small crystals of hedenbergite and ilmenite as well as alkali feldspar in optical continuity with the enveloping alkali feldspar. Two plagioclase crystals have been analysed by microprobe (Table 24 and Figure 24) and found to be andesine with a compositional range (4 analyses) of An36 to An44.

As noted in connection with alkali feldspar, quartz phenocrysts are only about one quarter as abundant as alkali feldspar

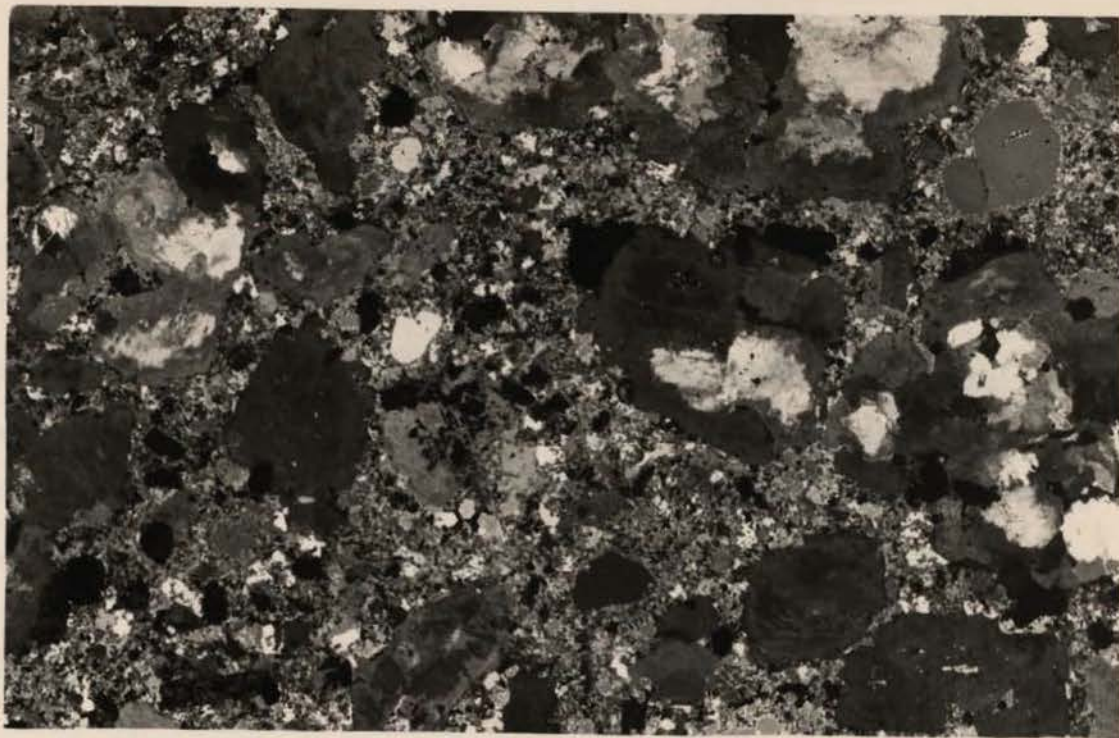


Plate 13. The texture and variable turbidity of alkali feldspars in the Zigau granite porphyry. Field width 30 mm; crossed polars. (ZG1)

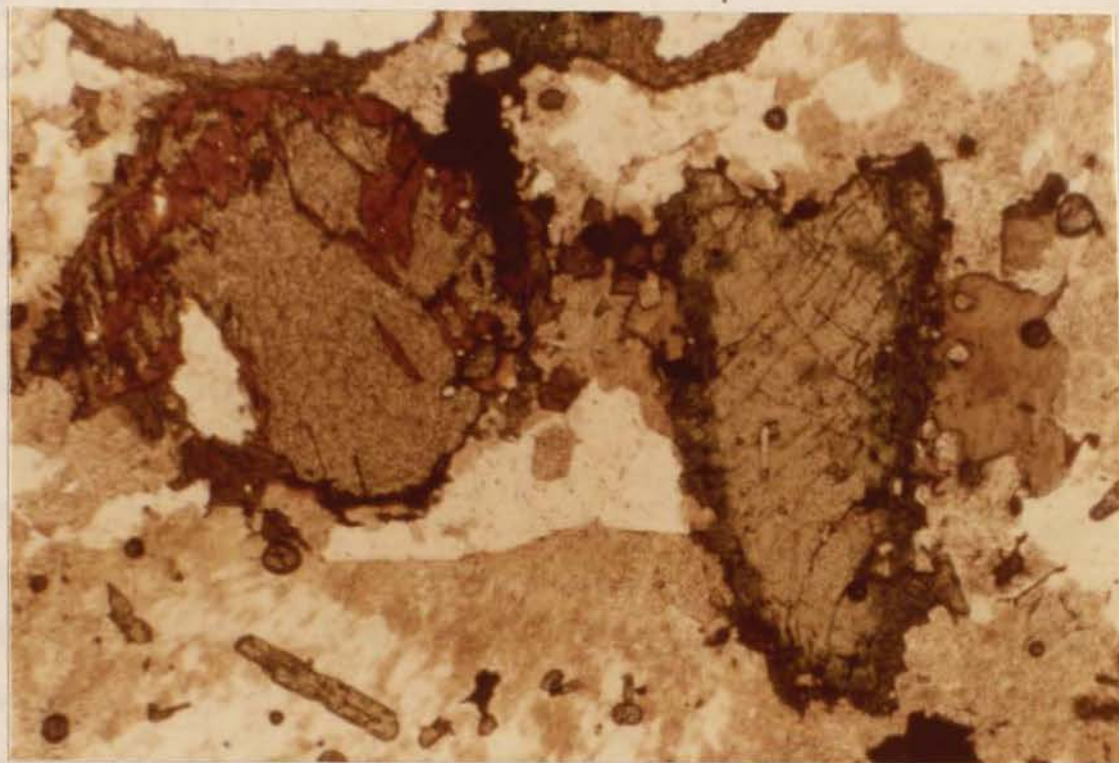


Plate 14. Fayalite and ferrohedenbergite phenocrysts in the Zigau granite porphyry. Fayalite is partly altered to orange iddingsite and rimmed by brown amphibole. Ferrohedenbergite has a dark green sodian rim. Field width 24 mm; plane light. (ZG2)

phenocrysts but the quartz-feldspar ratio in the matrix is about unity, indicating eutectic proportions for the latter stages of crystallisation. Quartz phenocrysts are subhedral or rounded, up to 3 mm diameter, and may include infrequent crystals of ferrohedenbergite or alkali feldspar. In plane light, the quartz phenocrysts appear to have sharp boundaries against the matrix, but under crossed polars it is evident that in the close vicinity of the phenocryst, anhedral quartz in the matrix has crystallised in optical continuity with the phenocryst, giving the impression of a ragged overgrowth.

Clinopyroxene occurs as euhedral or subhedral phenocrysts up to 1.5 mm in diameter (but usually less), and also as inclusions within alkali feldspar phenocrysts and rarely, in quartz. Microprobe analyses (Table 11 and Figure 15) show that core compositions are generally ferrohedenbergite, although a few analyses plot in the hedenbergite field close to the hedenbergite /ferrohedenbergite boundary. For all practical purposes however, they may be referred to as ferrohedenbergites. Typically, ferrohedenbergite crystals have very pale green cores with a relatively narrow, dark green, pleochroic rim of sodian ferrohedenbergite (Plate 14). The core has an extinction angle (c-X) of about 41 degrees while the rim is usually about 20 degrees less. The development of the green rim of sodian ferrohedenbergite is not equal around the crystal - it shows a patchy distribution such that areas around inclusions and along the longitudinal cleavage are usually best developed. In contrast, ferrohedenbergites which are completely enclosed by alkali feldspar may not develop a green sodic rim. An intermediate stage appears to occur when an elongate ferrohedenbergite crystal is only partially enclosed by alkali feldspar; the enclosed portion does not have a green rim whereas that part enclosed by matrix does. Also, small ferrohedenbergites enclosed by a single alkali feldspar crystal are very pale green in colour and homogeneous whereas

those crystals lying between two alkali feldspars in an aggregate usually show a green rim. Ferrohedenbergite is associated with fayalite (or iddingsite), ilmenite, amphibole, zircon, allanite and apatite in mafic mineral clusters. It may partly grow around an adjacent fayalite, while amphibole rims both minerals, and ilmenite, zircon, allanite and apatite are partially or completely enclosed.

Fayalite of composition Fa93-100 (Table 22) occurs as rounded crystals up to 1.5 mm across, or as groups of up to three crystals with a total diameter of 3 mm which may be part of a mafic aggregate. Fayalite may enclose ilmenite and zircon and itself be rimmed by grey to deep green or brownish, pleochroic amphibole, and sometimes biotite. Very commonly, fayalite is partly altered to deep red-brown iddingsite along fractures and around the margin, and the degree of alteration to iddingsite appears to be related to the turbidity of the alkali feldspars and abundance of green margins to ferrohedenbergite.

Amphibole occurs in two forms: as narrow rims to ferrohedenbergite or fayalite phenocrysts and as anhedral crystals in interstices or enclosing quartz and alkali feldspar in the matrix. It therefore appears to be the last mafic mineral to crystallise. It is pleochroic (1) from grey to brown-green, deep green or blue-green; larger, interstitial grains may be zoned with a green or brown-green centre and a deep blue-green rim. Crystal size rarely exceeds 0.4 mm and it does not polish well in microprobe sections. Therefore, comparatively few analyses have been made. The range in composition however, is from ferrorichterite to arfvedsonite (Table 3, Figure 6).

Ilmenite (Table 23, Figure 23), allanite, zircon, apatite and sometimes biotite form the accessory minerals.

(1) See section 3.2.5 for a discussion of the optical properties of Fe-rich alkali amphiboles.

3.1.2 Enclaves

Small (< 15 cm) enclaves (1) are found throughout the Zigau porphyry but are observed best in a quarry near Gabati. The enclaves may be porphyritic with phenocrysts of glassy feldspar and occasionally they have an outer, paler rim (1-2 cm wide) which is very similar to the host porphyry but contains fewer phenocrysts.

Subsequent to the field collection, a thin section study has shown that there are at least two types of enclave - a basaltic and a syenitic variety. It is not known whether any intermediate types of enclave exist, or the relative proportions of the two types.

Microscopic description The phenocryst-free enclave (ZG2B) has an ophitic texture; euhedral laths of plagioclase up to 0.6 mm long are heavily sericitised and poikilitically enclosed by augite pseudomorphs. These pseudomorphs contain occasional remnants of clear, birefringent augite which has been altered to pale brown biotite and scattered Fe-Ti oxides. Larger crystals of dark brown biotite and scattered apatite needles are also abundant. The margin with the host rock is sharp.

By contrast, enclaves containing sparse feldspar phenocrysts (ZG2A and ZG2C), bear a closer resemblance to the host porphyry. In hand specimen the alkali feldspar phenocrysts consist of aggregates up to 1 cm across. These crystals rarely show any perthitic texture but instead show the familiar variation in turbidity which may be distributed as irregular patches across a crystal or more abundantly near the margins and along fractures. Occasionally a small, clear plagioclase crystal in the centre of an alkali feldspar aggregate is seen. The alkali feldspar agglomerates contain fayalite and ferroaugite

(1) The term enclave is used because it may or may not be genetically related to the host rock. The term xenolith is defined (A.G.I.) as NOT being related to the host rock.

crystals (Table 11, Figure 15) both within and between individual grains. The feldspar margins contain a line of minute mafic inclusions which mark the beginning of a second period of mafic mineral growth. Two alkali feldspar analyses from the same phenocryst (AF1 and AF2, Table 25) within a porphyritic enclave (ZG2C) plot in the K-albite (anorthoclase) field (Figure 24).

Scarce plagioclase crystals of andesine composition (An44-An50, Table 24) occur as discrete phenocrysts; they are distinguished by their glass-like clarity and common euhedral form. They sometimes contain irregular inclusions of matrix and their margins are similarly marked by a line of minute mafic inclusions. They may also have overgrowths of alkali feldspar. Rarely, phenocrysts of olivine, ferroaugite and ilmenite may be found, but these minerals are principally confined to the matrix.

The dominant mafic mineral in the matrix is ferroaugite which is present as generally elongate, anhedral crystals up to 0.3 mm long; globular grains of Fe-Ti oxide, a little olivine and anhedral brown-green amphibole are also present. The rest of the matrix is composed of very slightly turbid alkali feldspar and a significant proportion of clear plagioclase which is rimmed by alkali feldspar. Only a trace of quartz is present. The feldspathic matrix is crowded with apatite needles in which many have well defined hollow centres - a form of skeletal structure. In fact, occasional Fe-Ti oxide 'phenocrysts' also show a pronounced skeletal habit.

3.1.3 Discussion

An important feature of the Zigau granite porphyry is the presence of synneusis aggregates of alkali feldspar. The selective development of turbidity around the margins and fractures within these phenocrysts, together with the fact that the matrix alkali feldspar is

thoroughly turbid indicates that this is a feature developed after the consolidation of the rock. Furthermore, the different extinction positions of clear and turbid zones in the same rock indicate that the development of alkali feldspar turbidity is accompanied by a structural change or reorganisation. On the scale of a bulk feldspar separate though, it has not been possible to identify more than one structural state; on a diffractogram the 131 and $\bar{1}\bar{3}1$ peaks are rudimentary, rounded peaks from which no accurate angular measurement can be made. Therefore, the potassic phase of alkali feldspar is probably a mixture of orthoclase and intermediate microcline.

The green, pleochroic sodic margins to the ferrohedenbergite crystals are not evenly developed as would be expected in growth zoning, but may be selectively developed around mineral inclusions and along the cleavage (shown to some extent in Plate 14). Such evidence points toward a secondary process. There is an approximate correlation between degree of turbidity in alkali feldspar and the presence of fresh fayalite (as opposed to partial or complete iddingsite pseudomorphs), implying that these changes are products of the same period of rock-fluid interaction.

The amphibole rims around fayalite and ferrohedenbergite phenocrysts do not appear to have been affected by any rock-fluid interaction, neither is there any textural evidence that the amphibole is replacing either mineral. Moreover, thermodynamic data indicate that it is most unlikely that fayalite or ferrohedenbergite could be replaced by a ferrorichteritic amphibole (Chapter 4). Instead, it would appear from the interstitial nature of the amphibole in the matrix and the rims to mafic phenocrysts, that ferrorichterite-arfvedsonite was the final mafic mineral to crystallise, in response to decreasing T and build up of volatiles. Afterwards, possibly as a continuation of the same late stage concentration of volatiles, a sub-solidus, sodic fluid may have interacted with the rock causing selective turbidity in alkali feldspar,

alteration of fayalite to iddingsite and sodic rims around ferrohedenbergite.

Very little petrographic or chemical research appears to have been done on enclaves within Younger Granites. The texture and mineralogy indicate that neither type of enclave is likely to have been derived from the basement since in the author's experience, the basement in N.Nigeria consists of metamorphic rocks or very coarse grained, two-feldspar biotite granite. In this respect, the ferroaugite enclaves are particularly interesting as they are syenitic, and they bear relatively calcic plagioclase phenocrysts (andesine) as well as plagioclase (of unknown composition) in the matrix, olivine, ilmenite, ferroaugitic pyroxene and a little quartz. This mineralogy is, in general, the same as the host rock but the more magnesian pyroxene (and olivine?) and virtual absence of quartz indicates a less fractionated rock. The question of whether the host rock and ferroaugite syenitic enclave have a direct connection with the basaltic enclave cannot be tackled here.

In a recent study of the Tibchi complex (Ike, 1979) very similar enclaves were found with an almost identical mineralogy (of plagioclase, alkali feldspar, fayalite (Fa 92), ilmenite, ferroaugite and abundant apatite) to that found here. The form of the Tibchi ferroaugite (Ike, op.cit., Plate 44) in particular, is similar to that at Zigau.

Two interesting points emerge: at Tibchi, the granite porphyry host to Ike's microferrodiorite and microsyenitic enclaves is the earliest sub-volcanic intrusion in a complex dominated by biotite granite. At Shira, the complex is mainly composed of peralkaline rocks, hence the Zigau porphyry is not necessarily connected with the genesis of the peralkaline rocks in the remainder of the complex. In the Zigau example therefore, this would imply that the

ferroaugite-ferrohedenbergite trend for the pyroxenes is continuous and that plagioclase-, ferroaugite- and apatite-rich enclaves would be expected to reduce the Ca, Mg and P content of any differentiates. These elements are generally very scarce in rocks of this province (see Chapter 5).

The habit of apatite may provide a partial clue to the origin of the microsyenite enclaves; experimental studies have shown that apatite needles with hollow form are indicative of rapid growth or quenching (Wyllie et al., 1962). Therefore, there is evidence to suggest that the microsyenite enclaves are chilled margins of the dyke or a magma chamber at depth, which was disrupted partially by the subsequent upward movement of magma. Supporting evidence for the cognate origin proposed for these enclaves comes from the writer's own observations on the Werram granite porphyry dyke in the Ropp complex; here, the granite porphyry dyke has narrow (10-20 cm) margins of dark, finer grained material. In thin section, these margins consist of alkali feldspar microsyenite with a few microphenocrysts of (heavily sericitised) plagioclase and a matrix of green hastingsitic pseudomorphs after pyroxene, Fe-Ti oxide, a little quartz and dominant, turbid alkali feldspar.

For the basaltic enclave which does not share common features of texture and mineralogy with the host rock, a different origin is likely. In many areas (e.g. Ningi, Jos, Banke) basaltic volcanism occurred very early in the evolution of a complex and could have erupted from central vents or along ring fractures. The Rafin Jaki granite porphyry (Buchanan et al., 1971) has a discontinuous basic margin, apparently up to 7 m wide, composed of plagioclase (up to An60 in the cores), augite, hornblende, Fe-Ti oxides and biotite. In the host granite porphyry, two types of enclaves are found, a doleritic or basaltic type and also a quartz microsyenitic variety - analogous to the

situation at Zigau.

Therefore, the basaltic enclaves at Zigau could be derived from a basic margin to the dyke, being the first magma to utilise the fracture, whether or not the basaltic magmatism was related to the genesis of the later granite porphyry.

3.2 Shira ferrorichterite alkali feldspar quartz syenite

The Shira quartz syenite is a white or cream coloured, coarse grained rock in which alkali feldspar is the dominant mineral with crystals averaging 0.5-1 cm in size. Quartz is glassy and more abundant than mafic minerals although both are interstitial with respect to alkali feldspar. On a sawn surface, alkali feldspar crystals are zoned and occasional crystals are packed with mafic inclusions.

Since petrographic descriptions of enclaves in the Nigerian peralkaline granitoids are lacking, some account of these is given below. Also, since the peralkaline, melanocratic dykes which cut the Shira quartz syenite appear to have a restricted geographic occurrence and are believed to have some significance with regard to the evolution of the magma chamber in this centre, they are dealt with in some detail.

3.2.1 Microscopic description

Alkali feldspar is the major rock forming mineral (Table 2), and it is a microperthite with a grain size up to 1.5 cm. Structurally, the microperthite is a low albite-maximum microcline with a triclinicity (Goldsmith and Laves, 1954) range of 0.80-0.94 (8 diffractograms run on 5 samples; Table 31). Five microprobe analyses (70 micron beam) from the host rock and one of an enclave feldspar indicate that chemically, the

microperthite bulk compositions plot mainly in the Na-sanidine field (Figure 24). The microperthite forms an interlocking framework of crystals between which the majority of the quartz and mafic minerals have crystallised interstitially. Alkali feldspar is usually evenly turbid across the width of any grain, but there are some clear cores (Plate 15); perthite lamellae are generally regular but the albitic component may often be enlarged into lensoid or irregularly shaped areas. Junctions between microperthite crystals are comparatively poor in albite films - indeed albite may often be absent altogether. Where such boundaries are highlighted by a narrow albite rim however, it commonly displays a 'swapped boundary' with one of the adjacent microperthite crystals.

In large thin sections there are usually one or two microperthite grains which display concentric growth zoning or a ring of small aegirine-hedenbergite crystals parallel to the margins. In plane light these growth zones are visible as parallel areas of variable turbidity according to the proportion of albitic component present in the microperthite (Plate 16). The growth zones are probably therefore, regions of alternating Na and K content.

In general, alkali feldspar contains few inclusions other than early formed aegirine-hedenbergite crystals in varying degrees of preservation, but under high power, microperthite is seen to be flecked with numerous minute crystals of aegirine and blue arfvedsonitic amphibole.

Quartz occurs interstitially relative to alkali feldspar and is aggregated. Characteristically, single crystals display undulose extinction with a number of rounded domains or sub-grains present, making the whole 'crystal' a polycrystalline aggregate in reality. The mafic minerals also occur interstitially; amphibole is characteristically zoned from a brownish or yellow-green to grey

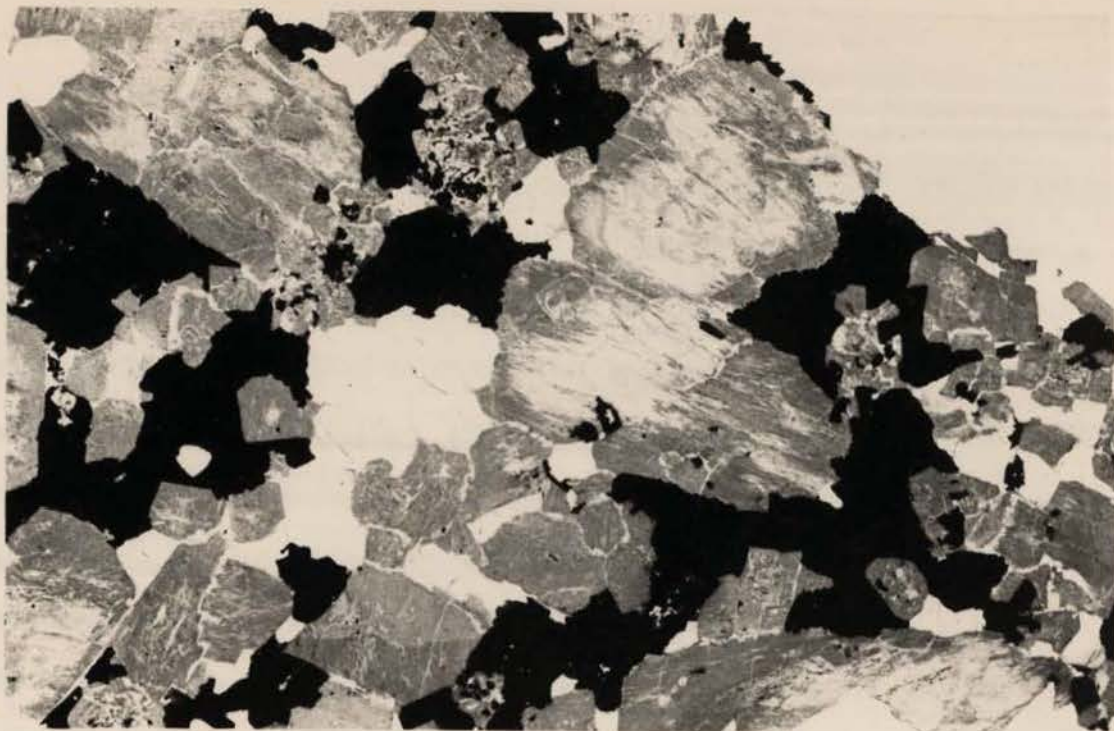


Plate 15. The texture and variable turbidity of alkali feldspars in the Shira quartz syenite. Note the interstitial nature of quartz and amphibole. Field width 30 mm; plane light. (SH105)



Plate 16. Growth zoning in alkali feldspar from the Shira quartz syenite caused by variable proportions of albitic (clear) and potassic (turbid) components in the microperthite. Field width 10 mm; crossed polars. (SH105)

pleochroic core with a deep green or deep blue-green margin (Plate 17). This colour zoning corresponds to a compositional change from a sodic-calcic amphibole (ferrorichterite) to a sodic amphibole (arfvedsonite), as shown in Chapter 4. Amphibole terminology therefore presents a problem and rather than use unwieldy prefixes, the term 'amphibole' will be used alone for the purposes of petrographic description. In fact, the amphibole zonation also leads to problems of nomenclature of the rock, and as a simplification, the scheme adopted in this work is to prefix the rock name with the name of the earliest formed (i.e. least sodic) amphibole. Amphibole crystals are generally around 2.5 mm in diameter but may reach 7 mm, and occur in interstitial clusters. Amphibole contains small inclusions of globular or elongate crystals of ilmenite, apatite and chevkinite and it may partly or completely enclose aegirine-hedenbergite, aenigmatite and quartz. Whilst it has clearly crystallised later than the majority of these minerals, it is common to find that the margins of an amphibole may partly enclose a quartz crystal, as well as the reverse relationship. Amphibole does not extinguish completely in most sections, but instead exhibits anomalous extinction with a brownish-red colour changing to a very dark blue on slight rotation, close to the extinction position. When viewed approximately normal to the c-axis however, and both cleavages are prominent, normal extinction occurs. In random orientations, amphibole often exhibits a domain-type of appearance in plane light, in which certain areas of a crystal are bluish. Commonly, green cores of amphiboles have blue-sided fractures traversing them and some crystals also possess a narrow, irregular overgrowth of deep blue amphibole; this overgrowth is visible only under high power when it appears to be growing at the expense of the adjacent alkali feldspar.

Two generations of pyroxene have crystallised in this rock: aegirine-hedenbergite and aegirine. The former is enclosed by alkali

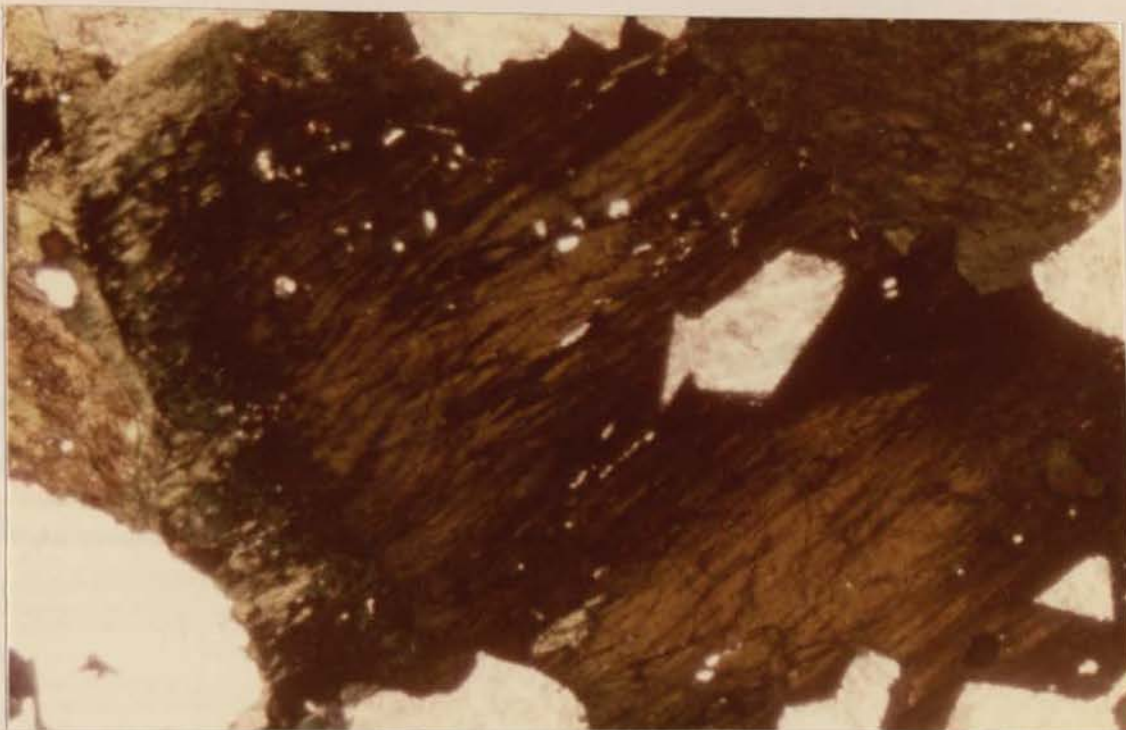


Plate 17. Zoned amphibole from the Shira quartz syenite. The yellow-brown core is ferrichterite which grades into dark blue-green arfvedsonite. Aegirine partly replaces the latter. Field width 10 mm; plane light. (SH105)

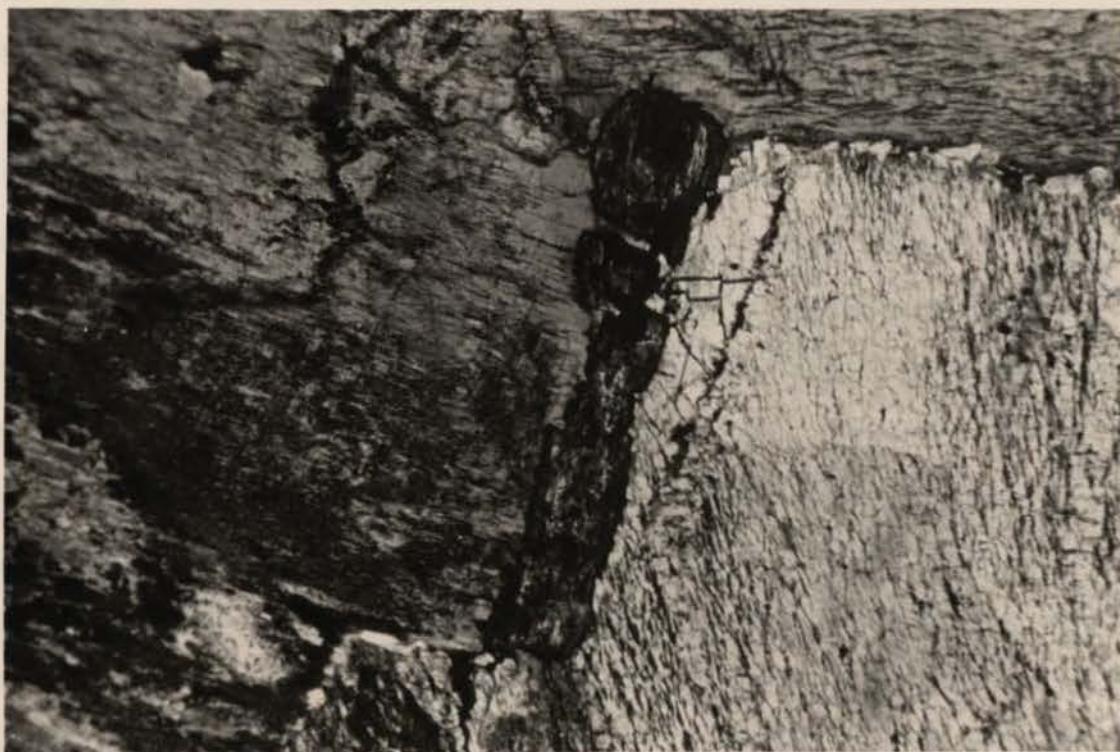


Plate 18. Aegirine-hedenbergite enclosed by alkali feldspar in the Shira quartz syenite. Field width 6 mm; plane light. (SH4)

feldspar (Plate 18), aenigmatite and amphibole and may be up to 3 mm long but is usually less; it is grass-green in colour, has an extinction angle (c-X) of up to 28 degrees and may be zoned, in which case the darker coloured rim may have an extinction angle of only 15 degrees. It is usually subhedral and elongate and although there are no distinct breakdown products, the core region especially is altered and heavily plucked during sectioning. Aegirine-hedenbergite is often mantled by amphibole and only a single example has been found where, from extinction angle measurements, there is a discontinuous variation towards aegirine. By contrast, aegirine is the last mafic mineral to crystallise and occurs as a partial rim around amphibole crystals or may replace amphibole. In addition, aegirine occurs, with arfvedsonitic amphibole as minute grains scattered throughout microperthite.

Aenigmatite occurs as deep blood-red coloured grains (up to 5 mm long) which may constitute as much as 2% by volume of the rock (Table 2). It encloses laths of aegirine-hedenbergite and apatite and is itself surrounded by amphibole. It is dominantly interstitial and yet in detail it appears as though minor indentations along its surface are filled by microperthite, perhaps indicating that the final period of alkali feldspar growth was in part later than that of aenigmatite. Typically, aenigmatite is anhedral and as a consequence the margins interdigitate with amphibole and aegirine, but a reaction between aenigmatite and other phases is not indicated. Chevkinite occurs as small globular or subhedral, brown crystals up to 0.15 mm long within amphibole; ilmenite has a similar mode of occurrence and has been found enclosed by amphibole even in sections containing abundant aenigmatite. Apatite occurs as short prisms enclosed by aenigmatite and amphibole. Zircon is found as a frequent accessory and occurs as localised aggregates of very small crystals enclosed by quartz. It is therefore one of the last minerals to crystallise.

Occasionally microenclaves (< 1 cm) consist of altered plagioclase, turbid alkali feldspar, turquoise amphibole, apatite and Fe-Ti oxide surrounded by a reaction rim of biotite (Plate 19). The turquoise amphibole occurs in aggregates which may be surrounded by small biotite crystals in a manner reminiscent of pyroxene pseudomorphs in the Amdulayi syenite (Section 3.5). These syenitic enclaves are small and infrequent but they may account for some of the mafic inclusions seen within alkali feldspar in hand specimen.

The foregoing description is typical of exposures near the centre of the intrusion but in other areas there are important petrographic variations which are described separately in the following section.

3.2.2 Particular features

An isolated enclave-rich exposure occurs approximately 1 km E of Dutsen Gabas, close to the inferred margin of the complex. Aenigmatite is found as small, usually globular crystals enclosed by brown-green or green ferrorichteritic amphibole, aegirine-hedenbergite and aegirine. One aegirine-hedenbergite occurs as a green subhedral crystal, 1.3 mm long, which is quite fresh and has an extinction angle (c-X) of 21 degrees; this crystal encloses aenigmatite and is itself mantled by aegirine (c-X, 7 degrees). Another crystal gave core-rim extinction angles of 19 degrees and 11 degrees respectively. Aegirine also crystallises around and partly replaces the amphibole. In one section, a few individual sericitised plagioclase crystals form cores to alkali feldspar; in other parts, the alkali feldspar itself is a lamellar microperthite which often has a clear centre surrounded by a more turbid margin. It is of interest to note, therefore, that (altered) plagioclase cores may be found, that aegirine may grow directly onto an aegirine-hedenbergite resulting in a zoned crystal and that aenigmatite



Plate 19. Microenclave in the Shira quartz syenite.
Field width 10 mm; plane light. (SH4)

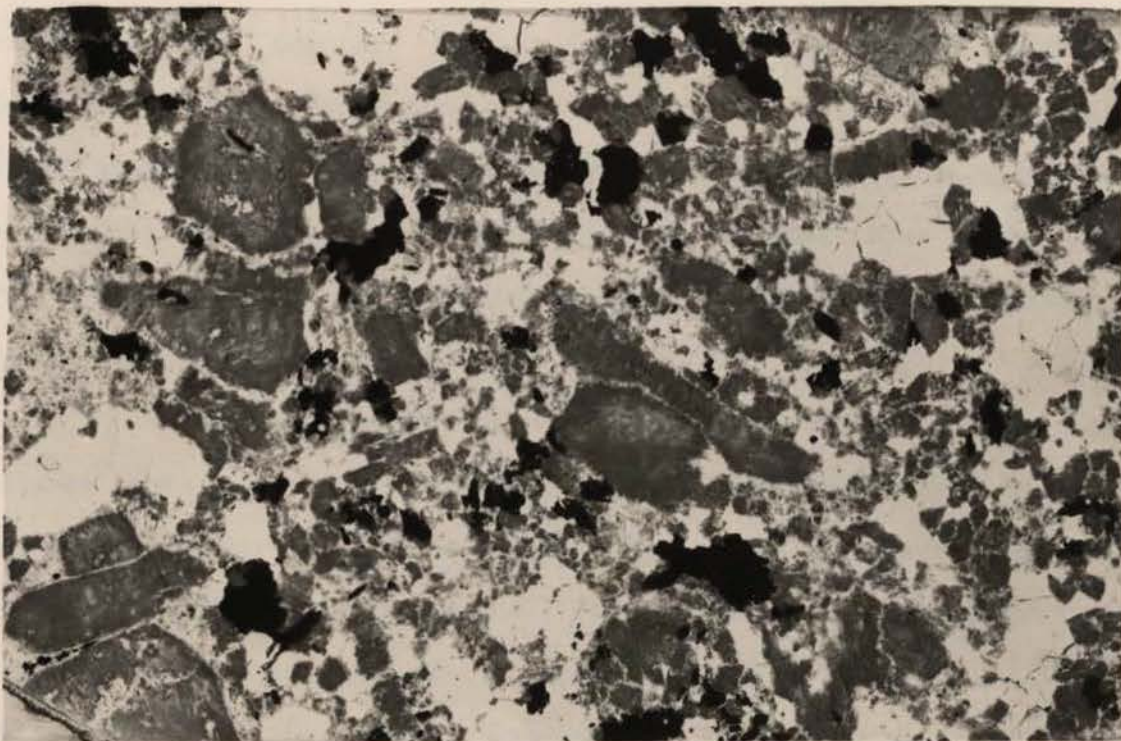


Plate 20. Texture of metasomatically altered Shira quartz syenite adjacent to the Birji granite. The turbid blastophenocrysts have a corroded appearance and are partly replaced by quartz and albite.
Field width 30 mm; plane light. (SH6)

crystallises earlier than aegirine-hedenbergite.

Close to the inferred N and NW margins of the quartz syenite at Dutsen Mainari, the exposures are relatively rich in enclaves. In the quartz syenite itself, many of the alkali feldspars are clear or pale blue in hand specimen, while others have a pronounced cream or pale yellow colour. In thin section the alkali feldspar may have clear cores and turbid margins or be uniformly turbid; occasional altered plagioclase cores are observed. Enclosed needles of aegirine and blue amphibole both tend to be larger (although still only 0.01 to 0.03 mm long) and more abundant than in other areas. Of particular interest in this area, however, are large (up to 2.5 mm) anhedral grains of Fe-Ti oxide (presumed to be ilmenite which is a common accessory), which are enclosed by ferrichterite, aenigmatite and aegirine-hedenbergite with no sign of a reaction relationship.

In hand specimen several partly filled miarolitic cavities contain aegirine needles. In thin section these cavities consist of a lining of extremely fine grained aegirine on which larger, euhedral (often radiating) aegirine needles grow into the void. In one such cavity a narrow rim of very fine grained acicular blue amphibole crystals grows on the aegirine aggregate, and the amphibole incipiently replaces an adjacent quartz crystal.

An arcuate exposure of quartz syenite which is rich in enclaves and has several granitic dykes, outcrops nearby and extends south-westwards. At Dutsen Elbegwa, close to a dyke, the quartz syenite has a 'tarnished' appearance due to numerous dark fractures in the feldspar. The 'fractures' however, are not readily visible in thin section although the alkali feldspar is more turbid than usual and albite is more abundant both as larger domains within the microperthite and along its boundaries. Aegirine is the major mafic mineral with only a trace of blue amphibole. Quartz, however, is more abundant than usual.

Near the south end of Dutsen Yola the quartz syenite is fresher than usual in appearance with clean, white alkali feldspar, and pegmatite is locally developed. In thin section, the rock displays the characteristic interlocking framework of lamellar microperthite with albitic margins. A peculiar feature here, is the presence of globular aenigmatite which is partly altered to a colourless mica; some enclosed opaque oxides may be associated with the breakdown. The pale green to deep blue-green pleochroic arfvedsonitic amphibole is altered to aegirine as usual, but it also contains numerous small inclusions of quartz and alkali feldspar.

In order to investigate any possible metamorphic or metasomatic effects on the quartz syenite by the intrusion of the arcuate Birji granite, a linear sampling traverse was made approximately normal to the contact. This south-westerly traverse was begun immediately west of Shira, at about 100 m from the north-eastern contact with the Birji granite. At this distance freshly broken surfaces of the quartz syenite had a somewhat tarnished appearance although on weathered surfaces some clear cores to K-feldspar could be seen. In thin section, several sericitised cores to microperthite are found in close association with Fe-Ti oxide rimmed by biotite and a turquoise-grey pleochroic amphibole - the familiar association of a microenclave. Aegirine-microperthite margins are marked by a line of projections of aegirine into the microperthite, where the potassic phase of the microperthite has been selectively replaced.

Closer to the Birji granite (approx. 50 m away), the quartz syenite develops a slightly porphyritic texture and there is a faint greenish colour to the alkali feldspar. In thin section, the alkali feldspar has enlarged albite domains and shows indefinite crystal boundaries embayed by quartz and discrete albite. Small needles of blue amphibole are abundant as inclusions and are oriented preferentially

normal to the microperthite lamellae. Aegirine and amphibole both show prominent overgrowths, replacing adjacent alkali feldspar. The amphibole, usually zoned and free of felsic inclusions, develops a poikilitic habit and encloses quartz and alkali feldspar.

Approximately half way between Shira and Bage, as the arcuate Birji granite is approached from the SW, textural changes in the quartz syenite are obvious in the field. Instead of a coarse grained equigranular texture, the rock becomes slightly porphyritic and quartz is noticeably more glass-like on a fresh surface. By comparing the texture of the quartz syenite in the central part of its exposure (Plate 15) with the modified version (Plate 20), it can be seen that the large alkali feldspar crystals are more turbid and less abundant (1). In fact, the alkali feldspars have a 'corroded' appearance in Plate 20, and the matrix has more quartz than usual while the boundaries between alkali feldspar crystals now have an appreciable albite rim. Junctions between microperthite crystals have changed from being even with very little intergranular albite, to relatively wide zones in which albite and quartz have grown. Plate 21 shows part of a 3 mm wide, growth zoned microperthite whose margin has been replaced by a fine grained aggregate of quartz and albite. A line encompassing this quartz/albite zone would be parallel to the present margins of the microperthite. In each case, the replacing albite is in optical continuity with the albitic component of the parent microperthite crystal. In a lamellar microperthite, it is common to see the clear, albitic component of the microperthite widening outwards to join up with a complete mantle of albite. In these cases, the potassic component has been depleted but quartz apparently has not replaced the microperthite. In many places, this albitisation process has proceeded to such an extent that only relic 'islands' of potassic

(1) Note that the proportion of mafic minerals in Plate 15 is well above average since that area was selected for microprobe analysis.



Plate 21. Quartz and albite replacement of growth zoned alkali feldspar in a metasomatically altered Shira quartz syenite. Field width 10 mm; crossed polars. (SH6)

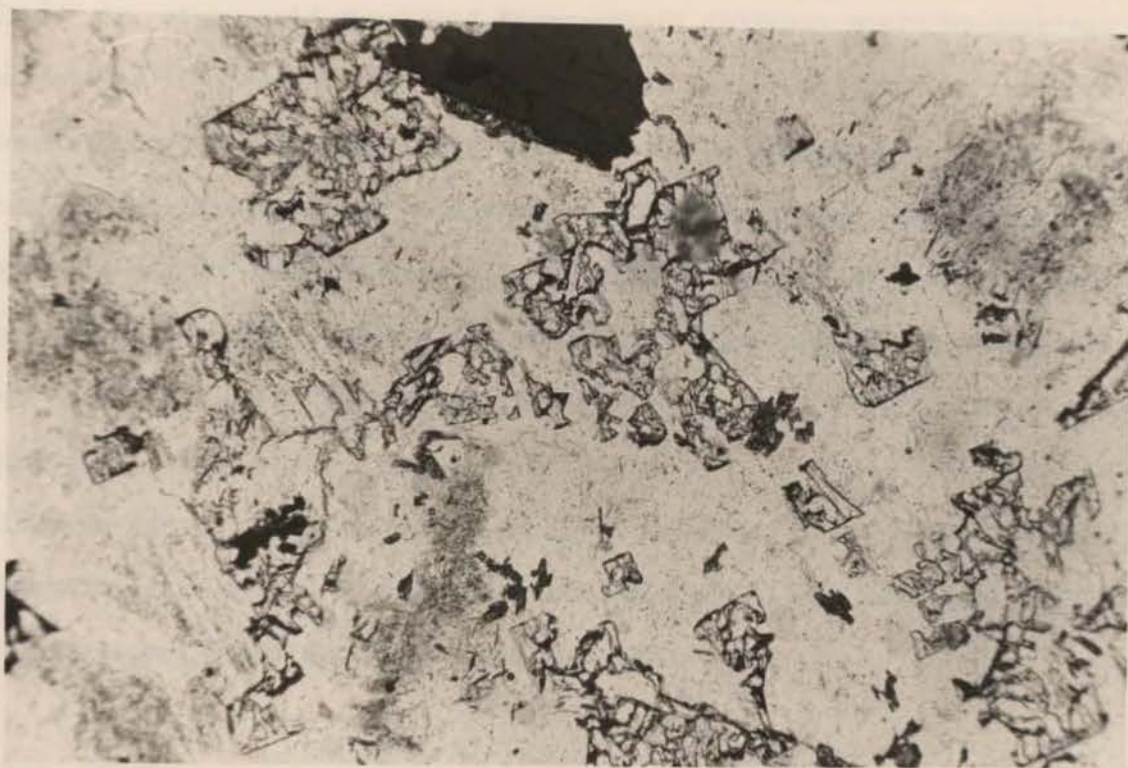


Plate 22. Narsarsukite in a granitic (?) dyke in the Shira quartz syenite. Field width 2.4 mm; plane light. (SH104)

feldspar remain. The arfvedsonitic amphibole shows a deep grey or grey-green to intense blue-green pleochroism and zoning is absent; the grain size is up to about 1.3 mm - much smaller than in the unaltered quartz syenite. Homogeneous aegirine laths and anheda up to 1.5 mm occur as single crystals or in aggregates with arfvedsonite but there is no indication of a reaction relationship; aegirine is much more abundant than usual, with respect to arfvedsonite, and the alkali feldspar is flecked with minute aegirine crystals in greater abundance than normal.

By analogy with the textural changes above, it is pertinent to note at this point that a similar texture occurs in a 3 m wide angular enclave of quartz syenite within the Birji granite, a short way south of Shira. Here, the enclave is cut by a thin (5 cm) pegmatitic vein and a narrow (12 cm) microgranite dyke. In thin section the alkali feldspar shows considerable enlargement of the albitic component and discrete albite is also well developed along alkali feldspar grain boundaries. Aenigmatite is present in minor amounts only, usually as altered globular crystals enclosed in deep green-blue amphibole. Aegirine can occur as anhedral crystals within amphibole but may also occur along the amphibole margin where it is clearly replacive. Specks of small aegirine needles are well developed in the alkali feldspar, and appear to replace both components of the microperthite. Most amphibole crystals are poikilitic and enclose alkali feldspar and quartz. Small alkali feldspars may be almost entirely replaced by albite while larger alkali feldspars have very enlarged albite domains. Albite is, in addition, well developed along perthite grain boundaries.

3.2.3 Enclaves

In the Shira quartz syenite as a whole, enclaves are comparatively rare and usually only a few centimetres in diameter, but in some areas close to the inferred margin of the intrusion (and near

Shira market) they may be both more abundant and larger. The enclaves have been fairly extensively sampled. It is convenient to describe the occurrence of enclaves (and dykes - Section 3.2.4) according to locality.

Gora enclave In the outcrops immediately north of Shira market there is an area of relatively depressed relief which is due to a large (approx. 1-200 m) xenolithic body of sparsely porphyritic microgranite. From the vicinity of the market, the enclave extends NNE to the margin of D.Gora overlooking the road to Azare where it is considerably fragmented by the intrusion of host Shira quartz syenite. It is texturally variable across the outcrop and this variation may be partly due to modification as a result of incorporation in the quartz syenite. However, a typical sample is a fine to medium grained granite having an average grain size of about 1-2 mm; a modal analysis is presented in Table 2.

Alkali feldspar is a turbid, lamellar microperthite in which there is a comparatively large number of amphibole and aegirine inclusions. Arfvedsonitic amphibole and aegirine form anhedral, interstitial crystals and accessory zircon occurs as aggregates of small, turbid crystals. In other specimens, aegirine, arfvedsonite and minor Fe-Ti oxide form aggregates up to 2.5 mm across with a large amount of intergranular albite. Aegirine may also be present as stellate clusters. In all sections examined, there is a greater abundance of aegirine relative to arfvedsonite than is normal for coarser grained granites and syenites in the rest of the complex.

Dutsen Kawaga Only two small (2-10 cm) syenitic enclaves have been sampled in this region due to sampling difficulty. One enclave (SH11) is dark grey-blue in hand specimen, sparsely porphyritic and has a narrow,

darker margin. In thin section, it consists dominantly of turbid, perthitic alkali feldspar, minor interstitial quartz and anhedral or subhedral arfvedsonite. Another, slightly larger enclave (SH13) is equigranular with regular grain boundaries and consists of turbid microperthite with well developed albite domains, rounded quartz, interstitial aegirine and deep blue-green arfvedsonite.

Mainari village Here, small (1-10 cm) slightly porphyritic, melanocratic enclaves occur in relative abundance. They are syenitic and medium grained and alkali feldspars usually have clear cores surrounded by turbid, microperthitic margins. Pale brown to green pleochroic ferrichterite-arfvedsonitic amphibole is abundant in the form of subhedral to anhedral crystals. Accessories include quartz, Fe-Ti oxide, aegirine and biotite.

Dutsen Dalliwo This locality lies a short way SW of Mainari village, close to Dalliwo. Here, several large (approx. 30 cm) porphyritic enclaves occur, which consist of medium grained syenite with an inequigranular texture in which quartz preferentially occurs in the coarser grained areas. Microperthite is the major mineral and may show marked concentration of albite towards the margins and/or an antiperthitic texture. Interstitial aegirine is the sole mafic mineral.

Dutsen Gora Close to the centre of the outcrop of quartz syenite, several small (1-10 cm) enclaves were collected. One enclave (SH76/1) is unusual in having well oriented tabular microperthite crystals. It contains interstitial quartz and amphibole, the latter being pleochroic from yellow-brown to dark green and poikilitically enclosing alkali feldspar; slight overgrowths grow into and replace the enclosed alkali feldspar. Interstitial deep green aegirine or aegirine-hedenbergite

occurs in greater abundance than arfvedsonite. Another enclave (SH76/3) is highly porphyritic with discrete and aggregated alkali feldspar phenocrysts; in one such aggregate there are several sericitised plagioclase cores, turquoise green to grey pleochroic amphibole and iron-ore rimmed by biotite. In the matrix the (plucked) remains of a single aenigmatite crystal occur, as well as quartz and dominant, turbid alkali feldspar in which albite preferentially exsolves towards the margins.

3.2.4 Dykes

In general, the abundance of dykes in the quartz syenite is very low, but they do occur preferentially close to the arcuate granites. It is of interest to note that whereas all the enclaves described are syenitic, the dykes are granitic. In this section and elsewhere, 'melanocratic' is used in the sense of a (dyke) rock having a significantly higher mafic mineral content than the major rock types in this complex.

Dutsen Elbegwa The N side of D.Elbegwa exhibits a 10-15 cm wide vertical dyke of melanocratic microgranite (SH69/2) traceable for a distance of 145 m. For about 100 m the strike is 040 degrees then a deviation of 025 degrees is observed, the dyke being approximately parallel to the nearby Birji granite. It is dilatational and in places there is a similar dyke parallel to it. As is common with melanocratic dykes, it is fresher than the host rock, and amphibole needles are clearly visible in hand specimen. In thin section, alkali feldspar is clear or slightly turbid and occasional microcline twinning is present; the margins are often albite-rich although no perthitic texture is evident, and discrete albite laths are scattered throughout the rock but are probably not replacive. Quartz is abundant as rounded or globular

crystals that have, in part, crystallised after alkali feldspar. Amphibole with yellow or grey-green to green-blue pleochroism forms larger crystals (approx. 1.0 mm) which may be acicular or anhedral and interstitial in which case they are moulded onto alkali feldspar. Anhedral aegirine is present in about the same abundance as amphibole and is intergrown with it with no apparent reaction relationship. Sporadic clusters of anhedral zircons are found. Occasional coarser grained (approx. 3 mm) areas exist in which euhedral aegirine crystals project into a cavity now filled with quartz and a few scattered albite laths. Aegirine encloses some small albite laths and turbid alkali feldspar. These coarser grained areas have the appearance of miarolitic cavities.

Further south, the dyke is not exposed for about 10 m but reappears as a narrow (2-3 cm) sinuous, discontinuous dyke (SH69/3) with a strike of 150 degrees. It does not appear to be dilatational and has marginal banding and a heterogeneous appearance due to the uneven distribution of aegirine which is partly surrounded by felsic material. The rock is sparsely porphyritic with alkali feldspar phenocrysts which have a patch or poorly lamellar perthitic texture, while the matrix consists of slightly turbid non-perthitic alkali feldspar, discrete albite, quartz, anhedral amphibole and large (up to 10 mm) aegirine crystals. The large size of these aegirine crystals should not be confused with large volume, since 50-70% of the area (in thin section) covered by one crystal is occupied by the enclosed quartz and feldspar.

Dutsen Eyagwel This hill contains the largest microgranite dyke (SH74/1) found in the quartz syenite. The dyke is 4 m wide on the surface, grey-blue in colour and dips 50 degrees SE at 028 degrees but the margins are obscured by scree since the dyke is more easily weathered than the host rock.

In nearby outcrops however, several parallel 8-10 cm wide dykes of similar material can be seen clearly; they are dilatational with sharp contacts, occasionally cross-cut one another and may be mafic-rich (SH74/3). The main (4 m) dyke has unusually clear, non-perthitic alkali feldspar with microcline twinning, discrete euhedral albite, quartz and scattered anhedral aegirine. Accessory arfvedsonite and zircon also occur. The clarity of the feldspars indicates that this rock is extremely fresh. Thin (1 cm) micropegmatitic veins (SH74/2) cut this dyke and consist of patch microperthite, quartz and euhedral aegirine, as well as exceptionally abundant clusters of anhedral zircon crystals.

Dutsen Gora Towards the southern tip of D.Gora at locality SH104, a loose boulder of unusual appearance was sampled; it is presumed to be a dyke rock with affinities to those described above. It is granitic with a medium grained texture, with aggregates of quartz grains in large groups up to 7 mm diameter. Alkali amphibole occurs as laths up to 2 mm long which may be perthitic or antiperthitic. The intergranular albite is notable in being composed of a mass of very small, irregularly oriented grains, instead of the usual dentate pattern. Aegirine and arfvedsonite occur as interstitial, anhedral grains up to 2 mm long which sometimes enclose a little aenigmatite. Some anhedral zircon also occurs. However, the main interest in this rock lies in the presence of narsarsukite which occurs as colourless, anhedral, interstitial grains in which a single crystal may sometimes be traced for up to 4 mm (Plate 22). The narsarsukite has been positively identified by microprobe (Table 20) and this is therefore the first Nigerian occurrence to be identified.

Dutsen Balkakori In the SE part of the complex a 30 cm wide blue-grey porphyritic, melanocratic microgranite dyke cuts the quartz

syenite. It dips 42 degrees SE at 078 degrees and is therefore approximately parallel to the nearby Birji granite. Phenocrysts are dominantly of quartz with minor alkali feldspar. In thin section, large (4 mm) quartz grains are globular and anhedral, and contain inclusions of alkali feldspar, albite and aegirine. Alkali feldspar is only faintly turbid, has microcline twinning and is a patch perthite. Aegirine is abundant as anhedral to euhedral crystals with subordinate arfvedsonite, together comprising about 20% of the rock.

3.2.5 Discussion

In thin sections of usual thickness, it is difficult or impossible to determine optical directions in alkali amphiboles and hence the precise pleochroic scheme has not been determined in this study. Optical data for Fe-rich amphiboles is hard to obtain because of strong absorption and dispersion, and anomalous extinction (Deer et al., 1963).

The intensity of colour increases with higher Fe content (Seitsaari, 1953; Bancroft and Burns, 1969) but the phenomenon of anomalous extinction requires some other explanation. In certain cases it has been attributed to elliptical polarisation of light (Shoda, 1958; Nickel and Mark, 1965) and equations have been devised to represent quantitatively the behaviour of light (Hori, 1942; Shoda, 1954). The anomalous extinction took place even in monochromatic light, so it is not related to dispersion of white light. An alternative explanation is that alkali amphiboles may have a sort of perthitic intergrowth of two components with slightly different cell dimensions (Sahama, 1956), but this idea has not been subsequently verified. More recent studies however, indicate that the pleochroism of alkali amphiboles is a function of charge transfer processes involving Fe²⁺ and Fe³⁺ ions (Bancroft and Burns, 1969; Faye and Nickel, 1970). However, Faye and

Nickel (op.cit.) found that the direction of maximum absorption in monoclinic amphiboles does not coincide with the 'c' axis, as would be the case if the absorption were due solely to Fe(2+)-Fe(3+) charge transfer. Instead, deviation of the direction of maximum absorption from 'c' may be due to charge transfer between oxygen and Fe³⁺ ions. Therefore, elliptical polarisation of light causing anomalous extinction could be due to the non-coincidence of the principal optical and absorption directions, and that anomalous extinction occurs preferentially in sections parallel to (010) i.e. a-c longitudinal sections.

The alkali feldspar crystals in the Shira quartz syenite are intergrown and are unique in this complex in exhibiting growth zoning (Plate 16). The zoning is oscillatory and is marked by concentric alternations in turbidity which reflect rhythmic variations in the clear (sodic) and cloudy (potassic) phases in the microperthite. In other crystals, there is a concentric ring of aegirine-hedenbergite inclusions. From the literature it appears that oscillatory zoning in alkali feldspar is rare compared to its occurrence in plagioclase. In calc-alkali granites such zoning has been attributed to variation in barium (Dickson and Sabine, 1967); similarly, zoned alkali feldspars attributable to Ba variation in trachytes associated with an ultramafic complex (Boettcher et al., 1967). However, in the low Ca, Sr, high Rb rocks of the Shira complex (see Table 26), Ba content is probably low since the Ba/K ratio falls and Ba decreases at a faster rate than Sr during fractionation (Taylor, 1965). The whole rock Ba contents of three samples of Shira quartz syenite have been determined by atomic absorption spectrophotometry (analyst, R.A. Batchelor) and the results are as follows:-

	SH2	SH4	SH105
Ba(ppm)	<25	332	407

Also, the Ba content of alkali feldspars analysed by electron microprobe (E.D.S.), was beneath the detection limit (Table 25). Thus, variation in Ba content is not likely to be the factor responsible for the zoning. In any case, the variation in turbidity would suggest that the zoning is due to Na/K oscillation. Should this be the case, it is perhaps surprising that the zoning is preserved at all, since the sodic and potassic regions of a microperthite can be easily homogenised (Orville, 1967). It is of interest to note, however, that Ba may stabilise the structure and prevent natural homogenisation (Smith, 1974, Vol.2, p.243). Oscillatory zoned alkali feldspar (and plagioclase) has been described from a small post-tectonic composite pluton in Maine (Boone, 1962). Boone accounts for the zoning as reflecting changes in the partial pressure of volatiles in the melt as a result of periodic volatile release during roof fracturing. In the high level ring complexes of Nigeria, such a concept appears quite feasible, and is the preferred explanation for alkali feldspar zoning found here. However, the zoning is comparatively rare in alkali feldspar from the Shira quartz syenite and is hardly ever exhibited among other rock types in this or other Nigerian complexes. A possible explanation for this is that subsequent postmagmatic changes within alkali feldspar such as Si/Al ordering, exsolution and albite enhancement, are not conducive to preservation of Na/K zoning.

Albite rims to alkali feldspar occur in the Shira quartz syenite. Such rims occur only between alkali feldspar crystals and they may be 'coherent' or 'swapped' (Smith, 1974, Vol.2, p.282). The rims are usually irregular and have a dentate appearance. There are two opposing opinions for the origin of such intergranular albite; the first considers that the albite results from preferential migration of the albite component to the margins of a microperthite during unmixing (e.g. Ramberg, 1962). The second view is that intergranular albite forms by

replacement of associated alkali feldspar by a residual magmatic fluid in the interstices of a crystal mush (e.g. Peng, 1970). In the case of the quartz syenite, there is very little change in the width or abundance of the perthitic lamellae as might be expected if there had been progressive migration of albite towards the margin during exsolution. Instead, the common, irregular dentate form of the intergranular albite is strongly suggestive of a late-stage, replacive origin, which is the mode of formation preferred here.

Quartz crystals are commonly aggregated but close inspection of each crystal near to extinction, shows that it is composed of numerous sub-grains or domains. The domain texture may be the result of recrystallisation from discrete centres of nucleation in an attempt to create strain-free areas from an originally strained quartz crystal (Phillips, 1965). However, these domains have sharp margins and the appearance is quite distinct from undulose extinction found in quartz from strained rocks. The idea that a single crystal has given rise to numerous sub-units would appear to be more plausible than the opposite, i.e. that the 'single' quartz crystal represents an aggregate of originally more (structurally) distinct grains, because the latter process would be expected to continue across other crystals in an aggregate. However, the former concept presupposes a strained crystal in the first place and the question therefore arises as to why strain might occur in largely interstitial quartz when it is not apparent in the other minerals. A possible explanation may be that a certain amount of strain occurs during the beta to alpha transition from a hexagonal to trigonal structure. From the intersection of the alpha/beta transition curve with the granite minimum in P-T space (Luth, 1976), it is apparent that in the case of shallow subvolcanic intrusions, quartz must have crystallised initially in the beta form and subsequently inverted. That quartz in this and other granitic rocks in the anorogenic province has

undergone recrystallisation, receives support from the common presence of dilute (non daughter salt bearing) fluid inclusions. It may therefore be possible that quartz is recrystallising as a result of inversion strain, with the aid of a post-magmatic fluid.

Alkali feldspar is clearly one of the earliest minerals to crystallise although some crystals may enclose small aegirine-hedenbergite grains, which are therefore also relatively early in the paragenesis. The accessory minerals apatite, chevkinite and ilmenite may be found enclosed by aenigmatite and amphibole and probably form the next group of minerals to crystallise, followed by aenigmatite, amphibole and quartz. Quartz and amphibole are probably the last major minerals to form and since zircon occurs as aggregates of small crystals which are always enclosed in quartz, it crystallises at about the same time. In some thin sections, Fe-Ti oxide (almost certainly ilmenite) has been found enclosed by aenigmatite. It is possible that the early formation, accessory status and effective removal of ilmenite from any fO_2 buffering capacity by virtue of being enclosed mainly by ferrichterite does not interfere with the crystallisation of the other Ti-rich phase, aenigmatite. However, the possible existence of a 'no-oxide' field in T- fO_2 space (Nicholls and Carmichael, 1969) in which aenigmatite crystallises instead of Fe-Ti oxides in a peralkaline rock, appears to have been contradicted to some extent.

It should be noted, however, that the comparatively unusual occurrence of aenigmatite (and amphibole) directly enclosing relatively large crystals of (probable) ilmenite with no sign of a reaction relationship, is restricted to one sample close to the margin of the quartz syenite. These marginal outcrops exhibit a number of other features not found in the central part of the intrusion. For example, some sericitised plagioclase cores have been found enclosed by alkali feldspar, and both mafic minerals and enclaves are more abundant and the

grain size may be less coarse. Occasional miarolitic cavities also occur.

Several textural features appear to be compatible with an origin after final consolidation of the rock: development of turbidity in the alkali feldspar, marginal alteration of amphibole to aegirine, blue-sided fractures across amphibole crystals, alteration of aegirine-hedenbergite crystals and intergranular albite along microperthite grain boundaries.

Dykes occurring within the quartz syenite are all granitic and exhibit textural, chemical and structural features which link them closely with the Birji granite, but the enclaves distributed throughout the quartz syenite are syenitic. A notable exception is the comparatively large Gora enclave which is a microgranite and possibly represents the only remaining occurrence of a preceding, granitic intrusion, and is now a roof pendant in the quartz syenite.

The syenitic enclaves however, may be found over most of the intrusion and are of a fairly uniform size (5-15 cm). They bear close textural and mineralogical similarity to the host rock and may have formed by chilling against the walls, with subsequent disruption and incorporation in the upward moving magma. Microenclaves which contain sericitised plagioclase, grey to turquoise-green amphibole and Fe-Ti oxide (probably magnetite) mantled by biotite, have been found in the syenitic enclaves and in the host rock. They are difficult to interpret but in view of the fact that biotite appears to be forming from the Fe-Ti oxide, the amphibole may also be a secondary mineral, possibly replacing pyroxene. Such a hypothesis would indicate that the microenclaves are, in reality, very similar to those in the Amdulayi syenite, for which a cognate origin is preferred (Section 3.5).

Along the western margin of the Birji granite, the quartz syenite shows good evidence for considerable textural (and chemical) modification.

3.3 The Birji arfvedsonite alkali feldspar granite

The Birji granite is the term used to describe two facies of arfvedsonite granite which occur in an arcuate, cone-sheet type of intrusion in the Shira quartz syenite. The two facies are distinguished by the habit of the amphibole and referred to as the acicular and poikilitic facies. In hand specimen the acicular facies has elongate laths of black amphibole up to 1 cm long, with very pale-grey coloured alkali feldspar and larger, globular, glassy quartz crystals. The poikilitic facies, as its name suggests, is characterised by arfvedsonite which is wholly interstitial and poikilitically encloses rounded quartz and subhedral alkali feldspar crystals. Both facies exhibit layering and a more detailed description of the layered rocks follows.

3.3.1 The acicular facies

Individual crystals of alkali feldspar may be up to 3.5 mm long but are commonly about 2 mm. They are cloudy, subhedral to euhedral patch microperthite/antiperthites in which twinned albite often dominates the crystal. However, the (exsolved) albite is not always evenly distributed and it is common to observe albite preferentially concentrated towards the margins. This feature is not to be confused with intergranular albite as, in the former case, albite is contained entirely within the subhedral or euhedral outline of the alkali feldspar and does not lie between adjacent microperthite crystals. In fact, intergranular albite in the usual sense is rare in this facies, although small groups of randomly oriented albite laths are common along perthite boundaries.

Alkali feldspar is the earliest mineral to crystallise and both quartz and arfvedsonite (+/- aegirine) are interstitial with respect to it. The generally subhedral alkali feldspars form a network

that is interlocking but not intergrown. That is, mutual penetration, implying intergrowth, is hardly developed but instead, the crystals merely rest against one another. There is not usually any preferred orientation to the crystals. Alkali feldspar is ubiquitously flecked with needles, stubby crystals or small anhedral crystals of replacing aegirine and/or blue arfvedsonitic amphibole, and both the sodic and potassic regions of the perthite are affected (Plate 23).

A common feature of all microperthite crystals in this complex is the presence of a turbid appearance which occurs selectively in the potassic component. Under a high power (x100) oil immersion objective the nature of the turbidity is apparently due to differing proportions of fluid inclusions. Plate 24 shows a pair of microperthitic lamellae; the albite lamella is clear and contains very few fluid inclusions although one in particular is in focus and the vapour bubble clearly visible. Conversely, the potassic lamella appears to be equally clear but is packed with fluid inclusions such that transmitted light becomes very diffuse and a turbid appearance results. The largest fluid inclusion visible in the albite lamella in Plate 24 is only of the order of 4 microns wide. The inclusions appear to be dilute and no daughter salts have so far been observed.

The globular, often aggregated nature of clear, glassy quartz is evident in hand specimen. In thin section, individual crystals may reach 3 mm in size or may occur in groups or chains of usually up to three individuals. Thus, quartz clusters may be up to 6-8 mm across and at times give the rock a porphyritic appearance. However, quartz is interstitial and its margins are defined by those of alkali feldspar. Mineral inclusions are rare except for small alkali feldspars which probably represent part of an adjacent crystal bordering and projecting into the quartz interstice. Although its general appearance is globular, in detail the margins of quartz are anhedral and it poikilitically



Plate 23. Aegirine and arfvedsonite needles replacing alkali feldspar in the Birji granite.
Field width 1.2 mm; crossed polars. (SH5)

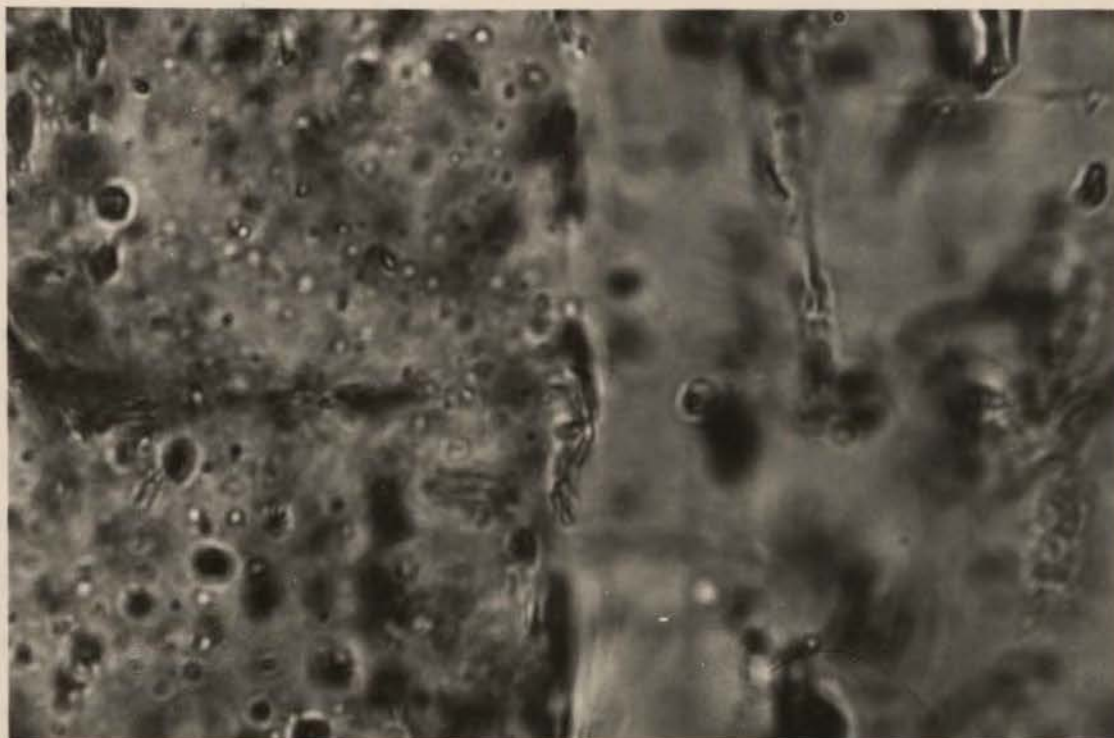


Plate 24. Fluid inclusions in potassic (left) and sodic lamellae in microperthite of the Birji granite. Inclusions are much less abundant in the albite lamella (right).
Field width 0.12 mm; plane light. (SH18)

encloses neighbouring feldspar. A characteristic feature of quartz under crossed polars is the presence of a type of undulose extinction, such that many different domains can be distinguished in a single crystal (Plate 25). This is a common feature of all the rock types in the complex and has already been discussed (Section 3.2.5).

The alkali amphibole has been analysed by microprobe and its composition found to be very close to end-member arfvedsonite (after Leake, 1978) (Table 5 and Figure 8). In this facies, arfvedsonite is acicular and sometimes has a sub-parallel orientation. The elongate arfvedsonite laths are nevertheless anhedral in the sense that a crystal may also extend into interstices between and partly surround, alkali feldspar. Therefore, the fact that the arfvedsonite laths are partly interstitial and show a subparallel orientation on some rock surfaces, is an unlikely combination. Individual crystals may be up to 5 mm long and 3 mm across and in some specimens there may be a crude parallelism producing a lineation in the rock. Sometimes, a single lath consists of two or more discrete crystals which are joined end to end with slight changes of orientation - the composite grain being up to 8 mm long. In addition, they may be aggregated into anhedral groups. Arfvedsonite has a grey or grey-green to deep blue-green pleochroism and a small extinction angle. However, it does not fully extinguish; instead a deep reddish colour is seen close to the extinction position, and consequently the extinction position cannot be determined with any accuracy (see Section 3.2.5). Irregular fractures cut across the cleavage of an acicular crystal and are distinctive because of their blue colour. Small projections often extend from an arfvedsonite across an otherwise straight boundary, into alkali feldspar and represent a late growth stage (or overgrowth) of the amphibole. Arfvedsonite may be partly overgrown by aegirine, which forms a narrow rim, or it may be preferentially replaced by aegirine down the cleavage or along fractures



Plate 25. Domain structure in quartz in the acicular facies of the Birji granite, close to the extinction position. Field width 2.4 mm; crossed polars. (5s)

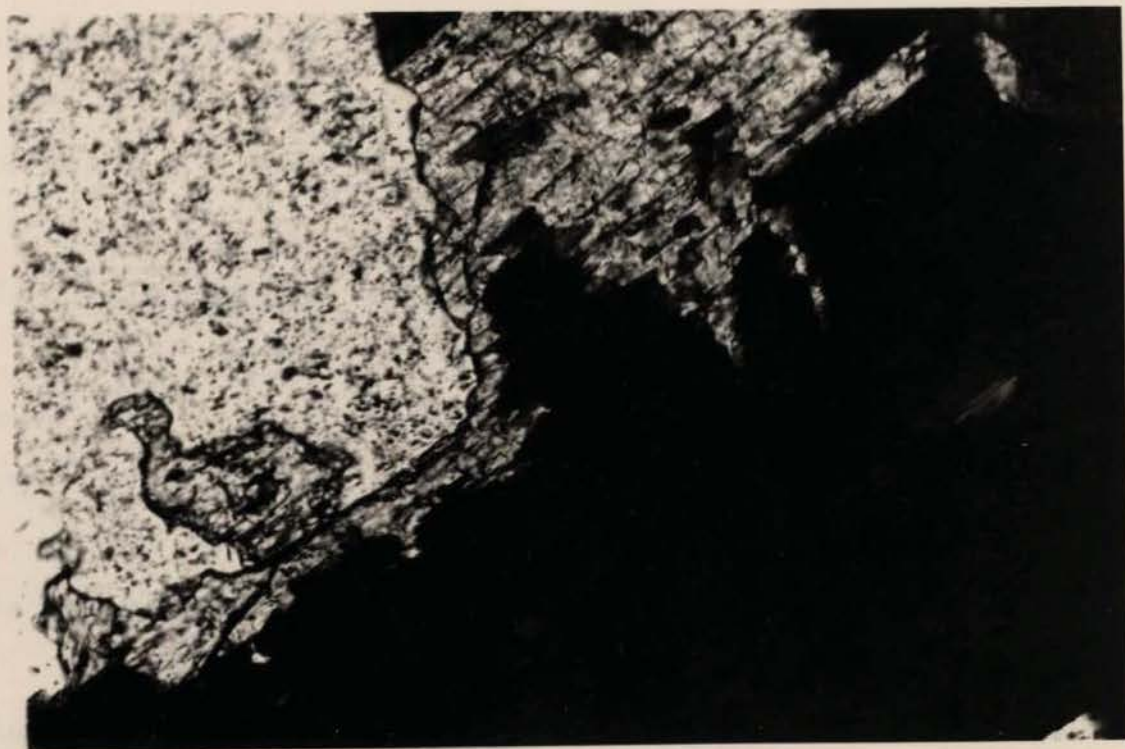


Plate 26. Aegirine replacement of arfvedsonite along the margin and fractures, acicular facies of the Birji granite. Field width 1.2 mm; plane light. (SH18)

(Plate 26). Apatite inclusions and colour zoning are noticeably absent. Quartz inclusions are also absent; quartz and arfvedsonite for the most part crystallise in discrete interstices and do not enclose one another. Where they are seen in contact though, quartz may have crystallised after arfvedsonite. This is an important distinction from the poikilitic facies in which arfvedsonite encloses globular quartz crystals.

Zircon is a frequent though not abundant accessory which is usually found as interstitial, aggregated anhedral grains enclosed within quartz (Plate 27). Zircon also occurs in interstitial areas along with a brown isotropic material which is visible in hand specimen as pink-brown spots, and may represent a breakdown assemblage from an earlier accessory (zirconium-bearing) mineral. In one specimen (SH5), there is a pale yellow, low possibly anomalously birefringent, fibrous or platy mineral which has an R.I. > quartz and may be an Fe-chlorite. In other samples a colourless, low birefringent, radiating and fibrous mineral which has straight extinction, positive elongation and an R.I. < quartz can be found in small, interstitial areas. This mineral is likely to be a zeolite, possibly natrolite (Plate 28).

3.3.2 The poikilitic facies

A comparison of the textures of the two facies of the Birji granite (Plates 29 and 33) shows that there is a close similarity in habit and grain size of both alkali feldspar and quartz. For this reason a separate description of the petrography of quartz and alkali feldspar in this facies is unnecessary.

The habit of arfvedsonite is evident in the field as well as in thin section (Plate 29), where large (1-3 cm) spongy crystals poikilitically enclose euhedral or subhedral alkali feldspar and globular quartz crystals. Closer examination of micropertthite grains enclosed by arfvedsonite reveals that there is often a narrow region (or

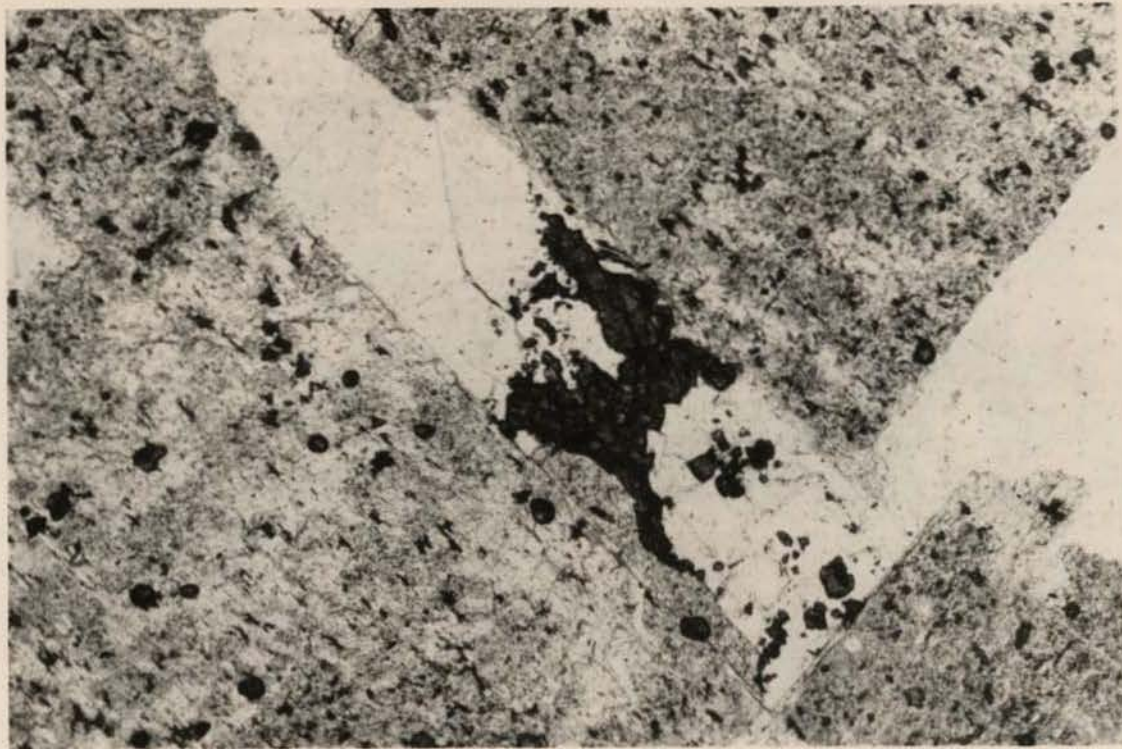


Plate 27. Late crystallising zircon aggregate in the acicular facies of the Birji granite. Field width 6 mm; plane light. (SH75/2)

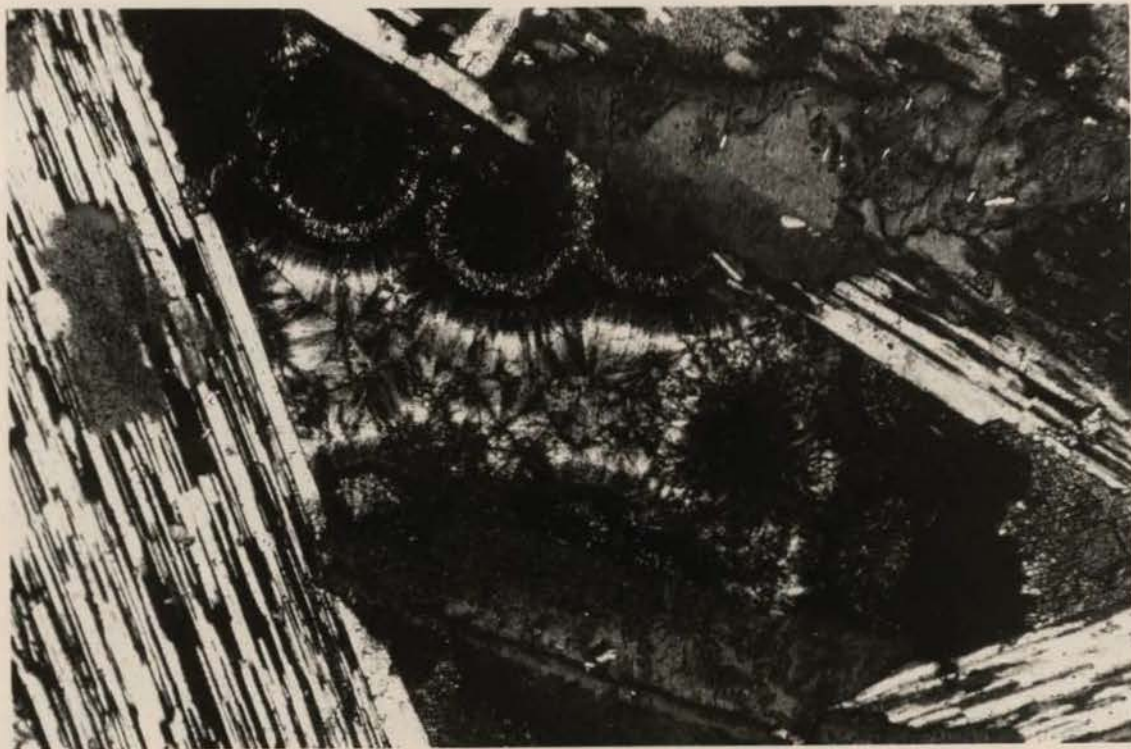


Plate 28. Zeolite filled miarolitic cavity in the poikilitic facies of the Birji granite. Field width 1.2 mm; crossed polars. (14s)

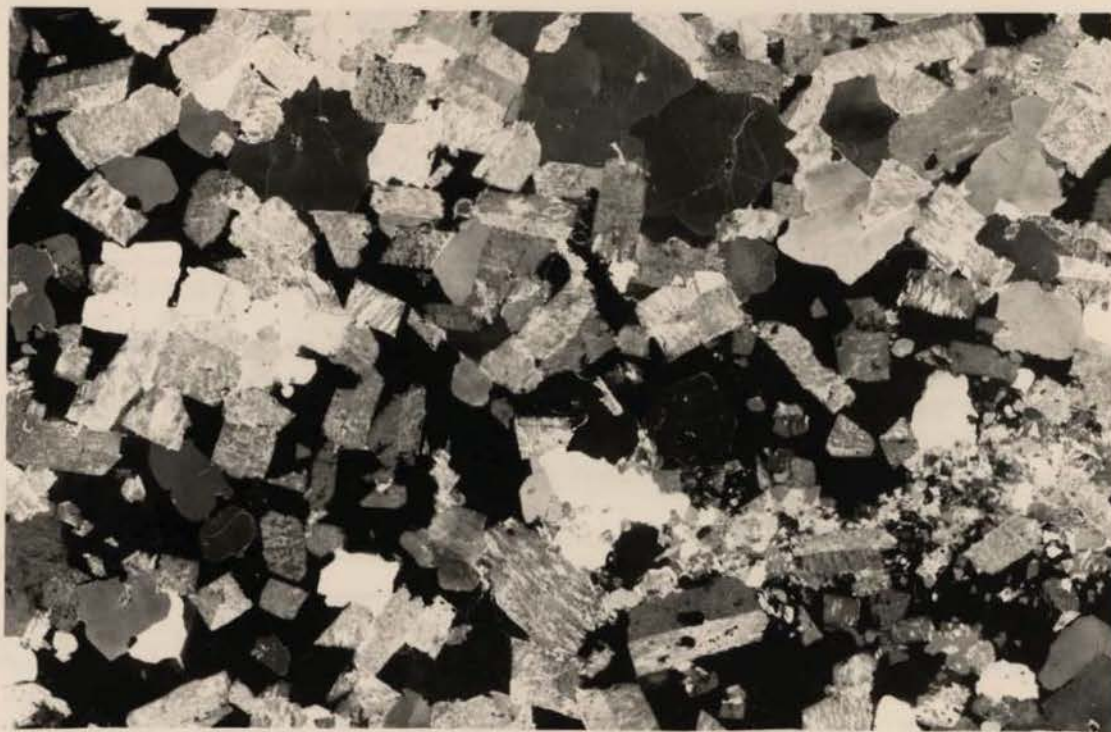


Plate 29. Texture of the poikilitic facies of the Birji granite. Note the euhedral-subhedral alkali feldspars and interstitial arfvedsonite. Field width 40 mm; crossed polars. (SH8)



Plate 30. Overgrowths of arfvedsonite replacing alkali feldspar in the poikilitic facies of the Birji granite. Field width 6 mm; plane light (SH30)

overgrowth) where small prolongations of arfvedsonite extend into and replace the feldspar (Plate 30), approximately at right angles to the microperthite-arfvedsonite interface.

Where quartz is enclosed by arfvedsonite, it appears that a different process has apparently taken place since along these junctions in particular, arfvedsonite has been replaced by aegirine, which occurs preferentially along the amphibole cleavage (Plate 31). In most cases, the outline of the enclosed (globular or rounded) quartz crystal is retained and is smooth and regular. Quartz does not therefore appear to be affected by the arfvedsonite/aegirine replacement process, even though quartz-arfvedsonite boundaries are selectively replaced. In rare (weathered?) specimens with abundant secondary haematite, aegirine has almost completely replaced arfvedsonite and only small cores of the latter remain. Apart from the grossly anhedral, poikilitic habit of the arfvedsonite in this facies, a further very important contrast with the acicular facies is that arfvedsonite encloses quartz and has clearly crystallised afterwards.

Aggregates of anhedral zircon crystals in quartz occur in an analogous form to the acicular facies. However, there may be a slightly greater abundance of interstitial areas (0.3-0.5 mm) carrying zircon and a brown isotropic (?amorphous) substance as well as (?)zeolite. In one section (SH72/4) (probable) zeolite has replaced an alkali feldspar crystal quite extensively and it has the following properties: acicular colourless laths show straight extinction, positive elongation, biaxial positive, first order birefringence (pale yellow), and an R.I. < quartz. The orthorhombic alkaline zeolites natrolite and mordenite are likely candidates. Similar material has once been observed (SH72/5) replacing aegirine in an area where layering is well developed. Aenigmatite has been found in only one thin section, where it occurs as small rounded grains in optical continuity and enclosed or adjacent to arfvedsonite.

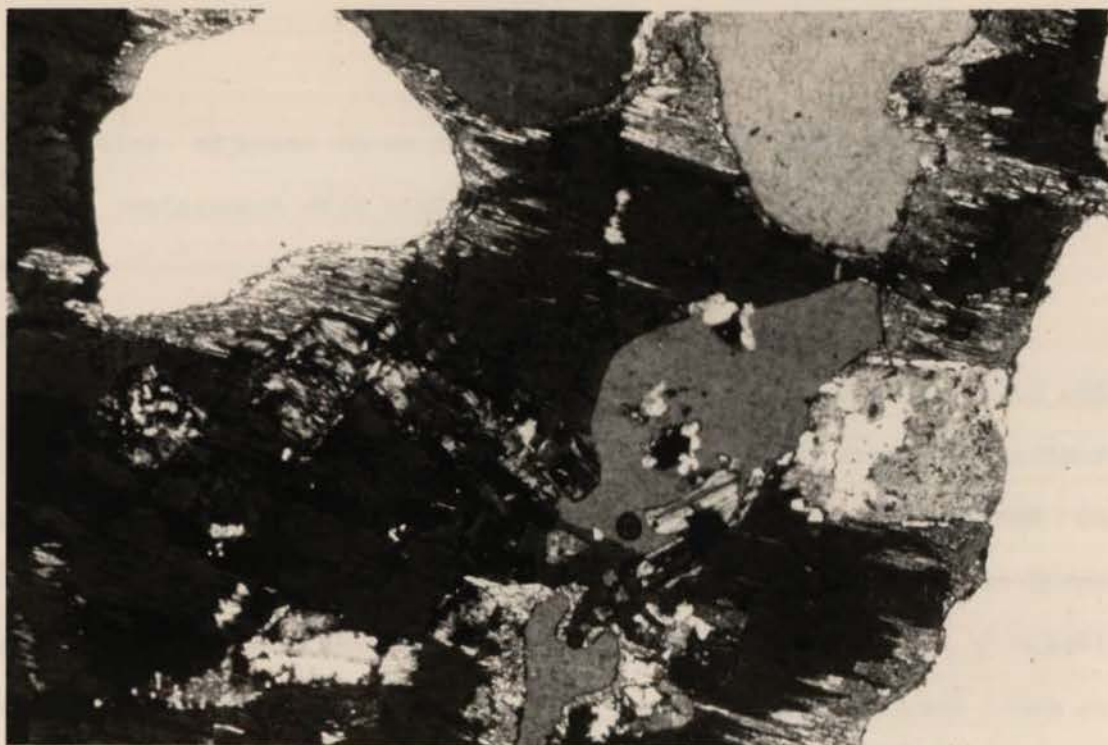


Plate 31. Aegirine preferentially replacing arfvedsonite around quartz crystals in poikilitic facies of the Birji granite.
Field width 2.4 mm; crossed polars. (22s)

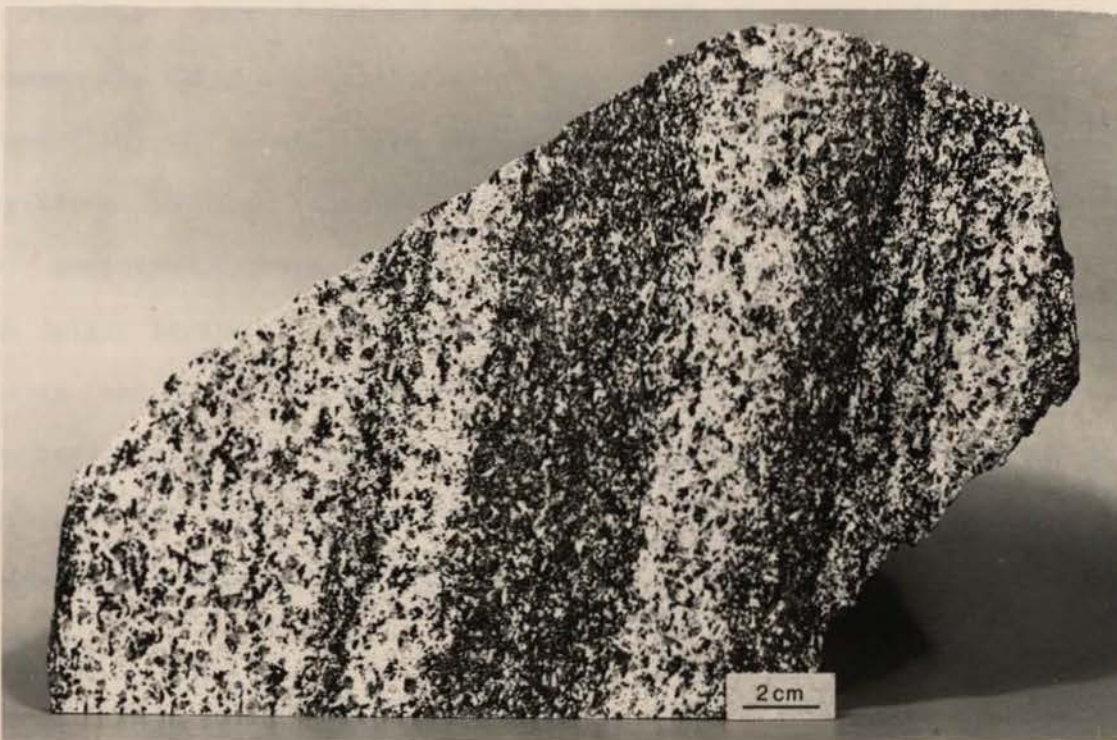


Plate 32. Layering in the Birji granite. (38s)

It is also adjacent to an aegirine crystal, but there is no sign of a reaction replacement with either.

3.3.3 Modal analysis of layered samples

In order to examine the modal variations between the mafic and felsic layers, a large thin section (Plate 33) was cut from the specimen shown in Plate 32, and point counted by the method outlined in Appendix 1. The modal data for this and a similar sample (39s) are given in Table 2. From this data, it can be seen that the proportion of alkali feldspar is virtually constant (within experimental error) and close to 70%. Thus, although alkali feldspar is an early, well formed mineral, it does not vary in proportion between the layers. Of equal interest however, are changes in the proportions of quartz and amphibole (+/- aegirine); in the felsic zones, quartz constitutes about 21-24% and amphibole about 8-9%. By contrast, in the mafic layers, quartz constitutes about 7-11% and amphibole 18-20%. Thus the modal variation between the mafic and felsic layers is due not to variation in the proportion of alkali feldspar (the first formed mineral), but to variation in the relative proportion of quartz and arfvedsonite (+/- aegirine). These two minerals reverse their abundances such that the felsic layers are relatively quartz-rich. Since these two minerals, quartz and arfvedsonite, are interstitial relative to alkali feldspar, the layering would appear to be due not to selective concentration of minerals by gravity but to selective crystallisation of either arfvedsonite or quartz in interstices within the feldspathic framework.

3.3.4 Dykes, pegmatite and enclaves

Dykes

The scarce dykes which cut the Birji granite are melanocratic medium grained granitic dykes. In these dykes, alkali feldspar

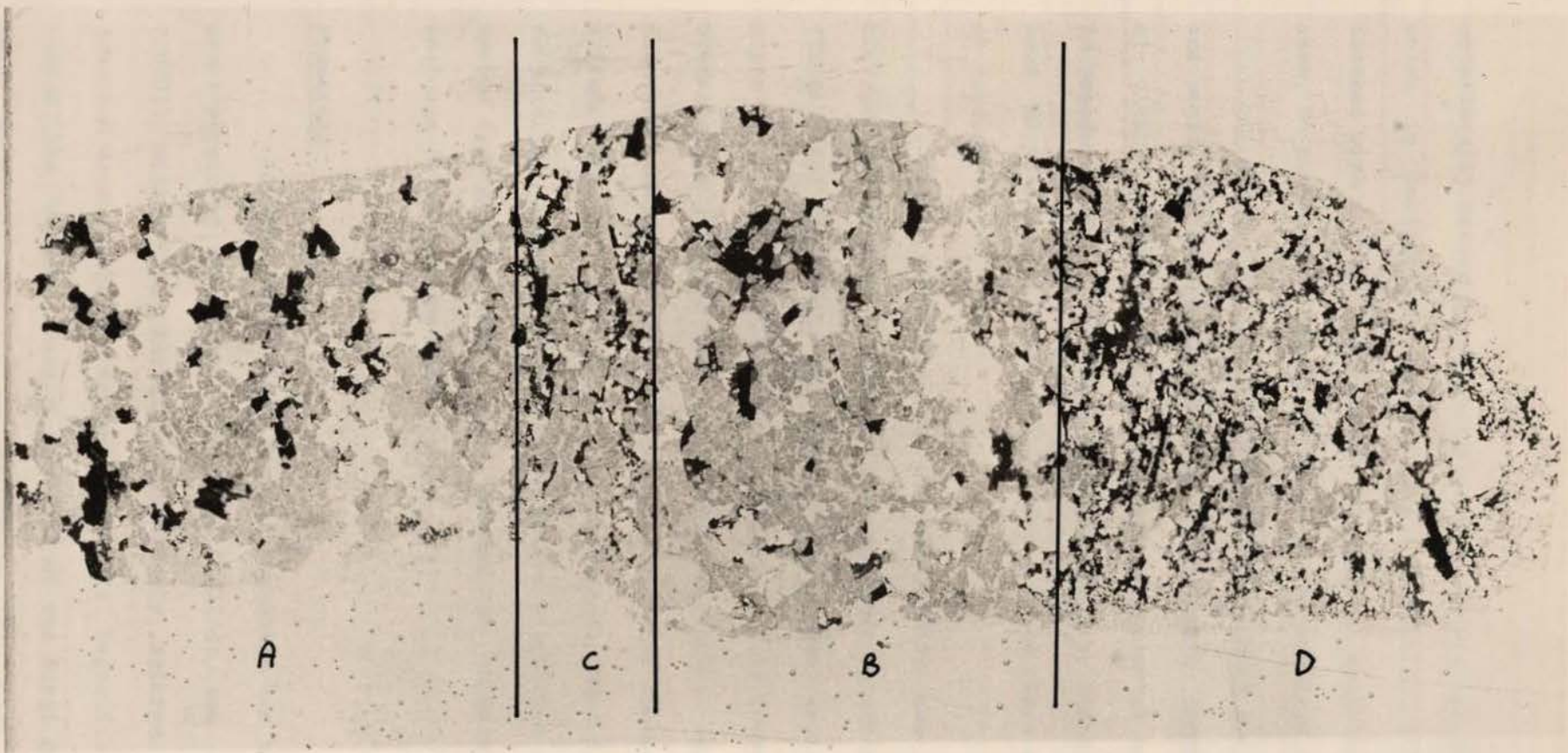


Plate 33. Texture of layered sample of the acicular facies of the Birji granite. Modal analyses of felsic zones A & B and mafic zones C & D are given in Table 2. Field width 80 mm; plane light. (38s)

occasionally occurs as phenocrysts (e.g. SH73/1) of patch microperthite which is turbid and anhedral, and generally 1-2 mm in size. It is flecked with aegirine needles and microcline twinning is occasionally seen, in contrast to alkali feldspar in the granites and syenites.

Quartz occurs as rounded grains which are evenly distributed and poorly aggregated. The margins often have a tangential arrangement of albite laths suggestive of a microphenocrystal occurrence, although in general, quartz has complex grain boundaries and appears in part to have crystallised after alkali feldspar since there are some inclusions of feldspar.

Alkali amphibole from one dyke (SH95) has been analysed by microprobe and has a composition very close to end-member arfvedsonite (Table 5 and Figure 8). The arfvedsonite shows typical grey to deep green or deep blue-green pleochroism, and is found as anhedral laths occasionally crossed by blue-sided fractures. Aegirine occurs as discrete subhedral to euhedral prisms and is commonly intergrown with arfvedsonite with little sign of replacement. There is usually a crude subparallel orientation and the relative proportion of the two minerals varies from dyke to dyke. Small groups of anhedral zircon crystals enclosed by quartz are commonly seen.

Pegmatite

Amphibole/aegirine bearing pegmatite has been found along the upper margin of the arcuate intrusion (SH72/3) and as loose boulders (SH101) within the intrusion apparently related to the gradational junction between the two facies of granite. Pegmatite dykes also occur toward the western margin (SH83/3) of the Birji granite. At locality SH101, amphibole crystals up to 20 cm long have been analysed by microprobe and are virtually pure arfvedsonite (Table 5 and Figure 8). It is the dominant mafic mineral and is euhedral and contains small

inclusions of quartz and alkali feldspar. There is some textural evidence that the arfvedsonite has crystallised at a relatively early stage compared to that in the associated granites, since it contains quartz and alkali feldspar inclusions. Alkali feldspar is a turbid lamellar or patch perthite, flecked with small aegirine and amphibole needles. Aegirine is present as a minor constituent and in the slide used for microprobe analyses, exhibits oscillatory green/brown zonation. Analyses AG4-7 in Table 13 indicate that Ti is strongly favoured in the green zones, whilst the brown areas represent a purer aegirine richer in Na and Fe (and relatively depleted in divalent and tetravalent cations).

Other pegmatite occurrences (e.g. at sample localities SH72/3 and SH83/3) also possess zoned aegirine, which may be the dominant mafic mineral. The zoning is marked by a large homogeneous (green) core surrounded by one or two narrow symmetrical zones marked by slightly different colour (also green) and pleochroism. The maximum difference in extinction angle between the core and margin is 6 degrees, the margin being less. Some cores to large, euhedral aegirine crystals have an extinction angle up to 15 degrees and should therefore properly be termed aegirine-hedenbergite. No analyses are available for these crystals. Occasional arfvedsonite crystals remain but are extensively replaced by aegirine. A small quantity of interstitial (?) natrolite occurs.

Enclaves

a) Volcanic rocks Nearly all volcanic rocks recorded in the Shira complex occur as enclaves within the Birji granite. These enclaves are not well exposed but at locality SH98 one such body may be traced for over 100 m. The rock at this locality, and nearby at locality SH96, consists of a very fine grained grey-blue flinty rock in which a foliated texture is apparent on weathered surfaces. The weathered crust

on such boulders is white and about 1 cm thick. These occurrences are apparently enclosed by the acicular facies although the poikilitic facies is close at hand. At localities SH17 and SH96 the grain size is about 0.02-0.04 mm and the rock consists largely of quartz, clear alkali feldspar and brown biotite with an equigranular texture in which the crystals have smooth outlines and are rounded or subhedral. The texture is thus typical of a hornfels. Iron-ore, zircon and apatite crystals are scattered throughout and white mica occurs as large, poikilitic flakes or as smaller, discrete areas which may represent feldspar pseudomorphs. At locality SH98 the enclave is very similar, although slightly coarser grained and bearing sparse microphenocrysts or porphyroblasts of quartz and turbid alkali feldspar. The alkali feldspar shows complex grain boundaries and encloses part of the matrix. In one section (SH98/3), biotite similarly forms abundant small, fresh equant plates and white mica forms larger anhedral plates or aggregates. In an adjacent sample (SH98/1) scattered iron-ore and amphibole with green to pale brown pleochroism occurs instead of biotite; the amphibole has equant grains and may be found enclosed by the turbid alkali feldspar porphyroblasts.

On the NW flanks of D.Gora at locality SH29, several different facies of volcanic rock occur among a number of separate enclaves. The largest occurrence (SH29/1) is an agglomerate consisting of clasts of crystal rich and aphyric volcanic rock fragments 1-3 cm in size. In thin section the clasts range from aphyric/spherulitic to trachytic varieties set in an extremely fine grained biotite bearing quartzofeldspathic matrix. No textures indicative of welding are seen. Some of the biotite is partly chloritised and white mica occurs as larger poikilitic plates. Enclaves may be of crystal-rich and crystal-poor varieties; in the crystal-poor facies (SH29/5) sparse quartz and alkali feldspar crystals are aggregated while the matrix is notable in being composed exclusively of a microgranophyric intergrowth of quartz and faintly turbid alkali

feldspar, which has a somewhat spherulitic appearance. There are scattered fluorite, iron-ore and zircon crystals but no mafic minerals. A crystal-rich enclave (SH29/4) has turbid, subhedral lamellar perthite grains up to 4 mm across which are aggregated into groups up to 1 cm across. Quartz crystals occur singly or in pairs and commonly have inclusions or deep embayments filled by the matrix. A notable feature in the rock however, is the presence of a 1 mm wide spherulitic margin to the phenocrysts and discrete 0.75 mm diameter spherules in the matrix. Scattered opaques occur but again there is an absence of mafic minerals.

b) Basement rocks No outer contacts of Younger Granite with basement (Older Granite) are seen in the Shira complex, but several occurrences of basement enclaves within the Birji granite have been found. At locality SH29 a 3 m wide basement enclave is a coarse grained granite with white alkali feldspar crystals up to 7 mm long; they are intergrown with a little plagioclase and are turbid, with poorly developed perthitic lamellae. Quartz is abundant and forms clusters and chains. Biotite is the dominant mafic mineral and forms aggregates of small crystals which are interstitial, but also appear to replace adjacent feldspar, particularly plagioclase. There is a little accessory green amphibole, fluorite and iron-ore. In one thin section there is a dark fracture along which there has been movement of about 0.5 mm and there is a concentration of amphibole, fluorite and iron-ore.

At locality SH89 a 20 m long basement outcrop is in contact with the poikilitic facies on the N side and has a number of narrow (1 cm) shear zones running through it. In these shear zones or veins, single crystals or aggregates of alkali feldspar exhibit a wide range in grain size from 5 mm down to the very fine grained matrix. Quartz is strained and fractured and has jagged crystal outlines. There is a little chloritised biotite and some white mica in the matrix.

At locality SH91, the leucocratic granite is foliated with a

preferred alignment of quartz and mafic minerals. In thin section, strained quartz aggregates form linear or lensoidal chains and are mainly responsible for the foliation observed in the rock. Alkali feldspar may be clear or turbid corresponding to crypto- or microperthite varieties, can reach 7 mm in diameter and is intergrown with a little plagioclase. The only mafic minerals observed were in a probable pseudomorph now consisting of biotite, chlorite and fluorite.

3.3.5 Discussion

The petrographic similarity of the two granite facies (with the exception of the habit of the amphibole), the gradational contacts between them and the occurrence of layering in both, implies a closely related origin. The fabric of both rocks is dominated by well formed alkali feldspar crystals that are interlocking, but only have a limited degree of intergrowth, around which quartz and arfvedsonite crystallise interstitially. The principal petrographic dissimilarity between the two facies is in the order of crystallisation of these two minerals; arfvedsonite encloses quartz in the poikilitic facies but does not do so in the acicular facies.

Among the alkali feldspars the strong development of a patch microperthite or antiperthite texture is probably due almost entirely to exsolution from an originally homogeneous, sodic alkali feldspar since there is virtually no intergranular albite. Arfvedsonite and aegirine have crystallised later than alkali feldspar, yet both these mafic minerals occur as minute crystals scattered throughout the microperthite and small overgrowths of arfvedsonite against microperthite are common. Some late stage pervasive replacement of alkali feldspar has evidently taken place. It does not appear to be restricted to either the sodic or potassic portions of the microperthite but a possible association in time between the development of a perthitic texture, replacement by

aegirine and arfvedsonite and Al/Si ordering of the alkali feldspar must be considered. Each event may be associated, enhanced or indeed caused by a sodic fluid phase.

It is noticeable that microcline ('tartan') twinning has not been observed in thin section yet X.R.D. data (Table 31 and Figure 25) indicate that microperthite from the Birji granite is structurally a low albite-maximum microcline. This 'anomaly' is found in all major rock types in the complex. Assuming that alkali feldspar initially crystallised above the solvus it presumably has unmixed subsequently to give a microperthite and at some stage also undergone a monoclinic to triclinic inversion to microcline. In the granites and syenites this inversion is therefore not necessarily accompanied by the development of 'tartan' twinning. However, in the highly peralkaline dyke rocks associated with the intrusion of the Birji granite, 'tartan' twinning is frequently seen in thin section. It may be significant therefore that the only other rock type in the province known to the writer where such twinning is readily seen, is an albite arfvedsonite granite. Since microcline twinning does not appear in the highly sodic (but nevertheless aluminous, i.e. P.I.<1) albite zinnwaldite granites (e.g. Odegi, Afu; C.A.Abernethy, pers. comm.), there would appear to be a connection between development of microcline twinning and highly peralkaline conditions, in this province.

In the poikilitic facies, aegirine replacement of arfvedsonite preferentially takes place around enclosed, rounded quartz grains. Quartz itself shows no sign of replacement and it does not seem likely that it has taken an active part in the replacement process. Instead, it appears more likely that quartz-arfvedsonite grain boundary has been preferentially exploited by a postmagmatic fluid. The latter suggestion would of course be strongly dependent on the relative rates of contraction of the three minerals arfvedsonite, alkali feldspar and

quartz since the pair with the greatest differential would be expected to have a grain boundary more easily exploited by a fluid during cooling. Experimental data given below may be used to test this hypothesis. ('Hornblende' is the only amphibole found with suitable data.)

Volume coefficients of expansion of minerals from 20-400 degrees C, with ratios relative to hornblende, from Skinner (1966):

<u>Mineral</u>	<u>Coefficient</u>	<u>Ratio</u>
Microcline	0.644	0.66
Hornblende	0.970	1.00
Quartz	1.890	1.95

Thus, during cooling, a larger grain boundary space will be expected to develop between an amphibole and quartz during cooling, than between amphibole and feldspar. This would encourage any postmagmatic fluid to utilise that junction and may result in alteration of arfvedsonite to aegirine.

As is characteristic of many peralkaline granites, zircon does not crystallise until a comparatively late stage and forms aggregates of anhedral crystals in interstices. The zircon sometimes occurs in similar form along with zeolite in which case the assemblage may represent the breakdown of a pre-existing interstitial, accessory mineral. Alternatively, the zeolite, being a hydrated mineral, may represent the result of limited postmagmatic rock-fluid interaction at a comparatively late stage at low temperature.

There have been several studies relating to zircon from this province, which have shown that in the aluminous mica granites, the

physical and optical properties of zircon can be modified by postmagmatic events (Williams et al., 1956; Jones, 1960; Mano, 1963). However, the comparatively large size and anhedral or subhedral nature of zircon from these rocks compared to the fine grained, aggregated zircon from the Shira quartz syenite, make extrapolations difficult or unwarranted. In a peralkaline magma however, the behaviour of Zr in the melt is quite distinct from an aluminous magma, and may lead to contrasting episodes of zircon crystallisation as a result. In experimental ZrO₂ bearing gels with compositions close to the Q-Ab-Or ternary minimum, well formed or skeletal zircon crystals can be precipitated (Dietrich, 1968). However, with the addition of sodium disilicate or sodium fluoride in amounts just slightly greater than the ZrO₂ content, the charge was peralkaline and zircon crystallisation was suppressed. In a similar way, it has been shown that in a non-peralkaline charge, the saturation level for Zr in the melt is comparatively low at around 57 ppm Zr, for whole rock Zr values greater than 200 ppm (Larsen, 1973).

In a more extensive study of the behaviour of Zr in felsic liquids, Watson (1979) confirmed Larsen's conclusion that less than 100 ppm Zr is required to saturate aluminous melts, but that in peralkaline melts the saturation level is considerably raised. In fact, the Zr solubility is mainly a function of the peralkalinity index and is not sensitive to temperature, SiO₂ or even the Na/K ratio (Watson, 1979). Thus in aluminous rocks, zircon can be expected to be a liquidus phase; in peralkaline rocks however, Zr will remain in solution for much longer due to the formation of alkali-zirconosilicate complexes and only precipitates at an advanced stage of crystallisation.

Although small zeolite filled interstices are found in each of the peralkaline rocks, they are perhaps displayed best in hand specimen in the Birji granite. The zeolite does not appear to be replacive but

perhaps an infilling of interstitial, miarolitic cavities. The optical properties suggest it is orthorhombic, and assuming that a sodic variety is most likely, then natrolite, gonnardite or mordenite are all possibilities. They each contain between 6 and 8 water molecules per formula unit and therefore presumably represent a period of minor, although pervasive rock-fluid interaction. The temperature at which this could have taken place must be relatively low - less than 300 degrees C (Coombs et al., 1959) and possibly lower. The zeolite filled miarolitic cavities are therefore interpreted as representing a period of low temperature rock-fluid interaction that appears to have been pervasive throughout the complex.

Layering has been defined as an igneous, planar phenomenon "dependent for its origin largely on the physical effects of gravity and the chemical effects of magmatic fractionation" (Wager and Brown, 1968, p.544). Thus, a genetic association between layering and crystal settling under the influence of gravity is clearly implied. Since rhythmic, igneous layering without any evidence of crystal settling has developed in the Birji granite, such a definition would have to be rejected. In fact, similar problems with the established crystal settling model for igneous layering have been pointed out by Campbell (1978), who also describes layering which may be parallel to the walls of an intrusion.

Among calc-alkaline granites, several examples of layering are known. Gilbert (1906) describes a "gravitational assemblage" of hornblende, biotite and feldspar in the Sierra Nevada batholith, which exhibits rhythmic layering with trough banding and truncated layers. In Ireland, Aucott (1965) reported that biotite layers in the Galway granite (adamellite) had sharp bases and could cross-cut one another. Further work on this granite showed that the biotite layers also contained hornblende, magnetite, sphene, apatite and allanite, all of

which crystallised earlier than quartz and alkali feldspar (if not plagioclase as well), and their origin was ascribed to crystal settling (Claxton, 1968). Subsequently, Leake (1974) similarly viewed the same biotite-rich layers as due to crystal settling but in addition, discovered a very coarse, near vertical type of layering. He attributed the latter to crystallisation in steep zones from the edge of the granite inward, during vertical movements of the magma which produced a sort of 'flow sorting' in much the same way as that envisaged by Wilshire (1969) for the Twin Lakes granodiorite. Similarly, Berger (1971) concluded that the geometry of the coarse banding in Donegal was compatible with formation during deformation of the magma.

In the Twin Lakes granodiorite, Wilshire (1969) describes what may be the type locality for vertical layering in marginal zones, which is explained by a process of flow sorting (differentiation) accompanying vertical shear flow during emplacement. Similar styles of layering ascribed to shearing during intrusion occur in Connecticut (Gates and Scheerer, 1963) and Nova Scotia (Smith, 1975).

Among anorogenic granites, layering has been described from granites in the Gardar province (Harry and Emeleus, 1960). In fluorite-rich biotite granites near Tigssaluk, they describe thin layers of biotite, sphene, opaque oxides and allanite which may be up to 100 m long with their best development near the outer contacts. They may be rhythmically layered, have a gentle dip, or be steeply dipping; sedimentary type structures occur, including slump folds, faults, graded bedding and trough banding. Large microcline crystals may be aligned within and parallel to the layering while preferred orientation is absent from the unlayered parts. With such well defined sedimentary-type structures, Harry and Emeleus (1960) ascribed the layering partly to the action of magmatic currents (for the complex types) and to an in situ kind of differentiation (for the rhythmic layers) aided perhaps by

variation in volatile content. The mafic and oxide minerals comprising the Tigssaluk layers are poikilitically enclosed by quartz, microcline microperthite, plagioclase and occasional fluorite, and it has been suggested that the layering here formed in a particularly fluid magma by bottom accumulation, with the help of magmatic currents (Emeleus, 1963). Similarly, syenites and other rock types of the Gardar province have been highlighted as exhibiting excellent mineral layering (Ferguson and Pulvertaft, 1963). In fact, the dominantly syenitic intrusion of Ilimaussaq is believed to have differentiated in situ with crystallisation from the roof downwards simultaneous with bottom accumulation of heavy minerals, which gave rise to an exceptionally well layered intrusion (Ferguson, 1970). These conclusions were supported by Sorensen (1969) who pointed out the rhythmic nature of layering in the Ilimaussaq intrusion, with a repetition of lower arfvedsonite, central eudialyte and upper alkali feldspar. Surprisingly however, Sorensen (1969) emphasised the extreme regularity of the layering in many Gardar intrusions while apparently being unaware of the sedimentary structures described by Harry and Emeleus (1960). More recently, Parsons (1979) has described a variety of sedimentary features from the Klokken intrusion including an exceptional development of flame structures.

Layering is perhaps the most important aspect of the Birji granite. An appreciation of the origin of this layering must incorporate essential features of both the field geology and petrography. The most significant points regarding the field geology of the Birji granite as a whole are that it is an inclined intrusion of cone-sheet form in which the central region consists of the acicular facies, but towards the margins there are a number of facies variations and layered localities. Both the facies variations and layering occur in essentially planar units that are sub-parallel to the margins of the intrusion and may therefore be considered concordant features. The acicular facies often

shows a weak lineation of arfvedsonite laths and both the acicular and poikilitic facies may be layered. There may be a gradational or relatively sharp junction between the two facies and a concordant pegmatite sheet sometimes occurs close to a facies change. Alkali feldspar is the first mineral to crystallise and occurs generally as well formed crystals of uniform grain size that exhibit little intergrowth and clearly were free to grow in a liquid. Despite this, detailed modal analysis has shown that the layering is not due to concentration of feldspar but to differential proportions of the interstitial minerals, quartz and arfvedsonite.

The principal difference between the acicular and poikilitic facies lies in whether arfvedsonite or quartz is the first interstitial mineral to crystallise. It becomes obvious that the alternation in the field between the acicular and poikilitic facies can be viewed as a large scale version (outcrop size) of the layering (hand specimen size). The two phenomena may therefore be closely related. In addition, it may be significant that both the layering and facies variation are absent from the central part of the intrusion but are concentrated closer to the margins. Proximity to the margins therefore appears to be important with respect to the development of each feature.

Considering a single mafic layer in which, as stated, arfvedsonite has crystallised in greater abundance than quartz, if for some reason, arfvedsonite began to crystallise along a particular plane in the crystal mush, the residual liquid would become enriched in silica. However, because the majority of crystal nuclei are those of arfvedsonite, this mineral will continue to extract the components it needs to crystallise from the magma, in preference to quartz. However, a point must eventually be reached where the silica content of the residual liquid away from the hypothetical plane has risen, and the iron content has fallen due to prolonged crystallisation of arfvedsonite,

such that quartz will preferentially crystallise. In fact, once selective crystallisation has taken place along a plane within a peralkaline magma at least, under stable thermal and gravitational conditions, alternate crystallisation of interstitial minerals could perhaps continue until solidification.

Similarly, the alternation of acicular and poikilitic facies granite sheets (given the fact that the relative positions of quartz and arfvedsonite in the crystallisation history of these two facies is different) may be analogous, and simply a larger scale version of the same process that gave rise to the layering.

In a crystallising magma in which a framework of early formed crystals has developed, essentially the same process of selective crystallisation of the interstitial phases probably takes place, but homogeneously; it is only when crystallisation is induced along an original plane that layering would appear. Thus, it is important to find the control to the initiation of crystallisation of the interstitial minerals along a plane. Since the layering and facies variations are broadly parallel to the margins of the intrusion, a control for selective crystallisation such as nucleation from the walls inward in a non-convecting magma is an obvious choice.

Although certain areas of the acicular facies develop a crude lineation due to the arfvedsonite laths, it is not well developed and a mechanism for the layering via any form of flowage differentiation (Bhattacharji and Smith, 1964) is not indicated. In any case, such a mechanism is limited to very narrow intrusions, probably of the order of less than 100 m (Barriere, 1976). Thus, cyclic layering as found in the Birji granite of the Shira complex, can probably be best explained by an oscillatory process of nucleation and crystal growth, which took place after the crystallisation of an alkali feldspar framework and which was governed by cooling from the inclined walls of the intrusion.

Thus it would appear that among granitic intrusions, two main explanations for layering have been proposed: gravity accumulation of crystals at either the base or top of an intrusion, or a type of flow or shear differentiation near the margins of an intrusion, due to deformation or movement of a crystal mush. In the Shira complex, the former hypothesis is totally rejected while the evidence for crystal lamination or mineral orientation is weak, such that a model for the layering based upon segregation of minerals by movement in a crystal mush, must therefore be insignificant.

The respective powers of nucleation of different minerals (in a basic magma) from a supercooled liquid was a mechanism favoured by Wager (1959), but in addition he suggested that they accumulated in a given order at the base of the liquid. However, for the Stillwater complex, Jackson (1961) believed that the cyclic layers could represent changing crystalline products with time (i.e. Wager's relative nucleation rates) but that sedimentation of crystals was not necessary; rather, a period of stability accompanied crystallisation which was followed by convective overturn. It has been pointed out that the liquid above a crystal cumulate should become supersaturated in those components not previously required for the cumulus minerals, resulting in a thin layer of crystals which form in situ above the cumulus pile (Kaniris- Sotiriou, 1974). That is, once a planar structure was developed, crystallisation can then occur parallel to it, but without crystal settling.

This concept has been taken a stage further by Lofgren and Donaldson (1975) to explain comb-layering; the change in modal importance from one layer to the next is ascribed to constitutional supercooling ahead of the growing crystals of any one layer. That is, when crystal 'A' grows, it accepts certain components from the liquid and rejects others; if the rate of crystal growth exceeds the rate of

diffusion of the rejected components, a boundary layer enriched in these components will form. These rejected components will modify (lower) the liquidus temperature and hence the term 'constitutional supercooling' is given. A point will ultimately be reached when the components rejected by crystal 'A' will supersaturate the boundary layer and crystal 'B' will crystallise instead. The major control for this process is believed to be the temperature gradient, and in fact, "comb layers occur preferentially near the margins of intrusive bodies, the regions most prone to supercooling" (Lofgren and Donaldson, 1975).

For some of the classic layered, basic intrusions, the concept of layering by gravitational settling of individual crystals at least, is untenable in certain instances (Campbell, 1978), and the concept of Jackson (1961) that most crystals in such intrusions grew in situ rather than settled to the bottom, has recently received enthusiastic support (McBirney and Noyes, 1979). Thus, even in basic magmas which were probably considerably less viscous than granitic ones, an alternative view of layering as being governed by the relative rates of nucleation and chemical diffusion (within the interstitial liquid) during cooling is now considered to be the dominant operative process for the production of layered rocks.

3.4 Andaburi ferrorichterite alkali feldspar granite

The Andaburi granite is a coarse grained, white or cream coloured rock in which the alkali feldspars are typically 5-8 mm long and may have a paler coloured core. Quartz is clear and glassy, and forms aggregates or chains of crystals. Amphibole occurs as black, anhedral or lath-like crystals. Dark green aegirine can sometimes be seen.

3.4.1 Microscopic description

Alkali feldspar constitutes over 60% of the rock (Table 2 and Plate 34) and occurs as crystals up to 8 mm long, but 3-5 mm is the most usual size. They are anhedral to subhedral, intergrown with one another and often have margins which are more turbid than the cores. The alkali feldspar is a microperthite but the perthitic lamellae are poorly developed in preference to the patch-perthite texture. Commonly the proportion of clear albite within the patch microperthite is sufficient to warrant the term 'antiperthite'.

Intergranular albite is only locally important on a grain-by-grain basis so that in general, intergranular albite between microperthite crystals is poorly developed. Under low power, alkali feldspar appears devoid of inclusions and it is only under high power (2-400x) that any become visible. These inclusions consist of very fine needles of blue amphibole about 40-50 microns long. Colourless needle-like inclusions with higher birefringence may be aegirine and it is possible that colourless, very low birefringent inclusions could be apatite. Dilute fluid inclusions are also visible. Structurally, the alkali feldspar is maximum microcline with triclinicity values (Goldsmith and Laves, 1953) of 0.85-0.88 (Table 31).

In contrast to other peralkaline rocks from this complex, the crystallisation of quartz does not appear to have been dominantly interstitial. In a single sample one can find evidence for alkali feldspar moulded on quartz as well as the reverse situation. A greater period of overlapping crystallisation than usual, is indicated. Quartz occurs as aggregated grains in which up to about 10 grains may be seen in any one aggregate, whose dimensions may be up to 7 mm. Component grains are anhedral or globular.

Amphibole crystals are partly interstitial, and up to 5 mm long, although 2-3 mm is more usual. They are anhedral and commonly have

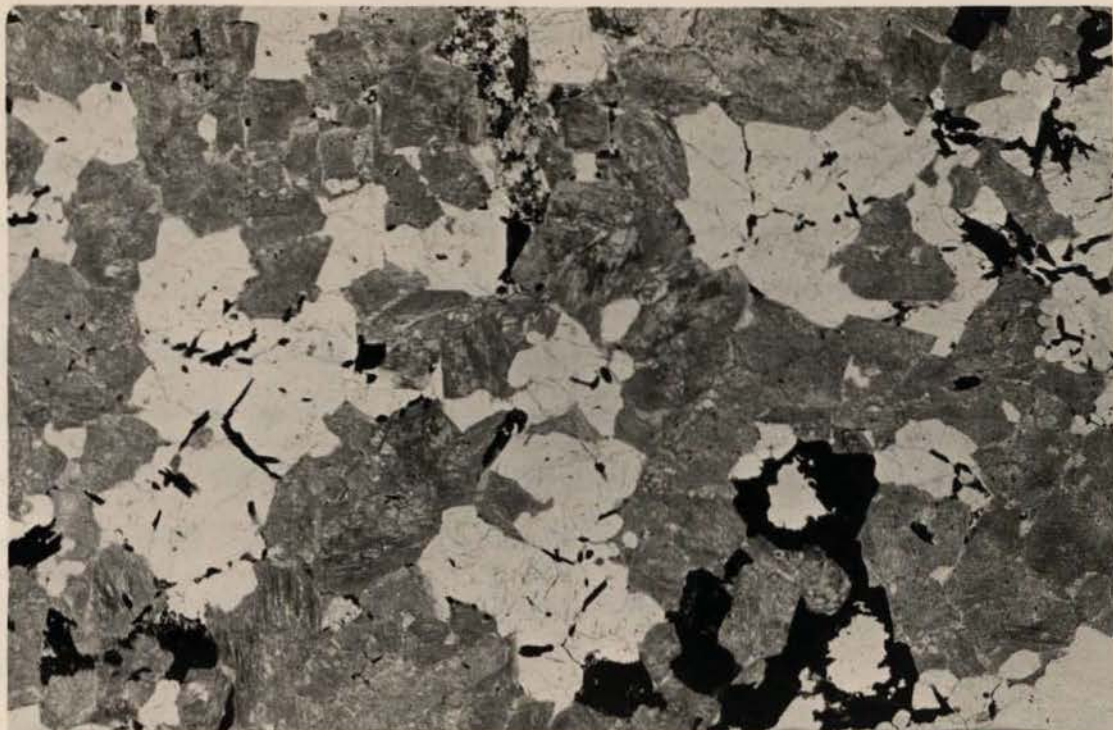


Plate 34. Texture of the Andaburi granite showing turbid alkali feldspar, aggregated quartz and interstitial amphibole. Field width 30 mm; crossed polars. (SH64)

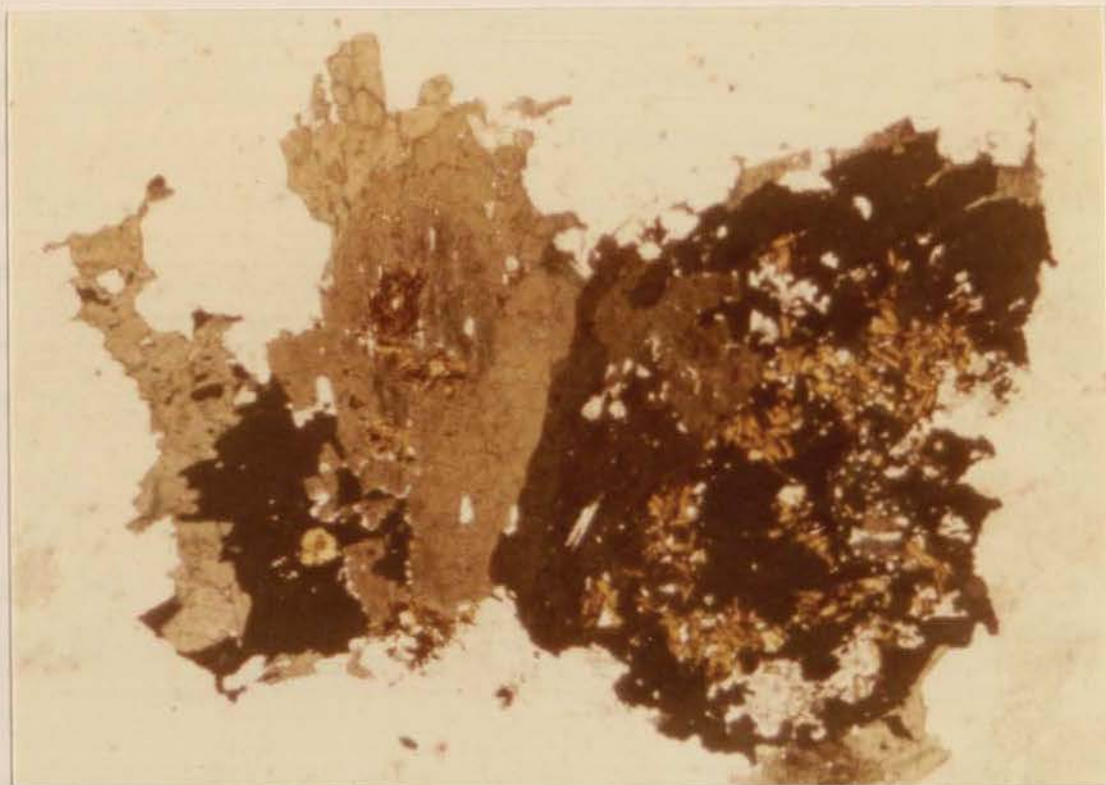


Plate 35. Localised astrophyllite replacement of arfvedsonite in the Andaburi granite. Field width 6 mm; plane light (SH54B)

an elongate shape with inclusions of alkali feldspar and small grains of apatite and Fe-Ti oxide. Crystals of amphibole may be discrete and up to several millimetres in length or occur in aggregates. Amphibole pleochroism is from a yellow-green or grey-green to a deep blue-green colour. There may be a colour zonation such that the core is less highly absorbing than the margin. Under high power (1-200x) it is common to see the margin of (and fractures within) a green amphibole coated with a narrow overgrowth of blue amphibole which replaces adjacent alkali feldspar and quartz.

In the Dutsen Gola outcrops particularly, there is a local development of astrophyllite which occurs solely within the arfvedsonite as irregularly distributed pale yellow or brown pleochroic plates. It is presumably replacing the amphibole (Plate 35).

The status of aegirine in this granite varies from an accessory to occurring in subequal quantities with amphibole. In many samples aegirine either forms discrete, anhedral to subhedral crystals and also rims amphibole, or (in other samples) shows extensive replacement of amphibole, particularly along the cleavage. Radiating laths of aegirine are sometimes encountered and may grow within amphibole or quartz. Aegirine also occurs along quartz-quartz crystal boundaries.

Globular Fe-Ti oxide (0.5 mm) and apatite (0.01-0.10 mm) occur as inclusions within amphibole. Zircon occurs sparsely, as single crystals or small groups, usually enclosed by quartz. Rarely, grains of Fe-Ti oxide have a reaction rim of brown biotite and in the Dutsen Gola area particularly, astrophyllite occurs enclosed by amphibole. Occasional small miarolitic cavities are lined with a colourless, radiating mineral which is probably a zeolite.

3.4.2 Microgranite dykes and related intrusions

Despite the superficial similarity in the field, the dark blue-grey, sparsely porphyritic microgranite dykes have two facies. Firstly, there is a sparsely porphyritic type (SH49) with a grain size of about 0.05-0.10 mm and an equigranular texture consisting of clear microperthite with well developed, parallel exsolution lamellae, quartz, anhedral crystals of arfvedsonite and some aegirine. This rock type has a very regular texture reminiscent of a metamorphic rock. The pale coloured streaks on the surface of hand specimens correspond to zones of turbidity in the feldspars and where aegirine is dominant over arfvedsonite. At locality SH48 in Jejin Dalli, the microgranite dykes are similar, although coarser grained and the alkali feldspar occasionally shows microcline twinning.

The second type (SH59/1) is much finer grained, has more mafic minerals and (still scarce) phenocrysts are slightly more abundant. The rock is dominated by small acicular crystals of aegirine about 0.04 mm long, and lesser quantities of similar sized blue arfvedsonitic amphibole needles set in a very fine grained quartzofeldspathic groundmass. Phenocrysts include euhedral crystals of alkali feldspar, quartz and deep blue-green arfvedsonite around which the matrix has eddy-like flow patterns (Plate 36). The arfvedsonite phenocrysts are fresh and unaltered; quartz may be aggregated and euhedral to subhedral or it can occur as discrete highly embayed grains. Alkali feldspar phenocrysts show signs of recrystallisation and aegirine has begun to replace them. The host granite close to the dykes shows a greater than usual abundance of aegirine relative to arfvedsonite but there is little evidence for any other change.

In addition to vertical microgranite dykes, the Andaburi granite is distinguished by granitic or pegmatitic sheets. One example, at the S end of D.Andaburi (SH55/1) is a 25 cm wide sheet which dips N



Plate 36. Eddy patterns shown by arfvedsonite and aegirine crystals in the matrix of a porphyritic microgranite dyke in the Andaburi granite.
Field width 2.4 mm; plane light. (SH59/1)



Plate 37. Stellate aegirine crystals in microgranite sheet in the Andaburi granite.
Field width 2.4 mm; plane light. (SH57/3)

at 26 degrees, and consists of fine grained (< 0.2 mm) aegirine laths, quartz and alkali feldspar which have a strongly foliated orientation. The quartz is without strain and the sheet may therefore have acquired its foliated appearance by flow. Some sheeted zones apparently represent multiple, narrow intrusions with several facies; however, all facies from one zone share a common mineralogy but exhibit different textures. At locality SH56, the most coarse grained part of the sheeted zone consists of turbid microperthite, albite, quartz and aegirine; the texture is reminiscent of that seen in the albite arfvedsonite granites of Nigeria. Both here and at the nearby SH57 locality, pegmatitic aegirine crystals have apparently grown at a late stage and contain inclusions of the other minerals. Sometimes, aegirine may occur in the form of rosettes (Plate 37).

In hand specimen however, there are numerous reddish-brown areas which in thin section compare with dark, highly turbid or brown interstices in which a low birefringent, colourless mineral sometimes occurs. In addition, there are abundant anhedral crystals and groups of slightly cloudy zircon; by comparison with the modal proportion of zircon in the Andaburi granite, it is apparent that zircon is considerably more abundant in the pegmatitic environment.

The SH58 locality is similarly banded with a lower pegmatitic zone in which up to 3 cm long mafic minerals contrast with a matrix with a graphic intergrowth of quartz and alkali feldspar. In thin section, the long mafic minerals exhibit an unusual texture in that acicular grey-blue to deep blue-green arfvedsonite has been extensively replaced by aegirine laths which sharply cross-cut the original amphibole. In the matrix, quartz and strongly antiperthitic alkali feldspar show complex intergrowth in which the K-feldspar patches are studded with birefringent aegirine crystals. Aegirine is not so abundant as in SH57. In the less coarse grained upper parts of the sheet-like intrusion, the texture and

mineralogy, in particular the abundance of discrete albite laths, once again have strong similarities to the albite arfvedsonite granites.

Finally, the greisen veins encountered close to the biotite granite consist of quartz, topaz, extremely fine grained pale green mica and fluorite. Occasional amphibole remnants from the host granite may also be found, but no alkali feldspar is preserved.

Towards the margin of the intrusion at D.Shenya, fine grained veins cut the granite; in thin section it is apparent that they are zones of cataclasis in which extremely turbid alkali feldspar is the dominant matrix mineral along with abundant quartz and small (approx. 0.04 cm) laths of pale yellow-brown to green pleochroic ferrichterite and a trace of aegirine. Commonly, slightly larger amphibole crystals are aggregated in a linear zone along with quartz. Under low power, sigmoidal amphibole-filled fractures extend from the most intensely crushed zones into adjacent 'augen' of less deformed rock. Quartz crystals show no strain.

In the host rock adjacent to the shear zone, grey or pale green to dark green amphibole shows slight oxidation to haematite and a little brown biotite. A single almost completely resorbed plagioclase crystal occurs in one thin section, and in one amphibole cluster several apatite crystals with hollow centres along half their length were observed.

3.4.3 Enclaves

At D.Shenya, several porphyritic enclaves occur. One of these (SH42/1) contains phenocrysts consisting of aggregates (up to 1 cm diameter) of anhedral to subhedral lamellar microperthite; quartz is also glomeroporphyritic but the aggregates are smaller and distinctly anhedral. The matrix consists of anhedral laths of turbid, lamellar microperthite about 0.5-0.75 mm long, intergranular quartz, anhedral

green ferrichterite and aegirine-hedenbergite, with some scattered ilmenite grains. Mineralogically it is identical to the host granite and is considered to be a cognate enclave, possibly from a chilled roof or other marginal zone. From the same exposure, an equigranular medium grained enclave is syenitic and composed of an intergrowth of turbid patch microperthite in which there are inclusions of small grains of Fe-Ti oxide (probably magnetite) often surrounded by brown biotite, aegirine-hedenbergite and pale yellow-brown or yellow-green to deep green ferrichteritic amphibole. Quartz is an accessory.

At D. Andaburi, another syenitic enclave occurs (SH57/1) which consists dominantly of alkali feldspar and aegirine with accessory quartz and alkali amphibole. Some cores to alkali feldspar contain altered and very turbid plagioclase. However the main feature of interest in the enclave is the presence of a spherulitic texture defined by radial aggregates of alkali feldspar laths. The interstices of the radial structures are filled by aegirine in which several 'arms' are in optical continuity.

In an aegirine granophyre enclave (SH47/4) only traces of alkali amphibole remain, the perthite is very turbid and intergrown with quartz and some albite, but once again a significant feature is the abundance of zircon as subhedral crystals up to 1.5 mm wide.

Another type of enclave sampled (SH44-1) is dark coloured and very fine grained. In thin section, this rock is dominated by 0.2-0.3 mm long brown biotite laths set in a matrix of only slightly turbid alkali feldspar and fluorite. Occasional groups of anhedral yellow-green to deep green ferrichteritic amphibole also occur. Also, there are prominent groups of globular, epidote crystals with unusually high birefringence indicating perhaps a high Fe content. Apatite needles and Fe-Ti oxide grains are scattered throughout, and rare, small rounded quartz crystals occur.

The mineralogy and texture of this enclave is compatible with it being a hornblende-epidote hornfels. Its origin however, is obscure as the only available country rocks in the Shira complex are enclaves themselves which consist of extremely coarse grained granite with minimal textural modification.

3.4.4 Discussion

In the Andaburi granite it is noticeable that quartz is often enclosed by alkali feldspar as well as being interstitial. This granite is also distinguished by the occasional development of aggregates of small astrophyllite and fluorite crystals enclosed by arfvedsonite. Astrophyllite is randomly orientated and is not related to cleavage direction in the arfvedsonite and therefore does not appear to be replacing the amphibole. Astrophyllite is triclinic, has a mica-type of structure and an ideal formula of $(K,Na)_3.(Fe,Mn)_7.Ti_2.Si_8.(O,OH)_{31}$ (Woodrow, 1967). However, astrophyllite from silica undersaturated rocks has higher Al, Ca, Mg, Mn, (OH+F), (K+Na) and Zr, and lower Li, Pb and Zn contents than from oversaturated rocks (Macdonald and Saunders, 1973) and therefore shows similar chemical variation to aenigmatite (Section 4.4). In fact, it has been suggested (P.Bowden, pers. comm.) that aenigmatite and astrophyllite may be antipathetic, since they are both Na, Fe, Ti minerals. While astrophyllite has not been noted in the aenigmatite-bearing rocks of this complex and aenigmatite is absent from the Andaburi granite, both minerals are entirely absent from the Birji granite and no definitive evidence can therefore be presented on this suggestion.

A similar occurrence of astrophyllite has been noted in a pegmatitic facies of the Quincy granite, Massachusetts, except that the astrophyllite was orientated parallel to the cleavage of the enclosing 'riebeckite' (Pirsson, 1910).

The Andaburi granite contains a distinctive suite of minor intrusions; the most prominent are dark blue, vertical microgranite dykes which are sparsely porphyritic (about 15% of phenocrysts of quartz, alkali feldspar and arfvedsonite). Sheet-like intrusions by contrast, are variable in texture from microgranitic to pegmatitic and there may be several facies within one sheeted zone. Whereas aegirine may coexist with arfvedsonite in the dykes and be flow oriented, aegirine commonly replaces arfvedsonite in the sheet-like intrusions. A possible link between the two types is provided by a microgranite sheet containing abundant, apparently flow orientated aegirine laths. The two types of minor intrusion have not been observed in contact and so definite age relations cannot be determined. They may therefore represent different periods of intrusion of the same residual liquid or they may have independent sources.

3.5 The Amdulayi ferrowinchite alkali feldspar syenite and quartz syenite

The Andaburi granite is intruded by three small syenitic outcrops which are discrete at the present erosional level and each of which has a different facies. It is not known whether these facies represent textural and mineralogical variations in the roof zone of a single body or whether there are two or more related intrusions. Each facies will therefore be described separately. Modal analyses of each are shown in Table 2.

3.5.1 Coarse grained ferrowinchite alkali feldspar syenite

This facies, with less than 4% quartz, is the most quartz-poor

rock found in the Shira complex. Crystals of alkali feldspar are anhedral and form an interlocking network that constitutes over 80% of the rock (Table 2). The alkali feldspar is generally turbid, has some clear cores, a poorly developed microperthitic texture and gently curving, intergrown crystal boundaries with little intergranular albite (Plate 38). Albite may be locally abundant near the margins where an antiperthitic texture may exist, but it is of exsolution rather than replacive origin. Individual grains may be up to 8 mm long. Two microprobe analyses (Table 25 and Figure 24) of clear cores to alkali feldspar crystals give K-albite (anorthoclase) compositions. An X-ray diffractogram of a feldspar separate gives a triclinicity of 0.85 (Table 31) and plots close to the maximum microcline position (Figure 25).

Amphibole occurs mainly as (up to 5 mm diameter) interstitial grains which have a yellow-brown to turquoise green or grey-green pleochroism (Plate 39). Microprobe analyses have shown that they vary in composition from ferrowinchite or ferrorichterite to arfvedsonite (Table 7 and Figure 10) and in common with the practice adopted elsewhere in this work, the amphibole is referred to generally by the least sodic composition, in this case ferrowinchite. The ferrowinchite contains anhedral inclusions of ilmenite (Plate 39) but smaller, nearly opaque zones oriented along the cleavage of some crystals have a reddish tint and are probably secondary haematite. The amphibole is also altered to aegirine to a minor extent and in some areas a grey-green to green pleochroic ferrowinchite or ferrorichteritic amphibole exists apparently as remnant islands within an aggregate of randomly oriented acicular crystals of deep blue-green arfvedsonitic amphibole.

Aenigmatite occurs as deep brown-red crystals up to 3 mm long which may be discrete and interstitial (Plate 40) or intergrown with ferrowinchite (Plate 41). Although mainly interstitial, aenigmatite may



Plate 38. Texture of the coarse grained Amdulayi syenite showing clear cores within mainly turbid alkali feldspar, and interstitial aenigmatite, ferrowinchite and quartz. Field width 30 mm; plane light. (SH51)

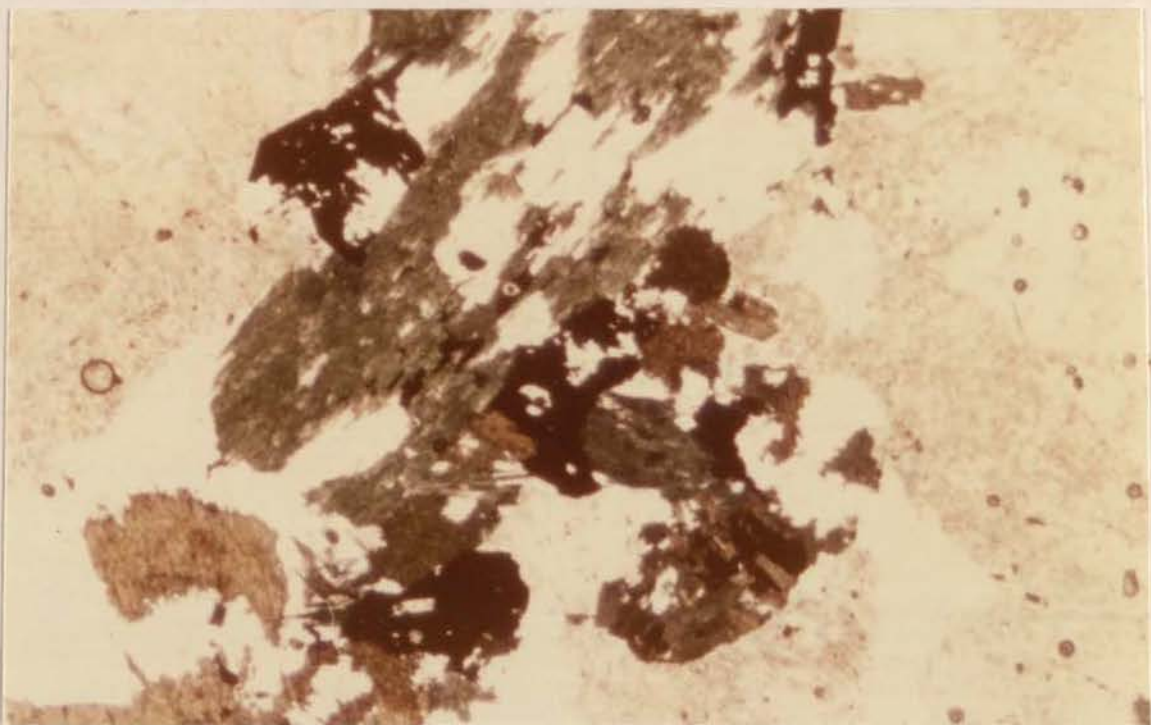


Plate 39. Intergrowth of ferrowinchite/ferrorichterite with ilmenite in the Amdulayi syenite. Clear areas within amphibole and ilmenite are holes. Field width 2.4 mm; plane light. (SH51)



Plate 40. Interstitial aenigmatite in the coarse grained Amdulayi syenite. Field width 6 mm; plane light. (SH51)

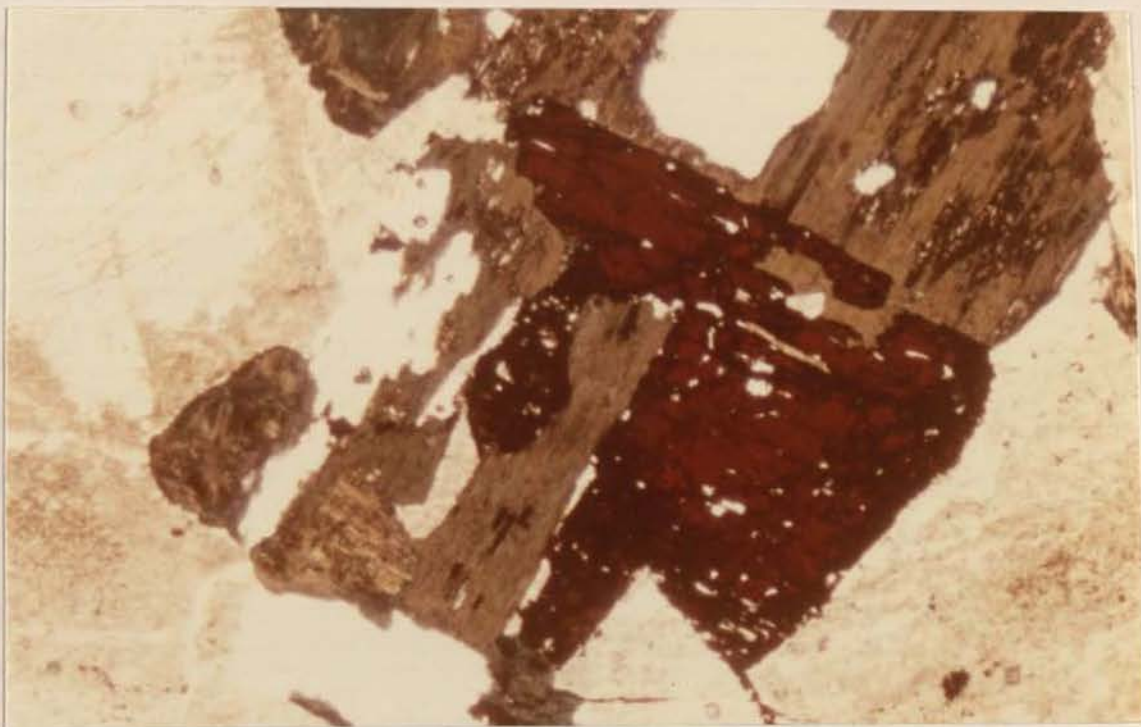


Plate 41. Intergrowth of aenigmatite and ferrowinchite/ferrorichterite in the coarse grained Amdulayi syenite. Field width 6 mm; plane light. (SH51)

show indentations which are filled by alkali feldspar in optical continuity with the crystal that aenigmatite is enclosing. Small, usually acicular quartz crystals and in one case, a zircon crystal, may be included within aenigmatite. In reflected light, some cleavages have a narrow lining of Fe-Ti oxide which has been analysed by microprobe and shown to be ilmenite (Table 23). Its mode of occurrence would suggest a secondary origin from oxidation of the aenigmatite.

Quartz occurs as comparatively rare, anhedral crystals whose shape is defined by the alkali feldspar network, but some small grains may be enclosed by ferrowinchite or aenigmatite.

3.5.2 Medium grained equigranular aegirine quartz syenite

Alkali feldspar occurs in this facies as 2.5 mm subhedral to euhedral crystals which are turbid and have a patch microperthite texture. Exsolved albite within alkali feldspar may be relatively abundant but there is little intergranular albite. The alkali feldspar crystals show very little intergrowth and they do not appear to have grown appreciably since they came into contact with one another (Plate 42). The texture is reminiscent of alkali feldspar in the Birji granite (Section 3.3). Some larger grains have clear cores where a perthitic texture cannot be seen. Alkali feldspar is flecked by small anhedral grains of haematite which probably represent the oxidised remnants of aegirine or alkali amphibole.

Aegirine is the dominant mafic mineral, occurring as anhedral to subhedral partly interstitial grains up to 1-3 mm long. Some of the larger, subhedral crystals contain an altered core that extinguishes at a larger extinction angle (up to 20 degrees) compared to the rim (0-5 degrees). A comparison of the occurrence of pyroxene in the Shira quartz syenite (Section 3.2.1) allows the inference that to a limited extent, aegirine-hedenbergite precipitated in this facies of the

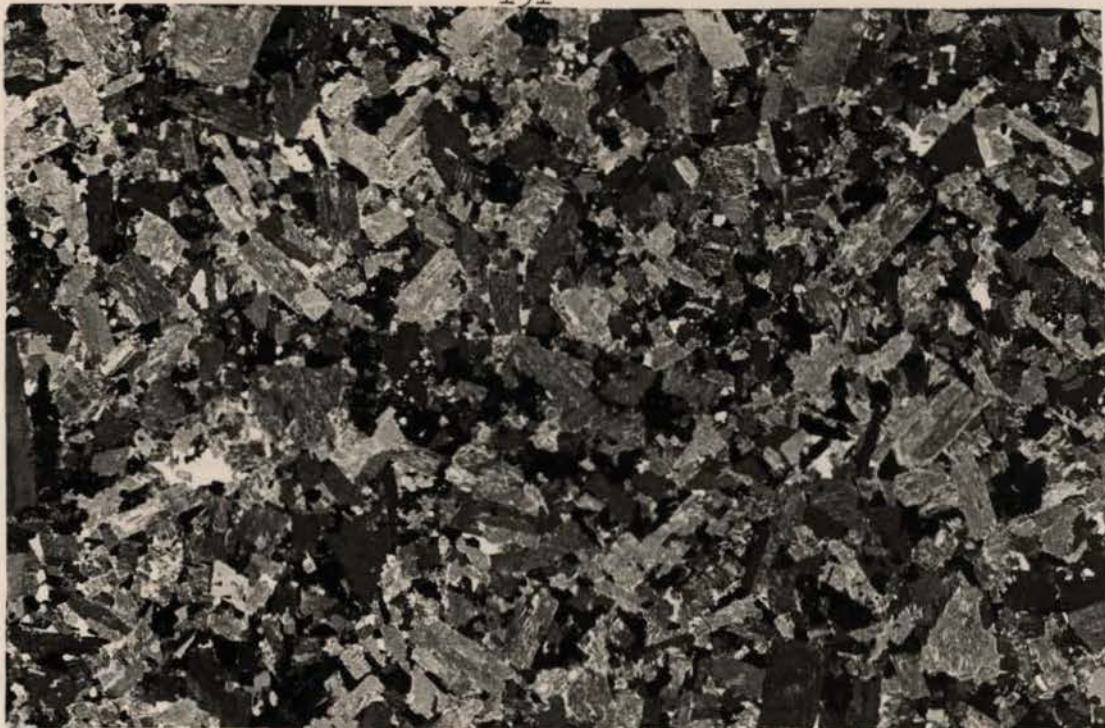


Plate 42. Texture of the equigranular facies of the Amdulayi quartz syenite showing subhedral alkali feldspar and interstitial quartz and aegirine. Field width 35 mm; crossed polars. (SH50)

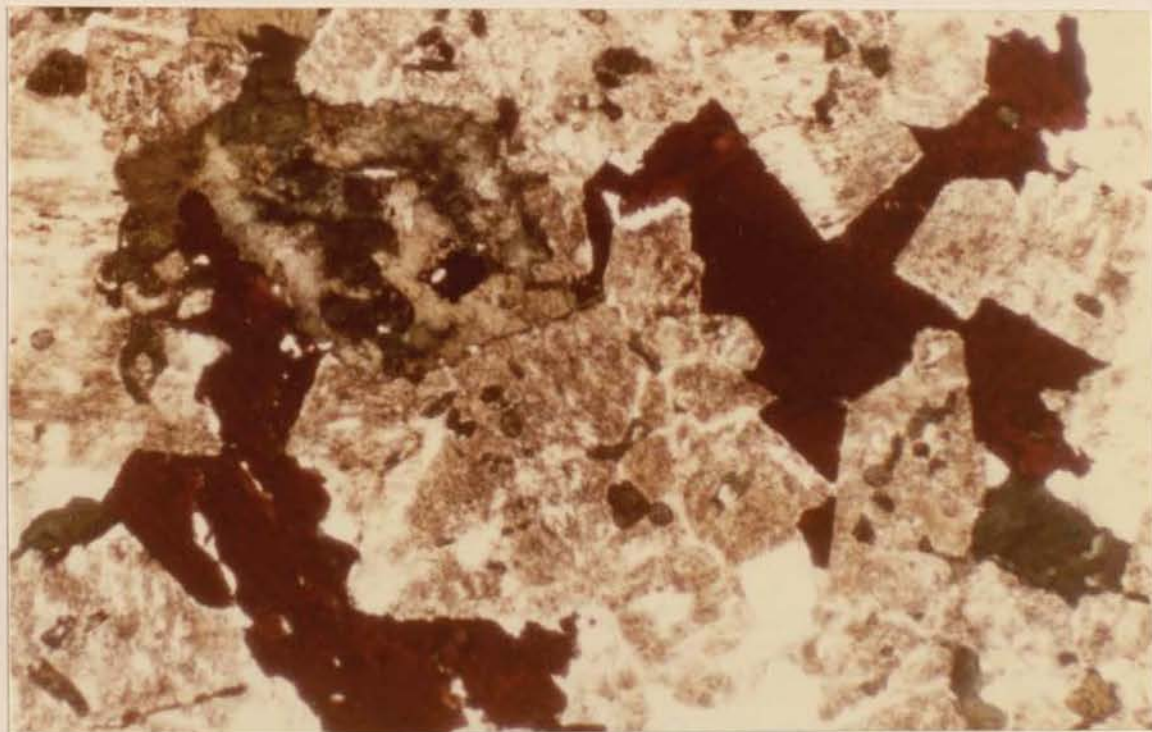


Plate 43. Interstitial aenigmatite in the porphyritic facies of the Amdulayi quartz syenite. Field width 2.4 mm; plane light. (SH25/1)

Amdulayi syenite and is represented by the partly altered, euhedral cores to aegirine crystals. Microprobe analyses of aegirine indicates that it is virtually the pure Na,Fe end-member (Table 14).

Arfvedsonitic amphibole occurs only very sparsely and is found as rare, interstitial crystals that are replaced by both aegirine and haematite along the cleavages.

Small, fine grained porphyritic, melanocratic enclaves occur in this facies in less abundance than in the porphyritic facies (Section 3.5.3), and will be described in a later section (3.5.4).

3.5.3 The porphyritic microsyenite facies

This facies is finer grained than the equigranular facies previously described, with an average grain size of a little under 1 mm.

In the matrix, alkali feldspar occurs as anhedral to subhedral turbid crystals up to 1.5 mm in size, which are intergrown with one another and which exhibit a patch microperthitic texture. Exsolved albite may sometimes give the feldspar an antiperthitic texture, but there is little or no albite along microperthite crystal margins. Interstitial areas filled by mafic minerals, are usually bounded by alkali feldspar with good crystal form. The matrix alkali feldspar contains frequent inclusions of aegirine-hedenbergite, 0.1-0.15 mm long.

The phenocrysts consist of glomeroporphyritic alkali feldspar in which individual crystals may be up to 5 mm long while the aggregate as a whole generally does not exceed 10 mm in diameter. These alkali feldspars are intergrown, clear or only very slightly turbid and without a visible perthitic texture. There is no intergranular albite. On some occasions a faint series of growth zones are visible (near the extinction position) and are distinguished by concentric zones of slightly different orientation. Towards the margins, there is an increase in turbidity and a microperthitic texture may be seen, and

small inclusions of aegirine-hedenbergite occur.

Two microprobe analyses have been made on the alkali feldspar phenocrysts and they both plot in the K- albite field of Smith (1974, Vol.2). A bulk feldspar separate has been X-rayed and it yields a comparatively low triclinicity value of 0.75 (Table 31) and plots away from the maximum microcline corner in Figure 25. It is therefore probably an intermediate microcline. Scarce altered plagioclase crystals occur enclosed by alkali feldspar and are regarded as xenocrysts derived from the small enclaves described later (Section 3.5.4).

Aenigmatite is deep brownish-red in colour, anhedral, and occurs as interstitial crystals moulded around alkali feldspar (Plate 43). Often, adjacent, apparently discrete anhedral crystals extinguish together, such that a single crystal may extend as far as 3 mm. A particular feature of aenigmatite is the near absence of included or intergrown minerals, and only rarely does one find amphibole in contact. In a few crystals, yellow-brown alteration cracks are present and in others, scarce grains of Fe-Ti oxide are enclosed; there is no indication of a reaction relationship between them.

Amphibole occurs as anhedral interstitial crystals up to 1.5 mm in diameter, with a grey to green pleochroism or it may be zoned with a yellow-brown core to a green or green-blue rim corresponding to a compositional variation from ferrorichterite towards arfvedsonite (Table 8, Figure 10). As in the coarse grained syenite, there are occasional areas where the amphibole may have recrystallised to an aggregate of small crystals which can enclose (?) ilmenite and a little fluorite. Amphibole is entirely interstitial and is not enclosed by alkali feldspar.

Pyroxene occurs as small (0.1-0.3 mm) subhedral, anhedral or rounded crystals that are mainly enclosed by alkali feldspar. It is pale green, slightly pleochroic and has an extinction angle (c-X) of up to

23 degrees. Its paragenesis, colour and extinction angle are diagnostic and it is an aegirine-hedenbergite under the classification used in the next chapter.

Quartz also occurs as anhedral, interstitial crystals which may be up to 2 mm in diameter but are usually much less. Accessory minerals include zircon and fluorite. It is occasionally possible to see small (0.5-1.0 mm) circular features which have an appearance similar to a miarolitic cavity but which contain a pale brown biotite and a pale green richterite in a zonal arrangement. These are more abundant in the enclaves however, and will be described further in the next section.

3.5.4 Enclaves

The porphyritic facies contains abundant, dark, fine grained, porphyritic enclaves which usually have a maximum diameter of 1-2 cm. In the enclaves, alkali feldspar occurs in aggregates up to 12 mm in diameter; individual crystals may be 5 mm long and are euhedral and tabular. Up to 9 crystals have been counted in a single aggregate. The alkali feldspar is largely clear and non-perthitic, although a microperthitic texture is weakly developed in some crystals. There are inclusions of apatite needles, Fe-Ti oxide, hedenbergitic pyroxene and sometimes a trace of amphibole along crystal boundaries particularly. These inclusions are commonly aligned in curvilinear trails of up to 3-5 crystals which extinguish together, and which are at a large angle to the longest margin of the feldspar. The alkali feldspar around these inclusions is slightly turbid. The enclaves also contain rare crystals of plagioclase which may be euhedral or anhedral and deeply corroded (Plate 44). Unfortunately, too few have been found to obtain an optical determination of composition. (Occasional altered plagioclase crystals found in the host rock are probably derived from these enclaves.) The plagioclase may be slightly turbid due to sericitic alteration or have



Plate 44. Partly resorbed plagioclase within an enclave in the porphyritic facies of the Amdulayi quartz syenite. Field width 2.4 mm; crossed polars. (SH25/1)

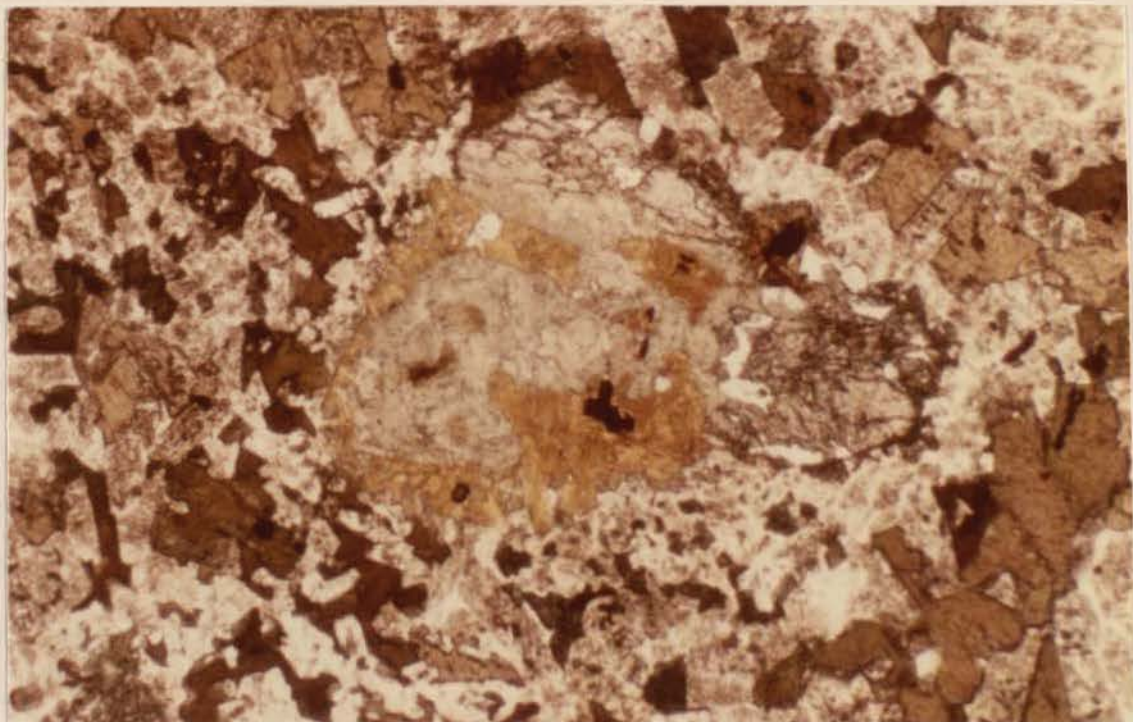


Plate 45. Ferroaugite crystal in the porphyritic facies of the Amdulayi quartz syenite, being replaced by biotite and richterite (pale green). Field width 2.4 mm; plane light. (SH25)

abundant small biotite flakes surrounding and apparently replacing it. Often, the margin is marked by a concentration of small hedenbergitic pyroxenes and the whole enclosed by a narrow rim of microperthite.

Small (usually less than 1 mm but occasionally up to 3 mm) zoned bodies are sometimes seen, which consist of an outer zone of pale brown (Mg-rich) biotite and a pale green richteritic amphibole in the centre (Tables 8 and 21). Ilmenite may occur within either phase. Although these features (which superficially resemble miarolitic cavities) are found in the host rock, their true nature as pseudomorphs is mainly revealed in the enclaves. Here, it is often possible to see an intermediate stage such that a rounded, colourless pyroxene crystal is partly altered to biotite, ilmenite and richterite (Plate 45). One pair of relatively unaltered globular (?)ferroaugite crystals is associated with magnetite which has a rim of dark brown biotite and coarse apatite crystals.

The matrix of the enclaves is extremely fine grained (around 30-50 microns) and consists of anhedral or globular grains of Fe-Ti oxide, apatite, pale green elongate hedenbergitic pyroxene and anhedral brown-green amphibole which are set in a clear alkali feldspar matrix in which a perthitic texture is only rarely seen. The pyroxene has been analysed by microprobe and the core regions are of ferroaugite/ferrosalite composition (Table 14, Figure 15). The matrix is extremely mafic-rich and contains perhaps 40% mafic minerals. Close to the margin of the alkali feldspar phenocrysts the mafic minerals of the matrix are smaller than usual and are enclosed by alkali feldspar of the matrix which has grown in optical continuity with the phenocryst.

3.5.5 Syenitic veins in the Andaburi granite

Narrow (2-5 cm) syenitic veins are common in the Andaburi granite and consist of two types. The first (SH25/2) is a quartz syenite

which is so similar to the equigranular facies of the Amdulayi quartz syenite that a separate description is unwarranted. It is however, slightly coarser grained. The second type of dyke (SH25/3) is aenigmatite-bearing but is not obviously directly related to either of the major syenitic phases. Alkali feldspar is the dominant mineral and occurs in the form of 1-2 mm intergrown often tabular, subhedral twinned laths which are mainly clear but have turbid patches and fractures. Perthitic texture is poorly developed in the larger grains and occurs preferentially in small grains or along the margins of larger crystals. Intergranular albite is rare.

Quartz occurs interstitially to alkali feldspar as small (up to 0.3 mm) rounded anhedral to subhedral grains.

Aegirine or aegirine-hedenbergite occurs in the interstices as anhedral grains up to 0.75 mm across. Extinction angles (c-X) of up to 17 degrees have been measured and the pyroxene may be moulded on aenigmatite or be intergrown with amphibole. Amphibole itself has a similar mode of occurrence as anhedral, interstitial grains which are arfvedsonitic with grey to deep blue-green pleochroism.

Aenigmatite is unusual in that it occurs as comparatively well formed subhedral, elongate crystals that are not obviously interstitial - its usual mode of occurrence. Commonly it is enclosed by aegirine.

3.5.6 Discussion

In the coarse grained alkali feldspar syenite, there is a virtual absence of any pyroxene except as slight alteration along amphibole cleavages. It is also unusual to find traces of haematite along amphibole cleavages and it appears likely that this is a weathering effect only. The ilmenite lined fractures or cleavages in aenigmatite may be similarly ascribed to the same near-surface oxidation conditions rather than to conditions that prevailed during

crystallisation. In this respect it may be significant that in the Nigerian province, syenitic rocks are commonly among the most deeply weathered and difficult to obtain fresh. Among interstitial amphibole it is noticeable that certain areas are characterised by aggregates of smaller blue crystals, possibly indicative of recrystallisation.

In the equigranular facies, unlike the coarse grained syenite or the porphyritic facies, alkali feldspar has a texture similar to the Birji facies where crystals are tabular and subhedral, with very little intergrowth. Pyroxene crystals are sometimes zoned with aegirine-hedenbergite cores to aegirine rims; there is a fairly abrupt transition from one to the other and although only a little arfvedsonitic amphibole remains (since it is heavily altered to aegirine), it is perhaps sufficient to suggest that there could have been an amphibole crystallisation period after aegirine-hedenbergite, in a similar manner to that in the Shira quartz syenite. Some small enclaves are found in this facies but although they are not as abundant as in the porphyritic facies, their presence is an important petrographic similarity despite for example, the difference in habit of alkali feldspar.

The porphyritic facies is characterised by synneusis of alkali feldspar phenocrysts in a microsyenite matrix, and abundant porphyritic, syenitic enclaves. In these enclaves, phenocrysts of clear (but usually altered) pyroxene are set in a matrix carrying plagioclase and abundant green ferroaugite to hedenbergitic pyroxene. Where similar plagioclase and phenocrystal pyroxene crystals occur in the host rock they are assumed to have been derived from these enclaves. Although the exact composition of the large pyroxenes is not known, it may be inferred from the fact that the biotite/richterite pseudomorphs are highly magnesian. This, together with the colour difference between the (analysed) ferroaugite/hedenbergite crystals in the matrix, strongly points to an

augitic composition.

The porphyritic and equigranular facies are related by virtue of the enclaves but the texture of all three facies is so different that it would be difficult (but not impossible) to relate them by textural variation across the roof zone of one particular body. However, geochemically the three facies are very similar (Table 26).

3.6 Eldewo biotite alkali feldspar granite

Due to the scarcity of exposure of the biotite granite, the following petrographic description is based upon outcrops which occur near the centre of the intrusion and which are assumed to be the most representative. However, towards the margins, there are important textural variants which will be described individually.

3.6.1 Coarse grained facies

This facies occurs close to Eldewo (SH21) near the centre of the biotite granite. In hand specimen, the coarse grained facies contains cream coloured alkali feldspar which often has pale brown margins and cleavage surfaces. Quartz is aggregated and biotite may have small red haematite patches associated with it.

In thin section, alkali feldspar is the dominant mineral (Plate 46), constituting over 60% of the rock (Table 2), and is composed of a turbid microperthite with a regular lamellar texture which is only slightly disturbed by the development of a patchy texture. The grain size varies between about 3 and 8 mm. There is only a limited amount of intergranular albite between the microperthite crystals (Plate 46). No microprobe analyses have been made, but from the relatively low

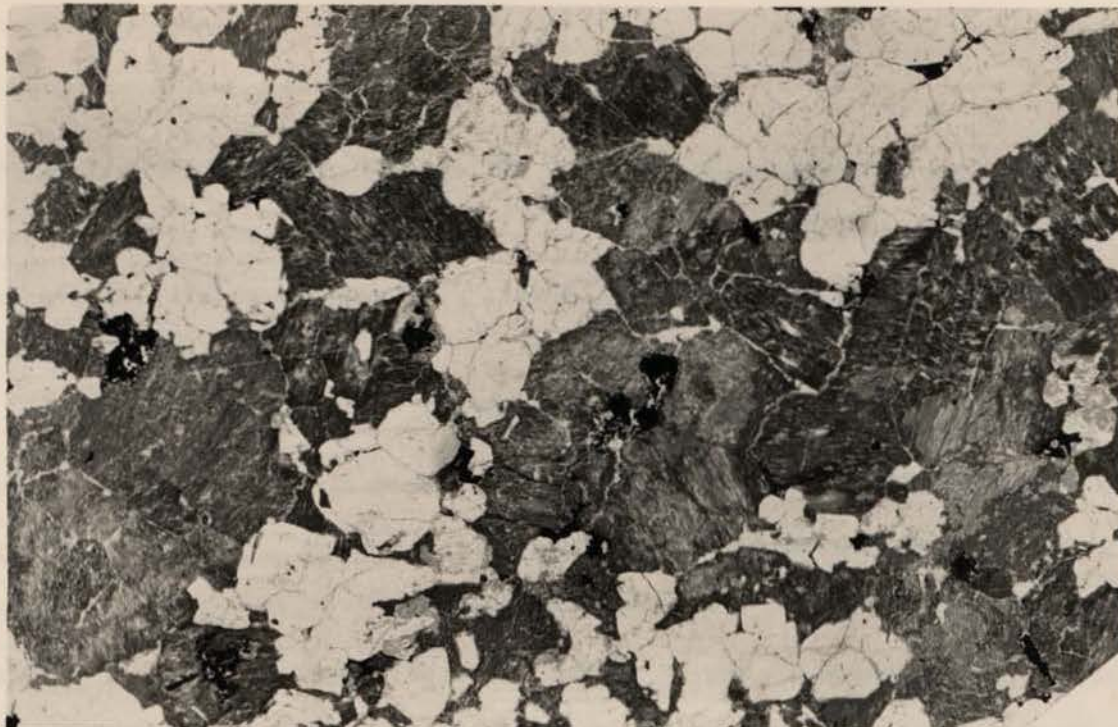


Plate 46. Texture of the coarse grained Eldewo biotite granite.
Field width 30 mm; plane light. (SH21)

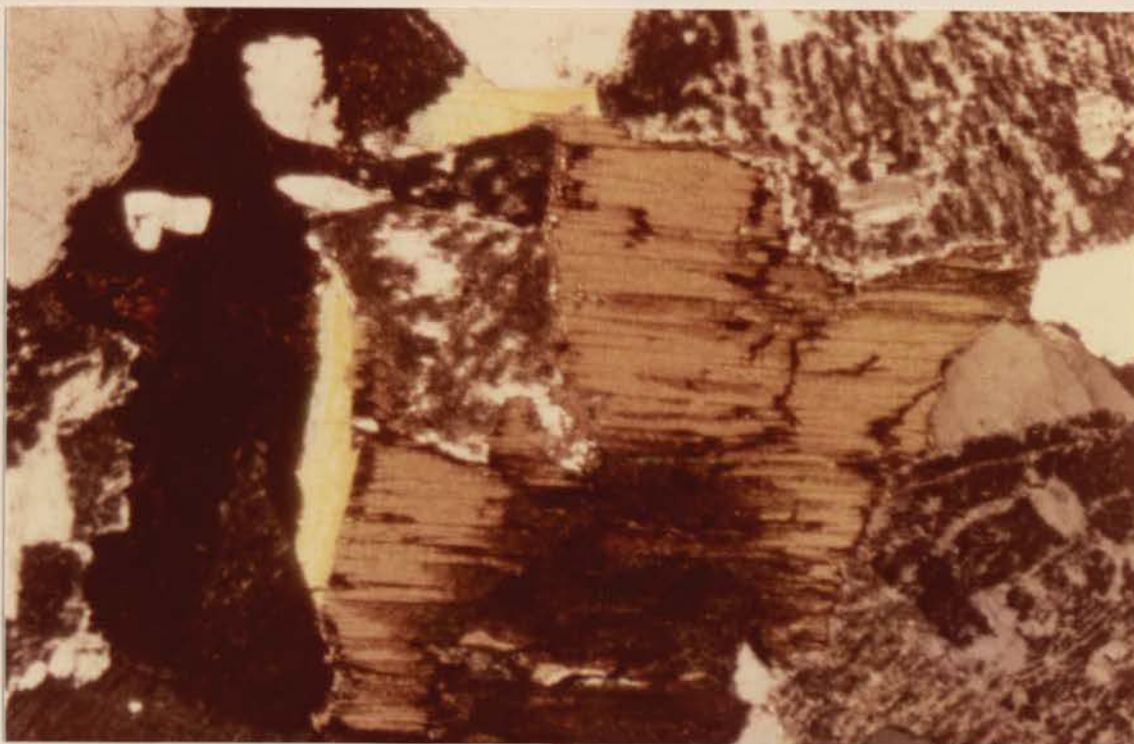


Plate 47. Zinnwaldite overgrowth around brown annitic
biotite, Eldewo biotite granite.
Field width 5 mm; crossed polars. (SH21)

proportion of clear albite lamellae in the microperthite it is probably more potassic than the majority of alkali feldspar so far described. It has a triclinicity of only 0.79 (Table 31) but it plots close to maximum microcline (Figure 25).

Quartz occurs as globular crystals which are aggregated into groups or chains up to 8 mm in diameter and which are usually enclosed by alkali feldspar. In contrast to the dominantly interstitial nature of quartz in the peralkaline granites and syenites, quartz in the biotite facies has crystallised earlier and it is not an interstitial phase. Commonly, embayments in a single crystal or junctions between quartz crystals are filled by microperthite. One crystal which was oriented normal to the 'c' axis showed an embayed, partially hexagonal outline indicating that it was free to grow in the liquid. Under high power, the quartz also shows two features which are in fact typical of all quartz grains from this complex (and indeed in granitic rocks elsewhere in the province): firstly, the presence of numerous domains within a single crystal and secondly, large numbers of randomly oriented, dilute, two-phase fluid inclusions. These inclusions are only a few microns across and are not related to fractures and do not appear to contain any daughter salts; the vapour bubble occupies only a relatively small part of the whole inclusion.

Biotite occurs as dominantly interstitial crystals which may be found as relatively large, discrete anhedral flakes up to 4 mm across or as aggregates of small crystals. It is annitic in composition (Table 21) and has a deep brown maximum absorption colour. Some of the cleavages are lined with an opaque or reddish material indicative of (?surface) oxidation to haematite. In the interstitial aggregates, biotite is moulded around quartz, globular magnetite (Table 23), and a little fluorite and zircon. The magnetite appears to be a primary accessory phase which crystallised before biotite and there is no sign

of reaction between the two phases. However, the interstitial occurrence of magnetite is notable since it is not found as inclusions in quartz or alkali feldspar, although in rare cases, individual magnetite or biotite crystals occur along microperthite grain boundaries. In some sections, a network of fine haematite veinlets radiate from around a biotite crystal or aggregate, although there is not necessarily any alteration visible in the biotite. Very occasionally the margin of a biotite shows an overgrowth of dark green mica which, in one instance, shows very clearly that it has selectively replaced the potassic component of the surrounding microperthite. Curiously, the overgrowth consists of narrow filaments which traverse an albitic zone close to the mica and then widen out into flakes the width of the potassic lamellae in the microperthite. In general though, mica overgrowths are better shown in the medium grained facies, but clearly it is a feature which post-dates exsolution of the alkali feldspar.

Biotite from this facies also exhibits a further type of overgrowth where a more or less even rim of clear zinnwaldite (Table 21) partially or completely encloses a brown biotite (Plate 47). The junction between the zinnwaldite and biotite is very sharp and there is no alteration of the latter. The width of the zinnwaldite overgrowth is relatively constant and it does not replace any adjacent mineral. It therefore appears to have grown freely into a void which is further enhanced by the fact that in two instances, a haematite filled cavity occurs alongside it (dark area on the left of Plate 47).

3.6.2 Medium grained biotite granite

In general, the medium grained biotite granite can be taken to include all other outcrops of the biotite granite which are finer grained than the Eldewo facies just described. However, it is perhaps better to consider one example of particular interest and then briefly

to examine samples from elsewhere in the granite.

The medium grained facies which occurs at locality SH47 (Plate 48) is modally indistinguishable from the coarse grained facies (Table 2) and as it occurs immediately beneath the Andaburi granite, it is probably a chilled facies. The adjacent Andaburi granite contains several thin greisen veins which consist of quartz, aggregates of green siderophyllitic mica (X = colourless, Z = pale grass green), some highly altered feldspar, topaz and a little fluorite and malacon (isotropic zircon).

Alkali feldspar of sample SH47 is a turbid, intergrown microperthite which has perhaps slightly more intergranular albite but otherwise is virtually identical to that in the coarse grained facies. The habit of quartz is also similar. Biotite in this facies has a slightly different colour and its maximum absorption colour (Z) is green-brown. Green filamentous overgrowths to the biotite are more abundant too (Plate 49), but in aggregates or single crystals it is obvious that enclosed grains of magnetite are very rare and fluorite has not been observed. Zircon is found along microperthite grain boundaries or enclosed within the mica. Microprobe analyses of the biotite (Table 21, Figure 22) show that, as expected from the colour difference, it has a slightly different composition from the coarser facies and is more Fe-rich.

3.6.3 Other exposures

At locality SH63 along the northern edge of the intrusion, the biotite granite is not quite as coarse grained as SH21 but it is very similar except that no zinnwaldite overgrowths have been found. Within a few hundred metres however, the granite is granophyric (SH63/2); a granophyric intergrowth of quartz and turbid alkali feldspar may extend outward from an alkali feldspar or quartz phenocryst and there are

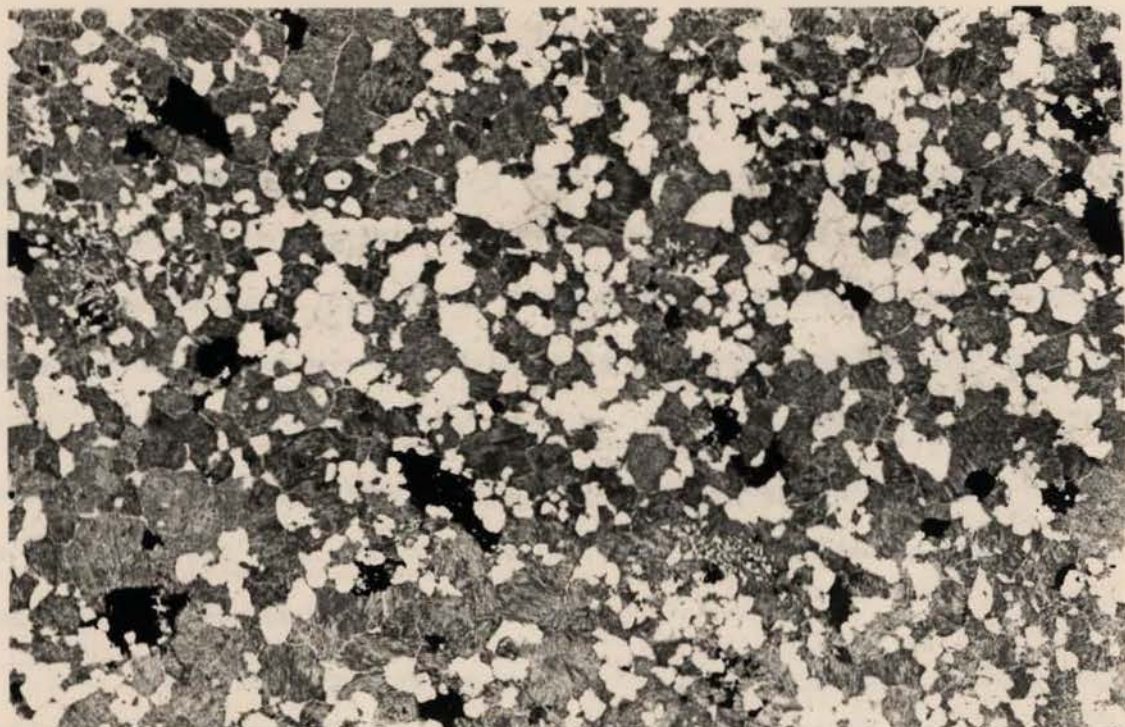


Plate 48. Texture of the medium grained facies of the Eldewo biotite granite.
Field width 30 mm; plane light. (SH47/6)

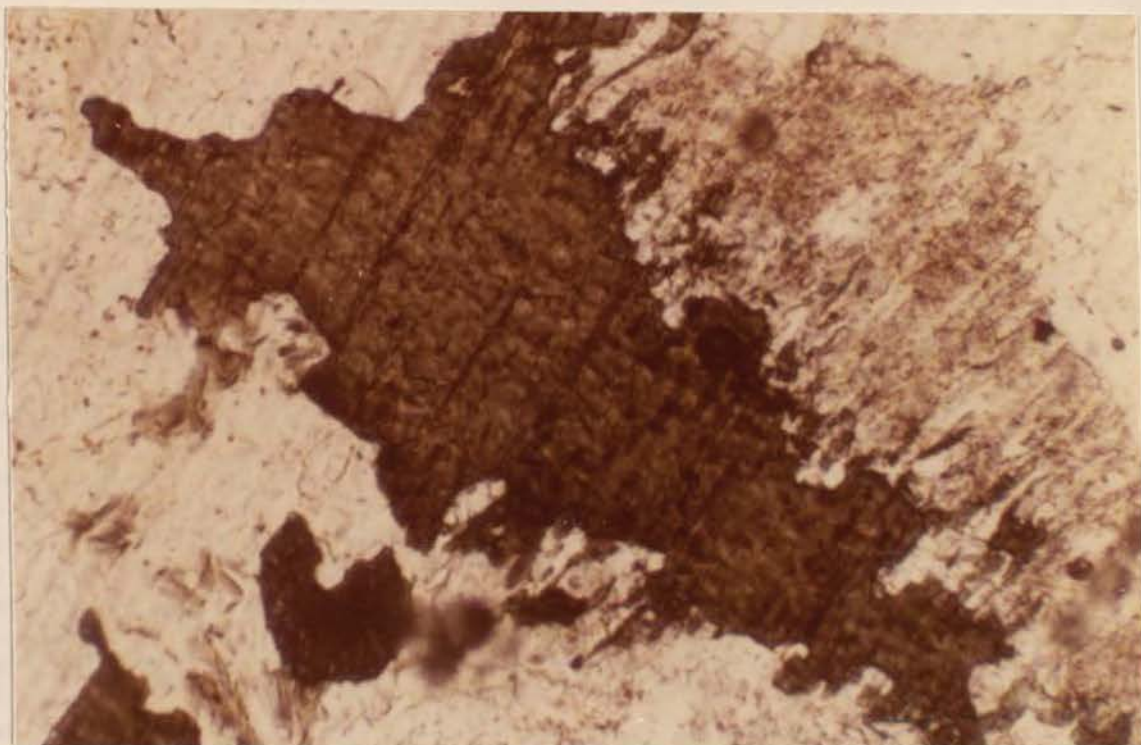


Plate 49. Green, filamentous overgrowths to annitic biotite in the Eldewo biotite granite.
Field width 2.4 mm; plane light. (SH47/6)

frequent inclusions of quartz in alkali feldspar. The biotite is highly absorbing with Z = very dark brown and X = light yellow-brown, rather than straw coloured. Biotite is associated with magnetite and fluorite. These two localities are also notable in containing an aegirine granite sheet and an arfvedsonitic granite sheet respectively. (Neither intrusion can be positively correlated with the Andaburi granite, but it is possible that they are related to the same suite of sheet-like intrusions which cut that granite also.)

The north-western outcrops of biotite granite occur to the north (SH66) and south (SH67) of Gwanawa village; both outcrops are deep pink in colour, medium grained and granophyric. In the case of SH66, all but a small trace of the biotite (and magnetite?) has been converted to haematite. Sample SH67 has a more prominent granophyric texture and contains a little more mica, the majority of which has been chloritised.

Towards the southern margin an isolated outcrop near Jan Dutse consists of highly altered biotite granite. In hand specimen, one sample (SH107/1) consists of quartz, aggregates of Fe-Ti oxide and a white (?) clay. In thin section there are numerous holes representing the clay, and aggregates or wisps of Fe-Ti oxide (?haematite). Often, the trails of opaque oxide are arranged in such a way that two outer edges are parallel to one another, strongly suggestive of mica pseudomorphs. The remainder of the rock consists of quartz with a grain size up to 2.5 mm in diameter. The grain boundaries are smooth and curving, often meeting at triple junctions and it is most noticeable that there are no domains within the quartz as is so typical of quartz in Younger Granites as a whole. The other sample collected (SH107/2) gives its name to the village (Jan Dutse = red rock) since it is an altered granite with brick-red alkali feldspar. In thin section, the alkali feldspar is more turbid than usual, but not coloured. However, in some places, the feldspar becomes nearly black due to a concentration of very fine

granules of opaque oxide. The red colour is therefore probably due to finely disseminated haematite.

In plane light the alkali feldspar has a lamellar microperthite pattern but in crossed polars is mottled, and no albitic component is visible. The granitic texture is preserved but once again, quartz shows none of the usual domain structure.

Mafic mineral aggregates up to 7 mm across are represented by pseudomorphing haematite; this haematite is heavily plucked in section but it is obvious that the original mafic mineral was either platy or acicular.

3.6.4 Discussion

The scarcity of exposure is not conducive to an intensive petrographic study but a number of interesting features emerge. The Eldewo biotite granite lacks plagioclase and may therefore be considered a hypersolvus biotite granite. In contrast to the peralkaline granites and syenites, quartz crystallises relatively early and is enclosed by alkali feldspar rather than being interstitial. The alkali feldspar is a lamellar microperthite with only a poor development of a patchy texture or intergranular albite, and is an intermediate or maximum microcline. In the centre of the intrusion the granite is coarse grained while towards the margins it is medium grained and equigranular or porphyritic and granophyric. These features are probably a function of the cooling rate and water content involving fairly rapid and simultaneous crystallisation of quartz and alkali feldspar which had a relatively high nucleation density. In the coarse grained granite, the biotite is deep brown and associated with magnetite and fluorite in interstitial areas. The biotite has experienced a second phase of growth (with or without simultaneous alteration itself) probably below the solidus, whereby green siderophyllitic mica filaments or a clear zinnwalditic

overgrowth may form. There is no evidence relating the relative age of the these two features, but in the former case, adjacent alkali feldspar is replaced whereas zinnwaldite appears to have grown unimpeded into a cavity. This cavity is also occupied by haematite and since the biotite in the coarse grained facies (SH21) is poorer in Fe than the medium grained facies (SH47/6) it is possible that there has been some leaching of Fe from biotite at the time of zinnwaldite formation. It is probable that the space in which the narrow zinnwaldite mantle formed was a miarolitic cavity.

Along the southern margins, in addition to textural modifications affecting quartz and alkali feldspar, biotite is often absent and pseudomorphed by haematite. Along the S margin, there is evidence for microclinisation of alkali feldspar and haematitisation of alkali feldspar and biotite, or alternatively, silicification and kaolinisation. In these altered rocks, the quartz has apparently recrystallised and shows none of the usual pattern of sub-grains within one crystal. The latter features are very similar to the 'reddened' granite associated with a mineralised lode from Ririwai (Jacobson and Macleod, 1977). Such alteration at the margins of a biotite may therefore be attributed to locally intense action of hydrothermal fluids. However, it should be noted that with the occurrence of only a few very narrow greisen veins in addition to marginal silicification and haematitisation, and only moderate postmagmatic changes occurring in the body of the granite, it cannot be regarded as having any economic potential.

3.7 Miscellaneous rock types

3.7.1 Yana agglomerate

This rock occurs as a low ridge near Yana and has a rubbly surface composed of rounded pebbles or clasts. The clasts contain rounded and angular fragments of quartz with a range of grain size up to about 0.5 mm (see Plate 50). There are no feldspar crystals of similar size, since feldspar appears to be confined to the very fine grained quartzofeldspathic groundmass only. The matrix is crudely laminated by virtue of trails of opaque oxide grains which are sinuous but run sub-parallel to one another, sometimes joining up with a larger grain. Small (1-2 mm) clasts of altered, pre-existing rock occur; judging by the relative abundance of Fe-Ti oxide in these small clasts, the original rock would have been mafic-rich.

3.7.2 Chida porphyritic granophyre

This rock occurs as deep pink coloured boulders a few hundred metres east of the Yana agglomerate. The granophyric texture is visible in hand specimen and is well displayed in thin section. Alkali feldspar is turbid and occurs as anhedral or subhedral crystals which may be aggregated into groups up to 10 mm wide. It displays only very faint lamellar texture and no intergranular albite is present. Quartz is found as up to 3.5 mm diameter globular crystals which are discrete rather than aggregated and they may be embayed, the embayments being filled by alkali feldspar.

Both quartz and alkali feldspar crystals may act as foci for the crystallisation of the granophyric matrix (as indicated in Plate 51) when the grain size of the granophyre increases away from the phenocryst. Ferrichteritic amphibole occurs as elongate crystals either alone or in groups associated with anhedral Fe-Ti oxide and euhedral zircon. The porphyritic granophyre therefore has peralkaline



Plate 50. Fragmental texture of the Yana agglomerate.
Field width 2.4 mm; crossed polars. (SH85)

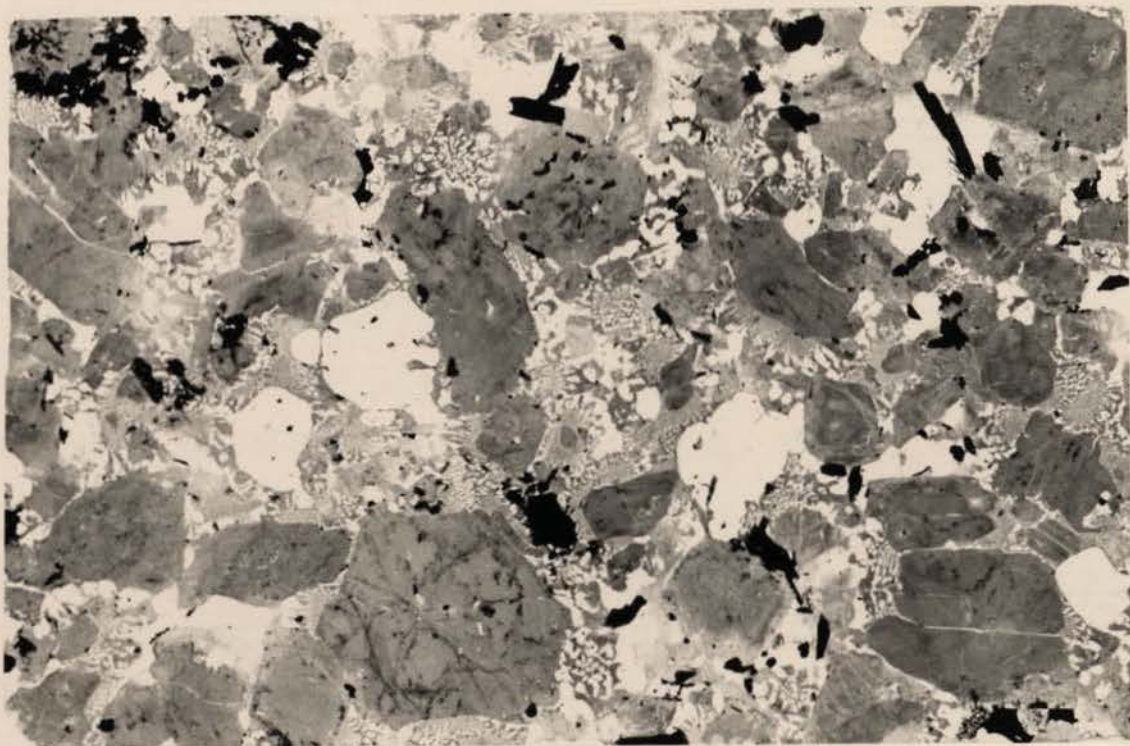


Plate 51. Texture of the Chida porphyritic granophyre.
Field width 30 mm; plane light. (SH84)

CHAPTER 4

4.1 Amphibole

Tables 3 to 8 contain 132 microprobe analyses of amphiboles from all the amphibole-bearing rocks in the Shira complex, together with

MINERAL CHEMISTRY4.1 Introduction

The object of this chapter is to define chemically the majority of minerals that have been described in the previous chapter, to investigate the chemical variation within distinct mineral species and to interpret the observed mineral chemistry as far as possible, in terms of the conditions of crystallisation of the magmas. A microscan V electron microprobe has been used to analyse the following minerals: amphibole, pyroxene, aenigmatite, chevkinite, narsarsukite, biotite, fayalite, Fe-Ti oxides, and alkali and plagioclase feldspar. In addition, a single pegmatitic arfvedsonite has been separated and analysed by classical means in order to provide accurate values for one specimen at least, of ferric and ferrous iron, Li, F, Cl and H₂O⁺. The analytical data together with structural formulae are presented, and in the case of the major mineral groups found in the Shira complex - amphiboles and pyroxenes, the analyses have been recalculated to include estimates of the ferric and ferrous iron contents.

Previous work on the chemistry of minerals from peralkaline rocks in the Younger Granite province is limited to classical analyses of mafic mineral separates (Borley, 1963a, 1963b). Therefore no information presently exists on mineral zoning, accessory minerals or alkali feldspars, and there is only a single analysis of an aenigmatite (Borley, 1976a).

This chapter deals primarily with the mineral chemistry of the mafic silicates of the peralkaline rocks (that is, amphibole, pyroxene and aenigmatite), approximately in order of their modal importance, then with biotite, fayalite, the accessories and the feldspars.

4.2 Amphibole

Tables 3 to 8 contain 132 microprobe analyses of amphiboles from all the amphibole bearing rocks in the Shira complex, together with structural formulae calculated on the anhydrous basis of 23 oxygens. Spot numbers AM1-79 represent analyses made using a wavelength dispersive spectrometer (WDS) which detected F, Zn and Zr in many cases; spot numbers AM100-156 are analyses made with an energy dispersive spectrometer (EDS) which was not sensitive enough to determine these elements in the quantities found in the Shira amphiboles (or in the case of F, EDS does not respond to the relatively long wavelengths). Calculation of the structural formulae of sodic amphiboles is a complex subject and is discussed in Appendix 3. It is sufficient to note here, however, that alkali amphiboles may not be stoichiometric and since this is an inherent assumption in the calculation of any structural formula, it represents a possible cause of the apparently low proportion of calculated ferric iron; consequently the other cations are believed to be slightly high. The requirement for a calculated ferric iron content is particularly important within the alkali amphibole group since the $Fe(3+)/Fe(3+)+Al$ ratio is necessary to accurately name the amphibole (Leake, 1978). In many microprobe analyses of arfvedsonite presented here, no Fe^{3+} has been calculated and the amphibole could therefore be classified as ferroeckermannite. However, this would imply an ideal Al:Si ratio of 1:7, whereas the Al content of the Shira amphiboles is generally extremely low and clearly ferroeckermannite is not present. Moreover, published wet chemical analyses of alkali amphiboles from Nigeria (Borley, 1963b) show high $Fe(3+)/Fe(3+)+Al$ ratios and the same is true for a pegmatitic arfvedsonite from the Birji granite (Appendix 3).

Problems related to non-stoichiometry and low calculated Fe^{3+} contents may also be largely responsible for the fact that many analyses

plot in a theoretically impossible region (e.g. Figure 11) where the B+A sites contain more than 3 cations. However, even where Fe³⁺ and Fe²⁺ have been determined separately, an excess of alkalis may still occur (Figure 11, Borley's data).

As over 90% of the amphibole analyses from the Shira complex are ferrichterites or arfvedsonites for which the dominant substitution is Na for Ca, it is most convenient to represent the amphibole compositions by means of Ca-alkalis diagrams as in Figures 6 to 11. Also, the end-members ferrowinchite, ferrichterite, riebeckite and arfvedsonite are easily shown on this type of diagram. Some authors use Si+Na+K along the abscissa (usually only where they wish to show subalkaline or aluminous compositions on the same diagram), but since Si is close to 8 cations in the amphiboles discussed here, it can be ignored for present purposes.

Figure 11 is a summary diagram on which all analysed amphiboles from the Shira complex have been plotted. This diagram shows effectively that the dominant compositional variation in the Shira amphiboles is from ferrichterite to arfvedsonite, with a subsidiary variation from ferrowinchite to arfvedsonite. Other data for Nigerian amphiboles (Borley, 1963b) display a trend along the ferrowinchite-arfvedsonite join, similar to some of the Shira amphiboles (Figure 38). Perhaps the most significant feature of both Figures 11 and 38, in view of the existing nomenclature of Nigerian alkali amphiboles (i.e. riebeckite and riebeckitic arfvedsonite), is the large vacant area around the riebeckite end-member. In fact, only one analysis from Shira is classified as a riebeckite (AM38) and that is a calcian variety.

In the Zigau granite porphyry, analyses AM112-113 (Table 3) are calcic amphiboles since their Na(B) contents are slightly less than 0.67 (Leake, 1978). Neighbouring crystals (AM114-117) have Na(B) contents slightly greater than this threshold and are therefore

Table 3 Electron microprobe analyses of amphiboles from the Zigau granite porphyry

Sample no.	ZG/2B			ZG/2D				
	1	2	3	4	5	6	7	
Crystal no.								
Spot no.	AM19	AM155	AM156	AM112 core	AM113 margin	AM114	AM116	AM117
SiO ₂	47.23	49.89	51.04	48.55	47.86	48.47	47.91	48.14
TiO ₂	2.16	0.60	0.28	1.49	1.66	1.50	1.80	1.55
Al ₂ O ₃	1.01	0.67	0.53	1.41	1.70	1.46	1.75	1.76
FeO _T	34.95	35.75	35.66	32.24	32.27	32.31	32.39	32.06
MnO	0.77	0.84	1.10	0.57	0.72	0.51	0.58	0.55
MgO	0.20	0.00	0.00	3.63	2.83	3.01	2.71	2.81
CaO	3.80	3.18	0.76	6.03	6.44	5.79	5.94	6.12
Na ₂ O	5.77	6.88	8.36	4.87	4.26	5.16	5.01	4.63
K ₂ O	1.33	1.41	1.09	1.15	1.19	1.10	1.17	1.22
ZnO	0.10	-	-	-	-	-	-	-
F	0.86	-	-	-	-	-	-	-
Cl	0.07	0.00	0.07	0.12	0.13	0.00	0.13	0.13
less O=F,Cl	0.38	-	0.02	0.03	0.03	-	0.03	0.03
	<u>97.87</u>	<u>99.22</u>	<u>98.87</u>	<u>100.03</u>	<u>99.03</u>	<u>99.31</u>	<u>99.34</u>	<u>98.94</u>
Fe ₂ O ₃ ^c	-	-	6.89	-	-	-	-	-
FeO	-	-	29.46	-	-	-	-	-
Formulae on the anhydrous basis of 23 oxygens								
Si	7.749	7.999	8.019	7.617	7.601	7.655	7.589	7.635
Al ^[IV]	0.195	0.001	-	0.261	0.318	0.272	0.327	0.329
Fe ³	-	-	-	-	-	-	-	-
Σ T	<u>7.944</u>	<u>8.000</u>	<u>8.019</u>	<u>7.878</u>	<u>7.919</u>	<u>7.927</u>	<u>7.916</u>	<u>7.964</u>
Al ^[VI]	-	0.125	0.098	-	-	-	-	-
Ti	0.266	0.072	0.033	0.176	0.198	0.178	0.214	0.185
Fe ³	-	-	0.815	-	-	-	-	-
Mg	0.049	-	-	0.849	0.670	0.709	0.640	0.664
Zn	-	-	-	-	-	-	-	-
Fe ²	4.673	4.794	3.871	3.975	4.132	4.113	4.146	4.151
Mn	-	0.009	0.146	-	-	-	-	-
Ca	-	-	0.037	-	-	-	-	-
Σ C/M ₁₋₃	<u>5.000</u>	<u>5.000</u>	<u>5.000</u>	<u>5.000</u>	<u>5.000</u>	<u>5.000</u>	<u>5.000</u>	<u>5.000</u>
Fe ²	0.123	-	-	0.255	0.154	0.155	0.145	0.102
Mn	0.107	0.105	-	0.076	0.097	0.068	0.079	0.074
Ca	0.668	0.546	0.091	1.014	1.096	0.980	1.008	1.040
Na	1.102	1.349	1.909	0.655	0.653	0.797	0.768	0.784
Σ B/M ₄	<u>2.000</u>	<u>2.000</u>	<u>2.000</u>	<u>2.000</u>	<u>2.000</u>	<u>2.000</u>	<u>2.000</u>	<u>2.000</u>
Na	0.734	0.790	0.637	0.825	0.658	0.783	0.770	0.639
K	0.278	0.288	0.219	0.230	0.241	0.222	0.236	0.247
Σ A	<u>1.114</u>	<u>1.078</u>	<u>0.856</u>	<u>1.055</u>	<u>0.899</u>	<u>1.005</u>	<u>1.006</u>	<u>0.886</u>
ENa + K	2.216	2.427	2.765	1.710	1.552	1.802	1.774	1.670
Mg/Mg + Fe ²	0.010	0.000	0.000	0.167	0.135	0.142	0.130	0.135
Class.	Na-Ca	Alk	Alk	Ca	Ca	Na-Ca	Na-Ca	Na-Ca
Name	FR	A	A	Si-Fe-E	Si-Fe-E	FR	FR	FR

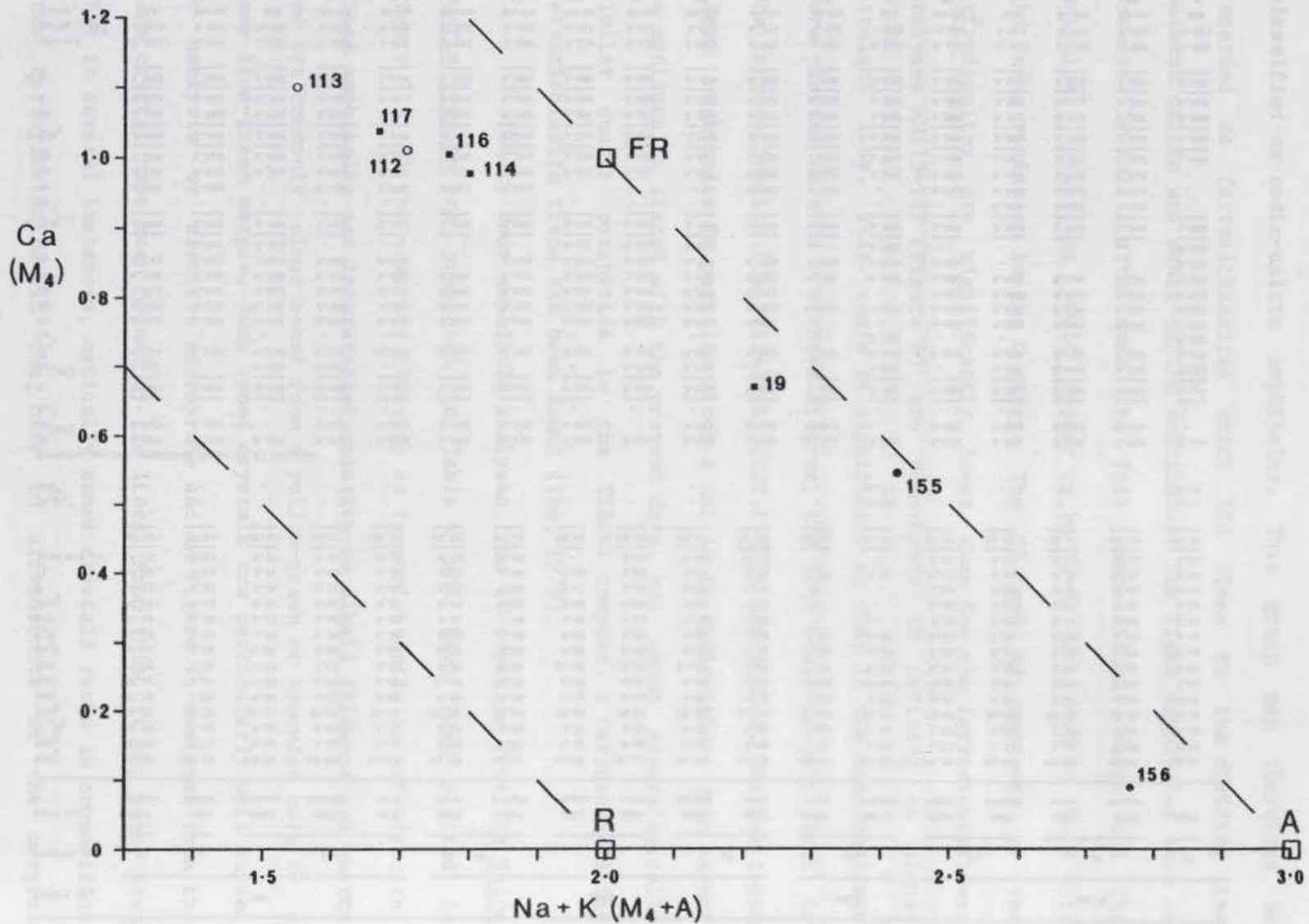


Figure 6 . Ca v alkalis diagram for amphiboles from the Zigau granite porphyry. Open circles = silicic ferroedenite. Squares = ferrowinchite. Dots = arfvedsonite.

Table 4 Electron microprobe analyses of amphiboles from the Shira alkali feldspar quartz syenite

Sample no.	SH4					SH19						SH19		SH105				
	3	9	10	11	12	13	14	15	16	17								
Crystal no.	3	9	10	11	12	13	14	15	16	17								
Spot no.	AM21 margin	AM22 core	AM23 margin	AM25 midway	AM24 core	AM13 core	AM14 margin	AM15 margin	AM16 core	AM17 margin	AM18 core	AM144 core	AM145 margin	AM26 core	AM27 margin	AM29 core	AM30 margin	AM31
SiO ₂	49.12	47.58	49.71	48.80	47.43	47.58	48.23	49.84	50.15	50.12	47.72	48.19	50.69	47.56	49.02	48.75	48.48	50.43
TiO ₂	1.79	1.71	2.13	1.61	2.06	2.03	1.67	0.55	0.58	0.63	2.09	1.91	1.93	1.73	1.71	1.46	1.54	2.31
Al ₂ O ₃	0.39	1.23	0.29	0.65	1.39	1.12	0.89	0.23	0.23	0.23	1.30	1.13	0.21	1.50	1.50	3.90	2.44	0.33
FeO _T	31.87	32.00	32.33	31.96	31.81	31.81	32.68	28.53	28.63	28.38	32.31	31.94	33.33	33.07	32.85	32.06	32.27	31.32
MnO	0.79	0.80	0.84	0.85	0.81	0.82	0.86	0.53	0.46	0.55	0.79	0.78	0.89	0.77	0.79	0.73	0.81	0.91
MgO	1.12	1.60	0.76	1.42	1.67	1.92	1.27	0.28	0.27	0.25	1.39	1.88	0.44	0.95	0.80	0.78	0.66	0.22
CaO	2.75	5.34	2.05	3.68	5.69	5.34	4.61	11.07	10.35	11.14	5.17	5.39	1.10	4.89	2.57	2.99	3.51	0.62
Na ₂ O	7.32	5.92	7.71	5.97	5.72	6.17	6.19	6.90	6.88	6.32	5.55	5.85	7.78	6.00	6.53	5.90	5.10	7.96
K ₂ O	1.53	1.17	1.70	1.36	1.18	1.21	1.38	0.03	0.04	0.10	1.27	1.25	1.68	1.19	1.60	1.46	1.42	2.02
ZnO	0.12	0.08	0.13	0.10	0.09	0.07	0.08	0.03	0.03	0.03	0.08	-	-	0.09	0.07	0.08	0.06	0.16
ZrO ₂	0.14	0.03	0.07	0.06	0.04	0.03	0.07	0.46	0.49	0.42	0.03	-	-	0.08	0.13	0.04	0.07	0.12
F	0.59	0.52	0.64	0.51	0.65	1.25	0.64	0.01	0.02	0.07	0.76	-	-	1.03	0.45	0.07	0.20	0.49
Cl	0.01	0.05	0.01	0.04	0.04	0.03	0.04	0.00	0.01	0.00	0.04	0.00	0.00	0.05	0.03	0.01	0.05	0.00
less O=Fe,Cl	0.25	0.23	0.27	0.22	0.28	0.53	0.28	-	0.01	0.03	0.33	-	-	0.44	0.20	0.03	0.09	0.00
	97.29	97.80	98.10	96.79	98.30	98.85	98.33	98.46	99.10	98.14	97.37	98.32	98.05	97.39	97.85	98.20	96.52	96.58
Fe ₂ O ₃	-	-	-	-	-	-	-	-	-	-	-	-	3.29	-	-	-	-	2.12
FeO ³	-	-	-	-	-	-	-	-	-	-	-	-	30.37	-	-	-	-	29.41
Formulas on the anhydrous basis of 23 oxygens																		
Si	7.977	7.710	8.008	7.941	7.651	7.662	7.794	7.949	8.004	7.989	7.709	7.715	8.042	7.708	7.901	7.731	7.860	8.134
Al ^[IV]	0.023	0.235	-	0.059	0.264	0.213	0.170	0.043	-	0.011	0.248	0.213	-	0.287	0.099	0.269	0.140	-
Fe ³	-	-	-	-	-	-	-	-	-	-	-	-	-	-	-	-	-	-
T	8.000	7.945	8.008	8.000	7.915	7.875	7.964	7.992	8.004	8.000	7.957	7.928	8.042	7.995	8.000	8.000	8.000	8.134
Al ^[VI]	0.051	-	0.055	0.066	-	-	-	-	0.043	0.032	-	-	0.039	-	0.186	0.460	0.326	0.063
Ti	0.219	0.208	0.258	0.197	0.250	0.245	0.203	0.066	0.070	0.076	0.253	0.230	0.230	0.210	0.207	0.174	0.188	0.280
Fe ²	-	-	-	-	-	-	-	-	-	-	-	-	0.393	-	-	-	-	0.257
Zr	0.011	0.002	0.006	0.005	0.003	0.002	0.006	0.035	0.038	0.033	0.002	-	-	0.006	0.010	0.003	0.006	0.010
Mg	0.271	0.386	0.183	0.344	0.402	0.461	0.305	0.066	0.064	0.059	0.335	0.448	0.104	0.230	0.192	0.184	0.159	0.053
Zn	0.015	0.010	0.015	0.012	0.011	0.008	0.010	0.004	0.004	0.010	-	-	-	0.011	0.008	0.010	0.007	0.019
Fe ²	4.328	4.337	4.356	4.310	4.291	4.284	4.417	3.806	3.822	3.783	4.365	4.276	4.030	4.482	4.427	4.169	4.314	3.968
Mn	0.105	0.055	0.114	0.066	0.026	-	0.059	0.072	0.062	0.074	0.035	0.046	0.120	0.061	-	-	-	0.111
Ca	-	0.002	0.013	-	-	-	-	0.951	0.939	0.975	-	-	0.082	-	-	-	-	0.107
C/H ₁₋₂	5.000	5.000	5.000	5.000	5.000	5.000	5.000	5.000	5.000	5.000	5.000	5.000	5.000	5.000	5.000	5.000	5.000	4.868
Fe ²	-	-	-	-	-	-	-	-	-	-	-	-	-	-	0.001	0.083	0.062	-
Mn	0.004	0.055	-	0.051	0.085	0.113	0.059	-	-	-	0.073	0.060	-	0.045	0.108	0.398	0.111	-
Ca	0.478	0.927	0.341	0.642	0.983	1.021	0.798	0.941	0.831	0.927	0.895	0.925	0.105	0.849	0.444	0.508	0.610	-
Na	1.518	1.018	1.659	1.307	0.932	0.866	1.143	1.059	1.169	1.073	1.032	1.015	1.895	1.106	1.447	1.311	1.217	2.000
B/H ₄	2.000	2.000	2.000	2.000	2.000	2.000	2.000	2.000	2.000	2.000	2.000	2.000	2.000	2.000	2.000	2.000	2.000	2.000
Na	0.786	0.842	0.749	0.577	0.857	0.951	0.797	1.074	0.960	0.880	0.707	0.801	0.498	0.780	0.593	0.503	0.387	0.489
K	0.317	0.242	0.349	0.282	0.243	0.248	0.284	0.006	0.008	0.020	0.262	0.255	0.340	0.246	0.329	0.295	0.294	0.416
A	1.003	1.084	1.098	0.859	1.100	1.209	1.081	1.080	0.968	0.900	0.969	1.056	0.838	1.026	0.922	0.798	0.681	0.905
Na + K	2.621	2.102	2.757	2.166	2.032	2.175	2.224	2.139	2.137	1.973	2.001	2.071	2.733	2.132	2.369	2.109	1.898	2.905
Mg/Mg + Fe ²	0.059	0.082	0.040	0.073	0.086	0.097	0.065	0.017	0.017	0.016	0.071	0.095	0.025	0.049	0.042	0.042	0.035	0.013
Class.	Alk	Na-Ca	Alk	Na-Ca	Na-Ca	Na-Ca	Na-Ca	Na-Ca	Na-Ca	Na-Ca	Na-Ca	Na-Ca	Alk	Na-Ca	Alk	Na-Ca	Na-Ca	Alk
Name	A	FR	A	FR	FR	FR	FR	FR	FR	FR	FR	FR	A	FR	A	FR	FR	A

classified as sodic-calcic amphiboles. This group may therefore be regarded as ferrorichterites which lie close to the dividing line between calcic and sodic-calcic amphiboles. The Zigau amphiboles show an essentially full A site over the full compositional range and the principal variations would appear to be Ca-Na variation in the B site and Fe/Mg variation in the C sites. The Ti and Al contents of the arfvedsonites are significantly lower than for the ferrorichterites. Analyses AM113-117 (Figure 6) are remarkable in defining an almost straight line. This could be significant in that if the same analyses were plotted on a Ca v Si+Na+K diagram, the line would project back to the ferroactinolite (Ca.Fe(2+)5.Si8.022.(OH)2) end-member. Whether these Zigau amphiboles in part lie along a calcic to sodic-calcic join cannot be equivocally stated with the present data, but among mineralogically similar quartz porphyries in the Tibchi complex, a ferroactinolite-ferrorichterite trend has been found (Ike, 1979).

Thirty four amphibole analyses from 20 crystals from the Shira quartz syenite are presented in Table 4 and have been plotted in Figure 7. All the analyses classify as ferrorichterite or arfvedsonite. These amphiboles are interstitial relative to alkali feldspar and quartz and are commonly colour zoned from a yellow-green or brownish core to a deep blue-green margin. Such zoned crystals are particularly well suited to analysis by electron microprobe and in Figure 7, analyses from the same crystal have been joined by tie lines. From this, it may be seen that in several instances, optically zoned crystals range in composition from ferrorichterite in the core to arfvedsonite at the margin. Therefore, individual amphiboles within the Shira quartz syenite may exhibit practically as great a range of composition as has been determined for the entire complex. A similar range of composition occurs among discrete amphiboles within a small enclave in sample SH11 (Table 4).

Table 4 continued. Electron microprobe analyses of amphiboles from the Shira alkali feldspar quartz syenite

Sample no.	SH11						SH11 xenolith			SH68/2				SH68/2 xenolith		
	18		19		20		21	22	23	24		25		26	27	
Crystal no.																
Spot no.	AM122 core	AM122/A core	AM123 core	AM124 midway	AM125 margin	AM126	AM127	AM119	AM120	AM121	AM128 core	AM129 margin	AM130 core	AM131 margin	AM132	AM133
SiO ₂	47.30	47.06	47.11	48.55	49.20	51.22	51.35	48.81	48.44	50.99	48.39	47.92	48.79	48.30	48.04	48.55
TiO ₂	1.78	1.74	2.05	1.73	1.72	2.63	1.90	1.69	1.64	1.89	1.99	1.72	1.76	1.82	1.88	1.81
Al ₂ O ₃	1.95	2.10	2.06	1.12	0.74	0.16	0.25	1.65	1.95	0.47	1.29	1.55	0.97	1.37	1.18	1.43
FeO _T	33.95	33.28	33.44	34.09	33.42	31.68	32.21	32.24	31.16	30.84	32.26	32.04	32.45	32.49	31.67	30.59
MnO	0.64	0.61	0.55	0.79	0.66	1.01	0.96	0.60	0.75	0.99	0.89	0.99	0.92	0.91	0.90	0.73
MgO	1.00	1.10	0.96	0.62	0.40	1.13	0.60	2.02	2.46	1.85	1.86	1.52	1.90	1.87	2.59	3.10
CaO	6.05	6.14	5.97	3.90	2.27	0.56	0.73	3.45	5.75	1.95	4.81	4.27	4.69	4.65	4.85	5.12
Na ₂ O	5.54	5.73	5.74	6.59	7.19	8.97	8.82	6.72	5.72	8.35	6.29	6.04	6.08	6.48	5.83	5.98
K ₂ O	1.05	1.06	1.08	1.23	1.49	1.66	1.67	1.34	1.09	1.49	1.15	1.43	1.26	1.19	1.28	1.27
Cl	0.11	0.10	0.00	0.00	0.00	0.00	0.00	0.09	0.09	0.00	0.00	0.09	0.00	0.00	0.00	0.06
less O=Cl	0.02	0.02	-	-	-	-	-	0.02	0.02	-	0.02	-	-	-	-	0.01
	99.35	98.90	98.96	98.62	97.09	99.02	98.49	98.59	99.03	98.82	98.93	97.55	98.82	99.08	98.22	98.64
Fe ₂ O ₃ ^C	-	-	-	-	-	0.80	1.86	-	-	-	-	-	-	-	-	-
FeO ^C	-	-	-	-	-	30.96	30.54	-	-	-	-	-	-	-	-	-
Formulae on the anhydrous basis of 23 oxygens																
Si	7.572	7.556	7.553	7.801	7.983	8.049	8.104	7.762	7.654	8.023	7.700	7.739	7.770	7.687	7.685	7.687
Al[IV]	0.368	0.398	0.389	0.199	0.017	-	-	0.238	0.346	-	0.247	0.261	0.182	0.257	0.223	0.267
Fe ³⁺	-	-	-	-	-	-	-	-	-	-	-	-	-	-	-	-
T	7.940	7.954	7.942	8.000	8.000	8.049	8.104	8.000	8.000	8.023	7.942	8.000	7.952	7.944	7.908	7.954
Al[VI]	-	-	-	0.013	0.124	0.030	0.046	0.071	0.017	0.087	-	0.034	-	-	-	-
Ti	0.214	0.210	0.247	0.209	0.210	0.311	0.225	0.202	0.195	0.224	0.238	0.209	0.211	0.218	0.226	0.215
Fe ²⁺	-	-	-	-	-	0.094	0.221	-	-	-	-	-	-	-	-	-
Mg	0.239	0.263	0.229	0.148	0.097	0.265	0.141	0.479	0.579	0.434	0.441	0.366	0.451	0.443	0.617	0.731
Fe ²⁺	4.545	4.469	4.484	4.581	4.535	4.069	4.031	4.248	4.118	4.058	4.293	4.328	4.322	4.325	4.157	4.051
Mn	0.002	0.058	0.040	0.049	0.034	0.134	0.128	-	0.091	0.132	0.028	0.063	0.016	0.014	-	0.003
Ca	-	-	-	-	-	0.094	0.123	-	-	0.065	-	-	-	-	-	-
C/M ₁₋₃	5.000	5.000	5.000	5.000	5.000	4.997	4.915	5.000	5.000	5.000	5.000	5.000	5.000	5.000	5.000	5.000
Fe ²⁺	-	-	-	-	-	-	-	0.040	-	-	-	-	-	-	-	0.080
Mn	0.085	0.025	0.035	0.059	0.057	-	-	0.081	0.009	-	0.092	0.072	0.108	0.109	0.122	0.095
Ca	1.038	1.056	1.026	0.671	0.395	-	-	0.588	0.973	0.264	0.820	0.739	0.800	0.793	0.831	0.869
Na	0.877	0.919	0.939	1.270	1.548	2.000	2.000	1.291	1.018	1.736	1.088	1.189	1.092	1.098	0.967	1.036
B/N ₄	2.000	2.000	2.000	2.000	2.000	2.000	2.000	2.000	2.000	2.000	2.000	2.000	2.000	2.000	2.000	2.000
Na	0.842	0.865	0.845	0.785	0.714	0.733	0.699	0.781	0.736	0.811	0.853	0.703	0.786	0.901	0.843	0.800
K	0.214	0.217	0.221	0.252	0.308	0.333	0.336	0.272	0.220	0.299	0.233	0.295	0.256	0.242	0.261	0.256
A	1.056	1.082	1.066	1.037	1.022	1.066	1.035	1.053	0.956	1.110	1.086	0.998	1.042	1.143	1.104	1.056
Na + K	1.933	2.001	2.005	2.307	2.670	3.066	3.035	2.344	1.974	2.846	2.174	2.187	2.134	2.241	2.071	2.092
Mg/Mg + Fe ²⁺	0.050	0.056	0.049	0.031	0.021	0.061	0.034	0.100	0.123	0.097	0.093	0.078	0.094	0.093	0.127	0.153
Class.	Na-Ca	Na-Ca	Na-Ca	Na-Ca	Alk	Alk	Alk	Na-Ca	Na-Ca	Alk	Na-Ca	Na-Ca	Na-Ca	Na-Ca	Na-Ca	Na-Ca
Name	FR	FR	FR	FR	A	A	A	FR	FR	A	FR	FR	FR	FR	FR	FR

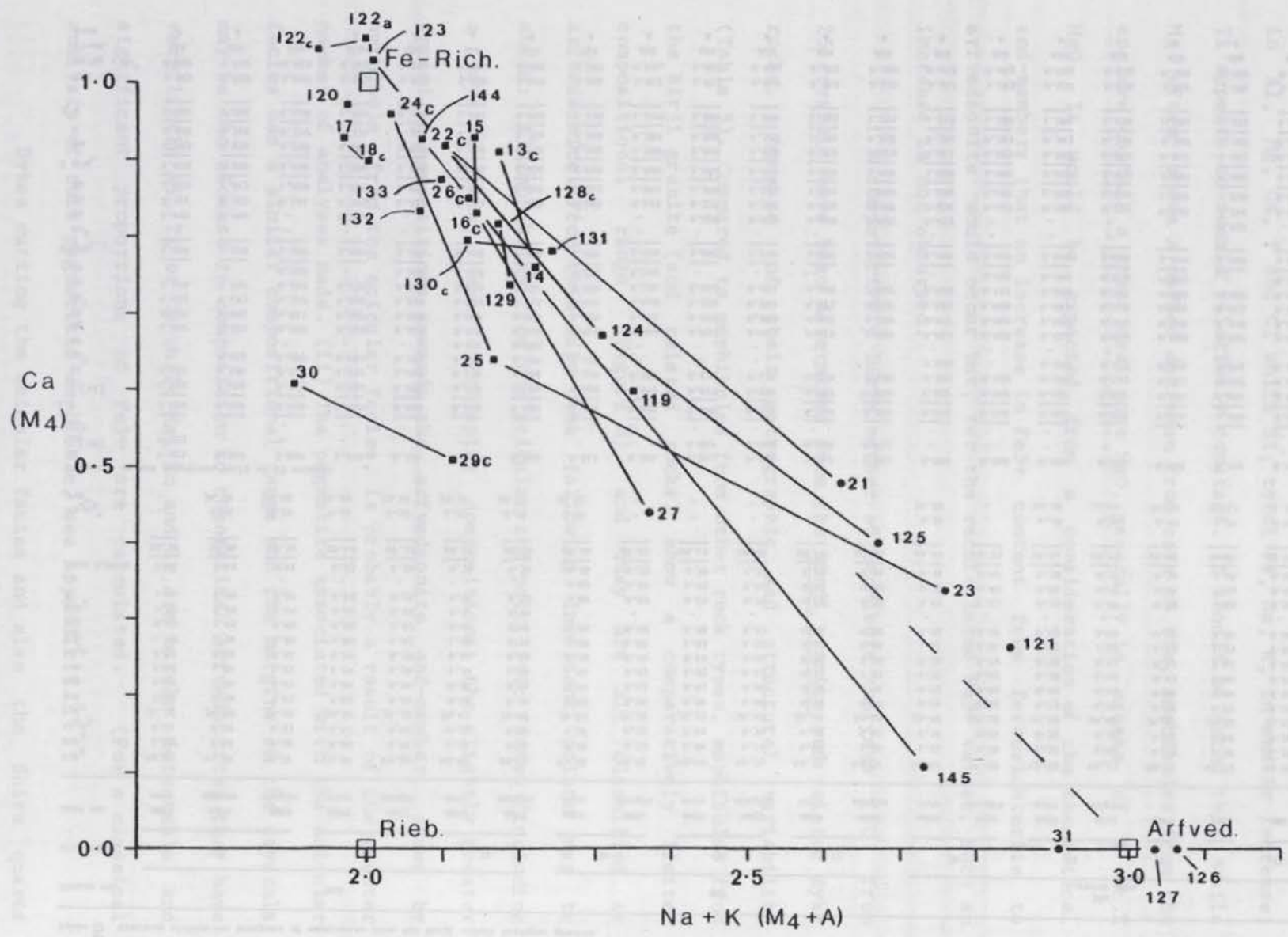


Figure 7. Ca v alkalis diagram for amphiboles from the Shira quartz syenite. Subscript c indicates the core of the crystal and it may be connected to the crystal margin by a tie line. [Symbols:Fig.6]

Chemically the variation from core to rim is due to a decrease in Al, Mg, Ca, F and Cl while Si, total Fe, Na, K, Zn and Zr increase; Ti appears to remain relatively constant. It should be noted that while Mg often shows a marked decrease from core to rim, amphiboles from the enclave contain a great deal more MgO, generally in excess of 2 wt.% MgO. It would be expected from a consideration of the theoretical end-members that an increase in Fe³⁺ content from ferrorichterite to arfvedsonite would occur but, for the recalculated Fe³⁺ values, such an increase is not observed.

A comparatively large number of amphibole analyses (40) from 25 crystals have been determined from the Birji granite and related dyke rocks, because of their petrographic and structural variability (Table 5). Compared to amphiboles from other rock types, amphiboles from the Birji granite (and related rocks) show a comparatively limited compositional range (Figure 8) and they are all classified as arfvedsonite. From this data the following important points may be noted: (i) Amphiboles from the acicular and poikilitic facies (including a layered zone) have overlapping compositions; the slightly greater spread of compositions towards the arfvedsonite end-member, shown by amphibole from the acicular facies, is probably a result of the greater number of analyses made. (ii) The pegmatite associated with the acicular facies has a similar compositional range and the margins of the crystals may be the closest in composition to theoretical arfvedsonite; they have very little Al, Ti or Ca while Mg, Zn and Zr are barely detectable and significant proportions of Fe³⁺ are calculated. (For a classical analysis of this pegmatitic amphibole, see Appendix 3.)

Dykes cutting the acicular facies and also the Shira quartz syenite close to the Birji granite have highly peralkaline whole rock compositions (see Table 26); correspondingly, the amphiboles are among the most sodic (and least calcic) found in the Shira complex.

Table 5 continued. Electron microprobe analyses of amphiboles from the Birji alkali feldspar granite.

Sample no.	SH101 Pegmatite associated with ancolular facies					SH95 Dyke cutting ancolular facies					SH8 Folklitic facies					SH90 Dyke cutting Shira quartz syenite								
	39		40		41	42		43		44	45		46		47		48		49		50	51	52	
Crystal no.																								
Spot no.	AM1 margin	AM2 core	AM3 margin	AM4 core	AM5 core	AM6 core	AM8 margin	AM9 core	AM10 core	AM11 core	AM14 core	AM15 margin	AM16 core	AM17 margin	AM18 margin	AM19 margin	AM20 core	AM22 core	AM23 core	AM24 core	AM25 core	AM26 core		
SiO ₂	50.33	49.05	49.57	50.10	50.41	45.51	49.86	50.01	50.43	50.25	50.78	49.00	49.40	50.08	49.77	49.82	50.29	52.00	51.51	51.61				
TiO ₂	0.89	1.01	0.91	1.01	0.86	1.13	1.35	1.14	1.11	1.38	1.50	1.48	1.64	2.09	1.76	1.54	1.73	1.02	1.02	0.75				
Al ₂ O ₃	0.23	0.33	0.58	0.16	0.11	0.55	0.35	0.30	0.32	0.41	0.64	0.62	0.47	0.30	0.37	0.44	0.27	0.25	0.21	0.34				
FeO ^T	34.56	34.79	35.10	34.79	34.61	35.43	34.62	34.41	34.71	34.12	34.68	34.49	34.58	34.44	35.44	35.20	34.75	32.96	32.34	32.68				
MnO	0.65	0.60	0.56	0.56	0.59	0.63	0.67	0.66	0.59	0.64	0.63	0.74	0.59	0.68	0.60	0.77	0.71	1.79	1.49	1.59				
MgO	0.02	0.03	0.04	0.00	0.04	0.04	0.03	0.05	0.04	0.09	0.24	0.00	0.00	0.00	0.00	0.00	0.00	0.22	0.29	0.31				
CaO	0.31	1.96	2.27	0.90	0.53	1.81	1.55	1.06	0.06	0.08	1.92	2.51	2.65	1.44	2.03	2.30	1.59	0.12	0.40	0.14				
Na ₂ O	8.28	8.01	7.70	8.19	8.11	8.52	8.32	8.76	9.06	9.05	7.74	7.56	7.63	8.38	7.71	7.58	8.20	9.52	9.58	9.63				
K ₂ O	1.69	1.48	1.49	1.99	2.35	1.55	2.02	1.75	1.64	1.63	1.72	1.53	1.59	1.71	1.60	1.55	1.65	1.99	1.93	1.96				
ZnO	0.07	0.02	0.05	0.03	0.05	0.07	0.08	0.07	0.08	0.09	-	-	-	-	-	-	-	-	-	-				
ZrO ₂	0.00	0.09	0.05	0.00	0.03	-	-	-	-	-	-	-	-	-	-	-	-	-	-	-				
F	0.86	0.79	0.59	0.68	0.21	0.79	0.54	0.83	0.85	0.85	-	-	-	-	-	-	-	-	-	-				
Cl	0.01	0.01	0.02	0.00	0.00	0.03	0.02	0.00	0.01	0.01	0.00	0.00	0.10	0.00	0.06	0.00	0.00	0.00	0.00	0.00				
loss O=F,Cl	0.36	0.33	0.25	0.29	0.01	0.34	0.23	0.35	0.36	0.36	-	-	0.02	-	0.01	-	-	-	-	-				
	97.54	97.84	98.68	98.12	97.91	95.72	98.98	98.69	98.54	99.03	99.85	97.93	98.63	99.12	99.33	99.20	99.19	99.87	98.77	99.01				
Fe ₂ O ₃ ⁰	5.96	0.95	0.64	3.78	4.90	-	0.92	1.76	4.31	1.24	1.30	-	-	0.02	-	-	1.04	3.36	2.15	3.18				
FeO ^T	29.20	33.94	34.52	31.39	30.20	-	33.79	32.82	30.83	33.01	33.51	-	-	34.42	-	-	33.81	29.94	30.41	29.82				
Formulae on the anhydrous basis of 23 oxygens																								
Si	8.063	8.000	8.000	8.049	8.075	7.748	8.019	8.039	8.044	8.041	8.000	7.948	7.958	8.000	7.968	7.978	8.009	8.121	8.147	8.129				
Al ^[IV]	-	-	-	-	-	0.110	-	-	-	-	-	0.052	0.042	-	0.032	0.022	-	-	-	-				
Fe ³⁺	-	-	-	-	-	-	-	-	-	-	-	-	-	-	-	-	-	-	-	-				
T	8.063	8.000	8.000	8.049	8.075	7.858	8.019	8.039	8.044	8.041	8.000	8.000	8.000	8.000	8.000	8.000	8.009	8.121	8.147	8.129				
Al ^[VI]	0.043	0.054	0.110	0.030	0.021	-	0.066	0.057	0.060	0.077	0.119	0.067	0.048	0.056	0.038	0.061	0.051	0.046	0.039	0.063				
Tl	0.107	0.114	0.110	0.122	0.104	0.145	0.139	0.138	0.133	0.166	0.178	0.181	0.199	0.251	0.212	0.185	0.207	0.120	0.121	0.089				
Fe ³⁺	0.718	0.106	0.078	0.457	0.591	-	0.112	0.213	0.517	0.149	0.154	-	-	0.003	-	-	0.125	0.395	0.255	0.377				
Zr	0.000	0.007	0.004	-	0.002	-	-	-	-	-	-	-	-	-	-	-	-	-	-	-				
Mg	0.005	0.007	0.005	0.010	0.010	0.007	0.012	0.010	0.010	0.002	0.056	-	-	-	-	-	-	0.051	0.068	0.073				
Zn	0.009	0.002	0.006	0.004	0.006	0.009	0.010	0.008	0.010	0.011	-	-	-	-	-	-	-	-	-	-				
Fe ²⁺	3.912	4.621	4.655	4.217	4.046	4.836	4.545	4.413	4.113	4.417	4.415	4.679	4.659	4.599	4.745	4.714	4.503	3.910	4.022	3.928				
Mn	0.088	0.073	0.032	0.076	0.080	-	0.091	0.090	0.080	0.087	0.078	0.073	0.080	0.091	0.005	0.040	0.096	0.237	0.200	0.212				
Ca	0.053	0.016	-	0.094	0.091	-	0.030	0.069	0.010	0.071	-	-	0.014	-	-	-	0.018	0.020	0.068	0.024				
C/M ₁₋₃	4.935	5.000	5.000	5.000	4.951	5.000	5.000	5.000	4.933	5.000	5.000	5.000	5.000	5.000	5.000	5.000	5.000	5.000	4.779	4.773	4.766			
Fe ²⁺	-	-	-	-	-	0.208	-	-	-	-	-	-	-	-	-	-	-	-	-	-				
Mn	-	-	0.045	-	-	0.091	-	-	-	-	0.006	0.029	-	0.001	0.076	0.064	-	-	-	-				
Ca	-	0.324	0.392	0.062	-	0.330	0.238	0.113	-	0.074	0.324	0.436	0.443	0.246	0.348	0.395	0.253	-	-	-				
Na	2.000	1.676	1.563	1.938	2.000	1.371	1.762	1.887	2.000	1.926	1.670	1.535	1.557	1.753	1.576	1.541	1.747	2.000	2.000	2.000				
R/R ₀	2.000	2.000	2.000	2.000	2.000	2.000	2.000	2.000	2.000	2.000	2.000	2.000	2.000	2.000	2.000	2.000	2.000	2.000	2.000	2.000				
Na	0.572	0.957	0.846	0.613	0.519	1.441	0.832	0.843	0.802	0.891	0.694	0.862	0.822	0.843	0.818	0.814	0.782	0.903	0.935	0.941				
K	0.345	0.308	0.307	0.408	0.480	0.337	0.414	0.359	0.333	0.333	0.346	0.317	0.327	0.348	0.327	0.317	0.335	0.396	0.389	0.394				
A	0.917	1.265	1.153	1.021	0.999	1.778	1.246	1.202	1.135	1.224	1.040	1.159	1.154	1.191	1.145	1.131	1.117	1.299	1.304	1.335				
Ena + K	2.917	2.941	2.716	2.959	2.999	3.149	3.008	3.089	3.135	3.150	2.710	2.694	2.711	2.944	2.721	2.672	2.864	3.299	3.304	3.335				
Mg/Mg + Fe ²⁺	0.001	0.002	0.002	0.000	0.002	0.002	0.002	0.003	0.002	0.005	0.001	-	-	-	-	-	-	0.013	0.017	0.018				
Class.	Alk	Alk	Alk	Alk	Alk	Alk	Alk	Alk	Alk	Alk	Alk	Alk	Alk	Alk	Alk	Alk	Alk	Alk	Alk	Alk				
Name	A	A	A	A	A	A	A	A	A	A	A	A	A	A	A	A	A	A	A	A				

Seventeen amphibole analyses from the Andaburi granite and dykes within the granite are presented in Table 6, together with three analyses of amphibole from a pegmatitic dyke in the nearby Eldewo biotite granite. The analyses are plotted in Figure 9. Amphiboles from the granite and dykes which intrude it fall into three groups on Figure 9: ferrorichterite, arfvedsonite and an intermediate group. Ferrorichterite occurs close to the supposed margin of the granite near Kakkaki village, where the rock is slightly porphyritic (SH44), whereas away from the contact (SH54) arfvedsonite occurs. (Both these samples however, come from the eastern part of the granite and unfortunately, polished thin sections from the central part of the body were not sufficiently good for analysis, so it is not known whether this is a real or an apparent compositional gap in the granite as a whole; with only 7 analyses though, it may be expected that the compositional range would be extended if more data were available). Amphiboles from fine grained, melanocratic dykes which cut the western and central parts of the Andaburi granite are arfvedsonites which lie intermediate in composition between the amphiboles from the two previously mentioned areas. These dyke-rock arfvedsonites have a range in Ca content from 0.2 to 0.6 cations and the total alkali content correspondingly varies from 2.9 to 2.5 cations. The very fine grained nature of the dykes is such that only one core-rim analysis pair was possible (AM100-101) and this shows a decrease in Ca towards the margin, like analyses AM65-66 from an arfvedsonite in the granite.

Amphibole from a pegmatitic sheet (SH65/1) within the Eldewo biotite granite (which dips away from the Andaburi granite) was analysed (AM77-79) in order to supplement field evidence for the relative ages of the two granites. These analyses have relatively low Ca and alkalis compared with the Andaburi granite or the dykes (Figure 9). On the evidence of the present data, the sheet would appear to be related more

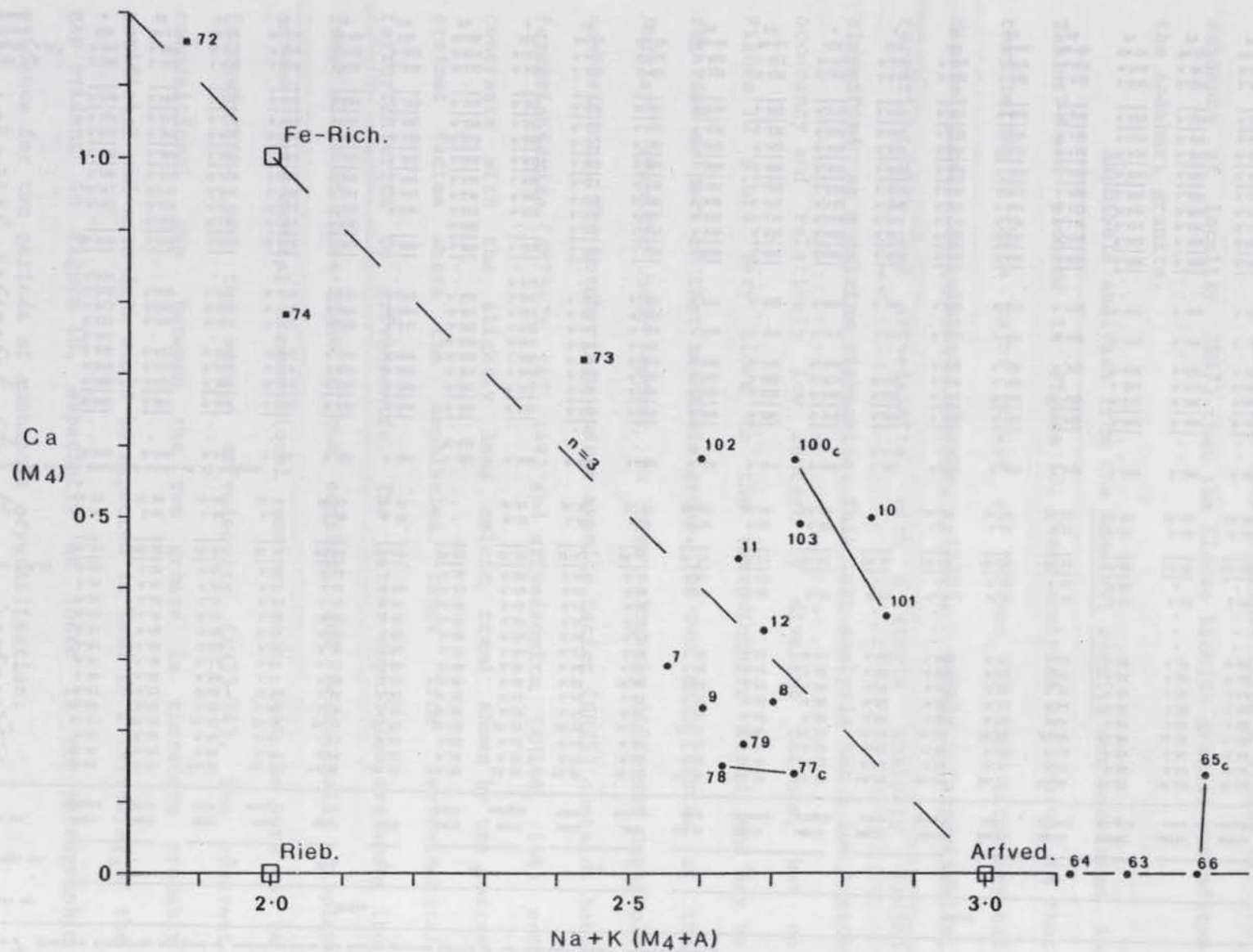


Figure 9. Ca v alkalis diagram for amphiboles from the Andaburi granite. Symbols as in Figs.6 & 7.

Table 7 Electron microprobe analyses of amphibole from the coarse grained facies of the Andulay alkali feldspar syenite

Sample no.	SH51A										SH51B										
	70		71		72		73		74		75		76		77		78		79		
	Spot no.	AM33 margin	AM34 core	AM35 core	AM36 margin	AM37	AM38	AM39 core	AM40 margin	AM41 core	AM42 margin	AM134 core	AM136 midway	AM135 margin	AM137 core	AM138 margin	AM139 core	AM140 midway	AM141 margin	AM142 core	AM143 margin
SiO ₂	49.69	49.39	49.35	49.39	49.71	50.52	49.31	50.27	49.28	50.17	49.74	49.37	50.52	49.59	49.78	50.15	49.54	49.83	50.53	50.65	
TiO ₂	0.64	0.09	0.08	0.14	0.45	0.20	0.57	0.77	0.03	0.20	0.42	0.54	0.25	0.46	0.41	0.50	0.00	0.34	0.42	0.20	
Al ₂ O ₃	0.45	0.52	0.45	0.47	0.63	0.42	0.61	0.25	0.49	0.50	0.52	0.60	0.52	1.15	0.80	0.53	0.46	0.70	0.46	0.42	
FeO _T	34.23	36.28	36.83	36.34	34.92	35.61	35.06	34.77	36.37	36.01	35.69	35.91	35.72	35.02	35.45	36.59	36.60	35.86	35.66	35.68	
MnO	1.48	1.41	1.27	1.41	1.08	0.77	0.90	1.50	1.44	0.97	1.17	0.98	0.88	1.04	0.94	0.99	1.14	1.07	0.94	0.89	
MgO	0.73	0.13	0.05	0.35	1.16	0.53	0.77	0.25	0.05	0.68	0.33	0.35	0.86	0.66	0.58	0.33	0.20	0.31	0.78	0.80	
CaO	1.40	4.16	4.81	3.41	4.18	3.20	3.64	0.56	4.80	4.68	2.88	2.77	0.84	2.18	2.10	3.93	4.35	4.02	3.92	3.62	
Na ₂ O	6.71	4.36	4.15	4.40	4.63	5.00	6.00	6.84	4.08	4.41	6.66	6.43	7.05	6.87	6.68	4.89	4.57	5.11	4.59	4.95	
K ₂ O	1.45	0.69	0.62	0.56	0.81	0.42	1.33	1.60	0.65	0.49	1.26	1.15	1.12	1.40	1.44	0.89	0.59	0.68	0.54	0.68	
ZnO	0.11	0.05	0.06	0.04	0.03	0.03	0.04	0.09	0.04	0.03	-	-	-	-	-	-	-	-	-	-	
ZrO ₂	0.03	0.00	0.00	0.00	0.00	0.00	0.07	0.14	0.05	0.05	-	-	-	-	-	-	-	-	-	-	
F	0.66	0.18	0.21	0.09	0.05	0.00	0.68	0.46	0.18	0.06	-	-	-	-	-	-	-	-	-	-	
Cl	0.04	0.05	0.07	0.04	0.06	0.02	0.05	0.03	0.06	0.02	0.06	0.07	0.00	0.00	0.00	0.06	0.09	0.13	0.00	0.00	
less O=F,Cl	0.29	0.09	0.11	0.05	0.03	-	0.30	0.20	0.09	0.04	0.01	0.02	-	-	-	0.01	0.02	0.03	-	-	
	97.33	97.22	97.84	96.59	97.68	96.72	98.73	97.33	97.43	98.23	98.72	98.15	97.76	98.37	98.18	98.85	97.52	98.02	97.84	97.89	
Fe ₂ O ₃ ^C	4.84	3.47	1.96	4.75	0.99	9.02	-	9.06	2.61	3.08	0.78	0.01	6.80	-	1.52	1.97	3.17	2.12	5.29	6.32	
FeO ^C	29.88	33.16	35.06	32.06	34.03	27.50	-	26.61	34.02	33.24	34.99	35.90	29.60	-	34.08	34.82	33.75	33.95	30.90	30.00	
Formulae on the anhydrous basis of 23 oxygens																					
Si	8.000	8.000	8.000	8.000	8.000	8.000	7.967	8.000	8.000	8.000	8.000	8.000	8.000	8.000	8.000	8.000	8.000	8.000	8.000	8.000	8.000
Al ^[IV]	-	-	-	-	-	-	0.033	-	-	-	-	-	-	0.021	-	-	-	-	-	-	-
Fe ³	-	-	-	-	-	-	-	-	-	-	-	-	-	-	-	-	-	-	-	-	-
T	8.000	8.000	8.000	8.000	8.000	8.000	8.000	8.000	8.000	8.000	8.000	8.000	8.000	8.000	8.000	8.000	8.000	8.000	8.000	8.000	8.000
Al ^[VI]	0.086	0.099	0.086	0.089	0.120	0.078	0.083	0.047	0.094	0.094	0.099	0.115	0.097	0.197	0.152	0.100	0.088	0.132	0.086	0.078	
Ti	0.078	0.011	0.010	0.017	0.054	0.024	0.069	0.092	0.319	0.024	0.051	0.066	0.030	0.056	0.060	-	0.184	0.236	0.385	0.256	0.630
Fe ³	0.586	0.423	0.240	0.580	0.120	1.077	0.000	1.086	0.004	0.370	0.094	0.002	0.810	-	0.184	0.236	0.385	0.256	0.630	0.751	
Zr	0.002	-	-	-	-	-	0.006	0.011	0.004	0.007	-	-	-	-	-	-	-	-	-	-	
Mg	0.175	0.031	0.012	0.085	0.278	0.125	0.185	0.059	0.012	0.162	0.079	0.084	0.203	0.158	0.139	0.079	0.048	0.074	0.184	0.188	
Zn	0.013	0.006	0.007	0.005	0.004	0.004	0.005	0.011	0.005	0.003	-	-	-	-	-	-	-	-	-	-	
Fe ²	4.023	4.430	4.645	4.224	4.424	3.642	4.652	3.542	4.562	4.340	4.677	4.733	3.860	4.589	4.475	4.525	4.479	4.497	4.050	3.959	
Mn	0.037	-	-	-	-	-	-	0.152	-	-	-	-	-	-	-	-	-	-	-	-	
Ca	-	-	-	-	-	-	-	-	-	-	-	-	-	-	-	-	-	-	-	-	
C	5.000	5.000	5.000	5.000	5.000	5.000	5.000	5.000	5.000	5.000	5.000	5.000	5.000	5.000	5.000	5.000	5.000	5.000	5.000	5.000	
Fe ²	-	0.062	0.109	0.119	0.156	-	0.086	-	0.056	0.093	0.034	0.132	0.060	0.123	0.106	0.121	0.079	0.062	0.041	0.003	
Mn	0.165	0.194	0.174	0.193	0.147	0.050	0.123	0.050	0.198	0.131	0.159	0.134	0.118	0.142	0.128	0.134	0.156	0.146	0.126	0.119	
Ca	0.241	0.722	0.835	0.592	0.721	0.543	0.630	0.096	0.835	0.800	0.496	0.481	0.342	0.376	0.362	0.672	0.753	0.691	0.665	0.613	
Na	1.594	1.022	0.882	1.096	0.976	1.407	1.161	1.854	0.911	0.976	1.311	1.253	1.680	1.359	1.404	1.073	1.012	1.001	1.168	1.265	
H	2.000	2.000	2.000	2.000	2.000	2.000	2.000	2.000	2.000	2.000	2.000	2.000	2.000	2.000	2.000	2.000	2.000	2.000	2.000	2.000	
Na	0.501	0.347	0.422	0.286	0.469	0.128	0.718	0.256	0.373	0.387	0.766	0.767	0.485	0.784	0.676	0.438	0.418	0.490	0.241	0.251	
K	0.297	0.142	0.128	0.116	0.166	0.085	0.274	0.325	0.135	0.099	0.258	0.238	0.226	0.287	0.295	0.181	0.122	0.139	0.109	0.137	
A	0.798	0.489	0.550	0.402	0.635	0.213	0.992	0.581	0.508	0.486	1.024	1.005	0.711	1.071	0.971	0.619	0.540	0.629	0.350	0.388	
Na + K	2.392	1.511	1.432	1.498	1.611	1.620	2.153	2.435	1.419	1.462	2.335	2.258	2.391	2.430	2.375	1.692	1.552	1.630	1.518	1.651	
Mg/Mg + Fe ²	0.042	0.007	0.003	0.019	0.057	0.033	0.038	0.016	0.003	0.035	0.016	0.017	0.049	0.033	0.029	0.017	0.010	0.016	0.043	0.045	
Class.	Alk	Na-Ca	Na-Ca	Na-Ca	Na-Ca	Alk	Na-Ca	Alk	Na-Ca	Na-Ca	Na-Ca	Na-Ca	Alk	Alk	Alk	Na-Ca	Na-Ca	Na-Ca	Na-Ca	Na-Ca	
Name	A	FW	FR	FW	FR	CR	FR	A	FR	FW	FR	FR	FR	A	A	A	FR	FR	FR	FW	

to the post-Andaburi granite dyke phase than to the granite itself and therefore does not contradict the field evidence (from a single critical exposure at locality SH47) that the Eldewo biotite granite post-dates the Andaburi granite.

Amphibole analyses from the Amdulayi syenite are presented in Tables 7-8 and plotted in Figure 10. These analyses are unusual in that they belong to three major groups as defined by the International Mineralogical Association (Leake, 1978), namely ferrowinchite, ferrorichterite and arfvedsonite, with a single analysis (AM38) classified as a calcian riebeckite. This last analysis has a low A site occupancy and relatively low content of divalent cations, but on Figure 10 plots very close to the ferrowinchite field and may be regarded as part of that amphibole group. The two main facies of the Amdulayi syenitic body appear to have slightly different amphibole compositions. The porphyritic quartz syenite facies (SH25) contains both ferrorichterite (AM75-76, 147, 149) and arfvedsonite (AM146, 148) and contrasts with the slightly less calcic trend shown by the coarse grained facies where the amphiboles range from ferrowinchite/ferrorichterite to arfvedsonite. The latter amphiboles are among the least sodic of those found in the complex, and occasionally display marked intra-crystal compositional zoning such that the core may be ferrowinchite and the margin arfvedsonite (AM33-34). The apparent compositional gap between the two groups is therefore probably artificial and more data would be expected to lead to a narrowing of the gap evident in Figure 10, especially as there is no petrographic evidence for two periods of amphibole crystallisation.

Analyses UN15-18 in Table 8 have not been included in Figures 10 or 11, or in the correlation matrix (Table 9) because they are pseudomorphs after (?augitic) pyroxene in the porphyritic facies. This amphibole is remarkable however, for its Mg content which is far

Table 8 Electron microprobe analyses of amphiboles from the Amdulayi alkali feldspar quartz syenite

Sample no.	SH25/1							SH25		
Crystal no.	pseudomorph									
	80	81	82	83	84	85	86	87	88	89
Spot no.	UN15	UN16	UN17	UN18	AM146	AM147	AM148	AM149	AM75	AM76
SiO ₂	54.65	53.78	54.22	54.81	51.00	50.20	50.52	48.91	49.12	48.57
TiO ₂	0.00	0.22	0.00	0.00	0.67	0.96	1.61	2.57	2.52	2.98
Al ₂ O ₃	0.49	0.57	0.42	0.30	0.55	0.67	0.39	1.48	1.26	1.37
FeO _T	15.03	17.77	15.49	12.14	31.98	32.03	32.18	28.87	31.56	30.54
MnO	0.41	0.60	0.47	0.36	1.09	1.03	1.08	0.82	0.93	0.89
MgO	14.52	12.66	14.01	16.69	2.57	2.31	1.86	3.82	2.25	2.65
CaO	6.28	6.17	5.86	6.29	2.98	3.34	2.27	5.64	4.68	5.42
Na ₂ O	5.69	5.60	6.34	5.44	6.07	6.03	6.75	5.54	5.24	5.33
K ₂ O	1.02	0.95	0.94	1.07	1.40	1.52	1.41	1.13	1.25	1.22
ZnO	-	-	-	-	-	-	-	-	0.04	0.08
F	-	-	-	-	-	-	-	-	0.47	0.56
Cl	0.00	0.00	0.00	0.06	0.12	0.14	0.00	0.00	0.03	0.02
less O=P,Cl	-	-	-	0.01	0.03	0.03	-	-	0.21	0.24
	<u>98.09</u>	<u>98.32</u>	<u>97.75</u>	<u>97.15</u>	<u>98.40</u>	<u>98.20</u>	<u>98.07</u>	<u>98.78</u>	<u>99.14</u>	<u>99.11</u>
Fe ₂ O ₃ ^c	-	-	-	-	3.12	-	1.64	-	-	-
FeO ^c	-	-	-	-	29.17	-	30.70	-	-	-
Formulae on the anhydrous basis of 23 oxygens										
Si	7.975	7.940	7.972	7.970	8.000	7.989	8.000	7.654	7.755	7.649
Al ^[IV]	0.025	0.060	0.028	0.030	-	0.011	-	0.273	0.234	0.254
Fe ³	-	-	-	-	-	-	-	-	-	-
T	<u>8.000</u>	<u>7.927</u>	<u>7.989</u>	<u>7.903</u>						
Al ^[VI]	0.059	0.039	0.044	0.021	0.102	0.115	0.073	-	-	-
Ti	-	0.024	-	-	0.079	0.115	0.192	0.303	0.299	0.353
Fe ³	-	-	-	-	0.368	-	0.195	-	-	-
Mg	3.158	2.786	3.070	3.617	0.601	0.548	0.439	0.891	0.529	0.622
Zn	-	-	-	-	-	-	-	-	0.005	0.009
Fe ²	1.783	2.151	1.886	1.362	3.827	4.222	4.066	3.778	4.167	4.016
Mn	-	-	-	-	0.023	-	0.035	0.028	-	-
Ca	-	-	-	-	-	-	-	-	-	-
C/M ₁₋₃	<u>5.000</u>									
Fe ²	0.051	0.043	0.019	0.114	-	0.041	-	-	-	0.006
Mn	0.051	0.075	0.058	0.044	0.122	0.139	0.110	0.080	0.124	0.119
Ca	0.982	0.976	0.923	0.980	0.501	0.569	0.385	0.946	0.792	0.915
Na	0.916	0.906	1.000	0.862	1.377	1.251	1.505	0.974	1.084	0.960
B/M ₄	<u>2.000</u>									
Na	0.693	0.697	0.808	0.672	0.469	0.609	0.568	0.707	0.520	0.668
K	0.190	0.179	0.176	0.198	0.280	0.309	0.285	0.226	0.252	0.245
A	<u>0.883</u>	<u>0.876</u>	<u>0.984</u>	<u>0.870</u>	<u>0.749</u>	<u>0.918</u>	<u>0.853</u>	<u>0.933</u>	<u>0.772</u>	<u>0.913</u>
ENa + K	1.799	1.782	1.984	1.732	2.126	2.169	2.358	1.907	1.856	1.873
Mg/Mg + Fe ²	0.633	0.559	0.617	0.710	0.136	0.114	0.097	0.191	0.113	0.134
Class.	Na-Ca	Na-Ca	Na-Ca	Na-Ca	Alk	Alk	Alk	Na-Ca	Na-Ca	Na-Ca
Name	Rt	Rt	Rt	Rt	A	A	A	PR	PR	PR

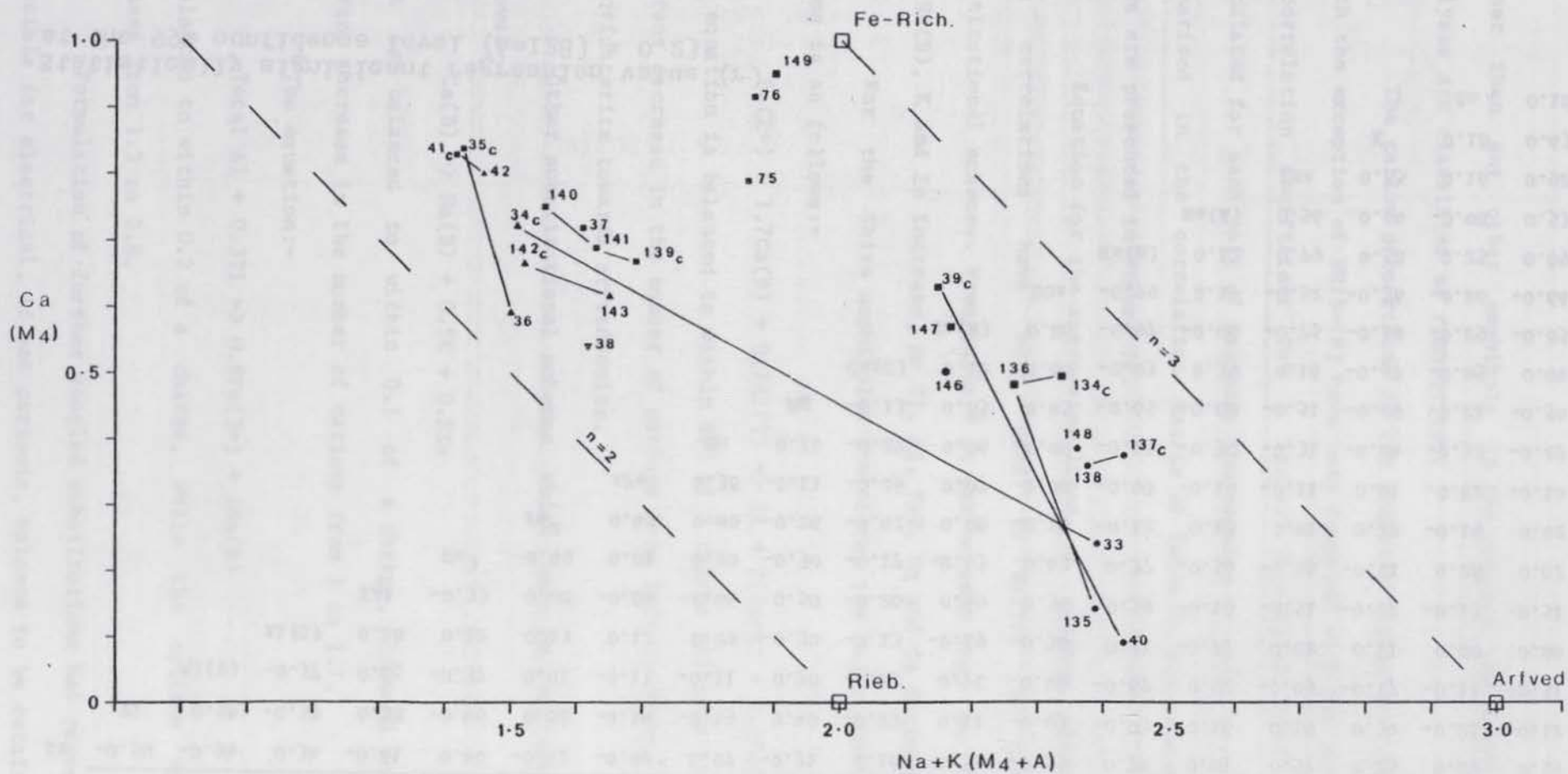


Figure 10. Ca v alkalis diagram for amphiboles from the Amdulayi syenite/quartz syenite. Upright triangle= ferrowinchite. Inverted triangle = calcian riebeckite. Other symbols as in Figures 6 & 7.

Table 9 Correlation matrix for microprobe analyses of amphiboles

	Ti	Al(T)	Al(C)	ΣAl	Fe ³	Fe ²	ΣFe	Mn	Mg	Ca(C)	Ca(B)	ΣCa	Na(B)	Na(A)	ΣNa	K	Zn	Na+K
Si	-0.50	-0.94	0.34	-0.81	0.40	-0.12	-0.07	0.07	-0.71	0.16	-0.79	-0.55	0.74	0.01	0.57	0.25	0.27	0.59
	Ti	0.54	-0.33	0.38	-0.46	0.06	-0.14	-0.19	0.40	-0.23	0.11	-0.03	-0.03	0.16	0.10	0.34	-0.06	0.12
		Al(T)	-0.37	0.85	-0.37	0.01	-0.11	-0.11	0.70	-0.17	0.71	0.48	-0.67	0.02	-0.49	-0.17	-0.11	-0.51
			Al(C)	0.18	0.12	0.13	0.12	0.09	-0.30	-0.13	-0.29	-0.30	0.21	-0.27	0.02	0.11	0.00	0.06
				ΣAl	-0.33	0.08	-0.04	-0.06	0.58	-0.26	0.59	0.34	-0.59	-0.13	-0.51	-0.12	-0.13	-0.51
					Fe ³	-0.49	0.01	0.20	-0.30	-0.17	-0.43	-0.43	0.37	-0.56	-0.05	-0.01	0.26	0.02
						Fe ²	0.43	0.00	-0.26	-0.42	0.08	-0.14	-0.12	0.13	0.01	0.27	-0.19	0.02
							ΣFe	0.38	-0.11	-0.26	0.07	-0.08	-0.08	-0.10	-0.11	0.01	-0.82	-0.10
								Mn	0.10	-0.27	0.06	-0.09	-0.13	-0.39	-0.31	-0.04	-0.32	-0.27
									Mg	-0.13	0.65	0.45	-0.65	-0.08	-0.51	-0.20	-0.21	-0.54
										Ca(C)	0.12	0.60	-0.03	0.39	0.16	-0.57	-0.05	0.04
											Ca(B)	0.86	-0.97	-0.06	-0.75	-0.59	-0.29	-0.85
												ΣCa	-0.79	0.14	-0.52	-0.76	-0.26	-0.66
													Na(B)	0.12	0.79	0.58	0.25	0.89
														Na(A)	0.56	0.04	-0.08	0.53
															ΣNa	0.55	0.16	0.92
																K	0.18	0.63
																	Zn	0.18

Statistically significant regression value (r)
at the 99% confidence level (n=128) = 0.23

higher than any other amphibole in the complex, and accordingly the analyses are classified as richterites.

The cation proportions in the analyses listed in Tables 3 to 8 (with the exception of UN15-18) have been compared with one another and a correlation coefficient for a linear regression line has been calculated for each pair of cations. The results of this procedure are summarised in the correlation matrix of Table 9, and selected cation pairs are presented in Figure 12.

Equation for the regression lines of cations pairs showing high correlations have been used to derive the most likely substitutional schemes. From Table 9 it can be seen that as Si, Fe³⁺, Mn, Na(B), K and Zn increase, so Ti, Al, Fe²⁺, Mg and Ca decrease.

For the Shira amphiboles therefore, the major substitutional scheme is as follows:-



This equation is balanced to within 0.3 of a charge although there is an apparent decrease in the number of cations from left to right, i.e. from ferrichterite towards arfvedsonite.

Other substitutional schemes which can be written are as follows:-



which is balanced to within 0.1 of a charge, although there is an apparent increase in the number of cations from 1 to 1.7.

The equation:-



is balanced to within 0.2 of a charge, while the cations apparently increase from 1.3 to 2.8.

Formulation of further coupled substitutions has proved almost impossible for electrical, if not cationic, balance to be retained. This situation contrasts markedly with that in the pyroxenes where electrical

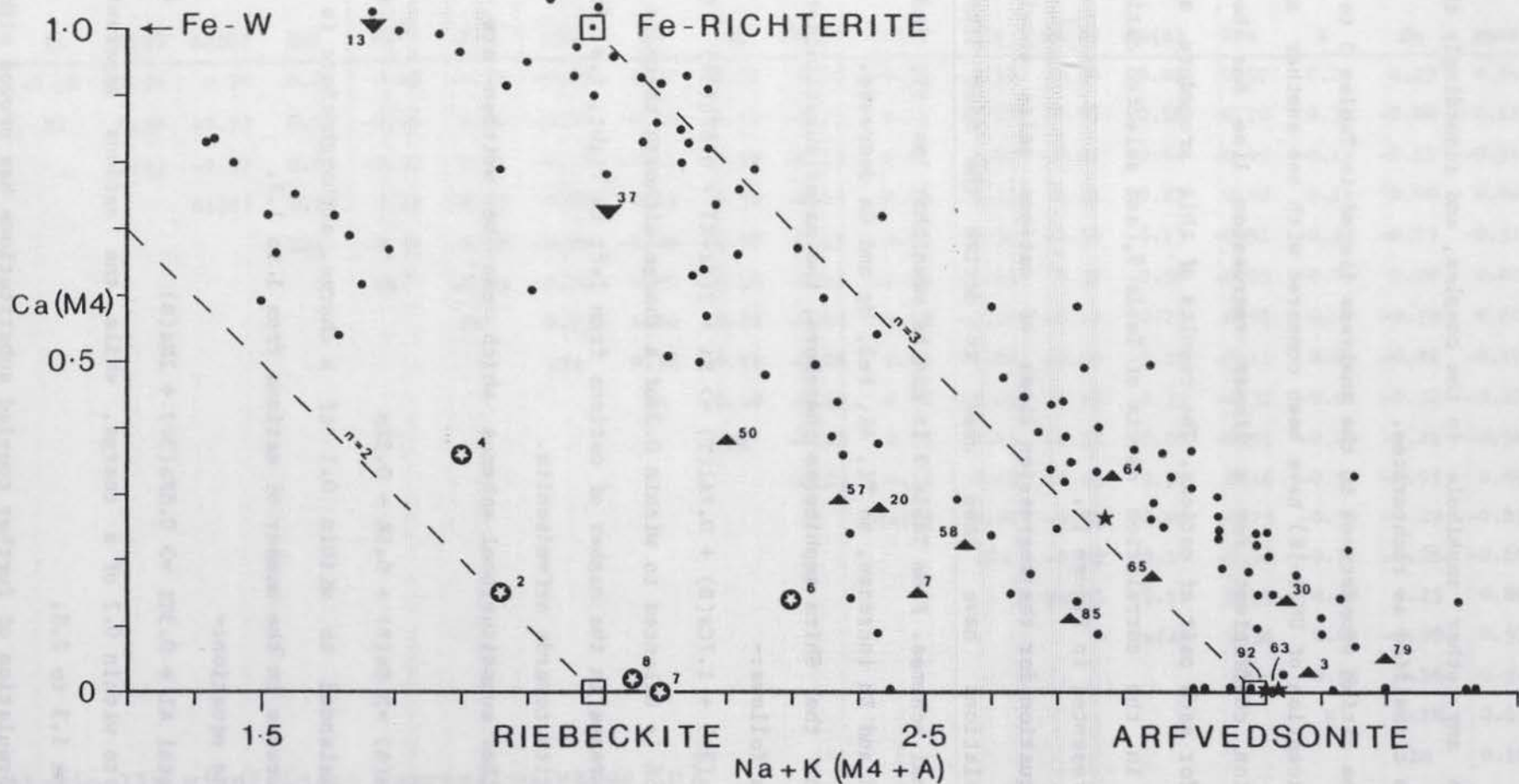


Figure 11. Ca v alkalis summary diagram for amphiboles from the Shira complex and elsewhere. Dots = Shira analyses. Upright and inverted triangles = arfvedsonite and ferrorichterite respectively (Borley, 1963b). Solid stars = arfvedsonite from Ailsa Craig (this work). Open stars = riebeckites from New Hampshire (Lyons, 1976).

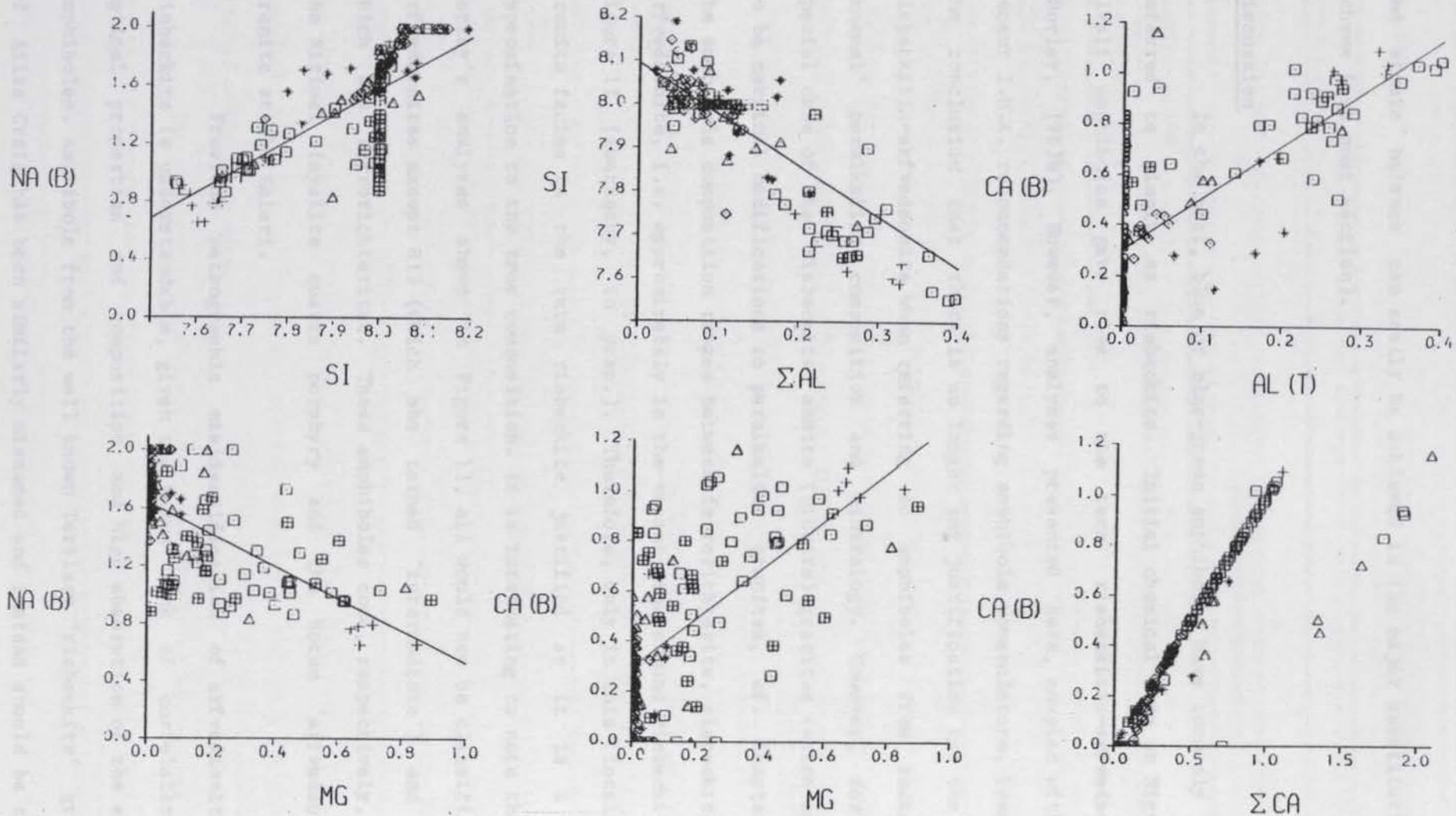


Figure 12. Cartesian diagrams of selected elements in amphiboles from the Shira complex and elsewhere in Nigeria. Stars = data from Borley (1963b). Crosses = Zigau granite porphyry. Plain squares = Shira quartz syenite. Diamonds = Birji granite. Triangles = Amdulayi granite. Squares with crosses = Amdulayi syenite/quartz granite.

and atomic balance can easily be achieved in the major substitutional scheme (see next section).

Discussion

In the past, blue or blue-green amphiboles have commonly been referred to simply as riebeckite. Initial chemical data on Nigerian alkali amphiboles gave rise to the term riebeckitic-arfvedsonite (Borley, 1963b). However, analyses presented here, coupled with the recent I.M.A. recommendations regarding amphibole nomenclature, lead to the conclusion that there is no longer any justification for the term riebeckitic-arfvedsonite when referring to amphiboles from rocks of 'normal' peralkaline composition and mineralogy. However, for the special case of the 'riebeckite' annite (biotite) granites (which appear to be marginal modifications to peralkaline granites, cf. Chapter 1), the amphibole composition ranges between ferrorichterite, riebeckite and arfvedsonite, i.e. approximately in the vacant area around riebeckite in Figure 11 (Abernethy, in prep.). Therefore, only in this (localised) granite facies is the term riebeckite justified as it is a good approximation to the true composition. It is interesting to note that of Borley's analyses shown in Figure 11, all would now be classified as arfvedsonites except R13 (which she termed 'intermediate') and R37, which are ferrorichterites. These amphiboles come, respectively, from the Ririwai fayalite quartz porphyry and the Hotum 'arfvedsonite' granite at Sha Kaleri.

Previous petrographic misidentification of arfvedsonite for riebeckite is understandable, given the known lack of correlation of optical properties and composition and high absorption of the alkali amphiboles. Amphibole from the well known Tertiary 'riebeckite' granite of Ailsa Craig has been similarly misnamed and instead should be termed arfvedsonite (Figure 11 and Table 10). In fact, it has proved difficult

Table 10 Electron microprobe analyses of amphibole from Ailsa Craig, W.Scotland

Sample no.	AC14			Formulae for 23 oxygens			
Crystal no.	1	2	3				
Spot no.	ACM1	ACM3	ACM4	ACM1	ACM3	ACM4	
SiO ₂	50.36	49.19	50.97	Si	8.149	8.005	8.179
TiO ₂	0.87	1.12	1.61	Al[IV]	-	-	-
Al ₂ O ₃	0.42	0.57	0.25	Fe ³	-	-	-
FeO _T	32.39	33.85	31.78	Σ T	8.149	8.005	8.179
MnO	0.90	0.96	0.97	Al[VI]	0.080	0.109	0.047
MgO	0.04	0.02	0.02	Ti	0.106	0.137	0.194
CaO	1.19	1.48	0.71	Fe ³	0.279	0.226	0.295
Na ₂ O	8.93	8.28	8.84	Zr	0.026	0.014	0.020
K ₂ O	1.04	1.26	1.34	Mg	0.010	0.005	0.005
ZnO	0.11	0.14	0.16	Zn	0.013	0.017	0.019
ZrO ₂	0.33	0.17	0.26	Fe ²	4.104	4.381	3.969
F	1.43	1.29	1.26	Mn	0.123	0.111	0.132
Cl	0.04	0.03	0.01	Ca	0.206	-	0.122
less O=F,Cl	0.61	0.55	0.53	Σ C/M ₁₋₃	4.947	5.000	4.803
	97.44	97.81	97.65	Fe ²	-	-	-
Fe ₂ O ₃ ^c	2.29	1.85	2.45	Mn	-	0.021	-
FeO ^c	30.33	32.19	29.58	Ca	-	0.258	-
				Na	2.000	1.721	2.000
				Σ B/M ₄	2.000	2.000	2.000
				Na	0.802	0.892	0.750
				K	0.215	0.262	0.274
				Σ A	1.017	1.154	1.024
				Σ Na+K	3.017	2.875	3.024
				Mg/Mg+Fe ²	0.002	0.001	0.001
				Class.	Alk	Alk	Alk
				Name	A	A	A

to find an occurrence of an amphibole compositional trend towards riebeckite, although a notable example is found in the granites of Massachusetts and Rhode Island (Lyons, 1976). These amphiboles plot close to the ferrowinchite-riebeckite join, as shown in Figure 11 (samples 1, 3 and 5 are not plotted because they are partial analyses only).

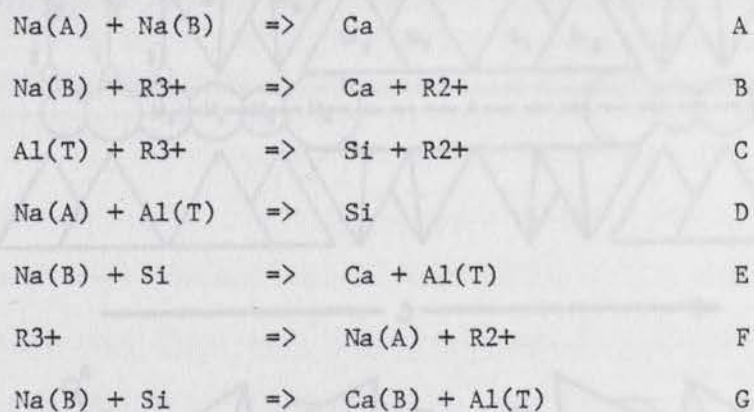
From a comparison of the theoretical end-member formulae for ferrorichterite ($\text{Na}_2\text{CaFe}^{2+}_5\text{Si}_8\text{O}_{22}(\text{OH})_2$) and arfvedsonite ($\text{NaNa}_2\text{Fe}^{2+}_4\text{Fe}^{3+}\text{Si}_8\text{O}_{22}(\text{OH})_2$) it is expected that arfvedsonite would contain more Fe^{3+} than ferrorichterite. Although there are limitations to the $\text{Fe}^{3+}/\text{Fe}^{2+}$ recalculation procedure (as discussed in Appendix 3), none of the ferrorichterites from the Shira quartz syenite have any calculated Fe^{3+} . By contrast, 70% of the arfvedsonites from the Birji granite have some calculated Fe^{3+} .

The disparity in amphibole compositions (from granite rather than dyke samples) from the Andaburi granite cannot be satisfactorily resolved at present. Both polished thin sections used for mineral analysis came from the eastern portion of the granite since samples from the central and western regions had an unsatisfactory polish and were not repeated. However, in the Shira quartz syenite and the Amdulayi syenite, a ferrorichterite to arfvedsonite compositional variation is commonly found in a single zoned crystal; thus it is quite feasible that the present 'compositional break' observed in amphiboles from the Andaburi granite is apparent rather than real, and is a function of limited analytical data.

The scatter of data about idealised linear relationships (even though the correlation coefficient may be quite high), together with known uncertainties regarding the calculated $\text{Fe}^{3+}/\text{Fe}^{2+}$ ratio and the complexity of coupled substitutions involving a total of 16 cations distributed among four different types of sites (T, M1-3 (or C), M4 (or

B) and A), perhaps combine to preclude the definition of simple substitutional schemes balanced in terms of charge and number cations, as in the case of the pyroxenes.

However, with these problems in mind, from equations 1 to 3 and Table 9, certain possible coupled substitutions which have been suggested, for example, by Fabriès (1966, 1978) can be considered. Fabriès proposes the following substitutional schemes between calcic and alkali amphiboles;-



From equations 1-3 and Table 9, scheme A is not appropriate to the Shira amphiboles because there is only a poor correlation between Na(A) and total Ca (0.14), although the substitution of Na(B) for total Ca has a good correlation (-0.79). In other words, an increase of Na in the B site for Ca occurs independently of Na in the A site. However, there is a good correlation between total Ca and K (-0.76) and so it is possible to restate equation (A) as:-



From equation (1) it can be seen that scheme B of Fabriès is valid here and has the form;-



Sodium and Si increase as Ca and Al(T) decrease in the Shira amphiboles and so scheme E is also appropriate. Since Al and Fe³⁺ have a negative relationship, scheme C is not appropriate nor are schemes D or F. Fabriès (1978) suggests that the substitution scheme G governs the

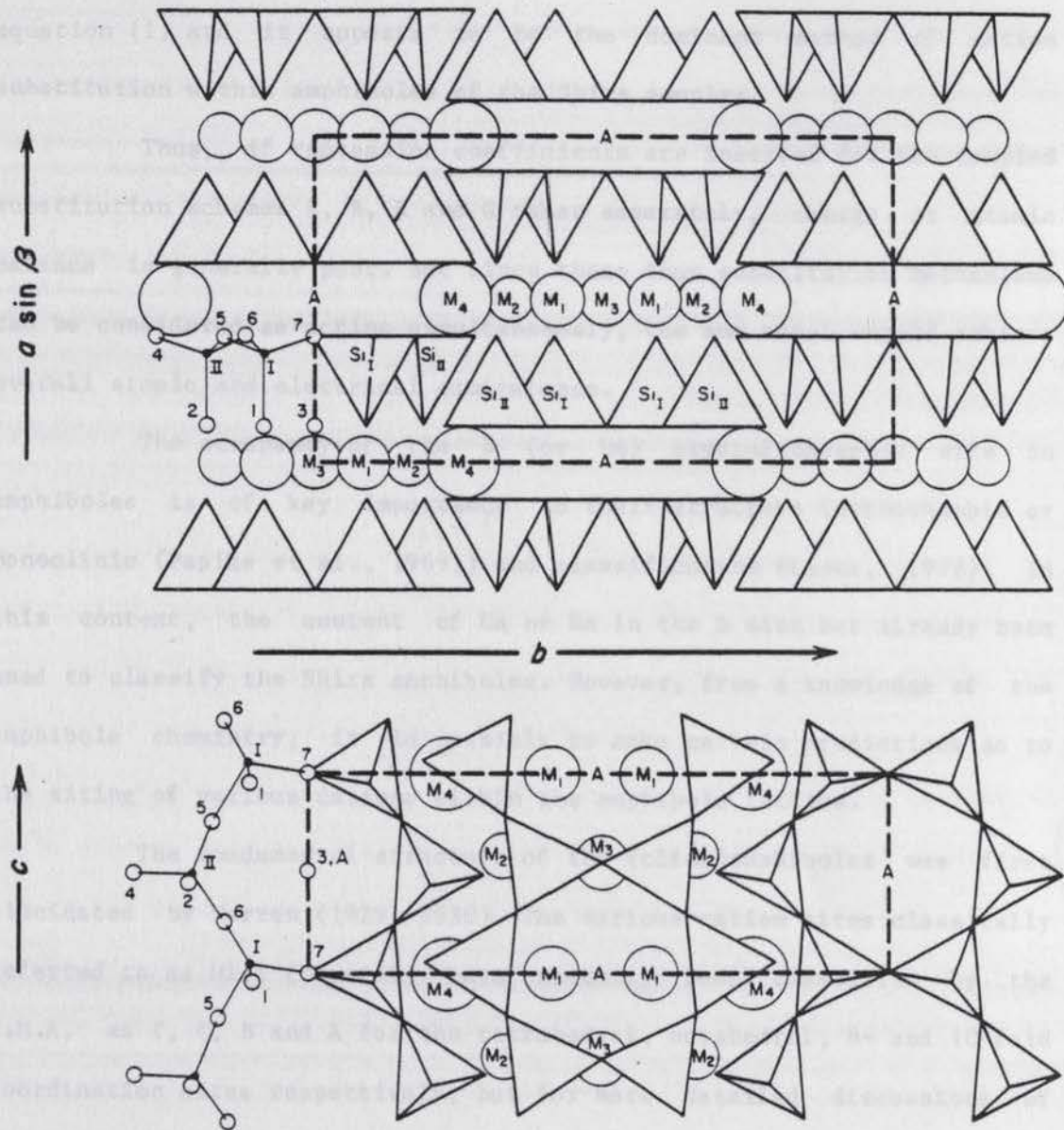


Figure 13. Schematic diagram for the structure of an amphibole (from Ernst, 1962). M_1-3 = octahedral sites. M_4 = 8-fold sites. A = 10-12-fold sites.

series hastingsite - taramite - katophorite - ferrorichterite - arfvedsonite. This scheme is essentially a simplified version of equation (1) and it appears to be the dominant method of cation substitution within amphiboles of the Shira complex.

Thus, if regression coefficients are inserted for the coupled substitution schemes A, B, E and G taken separately, charge or atomic balance is generally poor. But since these four substitution mechanisms can be considered as acting simultaneously, the sum total should achieve overall atomic and electrical equivalence.

The occupancy of the B (or M4) crystallographic site in amphiboles is of key importance to their structure (orthorhombic or monoclinic (Papike et al., 1969)) and classification (Leake, 1978). In this context, the content of Ca or Na in the B site has already been used to classify the Shira amphiboles. However, from a knowledge of the amphibole chemistry, it is possible to make certain predictions as to the siting of various cations within the amphibole lattice.

The fundamental structure of the (clino)amphiboles was first elucidated by Warren (1929, 1930). The various cation sites classically referred to as M1-4 (M=metal) have recently been classified by the I.M.A. as T, C, B and A for the tetrahedral, octahedral, 8- and 10-fold coordination sites respectively, but for more detailed discussions of site chemistry it is preferable to use the older, more established nomenclature of M(1)-(3) for the five C sites and M4 for the two B sites (see Figure 13). This nomenclature appears to derive from Whittaker (1949), and in general, the M(2) and (adjacent) M(4) sites in the amphiboles may be regarded as equivalent to the M1 and M2 sites respectively, in pyroxenes, while the M(1) and M(3) amphibole sites have no exact parallel since the anion octahedra around them includes hydroxyl or halogens (Whittaker, 1960).

When the M(4) site contains a monovalent ion such as Na, the

neighbouring M2 position is occupied by a trivalent ion to maintain local charge balance, while the octahedral ions will concentrate in the M(1) and M(3) sites (Whittaker, 1949; Ghose, 1966). Such conclusions regarding cation ordering in alkali amphiboles have been confirmed by Mossbauer studies and have shown in addition that in Fe³⁺ rich sodic amphiboles, Fe²⁺ tends to concentrate in M(1) relative to M(3) (Bancroft and Burns, 1969; Ernst and Wai, 1970). In riebeckite, a consideration of mean bond lengths has led to the conclusion that tetrahedral Al is strongly favoured in the T1 site, while octahedral trivalent ions are ordered into M(2), and Fe³⁺ in excess of that required to fill M(2) is favoured in M(1). In addition, octahedral Mn and Li are preferentially ordered in M(3) (Addison and White, 1968; Hawthorne, 1978). It is noticeable therefore, that the small Li cation probably occurs in the M(1) and M(3) octahedral sites rather than occurring in the larger M4 site where the similarly charged Na cation is found.

For arfvedsonite, trivalent cations are similarly considered to be ordered into the M(2) site while any small amount of Mg occurs in the M(1) site (Hawthorne, 1976). Hawthorne (op.cit.) also comes to the important conclusion that the sum of the normally accepted M(1)-(3) cations is <5 for arfvedsonite amphiboles and that this deficiency is about equal to excess (B+A) cations above 3.0. Therefore, he believes that in the special case of arfvedsonitic amphiboles, Ca may enter the M(1)-(3) sites.

There have been several experimental studies on the stability of alkaline amphiboles. Sodium-Mg amphiboles are readily synthesised hydrothermally at 6-700 degrees C and 3 kb water pressure in only six hours (Gier et al., 1964). 'Magnesioriebeckite' is stable at quite low temperature as indicated by its occurrence as blue authigenic overgrowths on detrital hornblende in the highly saline Green River formation (Milton and Eugster, 1959). Although authigenic, this

occurrence probably did not have a high f_{O_2} however (despite the presence of some Fe^{3+}), since a variety of sulphides and hydrocarbons are present. Later research has shown that the amphibole is more correctly termed magnesioarfvedsonite (Milton, 1974). Experimental work on magnesioriebeckite has confirmed that it is also stable at magmatic temperatures (Ernst, 1960). The Fe end-member riebeckite is however, less stable and decomposes at only 469 degrees C (at 0.25 kb P(f)) at an f_{O_2} controlled by the MH (magnetite-haematite) oxygen buffering pair (Ernst, 1962). This study also showed that as f_{O_2} decreased, so the amphibole became more arfvedsonitic (i.e. $Fe^{3+} = Fe^{2+} + Na$) and the intermediate riebeckite-arfvedsonite (arfvedsonite 40%, riebeckite 60%, approx.) was found to be stable up to 690 degrees C (1 kb P(f)) with the IW (iron-wustite) oxygen buffer. Ernst's results therefore indicate that as f_{O_2} decreases, the amphibole becomes more sodic and that despite the theoretical presence of approximately 30% of the iron as Fe^{3+} , arfvedsonitic amphibole is stable at extremely low oxygen pressures. Also, it appears that whereas an arfvedsonitic amphibole may crystallise at magmatic temperatures, riebeckite probably does not.

From richterite (the Mg end-member) to ferrorichterite, there is a predictable decrease in the maximum thermal stability limit from 1030 degrees C to 760 degrees C (WM buffer) and ferrorichterite (which theoretically has no Fe^{3+}) is most stable only at very low f_{O_2} , below the IW buffer curve (Charles, 1975). In fact, Charles found that ferrorichterite was very susceptible to changes in f_{O_2} ; at 1 kb P(H_2O) using the IW buffer it is stable to about 720 degrees C, whereas at the slightly higher f_{O_2} conditions of the QFM buffer it has a maximum stability of only about 530 degrees C (at 1 kb P(t)). In a more detailed consideration of richterite-ferrorichterite stability, Charles (1977) concluded that crystallisation of members of this series is favoured by a peralkaline environment which usually has normative quartz, a high

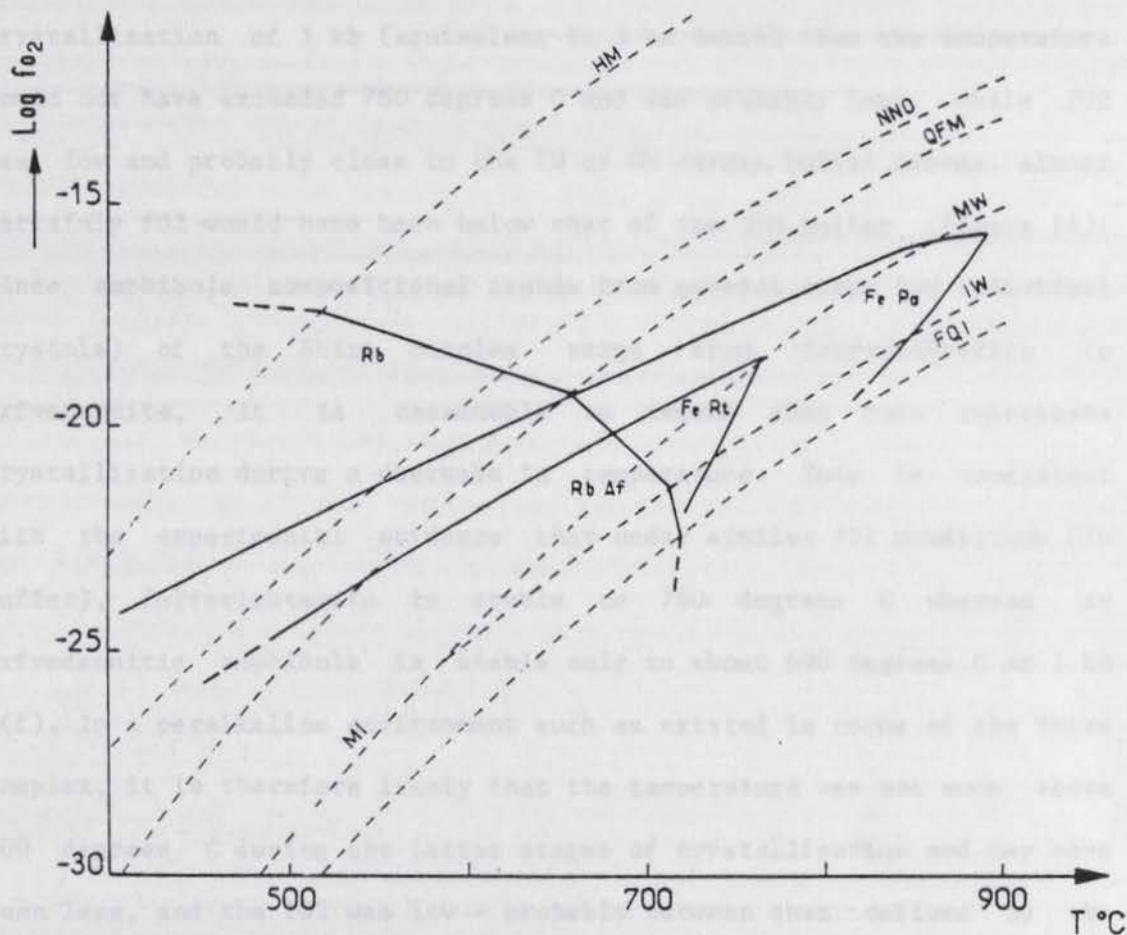


Figure 14. Temperature-oxygen fugacity diagram for alkali amphiboles. Rb = riebeckite. RbAf = riebeckitic arfvedsonite. FeRt = ferrorichterite. FePa = ferropargasite. Dashed lines are standard buffer curves (from Fabriès, 1978).

For example, in what variations can take place? How rigid are stability fields? (having compositions $\text{Rb}_{73}\text{Ac}_{27}$) are quite distinct from amphiboles from the Tighoudji complex in Niger, which show a ferrorichterite/arfvedsonite-riebeckite trend (Fabriès and Zanzi, 1972). As the experiments of Emat (1962) demonstrate, riebeckite is

volatile content and low fO_2 . Since, in rocks of the Shira complex, ferrichterite usually crystallised as an interstitial mineral, the experiments cited above allow some estimates of temperature and fO_2 for the latter stages of crystallisation. Assuming a pressure of final crystallisation of 1 kb (equivalent to 3 km depth) then the temperature could not have exceeded 760 degrees C and was probably less, while fO_2 was low and probably close to the IW or WM oxygen buffer curves. Almost certainly fO_2 would have been below that of the QFM buffer (Figure 14). Since amphibole compositional trends from several rocks (or individual crystals) of the Shira complex range from ferrichterite to arfvedsonite, it is reasonable to assume that this represents crystallisation during a decrease in temperature. This is consistent with the experimental evidence that under similar fO_2 conditions (IW buffer), ferrichterite is stable to 760 degrees C whereas an arfvedsonitic amphibole is stable only to about 690 degrees C at 1 kb P(f). In a peralkaline environment such as existed in rocks of the Shira complex, it is therefore likely that the temperature was not much above 700 degrees C during the latter stages of crystallisation and may have been less, and the fO_2 was low - probably between that defined by the QFM and MW or IW buffers.

Among other natural occurrences of alkali amphiboles it is difficult to make comparisons with the amphiboles discussed here, in the absence of precise compositions. However, a late stage pegmatitic/hydrothermal environment has been proposed for many so-called riebeckites (Phillips, 1926; Naganna, 1972; Fabriès and Rocci, 1972). For example, riebeckite from vein pegmatites in Precambrian granites in Mauritania (having mole proportions $Rb_{75}Arf_{25}$) are quite distinct from amphiboles from the Taghouadji complex in Niger, which show a ferrichterite/ferrowinchite-arfvedsonite trend (Fabriès and Rocci, 1972). As the experiments of Ernst (1962) demonstrate, riebeckite is

stable at lower temperature and higher fO_2 than arfvedsonite or ferrichterite, and so the absence of riebeckite in the majority of peralkaline granites of Niger-Nigeria is significant. However, riebeckitic amphiboles do occur in one particular alkaline/peralkaline granite in this province - the so-called riebeckite biotite granites or more correctly, the riebeckite annite granites (Abernethy, in prep.). These granites are unusual in that they appear to be marginal modifications of peralkaline granites (see Chapter 1) and may have a peralkalinity index (P.I.) either less than or greater than unity. The compositions of these 'riebeckites' define a trend away from the (magmatic) ferrichterite-arfvedsonite trend, and range from low Ca ferrichterites towards riebeckite, and have recently been interpreted as reflecting conditions of increasing oxidation (Abernethy, in prep.). The experimental evidence together with the field occurrence both tend to support such an interpretation.

Summary and conclusions

The dominant compositional trend shown by amphiboles from peralkaline rocks of the Shira complex and elsewhere in the Niger-Nigeria province (Borley, 1963b; Fabries and Rocci, 1965) is from ferrichterite to arfvedsonite or, in certain instances, from ferrowinchite to arfvedsonite. In fact, this trend may be typical of peralkaline rocks in a low P, anorogenic setting (Creasy, 1974; Giret et al., in prep.). The conditions of formation in terms of temperature and fO_2 (at 1 kb assumed) probably did not exceed 760 degrees C and the QFM buffer respectively, and may have been less. Amphibole zonation from ferrichterite to arfvedsonite indicates that the remaining Ca in the residual liquid was being rapidly depleted and the liquid was becoming increasingly peralkaline. Possibly the late magmatic to postmagmatic liquid was sufficiently peralkaline enabling aegirine to crystallise in

preference to arfvedsonite (Chapter 3). Alternatively or possibly in addition, the relative oxidation conditions (although fO_2 presumably decreases with falling temperature) were somewhat higher in the late stages of crystallisation or in the postmagmatic environment.

4.3 Pyroxene

Eighty microprobe analyses of clinopyroxenes from 69 crystals in rocks of the Shira complex are presented in Tables 11-14 together with structural formulae based upon 6 oxygens including calculated ferric iron contents (Appendix 3). The majority of these pyroxenes are alkaline and so the Di-Hd-Fs-En quadrilateral is not a suitable projection; the Na-Fe-Mg triangular diagram is therefore used as well (Figure 16). On the latter diagram the field of aegirine-augite analyses from Deer et al. (1978) is indicated, and clearly there is very little overlap with pyroxenes from the Shira complex. Under the existing classification scheme the Shira pyroxenes with Fe^{3+} contents between 0.2 and 0.8 cations (per 6 oxygens) would be termed aegirine-augites (Deer et al., 1978). The Shira pyroxenes are intermediate between ferroaugite/ferrohedenbergite and aegirine but the term aegirine-augite is clearly inappropriate as Figure 16 indicates.

A further difficulty with the existing nomenclature is that although the prefixes sodic or sodian are commonly used, there does not appear to be a strict definition. For these reasons the writer has devised a simple classification scheme based upon the commonly used Na-Fe-Mg triangular diagram, and the various fields are outlined in Figure 16. The basis of this scheme is the Na content (after summing $Na+(Fe(2+)+Mn)+Mg$ to 100); those pyroxenes with <10% Na are named

according to their position in the normal quadrilateral, those with 10-20% Na are the sodian equivalents and those with >80% Na are aegirines. For pyroxenes with Na values between 20% and 80% Na the nomenclature depends on the Mg content as shown in Figure 16. In cases where there is <10% Mg, the term aegirine-hedenbergite is suggested. The Na-Fe-Mg diagram (where Mn is understood to be combined with Fe₂) is not new, neither is the term aegirine-hedenbergite (von Wolff, 1904; Larsen, 1976) but the combination of both within this classification scheme does appear to be original.

Data from the Shira complex (Figures 15 and 16) are notable in that they comprise three apparently distinct groups - a feature to which later reference will be made. These three groups can be broadly classified as ferroaugite-ferrohedenbergite, aegirine-hedenbergite and aegirine. The first group is also plotted on a pyroxene quadrilateral (Figure 15) where it forms an approximately linear trend close to the ferrosalite/ferroaugite and hedenbergite/ferrohedenbergite boundaries. All the pyroxenes from this group come from the Zigau granite porphyry, and from enclaves of the Zigau granite porphyry and the Amdulayi syenite. The major rock types within the complex therefore contain only alkali pyroxenes; except for highly sodic rims to ferrohedenbergites, aegirine-hedenbergites are found entirely from the Shira quartz syenite and the Amdalayi syenite. Pyroxenes from the Birji and Andaburi granites are aegirine only.

Pyroxene phenocrysts or inclusions within alkali feldspar in the Zigau granite porphyry are commonly zoned with colourless cores and dark green rims. These rims are enriched in Na and Fe³⁺ relative to the cores and plot in the sodian ferrohedenbergite or just into the aegirine-hedenbergite field in Figure 16. Within the melanocratic enclaves at Zigau however, the pyroxenes are generally more magnesian and less sodic.

Table II Electron microprobe analyses of pyroxenes from the Zigau granite porphyry

Sample no.	ZG/2C				ZG/2B			
	within K-feldspar				within K-feldspar			
Crystal no.	1	2	3	4				
Spot no.	Hd1	Hd2	Hd3	Hd4	Hd5	Hd6	Hd7	Hd8
	green margin	core	green margin	core	unzoned core	unzoned margin	green margin	core
SiO ₂	48.63	47.76	47.93	47.15	46.82	47.25	49.00	47.56
TiO ₂	0.39	0.36	0.19	0.82	0.34	0.74	0.24	0.67
Al ₂ O ₃	0.24	0.30	0.22	0.91	0.27	0.78	0.35	0.62
FeO _T	29.76	31.18	29.55	31.04	28.66	29.96	28.68	30.29
MnO	0.74	1.02	0.79	1.02	1.07	1.05	1.03	1.11
MgO	0.18	0.12	0.28	0.14	1.46	0.86	0.54	0.60
CaO	15.30	19.00	17.06	19.19	19.58	19.28	19.20	19.15
Na ₂ O	3.45	0.46	1.27	0.46	0.33	0.34	0.44	0.34
K ₂ O	0.03	0.03	0.03	0.02	0.02	0.04	0.00	0.00
ZnO	0.07	0.07	0.07	0.06	0.04	0.05	0.02	0.04
ZrO ₂	0.16	0.05	0.05	-	-	-	-	-
	<u>98.95</u>	<u>100.35</u>	<u>97.44</u>	<u>100.81</u>	<u>98.59</u>	<u>100.35</u>	<u>99.50</u>	<u>100.38</u>
Fe ₂ O ₃ ^c	8.41	0.86	2.47	0.91	0.55	0.57	0.09	0.47
FeO ^c	22.19	30.40	27.32	30.22	28.16	29.45	28.60	29.87
Formulae on the basis of 6 oxygens								
Si	1.984	1.977	2.013	1.943	1.961	1.949	2.018	1.962
Al ^[IV]	0.012	0.015	-	0.044	0.013	0.038	-	0.030
Fe ³	0.004	0.008	-	0.013	0.017	-	-	0.008
Σ T	<u>2.000</u>	<u>2.000</u>	<u>2.013</u>	<u>2.000</u>	<u>1.991</u>	<u>1.987</u>	<u>2.018</u>	<u>2.000</u>
Al ^[VI]	-	-	0.011	-	-	-	0.017	-
Ti	0.012	0.011	0.006	0.025	0.011	0.023	0.007	0.021
Fe ³	0.254	0.019	0.078	0.015	-	0.003	0.003	0.004
Zr	0.003	0.001	0.001	-	-	-	-	-
Mg	0.011	0.007	0.018	0.009	0.091	0.053	0.033	0.037
Zn	0.002	0.002	0.002	0.002	0.001	0.002	0.001	0.001
Fe ²	0.718	0.960	0.884	0.949	0.906	0.919	0.939	0.937
Mn	-	-	-	-	-	-	-	-
Ca	-	-	-	-	-	-	-	-
Σ M1	<u>1.000</u>	<u>1.000</u>	<u>1.000</u>	<u>1.000</u>	<u>1.000</u>	<u>1.000</u>	<u>1.000</u>	<u>1.000</u>
Fe ²	0.039	0.093	0.076	0.093	0.081	0.097	0.046	0.093
Mn	0.026	0.036	0.028	0.036	0.038	0.037	0.036	0.039
Ca	0.669	0.843	0.768	0.847	0.879	0.852	0.847	0.846
Na	0.273	0.037	0.103	0.037	0.027	0.027	0.035	0.027
K	0.002	0.002	0.002	0.001	0.001	0.002	-	-
Σ M2	<u>1.009</u>	<u>1.011</u>	<u>0.977</u>	<u>1.014</u>	<u>1.026</u>	<u>1.015</u>	<u>0.964</u>	<u>1.005</u>
Na + Fe ³	0.527	0.056	0.181	0.052	0.027	0.030	0.038	0.031
Class.	A-H	PH	NaPH	PH	H	PH	PH	PH
Wo	-	44.29	44.00	44.66	44.92	44.36	45.42	44.23
En	-	0.39	1.00	0.45	4.66	2.75	1.78	1.93
Fs	-	55.32	55.00	54.89	50.43	52.89	52.81	53.85

Table II continued. Electron microprobe analyses of pyroxenes from the Zigau granite porphyry

Sample no.	ZG/2C								ZG/2C xenolith								ZG/2D			
	within alkali feldspar				matrix				phenocrysts				within alkali feldspar		phenocryst					
	5	6	7	8	9	10	11	12	13	14	15	16	17							
Crystal no.	5		6		7		8		9	10	11	12	13		14		15	16	17	
Spot no.	PX1 core	PX2 margin	PX3 core	PX4 margin	PX5 core	PX6 margin	PX7 core	PX8 margin	PX9	PX10	PX11	PX12	PX13 core	PX14 margin	PX15 core	PX16 margin	PX17	PX18	PX19 core	PX20 margin
SiO ₂	47.68	48.56	48.06	49.09	47.89	47.18	46.95	47.62	48.03	48.96	49.18	49.03	49.65	49.06	49.06	49.50	48.77	48.52	47.97	48.13
TiO ₂	0.44	0.25	0.87	0.24	0.44	0.40	0.50	0.31	0.51	0.45	0.21	0.21	0.79	1.66	0.19	0.14	0.41	0.26	0.82	0.88
Al ₂ O ₃	0.49	0.00	1.19	0.00	0.41	0.32	0.36	0.00	0.46	0.40	0.15	0.16	0.86	1.50	0.17	0.00	0.00	0.00	0.93	1.01
FeO _T	31.28	29.89	28.36	30.12	30.75	30.92	30.96	30.44	24.33	25.06	26.62	25.02	24.52	22.43	27.72	28.95	29.00	30.15	27.99	28.53
MnO	1.03	0.73	1.10	0.67	1.05	0.93	0.88	0.96	0.80	0.84	0.59	0.76	0.86	0.68	0.75	0.78	0.94	0.75	0.96	1.03
MgO	0.38	0.19	1.75	0.32	0.37	0.24	0.00	0.00	3.69	3.56	2.42	4.12	4.91	5.21	1.55	1.53	0.96	0.55	2.06	1.94
CaO	18.63	15.09	19.15	16.57	19.08	18.61	18.38	18.65	19.12	18.82	16.73	18.76	19.14	18.40	17.19	18.87	17.57	19.62	19.41	19.60
Na ₂ O	0.38	3.23	0.30	2.76	0.47	0.67	0.46	0.50	0.56	0.93	2.46	0.74	0.31	1.08	2.69	1.21	2.06	0.56	0.00	0.59
	100.31	97.94	100.78	99.77	100.46	99.27	98.49	98.48	97.50	99.02	98.36	98.80	101.04	100.02	99.32	100.98	99.71	100.41	100.14	101.71
Fe ₂ O ₃ ^c	0.87	7.82	0.30	6.63	0.97	1.43	0.75	0.67	1.02	1.93	5.98	1.74	0.03	0.92	6.82	2.84	4.49	0.92	0.00	1.34
FeO ^c	30.50	22.85	28.09	24.15	29.87	29.63	30.29	29.84	23.41	23.33	21.24	23.46	24.50	21.60	21.59	26.40	24.96	29.32	27.99	27.31
Formulae on the basis of 6 oxygens																				
Si	1.971	2.001	1.952	1.994	1.974	1.970	1.979	2.002	1.980	1.984	1.996	1.990	1.968	1.943	1.983	1.996	1.989	1.994	1.959	1.937
Al ^[IV]	0.024	-	0.048	-	0.020	0.016	0.018	-	0.020	0.016	0.004	0.008	0.032	0.057	0.008	-	-	-	0.041	0.048
Fe ³	0.005	-	-	0.006	0.006	0.014	0.003	-	-	-	-	0.002	-	-	0.009	0.004	0.011	0.006	-	0.015
T	2.000	2.001	2.000	2.000	2.000	2.000	2.000	2.002	2.000	2.000	2.000	2.000	2.000	2.000	2.000	2.000	2.000	2.000	2.000	2.000
Al ^[VI]	-	-	0.009	-	-	-	-	-	0.002	0.003	0.003	-	0.008	0.013	-	-	-	-	0.004	-
Ti	0.014	0.008	0.027	0.007	0.014	0.013	0.016	0.010	0.016	0.014	0.006	0.006	0.024	0.049	0.006	0.004	0.013	0.008	0.025	0.027
Fe ³	0.022	0.243	0.009	0.197	0.024	0.031	0.021	0.021	0.032	0.059	0.182	0.051	0.001	0.028	0.198	0.082	0.127	0.023	0.000	0.026
Mg	0.023	0.012	0.106	0.019	0.023	0.015	-	-	0.227	0.215	0.146	0.249	0.290	0.308	0.093	0.092	0.058	0.034	0.125	0.116
Fe ²	0.941	0.737	0.849	0.777	0.939	0.941	0.963	0.969	0.723	0.709	0.663	0.694	0.677	0.602	0.703	0.822	0.802	0.935	0.846	0.831
Mn	-	-	-	-	-	-	-	-	-	-	-	-	-	-	-	-	-	-	-	-
M1	1.000	1.000	1.000	1.000	1.000	1.000	1.000	1.000	1.000	1.000	1.000	1.000	1.000	1.000	1.000	1.000	1.000	1.000	1.000	1.000
Fe ²	0.113	0.050	0.105	0.044	0.091	0.094	0.105	0.080	0.084	0.082	0.058	0.102	0.135	0.114	0.027	0.068	0.049	0.073	0.110	0.089
Mn	0.036	0.025	0.078	0.023	0.037	0.033	0.031	0.034	0.028	0.029	0.020	0.026	0.029	0.023	0.026	0.027	0.032	0.026	0.033	0.035
Ca	0.825	0.666	0.833	0.721	0.843	0.833	0.830	0.840	0.844	0.817	0.727	0.816	0.813	0.781	0.745	0.815	0.768	0.864	0.849	0.845
Na	0.030	0.258	0.024	0.217	0.038	0.054	0.038	0.041	0.045	0.073	0.194	0.058	0.024	0.083	0.211	0.095	0.163	0.045	0.000	0.046
M2	1.004	0.999	1.000	1.005	1.009	1.014	1.004	0.995	1.001	1.001	0.999	1.002	1.001	1.001	1.009	1.005	1.012	1.008	0.992	1.015
Na + Fe ³	0.052	0.501	0.033	0.414	0.062	0.085	0.059	0.062	0.077	0.132	0.376	0.109	0.025	0.111	0.409	0.177	0.290	0.068	0.000	0.072
Class.	PH	A-H	PH	A-H	PH	PH	PH	PH	FA	FA	NaH	FA	FA	FA	A-H	H	NaH	H	PH	PH
Wo	43.36	-	44.01	-	44.46	44.23	43.74	44.47	44.96	44.83	45.62	43.83	42.45	43.29	-	45.36	45.77	45.34	43.99	44.93
En	1.23	-	5.59	-	1.20	0.79	0.00	0.00	12.07	11.80	9.18	13.39	15.15	17.05	-	5.12	3.48	1.77	6.49	6.19
Fs	55.41	-	50.39	-	54.34	54.98	56.26	55.53	42.97	43.37	45.21	42.78	42.40	39.66	-	49.53	50.75	52.89	49.51	48.88

177

Table 12 Electron microprobe analyses of pyroxenes from Shira alkali feldspar quartz syenite

Sample no.	SH11						SH68/2						SH68/2 xenolith		SH19		SH4		SH105			
Crystal no.	18	19	20	21	22	23	within alkali feldspar						29	30	31	32	33		34			
	PX21	PX22	PX23	PX24	PX25	PX26	PX27	PX28	PX29	PX30	PX31	PX32	PX33	PX34	PX35	AG9	AG10	AG11	AG12	AG13	AG14	
Spot no.							core	margin	core	core	core	core	margin	core	margin				green	green	brown	
SiO ₂	52.77	53.32	51.64	52.34	52.23	52.54	50.71	50.73	50.66	50.70	50.10	50.35	49.89	50.26	50.14	50.81	51.15	51.62	50.41	50.48	51.98	
TiO ₂	3.92	0.95	1.55	2.77	1.91	1.05	0.38	0.42	0.47	0.43	0.36	0.38	0.38	0.44	0.27	1.77	3.78	4.46	1.09	0.85	2.46	
Al ₂ O ₃	0.29	0.47	0.36	0.24	0.30	0.49	0.28	0.19	0.26	0.27	0.00	0.25	0.23	0.16	0.16	0.20	0.27	0.16	0.16	0.21	0.44	
FeO ^T	26.99	29.19	28.79	27.38	28.09	29.23	28.92	28.61	28.61	28.74	28.24	28.71	28.93	28.15	28.01	27.97	27.54	26.40	27.18	28.00	27.92	
MnO	0.33	0.38	0.27	0.29	0.22	0.28	0.63	0.61	0.79	0.65	0.83	0.75	0.87	0.69	0.81	0.13	0.21	0.28	0.43	0.47	0.18	
MgO	0.14	0.25	0.20	0.00	0.17	0.16	0.61	0.60	0.87	0.51	0.62	0.79	0.72	1.02	1.03	0.04	0.03	0.19	0.19	0.25	0.11	
CaO	2.61	1.19	5.11	3.01	4.85	1.22	11.29	10.78	13.33	11.59	13.24	13.03	13.38	13.60	13.59	1.33	1.99	2.49	8.15	9.89	1.72	
Na ₂ O	12.77	13.34	10.99	12.17	11.50	13.42	6.96	7.14	5.50	6.39	5.46	5.87	5.34	5.36	5.08	11.66	11.84	11.99	8.63	7.67	11.87	
K ₂ O	-	-	-	-	-	-	-	-	-	-	-	-	-	-	-	0.02	0.02	0.03	0.02	0.03	0.02	
ZnO	-	-	-	-	-	-	-	-	-	-	-	-	-	-	-	0.00	0.00	0.07	0.05	0.06	0.03	
ZrO ₂	-	-	-	-	-	-	-	-	-	-	-	-	-	-	-	1.61	1.49	0.13	1.98	1.22	0.10	
	99.82	99.09	98.85	98.20	99.27	98.39	99.78	99.08	100.49	99.28	98.85	100.13	99.74	99.68	99.09	95.54	98.32	97.82	98.29	99.13	96.83	
Fe ₂ O ₃ ^C	25.52	32.00	25.69	25.44	26.28	32.48	17.61	17.86	13.64	15.31	13.35	14.76	13.36	13.18	12.71	26.19	23.00	22.16	19.75	17.82	24.95	
FeO ^C	4.03	0.40	5.68	4.49	4.44	0.00	13.07	12.54	16.34	14.96	16.23	15.43	16.91	16.29	16.57	4.40	6.84	6.46	9.41	11.97	5.47	
Formulae on the basis of 6 oxygens																						
Si	1.981	1.996	1.979	2.000	1.983	1.983	1.981	1.990	1.985	1.998	1.997	1.978	1.978	1.986	1.994	2.022	1.993	1.992	2.007	1.999	2.014	
Al ^[IV]	0.013	0.004	0.014	-	0.013	0.017	0.013	0.009	0.012	0.002	-	0.012	0.011	0.007	0.006	-	0.007	0.007	-	0.001	-	
Fe ³	0.006	-	0.007	-	0.004	-	0.006	0.001	0.003	-	0.003	0.010	0.011	0.007	-	-	-	0.001	-	-	-	
T	2.000	2.000	2.000	2.000	2.000	2.000	2.000	2.000	2.000	2.000	2.000	2.000	2.000	2.000	2.000	2.022	2.000	2.000	2.007	2.000	2.014	
Al ^[VI]	-	0.017	-	0.011	-	0.005	-	-	-	0.011	-	-	-	-	0.001	0.009	0.005	-	0.008	0.009	0.020	
Ti	0.111	0.027	0.045	0.080	0.055	0.030	0.011	0.012	0.014	0.013	0.011	0.011	0.011	0.013	0.008	0.053	0.111	0.129	0.033	0.025	0.072	
Fe ²	0.715	0.902	0.734	0.732	0.747	0.923	0.512	0.526	0.402	0.454	0.398	0.426	0.388	0.385	0.380	0.784	0.674	0.645	0.594	0.531	0.728	
Zr	-	-	-	-	-	-	-	-	-	-	-	-	-	-	-	0.033	0.030	0.003	0.040	0.024	0.002	
Mg	0.008	0.014	0.011	-	0.010	0.009	0.036	0.035	0.051	0.030	0.037	0.046	0.043	0.060	0.061	0.002	0.002	0.011	0.011	0.015	0.006	
Zn	-	-	-	-	-	-	-	-	-	-	-	-	-	-	-	-	-	0.002	0.002	0.002	0.001	
Fe ²	0.126	0.012	0.182	0.143	0.141	-	0.427	0.412	0.533	0.492	0.541	0.507	0.558	0.538	0.550	0.119	0.178	0.206	0.312	0.396	0.171	
Mn	0.010	0.012	0.009	0.009	0.007	0.009	0.007	0.015	-	0.013	0.010	-	0.004	-	-	-	-	0.004	-	0.002	-	
Ca	0.030	0.016	0.019	0.025	0.040	0.024	-	-	-	-	-	-	-	-	-	-	-	-	-	-	-	
Σ MI	1.000	1.000	1.000	1.000	1.000	1.000	1.000	1.000	1.000	1.000	1.000	1.000	1.000	1.000	1.000	1.000	1.000	1.000	1.000	1.000	1.000	
Fe ²	-	-	-	-	-	-	-	-	0.002	0.001	-	0.003	-	0.001	0.001	0.028	0.045	-	-	-	0.005	
Mn	-	-	-	-	-	-	0.014	0.005	0.026	0.022	0.015	0.015	0.029	0.019	0.027	0.004	0.007	0.005	0.015	0.014	0.006	
Ca	0.075	0.032	0.191	0.098	0.157	0.025	0.473	0.453	0.560	0.489	0.566	0.548	0.569	0.576	0.579	0.057	0.083	0.103	0.348	0.420	0.071	
Na	0.930	0.968	0.817	0.902	0.847	0.982	0.527	0.543	0.418	0.488	0.422	0.447	0.411	0.411	0.392	0.900	0.895	0.897	0.666	0.589	0.892	
K	-	-	-	-	-	-	-	-	-	-	-	-	-	-	-	0.000	0.001	0.002	0.001	0.002	0.001	
Σ MZ	1.005	1.000	1.008	1.000	1.004	1.007	1.014	1.001	1.006	1.000	1.003	1.010	1.012	1.006	1.000	0.989	1.031	1.007	1.030	1.025	0.975	
Na + Fe ³	1.645	1.870	1.551	1.634	1.594	1.905	1.039	1.069	0.820	0.942	0.820	0.873	0.799	0.796	0.772	1.684	1.569	1.543	1.260	1.120	1.620	
Class.	A	A	A	A	A	A	A-H	A-H	A-H	A-H	A-H	A-H	A-H	A-H	A-H	A	A	A	A-H	A-H	A	

In the Shira quartz syenite there is only limited compositional variation within individual crystals and yet the pyroxenes fall into two apparently distinct groups with only slight overlap: aegirine-hedenbergites (AG12-13, PX27-35) and aegirines (AG9-11,14, PX21-26), with only a slight overlap of the 'aegirine' group into the aegirine-hedenbergite field.

For the aegirine-hedenbergites, examination of the polished thin sections shows that analyses PX27-33 are from discrete pyroxene crystals which are enclosed by alkali feldspar in several cases, and analyses AG12-13 are from a small crystal that is 'intergrown' with aenigmatite. By contrast, analyses AG9-11,14 and PX21-26 are from aegirine crystals which overgrow or replace ferrichterite-arfvedsonite amphibole. It is concluded therefore, that the aegirine-hedenbergite crystallised relatively early, while the aegirines crystallised later, following amphibole crystallisation.

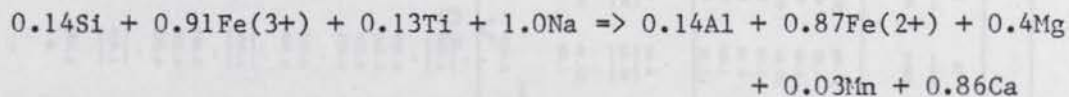
In the Gora enclave, the sole mafic mineral consists of almost pure aegirine (analyses AG30-31, Table 13).

The Birji granite contains aegirine which is also very pure and it has a Na content close to the theoretical maximum. Analyses AG4-7 are from an aegirine crystal (in a pegmatite associated with the Birji granite) which is concentrically zoned with alternate brown and green zones. Such colour zoning has not generally been observed except in the polished thin section used for microprobe analysis. The colour difference may be related mainly to the Ti content since the brown areas are Ti deficient (approx. 0.02 cations) while the green areas are Ti enriched (approx. 0.1 cations). There are corresponding, yet smaller changes in other elements, for example Al, Fe and Mn contents are lower in the green areas. The green margins to ferrohedenbergites in the Zigau granite porphyry however, are not richer in Ti than the cores, but the question of Ti enrichment in pyroxenes is of some interest and will be

discussed later.

In the Amdulayi syenite no pyroxene has been detected in the very coarse grained facies but in the medium grained, equigranular facies the pyroxene consists of almost pure aegirine (AG24-26), while the porphyritic, xenolithic facies contains three types of pyroxene. The small, porphyritic enclaves contain abundant pale green ferroaugite crystals; in one case there is a slightly larger, clear ferroaugite grain (PX47) which has a narrow, intensely green rim (PX48) that plots in the aegirine-hedenbergite field. Four analyses of pyroxenes from the matrix of this facies (PX38-41) have compositions which plot in both the aegirine and aegirine-hedenbergite fields. The data is insufficient to distinguish whether there are two distinct chemical groups or a continuous gradation. There are, however, no petrographic distinctions nor is any pyroxene forming by alteration of amphibole, so it seems likely that there is a continuous gradation in this case. Zn and Zr levels in the Shira pyroxenes are generally not detectable but the ZrO₂ content of samples PX38-41 is an exception and may reach up to 4 wt.%.

The overall chemical variation within the Shira pyroxenes, summarised in the correlation matrix in Table 15, shows that Si, Ti, Fe³⁺ and Na increase as Al, Fe²⁺, Mn and Ca decrease. These cations may be combined into a single equation which represents the dominant substitutional mechanism thus:-



(6)

This equation is balanced to within 0.13 of a charge - the difference probably being due to the minor cations such as Zn and Zr for which analyses are only available in a few cases and they have accordingly been omitted from the correlation matrix.

From equation 6, it is clear that the major cation exchange

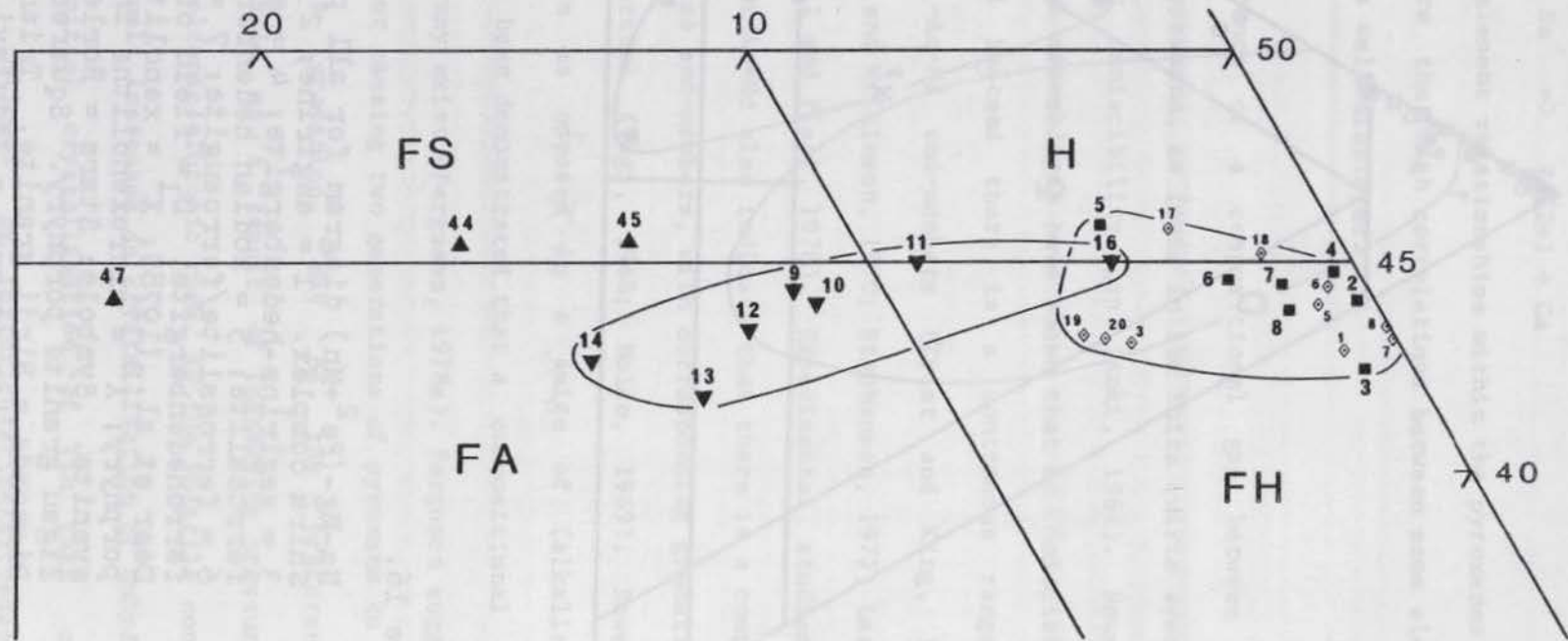
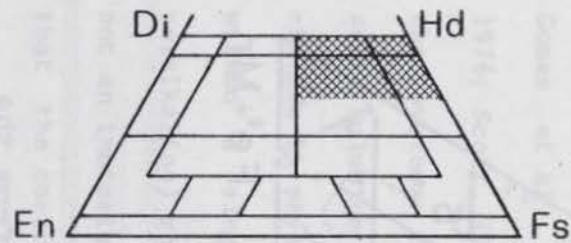


Figure 15. Di-Hd-En-Fs diagram for calcic pyroxenes from the Shira complex. FS = ferrosalite; FA = ferroaugite; H = hedenbergite; FH = ferrohedenbergite. Upright triangles = xenolith in Zigau granite porphyry. Squares and diamonds = phenocrysts in Zigau granite porphyry.

Mineral - mol %?
norm - wt %?

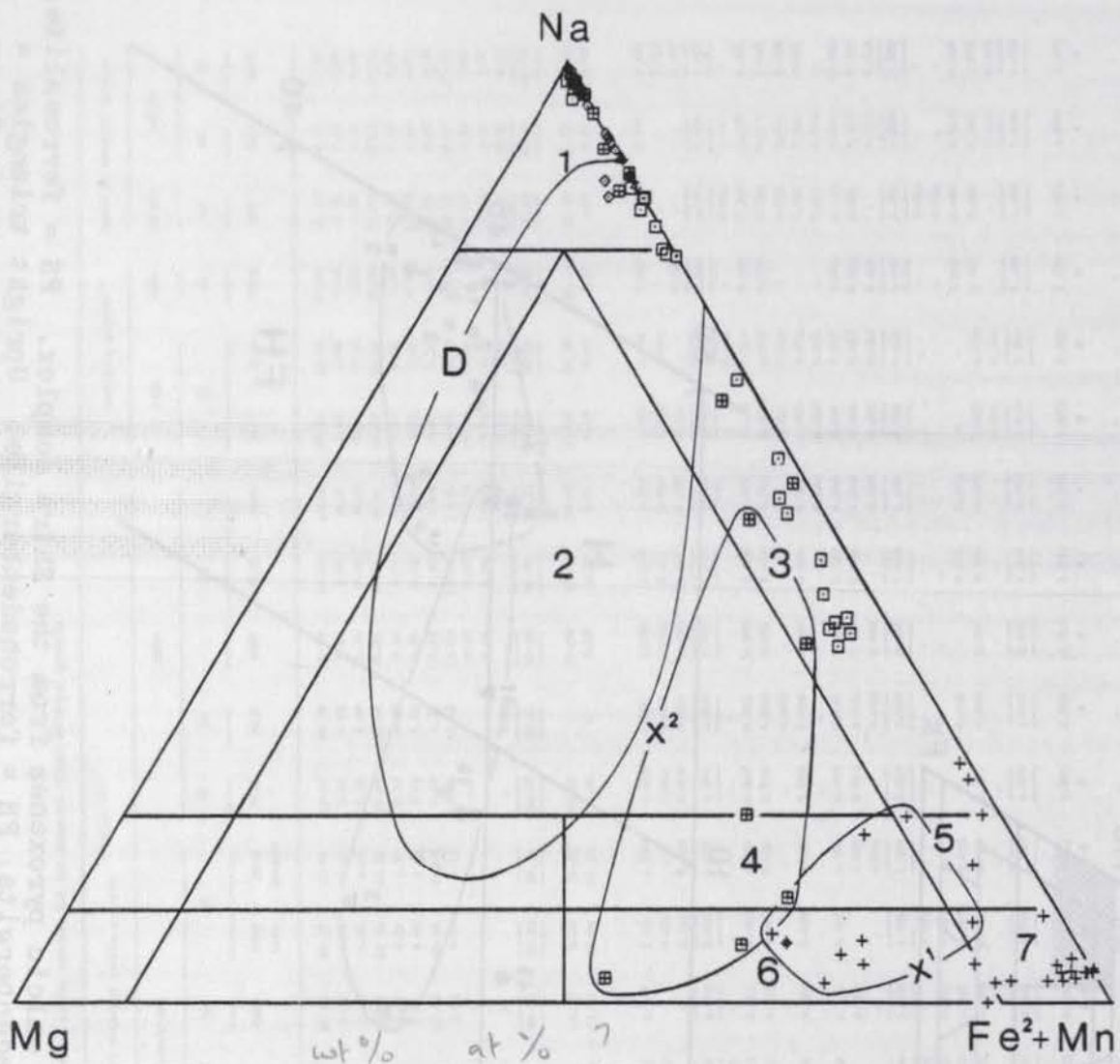


Figure 16.

Na-Mg-(Fe²⁺+Mn) diagram for all pyroxenes from the Shira complex. 1 = aegirine; 2 = aegirine augite; 3 = aegirine-hedenbergite; 4 = sodian ferroaugite/ferrosalite; 5 = sodian hedenbergite/ferrohedenbergite; 6 = ferrosalite/ferroaugite; 7 = hedenbergite/ferrohedenbergite. D₁ = field of aegirine-augites from Deer et al. (1978); X¹ = xenolith in Zigau granite porphyry; X² = microxenoliths in Amdulayi quartz syenite. Symbols: Stars = Borley (1963a). Crosses = Zigau granite porphyry. Squares = Shira quartz syenite. Diamonds = Birji granite. Triangles = Andaburi granite. Squares with crosses = Amdulayi syenite/quartz syenite.

mechanism is:



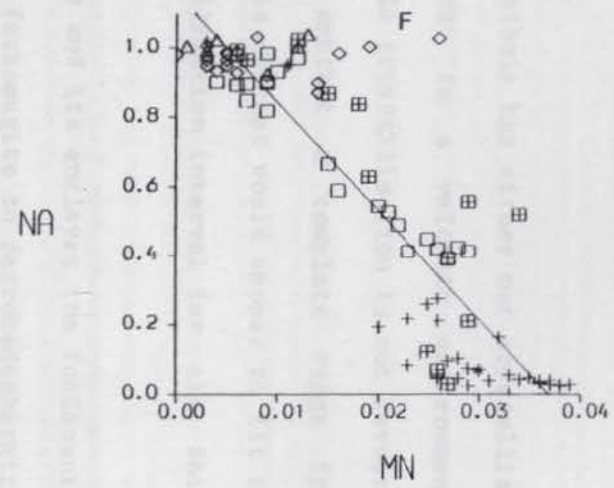
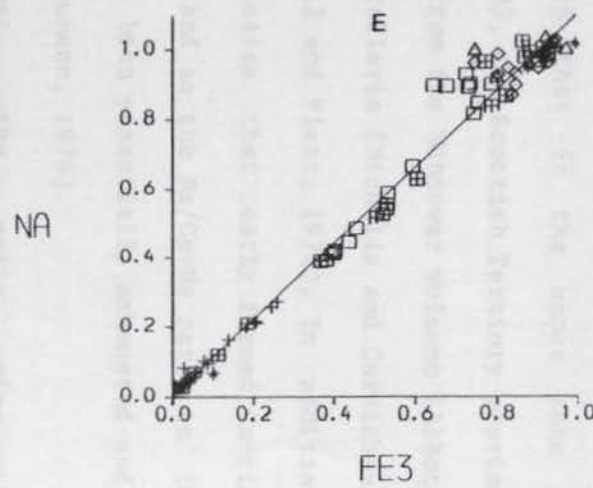
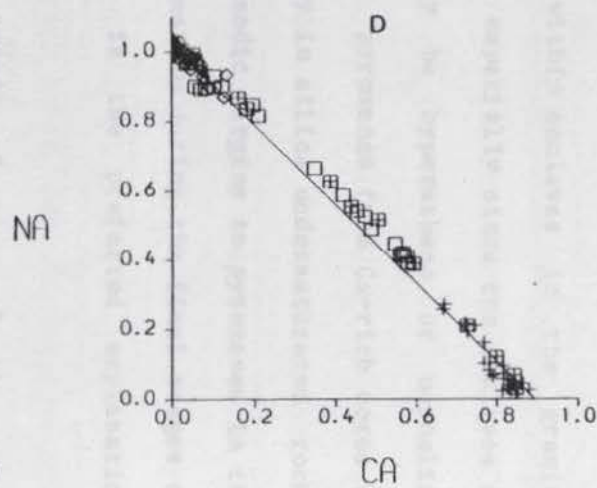
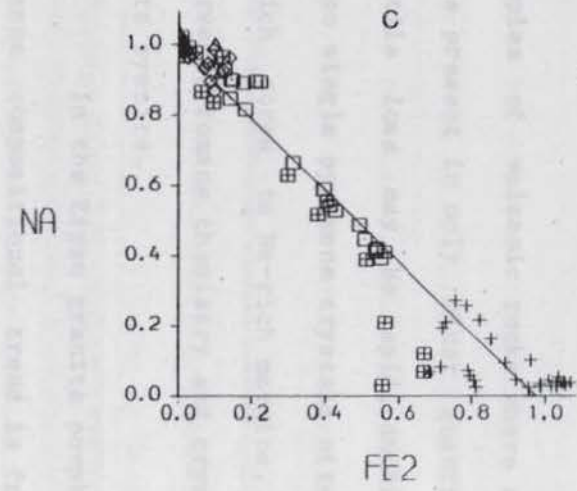
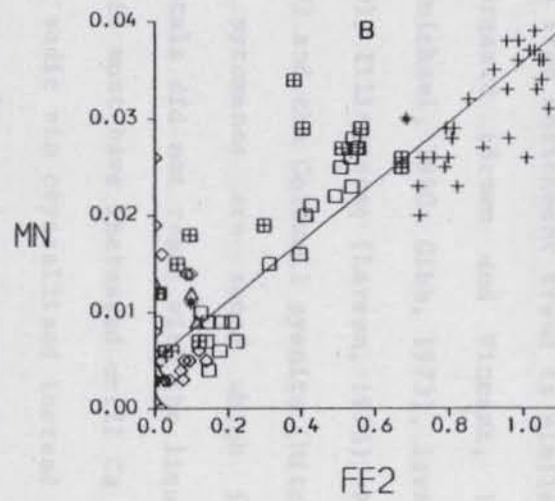
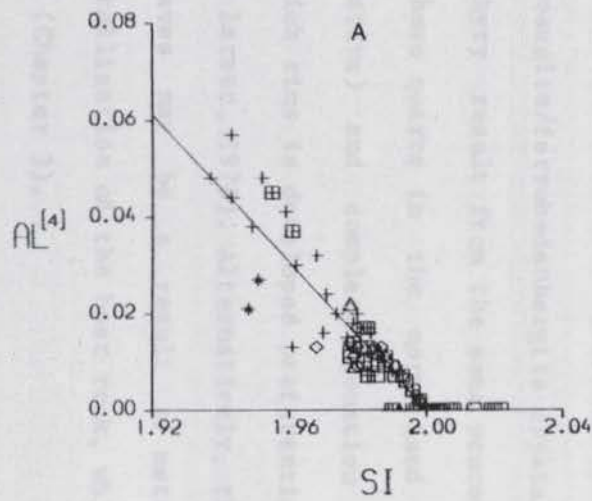
Specific inter-element relationships within the pyroxenes are shown in Figure 17 where the high correlations between some element pairs such as Ca and Na is well displayed.

Discussion The existence of a compositional gap between two generations of alkali pyroxene, as found in the Shira quartz syenite, has been interpreted as an immiscibility gap (Aoki, 1964). However, numerous studies of natural assemblages have shown that a miscibility gap does not exist and instead there is a continuous range in composition between the Di-Ac-Hd end-members (Tyler and King, 1967; Gomes et al., 1970; Nash and Wilkinson, 1970; Stephenson, 1972; Larsen, 1976; Scott, 1976; Mitchell and Platt, 1978). Experimental studies in the systems Di-Ac and Di-Ac-Hd also indicate that there is a complete solid solution between these end-members, with corresponding gradational changes in physical properties (Yagi, 1966; Nolan, 1969). However, within a single specimen as opposed to a suite of (alkaline or peralkaline) rocks, it has been demonstrated that a compositional (but not an immiscibility) gap may exist (Ferguson, 1978a). Ferguson suggests that the controlling factor causing two generations of pyroxene to form instead of a continuous gradation, may be the preferential crystallisation of amphibole as a result of increasing pressure of volatiles. Thus, in a subvolcanic/plutonic rock, as the volatile content (F, Cl, H₂O, etc.) of the melt increases as crystallisation of anhydrous minerals proceeds, so initial crystallisation of (in this case) aegirine-hedenbergite is followed by ferrichterite/arfvedsonite amphibole. Subsequently, increased peralkalinity and/or loss of volatiles may cause amphibole to become unstable with respect to aegirine. By way of support for this hypothesis, Ferguson (1978a) cites

Table 15. Correlation matrix for microprobe analyses of pyroxenes from the Shira complex.

	Ti	Al	Fe ₃	Fe ₂	Mn	Mg	Ca	Na
Si	0.07	-0.91	0.33	-0.30	-0.30	-0.41	-0.34	0.35
	Ti	-0.07	0.47	-0.52	-0.59	-0.26	-0.60	0.58
		Al	-0.38	0.32	0.33	0.52	0.37	-0.39
			Fe ₃	-0.98	-0.89	-0.57	-0.99	0.99
				Fe ₂	0.89	0.40	0.97	-0.97
					Mn	0.41	0.90	-0.90
						Mg	0.57	-0.58
							Ca	-1.00

Statistically significant regression value (r) at the 99% confidence level (n=80) = 0.28.



element
wt%

Figure 17. Cartesian diagrams of selected elements in pyroxenes from the Shira complex. [Symbols as in Figure 16.]

examples of volcanic rocks where amphibole has either not crystallised or is present in only minor quantities; in a volcanic environment, volatile loss may be rapid, amphibole crystallisation is not favoured and so single pyroxene crystals often exhibit a complete range from Ca-rich cores to Na-rich margins. This concept would appear to fit the observed pyroxene chemistry and crystallisation interval for the Shira quartz syenite.

In the Zigau granite porphyry and its enclaves the fundamental pyroxene compositional trend is from ferroaugite to ferrohedenbergite. This iron enrichment trend is similar to that in the upper zone at Skaergaard (Brown and Vincent, 1963), the Scottish Tertiary province (Carmichael, 1960; Gibb, 1973), lavas from the Nandewar volcano (Abbott, 1969), Illimaussaq (Larsen, 1976), Pantelleria (Nicholls and Carmichael, 1969) and the Coldwell syenite (Mitchell and Platt, 1978). In addition, the pyroxenes are zoned which indicates that early formed Ca-rich crystals did not react with the liquid and so the Na/Ca+Na ratio in the liquid must have increased until Ca had been essentially exhausted and a more sodic rim crystallised instead (Neumann, 1976).

It is possible that the sodic rims to ferroaugite/ferrohedenbergite crystals within enclaves in the granite porphyry result from the same process, especially since the enclaves do not have quartz in the norm (and may be hypersthene or nepheline normative) and complete zonation in pyroxenes from Ca-rich cores to Na-rich rims is developed preferentially in silica undersaturated rocks (see Larsen, 1976). Alternatively, the sodic margins to pyroxenes in the enclaves may be a result of metasomatism during the final stages of crystallisation of the host rock, which is the preferred explanation here (Chapter 3).

The pyroxene compositional trends of many of the areas previously mentioned (e.g. Nandewar), have been summarised by Larsen

(1976). It appears that the diopside-(ferro)hedenbergite trend occurs dominantly in silica oversaturated rocks while the diopside-aegirine trend is found in silica undersaturated rocks. However, while the latter trend occurs solely in silica undersaturated rocks, strong Fe enrichment trends are shown both by silica undersaturated rocks at Illimaussaq (Larsen, 1976) and silica oversaturated rocks at Coldwell (Mitchell and Platt, 1978), so Fe followed by Na enrichment is not dependent on the activity of silica in the magma, although the Mg to Na enrichment trend does appear to be so dependent. A possible characteristic of rocks with this pyroxene trend though, is a low pressure, sub-volcanic environment.

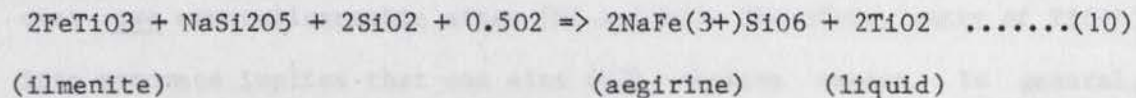
Hedenbergite is stable over a wide range of temperature and f_{O_2} , from the QFI to the NNO oxygen buffers. Above an f_{O_2} of 10(-13) bars at 800 degrees C and 10(-28) bars at 400 degrees C, hedenbergite breaks down to the assemblage andradite, magnetite and quartz (Kurchakova and Avetisyan, 1974; Gustafson, 1974). Hedenbergite (and presumably ferrohedenbergite) therefore has such a wide range of stability in f_{O_2} -T space that it is of little use in determining the conditions of crystallisation for the Zigau granite porphyry. Depending on bulk composition, the absence of the breakdown assemblage at least suggests that the f_{O_2} conditions were below those of the NNO buffer, and perhaps considerably lower. Furthermore, the presence of fayalite (Section 4.7) and quartz together with the absence of magnetite indicates that the f_{O_2} conditions during crystallisation of fayalite and ferrohedenbergite were probably below those of the QFM buffer, since an increase in f_{O_2} above the the QFM buffer would drive the equation:

$$3Fe(2+).SiO_4 + O_2 \Rightarrow 2Fe_3O_4 + 3SiO_2 \quad (8)$$

to the right.

In rocks of the Shira complex other than the Zigau granite porphyry, the absence of an experimentally calibrated f_{O_2} buffer assemblage means that no accurate prediction of f_{O_2} conditions during

environment as shown by authigenic occurrences (Milton and Eugster, 1959; Fortey and Mitchie, 1978). In a low P(t), silica oversaturated environment entry of Al into aegirine will be low (Popp and Gilbert, 1972), which is supported by the results presented here. Aegirine also appears to be stable in a low P-T, silica undersaturated environment as indicated by fenitised localities (Vartiainen and Woolley, 1976). Ernst (1962) and Bailey (1969) have demonstrated that aegirine (acmite) is stable at low f_{O_2} and Nielson (1979) favours an Fe(2+)-Na-Ti pyroxene at low f_{O_2} in a high level, peralkaline environment that is buffered by the reaction:-



Little work appears to have been done on the stability of aegirine-augite (or aegirine-hedenbergite) but it probably has a similar (but slightly greater) stability range to aegirine; in one (vein) locality it is regarded as a product of Na metasomatism of a calcic pyroxene (Watanabe, 1975).

The Ti content of aegirine in a pegmatite has been shown to vary systematically with colour in a zoned crystal, where it may reach 3.7 wt.% TiO₂. Similarly, aegirine in the medium grained equigranular facies of the Amdulayi syenite and the Andaburi granite commonly have TiO₂ values exceeding 2%. When oxides coexist with silicates, Ti will prefer the oxide phases at low f_{O_2} , and under these conditions, entry of Ti into pyroxenes will be favoured by high temperature of crystallisation (Verhoogen, 1962). This (thermodynamic) hypothesis would appear to be true for rocks of the Shira complex since the mean wt.% TiO₂ for calcic pyroxenes in the ilmenite bearing Zigau granite porphyry is 0.49, while the average for aegirine from the oxide free Birji arfvedsonite granite is 1.45.

Some experimental evidence indicates that entry of Ti into

aegirine is favoured by high fO_2 , when there is apparently simultaneous entry of Ti into the tetrahedral site (Flower, 1974). This substitutional scheme is not apparent in the Shira pyroxenes however, as Si and Ti increase while Al decreases. In addition, there appears to be little support for Flower's conclusions regarding either the (Ti+Al) substitutional pair, or for Ti-rich aegirines being favoured by high fO_2 (Pederson et al., 1975; Ferguson, 1977b).

Entry of a tetravalent cation such as Ti(4+) into pyroxene in fact causes immediate stoichiometric problems since only four positive charges (i.e. one Ti(4+) atom) are required (per 6 oxygens), distributed over two crystallographic sites (M1 and M2). Therefore, entry of Ti(4+) into pyroxene implies that one site (M2) remains vacant. In general, however, the assumption that the sum of cations in pyroxenes is 4.0 (i.e. stoichiometry) is valid, except perhaps for clinopyroxenes with less than 0.7 cations Ca per unit formula (i.e. sodic pyroxenes) (Cawthorn and Collerson, 1974). Since the existence of vacant M2 sites would be required for a significant amount of Ti(4+) in an aegirine, it is hardly surprising that the existence of Ti in the trivalent state has been proposed (Scott, 1976). However, this proposal has attracted much adverse comment (Ferguson, 1977a, 1977b; Ronsbo et al., 1977), principally because pyroxene with trivalent Ti has been synthesised only under the most extreme conditions of 65 kb pressure at 1550 degrees C (Prewitt et al., 1972). In addition, Ferguson (1977a) suggests that Ti³⁺ and Fe³⁺ are unlikely to exist together in a silicate lattice, since in aqueous solution at least, the pair Ti(4+)+Fe(2+) are more strongly favoured instead. Furthermore, optical absorption measurements have failed to confirm the existence of a Ti³⁺ cation in highly titanian aegirine (Ronsbo et al., 1977). Therefore there is no firm evidence whatsoever, at the present time, for the existence of Ti³⁺ in clinopyroxenes.

The substitution problem of Ti entry into aegirine has however, received an alternative explanation, that titanian aegirines belong to an aegirine-neptunite ($\text{Na}_2\text{Fe}(2+)\text{Ti}_4\text{Si}_4\text{O}_{12}$) solid solution series (Ferguson, 1977a, 1977b). Moreover, Ferguson (1977b) believes, in contrast to Flower (1974), that entry of Ti^{4+} into aegirine is favoured by low temperature (<600 degrees C) and is independent of silica activity in the magma. Rossi (1978) has criticised the concept of aegirine-neptunite solid solution because of the structural dissimilarity between the two; while Ferguson (1978c) agrees with Rossi on the structural dissimilarity between the two minerals, he nevertheless does not regard it as necessary that end members of a solid solution series should be isomorphs.

Another view, that Ti could be replacing Si in the tetrahedral site, is not supported by the analytical data which show a near maximum amount of Si. Hartman (1969) has also shown that such replacement is highly unlikely.

Therefore, the most likely explanation for Ti entry into pyroxenes would appear to be that it is accompanied by a corresponding number of vacancies in the M2 site.

Summary and conclusions Clinopyroxenes from the Shira complex may be divided into three compositional groups, namely aegirine, aegirine-hedenbergite and hedenbergite; only the small intrusion of Zigau granite porphyry contains calcic (hedenbergite) pyroxenes. There appears to be a compositional break between the crystallisation of aegirine-hedenbergite and aegirine, during which ferrichterite-arfvedsonite amphibole crystallises. Aegirine crystallisation is not necessarily linked with high oxidation conditions, but may be a result of the combined effect of f_{O_2} , volatile content, temperature and liquid composition - particularly peralkalinity

conditions. Both aegirine and hedenbergite/ferrohedenbergite have wide ranges of stability with respect to T-fO₂ space and are not particularly useful P-T-fO₂ indicators. However, the hedenbergite-aegirine trend does appear to be typical of a low P, sub-volcanic environment. Selected aegirine crystals have relatively high Ti contents and they may be non-stoichiometric as a result. In the ilmenite bearing Zigau granite porphyry, the Ti content of the associated pyroxene is significantly less than in the (mainly) oxide free granites and syenites.

4.4 Aenigmatite

Aenigmatite occurs in only two rock types in the Shira complex - the Shira quartz syenite and the Amdulayi syenite. In the Shira quartz syenite, aenigmatite occurs as relatively large, mainly interstitial, anhedral grains which have a deep blood-red colour. In the Amdulayi syenite, aenigmatite has a more marked poikilitic, interstitial habit and a brown-red colour.

In Table 16, nine microprobe analyses of aenigmatite from five crystals in the Shira quartz syenite and nine analyses from seven crystals in the Amdulayi syenite are presented. Structural formulae have been calculated on the basis of 40 oxygens after Kelsey and McKie (1964) and total iron as FeO, and the cations have been assigned to three major structural positions partly following the nomenclature of Cannillo et al. (1971).

It is apparent from this data that the compositional range of the Shira aenigmatites both within and between crystals, is relatively restricted compared to, for example, the amphiboles and pyroxenes. However, bearing in mind the slight colour difference between

aenigmatites from the two major host rocks, some slight chemical distinction would be expected. Closer inspection of the data in Table 16 shows that aenigmatite from the Amdulayi syenite is richer in Al, Fe, Mn, Mg and Ca, and has less Si and Ti than aenigmatite from the Shira quartz syenite. Na contents appear to be comparable. These observations have been summarised in Table 17, from which it appears that for Si, Al, Fe and Ca, there is much less scatter in the data from the Amdulayi syenite than the Shira quartz syenite, while for Ti, Mn, Mg and Na the reverse is true. Such variation as is present in aenigmatite from the Shira quartz syenite is at least partly due to slight differences in Al and Ca in particular, between the core and rim of some crystals.

Table 17. Means and standard deviations of aenigmatite analyses from the Shira complex.

	Shira quartz syenite		Amdulayi syenite	
	\bar{x}	σ	\bar{x}	σ
SiO ₂	41.51	0.58	41.19	0.28
TiO ₂	9.36	0.30	8.87	0.37
Al ₂ O ₃	0.40	0.30	0.57	0.13
FeO(T)	40.45	0.64	41.11	0.26
MnO	0.97	9.13	1.17	0.32
MgO	0.32	0.13	0.53	0.28
CaO	0.27	0.31	0.51	0.10
Na ₂ O	7.32	0.23	7.30	0.30

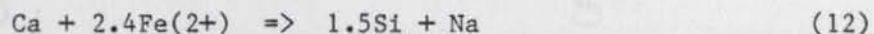
Since colour in transparent materials is a function of electron movements within transition element cations, the difference in colour between the two aenigmatite species is presumably dependent upon the relative Ti, Fe and Mn levels. It may therefore be significant that

the deep blood-red aenigmatite from the Shira quartz syenite has a higher Ti and lower Fe and Mn contents than the brown-red aenigmatite from the Amdulayi syenite.

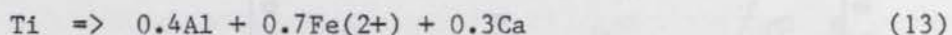
Compositional variation within the aenigmatites from the Shira complex is summarised in Figure 18 which shows the variation between specific pairs of elements. Of the major cations, Si, Mn and Na increase as Ti, Al, Fe, Mg and Ca decrease. Accordingly, the principal cation substitution mechanism appears to be as follows:



which is a modification of the aenigmatite-rhonite exchange $\text{Si} + \text{Na} = \text{Ca} + \text{Al}$. Subsidiary exchange mechanisms such as:

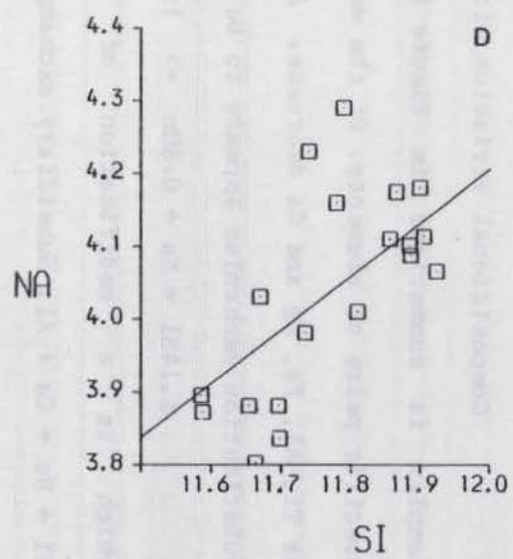
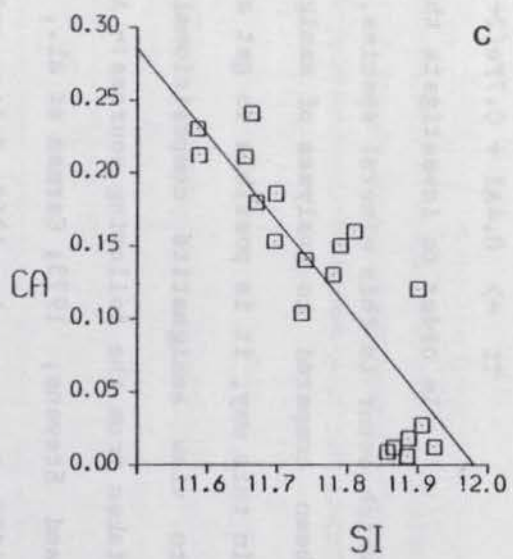
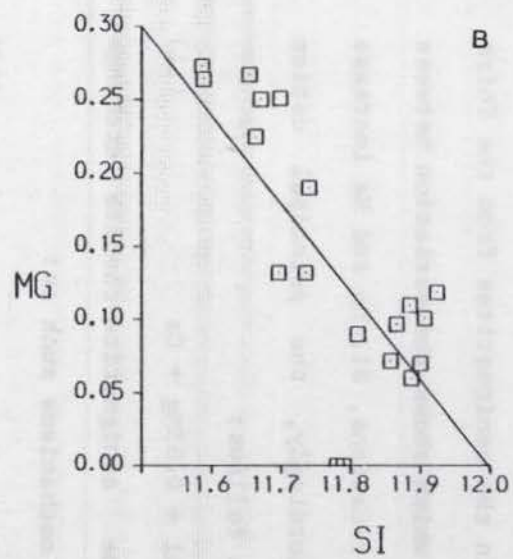
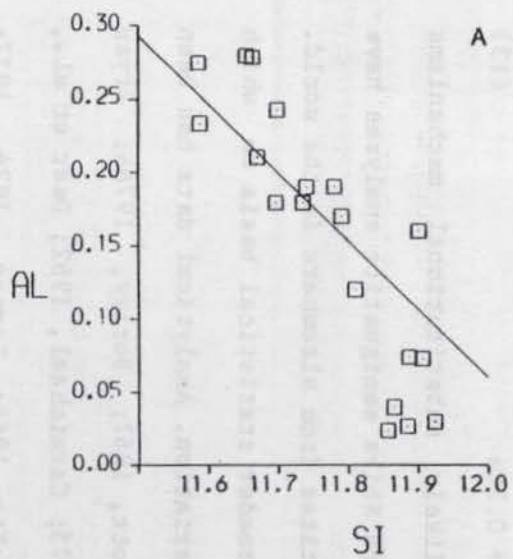


can also be envisaged. Although Ti has a negative relationship with Si, Al, Fe(T), Mn, Ca and Na, since these cations do not vary consistently within themselves it is not possible to write a simple substitutional equation for the behaviour of Ti. However, the following equation would appear to be the best compromise:



In order to investigate the likely substitutional mechanisms which occur in this mineral species, the Shira aenigmatite analyses have been compared to analyses of aenigmatites from elsewhere in the world. In this way, it is possible to get a broader statistical basis on which to view aenigmatite compositional variation. Analytical data has been taken from the following sources:- Abbott, 1967; Borley, 1976a; Bryan and Stevens, 1973; Carman et al., 1975; Carmichael, 1962; Deer et al., 1978; Ewart et al., 1968; Kelsey and McKie, 1964; Larsen, 1976, 1977; Lindsley et al., 1971; Marsh, 1975; Mitchell and Platt, 1978; Mitrofanov and Afanas'yeva, 1966 (1); Nash et al., 1969; Velde, 1978; Yagi and

(1) Although omitting analysis No.501 because of dubious CaO and Na₂O values.



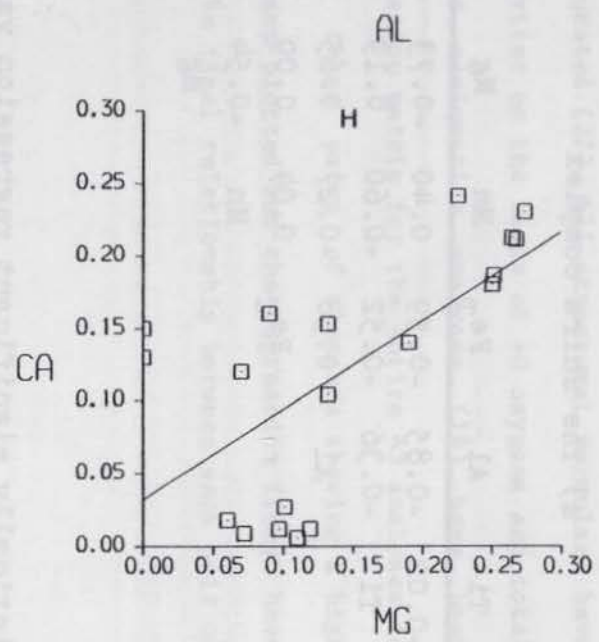
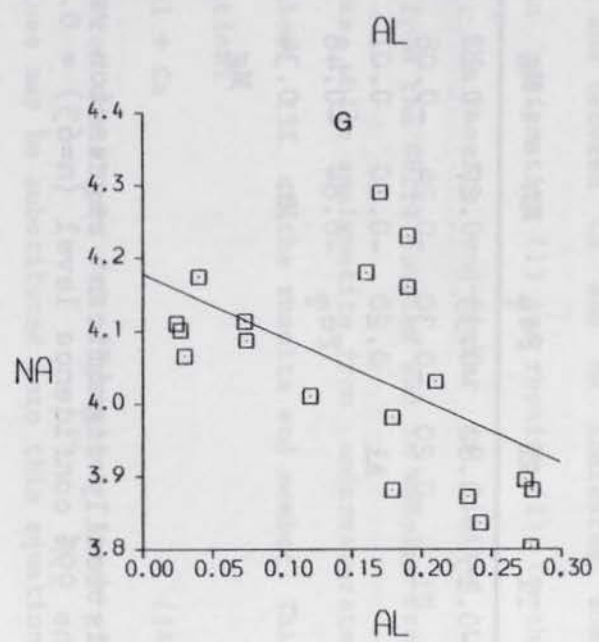
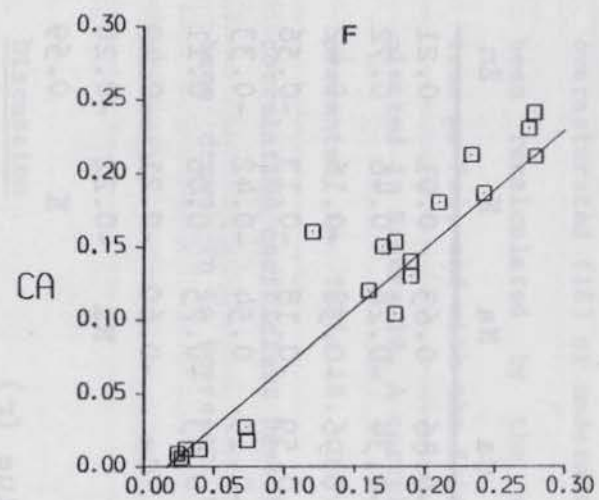
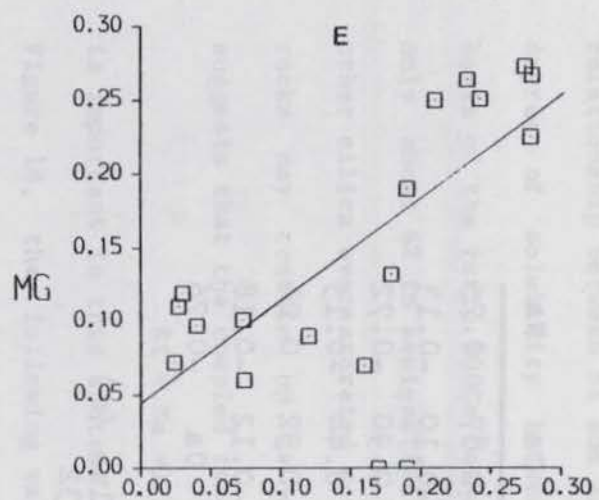


Figure 18. Cartesian diagrams of selected elements in anigmatite from the Shira complex.

Table 18. Correlation matrix for aenigmatite analyses from the Shira complex and elsewhere.

a) The Shira complex

	Ti	Al	Fe _T	Mn	Mg	Ca	Na	K	Zn
Si	-0.02	-0.85	-0.59	0.40	-0.73	-0.86	0.63	0.01	0.21
	Ti	-0.36	-0.52	-0.60	0.19	-0.34	-0.28	0.46	0.72
		Al	0.58	-0.27	0.65	0.96	-0.58	-0.16	-0.42
			Fe _T	0.04	0.09	0.59	-0.18	-0.13	-0.56
				Mn	-0.54	-0.19	0.54	-0.42	-0.33
					Mg	0.63	-0.75	0.06	0.11
						Ca	-0.60	-0.21	-0.49
							Na	-0.22	-0.20
								K	0.59

Statistically significant regression value (r) at the 95% confidence level (n=18) = 0.47

b) The Shira complex (18 analyses) and worldwide (45 analyses)

	Ti	Al	Fe _T	Mn	Mg	Ca	Na
Si	-0.15	-0.82	-0.33	0.27	-0.12	-0.87	0.75
	Ti	-0.20	-0.30	-0.24	-0.08	-0.10	-0.13
		Al	0.20	-0.10	0.01	0.90	-0.72
			Fe _T	-0.64	-0.48	0.44	-0.15
				Mn	0.34	-0.32	0.24
					Mg	-0.12	-0.18
						Ca	-0.76

Statistically significant regression value (r) at the 99% confidence level (n=63) = 0.32

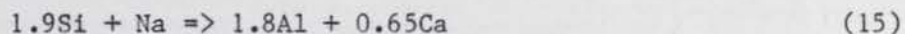
Souther, 1974; and Zies, 1966. These data (45 analyses) have been divided into two groups according to whether the host rock is silica oversaturated (18) or undersaturated (27). All structural formulae have been recalculated by the writer on the basis of 40 oxygens and total iron as FeO, and with the Shira aenigmatite analyses (19) have been plotted in Figure 19. A correlation matrix for the entire 63 analyses is presented in Table 18. Only those pairs of elements showing a high correlation coefficient have been plotted and the regression lines have been drawn in to represent the ideal relationship between each pair of elements.

Discussion

A fundamental feature of aenigmatite chemistry appears to be that aenigmatites from silica undersaturated rocks exhibit a wider compositional range than those from oversaturated rocks, an analogous situation to that found in fayalite (Section 4.7). The negative relationship between Si and Al and between Ca and Na indicates some degree of solubility between aenigmatite (1) and rhonite (2). On the basis of the ratio $100\text{Ca}/(\text{Ca}+\text{Na})$, the rhonite end-member is limited to only about 6% in aenigmatite from the Shira complex and in samples from other silica oversaturated rocks, while aenigmatite from undersaturated rocks may contain up to about 23% of the rhonite end member. This suggests that the coupled reaction:

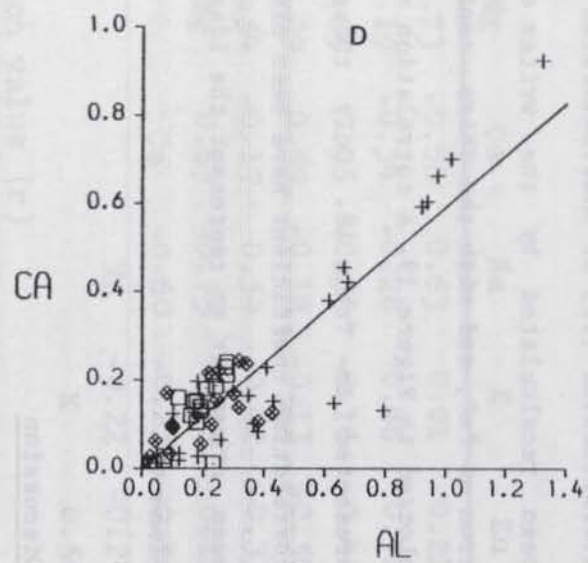
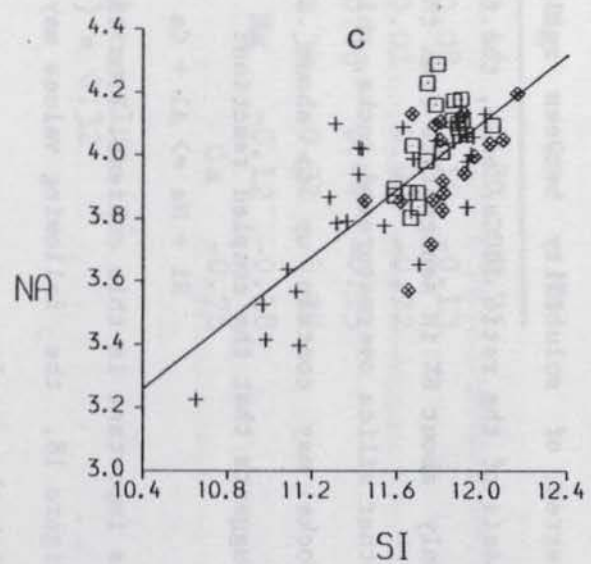
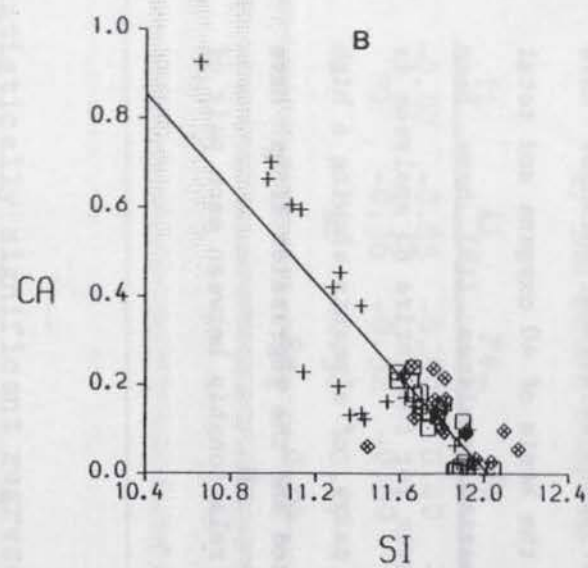
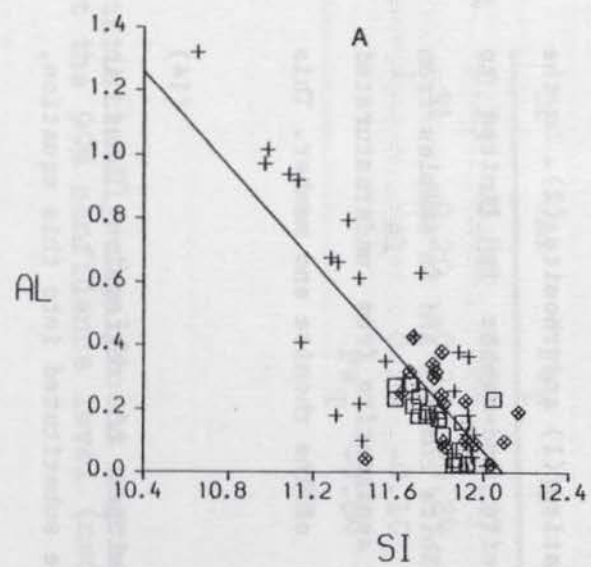


is important in this context. From the slopes of regression lines in Figure 18, the following values may be substituted into this equation, with the result:



(1) $\text{Na}_2.\text{Fe}(2)_5.\text{Ti}.\text{Si}_6.\text{O}_{20}$

(2) $\text{Ca}_2.(\text{Mg},\text{Fe}(2),\text{Fe}(3+))_5.\text{Ti}.\text{(Si,Al)}_6.\text{O}_{20}$



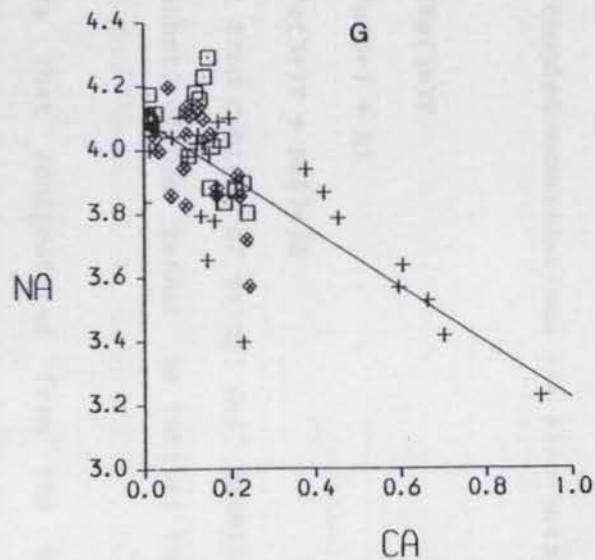
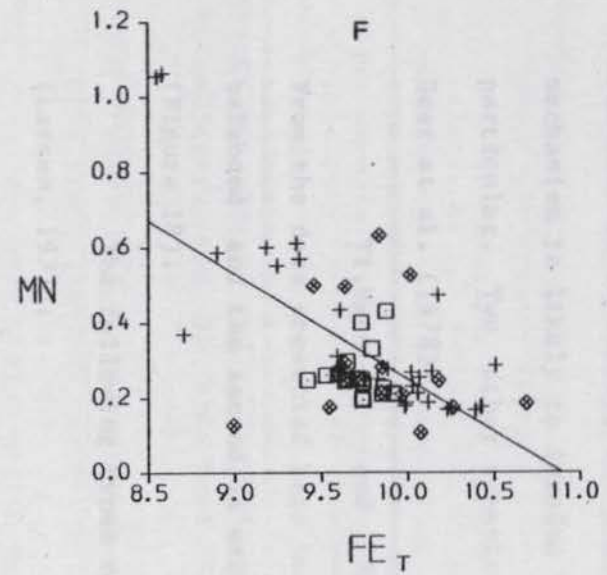
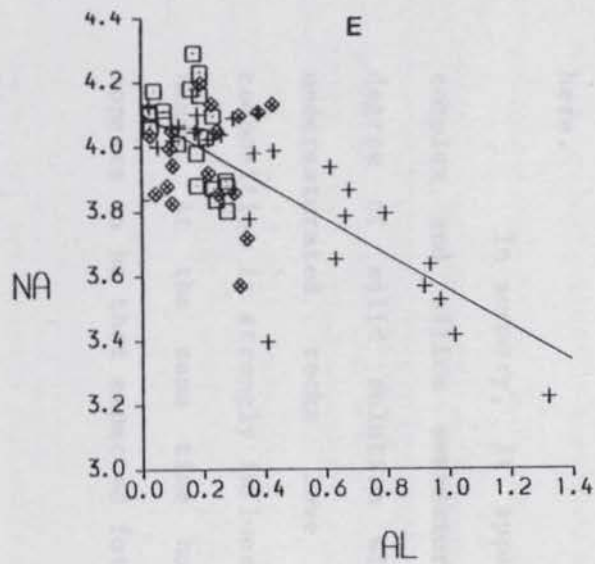
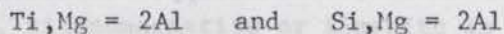


Figure 19. Cartesian diagrams of selected elements in aenigmatite from the Shira complex and elsewhere. Squares = Shira complex. Diamonds and crosses = aenigmatite from silica over- and undersaturated rocks respectively.

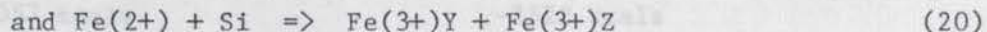
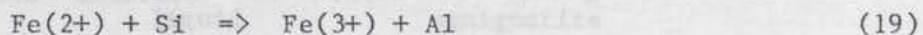
12/1/75

This equation involves only Z and X cations, and is obviously unbalanced. Therefore, the true rhonite-aenigmatite type substitutional mechanism is likely to involve Y cations also, probably Ti, Fe and Mg in particular. Two other substitutional mechanisms have been suggested by Deer et al. (1978):



From the data presented here however, the former equation is poorly balanced and the second is extremely unlikely since Mg increases with Al (Figure 18).

The following types of coupled substitutions are also possible (Larsen, 1977):



but without estimating the ferric iron content or using wet chemically analysed aenigmatites, these substitutions cannot be further tested here.

In summary, it appears that aenigmatites from the Shira complex and silica oversaturated rocks in general have a very modest degree of solid solution with rhonite, but aenigmatites from undersaturated rocks have significantly more. Thus, aenigmatite composition is strongly influenced by the activity of silica in the magma. At the same time however, the dominant substitution scheme appears to be that expected for a rhonite-aenigmatite solid solution.

Discussion

As aenigmatite has not been recorded from non-peralkaline rocks it would appear to form in response to peralkaline conditions. In addition, the general antipathetic relationship between Fe-Ti oxides (+/- fayalite) and aenigmatite has led to the suggestion that a

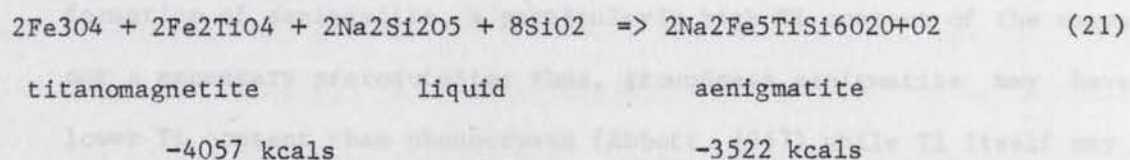
(1) The thermodynamic data used in this chapter concern the heats of formation of minerals from the elements at 298 degrees K, in kcal. per mole. Variation in the heat (or enthalpy) of formation with temperature is negligible and can be ignored for present purposes. Similarly the change in configurational entropy is also exceedingly small. A large negative value on the right hand side of the equation for example, indicates that heat has been lost from the system and hence the products are more stable than the reactants. However, these data are concerned with the relative stabilities of the solids only and such factors as the fugacity of oxygen or volatiles are not directly considered.

Discussion

The significance has not been mentioned in the preceding chapters. It would appear to form an important part of the general and specific relationships between the various (or) variables and variables has led to the suggestion that a

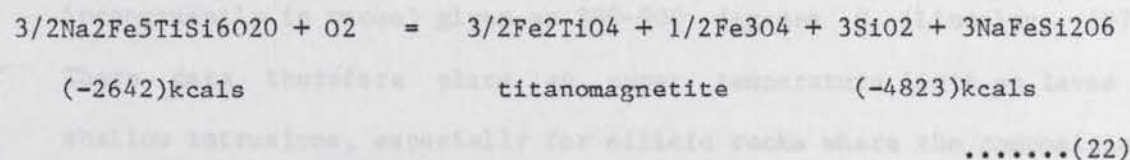
'no-oxide' field exists in fO_2 -T space, in which acmite (or other sodic pyroxene) and aenigmatite coexist instead of one or more oxide phases (Nicholls and Carmichael, 1969).

Certainly there is petrographic evidence for an oxide phase reacting with a peralkaline melt to form aenigmatite on a local scale: for example, titanomagnetite or ilmenite in the Nandewar oversaturated trachytes is rimmed by aenigmatite (Abbott, 1967) and in pegmatoid zones within thick tholeiitic basalt flows, ilmenite lamellae within titanomagnetites are selectively replaced by aenigmatite (Lindsley et al., 1971). Such a petrographic reaction may be expressed chemically (Marsh, 1975) as follows:-



For this reaction, information from Robie and Waldbaum (1968) has been added, and the data shows that for the reaction to proceed to the right would be energetically most unfavourable⁽¹⁾. However, the reaction is also dependent upon fO_2 such that very low fO_2 conditions would favour the reduction of the oxide to aenigmatite.

From experiments on the stability of aenigmatite (Lindsley, 1971), the following equation can be written for its breakdown (Marsh, 1975), again with thermodynamic data from Robie and Waldbaum (1968):



Therefore, aenigmatite can oxidise to titanomagnetite and the reaction is favourable energetically and it is also favoured by a high fO_2 . Such a reaction may therefore be expected to be commonplace.

It is these two reactions then, that are believed to define the lower and upper fO_2 stability limits of aenigmatite respectively,

and hence also define the limits of the supposed 'no oxide' field of Nicholls and Carmichael (1969). It is therefore of some interest to recall that ilmenite grains have been identified (by electron microprobe) within aenigmatite from the margin of the Shira quartz syenite and in the coarse grained facies of the Amdulayi syenite. In the former, ilmenite occurs as small euhedral or subhedral grains which have been enclosed by aenigmatite and show no sign of a reaction relationship. In aenigmatite within the Amdulayi syenite however, ilmenite occurs as narrow selvages along cleavages and it is probably secondary as a result of aenigmatite oxidation.

Whereas peralkaline conditions appear to be essential to the formation of aenigmatite, a particularly high Ti content of the magma is not a necessary prerequisite; thus, groundmass aenigmatite may have a lower Ti content than phenocrysts (Abbott, 1967) while Ti itself may not even be necessary, since a Ti-free 'aenigmatite' has been synthesised (Ernst, 1962). Synthetic aenigmatite is stable with quartz and acmite at a low f_{O_2} (MW and WI buffers) between 650-800 degrees C at a $P(f) < 1$ kb. Titaniferous aenigmatite synthesised under hydrothermal conditions at 700 degrees C and $P(f) = 1$ kb, using the WI buffer has, as expected, a larger stability field than Ernst's titanium free phase (Thompson and Chisholm, 1969). The synthesis of aenigmatite has since been confirmed and its maximum thermal stability (as determined by melting incongruently in vacuo) given as 880-900 degrees C (Lindsley, 1971). These data therefore place an upper temperature limit on lavas and shallow intrusions, especially for silicic rocks where the compositional variation within aenigmatite is small. The stability of natural aenigmatite as a function of oxygen fugacity has been estimated to be above that of the NNO buffer (Nicholls and Carmichael, 1962) despite the observation of Ernst (1962) that (Ti-free) aenigmatite was stable only at the lower f_{O_2} conditions defined by the MW and WI buffers. However,

Lindsley (1971) showed that aenigmatite exists only metastably at high (NNO) f_{O_2} and that, at 750 degrees C and 0.5 kb at least, the stability curve lies between the NNO and QFM buffer curves. In addition, Lindsley et al. (1971) found that synthetic aenigmatite was not stable at f_{O_2} conditions much above the QFM buffer. The fact that aenigmatite can be synthesised from anhydrous components in vacuum at atmospheric pressure suggests that f_{O_2} rather than $P(t)$ has the most significant influence on the stability of aenigmatite. At lower temperatures, aenigmatite breaks down to acmite and so the appearance of aenigmatite in the syenitic, but not the granitic rocks, in the Shira complex can be explained in terms of relatively high temperature and low f_{O_2} . The very limited development of ilmenite along cleavages within aenigmatite in the Amdulayi syenite probably reflects an f_{O_2} increase beyond the stability of aenigmatite for a short interval before final consolidation. Under the conditions of low f_{O_2} at which aenigmatite is stable therefore, magnetite and titanomagnetite cannot exist stably according to the equations given, so in a peralkaline environment, aenigmatite is the only Ti-rich phase possible. The fact that wet chemical analyses of aenigmatite from the literature show low Fe^{3+} contents while coexisting amphibole and aegirine have much higher oxidation ratios, and that the Shira aenigmatite is one of the earliest mafic silicates to crystallise, both tend to support the low f_{O_2} , high temperature environment in which aenigmatite crystallised within the Shira complex.

4.5 Chevkinite

Nine electron microprobe analyses of chevkinite are presented in Table 19, together with a structural formula for the mean. Chevkinite

Table 19. Electron microprobe analyses of chevkinite and allanite

	CV1	CV2	CV3	CV4 core	CV5 rim	CV6	CV7	CV8	CV9	Mean	a	
SiO ₂	19.75	19.59	19.95	19.72	19.61	19.66	19.74	19.74	20.04	19.76	Si	4.136
TiO ₂	18.70	18.32	18.51	18.19	17.53	18.54	18.68	18.61	18.83	18.43	Ti	2.902
ThO ₂	0.27	0.31	0.34	0.37	0.41	0.29	0.36	0.28	0.31	0.32	Th	0.015
Al ₂ O ₃	0.21	0.17	0.12	0.12	0.09	0.11	0.27	0.20	0.29	0.18	Al	0.045
La ₂ O ₃	12.69	12.67	12.49	12.29	11.92	11.84	12.35	12.79	12.48	12.39	La	0.956
Ce ₂ O ₃	23.74	23.74	23.72	23.34	24.21	23.51	22.86	23.46	23.18	23.53	Ce	1.804
Pr ₂ O ₃	2.05	2.08	1.18	2.08	2.22	2.06	1.95	2.05	2.05	1.97	Pr	0.151
Nd ₂ O ₃	7.20	7.19	7.37	7.52	8.24	7.45	7.04	7.15	6.96	7.35	Nd	0.548
Sm ₂ O ₃	0.66	0.72	0.78	0.84	1.00	0.82	0.55	0.68	0.57	0.74	Sm	0.053
FeO	11.16	11.17	11.14	11.25	11.70	11.20	11.05	11.08	11.30	11.23	Fe ²⁺	1.966
CaO	2.65	2.51	2.82	2.41	1.93	2.76	2.88	2.64	3.26	2.65	Ca	0.595
	<u>99.08</u>	<u>98.47</u>	<u>98.42</u>	<u>98.13</u>	<u>98.86</u>	<u>98.24</u>	<u>97.73</u>	<u>98.68</u>	<u>99.27</u>	<u>98.55</u>		<u>13.171</u>

	AL1 core	AL2 rim	AL3 core	AL4 rim	b	
SiO ₂	30.94	31.70	30.81	31.04	Si	3.959
TiO ₂	2.25	2.41	2.06	2.40	Ti	2.778
ThO ₂	0.48	1.51	0.60	0.95	Th	0.014
Al ₂ O ₃	12.11	11.49	12.38	11.27	Al	0.043
La ₂ O ₃	7.52	5.08	6.83	5.33	La	0.915
Ce ₂ O ₃	13.99	11.93	13.83	12.07	Ce	1.726
Pr ₂ O ₃	1.07	1.05	1.20	0.96	Pr	0.144
Nd ₂ O ₃	3.44	3.82	3.77	3.43	Nd	0.525
Sm ₂ O ₃	0.26	0.30	0.37	0.42	Sm	0.050
FeO	16.13	15.98	16.47	15.57	Fe ³⁺	1.881
CaO	9.37	9.51	9.38	9.14	Ca	0.570
	<u>97.56</u>	<u>94.78</u>	<u>97.70</u>	<u>92.56</u>		<u>12.605</u>

^a Structural formula of mean chevkinite analysis on the basis of 22 oxygens.

^b Structural formula of AL3 on the basis of 24 oxygens.

generally occurs as small (approx. 0.2 mm) subhedral or rounded grains enclosed by ferrichterite-arfvedsonite amphibole in the Shira quartz syenite, although one larger (0.4 mm) euhedral grain was found enclosed by quartz (CV4-5). Chevkinite is probably the first mafic mineral to crystallise in this rock and it is pleochroic from pale brown to deep red-brown and it may easily be mistaken for aenigmatite (or allanite), especially when aenigmatite occurs in the same rock. The paragenesis and small grain size are however, quite distinctive. Chevkinite has not previously been described from this province.

Chevkinite has an ideal formula of $A_4BC_4Si_4O_{22}$ where $A = REE, Th, Ca, Sr, Na, K$; $B = Fe_2, Mg, Mn, Ca$; and $C = Ti, Mg, Mn, Fe_2, Fe_3^+, Al$ (Segalstad and Larsen, 1978), but for simplicity it may be considered as a Ce, Fe, Ti silicate. The analyses show very little variation and the mineral appears to have a fairly constant composition, and in this way it is similar to aenigmatite. The high average total implies that there is not a significant content of Fe_3^+ or elements such as Sr, Na, K, Mg and Mn which were not analysed for. Perhaps the most obvious feature of the data is the familiar alternating abundances of REE with increasing atomic number.

When the average ionic radii (Shannon and Prewitt, 1969) for the A cations (1.010 Å) and the B+C cations (0.726 Å) from the mean chevkinite analysis in Table 19 are plotted on an extended diagram of the type shown by Segalstad and Larsen (1978, Fig.4), then the Shira analyses fall within the chevkinite field. So far, this updated version of a similar diagram by Ito (1967) is the only chemical way to distinguish between chevkinite and perrierite.

Given the small grain size of chevkinite in the Shira complex, its occurrence (largely) within alkali amphibole and its comparative rarity, it is not amenable to separation and X-ray diffraction, thereby giving positive identification. Despite this, one can be reasonably

certain of the present identification.

Discussion

The identification of chevkinite is not straightforward and under the microscope it can be mistaken for allanite and aenigmatite, but restrictions on the likely occurrence of chevkinite and allanite will be mentioned later. However, within chevkinite-related minerals, there is a further problem in that, under the microscope (as well as the microprobe) "it is practically impossible to distinguish between perrierite and chevkinite" (Bonatti, 1959).

The chevkinite-perrierite mineral pair are very closely related. The initial discovery of perrierite (Bonatti and Gottardi, 1950) indicated its close chemical similarity to chevkinite and also allanite (Bonatti and Gottardi, 1954). The structural similarity between chevkinite and perrierite has subsequently been confirmed (Calvo and Faggiani, 1974); in fact, the cell dimensions of the two minerals are almost identical and the main distinguishing feature between them is the monoclinic beta angle which is close to 100 degrees in chevkinite and 113 degrees in perrierite (Bonatti, 1959; Jaffe et al., 1956; Segalstad and Larsen, 1978). It has been proposed that this structural difference is due to slight compositional differences, such as larger cations in the B and C sites which expand the lattice of chevkinite (Ito, 1967; Segalstad and Larsen, 1978).

In an experimental study of numerous compositional variants, it has been found that the change from chevkinite to perrierite was accompanied by substitutions such as Ce by Ca or Sr, and Fe, Ti and Si by Al (Ito, 1967). Although the situation in nature may not be so simple, these conclusions indicate strongly that the Shira mineral is chevkinite rather than perrierite. From this, it appears that chevkinite favours an Al and Sr poor environment, but other workers (Ito and Arem,

1971) find that chevkinite is favoured by high Sm and Fe and high T, whereas perrierite is preferred at lower temperature and high Ce and Mg.

The occurrence of either mineral may give some guide as to the environment of formation of each; perrierite occurs in volcanic ash and some pegmatites (Bonatti and Gottardi, 1950; Izett and Wilcox, 1968; Mitchell, 1966; Segalstad and Larsen, 1978), whereas chevkinite has been found in volcanic ash, pegmatites, and in a quartz syenite from the White Mountain Magma Series (WMMS), New Hampshire (Kauffman and Jaffe, 1946; Jaffe et al., 1956; Young and Powers, 1960; Mitchell, 1966; Segalstad and Larsen, 1978). In addition, chevkinite occurs in 12 alkali feldspar syenites or quartz syenites (but only one granite) in the Kerguelen islands (Marot and Zimine, 1976). Both the Kerguelen islands and the WMMS (Greenwood, 1951) have close petrological links with this province. Thus, two significant points emerge: that chevkinite is favoured over perrierite in an iron rich magma, and it occurs predominantly in a syenitic environment.

Occurrence of allanite and chevkinite in the Younger Granites

In view of the common petrographic description of allanite within the Younger Granites and in view of its close optical similarity to chevkinite, the following data may help to alleviate possible confusion in the future. Four microprobe analyses of two allanite crystals from a hornblende biotite granite from the Afu complex (AF71) are presented in Table 19. This rock type was chosen because it is non-peralkaline and allanite has most frequently been petrographically identified from it, and a polished thin section was already available (from C.A. Abernethy). The polished section contained two relatively large 'allanite' crystals (approx. 0.4 mm), one of which was zoned with a deep brown core to a paler brown rim; the paler rim may be indicative of a partly metamict state (Jaffe et al., 1956). Analyses ALL-4 in

Table 19 are easily distinguishable from the chevkinite analyses, particularly by the Al content, and they may confidently be called allanites.

The totals in analyses AL1-4 are low by variable amounts and a structural formula has only been calculated for AL3. There are several possible reasons for these low totals; the mineral has an ideal formula of $(Ca,Ce)_2Al_2Fe(3+)_4Si_3O_{12}(OH)$ (Kostov, 1968) and so it is hydrated as well as theoretically being ferric iron bearing. Because of this, the structural formula is calculated assuming all iron is Fe^{3+} . Furthermore, several elements listed by Deer et al. (1962, Vol.1), for example Mn and Y, have not been analysed.

Therefore it is suggested that in the peralkaline Younger Granites, chevkinite is the most likely REE-bearing mineral to crystallise whereas in the aluminous hornblende biotite and probably the coarse grained biotite granites also, allanite will form instead. Such a hypothesis is in accord with evidence from extensive volcanic ash deposits, where allanite is an accessory mineral in the biotite bearing ashes and chevkinite occurs in the non-biotitic ashes (Izett and Wilcox, 1968).

4.6 Narsarsukite

Narsarsukite has been identified in a loose sample of a (probable) dyke intruded into the Shira quartz syenite and related to the Birji dyke. Narsarsukite occurs as colourless, moderate relief, interstitial highly anhedral grains associated with quartz, albite, microcline, aegirine, arfvedsonite and aenigmatite. It is the last mineral to crystallise in this association and it probably forms at a

Table 20. Electron microprobe analyses of narsarsukite, uncorrected for sodium volatilisation.

	N1	N2	N3	N4	N5
SiO ₂	63.58	62.17	62.19	62.10	62.39
TiO ₂	13.12	14.30	13.43	13.43	14.03
Al ₂ O ₃	0.53	0.43	0.48	0.48	0.63
FeO _T	5.01	4.13	4.69	4.68	4.75
MnO	0.10	0.00	0.12	0.12	0.00
MgO	0.00	0.00	0.00	0.00	0.00
CaO	0.00	0.00	0.00	0.00	0.00
Na ₂ O	11.18	10.67	11.14	11.13	10.98
K ₂ O	0.09	0.00	0.00	0.00	0.00
ZrO ₂	1.29	-	-	1.39	0.57
	<u>94.90</u>	<u>91.70</u>	<u>92.05</u>	<u>93.33</u>	<u>93.35</u>

relatively low temperature. In thin section, some areas show incipient alteration to a yellow-brown alteration product.

Narsarsukite has already been identified within this province, in highly peralkaline microgranites (probably recrystallised volcanics) in the Gouré complex of Niger where it was originally termed Goureite (Lacroix, 1934) but later correctly identified as narsarsukite (Jeremine and Christophe-Michel-Levy, 1961). Although the discovery at Shira is the first reported occurrence of narsarsukite in Nigeria, the author has also identified the mineral as a minor constituent of the Ririwai albite arfvedsonite granite and it appears likely that it may have been taken for amblygonite (Mackay and Beer, 1952), especially as amblygonite has never subsequently been verified. (The identification of pyrochlore, cryolite and its breakdown product thomsenolite in the albite arfvedsonite granites however, appears to be secure).

Five microprobe analyses of narsarsukite are presented in Table 20, which compare favourably with the analyses of Upton et al. (1976) except in one important respect; since the mineral was unknown at the time, no account was taken of the fact that narsarsukite is unstable under an electron beam. Consequently, the Na values reported are around 11% Na₂O whereas 15-16% would probably be the correct value. In addition, Upton et al. (1976) report appreciable Nb and F contents, although strangely they did not analyse for Zr. The Nigerian analyses are therefore presented as the best available at present but no structural formulae have been calculated.

Discussion

Narsarsukite is a very rare mineral with an ideal formula of Na₂Ti₂OSi₄O₁₀ (Peacor and Buerger, 1972) that was first recognised in Greenland (Flink, 1901) where it is "generally accompanied by the minerals which most frequently occur in the pegmatite veins of this

locality" (Boggild, 1953). In another Greenland occurrence (Upton et al., 1976), narsarsukite occurs within an oversaturated peralkaline trachyte dyke (near Illimaussaq). At this locality, narsarsukite is associated principally with albite and aegirine, and minor 'riebeckite', mica, oxides, calcite and zircon. In both the Greenland and Niger occurrences, narsarsukite consists of square or rectangular euhedra which are crowded with inclusions. During melting experiments of the chilled, apparently magmatic host dyke, all the major minerals crystallised except narsarsukite. This evidence together with some degree of metasomatic alteration in the host quartz diorite, was interpreted to indicate a lack of correspondence between the present rock and the original magma - that is, probable loss of alkalis and other elements (Upton et al., 1976).

Therefore, the euhedral narsarsukite may not be a phenocryst phase in the sense of growing from a magma, instead, it may have grown in the subsolidus under the influence of volatile components since lost from the system (Upton et al., 1976). This suggestion is supported by the Gouré occurrence, since although the host rock is described as a peralkaline 'microgranite', it does not resemble a true granite but in reality may be a series of thick, recrystallised peralkaline volcanic rocks (P. Bowden, pers. comm.) that are intruded by an 'alkaline' syenite (Black, 1963). The narsarsukite occurs in patches and pegmatitic veins and its habit is that of "pseudo-phenocrysts with distinct contours but riddled with small inclusions of quartz and feldspar" (Jeremie and Christophe-Michel-Levy, 1961).

In the Kola massif, narsarsukite occurs along an albitised zone between a nepheline syenite and the country rock. It is of relatively late formation and contains up to 50% by volume of albite inclusions (Vlasov et al., 1966). Similarly, narsarsukite occurs adjacent to nepheline syenite in Quebec, and also in the surrounding

hornfels and silicate vugs, where its formation has been attributed to Na and Ti metasomatism (Rajasekaran, 1966; Chao, 1967). The hornfels in particular, contains large (1 cm) euhedra of narsarsukite that are heavily crowded with inclusions.

In Montana, narsarsukite occurs close to an undersaturated syenite and is found in 5 mm wide veins or pegmatitic knots along with pectolite, calcite, quartz and galena (Graham, 1935; Stewart, 1959).

The predominant mode of occurrence of narsarsukite therefore appears to be the result of fluids emanating from an alkaline magma reacting with or trapped against the country rock. Furthermore, in Greenland (Flink, 1901) and Montana, there is a close association between narsarsukite and mineralised, hydrothermal veins.

The occurrence at Shira is in a loose boulder of distinctive appearance, whose origin is probably as a dyke related to the numerous, highly peralkaline dykes that are associated with the Birji granite, but perhaps with a higher proportion of alkalis which resulted in localised enrichment in Na and Ti particularly.

4.7 Olivine

Olivine occurs within the Shira complex only in the Zigau granite porphyry it may also be quite fresh and associated with ferrohedenbergite but is often heavily altered to deep red-brown iddingsite. Five microprobe analyses from four crystals are presented in Table 21 together with three analyses of two areas of iddingsite alteration. In the latter case, no formulae are presented as the mineral has no recognisable structure (Gay and Le Maitre, 1961). In addition, four analyses from two olivine crystals in the alkali feldspar syenite

from the nearby complex of Dutse are also presented in Table 21.

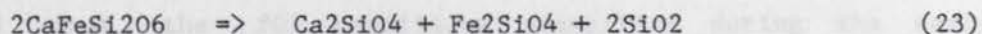
The proportion of end-member fayalite (Fe_2SiO_4) has been calculated on the basis of $\text{Fa} = (\text{Fe}(2+) + \text{Mn})$ and it may be seen that the Zigau olivine ranges from Fa 93.4-99.6 (those from Dutse also fall within this range). Analyses have been made from both the core and rim of three crystals but no detectable difference in composition was found. These results show that the Zigau (and Dutse) olivine is very close in composition to the theoretical end-member, although it must be remembered that had Mn been considered as belonging to the tephroite end-member, then the Fa values would range from Fa 90.6-96.1 in the case of Zigau, and Fa 89.8-91.0 for Dutse. By using a ferric iron calculation procedure the Fe^{3+} content was found to be negligible (NLSTFR program, Appendix 3).

Discussion

These data closely match other unpublished fayalite analyses (calculated on the same basis) from the Nigerian Younger Granite complexes. In quartz porphyries from the Tibchi complex a range of composition from Fa 97.3-99.3 for three samples has been found, while a single analysis from a micro-ferrodiorite enclave in the same rock gave a composition of Fa 92 (Ike, 1979). Apart from this enclave, Ike (op.cit.) found no significant variation within, or between grains. Fayalitic olivine is common in anorogenic granites and related rocks, since it also occurs in the Rapakivi granites of Finland (Simonen, 1961), the Pikes Peak batholith, Colorado (Barker et al., 1975), Corsica (Maluski, 1975), Skye (Kleeman, 1967), the Coldwell complex, Canada (Mitchell and Platt, 1978) and Ilimaussaq (Larsen, 1976). Within these various anorogenic granitic or syenitic complexes, fayalite may occur in both silica saturated and undersaturated rocks.

The Ca content of olivines in general appears to be partly

pressure dependent; the Ca content of the Zigau fayalites is relatively high compared to the data of Simkin and Smith (1970). Since the Ca content lies above 0.14 wt.% CaO (except OL2 = 0.11% CaO), these analyses fall outside the range for plutonic rocks and instead plot within the field of volcanic and hypabyssal rocks, in keeping with the high level nature of the Younger Granites. The Mn content, however, is not easily related to depth of crystallisation, although the data of Simkin and Smith (op.cit.) do show that the olivines with highest Mn content (2.8-3.4% MnO) are both fayalitic and from extrusive rocks. The Ca and Mn levels found in fayalitic olivines from the Igaliko undersaturated complex of the Gardar province are unusually high, a fact which Stephenson (1974) attributed to the high level of emplacement. However, Larsen (1976) proposed, in addition, that a high Ca content in fayalitic olivine is also dependent upon low silica activity in the magma, as suggested by the reaction:-



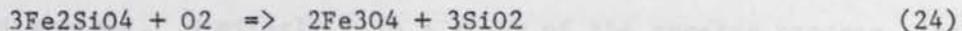
Simkin and Smith (op.cit.) also noted that highly undersaturated rocks carried olivines which were unusually rich in Mn and Ca.

Thus the range of Ca content in the Zigau fayalites from 0.11 to 0.35 %CaO can be considered quite normal for a silica oversaturated magma emplaced at a high structural level.

Despite the occurrence of fayalite as one of the first formed minerals in the Zigau porphyry, it can occur as a relatively low P-T mineral associated with hydrothermal fluorite and siderite in tension fractures related to granite (Pringle, 1975). In addition, fayalite has been synthesised over a range of temperature from 925 degrees C (the upper limit of the experiments) to 250 degrees C, below which hydrous phases (serpentine) were more stable (Flashen and Osborn, 1957).

The stability of fayalite as a function of temperature and f_{O_2} has been investigated by several workers but the results are

conveniently summarised by Eugster and Wones (1962), since the reaction:-



is commonly used as an oxygen buffering assemblage (QFM). The heat of reaction of the forward reaction is given by Wones and Gilbert (1968) as -117.4 kcals and it has been calculated by the writer as -125 kcals (i.e. -41.7 kcals per mole of fayalite at 25 degrees C) from data in Robie and Waldbaum (1968). Thus, the products of equation (24) are energetically favoured over the reactants. However, the fayalite may be rimmed by amphibole (which may or may not be replacing the fayalite) and definitely altered to iddingsite. No magnetite has been observed petrographically in association with fayalite, and for the Zigau porphyry, ilmenite is the only oxide phase identified by electron microprobe analysis. Thus, in view of these petrographic observations and the fact that the above reaction is dependent on $f\text{O}_2$, it may be concluded that the $f\text{O}_2$ conditions prevailing during the early crystallisation period of the Zigau granite porphyry were below that defined by the QFM buffer given in equation (25). No estimate of the temperature of crystallisation would be possible without an independent estimate of $f\text{O}_2$ however.

In Table 21, three microprobe analyses (UN1-3) of iddingsite pseudomorphs after fayalite are presented. In many cases remnants of fayalite can be found within an area which is dominantly iddingsite. Since iddingsite is therefore forming directly from fayalite, it is of interest to compare the analyses. The low totals are an indication that the iddingsite pseudomorph is considerably hydrated but in particular the levels of Fe and Mn and Mg decrease while Si, Ti and K increase, even if the analyses were to be recast on an anhydrous basis. Several studies of iddingsite are reported in the literature. Brown and Stephen (1959) found that iddingsite from a single olivine basalt was a

polycrystalline aggregate consisting largely of two components, goethite and a sheet silicate, in which the original olivine lattice had not been greatly disturbed. Similarly, in a study of the reverse process, that is, the artificial conversion of serpentine to olivine, Brindley and Zussman (1957) showed that few Si-O bonds were broken and the change involved only slight rearrangement of tetrahedra and some migration of Si. Thus, selective alteration of olivine, while adjacent minerals are unaffected, can be explained. In a more extensive study of iddingsite from a wider range of sources, Gay and Le Maitre (1961) found clear evidence that the mechanism for the alteration of olivine to iddingsite was one of ionic diffusion. The model favoured is that, under suitable PTX conditions, protons attach themselves to non-bridging oxygen ions which are capable of releasing Mg and Fe²⁺ cations as a result, and allowing their replacement by Fe³⁺, K etc. Also, these authors find only slight evidence of structural change, but Si atoms have apparently been free to move from their tetrahedral oxygen framework. The precise chemical environment of this alteration is unknown, but a strong oxidising environment seems essential. Gay and Le Maitre (op.cit.) suggest a temperature of alteration "below that necessary for structural reorganisation, and above that at which the rock has completely solidified". Thus a broadly late magmatic or 'deuteric' environment is likely, and as such, iddingsitization of the Zigau fayalite may be connected temporally and chemically with changes in coexisting clinopyroxene and alkali feldspar.

Fayalite and/or iddingsite is commonly surrounded by a ferrorichterite-arfvedsonite amphibole which has, however, not been affected by the formation of iddingsite. There is no petrographic sign that fayalite has altered to, say, ferrorichterite - rather, it appears as though the necessary growth conditions for fayalite were no longer available and ferrorichterite grew instead. In order to test this

Table 2.2 Electron microprobe analyses of micas

Sample no.	Eldewo alkali feldspar biotite granite										Zigau granite porphyry		Shira quartz syenite			Andulayi alkali feldspar syenite		
	SH21			SH47/6							ZG/2D		SH19 (xenolith)			SH25 (pseudomorph)		
	1		2	3	4		5		6		7	8	9	10	11	12	13	14
Crystal no.																		
Spot no.	B1 margin	B2 core	B4 colourless margin	B5 core	B6 core	B7 core	B8 margin	B9 core	B10 margin	B11 core	M1	M1A	M2	M3	M4	M5	M6	M7
SiO ₂	35.97	35.68	41.19	36.22	36.34	34.90	35.91	36.05	36.17	36.40	38.28	38.93	35.94	36.00	34.98	38.76	39.32	40.38
TiO ₂	2.73	2.60	0.50	2.23	1.91	1.83	1.76	1.59	1.56	2.22	0.00	0.00	4.53	4.43	4.18	3.27	1.16	1.05
Al ₂ O ₃	11.71	10.80	19.99	11.52	11.47	10.39	11.15	10.42	11.05	10.44	7.44	7.13	12.43	12.41	12.93	10.47	10.41	9.99
FeO _T	32.60	34.75	19.05	33.49	33.03	37.56	35.65	36.73	35.00	36.20	40.79	40.65	28.82	29.10	29.38	24.76	20.40	18.38
MnO	0.86	0.88	0.68	0.90	0.76	0.83	0.80	0.76	0.88	0.80	0.67	0.81	0.23	0.19	0.30	0.32	0.24	0.43
MgO	1.47	1.53	0.27	1.48	2.14	0.34	0.33	0.33	0.38	0.36	1.18	1.34	5.48	5.47	5.04	9.94	13.98	15.72
CaO	0.00	0.00	0.00	0.00	0.00	0.01	0.01	0.00	0.00	0.00	0.00	0.00	0.00	0.10	0.00	0.00	0.45	0.00
Na ₂ O	0.21	0.40	0.07	0.29	0.27	0.37	0.31	0.23	0.21	0.29	0.00	0.00	0.35	0.00	0.42	0.00	0.00	0.00
K ₂ O	8.81	8.58	9.93	8.60	8.95	8.50	8.56	8.66	8.76	8.60	7.10	6.61	8.71	8.67	8.97	9.28	9.56	9.84
ZnO	0.11	0.10	0.05	0.11	0.11	0.10	0.11	0.09	0.09	0.07	-	-	-	-	-	-	-	-
ZrO ₂	0.00	0.00	0.00	0.01	0.01	0.00	0.00	0.00	0.00	0.02	-	-	-	-	-	-	-	-
F	1.88	2.28	3.38	2.75	2.39	2.49	2.05	2.57	2.33	2.45	-	-	-	-	-	-	-	-
less O=F,Cl	0.79	0.96	1.42	1.16	1.00	1.05	0.86	1.08	0.98	1.03	-	-	-	-	-	-	-	-
	95.56	96.64	93.69	96.44	96.38	96.27	95.78	96.35	95.45	96.82	95.46	95.47	96.49	96.37	96.20	96.80	95.52	95.79
Structural formulae based on 22 oxygens																		
Si	5.957	5.929	6.389	5.991	5.995	5.933	6.030	6.073	6.090	6.070	6.445	6.513	5.687	5.702	5.594	5.977	6.029	6.109
Al ^[IV]	2.043	2.071	1.611	2.009	2.005	2.067	1.970	1.927	1.910	1.930	1.477	1.407	2.313	2.298	2.406	1.904	1.882	1.781
Σ Z	8.000	8.000	8.000	8.000	8.000	8.000	8.000	8.000	8.000	8.000	7.922	7.920	8.000	8.000	8.000	7.881	7.911	7.890
Al ^[VI]	0.243	0.045	2.045	0.238	0.226	0.015	0.237	0.143	0.283	0.122	-	-	0.006	0.020	0.031	-	-	-
Ti	0.340	0.325	0.058	0.277	0.237	0.234	0.222	0.201	0.198	0.278	-	-	0.539	0.529	0.503	0.380	0.134	0.120
Zr	-	-	-	0.001	0.001	-	-	-	-	0.002	-	-	-	-	-	-	-	-
Mg	0.363	0.379	0.062	0.365	0.526	0.086	0.083	0.083	0.095	0.089	0.297	0.330	1.294	1.293	1.202	2.284	3.196	3.544
Zn	0.013	0.012	0.006	0.013	0.013	0.013	0.014	0.011	0.011	0.009	-	-	-	-	-	-	-	-
Fe ²⁺	4.515	4.829	2.471	4.633	4.557	5.340	5.006	5.175	4.928	5.049	5.744	5.687	3.814	3.854	3.930	3.194	2.616	2.326
Mn	0.121	0.124	0.089	0.126	0.106	0.119	0.114	0.109	0.125	0.113	0.095	0.110	0.032	0.026	0.042	0.043	0.032	0.056
Ca	-	-	-	-	-	0.002	0.002	-	-	-	-	-	-	-	0.018	-	-	0.075
Σ X	5.595	5.714	4.731	5.653	5.666	5.809	5.678	5.722	5.640	5.662	6.136	6.127	5.685	5.740	5.708	5.901	6.053	6.046
Na	0.067	0.128	0.021	0.093	0.087	0.122	0.101	0.075	0.068	0.094	-	-	0.108	-	0.131	-	-	-
K	1.861	1.819	1.965	1.814	1.883	1.843	1.834	1.861	1.882	1.829	1.525	1.412	1.759	1.752	1.829	1.826	1.870	1.899
Σ Y	1.928	1.947	1.986	1.907	1.970	1.965	1.935	1.936	1.950	1.923	1.525	1.412	1.867	1.752	1.960	1.826	1.870	1.899
100Mg/Mg+Fe ²⁺	7.44	7.28	2.45	7.30	10.35	1.59	1.63	1.58	1.89	1.76	4.92	5.48	25.33	25.12	23.42	41.69	54.99	60.37

Perhaps the crucial point in the argument is that fayalite does not appear to have ceased to crystallise through an increase in f_{O_2} above the QFM buffer, since the expected reaction is not observed. However, at some later stage, fayalite probably become unstable, reacting with a deuteritic fluid to produce iddingsite.

4.8 Biotite

Biotites from both major facies of the Eldewo granite have been analysed by electron microprobe and the analyses are presented in Table 22. Other occurrences of biotites are of relatively minor importance and occur as xenolithic or pseudomorphic aggregates, which are much more Mg-rich than micas from the biotite granite.

On a Foster (1960) diagram (Figure 20) microprobe analyses of the Eldewo biotites plot in the $Fe(2+)$ -rich corner, away from the fields represented by micas from pegmatites of (dominantly calc-alkaline) granites. This position should be interpreted with some caution however, since the diagram was designed for wet chemically analysed micas in which Fe^{3+} is included at the apex of the diagram along with Ti and Al. However, for wet chemical analyses of similar annitic micas from Pikes Peak (Barker et al., 1975), and rapakivi granites (Simonen and Vormo, 1969), the Fe^{3+}/Fe^{2+} ratio is relatively low and averages 0.13. Thus the expected upward movement of the Shira microprobe analyses, were the Fe^{3+} content known, would be slight; possibly their 'true' position would lie close to the pegmatitic field. In addition, it is probable that the annitic micas from Shira and other high level, anorogenic granites contain >4 cations of Fe^{2+} per 22 oxygens, in contrast to Foster's claim that such micas are exceedingly rare.

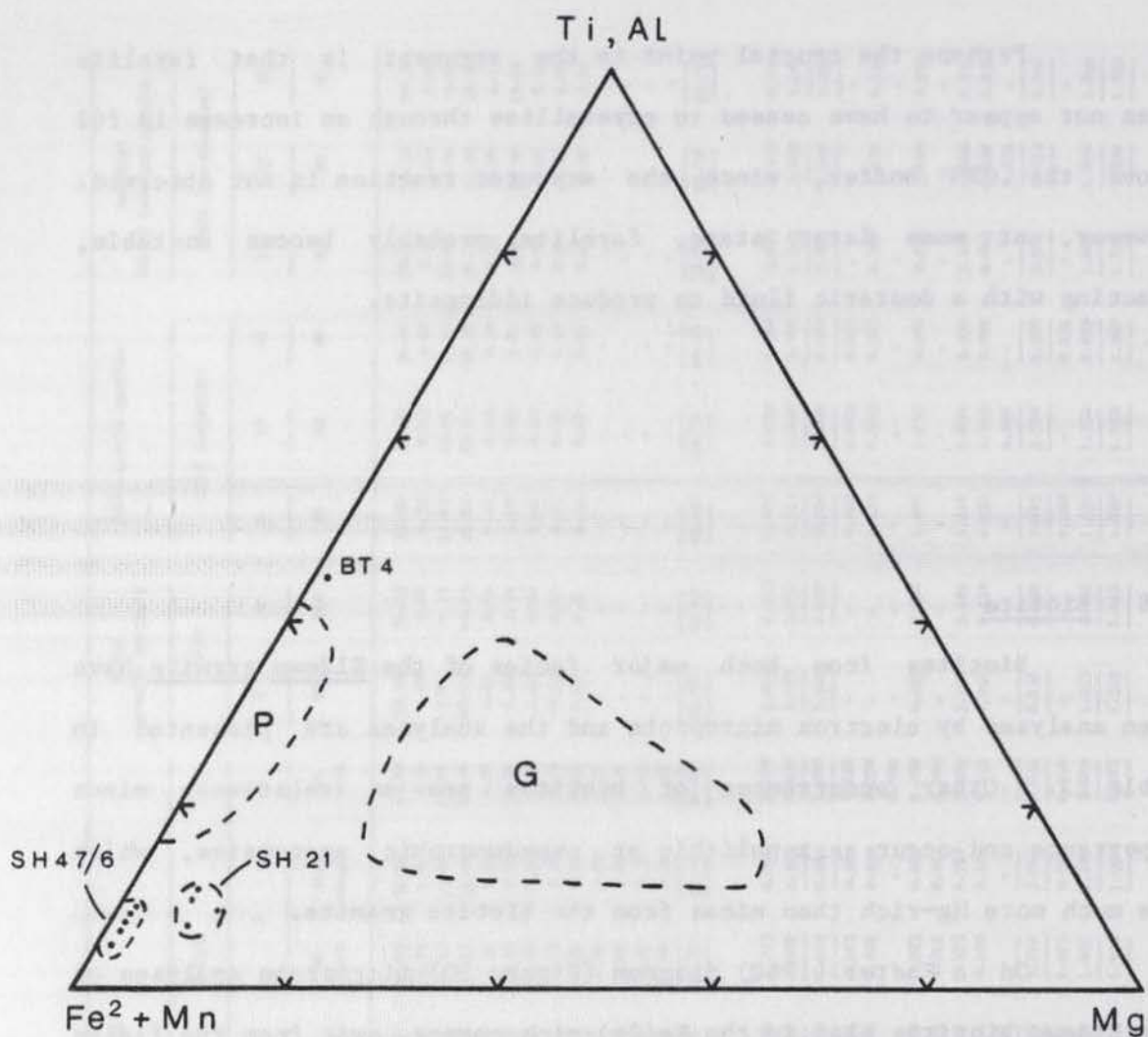


Figure 20. Modified Foster diagram for trioctahedral micas from the Eldewo biotite granite. Fields G and P are the approximate areas for granitic and pegmatitic micas from Foster (1960).

Other extremely Fe-rich biotites analysed from the Shira complex occur in the Zigau porphyry as narrow selvages around iddingsite pseudomorphs after fayalite (Table 21). These micas may have inherited an Fe-rich nature by reaction with the original fayalite. Other, non-analysed, occurrences in the Zigau porphyry, include narrow biotite rims to ilmenite crystals.

Biotite analyses from the Shira complex and elsewhere have been plotted in Figure 21, where the Fe-rich nature of those from the Eldewo granite is clearly illustrated. From Figure 21B, it can be seen that the two facies of biotite granite contain micas that are distinguishable from one another by their $Mg/(Mg+Fe)$ ratio; the coarse grained facies (Chapter 3) is the more magnesian. Analyses from the core and rim of several crystals (Figure 21) show that there is often a significant increase in Al towards the margins. This is accompanied by very little change in the $Mg/(Mg+Fe)$ ratio due to the very low content of Mg. Analysis B4 (Table 22) is unique among the mica analyses in that it comes from a colourless, probably postmagmatic overgrowth to a brown biotite. This overgrowth mica has over 2 cations of octahedral Al compared to less than 0.3 cations for the annitic biotites and it has an apparent sum of octahedral cations of only 4.7 cations, which is probably a reflection of the undetermined Li content. Analysis B4 is more appropriately plotted in Figure 22 which illustrates the approximate positions of ideal Li-Fe-Al mica varieties. This diagram illustrates the dominantly annitic nature of the Eldewo granite micas, with the exception of analysis B4 which plots close to the zinnwaldite variety. In thin section, many annitic micas have overgrowths of green filaments which symplectically replace adjacent alkali feldspar; however, the specimens used were not sufficiently well polished to enable microprobe analyses to be made. Despite this, by analogy with similar mica filaments in the Rishi biotite granite of the Saiya Shokobo

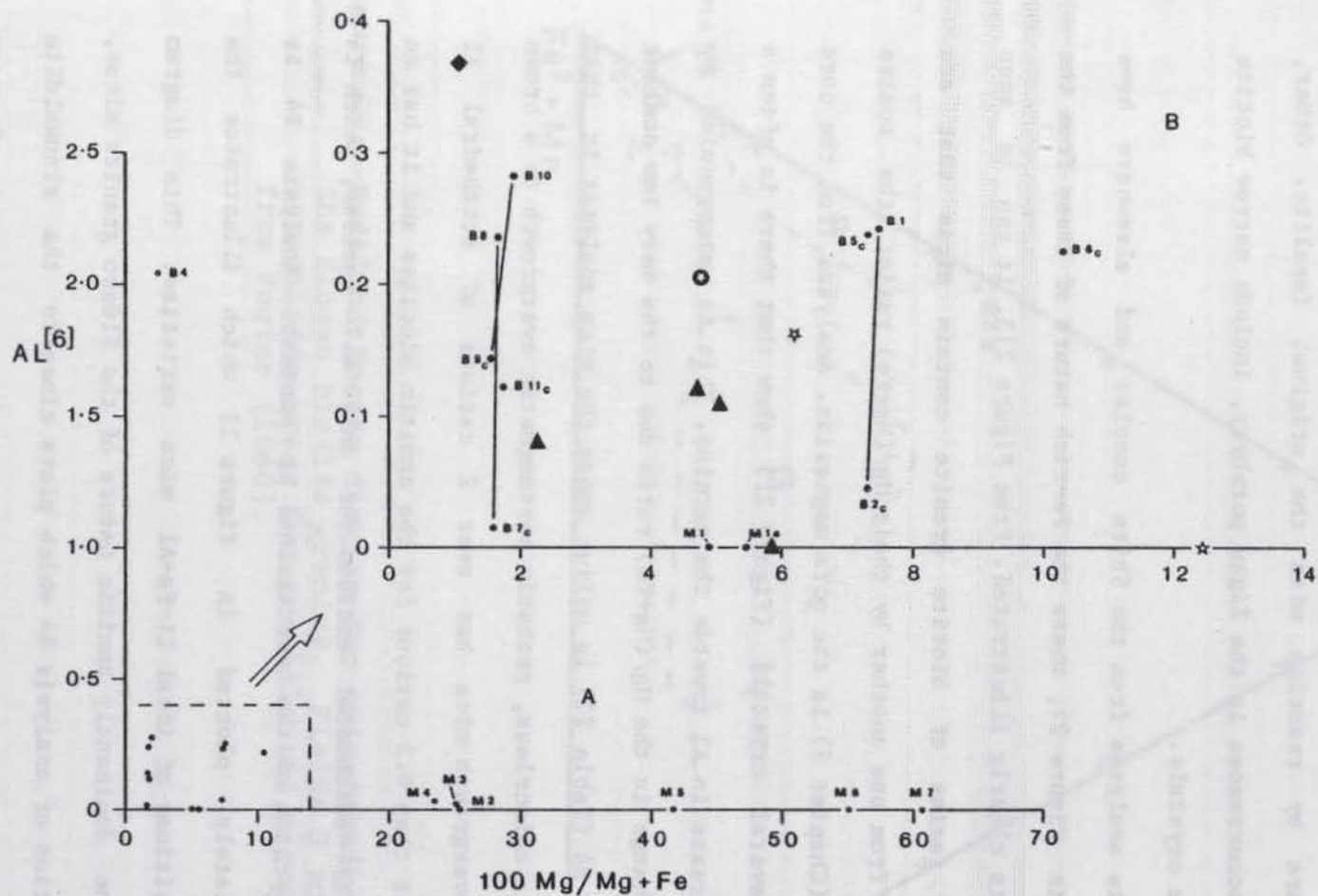


Figure 21. Al v 100Mg/Mg+Fe diagram for trioctahedral micas from the Shira complex and elsewhere. Dots = Shira complex. Diamond = Ririwai (Jacobson et al., 1958). Triangles = Pikes Peak batholith (Barker et al., 1975). Open star = Rapakivi granite (Simonen and Vormo, 1969). Star inside circle = Mourne mountains (Brown, 1956). Subscript c = core of crystal, joined to the margin by a tie line.

complex, it is expected that the green overgrowths are Al-rich annitic micas which will plot along the annite-ferroprotolithionite join in Figure 22.

At the eastern margin of the Shira quartz syenite, small (<1 cm), dark, mafic-rich xenolithic bodies occur; one such body (in SH19), enclosed by alkali feldspar, is composed almost entirely of ilmenite (Table 23) and dark brown biotite. This mineral assemblage is secondary after the original, presumably also highly mafic, enclave. Biotites from this enclave (M2-4 in Table 22 and Figure 21) are noticeably more magnesian than those from the Eldewo granite. It should be noted however, that this aluminous enclave appears to have been protected from any alteration within the peralkaline host rock, presumably by virtue of being enclosed within alkali feldspar.

Analyses M5-7 (Table 22) are of biotites from the xenolithic facies of the Amdulayi quartz syenite; here, biotite occurs in association with occasional ilmenite grains in the outer part of zoned pseudomorphs in which the centre is filled with richterite (Section 4.2). This association is interpreted as a breakdown assemblage and it is significant that both the mica and the amphibole are relatively Mg-rich. Analysis M5 is of a dark brown biotite close to an ilmenite grain, whereas analysis M6 is from the opposite side of the same pseudomorph where the mica is pale brown in colour. Analysis M7 is also a pale brown mica but from an ilmenite-free pseudomorph. The pale brown biotite, away from any ilmenite grains, is more magnesian than the dark brown biotite. These compositions lie approximately midway along the annite-phlogopite join and together with the central core of pale green richteritic amphibole, indicate that the pseudomorphed mineral was probably unusually Mg-rich (for this province). It is curious however that it should have two breakdown products (?plus ilmenite) which form concentric zones.

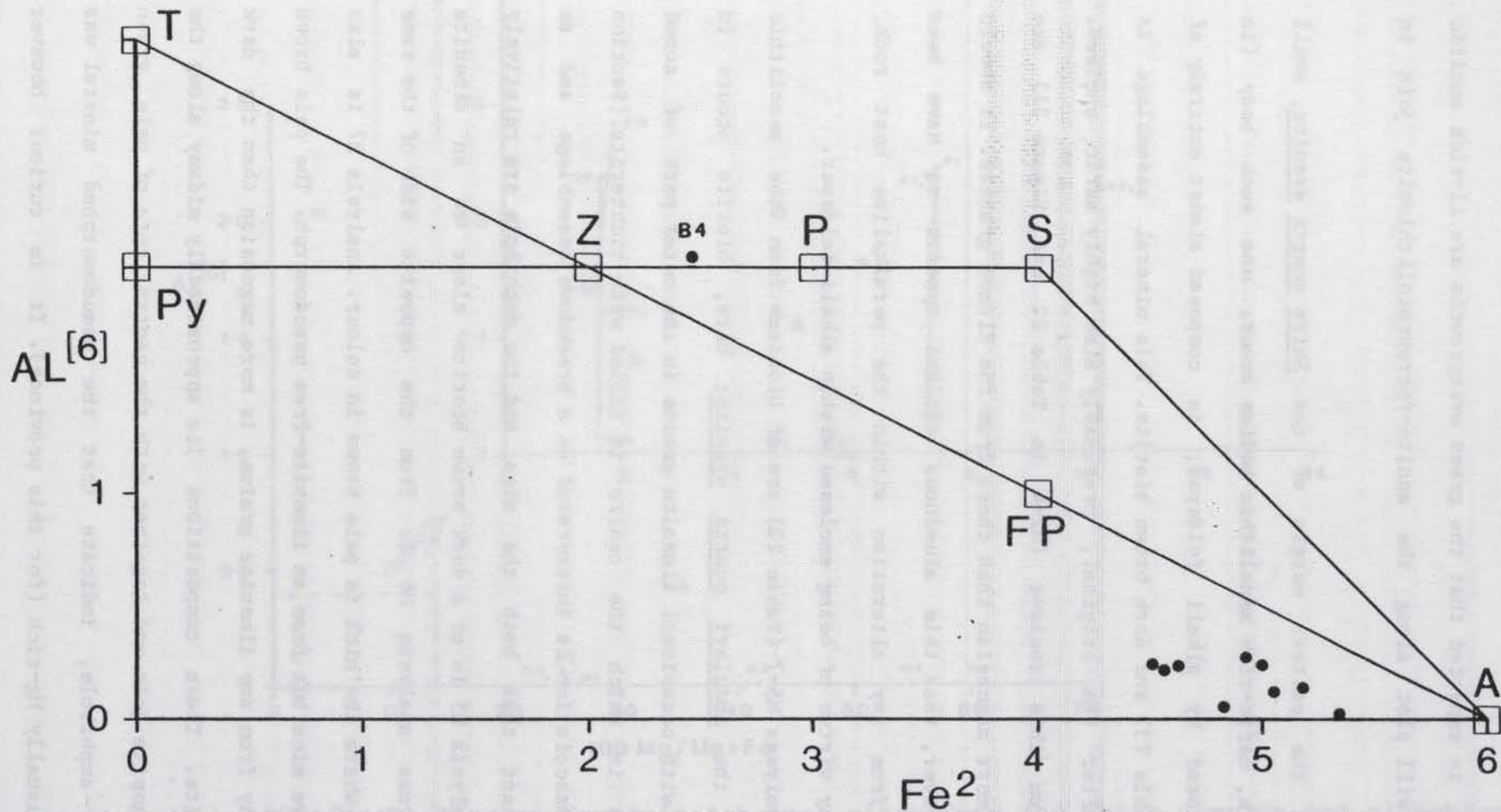


Figure 22. Al[6] v Fe² diagram for trioctahedral micas from the Shira complex (after Abernethy, in prep.). T = trillithionite; Py = polyolithionite; Z = zinnwaldite; P = protolithionite; S = siderophyllite; FP = ferroprotolithionite; A = annite.

13m/13

Discussion

As discussed in Chapter 3, the annite biotite in both facies of the Eldewo biotite granite is believed to be a product of magmatic crystallisation whilst the late magmatic and postmagmatic events are recorded in the green filaments or larger, zinnwalditic overgrowths. Several examples of annitic biotites from other parts of the world are plotted in Figure 21B, and the compositions are very close to those from Shira. A feature of these analyses from the literature is that they all occur in high level, anorogenic granites, including those in the Mourne mountains, Finnish Rapakivi granites and the Pikes Peak batholith. Within the Niger-Nigeria province it appears that analyses of dark brown, annitic biotites from alkali feldspar biotite granites are comparatively rare, which is probably in part a function of the degree of postmagmatic alteration suffered by these granites.

In an extensive study of micas from this province, Abernethy (in prep.) describes only a single dark brown, annitic biotite (from the relatively unaltered core of a crystal from the Rishi biotite granite, sample SS43). In contrast, the plagioclase bearing biotite and hornblende biotite granites appear to have biotites which are more magnesian - an expected result if the alkali feldspar biotite granites are fractionates of the plagioclase (+/- hornblende) bearing granites. Therefore, the Fe-rich nature of the biotite together with the absence of plagioclase in the Eldewo biotite granite both point to the rock being a highly fractionated aluminous granite. The slightly higher Mg/(Mg+Fe) ratio in biotite from the coarse grained facies could be the result of somewhat higher oxidation conditions (Wones and Eugster, 1965; Czamanske and Wones, 1973) or simply reflect bulk compositional differences. The scarcity of outcrop has limited geochemical sampling to the extent that the latter hypothesis cannot be tested with the present data.

The stability of biotite has been the subject of several studies. Annite [$K_2(Fe^{2+})_6Al_2Si_6(O)_{20}(OH)_4$] stability is lower in quartz bearing systems than those in which quartz is absent, and is sensitive to changes in pH_2O and fO_2 as well as temperature (Eugster and Wones, 1962). The maximum thermal stability of annite coexisting with quartz was found to be approximately 700 degrees C at an fO_2 defined by the QFM buffer, and the stability field widens considerably from this point with decreasing temperature and fO_2 . Subsequently, the Mg/Fe ratio of a biotite was also shown to be dependent upon fO_2 conditions (Wones and Eugster, 1965). Thus, biotite crystallising from a magma may become either more Mg-rich or Fe-rich depending on the fO_2 (and T) during crystallisation. An Fe-enrichment trend, as found in the Eldewo granite is probably accompanied by a decrease in fO_2 , in a water undersaturated magma.

Cations such as F, Al and Ti enhance biotite stability while Na decreases the stability (Rutherford, 1969, 1973; Robert, 1976). For Ti in particular, total pressure is also important; low pressure favours the entry of Ti into the mica lattice (Robert, 1976).

The octahedral Al content of the Shira biotites increases slightly from core to rim while the overall octahedral site occupancy apparently falls - presumably partly in response to a sympathetic increase in (undetermined) Li. However the average Al(6) content of the Eldewo granite micas is only 0.17 cations (per 22 oxygens) which is far below the level necessary to have a significant effect on the stability (Rutherford, 1973). However, whatever slight effect this small amount of Al(6) may have on biotite, stability will probably be augmented by the Ti content (average 0.26 cations, excluding B4), and perhaps the F content as well (Rutherford, 1969). The Na content of the Shira annitic micas is low and presumably has an insignificant effect on mica stability. Therefore, although the Shira annitic biotites are among the

nearest natural micas to the theoretical annite end-member, they will be expected to have slightly greater stability than their synthetic counterparts. However, maximum thermal stability is unlikely to have greatly exceeded 700 degrees C.

Since (almost pure) magnetite is present in the Eldewo biotite granite and it does not show any optical heterogeneity, fO₂ conditions during crystallisation and cooling probably lay between the QFM and HM fO₂ buffering curves.

For the Li-Fe micas there appears to be only an approximate compositional relationship between experimental compositions and those occurring in the Eldewo granite (B4). However, in a F-rich environment a Li-Fe mica will in general be more stable than an annitic mica (Rieder, 1971). In this context it should be noted that zinnwaldite B4 has a higher F content (3.38%) than the annitic micas (average 2.35%). The stability of micas along the join siderophyllite (1) - polyolithionite (2) given by Rieder (1971) is difficult to interpret for the zinnwalditic overgrowth B4 because of the absence of a Li analysis in particular, and also because neither of these synthetic end-members is close to natural (greisen mica) compositions. However, the synthetic Li-Fe micas have an extensive stability field below 550 degrees C and together with the mode of occurrence of analysis B4 as a possible hydrothermal overgrowth or an annitic biotite, a temperature of formation below 550 degrees C would be expected.

(1) $[K_2.Fe_{2+}.Al_2.Al_4.Si_4.O_{20}.(OH,F)_4]$

(2) $[K_2.Li_4.Al_2.Si_8.O_{20}.(OH,F)_4]$

Table 23 Electron microprobe analyses of ilmenite and magnetite

Sample no.	Zigau granite porphyry										Shira quartz syenite						Amdulayi syenite		Eidwe biotite gnt.			
	2G/2B				2G/2C					2G/2D		SH11		SH68/2		SH19		SH25	SH51		SH21	
					xenolith					within K-feld.	xenolith	xenolith		xenolith	within aenigm.	pseudo-morph	within aenigmatite		magnetite			
Crystal no.	1	2	3	4	5	6	7	8	9	10	11	12	13	14	15	16	17	18	19	20	21	
Spot no.	OX3	OX4	OX1	OX2	IL1	IL2	IL3	IL6	IL7	IL8	IL9	IL10	IL11	IL12	IL14	IL15	IL16	UN12	IL13	OX14	OX15	
SiO ₂	0.00	0.00	0.00	0.00	0.34	0.27	0.29	0.37	0.19	0.25	0.37	0.42	0.21	0.40	0.26	0.17	0.00	0.31	0.20	0.00	0.00	
TiO ₂	51.22	51.78	51.04	51.41	49.06	50.00	50.03	50.59	50.95	51.12	51.75	50.20	52.21	50.60	54.33	53.67	52.99	52.36	51.30	0.47	0.90	
Al ₂ O ₃	0.01	0.02	0.06	0.03	0.00	0.00	0.16	0.00	0.00	0.00	0.00	0.00	0.00	0.00	0.16	0.00	0.26	0.00	0.00	1.35	0.22	
FeO _T	47.07	47.28	45.99	46.96	47.68	47.41	47.12	47.06	47.94	47.81	42.39	47.66	45.30	46.08	41.58	41.46	42.31	45.98	46.12	82.06	85.74	
MnO	-	-	2.25	-	1.36	1.36	1.46	2.18	1.00	1.39	3.60	1.95	1.93	1.98	2.82	4.87	4.82	0.73	2.97	0.07	0.11	
MgO	0.01	0.01	0.02	0.03	0.00	0.00	0.00	0.00	0.00	0.00	0.00	0.00	0.00	0.00	0.00	0.00	0.28	0.00	0.00	0.12	0.03	
CaO	0.02	0.02	0.00	0.03	0.00	0.00	0.00	0.00	0.00	0.00	0.00	0.00	0.00	0.00	0.00	0.00	0.00	0.00	0.00	0.00	0.00	
	98.33	99.11	99.36	98.46	98.44	99.04	99.06	100.20	100.08	100.57	98.11	99.73	99.65	99.06	99.15	100.17	100.38	99.38	100.59	84.07	87.00	
Fe ₂ O ₃ ⁰	1.17	0.85	2.68	0.91	5.04	3.89	3.63	3.70	3.23	3.28	0.00	3.87	0.06	2.34	0.00	0.00	0.04	0.00	3.07	59.68	62.33	
FeO ^c	46.02	46.52	43.58	46.14	43.15	43.91	43.86	43.73	45.03	44.86	42.39	44.18	45.24	43.97	41.58	41.46	42.27	45.98	43.36	28.36	29.65	
Molecular proportions																						
SiO ₂	-	-	-	-	0.006	0.004	0.005	0.006	0.003	0.004	0.006	0.007	0.003	0.007	0.004	0.003	-	0.005	0.003	-	-	
TiO ₂	0.641	0.648	0.639	0.643	0.614	0.626	0.626	0.633	0.638	0.640	0.648	0.628	0.653	0.633	0.680	0.672	0.663	0.655	0.642	0.006	0.011	
Al ₂ O ₃	0.000	0.000	0.001	0.000	-	-	0.002	-	-	-	-	-	-	-	0.002	-	0.003	-	-	0.013	0.002	
Fe ₂ O ₃	0.007	0.005	0.017	0.006	0.032	0.024	0.023	0.023	0.020	0.021	-	0.024	0.000	0.015	0.000	0.000	0.000	0.000	0.019	0.374	0.390	
FeO	0.641	0.648	0.607	0.643	0.601	0.611	0.610	0.609	0.627	0.624	0.590	0.615	0.630	0.612	0.579	0.577	0.588	0.640	0.604	0.395	0.413	
MnO	-	-	0.032	-	0.019	0.019	0.021	0.031	0.014	0.020	0.051	0.020	0.027	0.028	0.040	0.069	0.068	0.010	0.042	0.001	0.002	
MgO	0.000	0.000	0.000	0.001	-	-	-	-	-	-	-	-	-	-	-	-	0.007	-	-	0.003	0.001	
CaO	0.000	0.000	-	0.001	-	-	-	-	-	-	-	-	-	-	-	-	-	-	-	-	-	
% TiO ₂ ⁽¹⁾	49.73	49.81	49.31	49.69	48.74	49.07	49.03	49.08	49.23	49.20	50.50	49.07	49.96	49.42	52.41	51.10	49.89	50.38	49.24	0.76	1.34	
% Fe ₂ O ₃ ⁽²⁾	0.54	0.38	1.39	0.46	2.52	1.87	1.94	1.77	1.54	1.60	0.00	1.85	0.00	1.16	0.15	0.00	0.23	0.00	1.45	48.86	47.86	
% FeO ⁽³⁾	49.73	49.81	49.31	49.85	48.74	49.07	49.03	49.16	49.23	49.20	49.50	49.07	50.04	49.42	47.43	48.90	49.89	49.62	49.31	50.38	50.79	

(1) TiO₂ + SiO₂ (2) Fe₂O₃ + Al₂O₃ (3) FeO + MnO + CaO

4.9 Iron-titanium oxides

Fe-Ti oxides are scarce in the dominantly peralkaline Shira complex. Previous work on the Fe-Ti oxides from the Younger Granite province as a whole is sparse and includes classical analyses of four ilmenites from a granite porphyry from Ririwai and two hornblende biotite granites from Sara-Fier and Jos-Bukuru (Borley, 1963a), and ilmenite, ferrian ilmenite, titanomagnetite, magnetite, and haematite microprobe analyses from the Tibchi complex (Ike, 1979).

Fe-Ti oxides within the Shira complex occur predominantly in the Zigau granite porphyry where discrete grains of ilmenite are often associated with fayalite or ferrohedenbergite, and may be partially or completely enclosed within these minerals or alkali feldspar. In addition, ilmenite occurs in greater abundance in enclaves within the Zigau granite porphyry. In the Eldewo biotite granite, small magnetite grains are found enclosed by, or in close association with biotite. In all other rock types in the complex, Fe-Ti oxides have either not been observed or they occur in very minor quantities. However, there may be a local abundance in certain areas such as the margins of the Shira quartz syenite and the Amdulayi granite. In these two rocks and in the Amdulayi syenite, the only Fe-Ti oxide identified optically by microprobe is ilmenite (Table 23). Thus, none of the rocks contains more than one Fe-Ti oxide and hence no estimate of temperature or fO_2 can be made using coexisting Fe-Ti oxides (Buddington and Lindsley, 1964). The analyses have been recalculated to molecular proportions by including a ferric iron estimation based on the method of Finger (1972) and have been plotted on an Fe-Ti oxide solid solution diagram (after Buddington and Lindsley) in Figure 23. Borley's ilmenite analyses are also plotted in Figure 23.

Compared to microprobe analyses by Ike (op.cit.) and those presented here, the ilmenite analyses of Borley exhibit a comparatively

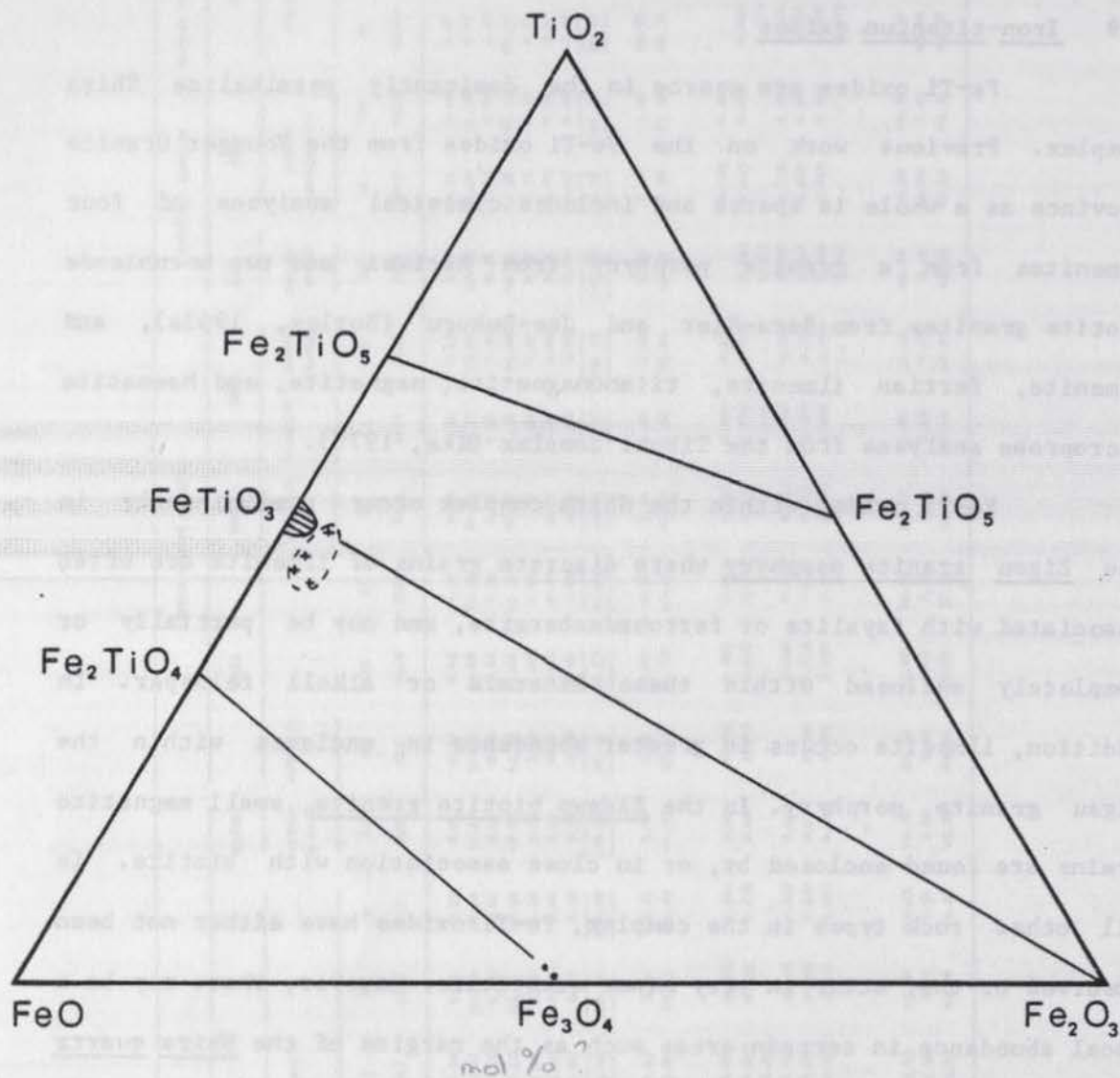


Figure 23. TiO_2 -FeO- Fe_2O_3 diagram for oxide minerals from the Shira complex and elsewhere. Shaded area = ilmenites. Dots = magnetites. Crosses = ilmenites from Borley (1963a).

wide scatter. This scatter is probably due to contamination (Borley herself states that the ilmenite contained inclusions of gangue minerals and were also associated with alteration products). Microprobe analyses need not suffer from these defects. Thus, Borley's observation that the Nigerian ilmenites are of unusual composition in containing a high proportion of ferric iron must be treated with caution. By contrast, the Shira ilmenites plot in a very restricted field and the essential feature of the Fe-Ti oxides from the Shira complex is their relative purity.

In Table 23 it can be seen that ilmenites from microenclaves, pseudomorphs and those which form along cleavages in aenigmatite (IL9, IL 12-13, IL14-16, but not apparently UN12) are relatively enriched in Ti and Mn and depleted in Fe. These particular environments apart, the remainder of the ilmenite analyses show a fairly uniform composition, which is in keeping with the fact that under reflected light they appear homogeneous. Such uniformity occurs despite the small diameter of the microprobe beam (approximately 1 micron). The occurrence of ilmenite with higher Ti and Mn contents and lower Fe values within pseudomorphs (after ferroaugite?) in the Amdulayi syenite and also as a probable breakdown product of aenigmatite (and amphibole) suggests different conditions of formation. The ilmenite-aenigmatite relationship here appears to be the reverse of that observed in a thick, tholeiitic basalt flow in which ilmenite oxidation-exsolution lamellae have been selectively replaced by aenigmatite in a reaction indicative of a reducing environment (Lindsley et al., 1971). In the Finnmarka ring complex, a trend of increasing Mn content in ilmenites with differentiation of the host rock has been ascribed to oxidation during magmatic differentiation (Czamanske and Mihalik, 1972). Furthermore, this conclusion has been confirmed by a parallel study of the mafic silicates (Czamanske and Wones, 1973). The ilmenite within the Finnmarka

complex occurs both as discrete grains and as oxidation exsolution lamellae in titanomagnetite grains. The enrichment in Mn relative to Fe²⁺ is interpreted to indicate that Fe²⁺ is more easily oxidised from the lattice (Czamanske and Mihalik, op.cit.; Snetsinger, 1969). Thus, at the time of formation of ilmenite-richterite pseudomorphs and oxidation of aenigmatite, fO₂ conditions are inferred to have been higher than at the time of crystallisation of the mafic silicate.

Finally, as Figure 23 shows, two magnetite analyses from the Eldewo biotite granite plot very close to the pure Fe₃₀₄ end member. Such a composition is typical of magnetites that form by oxidation of mafic silicates (Haggerty, 1976) but there is no evidence for such an origin here.

The distribution of Fe²⁺ and Mg between coexisting ilmenite and pyroxene has been shown to be a function of temperature and pressure (Bishop, 1980). However, for any coexisting ilmenite-pyroxene pair from Zigau, calculation of temperature of crystallisation assuming a pressure of 1 kb gives an unreasonably low temperature of approximately 300 degrees C. Any error in the assumed value for pressure is unlikely to influence the geothermometer greatly. It must therefore be assumed that the experimentally determined equation is not readily applicable to natural Fe-rich minerals where the Mg/(Mg+Fe) ratio is close to zero.

Table 25).

Alkali feldspars from the Eldewo granite granite range in composition from K-feldspar to the Na-feldspar field. Analyses from the Amuluri granite show that these feldspars can be more calcic and fall

4.10 Feldspars of K-feldspar and Ca-Na albite (Figure 24 and Table 25).

Alkali and plagioclase feldspars from selected rock types have been analysed by microprobe, and the structural states of alkali feldspars from all the major rock types have been investigated by X-ray diffraction using flat powder mounts. Information on the structural

Table 24 Electron microprobe analyses of plagioclase from the Zigau granite porphyry

Sample no.	ZG/2C xenolith				ZG/2D			
	1		2		3		4	
Crystal no.								
Spot no.	PL1	PL2	PL5	PL6	PL7	PL8	PL9	PL10
	core	margin	core	margin	core	margin	core	margin
SiO ₂	56.53	56.48	55.22	55.79	58.73	58.71	57.02	58.47
TiO ₂	0.11	0.14	0.00	0.00	0.20	0.16	0.13	0.17
Al ₂ O ₃	26.96	26.73	27.89	27.50	25.35	25.47	26.77	25.77
FeO _T	0.35	0.57	0.43	0.12	0.45	0.38	0.40	0.36
MgO	0.00	0.00	0.00	0.00	0.00	0.00	0.00	0.00
CaO	8.95	8.70	10.08	9.69	7.37	7.36	9.00	7.46
Na ₂ O	6.16	6.09	5.69	5.73	7.04	7.11	6.22	7.02
K ₂ O	0.23	0.31	0.23	0.14	0.33	0.42	0.50	0.33
	<u>99.29</u>	<u>99.02</u>	<u>99.54</u>	<u>98.97</u>	<u>99.47</u>	<u>99.61</u>	<u>100.04</u>	<u>99.58</u>
Formulae on the basis of 32 oxygens								
Si	10.226	10.250	10.007	10.125	10.565	10.551	10.257	10.507
Al	5.750	5.719	5.959	5.884	5.376	5.398	5.677	5.461
Ti	0.016	0.020	-	-	0.028	0.022	0.018	0.023
	<u>15.992</u>	<u>15.989</u>	<u>15.966</u>	<u>16.009</u>	<u>15.969</u>	<u>15.971</u>	<u>15.952</u>	<u>15.991</u>
Fe ²	0.054	0.086	0.065	0.018	0.068	0.057	0.061	0.055
Ca	1.735	1.693	1.958	1.885	1.421	1.418	1.736	1.436
Na	2.159	2.142	1.998	2.015	2.455	2.478	2.168	2.445
K	0.054	0.071	0.054	0.033	0.077	0.096	0.115	0.076
	<u>4.012</u>	<u>3.992</u>	<u>4.075</u>	<u>3.951</u>	<u>4.021</u>	<u>4.049</u>	<u>4.080</u>	<u>4.012</u>
% An	44.70	44.56	49.64	48.17	37.03	36.43	44.04	37.16
% Ab	53.95	53.68	49.03	51.00	61.05	61.20	53.14	60.94
% Or	1.35	1.78	1.33	0.83	1.92	2.37	2.82	1.89

states is included in this section, while the experimental conditions employed are given in Appendix 2.

For microprobe analysis of plagioclase crystals, a 1 micron diameter electron beam was used but for the majority of alkali feldspar analyses, the beam diameter was widened to 70 microns where possible. These analyses are therefore believed to be representative of the whole crystal and do not therefore simply reflect the sodic or potassic phases of a perthite. In addition, the area of an alkali feldspar crystal selected for microprobe analysis was clear (rather than turbid) in which no perthitic texture was visible. Chemical classification is after Smith (1974, Vol.1). In the Zigau granite porphyry plagioclase crystals occur as phenocrysts in both the host rock and in microsyenitic enclaves. Eight plagioclase analyses of such crystals are given in Table 24 and have been plotted in Figure 24; they range in composition from low to high calcic andesine (An_{36.4} - 49.6). As described in Section 3.1, these andesine crystals often show evidence of resorption and are clearly not in equilibrium with the enclosing matrix. It is possible that those crystals within the host rock are in fact (?cognate) xenocrysts from the microsyenite enclaves. The clear cores to alkali feldspar phenocrysts from the host rock and the microsyenitic enclaves exhibit a spread of composition from K-albite (anorthoclase) to Na-sanidine (Figure 24 and Table 25).

Alkali feldspars from the Shira quartz syenite range in composition from K-albite to the Na-sanidine field. Analyses from the Amdulayi syenite show that these feldspars can be more calcic and fall into the fields of K-albite and Ca-K albite (Figure 24 and Table 25). Analyses of alkali feldspars from the other rock types were not possible because the relatively coarse grained nature of the patch microperthites would have made representative analyses difficult to obtain, and the quality of polished thin sections was insufficient in many cases.

Table 25 Electron microprobe analyses of alkali feldspar

Rock type	Zigau granite porphyry						Shira alkali feldspar quartz syenite						Andulayi alkali feldspar quartz syenite									
	2G/2B		2G/2C		2G/2D		SH4	SH11		SH19		SH68/2	SH51		SH25				SH104 ¹			
Sample no.			xenolith				xenolith															
Beam size	1 μ	70 μ	1 μ	70 μ	70 μ	70 μ	70 μ	70 μ	70 μ	70 μ	70 μ	70 μ	70 μ	70 μ	70 μ	1 μ	1 μ	70 μ	70 μ	70 μ	1 μ	
Crystal no.	1	2	3	4	5	6	7	8	9	10	11	12	13	14	15		16	17	18		19	
Spot no.	FD1	AP28	AP1 core	AP2 margin	AP3	AP4 core	AP5 margin	AP27	AP6	AP7	AP11	AP12	AP8	AP9	AP10	AP13 core	AP14 margin	AP17 core	AP21 core	AP22 core	AP23 margin	AP24
SiO ₂	65.89	66.86	65.57	65.53	66.65	65.74	66.59	67.28	66.79	67.63	67.14	66.93	67.39	66.92	67.33	65.07	64.16	63.14	62.96	66.28	66.19	68.47
TiO ₂	0.03	0.00	0.34	0.25	0.00	0.00	0.00	0.00	0.00	0.00	0.00	0.00	0.00	0.00	0.00	0.00	0.00	0.00	0.00	0.00	0.00	0.00
Al ₂ O ₃	18.39	18.26	19.78	20.13	18.24	19.59	19.22	17.92	18.35	18.34	18.18	18.07	17.91	19.00	19.00	20.77	21.01	21.64	21.69	20.26	20.14	19.25
FeO _T	-	0.38	0.40	0.25	0.27	0.21	0.22	0.81	0.41	0.49	0.70	0.66	0.83	0.38	0.21	0.14	0.28	0.22	0.82	0.19	0.27	0.12
CaO	0.11	0.09	0.74	0.94	0.00	1.01	0.50	0.00	0.00	0.00	0.00	0.00	0.00	0.20	0.17	1.67	2.00	2.44	2.79	1.08	1.11	0.00
Na ₂ O	6.22	5.99	6.80	7.92	5.84	7.36	7.26	4.89	6.08	6.22	6.85	6.61	6.89	7.55	7.60	7.42	7.79	8.17	7.98	8.39	7.57	11.61
K ₂ O	7.46	7.53	5.61	3.92	7.64	4.71	5.61	9.42	7.86	7.88	7.06	7.32	6.67	5.78	5.56	4.09	3.22	2.28	2.40	3.99	4.92	0.00
BaO	-	0.00	0.00	0.00	0.00	0.44	0.46	0.00	0.00	0.00	0.00	0.00	0.00	0.00	0.00	0.84	1.35	1.84	1.66	0.35	0.40	0.00
	98.10	99.11	99.24	98.94	98.64	99.46	99.86	100.32	99.49	100.56	99.93	99.59	99.69	99.83	99.87	100.00	99.81	99.73	100.30	100.54	100.60	99.45
Formulae on the basis of 32 oxygens																						
Si	12.031	12.086	11.793	11.753	12.096	11.815	11.926	12.119	12.056	12.081	12.060	12.070	12.110	11.965	12.002	11.639	11.536	11.387	11.327	11.750	11.764	12.017
Al	3.959	3.892	4.194	4.257	3.904	4.152	4.058	3.805	3.906	3.862	3.850	3.843	3.795	4.006	3.993	4.382	4.454	4.601	4.602	4.235	4.221	3.984
	15.990	15.978	15.987	16.010	16.000	15.967	15.984	15.924	15.962	15.943	15.910	15.913	15.905	15.971	15.995	16.021	15.990	15.988	15.929	15.985	15.985	16.001
Ti	0.004	-	0.046	0.034	-	-	-	-	-	-	-	-	-	-	-	-	-	-	-	-	-	-
Fe ²⁺	-	0.057	0.061	0.038	0.041	0.032	0.034	0.122	0.062	0.073	0.106	0.099	0.125	0.057	0.032	0.021	0.043	0.034	0.124	0.029	0.041	0.018
Ca	0.021	0.019	0.144	0.181	-	0.195	0.097	-	-	-	-	-	-	0.038	0.033	0.320	0.385	0.472	0.538	0.206	0.212	-
Na	2.202	2.098	2.372	2.755	2.056	2.695	2.521	1.707	2.128	2.153	2.386	2.311	2.401	2.617	2.625	2.575	2.714	2.857	2.783	2.882	2.609	3.949
Ba	-	-	-	-	-	0.031	0.033	-	-	-	-	-	-	-	-	0.059	0.095	0.130	0.118	0.025	0.028	-
K	1.738	1.736	1.289	0.898	1.770	1.081	1.282	2.165	1.810	1.796	1.619	1.684	1.528	1.320	1.264	0.933	0.740	0.525	0.550	0.902	1.117	-
	3.965	3.910	3.912	3.906	3.867	4.034	3.967	3.994	4.000	4.022	4.111	4.094	4.054	4.032	3.954	3.908	3.977	4.018	4.113	4.044	4.007	3.967
% An	0.53	1.94	5.30	5.66	1.06	5.63	3.30	3.05	1.55	1.82	2.58	2.42	3.08	2.36	1.64	8.73	10.76	12.59	16.10	5.81	6.31	0.45
% Ab	55.59	53.66	61.36	71.15	53.17	66.81	63.55	42.74	53.20	53.53	58.04	56.45	59.23	64.91	66.39	65.89	68.24	71.11	67.66	71.27	65.11	99.55
% Or	43.88	44.40	33.34	23.19	45.77	27.57	33.15	54.21	45.25	44.65	39.38	41.13	37.69	32.73	31.73	25.38	21.00	16.30	16.24	22.92	28.58	0.00

¹ Narsarsukite bearing rock

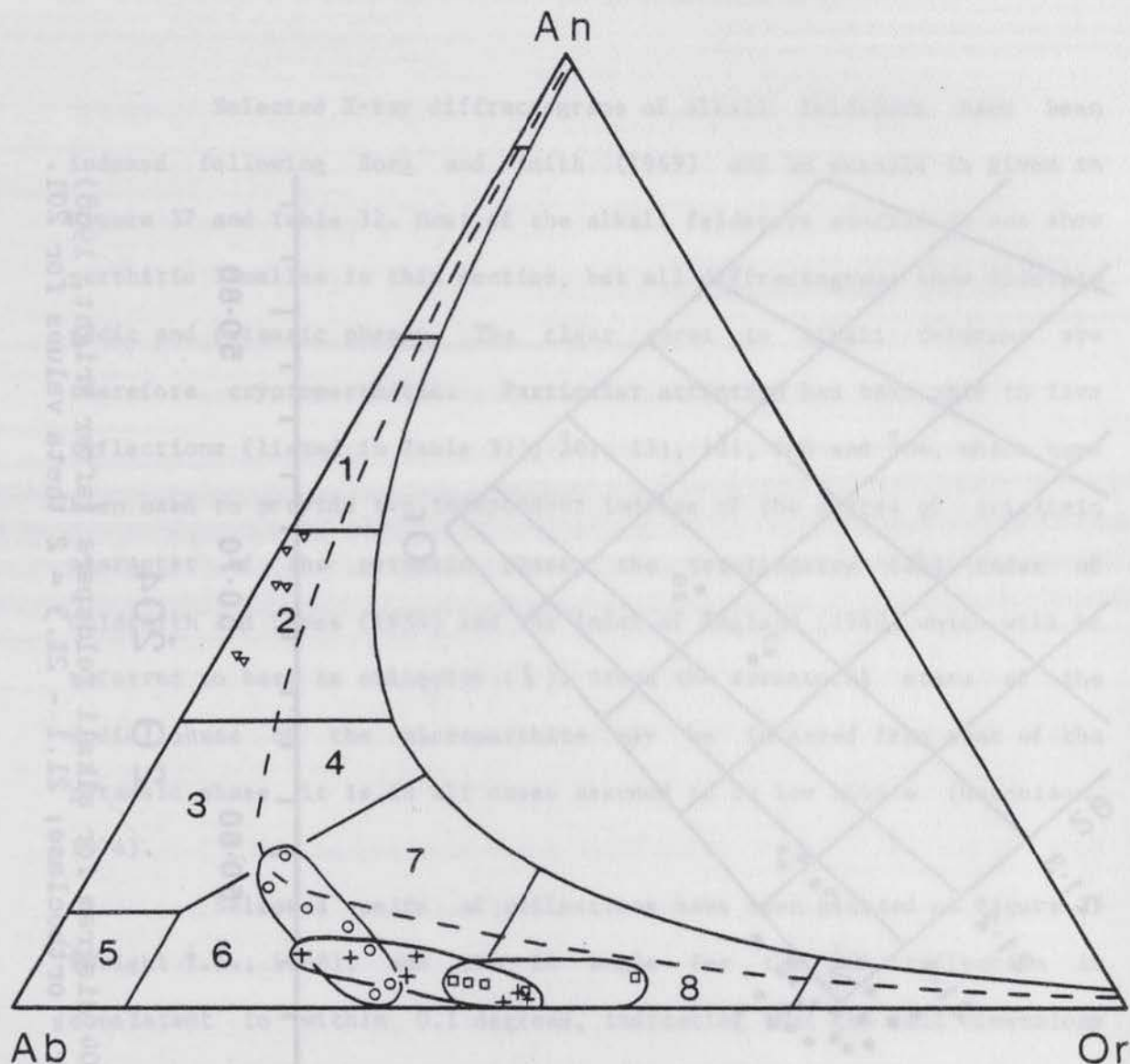


Figure 24. An-Ab-Or diagram for plagioclase and alkali feldspars from the Shira complex. 1 = labradorite; 2 = andesine; 3 = oligoclase; 4 = K-oligoclase; 5 = albite; 6 = K-albite; 7 = Ca-K-albite; 8 = Na-sanidine/microcline. Triangles and crosses = Zigau granite porphyry. Squares = Shira quartz syenite. Circles = Amdulayi syenite. Classification after Smith (1974, Vol.1).

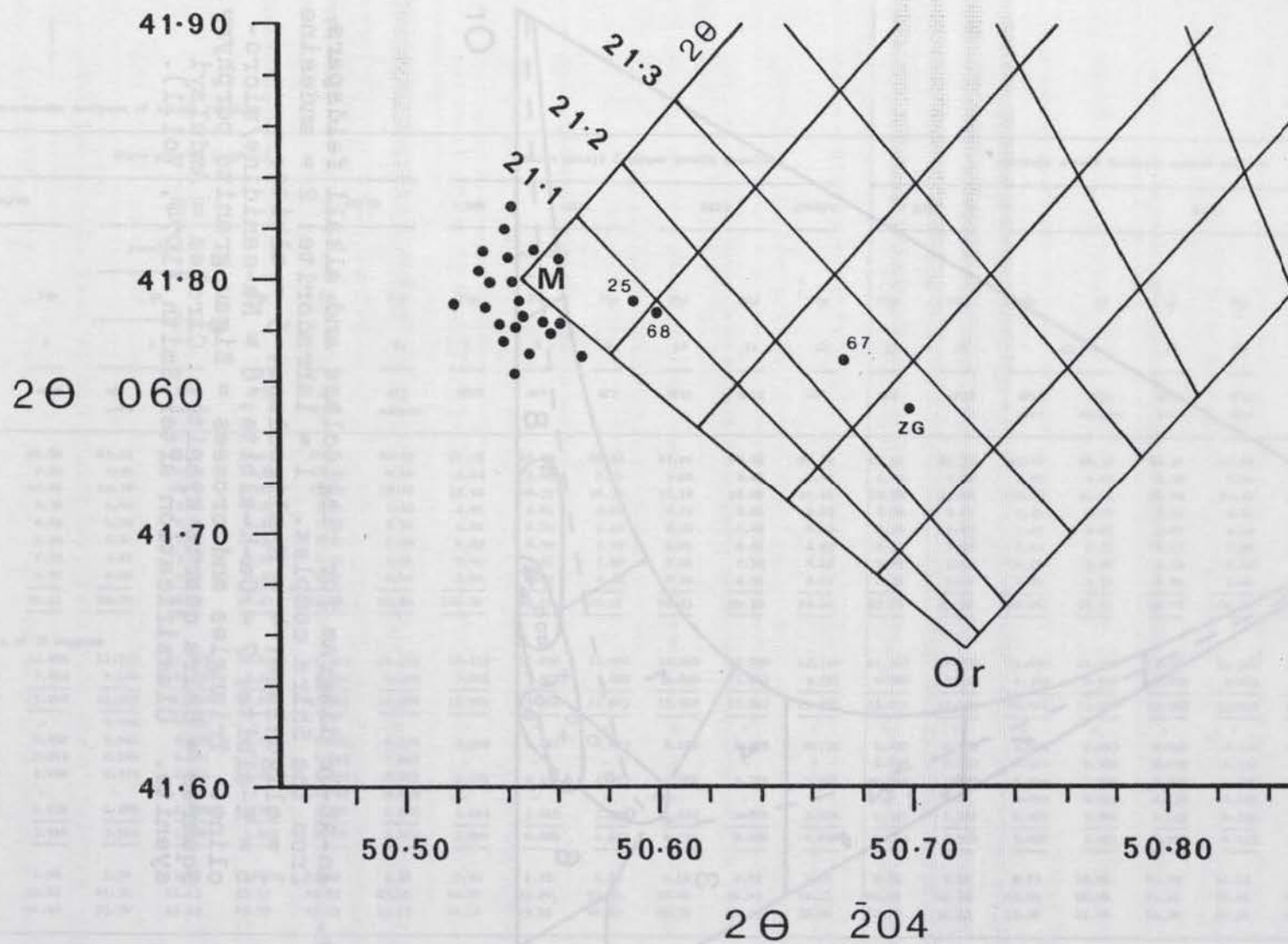


Figure 25. Two theta 060 v $\bar{2}04$ diagram for alkali feldspars (after Wright, 1968)
 M = microcline; Or = orthoclase; 21.1 - 21.3 = 2 theta values for $\bar{2}01$.

Selected X-ray diffractograms of alkali feldspars have been indexed following Borg and Smith (1969) and an example is given in Figure 37 and Table 32. Most of the alkali feldspars studied do not show perthitic lamellae in thin section, but all diffractograms show discrete sodic and potassic phases. The clear cores to alkali feldspar are therefore cryptoperthitic. Particular attention has been paid to five reflections (listed in Table 31), $\bar{2}01$, 131 , $1\bar{3}1$, 060 and $\bar{2}04$, which have been used to provide two independent indices of the degree of triclinic character of the potassic phase: the triclinicity (Δ) index of Goldsmith and Laves (1954) and the index of Ragland (1969) which will be referred to here as obliquity (δ). Since the structural state of the sodic phase of the microperthite may be inferred from that of the potassic phase, it is in all cases assumed to be low albite (Hutchison, 1974).

Selected pairs of reflections have been plotted on Figure 25 (Wright T.L., 1968), and the 2θ angle for the $\bar{2}01$ reflection is consistent to within 0.1 degrees, indicating that the cell dimensions are normal. For the major rock types, Figure 25 shows that the potassic phases of the microperthites concentrate close to the maximum microcline position and the microperthites are therefore regarded as belonging to the maximum microcline-low albite series. The average 2θ value for the $\bar{2}01$ reflection lies very close to 21.00 degrees, and substituting this value into the following equation (Wright T.L., 1968):

$$\text{Or\%} \Rightarrow 2031.77 - 92.19 \times 2\theta(\bar{2}01) \quad (27)$$

gives 96% orthoclase for the potassic component. This is consistent with the observation that microclines exsolve virtually all their albite and generally have less than 5% albite in solid solution (Goldsmith and Laves, 1961).

For those samples that do not plot close to the maximum microcline position, some caution regarding their interpretation is

necessary. Samples SH25 and ZG1-2 are bulk feldspar separates from porphyritic rocks and so if there is a difference in triclinicity between the phenocrysts and matrix (as is suggested by differences in turbidity) then an average value will result. For the Eldewo biotite granite, two samples have been X-rayed. Sample SH21 represents the coarse grained granite from the centre of the intrusion and the feldspar plots as a maximum microcline, but sample SH67 is from the margin of the intrusion and has a granophyric texture and an obliquity of only 0.51 (Table 31). Similarly, sample SH68 of the Shira quartz syenite is a marginal locality with a slightly porphyritic texture and the feldspar has a comparatively low obliquity of 0.74 (Table 31). Thus, samples with a porphyritic texture or a marginal position may have a lower triclinicity.

In the majority of cases the X-ray pattern in the region 29 to 31 degrees 2θ is similar to the type 4 of Parsons and Boyd (1971) or type V of Vorma (1971). In this region only four reflections are generally seen, being $K(131)$, $K(1\bar{3}1)$, $Na(0\bar{4}1,0\bar{2}2)$ and $K(022)$. Although the majority of bulk compositions of the Shira alkali feldspars are K-albites (anorthoclases) and correspond closely to the sodic microperthites of Loch Ailsh (Parsons, 1965), the $Ab(131)$ reflection is barely detectable and measurement of the Goldsmith and Laves (1954) triclinicity value is unimpeded.

Samples SH68 and SH44/2, being marginal facies of the Shira quartz syenite and Andaburi granite respectively, show patterns similar to type 2c of Parsons and Boyd (1971), and probably consist of microcline and some relic orthoclase. Similarly, the Zigau granite porphyry (sample ZG2) shows a broad (double) peak close to the $Or(131)$ position similar to type 2b of Parsons and Boyd. Sample SH67, a marginal variety of the Eldewo biotite granite also has a broad orthoclase peak, similar to type 2a. Both the last two samples probably therefore also

contain a mixture of relic orthoclase and microcline.

Discussion and the possible existence of a fluid phase

A fundamental assumption in the interpretation of the X-ray data on alkali feldspars is that they originally crystallised as homogeneous feldspars which have subsequently exsolved into crypto- or microperthites (Bowen and Tuttle, 1950). As such, a structural transition from monoclinic to triclinic symmetry during the cooling history of the rocks is also assumed to have taken place. Therefore, it is valid to plot the bulk composition of the alkali feldspars on a high temperature diagram such as Figure 24, after Smith (1974, Vol.2).

During cooling, the alkali feldspar is likely to undergo two other changes: ordering of Na and K atoms in the M sites and ordering of Al and Si atoms among the T sites. The former process results in the formation of sodic and potassic lamellae, whilst Al/Si ordering results in a slight collapse of the lattice and a change from monoclinic to triclinic symmetry in either phase. Neither process is instantaneous and both may be affected by such factors as rate of cooling and presence of volatiles. Intermediate steps in the Al/Si ordering process may produce domains of triclinic (ordered) feldspar within the original monoclinic material (Smith, 1974, Vol.1). Thus, the indices of triclinicity or obliquity as determined from X-ray diffractograms, are in effect estimates of how far the Al/Si ordering process has gone towards producing maximum microcline (and low albite).

Since a microperthitic texture is visible in several specimens in which the triclinicity is below maximum, it is likely that ordering of Na and K into discrete lamellae takes place faster than Al/Si ordering to produce a triclinic microcline. Such a view is supported by the known very slow rate of Al/Si ordering (Sipling and Yund, 1974), presumably attributable to the relative weakness of the Na/K-O bond

compared to the Al/Si-O bond. In terms of Na/K ordering, it would be expected that Na cations are more mobile in the feldspar lattice than K cations, since the former have a much lower activation energy of diffusion (19 Kcal/mole) compared to the latter (70 Kcal/mole) (Lin and Yund, 1972). In addition, the Al/Si ordering rates of the sodic and potassic regions of a perthite are not equal. Senderov et al. (1975) found that ordering rates for K-feldspars in experimental conditions were lower than for albites, and Parsons (1968) showed that at temperatures below 600 degrees C, anorthoclases are less well ordered than albite. Similarly, while low albite may be synthesised in the time span of laboratory experiments (Martin, 1969b), it has not so far been possible to synthesise a potassic feldspar more ordered than orthoclase (Martin, 1968; Senderov et al., 1975). Even rocks as old as Precambrian may contain K-feldspar no more ordered than can be produced in a laboratory in one year (Crosby, 1971). The reason for the different degrees of Al/Si order in coexisting sodic and potassic feldspars is believed to be a function of a higher activation energy for the potassic feldspars (about 99 Kcals/mole) compared to albite (74 Kcal/mole) (McConnell and McKie, 1960; Sipling and Yund, 1974). Therefore, since the majority of Shira feldspars contain maximum microcline, it is assumed that the sodic phase is low albite.

From Figure 25 it is apparent that the majority of alkali feldspars contain maximum microcline and yet no cross-hatched (or 'tartan') twinning has been observed in the major rock types. It has been stated that when monoclinic K-feldspar inverts to triclinic symmetry, "the microcline which forms is always intimately twinned on both the Pericline and Albite laws" (Ribbe, 1975, p.R-26). Laves (1950) and Goldsmith and Laves (1954b) also showed that cross-hatched twinning was indicative of inversion from an originally homogeneous, monoclinic alkali feldspar.

In the foregoing discussion it has been stated that relatively old (Precambrian) and/or very large intrusions often do not contain alkali feldspar which is more ordered than orthoclase. Therefore, time or very slow cooling rates may not by themselves be sufficient to produce fully ordered microcline. Small, high level intrusions such as those in the Scottish Tertiary province often do not contain well ordered alkali feldspar either (Mackenzie and Smith, 1962; Taylor and Forester, 1971), and the question of the means by which ordered microcline is attained in the Shira complex, remains.

In many studies, the importance of the composition of the whole rock has been demonstrated, such that feldspars with a greater degree of ordering correlate positively with decrease in Ca, Mg, Fe, Al, and Ti (e.g. Cherry and Trembath, 1978; Dietrich, 1962; Nilssen and Smithson, 1965; Parsons and Boyd, 1971; Ragland, 1970; and Vorma, 1970). Thus, in general, more ordered alkali feldspars are found in rocks which approach the granite minimum. However, this association may not be related directly to rock chemistry but to the presence of fluids which would be expected to be more abundant in more fractionated rocks (Parsons, 1978). In this regard, the presence and composition of a fluid phase may be more important than the host rock composition. Thus for example, Ragland (1970) attributes the increased triclinicity of the alkali feldspars in the more fractionated rocks to the catalysing action of water.

The role of alkali depletion or enrichment during crystallisation and cooling of alkali feldspars also appears to be of prime importance. Guidotti (1978) has shown that the Al content of the environment exerts a strong influence on the structural state attained by the K-feldspar. In contrast, several studies have shown that ordering is enhanced and more rapidly achieved in the presence of excess alkalis in a fluid phase (e.g. Martin, 1969a, 1969b, 1974; Parsons and Boyd,

1971; Senderov et al., 1975). Martin (1969a, 1969b) has demonstrated that the ordering rate of synthetic albite depends on the peralkalinity of the aqueous fluid accompanying recrystallisation, and suggested that this dependence applies to all feldspars. In fact, Martin (1974) is of the opinion that in the absence of water, ordering is probably precluded.

Thus, the dominance of maximum microcline in the Shira complex can be explained by the presence of highly fractionated host rocks which are, in addition, mainly peralkaline and so any residual peralkaline melt or fluid phase could have assisted in the Al/Si ordering of the alkali feldspar. Those samples which plot away from the maximum microcline position in Figure 25 come either from the margins of intrusions and exhibit distinctive textures, or from the small, dyke-like body of granite porphyry at Zigau. These rocks have probably cooled relatively quickly and lost any residual fluid. Similarly, Mackenzie and Smith (1962) attribute the preservation of orthoclase or sanidine in some high level intrusions to rapid cooling and loss of volatiles.

The mechanism by which a possible (?hydrous) peralkaline fluid may enhance ordering in alkali feldspars has been investigated by several authors. It has long been known that addition of water to a silicate melt has a marked effect on the viscosity, which drops. During devitrification experiments, Lofgren (1970) noted that the devitrification rate was enhanced by the presence of an alkali-rich solution. Both observations may be explained by the breaking of Si-bridging oxygen bonds to form Si-OH groups with a subsequent slight expansion of the lattice (or glass network), allowing diffusion of Na/K and Al/Si more easily (Lofgren, 1970; Burnham, 1975). Spectral studies have also shown the presence of (OH) ions in a hydrated silicate melt (Orlova, 1964). Therefore, although the separation of a discrete aqueous

phase is not to be expected in a cooling peralkaline magma, both quartz and alkali feldspar crystals are packed with minute, randomly oriented, dilute fluid inclusions of presumed aqueous nature. Since there are different concentrations of inclusions in the sodic and potassic components of microperthite (Plate 24), these fluid inclusions presumably post-date the feldspar exsolution, and were not included when the feldspar grew from a melt. Therefore, it is reasonable to assume that there is a connection between the need for feldspar ordering to take place in the presence of a fluid, and the presence of secondary fluid inclusions. However, it is difficult to reconcile the incompatibility of the experimental evidence (indicating continuous solubility of water to low temperatures in a peralkaline magma) and the demonstrably secondary nature of the fluid inclusions, indicative of a discrete hydrous fluid phase. However, since the inclusions probably post-date feldspar exsolution, they probably formed below the solidus and hence an aqueous fluid would not have coexisted with a melt. In this case, the aqueous fluid may represent water which was originally dissolved in the melt but which formed a discrete phase when the melt has completely crystallised; that is, magmatic rather than meteoric water.

It is concluded from the data on structural states of alkali feldspar and detailed petrographic observations that water which exsolved from the residual fluid at subsolidus temperatures was able to permeate quartz and alkali feldspars at least, and aid or cause Al/Si ordering. Meteoric water is not favoured as a suitable source mainly because of the writer's own observations on the basement rocks surrounding many complexes; these rocks consist of granites, migmatites and gneisses into which greisen veins which may be traceable for 1-200 m in the Younger Granite, die out within centimetres or metres of the contact. The basement thus appears extremely tough and impermeable.

Stable isotopic data for some Nigerian Younger Granites supports this argument, since they plot within the 'primary magmatic water' box on a hydrogen and oxygen isotopic diagram, whereas the greisens plot outside this area and the aqueous fluid associated with them may have had a different source (data from Sheppard, in Bowden, 1976).

At this stage it is pertinent to comment on the related feature of needles of aegirine and arfvedsonite which are scattered throughout alkali feldspar crystals. This feldspar replacement feature probably represents the action of an alkali rich silicate fluid, which may also be responsible for the development or enhancement of a patch perthite texture and intergranular albite. In this earlier replacement phase, only alkali feldspar appears to have been affected whereas at the aqueous fluid stage, alkali feldspar and quartz (at least) appear to have been affected. It is possible that the minor amount of zeolite found in the Shira rocks is also attributable to this aqueous fluid.

A further point to emerge from this discussion concerns the likelihood that, in a peralkaline rock, an aqueous fluid phase is unlikely to have existed above the solidus. Therefore, in a peralkaline granite or syenite, the probability of developing pegmatitic knots or miarolitic cavities would appear to be low and in fact, none are found in the Shira complex. In biotite granites however, such features are common especially near the margins of an intrusion where pegmatitic knots may be up to 1 m in diameter, and have been interpreted as representing water saturated conditions (Abernethy, in prep.). That is, the melt became water saturated above the solidus since the knots are an integral part of the rock fabric and are not replaceive features.

The model thus developed for the interaction of an aqueous fluid phase cannot easily be tested against many others in the literature as too few granite petrologists report on fluid inclusions. However, a notable exception concerns blocks of peralkaline granite

occurring on Ascension Island (Roedder and Coombs, 1967). Here, there is good evidence for a very highly saline aqueous fluid coexisting, but immiscible with the silicate melt. No comparable highly saline inclusions have been observed at Shira however, and one can speculate on whether there is a connection between an immiscible, highly saline aqueous fluid and the fact that the Ascension Island magma chamber would have been at a high level in an oceanic environment, raising the possibility of sea-water contamination. However, the aqueous inclusions at Ascension appear to be primary (i.e. included during crystal growth) whereas the less saline ones at Shira appear to be secondary, after exsolution of the alkali feldspar.

The Barker diagram is used as the principal means of displaying this data because of its simplicity and because since the range of chemical composition shown by the Shira complex is relatively limited (64-77% SiO₂), the data are compared with most values for the Niger-Nigeria province. As the Shira complex is dominated by quartz and peralkaline granitic rocks, a mean curve has been drawn through the respective average values for the province, for comparison only. These averages have been obtained by a geochemical review of the province which includes 756 analyses and which is discussed in detail in section 3-3.

3-2 The Shira complex

For the sake of clarity and brevity, only the average values for each rock will have been plotted on the Barker diagram although all data points have been included on the AFM and Q-Au-Or diagrams. For the major rock types, the oxides of Ti, Al, Fe, Mg, Ca, F and total alkalis

CHAPTER 5GEOCHEMISTRY5.1 Introduction

Fifty rocks from the Shira complex have been analysed for major and trace elements, mainly by X-ray fluorescence (X.R.F.), for which the experimental conditions are outlined in Appendix 4. Twenty-nine of these analyses are from samples of the six major rock units (i.e. Zigau, Shira, Birji, Andaburi, Amdulayi and Eldewo) and the remainder include dykes and enclaves, the Chida granophyre and a metasomatically altered variety of Shira quartz syenite. The analytical data together with CIPW norms, geochemical indices and averages, are presented in Tables 26 and 27.

The Harker diagram is used as the principal means of displaying this data because of its simplicity and common use. Since the range of chemical composition shown by the Shira complex is relatively limited (64-77% SiO₂), the data are compared with mean values for the Niger-Nigeria province. As the Shira complex is dominated by syenitic and peralkaline granitic rocks, a 'mean curve' has been drawn through the respective average values for the province, for convenience only. These averages have been obtained by a geochemical review of the province which includes 326 analyses and which is discussed in detail in Section 5.3.

5.2 The Shira complex

For the sake of clarity and brevity, only the average values for each rock unit have been plotted on the Harker diagrams although all data points have been included on the AFM and Q-Ab-Or diagrams. For the major rock types, the oxides of Ti, Al, Fe, Mg, Ca, P and total alkalis

Table 26. Analyses of rocks from the Shira complex.

For this and subsequent tables of rock analyses the following abbreviations are used;

For major and trace elements, a dash indicates 'not determined', a zero value indicates a value below the detection limit, and tr = trace amount. For the C.I.P.W. normative minerals, a dash indicates zero.

Ag.coeff. The Agpaitic coefficient or peralkalinity index (P.I.) is the sum of the mole proportions of the alkalis divided by the mole proportion of alumina, i.e. Ag.coeff. = $(\%Na_2O/61.98 + \%K_2O/94.20) \div (\%Al_2O_3/101.96)$

$\Sigma Fe/\Sigma Fe+Mg$ or I.E. (iron enrichment) $(\%Fe_2O_3 + \%FeO) \div (\%Fe_2O_3 + \%FeO + \%MgO)$

ΣFeO as FeO $\%FeO + (\%Fe_2O_3 \div 1.111)$

Σ alkalis $\%Na_2O + \%K_2O$

Diff.Index Thornton and Tuttle (1960) differentiation index (D.I.), being effectively the sum of the normative components Q, Or and Ab (and Ne, where present).

Oxid.ratio or O.R. $(100 \times \%Fe_2O_3) \div (\%FeO + \%Fe_2O_3)$

Table 26 Analyses of rocks from the Shira complex

Rock type	Zigau granite porphyry				Volcanic xenoliths				Shira alkali feldspar quartz syenite						Shira market xenolith		
	xenoliths														xenoliths		
	EG1	EG2	EG2A	EG2B	SH17	SH29/4	SH96	SH98/1	SH2	SH4	SH19	SH68/1	SH105	SH68/2B	SH76/3	SH108	SH109
SiO ₂	71.40	71.04	55.05	49.16	68.81	73.99	69.07	67.89	68.87	68.78	69.28	70.37	70.60	64.45	69.29	76.75	75.75
TiO ₂	40.10	0.36	2.09	1.84	0.43	0.28	0.43	0.36	0.46	0.46	0.45	0.37	0.32	0.33	0.30	0.16	0.13
Al ₂ O ₃	13.72	13.07	13.37	15.35	15.46	12.63	15.29	14.86	12.73	12.20	11.71	12.50	13.05	13.88	14.09	10.47	10.65
Fe ₂ O ₃	1.17	1.28	1.92	1.37	0.23	1.92	1.54	2.28	1.33	1.72	3.02	2.12	2.39	2.48	1.79	3.57	2.15
FeO	2.62	2.95	10.10	8.95	5.17	1.52	3.90	2.33	4.36	4.00	3.29	3.35	2.09	5.17	1.72	0.00	1.87
MnO	0.11	0.09	0.23	0.15	0.06	0.05	0.11	0.07	0.12	0.14	0.12	0.13	0.09	0.18	0.09	0.02	0.05
MgO	0.13	0.03	2.18	6.87	0.19	0.06	0.16	0.18	0.22	0.25	0.17	0.20	0.14	0.30	0.25	0.02	0.02
CaO	0.89	1.06	5.47	8.34	0.76	0.47	0.92	1.58	0.66	0.91	0.90	0.90	0.51	1.61	0.63	0.17	0.19
Na ₂ O	4.54	4.70	4.77	3.40	1.72	3.71	2.34	4.22	5.67	5.45	5.41	5.32	5.71	6.10	5.43	4.59	4.35
K ₂ O	5.13	5.07	3.26	2.38	5.96	5.70	5.70	5.69	4.80	4.67	4.71	4.75	4.77	5.38	5.42	4.23	4.49
P ₂ O ₅	0.05	0.03	1.03	0.34	0.06	0.02	0.07	0.04	0.07	0.07	0.06	0.07	0.03	0.13	0.06	0.01	0.00
H ₂ O ⁺	0.63	0.70	0.88	1.82	0.52	0.28	1.00	0.42	0.06	0.28	0.56	0.48	0.10	0.60	0.44	0.60	0.50
H ₂ O ⁻	0.11	0.12	0.08	0.12	0.08	0.08	0.14	0.08	0.10	0.10	0.12	0.10	0.10	0.08	0.12	0.10	0.06
	100.50	100.50	100.43	100.09	99.45	100.71	100.67	100.00	99.45	99.03	99.80	100.66	99.90	100.69	99.63	100.69	100.21
Li	33	27	71	334	51	2	39	7	55	43	46	9	44	38	29	14	35
Be	2	6	-	-	4	2	10	8	12	12	8	10	10	-	-	8	8
Zn	109	183	171	126	96	145	164	151	291	161	300	167	247	250	161	216	293
Nb	75	67	41	68	205	102	122	138	154	169	145	144	171	116	183	209	195
Sr	22	41	405	477	74	16	105	65	9	49	50	40	68	55	31	<8	8
Y	23	21	22	15	17	18	21	20	30	31	23	8	27	17	24	28	20
Zr	581	652	339	175	804	618	777	708	726	677	615	135	918	142	246	617	953
Agp. coeff.	0.95	1.01	0.85	0.53	0.60	0.97	0.66	0.88	1.14	1.15	1.20	1.11	1.12	1.14	1.05	1.16	1.13
IPa/IPa+Mg	0.97	0.99	0.84	0.60	0.97	0.98	0.97	0.96	0.97	0.96	0.98	0.97	0.97	0.96	0.93	0.99	1.00
IPa as FeO	3.67	4.10	11.83	10.18	5.37	3.25	5.28	4.38	5.55	5.55	6.01	5.26	4.16	7.40	3.35	3.21	3.81
I alkalis	9.67	9.77	8.03	5.78	7.68	9.41	8.04	9.91	10.47	10.12	10.12	10.07	10.48	11.48	10.85	8.82	8.84
Diff. Index	90.83	90.43	59.60	40.34	80.06	94.52	82.67	87.08	84.09	82.62	81.33	85.04	87.40	78.44	90.15	90.93	89.46
Oxid. ratio	30.87	30.28	15.97	13.28	4.26	55.81	28.30	49.46	23.37	30.07	47.86	38.76	53.35	32.42	51.00	100.00	53.48
CIPW norms																	
Q	22.12	21.40			30.30	29.46	29.20	17.77	16.98	18.28	19.49	19.18	18.65	5.21	15.83	35.64	33.15
Or	30.31	29.95	19.26	14.06	35.21	33.68	33.68	33.62	28.36	27.59	27.83	28.06	28.18	31.79	32.02	24.99	26.53
Ab	38.40	39.00	40.34	23.35	14.55	31.38	19.79	35.69	38.75	36.75	34.01	37.85	40.57	41.44	42.30	30.30	29.78
An	1.92		5.45	19.60	3.38	0.98	4.11	4.81									
Ms				2.93													
C					4.94		3.77										
An		0.66							3.85	4.98	8.74	6.13	6.81	7.17	3.20	7.50	6.18
KNo	0.91	2.11	6.25	8.16		0.51		1.16	1.18	1.69	1.70	1.67	0.97	2.98	1.14	0.06	0.39
DI KEn	0.08	0.04	1.83	4.53		0.08		0.23	0.09	0.16	0.13	0.15	0.10	0.25	0.26	0.05	0.01
SFe	0.93	2.34	4.69	3.32		0.47		1.01	1.22	1.72	1.75	1.71	0.98	3.06	0.95		0.44
Ky KEn	0.25	0.03	3.23		0.47	0.07	0.40	0.21	0.46	0.47	0.29	0.35	0.25	0.50	0.36		0.04
Ky SFe	2.95	1.78	8.29		8.70	0.37	5.38	0.92	6.25	5.13	3.77	4.07	2.47	6.22	1.31		2.86
Ol SFe			0.26	8.81													0.07
Ol SFe			0.74	7.12													
SFe																	
Nt	1.70	1.52	2.78	1.99	0.33	2.78	2.23	3.31					0.05		0.99		0.02
Ms																0.98	
Il	0.19	0.68	3.97	3.49	0.82	0.53	0.82	0.66	0.87	0.87	0.85	0.70	0.61	0.63	0.57	0.04	0.25
Ms									1.13	0.86	0.43	0.04					0.47
Ap	0.12	0.07	2.44	0.81	0.14	0.05	0.17	0.09	0.17	0.17	0.14	0.17	0.07	0.31	0.14		0.02

* plus 0.34 Zn

Table 26 continued

Rock type	Birji granite											
	Acicular facies						Poikilitic facies		Dyke in poik. facies	Dyke in acicular facies	Dykes in Shira quartz syenite	
	SH5	SH9	SH18	SH82	SH88	SH71/3	SH14	SH30	SH83/2	SH95	SH69/3	SH90
Sample no.	SH5	SH9	SH18	SH82	SH88	SH71/3	SH14	SH30	SH83/2	SH95	SH69/3	SH90
SiO ₂	74.95	72.86	68.10	72.61	72.52	70.57	73.36	75.99	70.44	69.35	71.40	70.50
TiO ₂	0.16	0.25	0.28	0.25	0.26	0.30	0.54	0.06	0.42	0.35	0.41	0.37
Al ₂ O ₃	9.11	9.10	9.61	9.25	8.99	8.07	9.20	10.18	7.67	8.24	8.10	7.37
Fe ₂ O ₃	1.04	3.03	2.65	3.70	3.87	4.93	4.78	2.52	5.35	4.55	5.26	8.53
FeO	4.01	4.95	7.69	4.28	4.00	6.08	2.15	1.83	5.27	7.02	4.88	2.77
MnO	0.10	0.12	0.17	0.13	0.13	0.17	0.12	0.05	0.20	0.17	0.19	0.20
MgO	0.07	0.02	0.03	0.06	0.06	0.02	0.04	0.05	0.10	0.00	0.16	0.05
CaO	0.29	0.47	0.52	0.43	0.49	0.45	0.33	0.41	0.28	0.34	0.42	0.19
Na ₂ O	4.19	4.49	5.15	4.49	4.50	4.27	4.34	4.67	5.01	5.62	5.04	5.69
K ₂ O	4.79	4.68	5.20	4.82	4.73	4.64	4.51	4.29	4.44	4.17	4.11	4.01
P ₂ O ₅	<0.01	0.01	0.01	0.01	0.00	0.01	0.01	0.00	0.00	0.00	0.02	0.01
H ₂ O ⁺	0.20	0.06	0.00	0.50	0.18	0.50	0.60	0.30	0.48	0.42	0.52	0.10
H ₂ O ⁻	0.08	0.10	0.10	0.08	0.12	0.12	0.10	0.12	0.10	0.10	0.14	0.14
	99.92	100.24	99.51	100.61	99.85	100.13	100.08	100.47	99.76	100.31	100.65	99.93
Li	58	61	100	82	80	32	52	36	222	146	195	166
Be	9	10	8	6	4	6	4	10	8	-	-	12
Zn	166	289	362	293	312	336	292	161	541	442	478	516
Rb	219	180	184	156	158	173	153	160	300	184	139	188
Sr	<8	8	8	<8	16	8	<8	17	16	25	8	16
Y	16	17	17	33	15	4	30	14	18	11	21	16
Zr	666	619	533	724	542	89	2240	560	897	430	286	1801
Agp. coeff.	1.33	1.37	1.47	1.36	1.39	1.49	1.31	1.21	1.70	1.67	1.57	1.86
EPe/EPe+Mg	0.99	1.00	1.00	0.99	0.99	1.00	0.99	0.99	0.99	1.00	0.98	1.00
EPe as FeO	5.76	7.68	10.07	7.61	8.09	10.44	6.45	4.10	10.08	11.12	9.61	10.45
E alkalis	8.98	9.17	10.35	9.31	9.23	8.91	8.85	8.96	9.45	9.79	9.15	9.70
Diff Index	83.58	79.23	73.75	78.95	78.28	71.73	81.30	87.69	70.37	69.53	72.57	67.89
Oxid. ratio	32.61	37.97	25.63	46.37	49.17	44.78	68.98	57.93	50.38	39.33	51.87	75.49
CIPW norms												
Q	35.09	30.83	21.54	29.73	30.42	28.64	32.44	33.86	29.41	25.72	29.51	28.62
Or	28.30	27.65	30.72	28.48	27.95	27.41	26.65	25.35	26.23	24.64	24.28	23.69
Ab	20.19	20.75	20.48	20.74	19.91	15.68	22.21	28.48	14.73	19.17	18.78	15.58
An												
Ne												
C												
Ac	5.61	8.76	7.67	10.70	11.19	14.26	12.77	7.29	15.48	13.16	15.22	24.67
%Wo	0.57	0.95	1.05	0.86	1.01	0.90	0.66	0.85	0.58	0.70	0.82	0.37
Di %En	0.02	0.01	0.01	0.02	0.02	0.02	0.02	0.03	0.02	0.02	0.04	0.01
%Fs	0.63	1.07	1.18	0.96	1.12	1.02	0.71	0.92	0.64	0.80	0.87	0.40
Hy %En	0.16	0.04	0.07	0.13	0.13	0.05	0.08	0.09	0.23	0.23	0.36	0.11
%Fs	6.65	7.83	12.79	6.73	6.03	9.96	2.26	2.43	8.72	11.83	7.76	4.44
Ol %Fo												
%Fa												
Wt							0.53					
Hm												
Il	0.30	0.47	0.53	0.47	0.49	0.57	1.03	0.11	0.80	0.66	0.78	0.70
Ns	2.07	1.69	3.35	1.18	1.27	0.99	0.64	0.64	2.34	3.13	1.53	1.06
Ap	0.02	0.02	0.02	0.02		0.02	0.02				0.05	0.02

Table 27 Mean values and standard deviations for rocks from the Shira complex

	(1)	(2)	(3)	(4)	(5)	(6)	(7)	(8)	(9)	(10)	(11)
SiO ₂	71.22 ± 0.18	69.58 ± 0.76	66.87 ± 2.42	76.25 ± 0.50	72.62 ± 2.29	70.42 ± 0.73	68.59 ± 0.51	73.43 ± 2.25	74.90 ± 0.88	64.57 ± 1.01	77.06 ± 0.38
TiO ₂	0.23 ± 0.13	0.41 ± 0.06	0.32 ± 0.02	0.15 ± 0.02	0.26 ± 0.13	0.39 ± 0.03	0.41 ± 0.03	0.31 ± 0.15	0.17 ± 0.00	0.67 ± 0.07	0.14 ± 0.03
Al ₂ O ₃	13.40 ± 0.32	12.44 ± 0.46	13.99 ± 0.11	10.56 ± 0.09	9.19 ± 0.56	7.85 ± 0.35	15.20 ± 0.25	11.83 ± 0.65	9.47 ± 0.96	13.60 ± 1.11	11.96 ± 0.21
Fe ₂ O ₃	1.22 ± 0.05	2.12 ± 0.58	2.14 ± 0.35	2.86 ± 0.71	3.43 ± 1.01	5.92 ± 1.54	1.35 ± 0.85	2.89 ± 0.96	3.76 ± 1.24	5.30 ± 2.06	0.88 ± 0.12
FeO	2.79 ± 0.16	3.42 ± 0.78	3.44 ± 1.73	0.94 ± 0.94	4.37 ± 1.80	4.99 ± 1.51	3.80 ± 1.16	1.21 ± 0.72	3.40 ± 1.20	2.56 ± 1.78	0.67 ± 0.07
MnO	0.10 ± 0.01	0.12 ± 0.02	0.14 ± 0.05	0.04 ± 0.02	0.12 ± 0.04	0.19 ± 0.01	0.08 ± 0.02	0.09 ± 0.03	0.12 ± 0.03	0.19 ± 0.02	0.03 ± 0.01
MgO	0.08 ± 0.05	0.20 ± 0.04	0.27 ± 0.02	0.02 ± 0.00	0.04 ± 0.02	0.08 ± 0.06	0.18 ± 0.01	0.14 ± 0.09	0.02 ± 0.03	0.18 ± 0.14	0.08 ± 0.03
CaO	0.98 ± 0.09	0.78 ± 0.16	1.12 ± 0.49	0.18 ± 0.01	0.42 ± 0.07	0.31 ± 0.08	1.09 ± 0.35	0.47 ± 0.32	0.33 ± 0.20	0.77 ± 0.45	0.42 ± 0.07
Na ₂ O	4.62 ± 0.08	5.51 ± 0.15	5.76 ± 0.33	4.47 ± 0.12	4.51 ± 0.28	5.34 ± 0.32	2.76 ± 1.06	4.94 ± 0.36	5.08 ± 0.32	6.34 ± 0.24	3.76 ± 0.07
K ₂ O	5.10 ± 0.03	4.74 ± 0.05	5.40 ± 0.02	4.36 ± 0.13	4.71 ± 0.25	4.18 ± 0.16	5.78 ± 0.12	4.61 ± 0.20	3.90 ± 0.38	5.02 ± 0.25	4.75 ± 0.11
P ₂ O ₅	0.04 ± 0.01	0.06 ± 0.02	0.09 ± 0.03	0.01 ± 0.01	0.01 ± 0.00	0.01 ± 0.01	0.06 ± 0.01	0.04 ± 0.05	0.01 ± 0.00	0.15 ± 0.11	0.02 ± 0.01
H ₂ O ⁺	0.67 ± 0.04	0.30 ± 0.20	0.52 ± 0.08	0.55 ± 0.05	0.29 ± 0.21	0.38 ± 0.16	0.65 ± 0.25	0.35 ± 0.22	0.33 ± 0.10	0.35 ± 0.01	0.43 ± 0.07
Li	30 ± 3	39 ± 16	34 ± 4.5	24 ± 11	63 ± 22	182 ± 29	32 ± 19	35 ± 13	189 ± 110	25 ± 5	33 ± 18
Be	4 ± 2	10 ± 1.5	-	8 ± 0	7 ± 2.3	10 ± 2	7 ± 2.5	13 ± 8	-	8 ± 1	12 ± 4
Zn	146 ± 37	233 ± 59	206 ± 45	255 ± 39	276 ± 69	494 ± 38	137 ± 29	257 ± 107	385 ± 86	269 ± 24	74 ± 11
Rb	71 ± 4	157 ± 11	150 ± 34	202 ± 7	173 ± 21	203 ± 59	155 ± 36	172 ± 48	198 ± 97	96 ± 23	234 ± 73
Sr	32 ± 10	43 ± 19	43 ± 12	8 ± 0	10 ± 3.7	16 ± 6	81 ± 17	25 ± 20	11 ± 4	22 ± 14	25 ± 10
Y	22 ± 1	24 ± 8	21 ± 3.5	24 ± 4	18 ± 8.6	17 ± 3.6	19 ± 1.7	22 ± 8	44 ± 29	24 ± 8	26 ± 6
Zr	617 ± 36	614 ± 260	194 ± 52	785 ± 168	747 ± 593	854 ± 592	763 ± 40	637 ± 238	961 ± 915	635 ± 226	179 ± 22
P.I.	0.98 ± 0.03	1.14 ± 0.03	1.10 ± 0.04	1.15 ± 0.02	1.37 ± 0.08	1.70 ± 0.10	0.71 ± 0.12	1.11 ± 0.05	1.36 ± 0.11	1.18 ± 0.11	0.94 ± 0.01
I.E.	0.98 ± 0.01	0.97 ± 0.01	0.95 ± 0.02	1.00 ± 0.00	1.00 ± 0.00	0.99 ± 0.01	0.97 ± 0.00	0.97 ± 0.01	1.00 ± 0.00	0.98 ± 0.01	0.96 ± 0.02
IFe as FeO	3.89 ± 0.21	5.31 ± 0.62	5.38 ± 2.02	3.51 ± 0.30	7.52 ± 1.98	10.32 ± 0.55	5.01 ± 0.45	3.82 ± 0.99	6.79 ± 1.49	7.33 ± 0.13	1.46 ± 0.13
F Alks	9.72 ± 0.05	10.25 ± 0.18	11.17 ± 0.32	8.83 ± 0.01	9.22 ± 0.45	9.52 ± 0.25	8.54 ± 0.98	9.55 ± 0.38	8.97 ± 0.07	11.34 ± 0.09	8.51 ± 0.11
D.I.	90.63 ± 0.20	84.10 ± 2.08	84.30 ± 5.86	90.20 ± 0.74	79.31 ± 4.77	70.09 ± 1.70	83.27 ± 2.90	89.76 ± 2.89	81.18 ± 4.36	80.53 ± 3.80	95.83 ± 0.51
O.R.	30.57 ± 0.31	38.68 ± 11.00	41.70 ± 9.30	76.70 ± 23.00	45.43 ± 13.00	54.27 ± 13.20	27.34 ± 18.40	69.65 ± 15.50	52.06 ± 13.18	66.58 ± 23.00	56.66 ± 4.10

(1) Zigau granite porphyry. (2) Shira quartz syenite. (3) Enclaves in Shira quartz syenite (4) Gora enclaves. (5) Birji granite. (6) Dykes related to Birji granite. (7) Volcanic enclaves in Birji granite (except SH29/4). (8) Andaburi granite. (9) Dykes in Andaburi granite. (10) Andulayi syenite and quartz syenite. (11) Eldowo granite.

show a steady decline in their abundance with increasing silica content and the Shira rocks follow the 'mean curve' for the province quite closely, except perhaps for MgO which is relatively low in the Shira samples (Figure 26d). However, for the minor rock types, dykes and enclaves, greater scatter away from the 'mean curve' is shown. For example, the dyke rocks (occurring in or associated with the Birji and Andaburi granites) are notably depleted in Al, Mg and P, and the basement enclave may be distinguished by high Al, Mg and Ca, and low Ti and Fe.

Figure 26a shows that the two aenigmatite bearing rocks, the Amdulayi syenite and Shira quartz syenite, contain the highest Ti contents of all the major rock types, while those rocks with the lowest Al content (Figure 26b) correlate with those having a relative excess of alkalis (i.e. high peralkalinity index or P.I., Figure 26g) but not necessarily an abnormal absolute alkali content (Figure 26h). These low Al rocks are the mafic rich dyke rocks and the Birji granite whose abundance of mafic minerals is reflected in the high total Fe contents (Figure 26c). In general, the Shira rocks have more Fe than the average for the province, and this coupled with a relatively low Mg content (Figure 26d) gives rise to very high iron enrichment (I.E.) ratios (Figure 26j). In fact, the average I.E. ratio for the major rock types is 0.97 or above. The presence of apatite only as a rare accessory is to be expected when the average P contents are around 0.06 wt% P₂O₅ (Figure 26e).

The relatively low Ca content of the Amdulayi syenite (0.77 wt% CaO) compared to the average for the province of 2.07 wt% CaO reflects the lack of plagioclase; the feldspar-poor dykes related to the Birji granite are also low in Ca.

Figure 26g shows that the Zigau granite porphyry, Eldewo biotite granite and (mica bearing) volcanic enclaves are the only

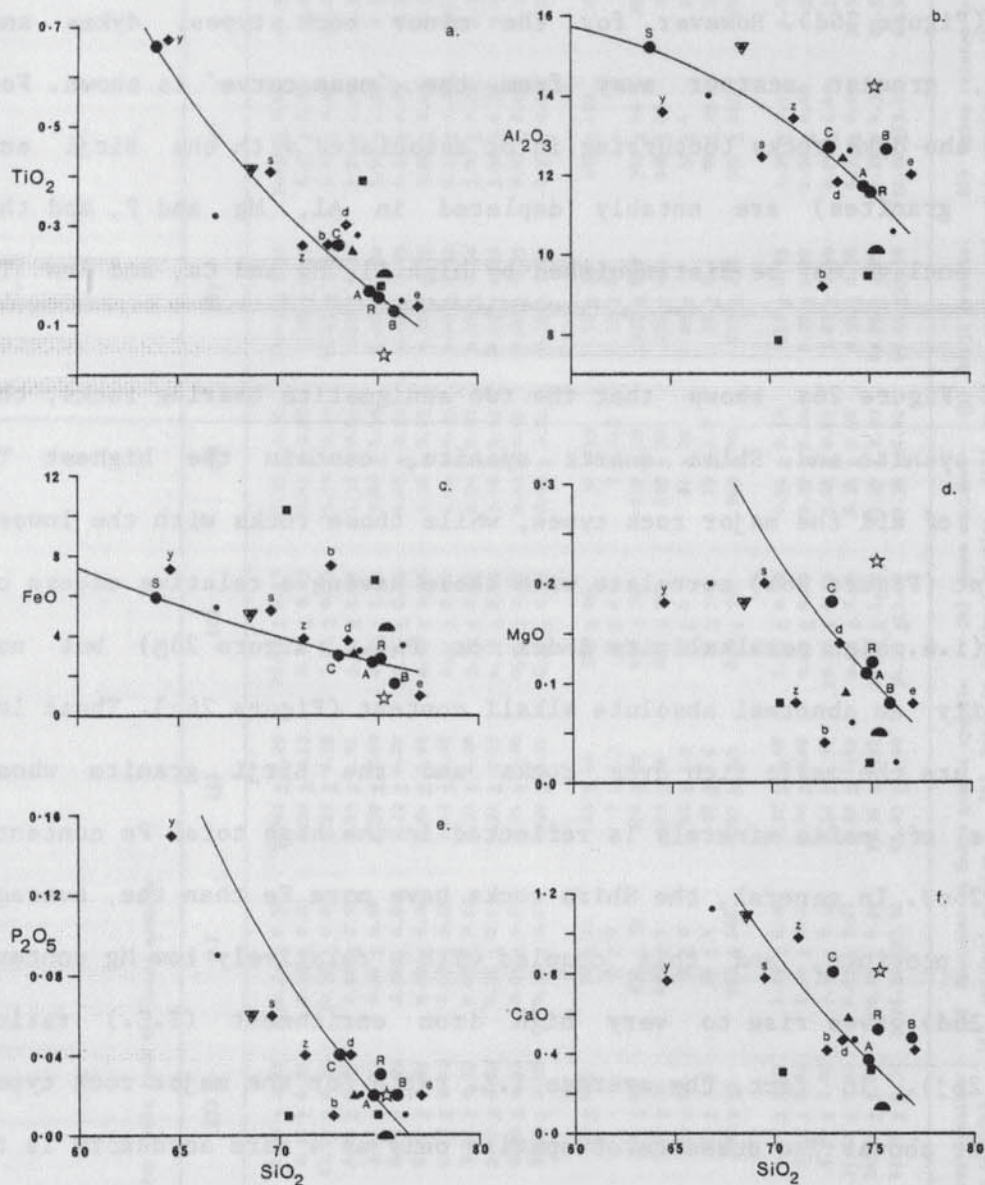
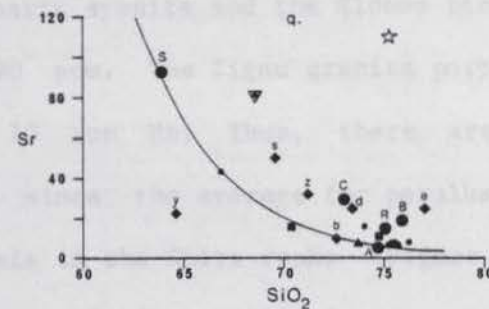
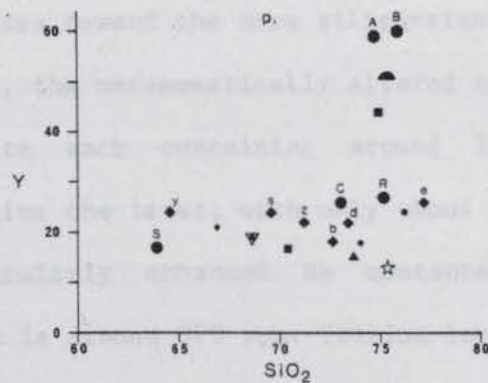
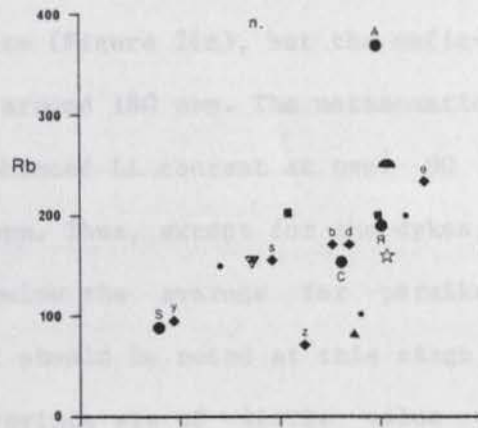
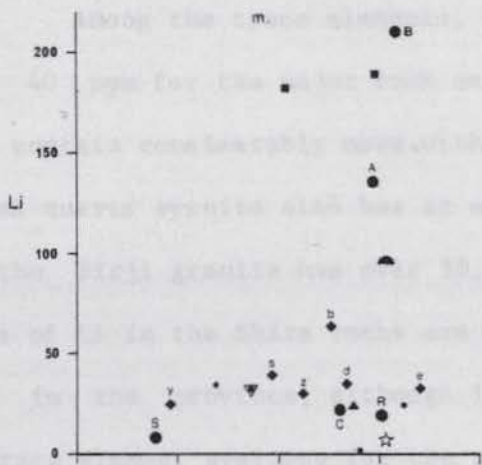
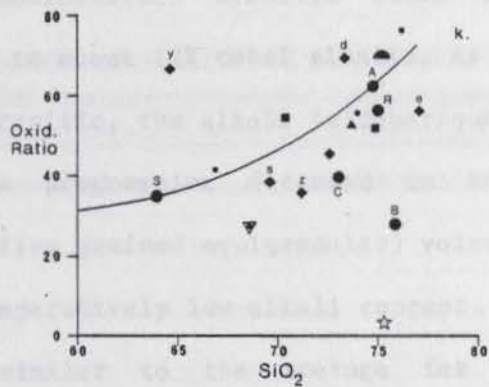
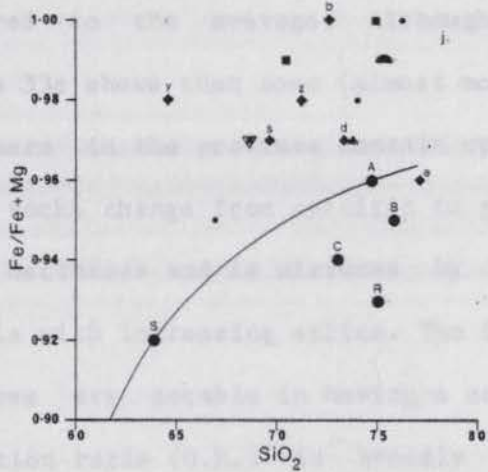
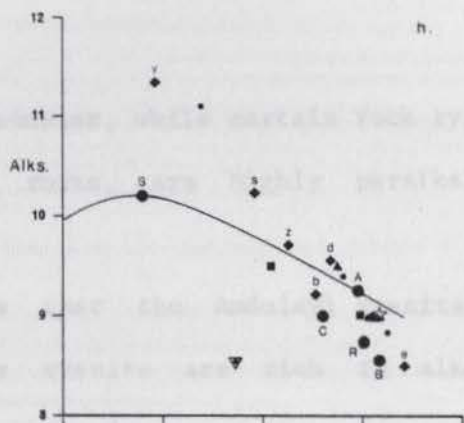
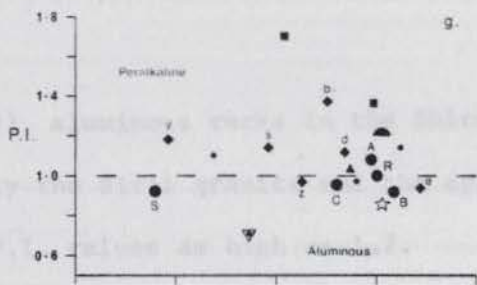


Figure 26.

Harker diagrams for averaged whole rock values from the Shira complex and the Niger-Nigeria province. Diamonds = major rock types : z = Zigau granite porphyry; s = Shira quartz syenite; b = Birji granite; d = Andaburi granite; y = Amdulayi syenite; e = Eldewo granite. Minor rock types : squares = dykes; dots = enclaves; dot within triangle = fine grained volcanic enclaves; filled semi-circle = metasomatically altered quartz syenite; triangle = Chida granophyre; open star = basement enclave. Large circles : averages for the Niger-Nigeria province, where S = syenites and trachytes; A = peralkaline granites; R = rhyolitic volcanics; C = Ca-amphibole granites and porphyries; B = biotite granites. (Averages listed in Tables 27 and 28.)



(major) aluminous rocks in the Shira complex, while certain rock types, notably the Birji granite and the dyke rocks, are highly peralkaline with P.I. values as high as 1.7.

From Figure 26h it appears that the Amdulayi syenite and syenitic enclaves from the Shira quartz syenite are rich in alkalis compared to the average. Although this is true to some extent, Figure 33c shows that some (almost monomineralic) syenitic rocks from elsewhere in the province contain up to about 12% total alkalis. As the Shira rocks change from syenitic to granitic, the alkali feldspar/quartz ratio decreases and is mirrored by a progressive decrease in total alkalis with increasing silica. The (fine grained equigranular) volcanic enclaves are notable in having a comparatively low alkali content. The oxidation ratio (O.R.) is broadly similar to the average for the province, except that the Amdulayi syenite is somewhat higher.

Among the trace elements, Li contents are modest and generally below 40 ppm for the major rock units (Figure 26m), but the mafic-rich dykes contain considerably more with around 180 ppm. The metasomatically altered quartz syenite also has an enhanced Li content at over 90 ppm, and the Birji granite has over 50 ppm. Thus, except for the dykes, the levels of Li in the Shira rocks are below the average for peralkaline rocks in the province, although it should be noted at this stage that the trace element averages for the province are of little value since the range of values is so great (Figure 31). For Rb, there is a general increase toward the more silica-rich rocks (Figure 26n) with the dyke rocks, the metasomatically altered quartz syenite and the Eldewo biotite granite each containing around 200 ppm. The Zigau granite porphyry contains the least, with only about 70 ppm Rb. Thus, there are no particularly enhanced Rb contents since the average for peralkaline rocks is around 370 ppm. Yttrium levels in the Shira rocks (Figure 26p) show very little change with increasing SiO₂ content and average about

20 ppm, except for the Andaburi dykes with 44 ppm and the metasomatically altered quartz syenite with 51 ppm.

As would be expected from the low Ca content of these rocks, the Sr content is also extremely low and decreases with increasing silica (Figure 26q) in an approximately exponential manner like the province average. The Li, Rb and Y contents of the basement enclave are generally very low, but it is noticeable that this enclave is comparatively rich in Sr with 110 ppm. The volcanic enclaves and the Eldewo biotite granite too may be comparatively rich in Sr. The Amdulayi syenite has a particularly low Sr content and clearly indicates that abundance of alkali feldspar is no indication of Sr content. In fact, the Sr levels quoted must be considered maximum values since the detection limit is relatively high at around 8 ppm. The general pattern for Zn values (not shown) is very similar to that of Li.

Therefore, from the trace element distribution patterns compared to the averages, the major Shira peralkaline rock types and the Eldewo aluminous granite are not enriched in the (lithophile) trace elements studied. Since in general, the most trace element enriched peralkaline granites also have a highly characteristic texture (often with abundant, discrete albite crystals), the generally low trace element contents of the Shira major rock units is compatible with the modest degree of textural modification which has taken place. The metasomatically altered quartz syenite (SH103) demonstrates this association however, since it shows enhanced levels of Li, Rb and Y, is depleted in Sr and has a higher peralkalinity index than the unaltered Shira quartz syenite.

The dykes associated with the Birji and Andaburi granites have abundant mafic minerals and are poor in alkali feldspar. Their chemistry reflects this, and they have high Fe and low Al and Mg contents and they contain relatively abundant Li and Rb but are depleted in Sr, while the

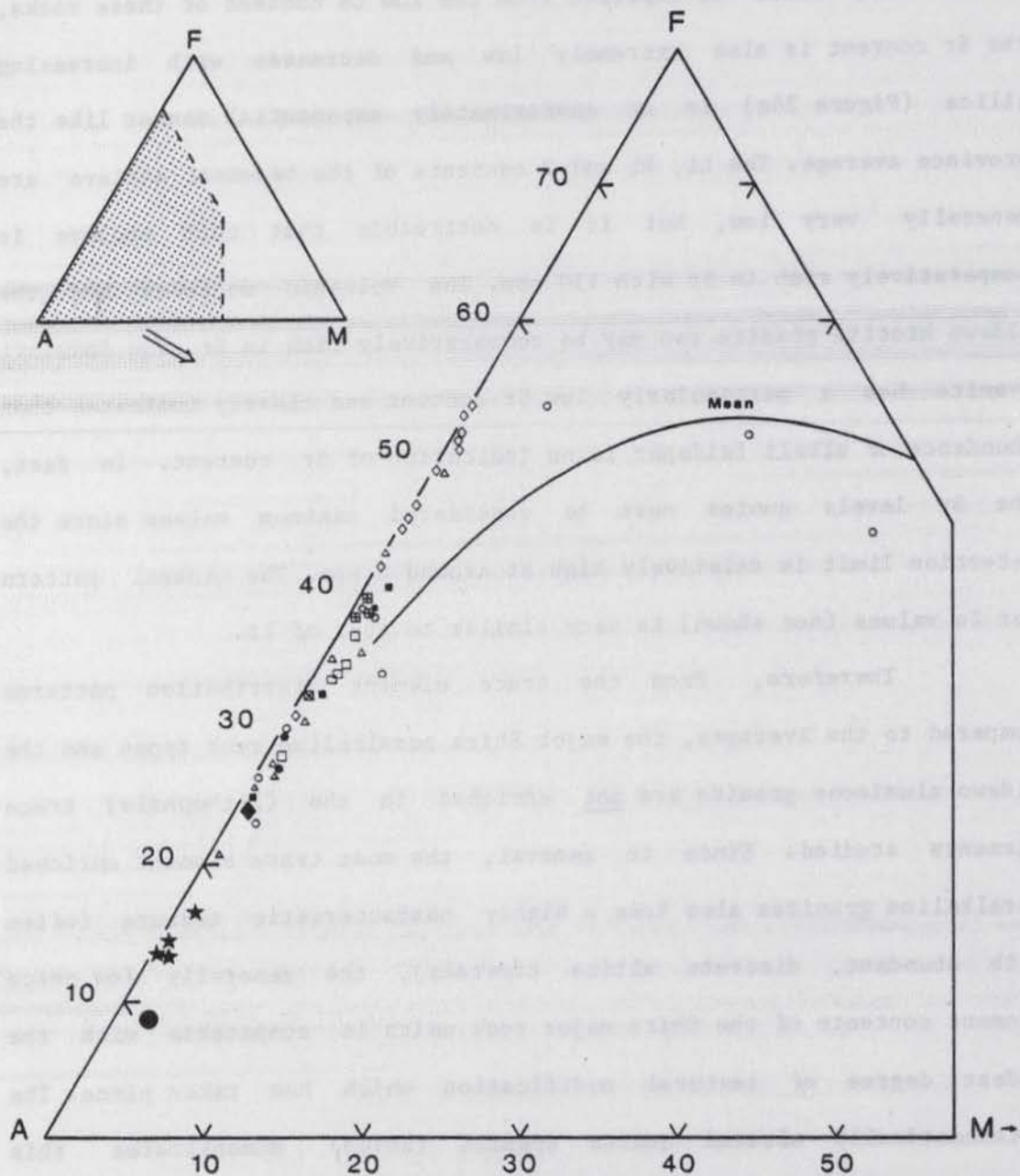


Figure 27.

AFM diagram for the Shira complex.

Filled circles = Zigau granite porphyry. Open squares = Shira quartz syenite. Open diamonds = Birji granite and related dykes. Open triangles = Andaburi granite and dykes. Squares enclosing crosses = Amdulayi syenite/quartz syenite. Stars = Eldewo granite. Large filled diamond = Chida granophyre. Large filled circle = basement xenolith. Square enclosing diagonal cross = metasomatically altered Shira quartz syenite. Open circles = enclaves. Mean = curve through the averaged rock types for the Niger-Nigeria province.

Andaburi dykes have among the highest Y contents. A possible explanation for the chemical features shown by these dykes will be given later.

The Chida granophyre has no clear field or petrologic associations but chemically it is mildly peralkaline and bears closest resemblance to the Andaburi granite, although such a link must be regarded as tentative.

The chemical nature of the fine grained (metamorphosed but probably not chemically altered) volcanic enclaves in the Birji granite is distinctive by virtue of a relatively aluminous composition (P.I. = 0.7), low alkali content and high levels of Ca and Sr. The aluminous nature is compatible with the fact that it contains biotite and larger, poikilitic white mica flakes. These enclaves therefore, have no close analogues among the Shira rocks. The porphyritic volcanic enclave (SH29/4) is texturally very similar to many Younger Granite quartz porphyries and, unlike the enclaves discussed above, it has no unusual chemical features. The basement enclave however, is very distinctive chemically, with relatively high Al, Mg, Ca and Sr, and low Ti, Fe, P.I., O.R., I.E., Li, Rb, Y and Zr.

On an AFM diagram (Figure 27) the low Mg content of the majority of samples is obvious as most samples fall very close to the A-F join. Only the enclaves in the Zigau granite porphyry (ZG2A/B) and one in the Andaburi granite (SH44/1) contain any appreciable Mg, but nevertheless it may be significant that they plot close to the curve representing the locus of averaged rocks from the whole province (Table 28). The remaining xenolithic samples then fall among the points for the other rock types. For the majority of samples therefore, their position on an AFM diagram reflects their ratio of alkalis to total iron (or the modal feldspar/mafic mineral ratio). Because alkali feldspar crystallises relatively early and the mafic minerals relatively late in the majority of rocks studied, the AFM diagram may provide a valuable

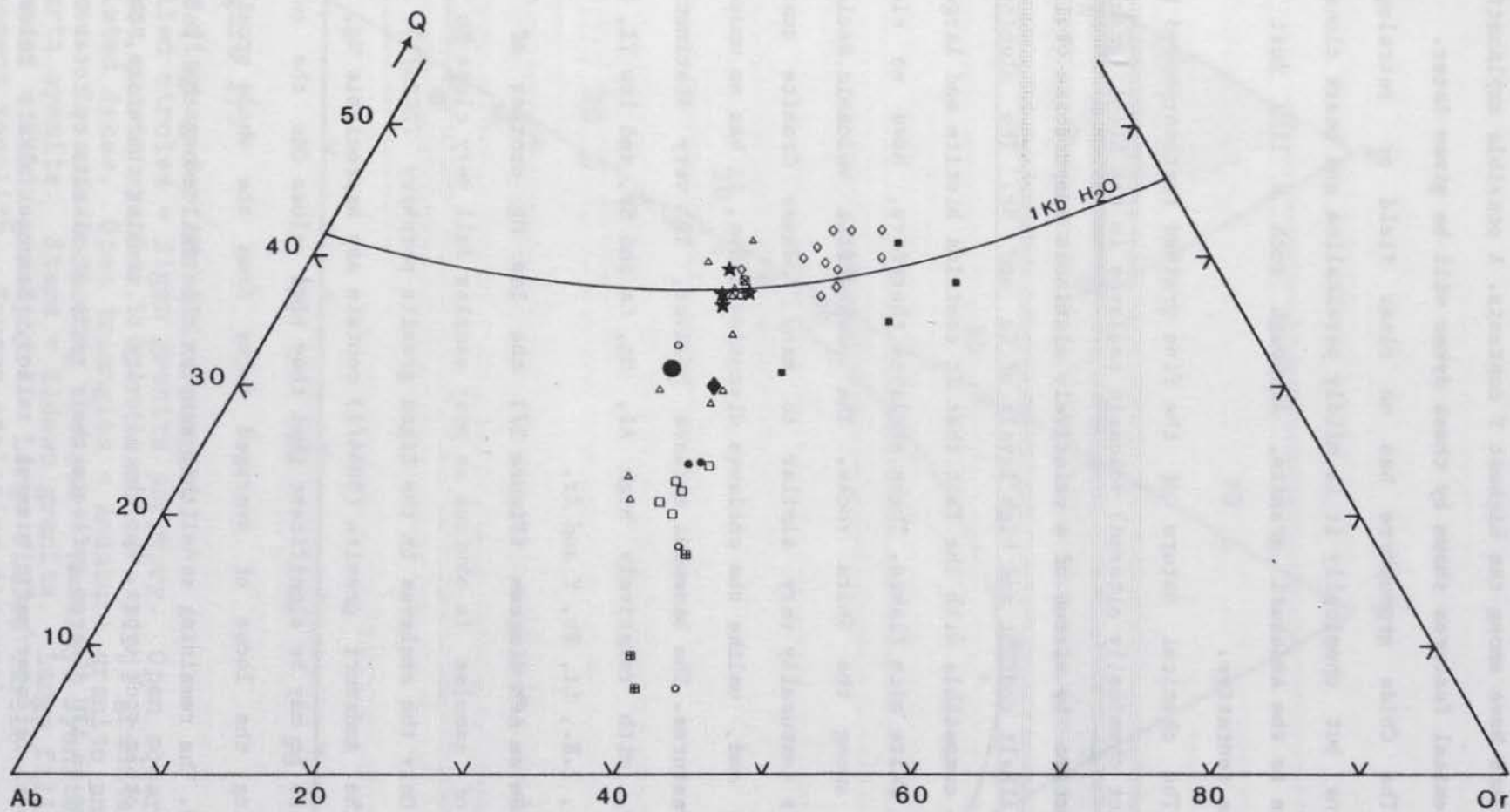


Figure 28. Normative Q-Ab-Or diagram for the Shira complex. [Symbols as in Figure 27.]

guide as to whether alkali feldspar fractionation has taken place. The diagram in addition, highlights the very low iron/alkalis ratio of the aluminous Eldewo biotite granite and basement granite.

With respect to the normative Q-Ab-Or diagram (Figure 28) it should be noted at this point that many of the samples plotted have a Thornton and Tuttle (1960) differentiation index (D.I.) of less than 80. Enclaves ZG2A/B and SH44/1 have not been plotted because they have very low D.I. values, but in the case of the mafic mineral-rich Birji granite, two facies of the Amdulayi syenite, the dykes and some enclaves, An is not present in the norm but the D.I. is usually a little below 80 because of the abundance of Ac, Hy and Ns in the norm. For these samples (Table 26), a cautious approach to any interpretation of their position on Figure 28 is therefore required. However, for these rocks certain experimental work can explain their anomalous position: normative sodium metasilicate (Ns) in the melt moves the granite minimum (and the thermal valley) away from the Ab apex towards the Q-Or join (Carmichael, 1962; Carmichael and Mackenzie, 1963) in a similar manner to the action of normative anorthite (An) (James and Hamilton, 1969). Carmichael and Mackenzie (op.cit.) also point out that natural pantelleritic liquids have a restricted range in composition and plot in a thermal valley toward the syenitic end, implying that "they must be derived from a liquid which itself lies in this valley".

Several deficiencies in the normative Q-Ab-Or projection for peralkaline compositions have been noted by Bailey and Macdonald (1964), in particular that by ignoring part of the Na in the liquid (i.e. as Ns) it conceals a relation between the liquid and the alkali feldspar phenocrysts. Thus, in contrast to Carmichael's (1962) findings that natural pantelleritic liquids crystallise a feldspar more sodic than the whole rock, Bailey and Schairer (1964) find that this is a misrepresentation and in fact feldspars in oversaturated silicic

	A. Basalts & gabbros n=34			B. Trachytes & syenites n=33			C. Rhyolitic volcanics n=31			D. Fay., pyx. & Ca-amph. granites n=60			E. Angrite & Na-amph. granites n=69			F. Biotite granites n=99		
	Mean	s.d.	Range	Mean	s.d.	Range	Mean	s.d.	Range	Mean	s.d.	Range	Mean	s.d.	Range	Mean	s.d.	Range
SiO ₂	50.05	4.06	43.76 - 58.80	63.92	2.76	59.20 - 69.76	75.06	1.64	71.70 - 77.60	73.03	2.14	67.63 - 77.40	74.73	1.97	68.20 - 78.50	75.83	1.59	72.37 - 78.60
TiO ₂	2.25	1.15	0.66 - 5.97	0.66	0.35	0.12 - 1.70	0.16	0.08	0.00 - 0.35	0.26	0.15	0.02 - 0.77	0.17	0.10	0.00 - 0.50	0.13	0.08	0.02 - 0.47
Al ₂ O ₃	16.26	1.88	13.33 - 20.57	15.20	1.66	11.21 - 18.33	11.55	0.59	10.46 - 13.03	12.67	0.78	11.07 - 14.93	11.66	0.99	9.94 - 14.50	12.60	0.93	11.09 - 16.98
Fe ₂ O ₃	3.04	2.29	0.51 - 10.96	2.14	1.02	0.48 - 5.09	1.75	0.84	0.52 - 3.58	1.22	0.61	0.14 - 2.74	1.82	0.78	0.25 - 4.98	0.45	0.37	0.00 - 1.48
FeO	7.90	2.29	2.30 - 12.10	3.95	1.67	1.23 - 6.74	1.34	1.04	0.00 - 6.02	1.85	0.83	0.28 - 3.97	1.09	0.56	0.07 - 2.71	1.14	0.41	0.00 - 2.67
MnO	0.20	0.16	0.08 - 0.67	0.14	0.08	0.05 - 0.28	0.10	0.11	0.02 - 0.76	0.07	0.04	0.00 - 0.22	0.05	0.04	0.01 - 0.27	0.03	0.02	0.00 - 0.18
MgO	5.34	2.89	0.83 - 12.70	0.56	0.42	0.04 - 1.62	0.12	0.09	0.02 - 0.36	0.18	0.16	0.01 - 0.79	0.11	0.11	0.00 - 0.45	0.08	0.08	0.01 - 0.35
CaO	8.32	2.22	3.49 - 13.28	2.07	1.19	0.25 - 4.65	0.52	0.26	0.09 - 1.02	0.81	0.43	0.06 - 2.14	0.37	0.24	0.01 - 1.20	0.48	0.21	0.01 - 1.25
Na ₂ O	3.24	0.82	1.87 - 5.67	5.25	0.90	3.26 - 6.94	3.75	0.57	1.94 - 4.64	4.04	0.57	2.86 - 5.60	4.58	0.86	3.19 - 7.23	3.94	0.46	2.94 - 5.06
K ₂ O	1.42	0.98	0.05 - 3.23	4.96	0.78	2.90 - 6.75	4.98	0.81	3.50 - 7.00	5.02	0.46	3.50 - 6.82	4.66	0.67	2.55 - 6.67	4.64	0.47	3.25 - 5.77
P ₂ O ₅	0.40	0.32	0.01 - 1.23	0.21	0.19	0.01 - 0.73	0.03	0.02	0.00 - 0.06	0.04	0.04	0.00 - 0.17	0.02	0.02	0.00 - 0.09	0.02	0.02	0.00 - 0.12
H ₂ O ⁺	0.97	0.49	0.34 - 2.27	0.57	0.29	0.16 - 1.30	0.29	0.15	0.01 - 0.65	0.44	0.23	0.03 - 1.21	0.39	0.20	0.08 - 0.98	0.28	0.13	0.01 - 0.79
	99.39			99.63			99.65			99.63			99.65			99.62		
Agp.-coeff.	0.44	0.13	0.15 - 0.67	0.92	0.11	0.75 - 1.20	1.00	0.09	0.86 - 1.18	0.95	0.08	0.76 - 1.16	1.08	0.12	0.85 - 1.49	0.92	0.07	0.69 - 1.07
EPe/EPe+Mg	0.69	0.13	0.35 - 0.94	0.92	0.04	0.86 - 0.99	0.93	0.17	0.90 - 0.99	0.94	0.04	0.80 - 1.00	0.96	0.04	0.83 - 1.00	0.95	0.04	0.61 - 1.00
EPe as FeO	10.94	2.77	5.66 - 19.68	5.88	1.83	2.80 - 10.00	2.92	1.34	1.20 - 6.75	3.04	1.10	1.08 - 6.44	2.76	0.91	1.24 - 5.20	1.57	0.48	0.93 - 2.82
E alkalis	4.69	1.54	1.92 - 8.43	10.21	1.26	7.55 - 12.30	8.73	0.76	7.47 - 10.28	9.06	0.79	7.34 - 10.54	9.24	0.86	7.68 - 12.20	8.57	0.44	7.43 - 9.67
Diff. index	38.10	13.04	16.77 - 66.15	81.67	6.97	63.64 - 91.23	92.08	2.93	83.34 - 97.42	90.04	2.82	83.39 - 97.03	91.63	2.93	83.87 - 96.11	94.11	1.76	87.72 - 96.53
Oxid. ratio	27.79	-	-	35.14	-	-	56.63	-	-	39.74	-	-	62.54	-	-	28.30	-	-
Trace elements	n=18			n=15			n=17			n=28			n=48			n=84		
Li	10	5	2 - 47	8	3	0 - 12	19	24	0 - 104	22	17	0 - 74	136	172	0 - 885	210	265	0 - 1482
Zn	103	39	33 - 165	120	46	56 - 247	109	57	28 - 230	109	48	35 - 284	304	229	42 - 988	173	176	29 - 828
Rb	25	26	0 - 80	88	29	50 - 149	191	87	105 - 470	155	59	86 - 280	368	330	105 - 1380	518	264	120 - 1472
Sr	434	110	164 - 618	92	85	3 - 274	14	17	0 - 65	29	34	0 - 137	6	9	0 - 38	17	28	0 - 190
Y	8	6	5 - 18	17	6	6 - 23	17	9	15 - 36	25	12	5 - 50	59	40	3 - 143	60	39	5 - 105
Zr	261	161	19 - 617	545	219	146 - 1060	466	230	200 - 1075	435	191	155 - 828	751	537	75 - 2170	207	212	58 - 1686
K/Rb (x10 ⁴)	458	488	180 - 2262	523	142	281 - 740	271	97	91 - 452	287	116	146 - 543						
Rb/Sr	0.06	-	0.01 - 0.23	0.96	-	0.19 - 28.00	14	-	4 - 94	5	-	1 - 43	157	92	27 - 426	99	61	21 - 371
Li/Mg	3	-	-	24	-	-	263	-	-	203	-	-	61	-	4 - 637	29	-	3 - 446
Ca/Sr (x10 ⁴)	137	-	-	161	-	-	265	-	-	200	-	-	2050	-	-	4353	-	-
													441	-	-	202	-	-
World averages																		
Li	10	-	-	10	-	-	51	-	-	40	-	-						
Zn	-	-	80 - 120	70	-	-	98	-	-	48	-	-						
Rb	-	-	2 - 36	-	-	110 - 124	217	-	-	170	-	-						
Sr	-	-	69 - 190	-	-	280 - 553	97	-	-	147	-	-						
Y	32	-	-	35	-	-	-	-	-	38	-	-						
Zr	-	-	66 - 330	310	-	-	-	-	-	-	-	50 - 700						

Table 28. Mean values, standard deviations and ranges for whole rock analyses of the major rock types from the Niger-Nigeria province.

peralkaline liquids are more potassic than the parental liquid. Hence fractional crystallisation of alkali feldspar, they suggest, can lead to strongly peralkaline and sodic residual liquids - the so-called 'orthoclase effect'. Since in the Shira peralkaline rocks the interstices are occupied by Na-rich mafic minerals, the entry of K preferentially into alkali feldspar is established and operation of the 'orthoclase' (i.e. perthite) effect is a possibility.

From Figure 28 it may be seen that there is a progression (close to the low temperature trough in the feldspar region) from the Amdulayi syenite / quartz syenite, through the Shira quartz syenite and Zigau granite porphyry, to the Andaburi granite, Gora enclave and the Eldewo biotite granite. The Birji granite and most dyke rocks have high Fe contents and D.I.'s of less than 80, and plot along the quartz-feldspar cotectic towards the Q-Or side. The volcanic enclaves are equally distinctive and are among the most Ab-poor rocks analysed. The syenitic enclaves fall within the range shown by the major rock types and by comparison with Figure 27, the data are compatible with the view that there is a progressive evolution from syenitic to granitic rocks in the Shira complex.

5.3 Geochemistry of the Niger-Nigeria province Introduction

In order to gain a better understanding of the geochemistry of the Shira complex and to view it in a wider context, a geochemical review of the Younger Granite province has been undertaken with the aid of many unpublished analyses and computer manipulation of data. In all, 326 published and unpublished analyses have been compiled into 6 groups and the averages, standard deviations and ranges for each of these groups are listed in Table 28. The selection of the 6 groups of rocks follows an established classification (Jacobson et al., 1958) and is based mainly on mineralogy, although in one case, rhyolitic (as distinct

from trachytic or basaltic) volcanic rocks are treated as a distinct group even though many of their mineralogical features are the same as in the calcic amphibole bearing granites and porphyries.

No attempt has been made to exclude samples for which accompanying descriptions indicate that they have undergone a 'deuteric' albitisation event, as such processes probably operate on a continuum from truly magmatic processes and are therefore regarded as an integral geochemical part of the rocks. However, it is first necessary to consider some possible shortcomings inherent in any geochemical data and the diagrams used to summarise that data.

The simple Harker diagram was used initially as the principal means of graphically expressing the geochemical variation of the Niger-Nigeria province. Later, the Thornton and Tuttle differentiation index (D.I.) was tried, but as the corresponding graphs were so similar in these dominantly oversaturated rocks, the Harker diagram was retained. The modified D.I. of Upton et al. (1971) whereby normative Ac and Ns are added to $Q+Ab+Or$, may be a way of spreading out points at the high silica end of the spectrum but it was not tried here. Given that the Harker diagram cannot be used to distinguish between different processes that may act to produce a sequence of rocks (Chayes, 1964), Cox et al. (1979) find the use of such diagrams satisfactory as long as other evidence is provided to support a particular model. On the subject of Harker diagrams, Chayes (1962) advocates the retention of Fe_2O_3 and FeO as independent variables, whether or not a pooled (total) iron variable is used. He suggested that a pooled iron variable is preferred by some workers because it provides a better correlation with silica than either Fe_2O_3 or FeO . This is true for the Niger-Nigeria province but the use of the total iron variable is justified here on the basis that the oxidation ratio may be slightly altered in some specimens although the total iron content will remain the same. Also, there is

some evidence to indicate that the ferrous/ferric ratio is dependent upon the fluorine content of the melt (Belyaev, 1959), the type of alkali and the alkali concentration (Paul and Douglas, 1965; Thornber et al., 1980) as well as temperature and fO_2 .

The presentation and interpretation of chemical data has been discussed by Wright (1974), who regards the use of a complete set of oxide variation diagrams as the only way of presenting all the chemical data for a rock suite. Wright objects to the use of triangular AFM diagrams for petrogenetic conclusions because only about half the data is plotted, but Barker (1978) justifies their use on the grounds that if mineral compositions are plotted as well, information on which cumulate minerals could give the resulting whole rock trend, can be obtained. However, Butler (1979) regards the trends on ternary diagrams as being due to a more complex set of interactions than those proposed by Barker (1978). It is therefore concluded that this geochemical review should include several different types of diagram to represent the data, bearing in mind the shortcomings of each.

In the case of volcanic and peralkaline rocks particularly it is pertinent to consider the possibility that their chemical composition no longer reflects that of the magma, because of modification by later intrusions or volatile loss. In the first instance, it should be borne in mind that the 326 samples used in the geochemical survey of the province represent only about 90% of available analyses. Of the rejected analyses, many may be the result of printing errors, bad analyses, etc., but in at least a few cases when such an analysis was matched with a thin section, clear evidence of secondary alteration was observed. Such alteration may be more common among basalts and trachytes which lie at the base of the volcanic pile (e.g. Turner and Bowden, 1979). For the rhyolitic volcanics however, the initial anhydrous mineralogy is usually preserved and secondary chemical changes induced by intrusion of nearby

granites, are thought to be insignificant in the present context. Similarly, selective loss of lighter pumice fragments from an ignimbritic eruption can cause significant compositional changes (Flood et al., 1980) but the frequent abundance of flattened pumice fragments in the Nigerian ignimbrites and their preservation within a cauldron (implying that the distance from source to deposition was small), suggests that this effect is also insignificant.

In the case of peralkaline volcanic rocks, many workers have recorded chemical changes accompanying devitrification (e.g. Noble et al., 1967; Noble, 1970; Macdonald and Bailey, 1973; Baker and Henage, 1977), and in peralkaline dykes in the Gardar province, devitrification is accompanied mainly by alkali and halogen loss (Macdonald and Parker, 1970). For the central Kungnat complex, alkali loss has also been proposed (Upton et al., 1971), although there is no supporting field evidence such as metasomatism of the country rocks. If the peralkaline granites of the Shira complex are typical then the role of metasomatic loss of alkalis for example, from the coarse grained syenites and granites as witnessed by chemically unaltered enclaves, must be regarded as unproven for these rocks.

In common with many others, the author initially used the term apgaitic coefficient as being synonymous with peralkalinity index. The former term has been used in Table 28 and Figure 29, but in the text and for all reference to the Shira rocks, the term peralkalinity index (P.I.) is used, in accordance with Edgar (1974).

For reasons which will be given later and which are also discussed at greater length in Chapter 6, the geochemical data is believed to contain two distinct trends - aluminous (biotite and Ca-amphibole granites) and peralkaline. Although the data for each shows a large measure of overlap, where possible the distinctions are highlighted.

Summary

Figure 29 shows selected Harker diagrams for the province and Figure 30 is a combined Harker diagram for the major and minor oxides using the averages listed in Table 28. Similar diagrams for trace elements are presented in Figure 31. AFM and AFA diagrams for the province are shown in Figure 32, and a summary AFM diagram together with total alkali and iron enrichment graphs can be seen in Figure 33. In addition, a simplified normative Q-Ab-Or diagram is presented in Figure 34 and a correlation matrix for the major, minor and trace elements, P.I. and K/Rb is given in Table 29. From this data, the significant points related to the geochemistry of the Younger Granite province may therefore be stated as follows:

From the Harker diagrams,

1. TiO_2 , MgO and CaO show an initial rapid decrease with increasing SiO_2 , and then show only a very modest decrease.
2. Total iron shows a virtually constant rate of decline.
3. The Al_2O_3 content remains constant or only very slightly decreases between about 50% and 60% SiO_2 , but then decreases at a faster but fairly constant rate.
4. The MnO and P_2O_5 contents are low in all rocks and change comparatively little but these oxides are most depleted in the granitic rocks.
5. The alkalis Na_2O and K_2O show a steady increase and reach maxima in the syenitic rocks close to about 65% SiO_2 , but then decrease toward the granitic rocks.
6. Li and Zn contents are low in all rock types except the biotite and peralkaline granites, where a very large range is encountered. Li is generally more abundant, and reaches the highest concentrations, in the biotite granites.
7. Rb and Y have a similar behaviour and there is a steady increase

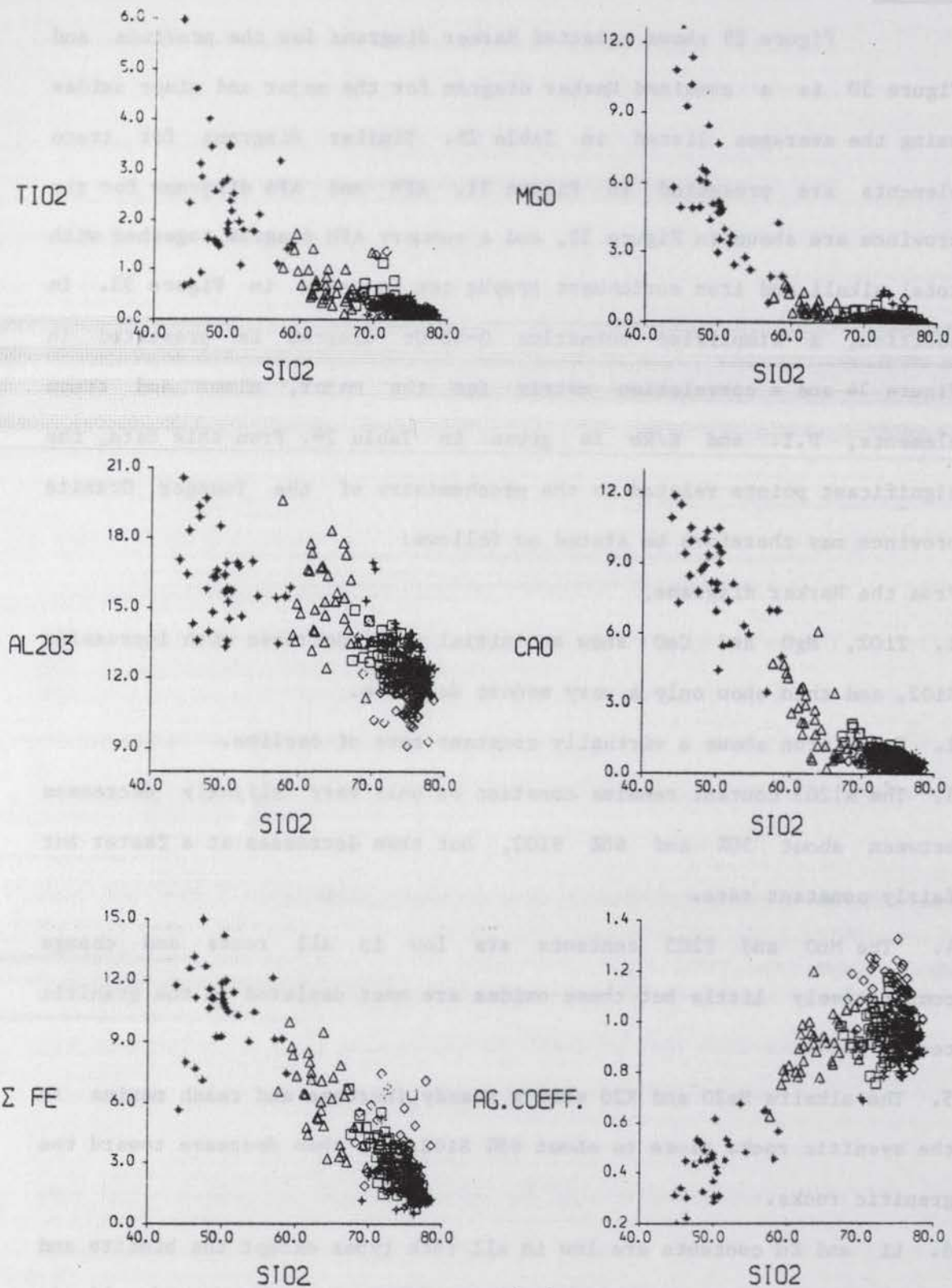


Figure 29. Harker diagrams for selected oxides from 326 samples from the Niger-Nigeria province. Stars = gabbros, dolerites and basalts. Triangles = syenites and trachytes. Squares = Ca-amphibole granites and porphyries. Crosses with central dot = rhyolitic volcanics. Diamonds = peralkaline granites. Crosses with central diamond - biotite granites.

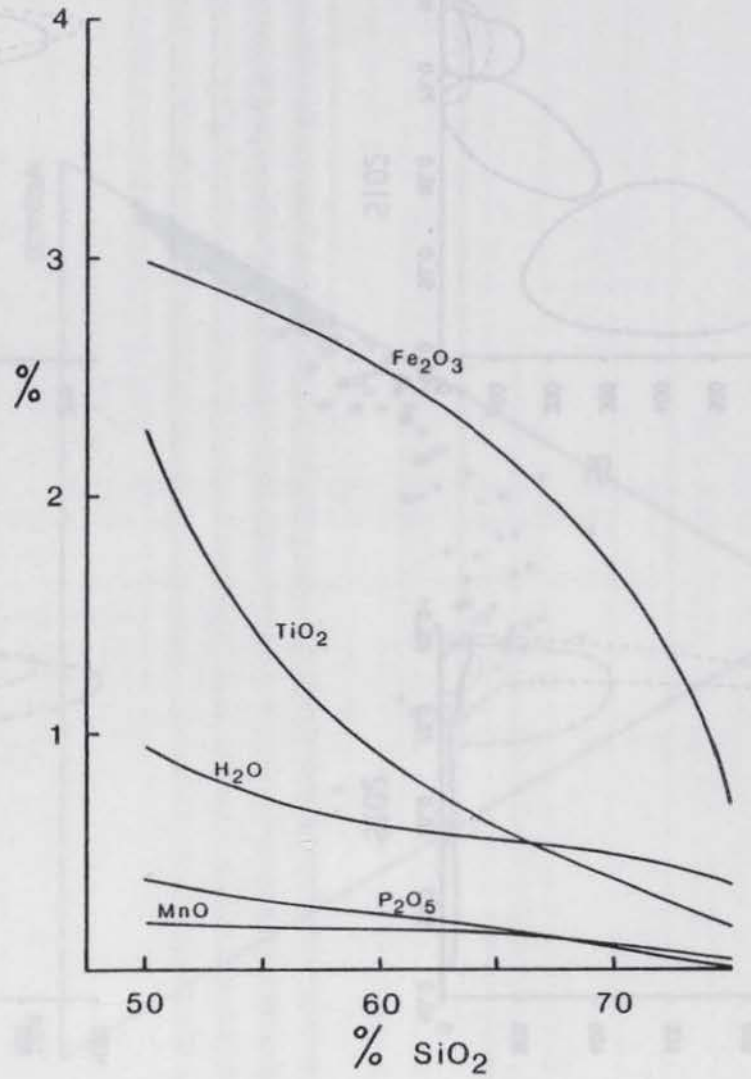
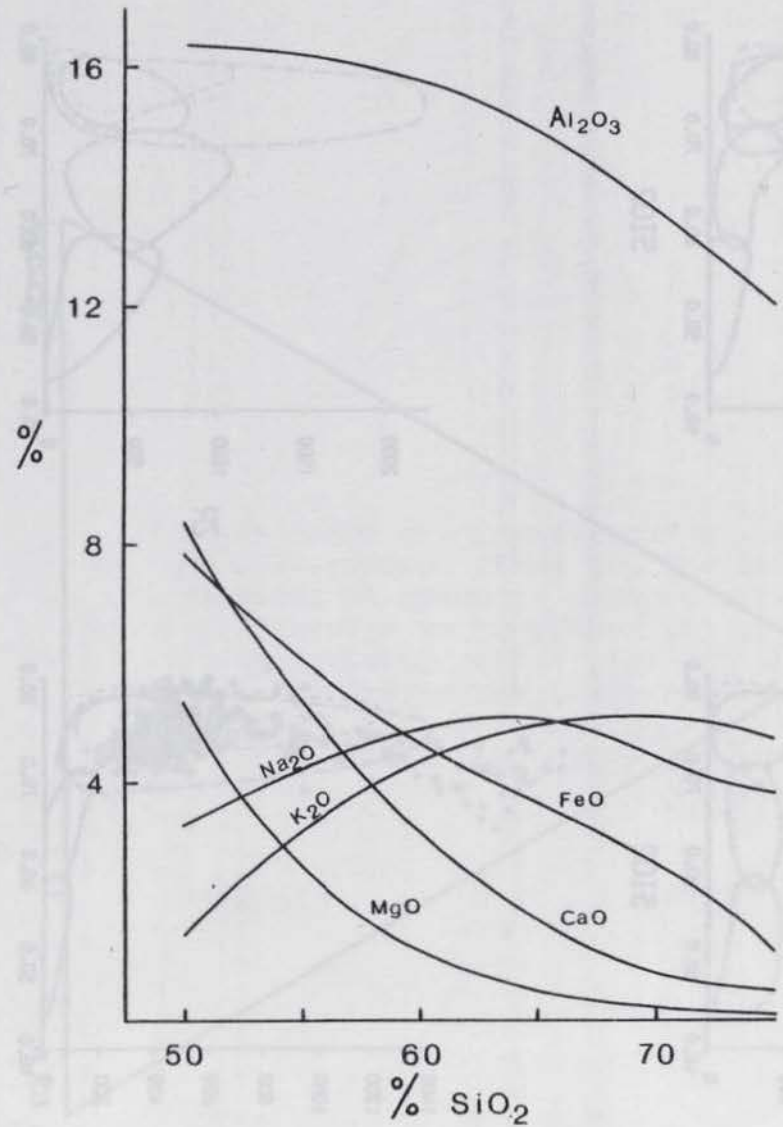


Figure 30. Summary Harker diagrams of averaged values for the Niger-Nigeria province.

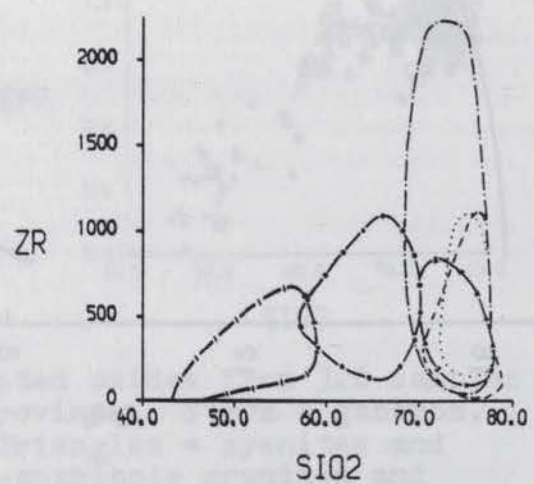
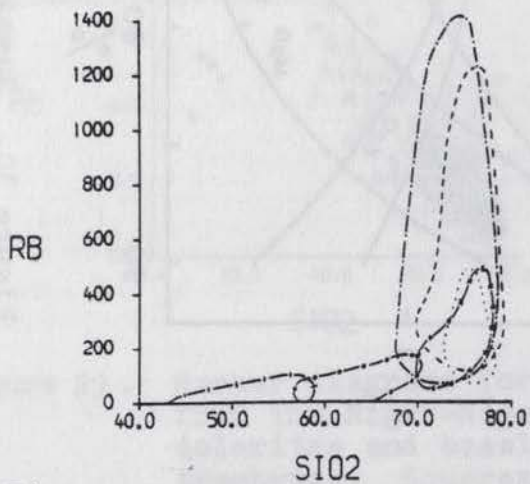
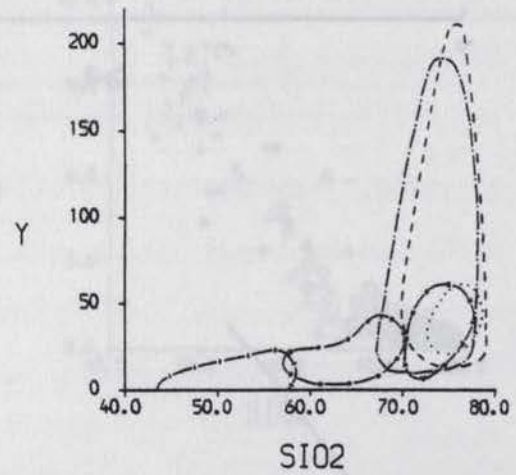
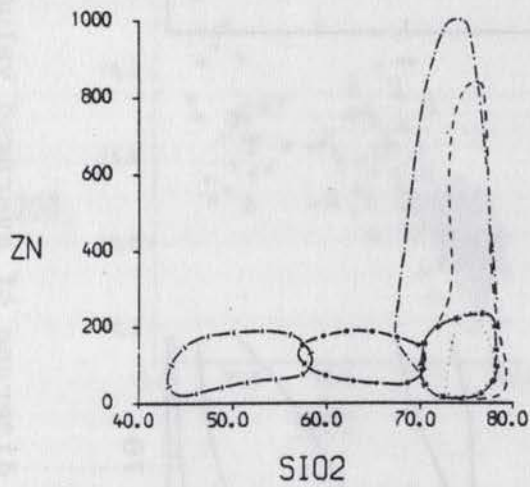
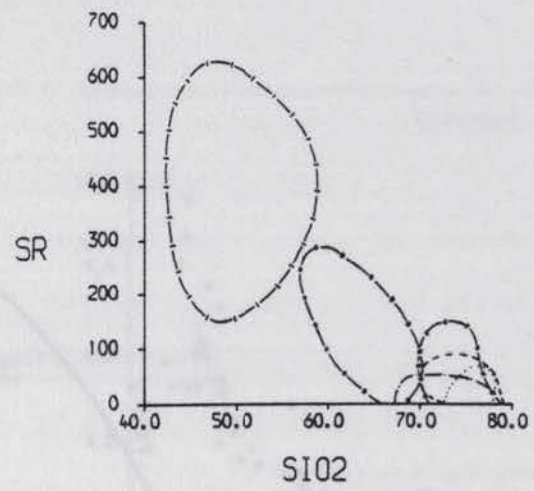
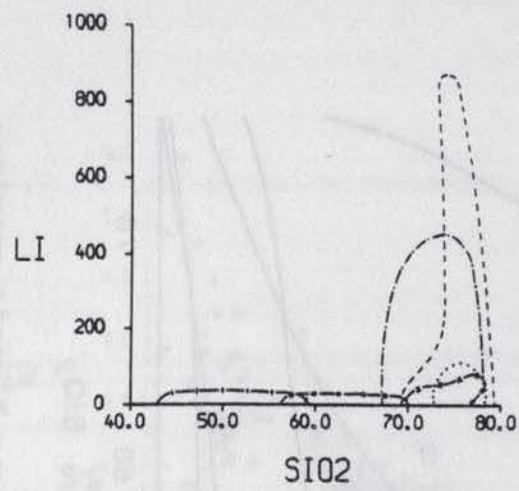


Figure 31.

Summary Harker-type diagrams for trace elements in the Niger-Nigeria province. Symbols as in Figure 34, except dashed lines with vertical marks = basaltic rocks.

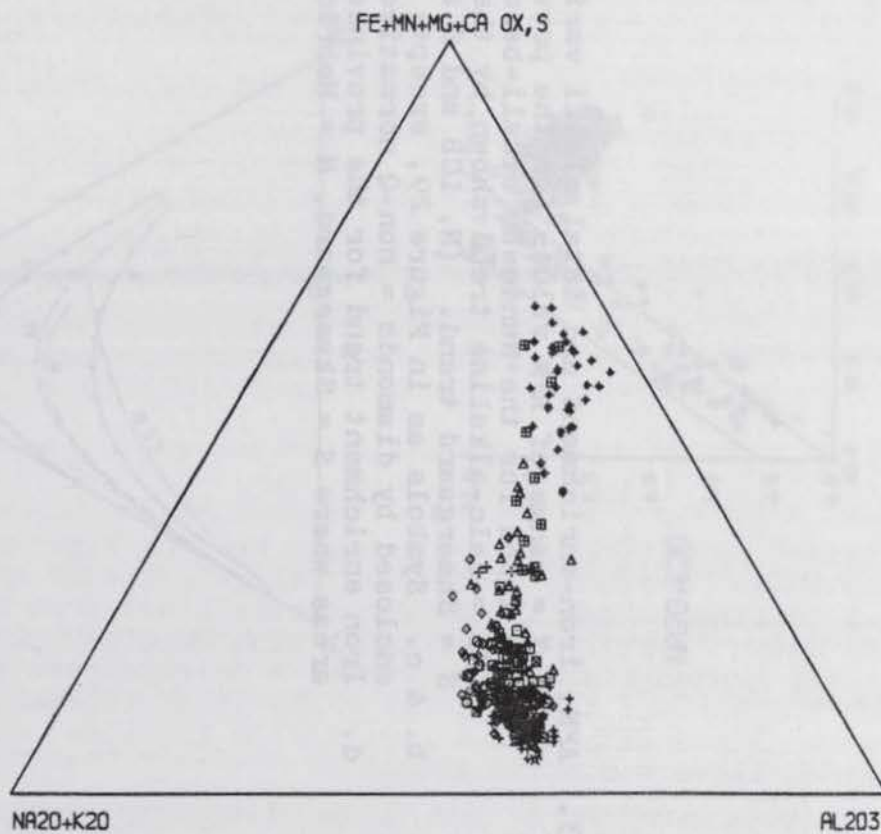
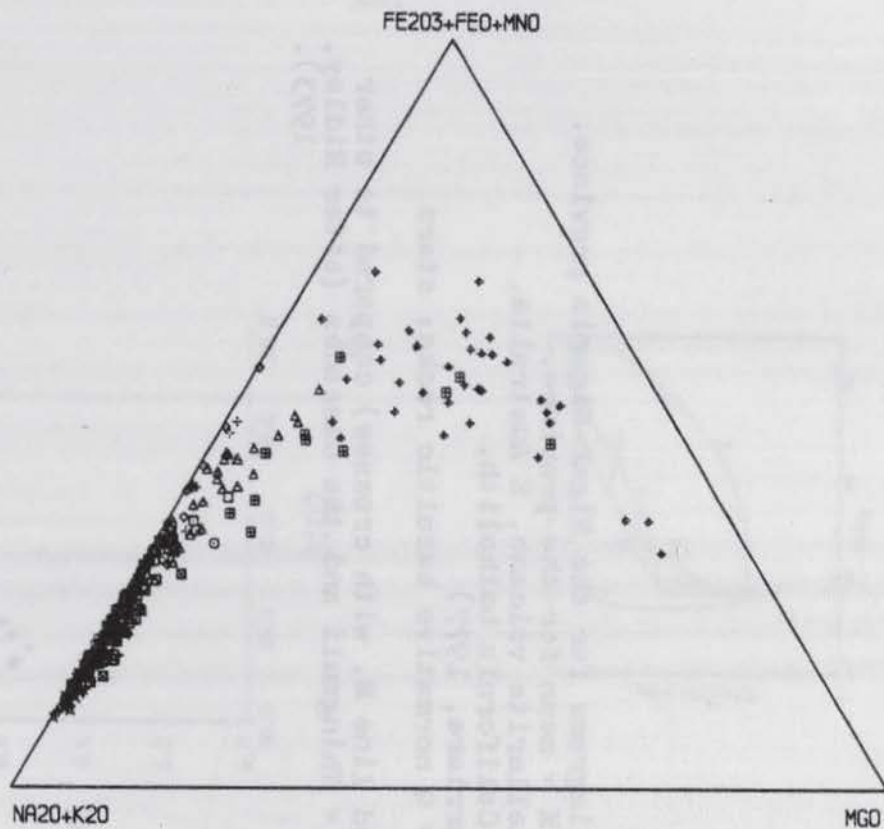
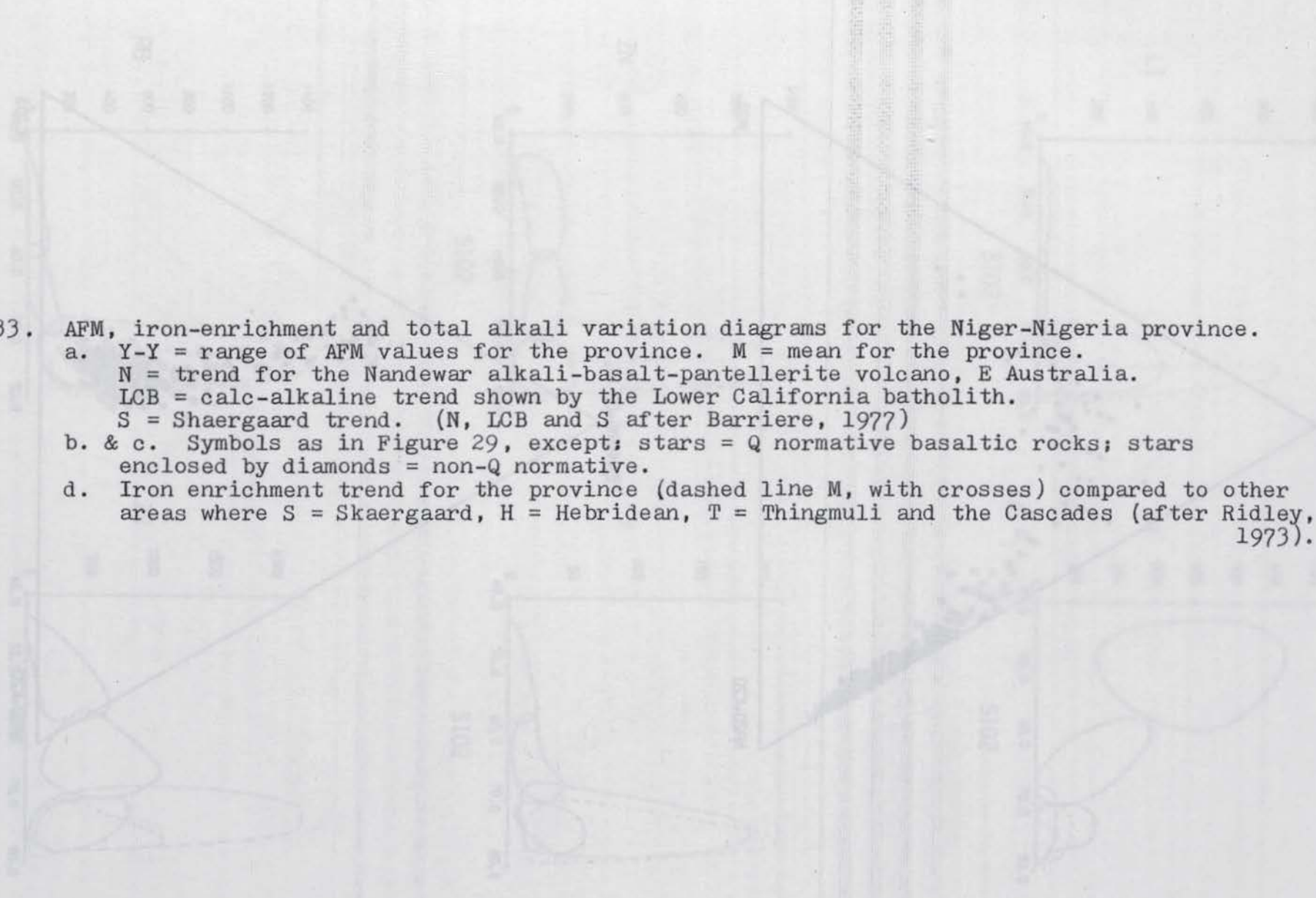


Figure 32.

AFM and AFA diagrams for the Niger-Nigeria province. Symbols as in Figure 29, and squares with crosses = metasomatically altered basic rocks from Sara-Fier; squares with diagonal crosses = riebeckite annite granites.

- 
- Figure 33. AFM, iron-enrichment and total alkali variation diagrams for the Niger-Nigeria province.
- Y-Y = range of AFM values for the province. M = mean for the province.
N = trend for the Nandewar alkali-basalt-pantellerite volcano, E Australia.
LCB = calc-alkaline trend shown by the Lower California batholith.
S = Shaergaard trend. (N, LCB and S after Barriere, 1977)
 - & c. Symbols as in Figure 29, except; stars = Q normative basaltic rocks; stars enclosed by diamonds = non-Q normative.
 - Iron enrichment trend for the province (dashed line M, with crosses) compared to other areas where S = Skaergaard, H = Hebridean, T = Thingmuli and the Cascades (after Ridley, 1973).

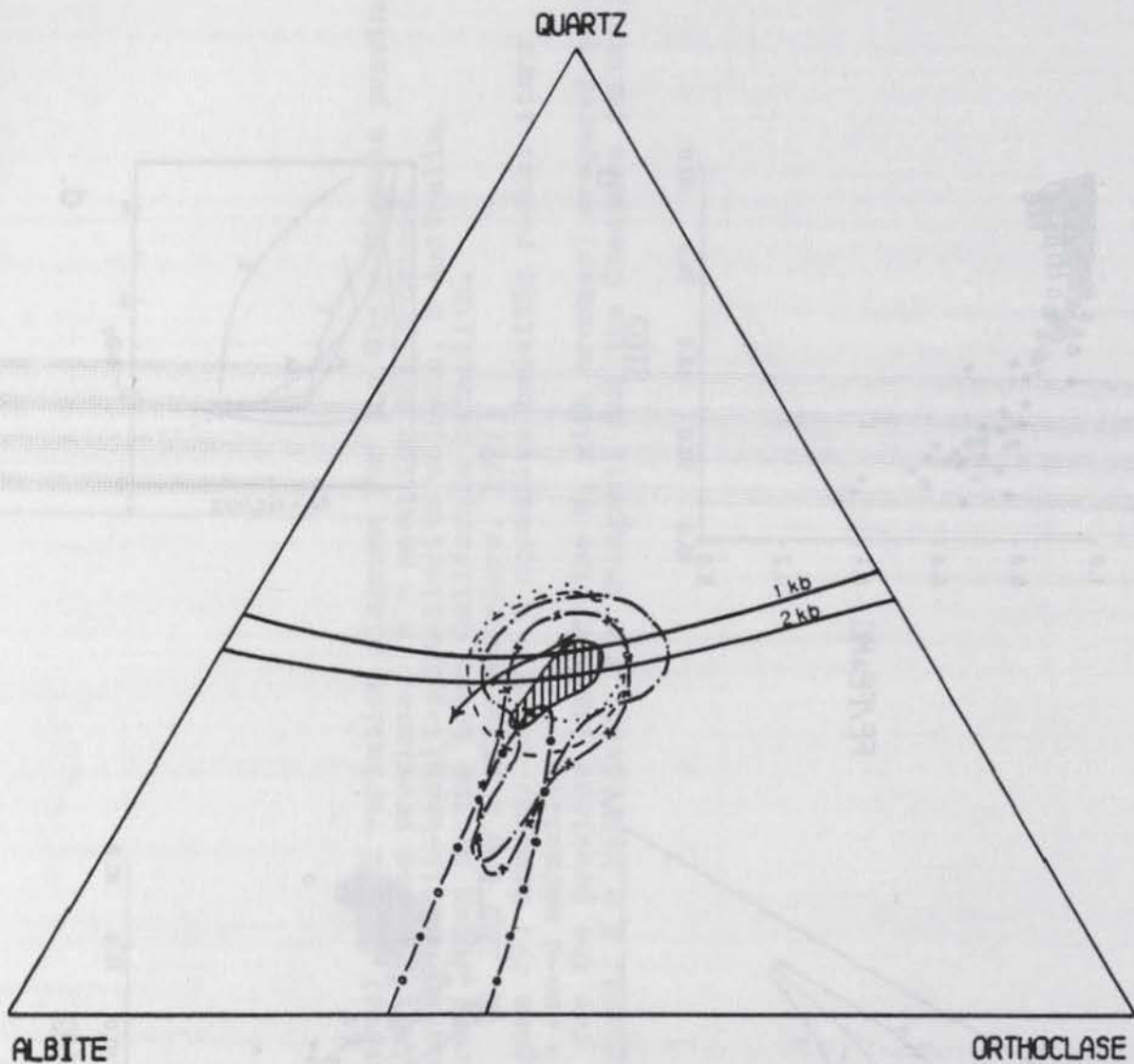


Figure 34.

Summary normative Q-Ab-Or diagram for the Niger-Nigeria province. Vertical shading = average granitic rocks and 1-2 kb lines = positions of cotectic lines from Tuttle and Bowen (1958). Dashed lines with circles = syenitic rocks; dashed lines with crosses = Ca-amphibole granites and porphyries; dotted lines = rhyolitic volcanics; dashed lines with dots = peralkaline granites; short dashed lines = biotite granites.

towards the rhyolitic volcanics and Ca-amphibole granites, but both elements can be highly enriched in the peralkaline and biotite granites.

8. The Zr content of each of the rock types shows a relatively large range. However, it is notable that the syenitic rocks show as great a range as the granitic rocks, with the exception of the peralkaline granites which may have very enhanced Zr values.

9. The Sr content of basaltic rocks shows a wide range but nevertheless there is an almost linear decrease with increasing silica.

10. On a summary AFM diagram (Figure 33a) the range and the mean curves for the province are drawn. The distribution is quite distinct from either the tholeiitic or calc-alkaline trends and in fact, the mean curve lies very close to that for the alkali basalt-pantellerite sequence of the Nandewar volcano in Australia.

11. The iron enrichment (I.E.) trend (Figure 33b) shows a rapid increase in I.E. in the basaltic rocks and then it levels off at a value of around 0.9 or above. This trend is compared to other provinces in Figure 33d.

12. On a SiO₂ v total alkalis diagram (Figure 33c), a postulated silica saturation line falls between those for the Gardar and Hawaii provinces, but there are very few Ne normative rocks in the province and not all basaltic samples which lie above the line are Ne normative.

13. On a summary normative Q-Ab-Or diagram (Figure 34) it is apparent that the syenites, and the Ca-amphibole and peralkaline granites extend along the low temperature feldspar trough but that the biotite granites and volcanic rocks do not. All the granitic and rhyolitic groups, though, cluster around the granite minimum (at 1-2 kb H₂O pressure; Tuttle and Bowen, 1958).

14. The coincidence of compositions of the Ca-amphibole granites and porphyries (particularly Figure 31), and the rhyolitic volcanics (which share many common mineralogical features), implies a closely related

origin.

15. Although there is a comparative scarcity of published information on the distribution of rare earth elements (REE) in the province, they are nevertheless an important trace element group. In particular, it has been convincingly demonstrated that there is a clear distinction between the aluminous biotite granites which may or may not have a (negative) Eu anomaly, and the peralkaline (including riebeckite annite) granites which have generally higher total REE abundances together with a marked negative Eu anomaly (Bowden and Whitley, 1974; Bowden et al., 1979). In the Ningi complex, basalts and a plagioclase-rich syenite (close to the border with monzonite) do not exhibit Eu anomalies, while the granite porphyries and rhyolitic ignimbrites show Eu anomalies but they are not nearly so prominent as in the peralkaline granites (Bennett, unpublished data). Such Eu depletions are usually interpreted as indicating plagioclase fractionation (e.g. Buma et al. 1971; Ewart et al., 1968), particularly if the magma has a low f_{O_2} favouring Eu in the divalent rather than trivalent state.

5.4 Discussion

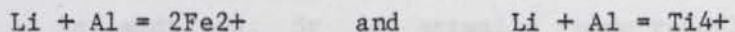
In this section, an attempt will be made to explain the generalised variations in major, minor and trace element variations which occur in the Younger Granite province and to determine whether these explanations are appropriate for the geochemical variation observed in the Shira complex. With regard to the trace element contents of the granitic rocks (notably the biotite and peralkaline granites), several interesting points emerge from their distribution patterns. Lithium may be considered as an example of one of several trace elements that can become enriched in the biotite and peralkaline granites (Figure 31) while Sr is markedly depleted.

By reference to Figure 31 and Table 28 it may be seen that in

the rock series basalt - syenite - Ca-amphibole granite - rhyolitic volcanic, the Li content is low at around 20 ppm or less, while the biotite granites in particular may contain up to 1500 ppm. Lithium is the smallest of the alkali metals with a 6-fold radius of 0.82 Å (considerably smaller than the next alkali metal, Na, with an 8-fold radius of 1.24 Å), and which is very similar to the common octahedral cations such as Fe²⁺ (0.86 Å; Whittaker and Muntus, 1970). Li contents of mafic minerals increase in the order orthopyroxene - clinopyroxene - amphibole - mica (Rankama and Sahama, 1950) while the Li content of quartz and feldspar is negligible (Heier and Taylor, 1959).

From Table 28, the Li content of peralkaline granites can be over 800 ppm. The major mafic mineral phases in these rocks are aegirine and alkali amphibole. Lithium is unlikely to substitute into aegirine however, because on the basis of ionic size it would most probably replace an Fe³⁺ cation (at 0.73 Å), leaving an impossible imbalance of 2 charges. On the other hand, Li fits into the octahedral (M1-3) sites in alkali amphiboles, substituting mainly for Fe²⁺ (Borley, 1963b). Presumably some remaining iron will oxidise to the trivalent state to maintain neutrality.

Similarly, Li is easily accommodated into the mica lattice and in Nigerian trioctahedral micas the substitution schemes:



are believed to operate (Abernethy, in prep.).

Thus, appreciable Li contents of the biotite and peralkaline granites can be readily accommodated in the mica and amphibole lattices respectively. However, the very modest increase in Li from basaltic rocks through to the Ca-amphibole granites and, in some samples, a remarkable increase in Li content for an increase in SiO₂ of only 1-2% demands explanation. Similarly, the Li/Mg ratio rises from 3 to 263 in the basalt - Ca-amphibole granite series but may be over 2000 in the

peralkaline granites. Such an increase (assuming the majority of these rocks represent a comagmatic suite) cannot be explained solely by crystal-liquid fractionation. Rocks with Li contents greater than 100 ppm have been used to indicate that the rock is a late stage, high level differentiate (Taylor, 1965), and high Li (and F) levels in the Nigerian Younger Granites are believed to be the result of late magmatic or postmagmatic processes (Bowden, 1966). Also, since many workers have noticed a connection between high Li content and extensive textural modification and/or pervasive Nb mineralisation in particular (e.g. Macleod et al., 1971; Abernethy, in prep.), the association between enrichment in Li (and other trace elements such as Zn, Rb, Y and selectively, Zr) and deuteric or postmagmatic rock-fluid (1) rather than magmatic crystal-liquid interaction, appears to be valid.

Strontium contents on the other hand, decrease very rapidly from an average of over 400 ppm in the basaltic rocks to less than 100 in the syenitic rocks to generally less than 20 ppm for the granites.

Strontium has an 8-fold coordination radius of 1.33 Å which is close to that of Ca at 1.20 Å (Whittaker and Muntus, 1970) and it is therefore readily accommodated into plagioclase. Since the Sr content of silicates other than feldspars is low (Steuber, 1978), fractionation of plagioclase will deplete the residual liquid in Sr.

In addition, Sr is actually more readily partitioned into plagioclase than Ca (Berlin and Henderson, 1968), although in practice, there appears to be a tendency for maximum Sr concentration to occur in the An₄₀₋₅₅ range (Heier, 1962; Ewart and Taylor, 1969), similar in composition to the Niger anorthosites which contain up to 1000 ppm Sr (Reay, 1976). Strontium is also more easily accommodated into alkali feldspar than Ca (Heier and Taylor, 1969).

(1) In general, a residual 'deuteric' silicate fluid generated within the rock itself is envisaged, rather than extraneous meteoric fluid.

Thus, fractional crystallisation of plagioclase (for which there is ample field evidence in Niger) can explain the rapid decline in Sr with increasing fractionation and the average Sr content of syenites at 92 ppm (Table 28) is higher than the granites because of the presence of plagioclase and/or greater abundance of alkali feldspar. Therefore, if the peralkaline granites, for example, lie at the end of a prolonged fractional crystallisation sequence in which plagioclase has been continuously removed, they will be expected to have very low Sr contents. At this point it is worth noting that the Ca-amphibole and biotite granites frequently contain magmatic plagioclase (Chapter 1) and their Sr contents are correspondingly higher than the peralkaline granites.

Finally, it is perhaps significant that in Figure 31, Sr is the only trace element to show virtually a linear trend against silica, which may be attributable solely to crystal-liquid equilibria whereas the others require a period of deuteric or post-magmatic, rock-fluid interaction to satisfactorily explain the observed enrichments.

The iron enrichment ratio (Figure 33) rapidly increases with increasing silica content. Such a trend has been modelled experimentally by Osborn (1959) who found that a rapidly increasing iron enrichment trend was the result of fractional crystallisation under conditions of decreasing partial pressure of oxygen. This is consistent with fractional crystallisation under buffered oxygen fugacity conditions when f_{O_2} falls with temperature.

The chemistry of the peralkaline rocks (see also Macleod et al., 1971) is very similar to that of pantellerites and comendites (Noble, 1965; Noble and Haffty, 1969; Ewart et al., 1968; Weaver et al., 1972; Ferrara and Treuil, 1974; Villari, 1974). The pantelleritic rocks show enhanced levels of Li, F, Na, Cl, K, Zn, Rb, Y, Zr, Nb, Mo, Sn, Cs, REE, Hf, Th and U, and are strongly depleted in Mg, Ca, Sr, Ba, Eu and

the transition elements. Such characteristics are usually interpreted as the result of protracted fractional crystallisation (e.g. Noble, 1965; Noble et al., 1969; Villari, 1974). The geochemical similarities between pantellerites and the peralkaline rocks from this province probably indicate that they have evolved in a similar way. This likelihood is enhanced by the fact that in several areas including Pantelleria itself, there is a complete gradation between basaltic, aluminous and peralkaline trachytes, and comendites and pantellerites (Gibson, 1974; Barberi et al., 1975; Abbott, 1969; Villari, 1974) as appears to be the case in this province.

Most, if not all, of the alkalis and trace elements mentioned above, have the common characteristic that they are generally partitioned towards the liquid and will therefore concentrate in the residual liquids in a fractional crystallisation scheme (e.g. Dostal and Capedri, 1975) or become concentrated in the apical parts of an intrusion (Tauson, 1967; Volkov et al., 1978). (The latter point is of considerable importance with respect to concentration of Rb and its effect on the Rb/Sr systematics, as discussed in Chapter 6.)

The variation in trace element content of rocks from the same province with similar major element chemistry, may be due not so much to a different source or a different fractionation mechanism, but to the efficiency of that mechanism with respect to the particular history of any single rock. Thus, the degree of enrichment of residual trace elements is dependent upon the effectiveness of removal of the solid phases during fractional crystallisation (McCarthy and Hasty, 1976). The concentration of some of these elements in well fractionated magmas also has certain implications regarding ore deposits (Bonin et al., 1979) and lowering of the solidus (Manning, 1979).

Almost identical trace element distribution patterns to those in this province, may be found in a suite of trachydolerite through to

aegirine microgranite dykes in the Gardar province (Macdonald and Edge, 1970). In these dykes, Li, Rb, Y, Zr, La and Ce all show exponential-type distribution patterns with increasing fractionation, while the K/Rb ratio shows a maximum (as does that from the Niger-Nigeria province) and the Sr and water contents decrease.

The low water content of the peralkaline granites and syenites in the Niger-Nigeria province is of some significance. Experimental work (Bailey et al., 1974; Bailey and Cooper, 1978) has shown that under hydrous conditions, the normal mafic mineral crystallisation sequence of pantellerite liquids is reversed, and aegirine appears on the liquidus in place of arfvedsonitic amphibole. Since the usual sequence is for ferrichterite-arfvedsonite to crystallise as the dominant mafic mineral (although it is commonly partially altered to aegirine), one may conclude that there is good agreement between the experimental and natural observations, and that the Shira magmas for example, were relatively dry. The same evidence may be applicable to the aegirine granites at Kila Warji and Dogo Dutse for example, where large euhedral or subhedral aegirine crystals occur which do not appear to be the result of alteration of a pre-existing amphibole. Perhaps in these few instances, the peralkaline magma was more water-rich than usual.

The aluminous biotite granites (and probably the aluminous Ca-amphibole granites) are geochemically distinct from the basalt-syenite-peralkaline granite trend in the following respects: the peralkalinity index, oxidation ratio, Ca/Sr ratio and Zr content are low, while SiO₂ is high and the Eu depletion is relatively small or non-existent. Other distinctive features of the biotite granites are that they commonly contain mineralised replacement veins and, like many of the Ca-amphibole granites, they often contain appreciable quantities of plagioclase and tend to occur as larger intrusions with shallower contacts than the peralkaline granites and syenites. The mineralogical

differences are obvious from the nomenclature but it is also apparent that in the Niger sub-province peralkaline granites, syenites, anorthosites and gabbros are dominant (Black et al., 1967) whereas these rocks are of minor importance in Nigeria, compared to the aluminous granites. Since the rhyolitic volcanics show virtually identical chemical characteristics to the Ca-amphibole granites, they are regarded as petrographically different aspects of the same magma type, and therefore to be genetically related.

Since a large part of the geochemical variation within the province occurs in basaltic rocks, (gabbros as well as lavas) it is relevant to look at the mineralogy of these rocks. Unfortunately these rocks occur in only minor quantities in Nigeria and have been comparatively neglected. However, in Niger they occur (along with anorthosites) in greater abundance and have recently been the subject of a comparatively detailed study (Husch and Moreau, in prep.). This work (supplemented by the writer's own field experience in Niger) has shown that olivine (Fo₆₅₋₄₅), clinopyroxene (augite) and titanomagnetite (titaniferous magnetite with exsolved ilmenite lamellae) are the major phases while orthopyroxene and pigeonite do not occur. Of these minerals, augite usually subophitically encloses the others. Layering is common in these basic rocks and reaches perhaps its best development in the Ofoud complex where layers or lenses of titanomagnetite occur up to 10 m thick, and which may "contain in places up to 50 modal percent euhedral, apparently cumulative, olivine" (Husch and Moreau, in prep.).

Therefore, there is evidence to suggest that the observed marked decrease in TiO₂, total FeO and MgO may be due to fractional removal of olivine and titanomagnetite in particular. The decrease in CaO is more marked than the early decrease in Al₂O₃ (Figure 30) which suggests that initially, CaO was being removed preferentially by augite and plagioclase removal only became dominant at a slightly later stage.

If fractional crystallisation of these minerals occurs, as indeed the field evidence in Niger would indicate, then the alkalis and silica would be expected to increase in the liquid. It may therefore be significant that Husch and Moreau describe 'monzoanorthosites' at Ofoud and Taguei which have up to 15% of quartz and alkali feldspar and which may represent a transitional stage towards a syenite.

5.5 Conclusions

The major element geochemistry for the province therefore may be explained as being due to olivine and titanomagnetite followed by clinopyroxene and plagioclase fractionation, and finally possibly alkali feldspar fractionation leading towards a peralkaline residuum. The general trend of trace element variation from basaltic to granitic rocks supports this view but in certain peralkaline and biotite granites a period of late or postmagmatic rock-fluid interaction is necessary to explain the enhanced values (and indeed the evidence of textural modifications).

For the Shira complex, there is a close correspondence between the major element chemistry and the average for the respective rock types in the province and the complex may therefore be regarded as representing the latter stages of fractionation from a basaltic magma by the processes outlined. For the trace element geochemistry, the major rock types show a linear increase with increasing silica, from syenitic to granitic samples and there is no evidence for a significant period of enrichment by late or postmagmatic fluids, except in specific examples referred to. The geochemical characteristics of the small, syenitic enclaves found in several rocks are compatible with a cognate origin. The mafic-rich, melanocratic dykes which cut and/or are related to the Birji and Andaburi granites show evidence for being the product of strong alkali feldspar fractionation, and they are regarded as iron-rich

residual liquids resulting from the crystallisation of the bulk of the alkali feldspar in the respective rock types.

CONCLUSIONS

6.1 Introduction

The object of this chapter is to summarise the problems related to the nature and genesis of the anorthositic, tholeiitic igneous provinces that were outlined in Chapter I, and to discuss, in particular, a tectonostratigraphic framework for the three complexes and the province as a whole, by presenting a series of points which should be considered as features of the province as a whole:

1. The persistence of igneous activity from Eocene to Cretaceous.
 2. The generally unconfined, overlapping, and yet a distinct grouping of ring complexes into three zones.
 3. The frequent similarity in size of complexes, centres of separate intrusions.
 4. The frequent migration of centres within one complex and repetition of rock types or intrusive sequences.
 5. The coexistence of basic, intermediate and peralkaline rocks together with anorthositic and related layered rocks in Niger while alkaline rocks are absent in Nigeria.
 6. The range of initial or isochronous values encompassed within a single ring complex.
 7. The geochemically highly fractionated nature of the granitic rocks.
 8. The relationship between texture, mineralogy, and trace element content.
 9. $^{87}\text{Sr}/^{86}\text{Sr}$ -vein mineralization associated with some biotite granites.
- Some of these features, for example the repetition of rock types from centre to centre within a single ring complex, probably reflect the

CHAPTER 6

PETROGENESIS6.1 Introduction

The object of this chapter is to examine the problems related to the nature and genesis of the anorogenic, Niger-Nigeria igneous province that were outlined in Chapter 1, and consequently, to establish a petrogenetic framework for the Shira complex and the province as a whole. Any petrogenetic theory must account for certain fundamental features of the province such as:

1. The persistence of igneous activity from L.Ordovician to U.Cretaceous.
2. The generally southward decreasing age trend and yet a regional grouping of ring complexes into three areas.
3. The frequent similarity in size of complexes, centres or separate intrusions.
4. The frequent migration of centres within one complex and repetition of rock types or intrusive sequences.
5. The dominance of basic, intermediate and peralkaline rocks together with anorthosites and related layered rocks in Niger while aluminous rocks are dominant in Nigeria.
6. The range of initial Sr isotopic ratios encountered within a single ring complex.
7. The geochemically highly fractionated nature of the granitic rocks.
8. The relationship between texture, mineralogy and trace element content.
9. Zn/Sn/W vein mineralisation associated with some biotite granites.

Some of these features, for example the repetition of rock types from centre to centre within a single ring complex, probably reflect the

similar development and evolution of individual magma chambers beneath each centre (Turner, 1963) and do not have a direct bearing on the genesis of the magma(s). Similarly, the nature of various structural features such as ring faulting, cauldron subsidence and the preservation of volcanic rocks are not germane to petrogenesis.

However, a few features of the province as a whole and of peralkaline and aluminous granites in particular, are of crucial importance to a petrogenetic theory and will therefore be discussed below.

6.2 Geochronology and possible mantle plumes

Until comparatively recently, the Younger Granites of Nigeria (and Niger) were presumed to be of Precambrian age (Jacobson et al., 1958), but with the advent of radiometric age dating, a much younger age of 159(+/-25) my was obtained on accessory fergusonite from Ca-amphibole granites (Darnley et al., 1962). Subsequent work using a variety of samples and techniques confirmed this Jurassic age for the central Nigerian complexes (Jacobson et al., 1963; Grant, 1971) although common lead ages from galena mineralisation associated with some Younger Granites gave older, Panafrican ages (Jacobson et al., 1963; Tugarinov et al., 1968). Preliminary K-Ar ages on some Niger complexes were also older, at around 295 my (Schetcheglov et al., 1965 - quoted in Black and Girod, 1970), and around 460 my for the Elmeki biotite granite (Brunnschweiler, 1974).

More detailed Rb/Sr age determinations showed that there was a southerly decreasing age trend from 170 to 151 my (1) (van Breemen and Bowden, 1973) within central Nigeria, while the province as a whole had a N-S age variation from 420 my to 141 my (Bowden et al., 1976a). The

(1) All Rb/Sr ages are recalculated to a (^{87}Rb) decay constant of 1.42×10^{-11} my, after Steiger and Jager (1977)

age range has recently been shown to extend as far back as the Ordovician (487 my; Karche and Vachette, 1976, 1978) and it is now generally accepted that the mixed whole rock-mineral isochron of Bowden et al. (1976a) which gave an age of 420 my for the Adrar Bous complex, may indicate a slightly younger event. Furthermore, extrapolation of the age trend for the Nigerian complexes, southwards towards the coast, gives an 'age' of about 90 my which is close to estimates for the age of opening of the S. Atlantic (Wright, 1968; Larson and Ladd, 1973; Offodile, 1976). Similarly, the Cabo Santo Agostinho granite on the coast of Brazil has been dated at about 90 my (de Almeida et al., 1967).

The southerly decreasing age trend and generalised N-S alignment of ring complexes has been interpreted (van Breemen and Bowden, 1973) as a record of magmatism as a result of the progressive northward shift of the African plate over a stationary mantle plume (see Wilson, 1965, 1973; Morgan, 1971; Rhodes, 1971). However, there are problems with this hypothesis, since extrapolation of the rate of apparent plate movement, based on the age trend in central Nigeria, gives an apparent age for the N. Niger complexes which is far too young. Therefore, it has been suggested (Bowden et al., 1976) that the three geographical regions of Younger Granite magmatism (N and S Niger, Nigeria) reflect periods of relatively slow plate movement which correspond to the quasistatic intervals suggested by Briden (1967).

In fact, these three regions correspond at the present day, to topographically high areas which are separated by sedimentary basins (see Unesco 1:10 m maps of Africa, 1968). These basins contain Permo-Triassic, Carboniferous and Devonian sediments which are absent in the three regions mentioned, and yet Cretaceous sediments at one time covered the ring complexes (Black et al., 1967). Thus, there is some evidence to indicate that the areas with anorogenic magmatism were topographically emerged at the time of their activity, as well as the

present day, which is significant because of the association between peralkaline volcanism (at least) and crustal swelling (Le Bas, 1971).

A further problem with the ring complexes being a plume scar trace is that the apparent rate of movement by the African plate (0.43 cm/yr) is less than that indicated by palaeomagnetism (2 cm/yr). If the palaeomagnetic data quoted by Karche and Vachette (1976) is accepted as accurate, then a likely explanation for the discrepancy in the apparent and real rates of plate motion could be due to the slow movement of the hot spot or plume in the same direction as the plate (Karche and Vachette, 1978). This appears to be quite feasible as hot spots are believed to be mobile with respect to one another (Molnar and Atwater, 1973) although in certain cases this may diminish their value as a frame of reference for plate movement.

The separate geographical/temporal groupings of ring complexes in Niger correspond in time to similar anorogenic magmatism in the N.Appalachians (Taylor, 1979) and also to the Caledonian and Hercynian orogenies and to Briden's quasistatic intervals for Africa. These points suggest that when orogeny was in progress at plate margins, magmatic activity proceeded (on a comparatively small scale) in the central parts. Therefore, the term 'anorogenic' is used to mean unrelated spatially to an orogeny but not in time (Karche and Vachette, 1978).

The association of magmatic activity and restricted plate motion appears to be strong in Africa. Briden and Gass (1974) consider that a sublithospheric heat source "can only produce recognisable effects in the upper crust if focused for long periods on the same part of the lithosphere". Similarly, Wilson and Burke (1975) suggest that quiescent periods of African plate movement correspond to igneous activity, topographically high features and ultimately the breakup of Gondwana. This aspect is taken further by Bonin (1974) who suggests that the ring complex provinces around the Atlantic, namely the White

Mountains, British Tertiary, Corsica and Niger-Nigeria, are all related to a tensional environment caused by attempted or actual continental disruption. Apparently, there is also a good correlation between the peak of igneous activity and continental disruption (Scrutton, 1973).

Moreover, since the extrapolated Nigerian age trend seems to correspond with the age of opening of the S. Atlantic, there could be a connection between mantle plumes, anorogenic magmatism and plate rifting and/or separation. This view is supported by Emslie (1978) who considers the late Precambrian Elsonian magmatism was a precursor to a sequence of events which led to incipient continental rifting. Similarly, Philpotts (1978) identifies rift-like systems in the eastern U.S.A. whose origins are traceable into the Precambrian (although the dominant features are of Triassic-Cretaceous age), and which had associated episodic igneous activity. Also, Philpotts accounts for the SE decreasing age trend of the White Mountain Magma Series as due to the plate moving over a hot spot, while the older St. Lawrence rift valley rocks include gabbro, anorthosite and alkaline granites - analogous to Niger. Indeed, composite plutonic ring complexes may be characteristic of rift-zone plutonism since Peterson (1978) finds that "they occur in distinct structural belts, which, according to global tectonic models, define major continental rupture lineaments associated with former triple junctions. Their origin therefore seems to be related to processes of crustal rifting". Obviously, the rifts and associated magmatism that are preserved have to be, by their nature, "failed rifts" (Burke, 1978), but it may be significant that the youngest anorogenic complex in the province (Afu) lies closest to the Benue trough which is believed to be a 'failed' rift valley (Cratchley and Jones, 1965; Burke, 1978) which extends up into Chad and has an 800 km long positive gravity anomaly (Cratchley and Louis, 1975). Perhaps the reason for the failure of the Benue trough to become a rift valley may be found in the very thick

lithosphere in central/northern Nigeria and Niger (Fairhead and Reeves, 1977).

The geochronological data indicate that magmatism in the Niger-Nigeria province has been periodically active for a long period, from at least the L.Ordovician to U.Jurassic. In fact, if the alkaline magmatism in the Hoggar region of Algeria is related (Boissonas et al., 1969), then the activity can be extended as far back as the Cambrian - at 560 my. If the magmatism is related to sub-lithospheric plumes, hot spots or thermal anomalies, then obviously the life span of such features has to be at least as great. If a mantle plume is accepted as responsible for the generation of heat necessary for the initiation of anorogenic magmatism seen in this province, then there is evidence for its continuing existence in the guise of the 'granites ultimes' of Cameroun and the chain of volcanic islands extending seawards from Fernando Po (Gazel et al., 1963; Lasserre, 1966; Dunlop and Fitton, 1979). Since the central Cameroun complexes have been dated at around 58 my (Gazel et al., 1963) while the oldest lavas on Principe are about 30 my old (Dunlop and Fitton, 1979) the possibility of an analogous age trend exists. A further implication of possible mantle plumes beneath this province is that, as Sillitoe (1974) suggests, the mantle has contributed Sn and other elements which later find expression in mineralisation associated with the biotite granites.

An alternative explanation for the age trend is that of a propagating fracture which could also be linked to tensional stresses ultimately leading to continental fracture (Turcotte and Oxburgh, 1973). Although the tectonic fabric of the upper crustal rocks may play a part in controlling the alignment of individual centres within a ring complex, the concept of membrane tectonics has not apparently found much favour among students of the Niger-Nigeria province.

The association between continental magmatism and oceanic

geologic events may also be viewed in the context of the relationship between transform faults and chains of ring complexes (Marsh, 1973) or of transform faults and continental faults (Blundell, 1976). Geochronological data therefore provides very strong clues to the possible, indeed likely, connection between events in the mantle which may ultimately be associated with continental break-up and the genesis of anorogenic ring complexes.

6.3 Radiogenic and stable isotopes

Although Rb/Sr and Pb isotopic data for the Nigerian sub-province has been available for over a decade, there is as yet no coherent petrogenetic model based upon this particularly crucial evidence either alone, or with other geochemical evidence. For example, Tugarinov et al. (1968) found that the isotopic composition of lead from the basement, Younger Granites and mineralised localities was identical and consequently supposed the Younger Granites were derived by partial melting from the basement. Such data must however, be regarded with caution as there is approximately a 50:1 ratio for average lead contents in the upper crust and mantle respectively, which means that a mantle-derived magma would need only a very small amount of upper crustal contamination to achieve a highly modified Pb isotopic ratio (Doe and Zartman, 1979). The situation with Rb/Sr isotopic data is also inconclusive and a variety of different sources have been proposed.

Bowden and van Breemen (1972) suggested that both peralkaline and peraluminous rocks had a common, upper crustal source; the initial liquid was peralkaline whereas more extensive melting yielded the aluminous rocks. Subsequent data (determined in 1973) showed that the Younger Granites had a range of initial ratios (I.R.'s) and no satisfactory source could be defined (Bowden et al., 1976b). In a review of the province, Bowden and Turner (1974) regarded the aluminous

granites as being derived by partial melting of the lower crust whereas the syenites and peralkaline granites (they are commonly associated) were derived from melting of the upper crust. In a deeper consideration of the matter, van Breemen et al. (1975) concluded that the coarse grained biotite granites with low I.R.'s were either partial melts of the lower (dioritic) crust, or modifications of mantle derived syenitic liquids. For the syenites (with low I.R.'s) and the associated peralkaline granites (with high I.R.'s), they postulated increasing degrees of crustal contamination of mantle derived syenitic liquids.

No further work on the initial isotopic ratios of this province has been completed and from this brief summary, it would seem that no viable petrogenetic scheme has been devised. Nevertheless, it is possible that some order can still be achieved.

In many regions there is a variation of I.R. with rock chemistry in a related series of rocks; for example, trachytes from Ascension, Gough and Hawaii have higher I.R.'s than basalts (e.g. Gast et al., 1964; Lessing and Catanzaro, 1964), whereas in Corsica and Marangudzi (Zimbabwe), rock chemistry appears to be unrelated to the age or I.R. within the suite (Foland and Henderson, 1976; Bonin et al., 1978). Where there is a variation of I.R. with rock chemistry, it may occur within a single magma chamber, where the upper portions are more radiogenically enriched (Noble and Hedge, 1969; Dickinson and Gibson, 1972). The variation in composition and I.R. with height in a high level magma chamber may imply that the I.R. is in some way linked to fractionation within the chamber rather than selective contamination.

Ferrara and Treuil (1974) derived a model for achieving peralkaline acid rocks with more radiogenic Sr than cogenetic basic and intermediate rocks, by the production of variable Rb/Sr ratios in different portions of a magma chamber, when that magma had a long history. Hence, with time, different portions of the magma could achieve

different initial ratios but have the same age within experimental error. Similarly, in the Gardar province, Blaxland et al. (1978) found that in 9 complexes studied, the I.R.'s fall into three groups: a) the gabbros and syenite, 0.702-0.704 indicative of a primitive mantle origin, b) a few centres with a range from 0.704-0.707 which they attribute to the action of closed system enrichment of radiogenic Sr during a long crystallisation history, and c) two mineralised complexes with ratios up to 0.712. This study is important because many workers (e.g. Upton and Thomas, 1980) have shown that there is an evolutionary trend from gabbroic to granitic compositions within the Gardar province, and so the variations in I.R. are unlikely to reflect different source materials. In the mineralised Ivigtut granite, Blaxland (1976) has further shown that the bulk of the rock has a lower I.R. (0.705-0.710 or less) than the interstitial cryolite (approx. 0.720). Although Blaxland favours this enrichment in radiogenic Sr as resulting from basement interaction via a hydrothermal fluid, since there is no field evidence for fluid interaction between the peralkaline granites (at least) and the basement in Nigeria, an alternative proposal is that the magma itself can generate high initial ratios.

Vidal et al. (1979) propose that if a magma with a high Rb /Sr ratio remains liquid for a relatively long time, the I.R. "of a liquid with a Rb/Sr ratio of 500 grows from 0.705 to 0.750 in about only 2 my". Obviously, with an Rb/Sr ratio of up to 1200 in some of the Nigerian rocks, the time interval required to alter the I.R. significantly will be correspondingly reduced. This process, Vidal et al. suggest, has been much underestimated in Sr isotope geochemistry, but has recently been discussed in detail by McCarthy and Cawthorn (1980). Their thesis is essentially the same as Vidal et al. (op.cit.), that the Rb/Sr ratios of magmas increase significantly during fractional crystallisation, so the rate of change of I.R. in successive liquids increases as

crystallisation proceeds.

Within the Ririwai complex, Nigeria, I.R.'s for discrete rock types range from 0.708 for a fayalite granite porphyry to 0.729 for a mineralised biotite granite and 0.752 for an albite arfvedsonite granite (van Breemen et al., 1975). In a review of strontium isotope geology, Faure and Powell (1972) do not cite such high I.R.'s, and their field for peralkaline rocks ranges only up to an I.R. of 0.708; however, they regarded relatively high I.R.'s in granites as representing sialic melts.

Therefore the initial ratios in the Niger-Nigeria province show a very wide range of values. Whereas low (perhaps <0.706) I.R.'s indicate a mantle source, the high ratios up to 0.752 do not necessarily indicate a crustal source or even crustal contamination (for which there is no field or petrographic evidence). Therefore, high I.R.'s in the peralkaline granites are probably indicative of a long fractional crystallisation history from a similar source as those rocks with a low I.R.

So far, there has been little research work on the stable isotopic composition of rocks and minerals from this province. However, one study (Borley et al., 1976) is particularly important in that it concerns the Ririwai albite arfvedsonite granite for which an origin by interaction between the granite and an albitising fluid has often been proposed. Borley et al. (op.cit.) found that despite the petrographic and chemical heterogeneity displayed by the granite, it had a normal oxygen isotopic composition. Therefore, the evidence suggests that the albitizing fluid had an isotopic composition identical to that of the host granite. If a significant meteoric/hydrothermal circulatory system had been created, a depletion in $O(18)$ would be expected (e.g. Taylor, 1977).

Oxygen and hydrogen isotopic data determined by S.M.F. Sheppard

(Bowden, 1976, Fig.5) show that non-mineralised Nigerian granites have 'normal' isotopic ratios whereas the greisens are depleted in deuterium and slightly depleted in $O(18)$. Thus, the fluid involved in the albitization of peralkaline granites at least, is unlikely to have an extraneous source - rather it is deuteritic in the sense of being derived from within the granite body itself. By contrast, it would appear that the fluids associated with greisen vein formation (Zn/Sn/W mineralisation) may have an extraneous water component. These hypotheses ideally fit the field evidence; neither the albite arfvedsonite or albite zinnwaldite granites (Jacobson and Macleod, 1977; Abernethy in prep.) show signs of more than a minor amount of metasomatic activity in the surrounding rocks, whilst the greisen veins may be found both in biotite granites and in the basement, and in one prominent case (Ririwai) there is evidence of considerable metasomatic alteration of the host biotite granite.

The high strontium initial ratios are probably not indicative of significant crustal interaction or anatexis but may result solely from prolonged fractionation and magmatic-deuteric effects.

6.4 Paucity of intermediate and basic rocks

It has often been stated that a crustal anatexic origin for the Younger Granites has been favoured primarily because of the dominance of granitic and in particular, aluminous rocks. Whilst this may be true for central Nigeria where most of the research has so far been carried out, aluminous granites are not so abundant in northern Nigeria (author's own work), S.Niger (Black, 1963), or in the Air mountains (Black et al., 1967), where peralkaline granites, syenites and basic rocks are increasingly abundant. Nevertheless, it is probably still true to say that the abundance of intermediate, and perhaps basic rocks too, is not particularly high in the province overall. This is a

familiar problem in other areas where a 'Daly gap' exists.

The relative paucity of intermediate rocks (53-58% SiO₂) among oceanic islands has been highlighted by Chayes (1963), whose work subsequently attracted much adverse comment (Harris, 1963; Macdonald, 1963; Bryan, 1964). The major criticism was directed toward the assumption that the statistical analysis of Chayes rests on a systematic sampling approach and thus is representative of the relative areas of oceanic island lavas. Bryan (1964) also points out that where a Daly gap does exist, its explanation "may be sought as much in the mechanism of eruption as in crystal-melt equilibriums".

Jones (1979a) suggests that the scarcity of benmoreite lavas in a sequence from basalt to trachyte in Kenya, is due to difficulty of eruption because viscosity reached a maximum, while the small volume of basic magma reaching the surface of Pantelleria may simply be a function of greater density (Korringa and Noble, 1972). This suggestion receives support from Sparks et al. (1977) and also Hildreth (1979).

Whereas modal analyses from Pantelleria strongly suggested a bimodality (Rittman, 1967), recent geochemical analyses have shown that intermediate members are present (Villari, 1974). The evolutionary stage which a volcano has reached may also be significant. Among the early lavas of Jebel Khariz (S.Arabia), for example, a classic bimodality exists, but the youngest lavas consist dominantly of trachytes (Gass and Mallick, 1968).

A different approach is taken by Baker (1968), Baker et al. (1978) and Clague (1978) who point out that the existence of a Daly gap assumes that there is a steady increase in SiO₂ with degree of differentiation. In a plot with these parameters, they find a sharp rise in the 50-60 % SiO₂ range which, for the rocks concerned, would account for the paucity of intermediate members. Similarly, Wood (1978) regards intermediate differentiates in Iceland as only forming in a narrow

crystallisation interval. On a chemical basis, Martin and Piwinski (1972) and Martin and Bonin (1976) find that anorogenic suites are bimodal, which Martin (1974b) explained by the direct genesis of a silicic extract from a basaltic or peridotitic source by reaction with water. These results may not have relevance in nature however, and in any case the bimodality hypothesis suffers from the same shortcomings as were levelled against Chayes (1963). Also, the concept is in direct conflict with the continuum of geochemical data presented here.

The British Tertiary Province is perhaps the classic area for contemporaneous acid and basic rocks with a distinct scarcity of intermediate rocks. Early isotopic data indicated a significant crustal component in the felsic rocks and so the bimodality was conveniently explained by melting of country rocks (Moorbath and Bell, 1965; Moorbath and Welke, 1969). However, stable isotopic studies indicated that these igneous rocks had undergone large-scale interaction with meteoric-hydrothermal fluid which had altered their stable isotope ratios and possibly their radiogenic isotopic ratios as well (Taylor and Forester, 1971; Forester and Taylor, 1976). Therefore the apparently sound (radiogenic) isotopic arguments for a crustal origin for the felsic rocks came into question although some form of crustal contamination was confirmed. Added to this, recent trace element studies indicate that the local country rocks are unsuitable source rocks and fractional crystallisation from a basic parent is a distinct possibility (Thorpe et al., 1977; Thorpe, 1978; Meighan, 1976, 1979, 1980). So, the conclusions to be drawn in the British Tertiary province are that even where intermediate rocks are scarce, a fractional crystallisation origin of the acid rocks is still a possibility.

Thus, the present writer agrees with Weaver et al. (1972) who suggested, on the basis of trace element similarities between basaltic, trachytic and pantelleritic lavas, that the relative volumes of rock

types (from one volcano or province) has little bearing on the petrogenetic glassy residua from an alkali olivine basalt, processes concerned. Similarly, on the basis of the alkali trachytic Wilkinson (1966) states that "salic liquids can be produced by fractional crystallisation of basic liquids and that the production of these differentiates need not be accompanied by significant quantities of differentiates with intermediate compositions", since there can be a strong contrast in composition between residual glass and the host rock.

6.5 Peralkaline granites

Peralkaline granites or volcanic equivalents such as comendites and pantellerites are found in both oceanic and continental environments, and are often associated with intermediate and basic rocks. It is proposed to examine some of these areas with a view to establishing features which they may have in common with the Niger-Nigeria province.

In many areas of the world, there is a progression from basaltic to syenitic rocks only, whereas in other areas there is a progression of rock types through to peralkaline rhyolites. Among the former group may be mentioned Iceland (Walker, 1965; Wood, 1978), Gough island (Le Maitre, 1962; Zielinski and Frey, 1970) and Tristan da Cunha (Baker et al., 1964). A fractional crystallisation model has been invoked for each of these areas, whether the evolutionary trend be akin to the alkali basalt-hawaiite-mugearite-benmoreite-trachyte trend envisaged by Coombs and Wilkinson (1969), or similar to the tholeiitic basalt-rhyolite sequence found in Iceland. Moreover, as mentioned above, the glassy residua from an alkali olivine basalt and nepheline basanite in New South Wales, has been shown to have an alkali trachytic or phonolitic composition respectively (Wilkinson, 1966), showing that fractional crystallisation is readily possible. Further evidence comes

from pegmatoid zones in basalt which may have a peralkaline nature and contain aenigmatite (Lindsley et al., 1971) or arfvedsonite (Henley, 1978), or have granophyric interstices (Sinton and Byerly, 1980). Trachyte flows show similar features (Abbott, 1967; Ferguson, 1978b; Velde, 1978).

Volcanic rocks of the hawaiite-comendite kindred are also found on the continents, for example E.Australia, where plate migration over a hot-spot is the mechanism proposed to account for a 750 km line of volcanoes (Middlemost, 1980).

A number of oceanic volcanic islands contain sparse peralkaline trachytes or rhyolites which have associated basic and intermediate lavas, for example Easter, Pitcairn, Socorro, Ascension, Bouvet, Canaries and Kerguelen (Baker, 1974). In both oceanic and continental peralkaline volcanoes it is possible to find ejected coarse grained blocks of syenite or granite, which suggest a close analogy to subvolcanic ring complexes (Cann, 1965; Jones, 1979b; Black et al., 1972). On Pantelleria itself and on the continents, peralkaline volcanoes are found in rift environments (e.g. Villari, 1974; Gibson, 1972).

In some cases there is evidence for zoned magma chambers with pantellerite at the top changing to trachyte at the base (Gibson, 1970) but in most cases the consensus view is that the peralkaline rocks are fractional crystallisation derivatives of a basalt, probably a mildly alkaline transitional basalt (Weaver et al., 1972; Barker et al., 1975; Bizouard et al., 1980). At Pantelleria, strontium isotopic evidence rules out the possibility that the peralkaline silicic liquids were derived from older sialic crust (Korringa and Noble, 1972), and it is interesting to note that comparatively young peralkaline lavas do not appear to have had a prolonged liquid life which might have increased their initial ratios.

Similarly, among older sub-volcanic complexes, peralkaline granites and less fractionated rocks are commonly assigned to a fractional crystallisation scheme from a basic parent, often in a defined rift-related zone, for example, in the Kola peninsula (Batieva and Bel'kov, 1972), Sudan (Curtis and McCormac, 1980), the Gardar province of S.W.Greenland (e.g. Upton and Thomas, 1980) and New England (Buma et al., 1971). In some cases such complexes may be associated with denser rocks at depth, e.g. New England (W.B.Joyner, quoted in Buma et al., 1971), Gardar (Blundell, 1978) and Oslo (Heier and Compston, 1969; Ramberg, 1976). In the Nigerian sub-province the coverage for gravity data is mainly from the Jos Plateau region which is dominated by aluminous granites but it is significant that the region with the smallest negative gravity anomaly lies close to the Kila-Warji and Shira complexes (Ajakaiye, 1970) which contain the greatest concentration of syenitic and peralkaline rocks in Nigeria (Turner, 1968; this work).

The probability of closed system fractionation from a basaltic melt is disputed by Bailey (1970, 1974, 1978), who suggests that ingress of volatiles at the source region would aid partial melting and the development of a peralkaline trend. Support for his model comes from evidence of metasomatism in the upper mantle by fluids rich in Ti, K, Fe and H₂O particularly, which may be a necessary precursor to the genesis of alkali basalts (Boettcher et al., 1979). Such fluid concentration to provide metasomatism and partial melting could, according to Boettcher et al., be due to the action of thermal plumes in the mantle.

Peralkaline granites are occasionally mineralised and undersaturated varieties have been explored for their uranium potential (Sorensen, 1970). In Nigeria the Ririwai albite arfvedsonite granite is the most richly mineralised peralkaline granite and contains dispersed U and Th in the form of pyrochlore, cryolite and minor zircon, monazite and thorite (Beer, 1952; Mackay and Beer, 1952). In the Kigom complex,

an arfvedsonite granite contains dispersed molybdenite mineralisation (Buchanan et al., 1971), and minor quantities of chevkinite are recorded (this study) from the peralkaline quartz syenite at Shira. Significantly, pyrochlore, chevkinite and molybdenite may be found in the oceanic environment (Cann, 1965; Giret, 1980) and hence leaching from the continental crust for example, is not a necessary source for Mo, REE, Th and U enrichment or mineralisation. It is also relevant to note that in Kerguelen, as in Nigeria and the Gardar province (Macdonald, 1969), there are two types of syenite - aluminous and peralkaline (Vidal et al., 1979) and continental crust therefore does not appear to be necessary for the production of either.

For the genesis of peralkaline liquids, paying due regard to the possible reasons for the absence or paucity of intermediate rocks mentioned earlier, most authorities regard a model of fractional crystallisation from a basaltic parent as most likely. Indeed "the large-scale involvement of normal sialic crust in the generation of peralkaline sialic rocks seems to be unnecessary on the following grounds: (i) Sr isotope ratios and the characteristic pattern of trace elements in these rocks, and (ii) the formation of peralkaline rocks in truly oceanic settings" (Macdonald et al., 1974). In particular, "the similarity of alkaline volcanic suites and of their silic differentiates in continental and oceanic environments suggests that both are results of similar petrogenetic processes" (Baker et al., 1978). These authors estimate that 97-98% crystallisation of a basalt is required to produce trachytic or peralkaline silicic liquids, and that input of extraneous volatiles is not necessary to the genesis of peralkaline rocks.

In the Gardar province, dyke rocks form an almost continuous series from trachydolerite through hastingsite and 'riebeckite' bearing microsyenites to peralkaline granites (Macdonald, 1969). Experimental evidence suggests that a peralkaline granite composition can be derived

from partial melting of oversaturated syenite (which itself could be part of an evolutionary scheme) or progressive melting of alkali basalt (Bailey and Schairer, 1966).

Similarly, for undersaturated lavas in Kenya, "the peralkaline nature of the magmas would seem to rule out generation by fusion or major assimilation of normal, relatively alumina-rich, crustal material" (Nash et al., 1969).

For the peralkaline silicic volcanic rocks of western U.S.A., Noble (1965) and Noble and Parker (1974) find that the initial Sr ratios are virtually the same as associated basalts, and they regard them as originating by fractionation from a basalt which itself was a partial melt from the mantle by the action of a localised thermal plume. By contrast, aluminous ash flow tuffs in California are ascribed an origin by crustal melting, with basalt acting only as a heat source (Hildreth, 1979).

Although peralkaline rocks are generally considered typical of stable crustal areas, there may be a surprisingly small time gap between orogenic activity and the onset of peralkaline volcanism (Branch, 1966; Kempe, 1973; Smith et al., 1977) and Noble (1970b) has stressed the common association of peralkaline and subalkaline (aluminous) silicic rocks in anorogenic terrain such as Niger-Nigeria, Oslo, White Mountains and the western U.S.A. Since peralkaline rocks are characteristically related to tensional crustal environments, the occurrence of peralkaline rhyolites in an andesitic arc has been interpreted as representing a fundamental change in the tectonic environment (Smith et al., 1977).

It is apparent therefore, that in the major areas of peralkaline volcanism or plutonism a genetic scheme independent of the crust is favoured.

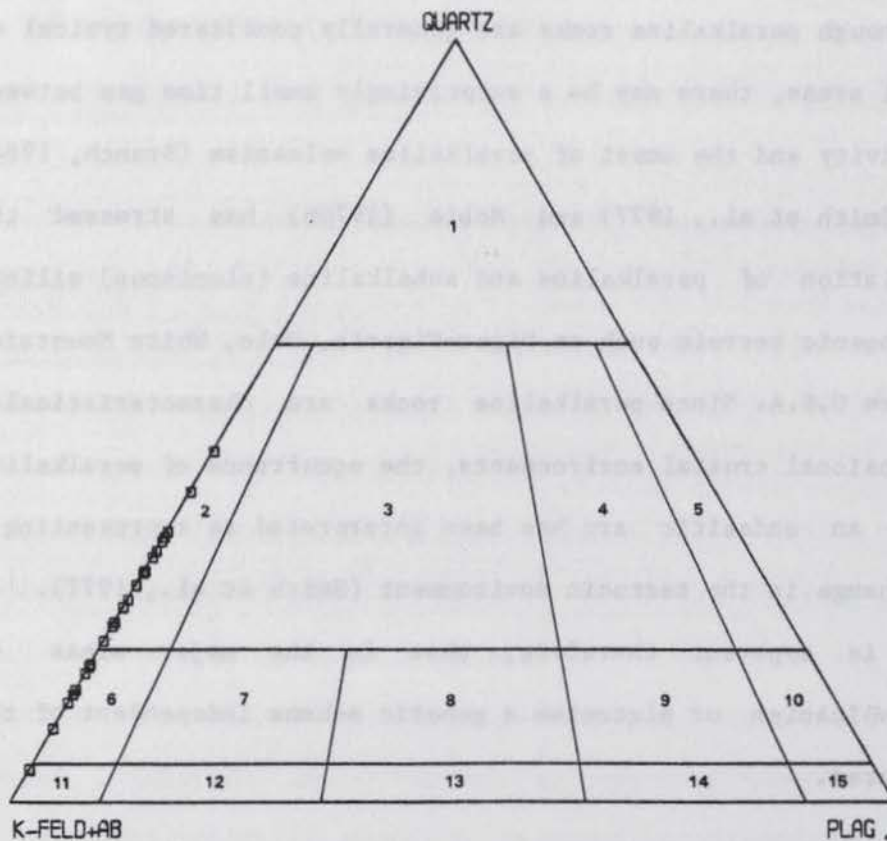
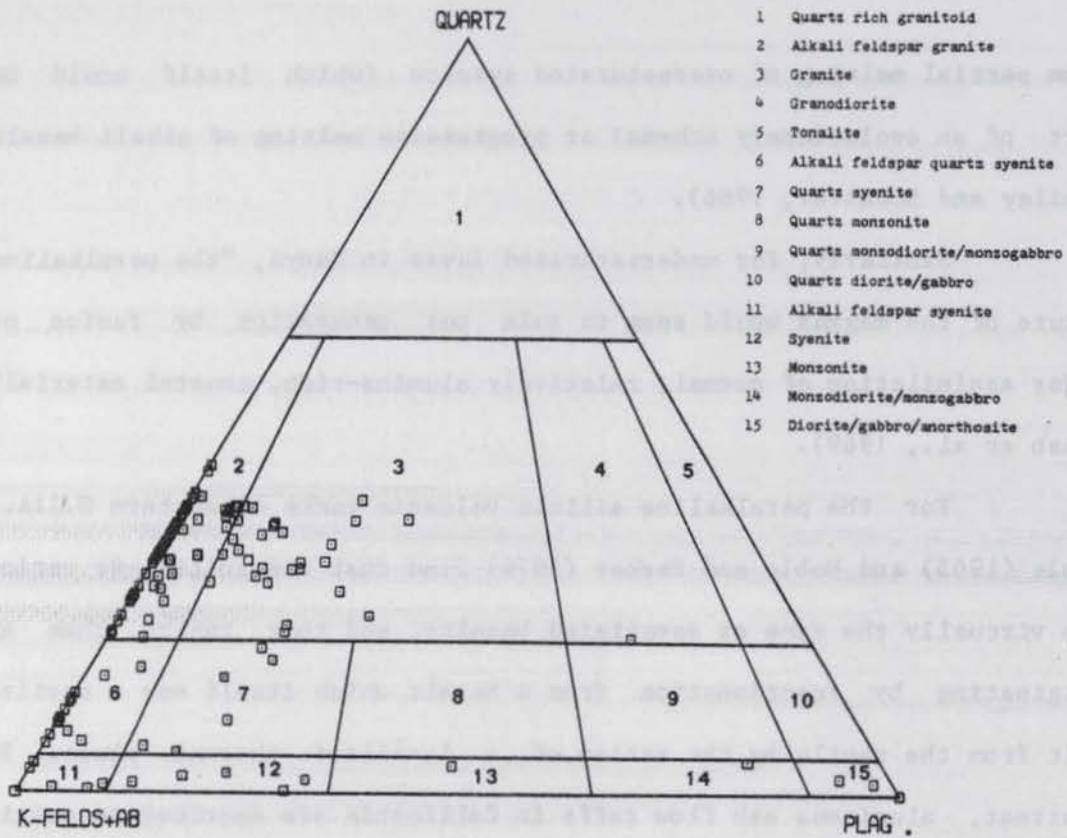


Figure 35.

I.U.G.S. classification diagrams for modal analyses from
 a) the Niger-Nigeria province and b) the Shira complex.

6.6 Aluminous rocks and mineralisation

As is common in several anorogenic provinces (Noble, 1970b) the peralkaline rocks of the Niger-Nigeria complex are closely associated with aluminous granites, porphyries and volcanic rocks. However, whereas an origin for the peralkaline rocks via fractional crystallisation from a basaltic parent is most likely and is supported by the trend of modal analyses in Figure 35a (see also Figure 36), an origin for the aluminous rocks by crustal melting is a more likely origin.

One of the strongest pieces of evidence for this hypothesis is the absence of aluminous granitic rocks on the oceanic islands mentioned previously, and the absence also of the Zn/Sn/W vein mineralisation. The presence of plagioclase too is a highly distinctive feature of many of the Ca-amphibole and biotite granites in this province, and it is this that gives the group as a whole a distinctive position on the modal diagram of Figure 35a. This position corresponds to the leucogranites of Lameyre (1980).

The aluminous Pliny Range complex of the White Mountain Magma Series (WMMS) includes syenites, diorite, quartz monzodiorite, hastingsite biotite granite and biotite granite. From whole rock and mafic mineral $Fe/(Fe+Mg)$ ratios, the amphibole chemistry and the Mn content of ilmenites, Czamanske et al. (1977) concluded that these rocks could not have originated by continuous differentiation from a single parent magma. Instead, the complex chemical data could best be explained by different levels of fusion of crustal rocks. Rocks from the Pliny Range all bear plagioclase, hastingsite and biotite in varying proportions, and sometimes a little pyroxene, and they appear to be petrographically similar to the Nigerian Ca-amphibole and biotite granites.

In the Holterkollen complex of the Oslo Permian rift valley, a

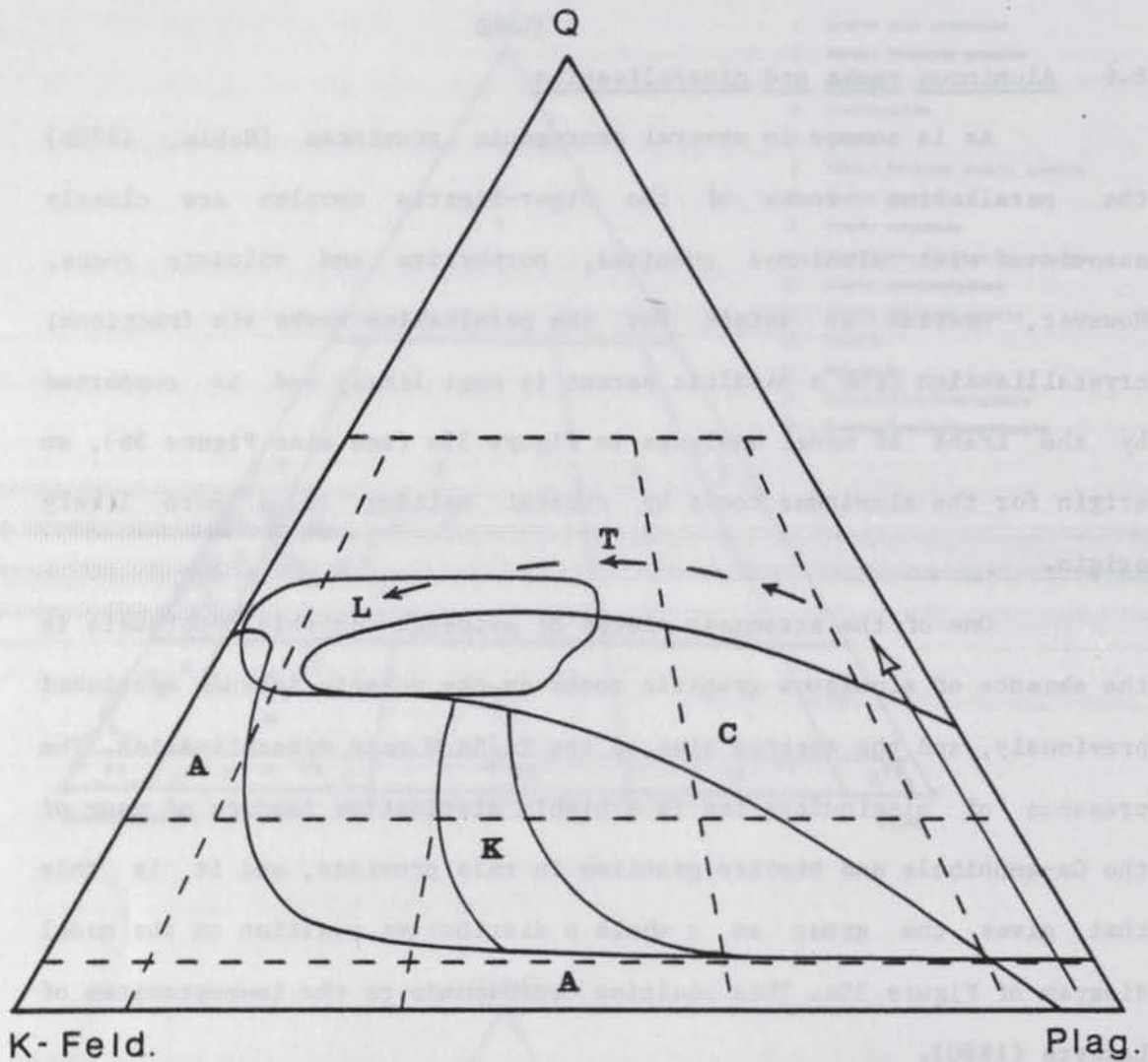


Figure 36.

Generalised evolutionary diagram for various igneous suites (after Lameyre, 1980). A = alkaline; K = highly potassic; C = calc-alkaline; L = leucogranites; T = tholeiitic.

More detail needed. modal vol% - structure etc!

biotite granite has 10-15 modal % oligoclase, while plagioclase is present to the extent of about 5% in a quartz porphyry. These feldspars are rimmed by alkali feldspar and show evidence of disequilibrium stages producing corrosion textures, indicative of a complex history. In the quartz porphyry, the quartz phenocrysts (by analogy with experimental systems) are indicative of crystallisation under a vapour pressure near 10 kb, and for the quartz porphyry at least, an anatectic origin is favoured (Neff and Khalil, 1978).

A comprehensive study of the abundance of K, Th and U in the igneous rocks of the Oslo province has shown that there are two statistically separable populations (Raade, 1978). This data, taking into account the Rb-Sr isotopic compositions and geophysical considerations, suggest to Raade that one group with uniform Th/U ratios originated directly from a mantle-derived source whereas rocks with variable Th/U ratios had a different origin. Of the latter group, Raade postulates some crustal contamination to upset the previous Th/U ratio, but in the case of the biotite granites, he thinks that a direct crustal source is most likely (Raade, 1978, Fig.3).

The Sudan anorogenic province has very close structural and petrologic similarities to the Niger-Nigeria province (Delany, 1955, 1958; Almond, 1971, 1979; Vail, 1978). In the Bayuda district, the ring complexes are dominantly peralkaline with only minor biotite granite and there is a trace of Sn/W mineralisation (Almond, 1967; Almond et al., 1977). Peralkaline and aluminous trends are recognised (McCormac, 1979), with the former group attributable to an origin by fractional crystallisation from a basic parent and the aluminous types representing crustal contamination or anatexis (Ahmed, 1977; Curtis, 1979; Curtis and McCormac, 1980).

In Arabia, 45 post-orogenic alkaline granites have been recognised in the same (Arabian-Nubian) shield area as Sudan, and yet

curiously there is a geographical separation between the peralkaline and aluminous varieties (Stoeser and Elliot, 1979).

The late Precambrian rapakivi granites of N. Wisconsin are considered to be examples of anorogenic magmatism which resulted from thermal doming in an extensional tectonic regime (Anderson and Cullers, 1978). As such, they are comparable to many of the younger anorogenic provinces under discussion, but rapakivi granites in general appear to be largely or wholly aluminous, with Fe-rich biotite and hastingsite as the chief mafic minerals (Simonen and Vormo, 1969) and greisen type vein mineralisation (Haapala, 1977). On the basis of age and geochemistry, the Parguaza rapakivi granite in Venezuela is believed to have a crustal anatexic origin (Gaudette et al., 1978). Similarly, the Precambrian Pikes Peak batholith, Colorado is composed mainly of biotite and hornblende biotite granites, which, on the basis of geochemistry and mineral chemistry, are believed to be derived by crustal melting (Barker et al., 1975).

Thus, for the aluminous granites such as fayalite, hornblende and biotite granites which are not found on oceanic islands, a continental environment appears to be necessary. Further, in many different anorogenic provinces, such aluminous granites have been ascribed to an origin by crustal melting. This evidence, together with evidence discussed above concerning the geochemistry, isotope geochemistry and mineralisation, indicate very strongly that the aluminous granites in the Niger-Nigeria province are the products of crustal anatexis, presumably as a by-product of basalt magma which may have collected at or near the base of the crust and which by differentiation, gave rise to the anorthosites, 'monzoanorthosites', monzonites, syenites and peralkaline syenites and granites which are so typical of anorogenic magmatism.

In the Niger-Nigeria province, Zn/Sn/W vein mineralisation is

associated with the biotite granites, and preferentially with the medium grained facies. Since biotite granites are absent from oceanic islands it therefore follows that this type of mineralisation is also absent. This point and its implications has been put succinctly by Mitchell and Garson (1976) who state that "the absence of tin and tungsten from most island arcs, which lack exposed pre-Mesozoic rocks, provides evidence that crust of continental thickness, perhaps with a lower layer of high grade metamorphic rocks typical of Precambrian rocks on the continents, is necessary for the generation of tin-bearing magmas".

This suggestion is completely in accord with the views expressed above that the biotite (and other aluminous) granites are derived by anatexis, in which case the source of the metals is also crustal. The concentration of Zn, Si and W particularly, in late stage hydrothermal greisen vein deposits (Haag, 1943; Bowden and Jones, 1974) can be correlated with the separation of discrete late stage, water-rich fluid in an aluminous environment whereas such phase separation does not occur in the peralkaline environment (Luth and Tuttle, 1969).

The fact that both peralkaline and aluminous granites can exhibit very similar 'albitised' textures in small bodies that are both enriched in Nb and other metals, has long been regarded, like the riebeckite annite granites, as an important link between the two geochemical types of magma. As late as 1978, the peralkaline and aluminous granites were thought to have a common origin, and so the fact that they both had dispersed phases of mineralisation was therefore expected (Bowden and Kinnaird, 1978).

However, it has recently been demonstrated that among the biotite granites there are certain elements that are partitioned preferentially into a silicate phase and others that are partitioned into a water-rich fluid (Abernethy, in prep.). Niobium appears to prefer the silicate phase and where the magma has had a long liquid life, in a

very few small bodies its concentration has built up to economic proportions, irrespective of an aluminous or peralkaline environment. Thus it would appear that the development of pyrochlore, zircon, and thorite-bearing (peralkaline) albite arfvedsonite granites has been the result of a parallel petrologic process to that in the columbite-thorite-xenotime bearing (aluminous) 'biotite' (actually Li-mica) granites. However, this does not, as has been assumed in the past, necessarily indicate a common source for the two rock types.

6.7 Conclusions

In the Shira complex, the Zigau granite porphyry, the Eldewo biotite granite and the volcanic enclaves are of aluminous composition and in view of the evidence cited above, are thought to represent well fractionated products of crustal melting. Variations in texture and mineralogy can be explained by such factors as degree of partial melting, rapidity of ascent and effectiveness of removal of the early crystallising minerals.

By contrast, the Shira quartz syenite, the Birji and Andaburi granites and the Amdulayi syenite and their associated dyke rocks are all peralkaline. When the field, geochemical and geochronological evidence from this complex and elsewhere is assessed, it is considered that the origin of these rocks can best be explained by extensive fractionation from basaltic liquids which were ultimately derived from the mantle. The association of aluminous and peralkaline rocks in the Shira complex (and elsewhere) is probably due to the basaltic liquid acting as a heat source for crustal fusion as well as being capable of extensive fractionation itself.

REFERENCES

- Abaa S.I. (1976) Geochemistry and petrology of mineralisation at Ririwai, Gindi Akwati and Dutsen Wai in the Nigerian Younger Granite Province. Unpubl. M.Sc. thesis. Ahmadu Bello Univ., Zaria, Nigeria.
- Abbey S. (1977) Studies in 'standard samples' for use in the general analysis of silicate rocks and minerals. Part 5: 1977 edition of 'usable' values. Geol. Surv. Can. Paper No.77-34, 31pp.
- Abbott M.J. (1967) Aenigmatite from the groundmass of a peralkaline trachyte. *Am. Mineral.* 52, 1895-1901.
- (1969) Petrology of the Nandewar volcano, N.S.W., Australia. *Contrib. Mineral. Petrol.* 20, 115-34.
- Abernethy C.A. (in prep.) The mineralogy and petrology of biotite granites in the Nigerian Younger Granite province. Unpubl. Ph.D. thesis, Univ. of St. Andrews.
- Addison W.E. and White A.D. (1968) Spectroscopic evidence for the siting of lithium ions in a riebeckite. *Mineral. Mag.* 36, 743-5.
- Ahmed F. (1977) Petrology and evolution of the Tehilla igneous complex, Sudan. *J. Geol.* 85, 331-44.
- Ajakaiye D.E. (1968) A gravity interpretation of the Liruei Younger Granite ring complex of N.Nigeria. *Geol. Mag.* 105, 256-63.
- (1970) Gravity measurements over the Nigerian Younger Granite Province. *Nature* 225, 50-2.
- (1974) A gravity profile across the Banke ring complex. *Geoexploration* 12, 59-66.
- and Sweeney J.F. (1974) Three dimensional gravity interpretation of the Dutsen-Wai Complex, Nigerian Younger Granite province. *Tectonophysics* 24, 331-41.
- Aleksiyev E.I. (1970) Genetic significance of the REE in the Younger Granites of N.Nigeria and the Cameroons. *Geochem. Int.* 7, 127-32.
- de Almeida F.F.M., Leonardos O.H. and Valenca J.G. (1967) Notes on the granitic rocks of northeastern Brazil. Symposium on the granites and basement of northeastern Brazil and their comparison with those of West Africa. Recife, Oct. 1967.
- Almond D.C. (1967) Discovery of a tin-tungsten mineralisation in northern Khartoum province, Sudan. *Geol. Mag.* 104, 1-12.
- (1971) Ignimbrite vents in the Sabaloka cauldron, Sudan. *Geol. Mag.* 108, 159-76.
- (1979) Younger Granite complexes of Sudan. In 'Evolution and mineralization of the Arabian-Nubian Shield', Vol.1, King Abdulaziz Univ., Jeddah. 151-63.
- , O'Halloran D., Ahmed F., Curtis P., McCormac M. and Vail J.R. (1977) Concentrations of Younger Granite ring complexes and of small Cainozoic volcanic fields in the Bayuda desert, Sudan. 20th Ann. Rep. Res. Inst. Afr. Geol., Leeds Univ. 61-5.
- Anderson J.L. and Cullers R.L. (1978) Geochemistry and evolution of the Wolf river batholith, a late Precambrian rapakivi massif in north Wisconsin. *Precambrian Res.* 7, 287-324.
- Aoki K. (1964) Clinopyroxenes from alkaline rocks of Japan. *Am. Mineral.* 49, 1199-223.
- Aucott J.W. (1965) Layering in the Galway granite. *Nature* 207, 929-30.
- Badejoko T.A. (1977) The composition and structural state of the K-feldspars and their bearing on the petrogenesis of the Younger Granites of Nigeria. Unpubl. Ph.D. thesis, Univ. of

- Ibadan, Nigeria.
- Bailey D.K. (1963) The stability relations of acmite. *Carnegie Inst. Wash. Yearbk.* 62, 131-3.
- (1969) The stability of acmite in the presence of H₂O. *Am. J. Sci.* 267A, 1-16.
- (1970) Volatile flux, heat-focussing and the generation of magma. In 'Mechanisms of igneous intrusion', Eds. G.Newall and N.Rast. *Geol. J. Spec. Issue No.2*, Gallery Press, Liverpool. 177-86.
- (1974) Continental rifting and alkaline magmatism. In 'The alkaline rocks', Ed. H.Sorensen; J.Wiley, London. 148-59.
- (1978) Continental rifting and mantle degassing. In 'Petrology and geochemistry of continental rifts', Eds. E-R.Neumann and I.B.Ramberg, D.Reidel Publ. Co., Dordrecht. 1-13.
- and Cooper J.P. (1978) Comparison of the crystallisation of pantelleritic obsidian under hydrous and anhydrous conditions. In 'Progress in experimental petrology 1975-8', Ed. W.S.Mackenzie, 4th report N.E.R.C. Series D, 230-3.
- , ----- and Knight J.L. (1974) Anhydrous melting and crystallisation of peralkaline obsidians. *Bull. Volc.* 38, 653-65.
- and Schairer J.F. (1964) Feldspar liquid equilibria in peralkaline liquids - the orthoclase effect. *Am. J. Sci.* 262, 1198-1206.
- and ----- (1966) The system Na₂O-Al₂O₃-Fe₂O₃-SiO₂ at 1 atmosphere and the petrogenesis of alkaline rocks. *J. Petrol.* 7, 114-70.
- Bain A.D.N. (1934) The younger intrusive rocks of the Kudaru Hills, Nigeria. *Quart. J. Geol. Soc.* 90, 201-39.
- Baker B.H. (1978) A note on the behaviour of incompatible trace elements in alkaline magmas. In 'Petrology and geochemistry of continental rifts', Eds. E-R.Neumann and I.B.Ramberg, D.Reidel Publ. Co., Dordrecht, 15-25.
- , Crossley R. and Goles G.G. (1978) Tectonic and magmatic evolution of the southern part of the Kenya rift valley. In 'Petrology and geochemistry of continental rifts', Eds. E-R.Neumann and I.B.Ramberg, D.Reidel Publ. Co., Dordrecht, 29-50.
- and Henage L.F. (1977) Compositional changes during crystallisation of some peralkaline silicic lavas of the Kenya rift valley. *J. Volc. Geotherm. Res.* 2, 17-28.
- Baker I. (1968) Intermediate oceanic volcanics and the 'Daly Gap'. *Earth Planet. Sci. Lett.* 4, 103-6.
- Baker P.E. (1974) Peralkaline acid volcanic rocks of oceanic islands. *Bull. Volc.* 38, 737-54.
- , Gass I.G., Harris P.G. and Le Maitre R.W. (1964) The volcanological report of the Royal Society expedition to Tristan da Cunha. *Phil. Trans. Roy. Soc. Lond.* 256A, 439-578.
- Bancroft G.M. and Burns R.G. (1969) Mossbauer and absorption spectral study of alkali amphiboles. *Mineral. Soc. Am. Spec. Pap.* 2, 137-48.
- Barberi F., Ferrara G., Santacroce R., Treuil M. and Varet J. (1975) A transitional basalt-pantellerite sequence of fractional crystallisation, the Boina centre (Afar Rift, Ethiopia). *J. Petrol.* 16, 22-56.
- Barker D.S. (1978) Magmatic trends on alkali-iron-magnesium diagrams. *Am. Mineral.* 63, 531-4.
- Barker F., Wones D.R., Sharp W.N. and Desborough G.A. (1975) The Pikes Peak batholith, Colorado Front Range, and a model for the origin of the gabbro-anorthosite-syenite-potassic granite

- suite. Precambrian Res. 2, 97-160.
- Barrière M. (1976) Flowage differentiation : limitation of the Bagnold effect to the narrow intrusions. *Contrib. Mineral. Petrol.* 55, 139-45.
- (1977) Le Complexe de Ploumanac'h (massif Armoricaïn). These de Docteur-es-Sciences, Univ. Bretagne Occidentale (Brest).
- Batchelor R.A. (1979) Analysis of major, minor and selected trace elements in silicate rocks and minerals. Univ. of St. Andrews, Dept. of Geology, Internal publ. No.79/1.
- Batieva I.D. and Bel'kov I.V. (1972) Origin of alkaline granites of the Kola peninsula. *Chem. Abs.* 73-46183.
- Bawden M.G. and Jones J.A. (1973) The physiography of the Northern Plains. Misc. report No.154, Land Resources Division, Overseas Devt. Admin. 74pp.
- Beer K.E. (1952) The petrography of some of the riebeckite-granites of Nigeria. *Rep. Geol. Surv. U.K., At. Energy Div. H.M.S.O., London.* 38pp.
- Belyaev G.I. (1959) The action of fluorine on some properties of ground enamel. Quoted in Kogarko L.N., 'The role of volatiles'. In 'The alkaline rocks', Ed. H.Sorensen, J.Wiley and Sons, London, (1974), 474-87. (Chem. Abs. 53-11788)
- Berger A.R. (1971) The origin of banding in the main Donegal granite, NW Ireland. *Geol. J.* 7, 347-58.
- Berlin R. and Henderson C.M.B. (1968) A reinterpretation of Sr and Ca fractionation trends in plagioclase from basic rocks. *Earth Planet. Sci. Lett.* 4, 79-83.
- Bhattacharji S. and Smith C.H. (1964) Flowage differentiation. *Science* 145, 150-3.
- Bishop F.C. (1980) The distribution of Fe²⁺ and Mg between coexisting ilmenite and pyroxene with applications to geothermometry. *Am. J. Sci.* 280, 46-77.
- Bizouard H., Barberi F. and Varet J. (1980) Mineralogy and petrology of Erta Ale and Boina volcanic series, Afar rift, Ethiopia. *J. Petrol.* 21, 401-36.
- Black R. (1963) Note sur les complexes annulaires de Tchouni-Zarniski et de Gouré, Niger. *Bull. Bur. Rech. Geol. Min. Paris* 1, 3-45.
- (1965) Sur la signification petrogénétique de la découverte d'anorthosites associées aux complex annulaires subvolcanique du Niger. *C. R. Acad. Sci. Paris* 260, 5829-31.
- and Girod M. (1970) Late Palaeozoic to Recent igneous activity in West Africa and its relationship to basement structure. In 'African Magmatism and Tectonics', Eds. T.N.Clifford and I.G.Gass, Oliver and Boyd, Edinburgh. 185-210.
- , Janjou M. and Pellaton C. (1967) Notice explicative sur la carte géologique de l'Air, à l'échelle de 1:500,000. *Dir. Mines Geol. Niger.* 62pp.
- , Morton W.H., Rex D.C. and Shackleton R.M. (1972) Sur la découverte en Afar (Ethiopie) d'un granite hyperalkalin Miocene : le massif de Limmo. *C.R. Acad. Sci. Paris* 274, 1453-6.
- Blaxland A.B. (1976) Rb-Sr isotopic evidence for the age and origin of the Ivigtut granite and associated cryolite body, south Greenland. *Econ. Geol.* 71, 864-9.
- , van Breemen O., Emeleus C.H. and Anderson J.G. (1978) Age and origin of the major syenite centers in the Gardar province of south Greenland : Rb-Sr studies. *Geol. Soc. Am. Bull.* 89, 231-44.
- Blundell D.J. (1976) Active faults in West Africa. *Earth Planet. Sci.*

- Let. 31, 287-90.
- (1978) A gravity survey across the Gardar igneous province, SW Greenland. *J. Geol. Soc. Lond.* 135, 545-54.
- Boettcher A.L., O'Neil J.R., Windon K.E., Stewart D.C. and Wilshire H.G. (1979) Metasomatism of the upper mantle and the genesis of kimberlites and alkali basalts. In 'The mantle sample: Inclusions in kimberlites and other volcanics' (Proc. Sec. Int. Kimb. Conf., Vol.2), Eds. F.R. Boyd and H.O.A. Meyer. Am. Geophys. Union, Wash. 173-82.
- , Piwinski A.J. and Knowles C.R. (1967) Zoned potash feldspars from the Rainy Creek complex near Libby, Montana. *Earth Planet. Sci. Lett.* 3, 8-10.
- Boggild O.B. (1953) The mineralogy of Greenland. *Medd. Gronland* 149, 1-442.
- Boissonas J., Borsi S., Ferrara G., Fabre J., Fabries J. and Gravelle M. (1969) On the early Cambrian age of two late orogenic granites from West-central Ahaggar (Algerian Sahara). *Can. J. Earth. Sci.* 6, 25-37.
- Bonatti S. (1959) Chevkinite, perrierite and epidotes. *Am. Mineral.* 44, 115-37.
- and Gottardi G. (1950) Perrierite, nuovo minerale ritrovato nella sabbia di Nettuno (Roma). *Acc. Naz. Lincei. Rend. Sc. Fis. Mat. e Nat.* 9, 361-68. (Mineral. Abs. 11-310)
- and ----- (1954) Nuovi dati sulla perrierite. *Relazioni tra perrierite, chevkinite e epidoti.* *Rend. Soc. Min. Ital.* 10, 208-25. (Mineral. Abs. 12-498)
- Bonin B. (1974) Hypersolvus subvolcanic complexes and the youthful Atlantic basin. *Geol. Mediterraneene* 1, 139-42.
- , Bowden P. and Vialette Y. (1979) Le comportement des éléments Rb et Sr au cours des phases de minéralisation : l'exemple de Ririwai (Liruei), Nigéria. *C.R. Acad. Sci. Paris* 289D, 707-10.
- , Grelou-Orsini C. and Vialette Y. (1978) Age, origin and evolution of the anorogenic complex of Evisa (Corsica) : a K-Li-Rb-Sr study. *Contrib. Mineral. Petrol.* 65, 425-32.
- Boone, G.M. (1962) Potassic feldspar enrichment in magma : origin of syenite in Deboullie district, Northern Maine. *Geol. Soc. Am. Bull.* 73, 1151-76.
- Borg I.Y. and Smith D.K. (1969) Calculated X-ray powder patterns for silicate minerals. *Geol. Soc. Am. Mem.* 122, 896pp.
- Borley G.D. (1963a) Geochemistry of the mafic minerals in some Younger Granites of Nigeria. Unpubl. Ph.D. thesis, Univ. of London.
- (1963b) Amphiboles from the Younger Granites of Nigeria. Part I. Chemical classification. *Mineral. Mag.* 33, 358-76.
- (1976a) Aenigmatite from an aegirine riebeckite granite, Liruei complex, Nigeria. *Mineral. Mag.* 40, 595-8.
- (1976b) Ferromagnesian mineralogy and temperatures of formation of the Younger Granites of Nigeria. In 'Geology of Nigeria', Ed. C.A. Kogbe. Elizabethan Publ. Co., Nigeria. 159-76.
- , Beckinsale R.D., Suddaby P. and Durham J.J. (1976) Variations in composition and d_{018} values within the Kaffo albite riebeckite granite of Liruei Complex, Younger Granites of Nigeria. *Chem. Geol.* 18, 297-308.
- and Frost M.T. (1963) Some observations on igneous ferrohastingsite. *Mineral Mag.* 33, 646-62.
- Bowden P. (1964) Gallium in Younger Granites of N. Nigeria. *Geochim. Cosmochim. Acta* 28, 1981-8.
- (1966a) Lithium in Younger Granites of N. Nigeria. *Geochim. Cosmochim. Acta* 30, 555-64.

- (1966b) Zirconium in Younger Granites. *Geochim. Cosmochim. Acta* 30, 985-93.
- (1970) Origin of the Younger Granites of Northern Nigeria. *Contrib. Mineral. Petrol.* 25, 153-62.
- (1976) Granites and their mineralisation. Eighth Tomkeieff Memorial Lecture. Univ. of Newcastle, Geol. Dept. 24pp.
- , Bennett J.N., Whitley J.E. and Moyes A.B. (1979) Rare earths in Nigerian Mesozoic granites and related rocks. In 'Origin and distribution of the elements', 2nd Edition, Ed. L.H.Ahrens, Pergamon Press, Oxford, 479-91.
- and van Breemen O. (1972) Isotopic and chemical studies on Younger Granites from Northern Nigeria. In 'African Geology', Eds. T.F.J.Dessauvague and A.J.Whiteman, Univ. of Ibadan, Nigeria, 105-20.
- , -----, Hutchison J. and Turner D.C. (1976a) Palaeozoic and Mesozoic age trends for some ring complexes in Niger and Nigeria. *Nature* 259, 297-9.
- and Jones J.A. (1974) Mineralisation in the Younger Granite Province of Northern Nigeria. In 'Mineralisation associated with Acid Magmatism', Eds. M.Stemprok, L.Burnol and G.Tischendorf, I.G.C.P. Geol. Surv. Prague. 179-90.
- and Kinnaird J.A. (1978) The Younger Granites of Nigeria - a zinc-rich tin province. *Trans. Inst. Min. Metall. Sect.B*, 87, B66-9.
- and Turner D.C. (1974) Peralkaline and associated ring complexes in the Nigeria-Niger province, W.Africa. In 'The alkaline rocks', Ed. H.Sorensen, John Wiley and Sons, London, 330-51.
- and Whitley J.E. (1974) Rare earth patterns in peralkaline and associated granites. *Lithos* 7, 15-21.
- , Whitley J.E. and van Breemen O. (1976b) Geochemical studies on the Younger Granites of Northern Nigeria. In 'Geology of Nigeria', Ed. C.A.Kobe, Elizabethan Publ. Co., Nigeria, 177-93.
- Bowen N.L. and Tuttle O.F. (1950) The system NaAlSi₃O₈- KAlSi₃O₈-H₂O. *J. Geol.* 58, 489-511.
- Branch C.D. (1966) Volcanic cauldrons, ring complexes and associated granites of the Georgetown inlier, Queensland. *Aust. Bur. Min. Res. Bull.* 76, 160pp.
- van Breemen O. and Bowden P. (1973) Sequential age trends for some Nigerian Mesozoic granites. *Nature* 242, 9-11.
- , Hutchinson J. and Bowden P. (1975) Age and origin of the Nigerian Mesozoic Granites - a Rb-Sr isotopic study. *Contr. Mineral. Petrol.* 50, 157-72.
- , Pidgeon R.T and Bowden P. (1977) Age and isotopic studies of some Pan-African granites from north-central Nigeria. *Precambrian Res.* 4, 307-19.
- Briden J.C. (1967) Recurrent continental drift of Gondwanaland. *Nature* 215, 1334-9.
- and Gass I.G. (1974) Plate movement and continental magmatism. *Nature* 248, 650-3.
- Brindley G.W. and Zussman J. (1957) A structural study of the thermal transformation of serpentine minerals to forsterite. *Am. Mineral.* 42, 461-74.
- Brown G. and Stephen I. (1959) A structural study of iddingsite from New South Wales, Australia. *Am. Mineral.* 44, 251-60.
- Brown G.C. and Bowden P. (1973) Experimental studies concerning the genesis of the Nigerian Younger granites. *Contr. Mineral. Petrol.* 40, 131-9.
- Brown G.M. and Vincent E.A. (1963) Pyroxenes from the late stages of

- fractionation of the Skaergaard intrusion, east Greenland. *J. Petrol.* 4, 175-97.
- Brown P.E. (1956) The Mourne Mountains granites - a further study. *Geol. Mag.* 93, 72-84.
- Brunnschweiler R.O. (1974) New K-Ar age determinations from the West African shield in the Niger Republic. *Geology* 2, 17-20.
- Bryan W.B. (1964) Relative abundance of intermediate members of the oceanic basalt-trachyte association; evidence from Clarion and Socorro Islands, Revillagigedo Islands, Mexico. *J. Geophys. Res.* 69, 3047-9.
- and Stevens N.C. (1973) Holocrystalline pantellerite from Mt. Ngungun, Glass House mountains, Queensland, Australia. *Am. J. Sci.* 273, 947-57.
- Buchanan M.S., Macleod W.N. and Turner D.C. (1971) The geology of the Jos Plateau. *Geol. Surv. Nigeria Bull* 32, Vol.2 - Younger Granite Complexes. 159pp.
- Buddington A.F. and Lindsley D.H. (1964) Iron-titanium oxide minerals and synthetic equivalents. *J. Petrol.* 5, 310-57.
- Buma G., Frey F.A. and Wones D.R. (1971) New England granites : trace elements regarding their origin and differentiation. *Contrib. Mineral. Petrol.* 31, 300-20.
- Burke K. (1978) Evolution of continental rift systems in the light of plate tectonics. In 'Tectonics and geophysics of continental rifts', Eds. I.B.Ramberg and E-R.Neumann, D.Reidel Publ. Co., Dordrecht. 1-9.
- Burnham C.W. (1975) Water and magmas; a mixing model. *Geochim. Cosmochim. Acta* 39, 1077-84.
- Butler J.C. (1979) Trends in ternary petrologic variation diagrams - fact or fantasy? *Am. Mineral.* 64, 1115-21.
- Butler J.R., Bowden P. and Smith A.Z. (1962) K/Rb ratios in the evolution of the younger granites of northern Nigeria. *Geochim. Cosmochim. Acta* 26, 89-100.
- Calvert A.F (1912) Nigeria and its tinfields. Stanford, London. 488pp.
- Calvo C. and Faggiani R. (1974) A re-investigation of the crystal structures of chevkinite and perrierite. *Am. Mineral.* 59, 1277-85.
- Campbell I.H. (1978) Some problems with the cumulus theory. *Lithos* 11, 311-23.
- Cann J.R. (1965) Preliminary investigations of the acid ejected blocks of Ascension Island. *Geol. Soc. Lond. Proc.* 1621, 62-3.
- Cannillo E., Mazzi F., Fang J.H., Robinson P.D. and Ohya Y. (1971) The crystal structure of aenigmatite. *Am. Mineral.* 56, 427-46.
- Carman M.F., Cameron M., Gunn B., Cameron K.L. and Butler J.C. (1975) Petrology of Rattlesnake Mountain Sill, Big Bend National Park, Texas. *Geol. Soc. Am. Bull.* 86, 177-93.
- Carmichael I.S.E. (1960) The pyroxenes and olivines from some Tertiary acid glasses. *J. Petrol.* 1, 309-36.
- (1962) Pantelleritic liquids and their phenocrysts. *Mineral. Mag.* 33, 86-113.
- and Mackenzie W.S. (1963) Feldspar-liquid equilibria in pantellerites : an experimental study. *Am. J. Sci.* 261, 382-96.
- Carter J.D. (1964) Geological map of Nigeria at 1:2 m scale. *Geol. Surv. Nigeria, Kaduna.*
- Cawthorn R.G. and Collerson K.D. (1974) The recalculation of pyroxene end-member parameters and the estimation of ferrous and ferric iron content from electron microprobe analysis. *Am. Mineral.* 59, 1203-8.
- Chao G.Y. (1967) Leucophanite, elpidite and narsarsukite from the

- Desourdy Quarry, Mont St.Hilaire, Quebec. *Can. Mineral.* 9, 286-7.
- Charles R.W. (1975) The phase equilibria of richterite and ferrichterite. *Am. Mineral.* 60, 367-74.
- (1977) The phase equilibria of intermediate compositions on the pseudobinary $\text{Na}_2\text{CaMg}_5\text{Si}_8\text{O}_{22}(\text{OH})_2 - \text{Na}_2\text{CaFe}_5\text{Si}_8\text{O}_{22}(\text{OH})_2$. *Am. J. Sci.* 277, 594-625.
- Chayes F. (1962) The treatment of FeO and Fe₂O₃ on Harker diagrams. *Carnegie Inst. Wash. Yearbk.* 62, 119-21.
- (1963) Relative abundance of intermediate members of the oceanic basalt-trachyte association. *J. Geophys. Res.* 68, 1519-34.
- (1964) Variance-covariance relations in some published Harker diagrams of volcanic suites. *J. Petrol.* 5, 219-37.
- Cherry M.E. and Trembath L.T. (1978) Structural state and composition of alkali feldspars in granites of the St. George pluton, south-western New Brunswick. *Mineral Mag.* 42, 391-9.
- Clague D.A. (1978) The oceanic basalt-trachyte association: an explanation of the Daly gap. *J. Geol.* 86, 739-43.
- Claxton C.W. (1968) Mineral layering in the Galway granite, Connemara, Eire. *Geol. Mag.* 105, 149-59.
- Coombs D.S., Ellis A.J., Fyfe W.S. and Taylor A.M. (1959) The zeolite facies; with comments on the interpretation of hydrothermal synthesis. *Geochim. Cosmochim. Acta.* 17, 53-107.
- and Wilkinson J.F.G. (1969) Lineages and fractionation trends in undersaturated volcanic rocks from the East Otago Volcanic province (New Zealand) and related rocks. *J. Petrol.* 10, 440-501.
- Cox K.G., Bell J.D. and Pankhurst R.J. (1979) 'The interpretation of igneous rocks'. George Allen and Unwin, London. 450pp.
- Cratchley C.R. and Jones G.P. (1965) An interpretation of geology and gravity anomalies of the Benue valley, Nigeria. *Overseas Geol. Surv. Geophys. Paper No.1*, HMSO, London.
- and Louis P. (1975) Interpretation of the principal gravity anomalies of the Chad basin. 7th Int. Colloq. African Geol., Florence, 1973. *Trav. Lab. Sci. Terre. Marseille* 11, 52-3.
- Creasy J.W. (1974) Amphibole compositional variation, White Mountain batholith, New Hampshire. (Abs.) *Trans. Am. Geophys. Union.* 55, p477.
- Crosby P. (1971) Composition and structural state of alkali feldspar from charnockitic rocks on Whiteface Mountain, New York. *Am. Mineral.* 56, 1788-811.
- Curtis P. (1979) The mineralogy and geochemistry of the Sultaniyat Younger Granite complex, Baiyuda desert, Sudan. 10e Colloque de Geol. Africaine, Montpellier. 83-4. (Abs.)
- and McCormac M. (1980) Some aspects of the petrology and geochemistry of the Muweilih and Sultaniyat sub-volcanic ring complexes, Buyuda desert, Sudan. *J. Geol. Soc. Lond. (Proc.)* 137, p.519. (Abs.)
- Czamanske G.K. and Mihalik P. (1972) Oxidation during magmatic differentiation, Finnmarka complex, Oslo area, Norway: Part 1, the opaque oxides. *J. Petrol.* 13, 493-509.
- and Wones D.R. (1973) Oxidation during magmatic differentiation, Finnmarka, Oslo area, Norway: Part 2, the mafic silicates. *J. Petrol.* 14, 349-80.
- , ----- and Eichelberger J.C. (1977) Mineralogy and petrology of the intrusive complex of the Pliny range, New Hampshire. *Am. J. Sci.* 277, 1073-1123.
- Darnley A.G., Smith G.H., Chandler T.R.D. and Dance D.F. (1962) The age of fergusonite from the Jos area, Northern Nigeria. *Mineral.*

- Mag. 33, 48-51.
- Deer W.A., Howie R.A. and Zussman J. (1962) Rock forming minerals. Vol.1. Ortho- and ring silicates. Longman, London. 333pp.
- , ----- and ----- (1963) Rock forming minerals. Vol.2. Chain silicates. Longman, London. 379pp.
- , ----- and ----- (1978) Rock-forming minerals. Vol.2A. Single chain silicates. Second edition. Longman, London. 668pp.
- Delany F.M. (1955) Ring structures in the N.Sudan. *Eclog. Geol. Helvet.* 48, 133-48.
- (1958) Observations on the Sabaloka series of the Sudan. *Trans. Geol. Soc. S.Africa LXI*, 111-24.
- Dickinson D.R. and Gibson I.L. (1972) Feldspar fractionation and anomalous $^{87}\text{Sr}/^{86}\text{Sr}$ ratios in a suite of peralkaline silicic rocks. *Geol. Soc. Am. Bull.* 83, 231-39.
- Dickson F.W. and Sabine C. (1967) Barium zoned large K-feldspars in quartz monzonites of eastern and south eastern California. *Geol. Soc. Am. Abs. with Progr.* p.323.
- Dietrich R.V. (1962) K-feldspar structural states as petrogenetic indicators. *Nor. Geol. Tidsskr.* 42, 394-414.
- (1968) Behaviour of zirconium in certain articial magmas under diverse P-T conditions. *Lithos* 1, 20-9.
- Doe B.R. and Zartman R.E. (1979) Plumbotectonics, the Phanerozoic. In 'Geochemistry of hydrothermal ore deposits', Ed. H.L.Barnes, Second Edition, John Wiley and Sons, New York, 22-70.
- Dostal J. and Capedri S. (1975) Partition coefficients of uranium for some rock forming minerals. *Chem. Geol.* 15, 285-94.
- Dunlop H.M. and Fitton J.G. (1979) A K-Ar and Sr-isotope study of the volcanic rocks of the island of Principe, West Africa - evidence for mantle heterogeneity beneath the Gulf of Guinea. *Contrib. Mineral. Petrol.* 71, 125-31.
- Edgar A.D. (1974) On the use of the term 'agpaitic'. *Mineral. Mag.* 39, 729-30.
- Edwards A.C. (1976) A comparison of the methods for calculating Fe^{3+} contents of clinopyroxenes from microprobe analysis. *Neues Jahrb. Min. Monats.* 11, 508-12.
- Emeleus C.H. (1963) Structural and petrographic observations on layered granites from southern Greenland. *Mineral. Soc. Am. Spec. Paper* 1, 22-9.
- Emslie R.F. (1978) Elsonian magmatism in Labrador : age, characteristics and tectonic setting. *Can. J. Earth Sci.* 15, 438-53.
- Ernst W.G. (1960) The stability relations of magnesioriebeckite. *Geochim. Cosmochim. Acta* 19, 10-40.
- (1962) Synthesis, stability relations and occurrences of riebeckite and riebeckite-arfvedsonite solid solutions. *J. Geol.* 70, 689-736.
- and Wai C.M. (1970) Mossbauer, infrared, X-ray and optical study of cation ordering and dehydrogenation in natural and heat-treated sodic amphiboles. *Am. Mineral.* 55, 1226-58.
- Eugster H.P. and Wones D.R. (1962) Stability relations of the ferruginous biotite, annite. *J. Petrol.* 3, 82-125.
- Ewart A. and Taylor S.R. (1969) Trace element geochemistry of the rhyolitic volcanic rocks, central North Island, New Zealand. Phenocryst data. *Contrib. Mineral. Petrol.* 22, 127-46.
- , ----- and Capp A.C. (1968) Geochemistry of the pantellerites of Mayor Island, New Zealand. *Contrib. Mineral. Petrol.* 17, 116-40.
- Fabriès J. (1966) Une représentation graphique des principales substitutions rencontrées dans les amphiboles calciques et sodiques. *C. R. Acad. Sci. Paris* 262D, 1824-7.

- (1978) Les types paragénetiques des amphiboles sodiques dans les roches magmatiques. *Bull. Mineral.* 101, 155-65.
- and Rocci G. (1965) Le massif granitique du Tarraouadji (Republic du Niger). Etude et signification pétrogénétique des principaux minéraux. *Bull. Soc. Franc. Miner. Crist.* 88, 319-40.
- and ----- (1972) Evolution cristallogénétique des amphiboles dans la série granitique de Fort-Trinquet (Mauritanie). *Contrib. Mineral. Petrol.* 35, 215-25.
- Fairhead J.D. and Reeves C.V. (1977) Teleseismic delay times, Bouguer anomalies and inferred thickness of the African lithosphere. *Earth Planet. Sci. Lett.* 36, 63-76.
- Falconer J.D. (1910) Outlines of the geology of Nigeria. *Geol. Mag.* 7, 519-20.
- (1911) The geology and geography of Northern Nigeria. MacMillan, London. 295pp.
- (1921) Geology of the Plateau tinfields. *Geol. Surv. Nigeria Bull. No.1.* 55pp.
- and Raeburn C. (1923) The Northern tinfields of Bauchi Province. *Geol. Surv. Nigeria Bull. No.4.* 67pp.
- , Raeburn C. and Bain A.D.N. (1926) The southern plateau tinfields. *Geol. Surv. Nigeria Bull. No.9.* 67pp.
- Faure G. and Powell J.L. (1972) Strontium isotope geology. Springer Verlag, Heidelberg. 188pp.
- Faye G.H. and Nickel E.H. (1970) The effect of charge-transfer processes on the colour and pleochroism of amphiboles. *Can. Mineral.* 10, 616-35.
- Ferguson A.K. (1977a) Titanium in aegirine - a comment on: Crystallisation trends of pyroxene from the alkaline volcanic rocks of Tenerife, Canary Islands, by P.W.Scott. *Mineral. Mag.* 41, 553-4.
- (1977b) The natural occurrence of aegirine-neptunite solid solution. *Contrib. Mineral. Petrol.* 60, 247-53.
- (1978a) The crystallisation of pyroxenes and amphiboles in some alkaline rocks and the presence of a pyroxene compositional gap. *Contrib. Mineral. Petrol.* 67, 11-15.
- (1978b) Hollow aenigmatite and amphibole crystals from a late-stage vein in a trachyte flow near Turritable Falls, Upper Macedon, Victoria. *Mineral Abs.* 80-0859.
- (1978c) Reply to G.Rossi on the "pretended" occurrence of aegirine-neptunite solid solution. *Contrib. Mineral. Petrol.* 66, 111-2.
- Ferguson J. (1970) The significance of the kakortokite in the evolution of the Ilimaussaq intrusion, south Greenland. *Medd. Gronland* 190, 193pp.
- and Pulvertaft T.C.R. (1963) Contrasted styles of igneous layering in the Gardar Province of south Greenland. *Mineral. Soc. Am. Spec. Paper* 1, 10-21.
- Ferrara G. and Treuil M. (1974) Petrological implications of trace element and Sr isotope distributions in basalt-pantellerite series. *Bull. Volc.* 38, 548-74.
- Finger L.W. (1972) The uncertainty in the calculated ferric iron content of a microprobe analysis. *Carnegie Inst. Wash. Yearbk.* 71, 600-3.
- Flaschen S.S. and Osborn E.F. (1957) Studies of the system iron oxide-silica-water at low oxygen partial pressures. *Econ. Geol.* 52, 923-43.
- Flink, G. (1901) Undersøgelser af Mineralen fra Julianehaab. Part 1: On the minerals. *Medd. Gronland* 24, 9-180.

- Flood R.H., Shaw S.E. and Chappell B.W. (1980) Mineralogical and chemical matching of plutonic and associated volcanic units, New England batholith, Australia. *Chem. Geol.* 29, 163-70.
- Flower M.F.J. (1974) Phase relations of titan-aegirine in the system $\text{Na}_2\text{O}-\text{Fe}_2\text{O}_3-\text{Al}_2\text{O}_3-\text{TiO}_2-\text{SiO}_2$ at 1000 bars total water pressure. *Am. Mineral.* 59, 536-48.
- Foland K.A. and Henderson C.M.B. (1976) Application of age and Sr isotopic data to the petrogenesis of the Marangudzi ring complex, Rhodesia. *Earth Planet. Sci. Lett.* 29, 291-301.
- Forester R.W. and Taylor H.P. (1976) (18)O depleted igneous rocks from the Tertiary complex of the Isle of Mull, Scotland. *Earth Planet. Sci. Lett.* 32, 11-17.
- Fortey N.J. and Michie U.M. (1978) Aegirine of possible authigenic origin in Middle Devonian sediments in Caithness, Scotland. *Mineral. Mag.* 42, 439-42.
- Foster M.D. (1960) Interpretation of the composition of trioctahedral micas. *U.S. Geol. Surv. Prof. Paper* 354-B.
- Frost M.T. (1963) Amphiboles from the Younger Granites of Nigeria. Part II: X-ray data. *Mineral. Mag.* 33, 377-84.
- Gass I.G. and Mallick D.I.J. (1968) Jebel Khariz : an Upper Miocene strato-volcano of comenditic affinity on the South Arabian coast. *Bull. Volc.* 32, 33-88.
- Gast P.W., Tilton G.R. and Hedge C. (1964) Isotopic composition of lead and strontium from Ascension and Gough Islands. *Science* 145, 1181-5.
- Gates R.M. and Scheerer P.E. (1963) The petrology of the Nonewaug granite, Connecticut. *Am. Mineral.* 48, 1040-69.
- Gaudette H.E., Mendoza V., Hurley P.M. and Fairbairn H.W. (1978) Geology and age of the Parguaza rapakivi granite, Venezuela. *Geol. Soc. Am. Bull.* 89, 1335-40.
- Gay P and Le Maitre R.W. (1961) Some observations on "iddingsite". *Am. Mineral.* 46, 92-111.
- Gazel J., Lasserre M., Limasset J-C. and Vachette M. (1963) Age absolus des massifs granitiques ultimes et de la mineralisation en etain du Cameroun central. *C.R. Acad. Sci. Paris* 256, 2875-8.
- Ghose S. (1966) A scheme of cation distribution in the amphiboles. *Mineral. Mag.* 35, 46-54.
- Gibb F.G.F. (1973) The zoned clinopyroxenes of the Shiant Isles Sill, Scotland. *J. Petrol.* 14, 203-30.
- Gibson I.L. (1970) A pantelleritic welded ash flow tuff from the Ethiopian Rift valley. *Contrib. Mineral. Petrol.* 28, 89-111.
- (1972) The chemistry and petrogenesis of a suite of pantellerites from the Ethiopian rift. *J. Petrol.* 13, 31-44.
- (1974) A review of the geology, petrology and geochemistry of the volcano Fantale. *Bull. Volc.* 38, 791-802.
- Gier T.E., Cox N.L. and Young H.S. (1964) The hydrothermal synthesis of sodium amphiboles. *Inorg. Chem.* 3, 1001-4.
- Gilbert G.K. (1906) Gravitational assemblage in granite. *Geol. Soc. Am. Bull.* 17, 321-8.
- Giret A. (1980) Notice de la carte geologique au 1:50,000 de la Peninsule Rallier du Baty, Isles Kerguelen. *Comite National Francais des Recherches Antarctiques* No.45.
- , Bonin B. and Leger J-M. (in prep.) Amphibole compositional trends in oversaturated and undersaturated alkaline igneous ring complexes.
- Gol'dman M.M., Bunchuk Z.V. and Ni L.P. (1968) Aegirine obtained by hydrothermal synthesis. *Zap. Vses. Min. Obsh.* 97, 497-500. (Chem. Abs. 69-102572)
- Goldsmith J.R. and Laves F. (1954a) The microcline-sanidine stability

- relations. *Geochim. Cosmochim. Acta* 5, 1-19.
- and ----- (1954b) Potassium feldspars structurally intermediate between microcline and sanidine. *Geochim. Cosmochim. Acta* 6, 100-18.
- and ----- (1961) The sodium content of microclines and the microcline-albite series. *Mineral. Abs.* 16, p75.
- Gomes C.de B., Moro S.L. and Dutra C.V. (1970) Pyroxenes from the alkaline rocks of Itapirapua, Sao Paulo, Brazil. *Am. Mineral.* 55, 224-30.
- Graham W.A.P. (1935) An occurrence of narsarsukite in Montana. *Am. Mineral.* 20, 598-601.
- Grant N.K. (1969) The Late Precambrian to early Paleozoic Pan-African orogeny in Ghana, Togo, Dahomey and Nigeria. *Geol. Soc. Am. Bull.* 80, 45-56.
- (1970) Geochronology of Precambrian basement rocks from Ibadan, Southwestern Nigeria. *Earth Planet. Sci. Lett.* 10, 29-38.
- (1971) A compilation of radiometric ages from Nigeria. *Nig. J. Mining and Geol.* 6, 37-54.
- Grapes R., Yagi K. and Okumura K. (1979) Aenigmatite, sodic pyroxene, arfvedsonite and associated minerals in syenites from Morotu, Sakhalin. *Contrib. Mineral. Petrol.* 69, 97-103.
- Greenwood R. (1951) Younger intrusive rocks of Plateau Province, Nigeria compared with the alkalic rocks of New England. *Geol. Soc. Am. Bull.* 62, 1151-78.
- Gustafson W.I. (1974) The stability of andradite, hedenbergite and related minerals in the system Ca-Fe-Si-O-H. *J. Petrol.* 15, 455-96.
- Haag H.L. (1943) Wolfram in Nigeria; with notes on cassiterite, wolfram and columbite zones. *Trans. Inst. Min. Metal.* 52, 119-83.
- Haapala I. (1977) Petrography and geochemistry of the Eurajoki stock, a rapakivi-granite complex with greisen type mineralization in SW Finland. *Bull. Geol. Surv. Finland* No.286.
- Haggerty S.E. (1976) Opaque mineral oxides in terrestrial igneous rocks. In 'Oxide Minerals', Ed. D.Rumble, *Mineral. Soc. Am. Short Course Notes*, Vol.3. Southern Printing Co., Blacksburg, Virginia. Hgl01-276.
- Harris P.G. (1963) Comments on a paper by F.Chayes, 'Relative abundances of intermediate members of the oceanic basalt-trachyte association'. *J. Geophys. Res.* 68, 5103-7.
- Harry W.T. and Emeleus C.H. (1960) Mineral layering in some granite intrusions in SW Greenland. *21st Int. Geol. Congr.*, Part 14, 172-81.
- Hartman P. (1969) Can Ti^{4+} replace Si^{4+} in silicates? *Mineral. Mag.* 37, 366-9.
- Hawthorne F.C. (1976) The crystal chemistry of the amphiboles : V. The structure and chemistry of arfvedsonite. *Can. Mineral.* 14, 346-56.
- (1978) The crystal chemistry of the amphiboles : VIII. The crystal structure and site chemistry of fluor-riebeckite. *Can. Mineral.* 16, 187-94.
- Heier K.S. (1962) Trace elements in feldspars - a review. *Nor. Geol. Tidsskr.* 42, 415-54.
- and Compston W. (1969) Rb-Sr isotopic studies of the plutonic rocks of the Oslo Region. *Lithos* 2, 133-45.
- and Taylor S.R. (1959) The distribution of Li, Na, K, Rb, Cs, Pb and Tl in southern Norwegian pre-Cambrian alkali feldspars. *Geochim. Cosmochim. Acta* 15, 284-304.
- Henley R.W. (1978) Arfvedsonite in basalt dykes, Buchans, Newfoundland. *Am. Mineral.* 63, 413-4.

- Higuchi H. and Nagasawa H. (1969) Partition of trace elements between rock forming minerals and the host volcanic rocks. *Earth Planet. Sci. Lett.* 7, 281-7.
- Hildreth W. (1979) The Bishop Tuff : evidence for the origin of compositional zonation in silicic magma chambers. In 'Ash flow tuffs', Eds. C.E.Chapin and W.E.Elston, *Geol. Soc. Am. Spec. Pap.* 180, 43-75.
- Hori S. (1942) On an abnormal optical phenomenon of alkali amphibole. *J. Geol. Soc. Japan.* 49, 451-2.
- Husch J.M. and Moreau C. (in prep.) Geology and major element geochemistry of anorthositic rocks associated with Palaeozoic hypabyssal ring complexes, Air massif, Niger, West Africa.
- Hutchison C.S. (1974) Laboratory handbook of petrographic techniques. J.Wiley and Sons, New York. 527pp.
- Ike E.C. (1979) The structure, petrology and geochemistry of the Tibchi Younger Granite ring complex, Nigeria. Unpubl. Ph.D. thesis, Univ. of St.Andrews. 333pp.
- International tectonic map of Africa. (1968) *Assoc. Afr. Geol. Survs./Unesco.* 1:5m scale. 9 sheets. G.Choubert, general coordinator.
- Ito J. (1967) A study of chevkinite and perrierite. *Am. Mineral.* 52, 1094-104.
- and Arem J.E. (1971) Chevkinite and perrierite : synthesis, crystal growth and polymorphism. *Am. Mineral.* 56, 307-19.
- Izett G.A. and Wilcox R.E. (1968) Perrierite, chevkinite and allanite in upper Cenozoic ash beds in the western United States. *Am. Mineral.* 53, 1558-67.
- Jackson E.D. (1961) Primary textures and mineral associations in the ultramafic zone of the Stillwater complex, Montana. *U.S. Geol. Surv. Prof. Paper* 358, 106pp.
- Jacobson R.R.E. (1947) The Younger Granite complex of the Liruei Hills, Nigeria. Unpubl. Ph.D. thesis, Univ. of London.
- , Macleod W.N. and Black R. (1958) Ring complexes in the Younger Granite province of Northern Nigeria. *Geol. Soc. Lond. Mem.* No.1. 117pp.
- and Macleod W.N. (1977) The Liruei, Banke and adjacent Younger Granite complexes. *Geol. Surv. Nigeria Bull.* No.33. 117pp.
- , Snelling N.J. and Truswell J.F. (1963) Age determination in the geology of Nigeria, with special reference to the Older and Younger Granites. *Overseas Geol. Min. Resources* 9, 168-82.
- Jaffe J.W., Evans H.T. and Chapman R.W. (1956) Occurrence and age of chevkinite from the Devil's slide fayalite quartz syenite near Stark, New Hampshire. *Am. Mineral.* 41, 474-87.
- James R.S. and Hamilton D.L. (1969) Phase relations in the system $\text{NaAlSi}_3\text{O}_8\text{-KAlSi}_3\text{O}_8\text{-CaAl}_2\text{Si}_2\text{O}_8\text{-SiO}_2$ at 1 kilobar water vapour pressure. *Contrib. Mineral. Petrol.* 21, 111-41.
- Jenkins R. and de Vries J.L. (1970) Practical X-ray spectrometry. MacMillan Press, London. 180pp.
- Jérémine E. and Christophe-Michel-Levy, M. (1961) Un nouveau gisement de narsarsukite. (Identification d'un minéral dénommé provisoirement "goureite" par A.Lacroix en 1934.) *Bull. Soc. Franc. Miner. Crist.* 84, 191-4.
- Jones M.P. (1960) Mineral dressing tests on the extraction of columbite and other heavy minerals from the Odegi Younger Granite. *Records Geol. Surv. Nigeria for 1957*, 36-59.
- Jones W.B. (1979a) Mixed benmoreite/trachyte flows from Kenya and their bearing on the Daly gap. *Geol. Mag.* 116, 487-9.
- (1979b) Syenite boulders associated with Kenyan trachyte volcanoes. *Lithos* 12, 89-97.

- Kaniris-Sotiriou R. (1974) Fine-scale layering in igneous intrusions : a possible mechanism for a non-depositional origin. *Geol. Mag.* 111, 157-62.
- Karche J-P. and Moreau C. (1977) Note préliminaire sur le massif subvolcanique à structure annulaire d'Abontorok (Air-Niger). *C.R. Acad. Sc. Paris* 284, 1259-62.
- and Vachette M. (1976) Migration des complexes subvolcaniques à structure annulaire du Niger. *Conséquences. C.R. Acad. Sc. Paris* 282, 2033-6.
- and ----- (1978) Age et migration de l'activité magmatique dans les complexes paléozoïques du Niger. *Conséquences. Bull. Soc. Geol. France* 20, 941-53.
- Kauffman A.J. and Jaffe H.W. (1946) Chevkinite (tscheffkinite) from Arizona. *Am. Mineral.* 31, 582-8.
- Kelsey C.H. and McKie D. (1964) The unit cell of aenigmatite. *Mineral. Mag.* 33, 986-1001.
- Kempe D.R.C. (1973) The petrology of the Warsak alkaline granites, Pakistan, and their relationship to other alkaline rocks in the region. *Geol. Mag.* 110, 385-405.
- Kleeman A.W. (1967) The origin of granitic rocks : Skye and Rhum. A reply. *J. Geol. Soc. Aust.* 14, 345-7.
- Korringa M.K. and Noble D.C. (1972) Genetic significance of chemical, isotopic, and petrographic features of some peralkaline salic rocks from the island of Pantelleria. *Earth Planet. Sci. Lett.* 17, 258-62.
- Kostov I. (1968) *Mineralogy.* Oliver and Boyd, Edinburgh. 587pp.
- Kurshakova L.D. and Avetisyan Ye.I. (1974) Stability and properties of synthetic hedenbergite. *Geochem. Int.* 11, 338-46.
- Lacroix A. (1905) Sur les microgranites alcaline du territoire de Zinder. *C.R. Acad. Sci. Paris* 140, 22-6.
- (1934) Mission au Tibesti : volcanisme et lithologie. *Memoires Acad. Sci. Paris* 61, 171-367.
- Lameyre J. (in press.) Les magmas granitiques : leur comportements, leurs associations et leurs sources. *Memoire Spec. 'Centenaire Soc. Geol. France'*.
- Larsen L. (1973) Measurement of solubility of zircon ($ZrSiO_4$) in synthetic granitic melts. *Trans. Am. Geophys. Union* 54, p479.
- (1976) Clinopyroxenes and co-existing mafic minerals from the alkaline Ilimaussaq intrusion, South Greenland. *J. Petrol.* 17, 258-90.
- (1977) Aenigmatites from the Ilimaussaq intrusion, South Greenland : chemistry and petrological implications. *Lithos* 10, 257-70.
- Larson R.L. and Ladd J.W. (1973) Evidence for the opening of the South Atlantic in the Early Cretaceous. *Nature* 246, 209-12.
- Lasserre M. (1966) Confirmation de l'existence d'une série de granites Tertiaires au Cameroun. *Bull. Bur. Rech. Geol. Min.* 3, 141-8.
- Laves F. (1950) The lattice and twinning of microcline and other potash feldspars. *J. Geol.* 58, 548-71.
- Leake B.E. (1974) The crystallisation history and mechanism of emplacement of the western part of the Galway granite, Connemara, Western Ireland. *Mineral. Mag.* 39, 498-513.
- (1978) Nomenclature of amphiboles. *Can. Mineral.* 16, 501-20.
- Le Bas M.J. (1971) Per-alkaline volcanism, crustal swelling and rifting. *Nature* 230, 85-7.
- Lehmann B. and Pichler H. (1980) Tin distribution in mid-Andean volcanic rocks. *Mineral. Deposita* 15, 35-9.
- Le Maitre R.W. (1962) Petrology of volcanic rocks, Gough island, south Atlantic. *Geol. Soc. Am. Bull.* 73, 1309-40.

- Lessing P. and Catanzaro E.J. (1964) Sr87/Sr86 ratios in Hawaiian lavas. *J. Geophys. Res.* 69, 1599-601.
- Lin F.H. and Yund R.A. (1972) Potassium and sodium self-diffusion in alkali feldspar. *Contrib. Mineral. Petrol.* 34, 177-84.
- Lindsley D.H. (1971) Synthesis and preliminary results on the stability of aenigmatite. *Carnegie Inst. Wash. Yearbk.* 69, 188-90.
- , Smith D. and Haggerty S.E. (1971) Petrography and mineral chemistry of a differentiated flow of Picture Gorge Basalt near Spray, Oregon. *Carnegie Inst. Wash. Yearbk.* 69, 264-85.
- Lofgren G.E. (1970) Experimental devitrification rate of rhyolite glass. *Geol. Soc. Am. Bull.* 81, 553-9.
- and Donaldson C.H. (1975) Curved branching crystals and differentiation in comb-layered rocks. *Contrib. Mineral. Petrol.* 49, 309-19.
- Luth W.C. (1976) Granitic rocks. In 'The evolution of the crystalline rocks'. Eds. D.K. Bailey and R. Macdonald, Academic Press, London, 335-417.
- and Tuttle O.F. (1969) The hydrous vapor phase in equilibrium with granite and granite magmas. *Mem. Geol. Soc. Am.* 115, 513-48.
- Lyons P.C. (1976) The chemistry of riebeckites of Massachusetts and Rhode Island. *Mineral. Mag.* 40, 473-9.
- Macdonald G.A. (1963) Relative abundance of intermediate members of the oceanic basalt-trachyte association - a discussion. *J. Geophys. Res.* 68, 5100-2.
- Macdonald R. (1969) The petrology of alkaline dykes from the Tugtutoq area, south Greenland. *Bull. Geol. Soc. Denmark* 19, 257-82.
- and Bailey D.K. (1973) The chemistry of the peralkaline oversaturated obsidians. *U.S. Geol. Surv. Prof. Paper* 440-N-1, 1-37.
- and Saunders M.J. (1973) Chemical variation in minerals of the astrophyllite group. *Mineral. Mag.* 39, 97-111.
- , ----- and Barberi F. (1974) Recommendations for further studies on the peralkaline oversaturated volcanic rocks. *Bull. Volc.* 38, 828-36.
- and Edge R.A. (1970) Trace element distribution in alkaline dykes from the Tugtutoq region, south Greenland. *Bull. Geol. Soc. Denmark* 20, 38-58.
- and Parker A. (1970) Zirconium in alkaline dykes from the Tugtutoq region, south Greenland. *Bull. Geol. Soc. Denmark* 20, 59-63.
- and Saunders M.J. (1973) Chemical variation in minerals of the astrophyllite group. *Mineral. Mag.* 39, 97-111.
- Mackay R.A. and Beer K.E. (1952) The albite riebeckite granites of Nigeria. *U.K. Geol. Surv., At. Energy Div. Report No.95*, H.M.S.O., London.
- Mackenzie W.S. (1957) The crystalline modifications of NaAlSi3O8. *Am. J. Sci.* 255, 481-516.
- and Smith J.V. (1962) Single crystal X-ray studies of crypto- and micro-perthites. *Nor. Geol. Tidsskr.* 42, 72-103.
- Macleod W.N., Turner D.C. and Wright E.P. (1971) The geology of the Jos Plateau. *Geol. Surv. Nigeria Bull. No.32. Vol.1. General Geology.* 110pp.
- Mai Manga B. (1979) Les granites et les syenites du complexe annulaire Silurien de l'Iskou, dans l'Air (Republique du Niger). These 3e cycle, Paris VI, 133pp.
- Maluski H. (1975) Sur la présence de fayalite en mégacristaux dans les microgranites a riebeckite d'Evisa (Corse). *C.R. Acad. Sci. Paris* 281, 5-7.

- Manning D.A.C. (in press) An experimental study of the effects of fluorine on the crystallisation of granitic melts. In 'Problems of Mineralisation Associated with Acid Magmatism', Exeter Mawam volume, Ed. A.M.Evans, John Wiley and Sons, London.
- Mano J. (1963) Les minéraux lourds accessoires des granites alcalins centraux du Tarraouadji (Air-Niger) : intérêt pétrogénétique des zircons. C.R. Acad. Sci. Paris 256, 4475-7.
- Marot A. and Zimine S. (1976) Les complexes annulaires de syenites et granites alcalins dans la peninsule Rallier du Baty, Iles Kerguelen (TAAF). These 3eme Cycle, Universite Pierre et Marie Curie, Paris. Tome 1.
- Marsh J.S. (1973) Relationships between transform directions and alkaline igneous rock lineaments in Africa and South America. Earth Planet. Sci. Lett. 18, 317-23.
- (1975) Aenigmatite stability in silica undersaturated rocks. Contrib. Mineral. Petrol. 50, 135-44.
- Martin R.F. (1968) Hydrothermal synthesis of low albite, orthoclase and non-stoichiometric albite. Unpubl. Ph.D. thesis, Stanford Univ.
- (1969a) Effect of fluid composition on structural state of alkali feldspars. Trans. Am. Geophys. Union 50, p.350.
- (1969b) The hydrothermal synthesis of low albite. Contrib. Mineral. Petrol. 23, 323-39.
- (1974a) Controls of ordering and subsolidus phase relations in the alkali feldspars. In 'The Feldspars', Eds. W.J.Mackenzie and J.Zussman, Manchester Univ. Press, 313-36.
- (1974b) Role of water in pantellerite genesis. Bull. Volc. 38, 666-79.
- and Bonin B. (1976) Water and magma genesis : the association hypersolvus granite - subsolvus granite. Can. Mineral. 14, 228-37.
- and Piwinski A.J. (1972) Magmatism and tectonic settings. J. Geophys. Res. 77, 4966-75.
- McBirney A.R. and Noyes R.M. (1979) Crystallization and layering of the Skaergaard intrusion. J. Petrol. 20, 487-554.
- McCarthy T.S. and Cawthorn R.G. (1980) Changes in initial $87\text{Sr}/86\text{Sr}$ ratio during protracted fractionation in igneous complexes. J. Petrol. 21, 245-64.
- and Hasty R.A. (1976) Trace element distribution patterns and their relationship to the crystallisation of granitic melts. Geochim. Cosmochim. Acta 40, 1351-8.
- McConnell J. and McKie D. (1960) The kinetics of the ordering process in triclinic $\text{NaAlSi}_3\text{O}_8$. Mineral. Mag. 32, 436-454.
- McCormac M. (1979) Observations on alkali feldspars in a peralkaline environment. 10e Colloque de Geol. Africaine, Montpellier. 93-4. (Abs.)
- Meighan I.G. (1976) The Coire Uaigneich granophyre, Isle of Skye. J. Geol. Soc. Lond. (Proc.) 132, p.114.
- (1979) The acid igneous rocks of the British Tertiary province. Bull. Geol. Surv. G.B. 70, 10-22.
- (1980) The alkaline acid rocks of the British Tertiary province. J. Geol. Soc. Lond. (Proc.) 137, p.519.
- Middlemost E.A.K. (1980) Rocks of the hawaiite-comendite kindred in a continental environment. 26e Congres Geol. Int., Paris, Vol.1, p.66. (Abs.)
- Milton C. (1974) Authigenic magnesioarfvedsonite from the Green River formation, Duchesne County, Utah. Am. Mineral. 59, 830-6.
- and Eugster H.P. (1959) Mineral assemblages of the Green River

- formation. In 'Researches in Geochemistry', Ed. P.H. Abelson, John Wiley and Sons, New York. 118-50.
- Mitchell A.H.G. and Garson M.S. (1976) Mineralisation at plate boundaries. *Minerals Sci. Engng.* 8, 129-69.
- Mitchell R.H. and Platt R.G. (1978) Mafic mineralogy of ferroaugite syenite from the Coldwell alkaline complex, Ontario, Canada. *J. Petrol.* 19, 627-51.
- Mitchell R.S. (1966) Virginia metamict minerals : perrierite and chevkinite. *Am. Mineral.* 51, 1394-405.
- Mitrofanov F.P. and Afanas'eva L.I. (1966) Aenigmatite from alkaline syenites of the Eastern Sayan Mountains. *Dokl. Acad. Nauk. SSSR* 166, 444-6. (In Russian)
- Molnar P. and Atwater T. (1973) Relative motion of hot spots in the mantle. *Nature* 246, 288-91.
- Moorbath S. and Bell J.D. (1965) Strontium isotope abundance studies and rubidium-strontium age determinations on Tertiary igneous rocks from the Isle of Skye, NW Scotland. *J. Petrol.* 6, 37-66.
- and Welke H. (1969) Lead isotope studies on igneous rocks from the Isle of Skye. *Earth Planet. Sci. Lett.* 5, 217-30.
- Moreau C., Karche J-P. and Trichet J. (1978) Remarques sur les anorthosites des complexes subvolcaniques de L'Air (Niger). *C.R. Somm. Soc. Geol. Fr.* 1, 21-3.
- Morgan W.J. (1971) Convection plumes in the lower mantle. *Nature* 230, 42-3.
- Naganna C. (1972) Alkali amphiboles from syenites of Idamakallu-Racherla, Andhra Pradesh, India. *Krystalinikum* 9, 133-9.
- Nash W.P. and Wilkinson J.F.G. (1970) Shonkin Sag laccolith, Montana. 1. Mafic minerals and estimates of temperature, pressure, oxygen fugacity and silica activity. *Contrib. Mineral. Petrol.* 25, 241-69.
- , Carmichael I.S.E. and Johnson W.P. (1969) The mineralogy and petrology of Mount Suswa, Kenya. *J. Petrol.* 10, 409-39.
- Neff T.R. and Khalil S.O. (1978) Petrogenesis of the Holterkollen plutonic complex, Norway. In 'Petrology and geochemistry of continental rifts', Eds. E-R. Neumann and I.B. Ramberg, D. Reidel Publ. Co., Dordrecht. 237-44.
- Neumann E-R. (1976) Compositional relations among pyroxenes, amphiboles and other mafic phases in the Oslo Region plutonic rocks. *Lithos* 9, 85-109.
- Nickel E.H. and Mark E. (1965) Arfvedsonite and aegirine-augite from Seal Lake, Labrador.
- Nielson T.F.D. (1979) The occurrence and formation of Ti-aegirines in peralkaline syenites. An example from the Tertiary ultramafic alkaline Gardiner complex, east Greenland. *Contrib. Mineral. Petrol.* 69, 235-44.
- Nicholls J. and Carmichael I.S.E. (1969) Peralkaline acid liquids : a petrological study. *Contrib. Mineral. Petrol.* 20, 269-94.
- Nilssen B. and Smithson S.B. (1965) Studies of the Precambrian Herefoss granite. *Nor. Geol. Tidssk.* 45, 367-96.
- Noble D.C. (1965) Gold flat member of the Thirsty Canyon Tuff - a pantellerite ash-flow sheet in southern Nevada. *U.S. Geol. Soc. Prof. Paper* 525-B, 85-90.
- (1970a) Loss of sodium from crystallised comendite welded tuffs of the Miocene Grouse Canyon member of the Belted range tuff, Nevada. *Geol. Soc. Am. Bull.* 81, 2677-87.
- (1970b) Pantellerite in the Palaeozoic volcanics of the Georgetown inlier, Queensland, and the close association of

- peralkaline and subalkaline silicic magmas. *J. Geol. Soc. Aust.* 16, 765-6.
- and Haffty J. (1969) Minor-element and revised major-element contents of some Mediterranean pantellerites and comendites. *J. Petrol.* 10, 502-9.
- , ----- and Hedge C.E. (1969) Strontium and magnesium contents of some natural peralkaline silicic glasses and their petrogenetic significance. *Am. J. Sci.* 267, 598-608.
- and Hedge C.E. (1969) (87)Sr/(86)Sr variations within individual ash flow sheets. *U.S. Geol. Surv. Prof. Paper* 650-C, 133-9.
- and Parker D.F. (1974) Peralkaline silicic volcanic rocks of the western United States. *Bull. Volc.* 38, 803-27.
- , Smith V.C. and Peck L.C. (1967) Loss of halogens from crystallised and glassy silicic volcanic rocks. *Geochim. Cosmochim. Acta.* 31, 215-23.
- Nolan J. (1969) Physical properties of sythetic and natural pyroxenes in the system diopside-hedenbergite-acmite. *Mineral. Mag.* 37, 216-29.
- Offodile M.E. (1976) The geology of the Middle Benue, Nigeria. *Spec. Publ. Palaeont. Inst. Univ. Uppsala* No.4. 166pp.
- Onuma N., Higuchi H., Wakita H. and Nagasawa H. (1968) Trace element partition between two pyroxenes and the host lava. *Earth Planet. Sci. Lett.* 5, 47-51.
- Orlova G.P. (1964) The solubility of water in albite melts. *Int. Geol. Rev.* 6, 254-8.
- Orville P.M. (1967) Unit-cell parameters of the microcline-low albite and the sanidine-high albite solid solution series. *Am. Mineral.* 52, 55-86.
- Osborn E.F. (1959) Role of oxygen pressure in the crystallization and differentiation of basaltic magma. *Am. J. Sci.* 257, 609-47.
- Oyawoye M.O. (1968) The geology of the Zaranda ring complex, N.Nigeria. *Nigerian J. Mining Geol.* 3, 33-47.
- Papike J.J., Cameron K.L. and Baldwin K. (1974) Amphiboles and pyroxenes : characterisation of other than quadrilateral components and estimation of ferric iron content from microprobe data. *Geol. Soc. Am. Abstr. with Progr.* 6, 1053-4.
- , Ross M. and Clark J.R. (1969) Crystal-chemical characterisation of clinoamphiboles based on five new structure refinements. *Mineral. Soc. Am. Spec. Paper* 2, 117-36.
- Parsons I. (1965) The feldspathic syenites of the Loch Ailsh intrusion, Assynt, Scotland. *J. Petrol.* 6, 365-94.
- (1968) An experimental study of ordering in sodium rich alkali feldspars. *Mineral. Mag.* 36, 1061-77.
- (1978) Feldspars and fluids in cooling plutons. *Mineral. Mag.* 42, 1-17.
- (1979) The Klokken gabbro-syenite complex, South Greenland : cryptic variation and origin of inversely graded layering. *J. Petrol.* 20, 653-94.
- and Boyd R. (1971) Distribution of potassium feldspar polymorphs in intrusive sequences. *Mineral. Mag.* 38, 295-311.
- Paul A. and Douglas R.W. (1965) Ferrous-ferric equilibrium in binary alkali silicate glasses. *Phys. Chem. Glasses* 6, 207-11.
- Peacor D.R. and Buerger M.J. (1962) The determination and refinement of the structure of narsarsukite Na₂Ti₁₀Si₄O₁₀. *Am. Mineral.* 47, 539-56.
- Pederson A.K., Engell J. and Ronsbo J.G. (1975) Early Tertiary volcanism in the Skagerrak : new chemical evidence from ash layers in the mo-clay of northern Denmark. *Lithos* 8, 255-68.
- Peng C.C.J. (1970) Intergranular albite in the granite and syenites of

- Hong Kong. *Am. Mineral.* 55, 270-82.
- Peterson J.S. (1978) Composite plutonic ring-complexes : a structural characteristic of rift zone plutonism. In 'Petrology and geochemistry of continental rifts', Eds. E-R. Neumann and I.B. Ramberg, D. Reidel, Dordrecht. 217-29.
- Phillips F.C. (1926) Note on a riebeckite-bearing rock from the Shetland Islands. *Geol. Mag.* 63, 72-7.
- Phillips W.J. (1965) The deformation of quartz in a granite. *Geol. J.* 4, 391-414.
- Philpotts A.R. (1978) Rift-related igneous activity in eastern North America. In 'Petrology and geochemistry of continental rifts', Eds. E-R. Neumann and I.B. Ramberg, D. Reidel Publ. Co., Dordrecht. 133-54.
- Philpotts J.A. (1978) The law of constant rejection. *Geochim. Cosmochim. Acta* 42, 909-20.
- Pirsson L.V. (1910) Note on the occurrence of astrophyllite in the granite at Quincy, Mass. *Am. J. Sci.* 29, 215-6.
- Popp R.K. and Gilbert M.C. (1972) Stability of acmite-jadeite at low pressure. *Am. Mineral.* 57, 1210-31.
- Prewitt C.T., Shannon R.D. and White W.B. (1972) Synthesis of a pyroxene containing trivalent titanium. *Contrib. Mineral. Petrol.* 35, 77-82.
- Pringle I.C. (1975) An occurrence of hydrothermal fayalite in the epicrustal rocks of the Bushveld igneous complex. *Mineral. Mag.* 40, 418-9.
- Raade G. (1978) Distribution of Th, U, K in the plutonic rocks of the Oslo region, Norway. In 'Petrology and geochemistry of continental rifts', Eds. E-R. Neumann and I.B. Ramberg, D. Reidel Publ. Co., Dordrecht. 185-92.
- Raeburn C., Bain A.D.N. and Russ W. (1927) The tinfields of Zaria and Kano provinces. *Geol. Surv. Nigeria Bull. No. 11.* 69pp.
- Ragland P.C. (1969) Composition and structural state of the potassic phase in perthites as related to petrogenesis of a granitic pluton. *Lithos* 3, 167-89.
- (1970) Composition and structural state of the potassic phase in perthites as related to petrogenesis of a granitic pluton. *Lithos* 3, 167-89.
- Rajasekaran K.C. (1966) Narsarsukite from Mont St. Hilaire, Quebec, Canada. *Can. Mineral.* 8, 506-14.
- Ramberg H. (1962) Intergranular precipitation of albite formed by unmixing of alkali feldspar. *Neues. Jahrb. Min. Abt.* 98, 14-34.
- Ramberg I.B. (1976) Gravity interpretation of the Oslo Graben and associated igneous rocks. *Norges Geol. Unders.* 325, 1-194.
- Ramberg I.B. (1976) Gravity interpretation of the Oslo Graben and associated igneous rocks. *Norges Geol. Unders.* 325, 1-194.
- Rankama K. and Sahama Th.G. (1950) *Geochemistry.* Chicago Univ. Press, Chicago. 912pp.
- Raulais M. (1946) La série granitique ultime de l'Air au Niger et sa minéralisation stannifère. *C.R. Acad. Sci. Paris* 223, 96-8.
- (1948) Sur la découverte de wolfram dans le jeune granite à biotite de l'Air (Niger). *C.R. Acad. Soc. géol. Fr.* 113-4.
- (1957) La minéralisation de l'Air (Territoire du Niger) et ses relations avec la tectonique. *C.R. Acad. Sci. Paris* 224, 913-6.
- Reay D.M. (1976) Some aspects of the geology of Adrar Bous and Agueraguer, two ring complexes in the Air (N. Niger) subprovince of the Nigeria-Niger Younger Granite province. Unpubl. B.Sc. thesis, Univ. of St. Andrews.

- Rhodes R.C. (1971) Structural geometry of subvolcanic ring complexes as related to pre-Cenozoic motions of continental plates. *Tectonophys.* 12, 111-7.
- Ribbe P.H. (1975) The chemistry, structure and nomenclature of feldspars. In: Mineral. Soc. Am. Short Course Notes. Southern Printing Co., Blacksburg, Virginia. R1-72.
- Ridley W.I. (1973) The petrology of volcanic rocks from the Small Isles of Inverness-shire. *Inst. Geol. Sci. Lond. Report* 73/10, 55pp.
- Rieder M. (1971) The phase relations of aluminous iron biotites in the system $KAlSi_3O_8$ - $KAlSiO_4$ - Al_2O_3 - Fe - O - H . *J. Petrol.* 14, 159-80.
- Rittman A. (1967) Studio Geovulcanologico e magmatologico dell'isola de Pantelleria. *Rivista Mineraria Siciliana* 106-8, 147-82. (In Italian)
- Robert J-L. (1976) Titanium stability in synthetic phlogopite solid solution. *Chem. Geol.* 17, 213-27.
- Robie R.A. and Waldbaum D.R. (1968) Thermodynamic properties of minerals and related substances at 298.15 degrees K (25 degrees C) and one atmosphere (1.013 Bars) pressure and at higher temperatures. *U.S. Geol. Surv. Bull.* 1259, 256pp.
- Rocci G. (1960) Le massif de Tarrouaudji, étude géologique et pétrographique. *Notes Bureau Rech. Geol. Min. Dakar* 6, 5-39.
- Roedder E. and Coombs D.S. (1967) Immiscibility in granitic melts, indicated by fluid inclusions in ejected granitic blocks from Ascension Island. *J. Petrol.* 8, 417-51.
- Ronsbo J.G., Pederson A.K. and Engell J. (1977) Titan-aegirine from early Tertiary ash layers in northern Denmark. *Lithos* 10, 193-204.
- Rossi G. (1978) On the pretended occurrence of aegirine-neptunite solid solution. *Contrib. Mineral. Petrol.* 66, p.109.
- Rutherford M.J. (1969) An experimental determination of iron biotite-alkali feldspar equilibria. *J. Petrol.* 10, 381-408.
- (1973) The phase relations of aluminous iron biotites in the system $KAlSi_3O_8$ - $KAlSiO_4$ - Al_2O_3 - Fe - O - H . *J. Petrol.* 14, 159-80.
- Sahama Th.G. (1956) Optical anomalies in arfvedsonite from Greenland. *Am. Mineral.* 41, 509-12.
- Schetcheglov A.D., Ovtcharenko E.F. and Ivanov T.I. (1965) Conclusions des experts géologues soviétiques concernant les problèmes du développement des travaux géologiques en République du Niger. *Arch. Bibl. Serv. Mines de Niamey* No.175.
- Scott P.W. (1976) Crystallisation trends of proxenes from the alkaline volcanic rocks of Tenerife, Canary Islands. *Mineral. Mag.* 40, 805-16.
- Scrutton R.A. (1973) The age relationship of igneous activity and continental break-up. *Geol. Mag.* 110, 227-34.
- Segalstad T.V. and Larsen A.O. (1978) Chevkinite and perrierite from the Oslo region, Norway. *Am. Mineral.* 63, 499-505.
- Seitsaari J. (1953) Blue-green hornblende and its genesis from the Tampere schist belt, Finland. *Bull. comm. geol. Finlande* 159, 83-98.
- Senderov E.E., Yas'kim G.M. and Bychkov A.M. (1975) Effects of alkaline solutions on Si-Al ordering in potash feldspar. *Geochem. Int.* 12, 116-25.
- Shannon R.D. and Prewitt C.T. (1969) Effective ionic radii in oxides and fluorides. *Acta Cryst.* B25, 925-46.
- Shoda T. (1954) On the anomalous optical properties of heikolite. *Mineral. J. Japan* 1, 69-83.
- (1958) Elliptic vibration of light in some alkali amphiboles. *Mineral. J. Japan* 2, 269-78.

- Sillitoe R.H. (1974) Tin mineralisation above mantle hot spots. *Nature* 248, 497-99.
- Simkin T. and Smith J.V. (1970) Minor element distribution in olivine. *J. Geol.* 78, 304-25.
- Simonen A. (1961) Olivine from Rapakivi. *Bull. Comm. Geol. Finlande* 196, 371-6.
- and Vormaa A. (1969) Amphibole and biotite from Rapakivi. *Bull. Comm. Geol. Finlande* 238, 28pp.
- Singh S.K. and Bonardi M. (1972) Mossbauer resonance of arfvedsonite and aegirine-augite from the Joan Lake agpaitic complex, Labrador. *Lithos* 5, 217-25.
- Sinton J.M. and Byerly G.R. (1980) Silicic differentiates of abyssal oceanic magmas : evidence for late-magmatic vapor transport of potassium. *Earth Planet. Sci. Lett.* 47, 423-30.
- Sipling P.J. and Yund R.A. (1974) Kinetics of Al/Si disordering in alkali feldspars. In 'Geochemical transport and kinetics', Eds. A.W.Hofman et al., Carnegie Inst. Wash., Publ. No. 634, 185-94.
- Skinner B.J. (1966) Thermal expansion. In 'Handbook of physical constants', Ed. S.P.Clark, revised edition, Geol. Soc. Am. Mem. 97, 75-96.
- Smith I.E.M., Chappell B.W., Ward G.K. and Freeman R.S. (1977) Peralkaline rhyolites associated with andesitic arcs of the southwest Pacific. *Earth Planet. Sci. Lett.* 37, 230-6.
- Smith J.V. (1974) Feldspar minerals. Vols. 1 and 2. Springer-Verlag, Berlin. 627pp and 690pp.
- Smith T.E. (1975) Layered granitic rock of Chebucto Head, Halifax County, Nova Scotia. *Can. J. Earth Sci.* 12, 456-63.
- Snetsinger K.G. (1969) Manganoan ilmenite from a Sierran adamellite. *Am. Mineral.* 54, 431-6.
- Sorensen H. (1969) Rhythmic igneous layering in peralkaline intrusions. *Lithos* 2, 261-83.
- (1970) Occurrence of uranium in alkaline igneous rocks. In 'Uranium exploration geology', Int. At. Energy Authority, Vienna. 161-8.
- Sparks R.S.J., Sigurdsson H. and Wilson L. (1977) Magma mixing : a mechanism for triggering acid explosive eruptions. *Nature* 267, 315-8.
- Statham P.J. (1975) Quantitative energy spectrometry : the application of a Si(Li) detector to electron microprobe analysis. Unpubl. Ph.D. thesis, Univ. of Cambridge.
- Steiger R.H. and Jager E. (1977) Subcommittee on geochronology : convention on the use of decay constants in geo- and cosmochemistry. *Earth Planet. Sci. Lett.* 36, 359-62.
- Stephenson D. (1972) Alkali pyroxenes from nepheline syenites of the South Qôroq Centre, south Greenland. *Lithos* 5, 187-201.
- (1974) Mn and Ca enriched olivines from nepheline syenites of the South Qôroq Centre, south Greenland. *Lithos* 7, 35-41.
- Steuber A.M. (1978) Strontium. In 'Handbook of geochemistry', Vol.II/4, Ed. K.H.Wedepohl, Springer-Verlag, Berlin.
- Stewart D.B. (1959) Narsarsukite from Sage Creek, Sweetgrass Hills, Montana. *Am. Mineral.* 44, 265-73.
- Streckeisen A. (1976) To each plutonic rock its proper name. *Earth Sci. Rev.* 12, 1-33.
- Stoeser D.B. and Elliott J.E. (1979) Post-orogenic peralkaline and calc-alkaline granites and associated mineralization of the Arabian Shield, Kingdom of Saudi Arabia. *Bull. Inst. Appl. Geol. Saudi Arabia* 3, 1-23.
- Stull R.J. (1978) Mantled feldspars from the Golden Horn batholith,

- Washington. *Lithos* 11, 243-9.
- Sweatman T.R. and Long J.V.P. (1969) Quantitative electron-probe microanalysis of rock-forming minerals. *J. Petrol.* 10, 332-79.
- Tauson L.V. (1967) Geochemical behaviour of rare elements during crystallisation and differentiation of granitic magmas. *Geochem. Int.* 4, 1067-75.
- Taylor H.P. (1977) Water/rock interactions and the origin of H₂O in granitic batholiths. *J. Geol. Soc. Lond.* 133, 509-58.
- and Forester R.W. (1971) Low-O₁₈ igneous rocks from the intrusive complexes of Skye, Mull and Ardnamurchan, Western Scotland. *J. Petrol.* 12, 465-97.
- Taylor J. (1959) Occurrence of beryllium in the Younger Granites of N.Nigeria. Unpubl. Rep. Geol. Surv., U.K. Atomic Energy Div., No.221.
- Taylor R.P. (1979) Topsails igneous complex - further evidence of middle Paleozoic epeirogeny and anorogenic magmatism in the northern Appalachians. *Geology* 7, 488-90.
- Taylor S.R. (1965) The application of trace element data to problems in petrology. In 'Physics and chemistry of the earth', Eds. L.H.Ahrens et al., Vol.6, Pergamon Press., Oxford.
- Thompson R.N. and Chisholm J.E. (1969) Synthesis of aenigmatite. *Mineral. Mag.* 37, 253-5.
- Thornber C.R., Roeder P.L. and Foster J.R. (1980) The effect of composition on the ferric-ferrous ratio in basaltic liquids at atmospheric pressure. *Geochim. Cosmochim. Acta* 44, 525-32.
- Thornton C.P. and Tuttle O.P. (1960) Chemistry of igneous rocks. 1. Differentiation Index. *Am. J. Sci.* 258, 664-84.
- Thorpe R.S. (1978) The parental basaltic magma of granites from the Isle of Skye, NW Scotland. *Mineral. Mag.* 42, 157-8.
- and Francis P.W. (1979) Variations in Andean andesite compositions and their petrogenetic significance. *Tectonophys.* 57, 53-70.
- , Potts P.J. and Sarre M.B. (1977) Rare earth evidence concerning the origin of granites of the Isle of Skye, northwest Scotland. *Earth. Planet. Sci. Lett.* 36, 111-20.
- Tugarinov A.I., Kovalenko V.I., Znamensky E.B., Legeido V.A., Sobatovich E.V., Brandt S.B. and Tsyhansky V.D. (1968) Distribution of Pb-isotopes, Sn, Nb, Ta, Zr and Hf in granitoids of Nigeria. In 'Origin and distribution of the elements', Ed. L.H.Ahrens, Pergamon Press, Oxford, 687-99.
- Turcotte D.L. and Oxburgh E.R. (1973) Mid-plate tectonics. *Nature* 244, 337-9.
- Turner D.C. (1962) The geology of the Younger Granite ring complex of the Sara-Fier and Pankshin Hills, Northern Nigeria. Unpubl. Ph.D. thesis, Univ. of London.
- (1963) Ring structures in the Sara-Fier Younger Granite complex, N.Nigeria. *J. Geol. Soc. Lond.* 119, 345-66.
- (1968) Volcanic and intrusive structures in the Kila-Warji ring complex, N.Nigeria. *J. Geol. Soc. Lond.* 124, 81-9.
- (1971) A note on the occurrence of trachytes in the Zaranda ring complex. *Nigerian J. Mining Geol.* 6, 61-3.
- (1973) Structure and tectonic setting of the Younger Granite ring complexes of Nigeria and S.Niger. *Savanna* 2, 51-60.
- (1974a) The Younger Granites of the Matsena area, Bornu Province, Northern Nigeria. *Records Geol. Surv. Nig.* 8, 5-15.
- (1974b) Petrology of the Kila Warji complex. Unpubl. manuscript.
- and Bowden P. (1979) The Ningi-Burra complex, Nigeria : dissected

- calderas and migrating magmatic centres. *J. Geol. Soc. Lond.* 136, 105-19.
- and Webb P.K. (1974) The Daura igneous complex, N.Nigeria - a link between the Younger Granite districts of Nigeria and S.Niger. *J. Geol. Soc. Lond.* 130, 71-7.
- Tuttle O.F. and Bowen N.L. (1958) Origin of granite in the light of experimental studies in the system albite-orthoclase-SiO₂-H₂O. *Geol. Soc. Am. Mem.* 74, pp.153.
- Tyler R.C. and King B.C. (1967) The pyroxenes of the alkaline igneous complexes of Eastern Uganda. *Mineral. Mag.* 36, 5-22.
- Upton B.G.J., Macdonald R., Hill P.G., Jefferies B. and Ford C.E. (1976) Narsarsukite: a new occurrence in peralkaline trachyte, south Greenland. *Mineral. Mag.* 40, 737-46.
- and Thomas J.E. (1980) The Tugtutoq Younger Giant Dyke Complex, south Greenland: fractional crystallisation of transitional olivine basalt magma. *J. Petrol.* 21, 167-98.
- , ----- and Macdonald R. (1971) Chemical variation within three alkaline complexes in south Greenland. *Lithos* 4, 163-84.
- Vail J.R. (1978) Outline of the geology and mineral deposits of the Democratic Republic of the Sudan and adjacent areas. *Overseas Geol. and Min. Resources*, No.49, 68pp.
- Vartiainen H. and Woolley A.R. (1976) The petrography, mineralogy and chemistry of the fenites of the Sokli carbonatite intrusion, Finland. *Geol. Surv. Finland Bull.* 280, 87pp.
- Velde D. (1978) An aenigmatite-richterite-olivine trachyte from Puu Koae, West Maui, Hawaii. *Am. Mineral.* 63, 771-8.
- Verhoogen J. (1962) Distribution of titanium between silicates and oxides in igneous rocks. *Am. J. Sci.* 260, 211-20.
- Vidal P., Dosso L., Bowden P. and Lameyre J. (1979) Strontium isotope geochemistry in syenite-alkaline granite complexes. In 'Origin and distribution of the elements', Second edition, Ed. L.H.Ahrens, Pergamon Press, Oxford, 223-31.
- Villari I. (1974) The Island of Pantelleria. *Bull. Volc.* 38, 680-724.
- Vlasov K.A., Kuz'menko M.Z. and Eskova E.M. (1966) The Lovozero alkali massif. Oliver and Boyd, Edinburgh. 61pp.
- Volkov V.N., Gavrilin R.D. and Kotel'nikova Z.A. (1978) Distribution of K, Na, Li and Rb in vertical section, by facies and age sequence of a multiphase granite massif. *Geochem. Int.* 15, 69-82.
- Vorma A. (1970) Alkali feldspars of the Wiborg rapakivi massif in southeastern Finland. *Bull. Comm. Geol. Finlande* 246, 72pp.
- Wager L.R. (1959) Differing powers of crystal nucleation as a factor producing diversity in layered igneous intrusions. *Geol. Mag.* 96, 75-80.
- and Brown G.M. (1968) Layered igneous rocks. Oliver and Boyd, Edinburgh. 588pp.
- Walker G.P.L. (1965) Acid rocks of Iceland. *Geol. Soc. Lond. Proc.* 1621, 61-2.
- Warren B.E. (1929) The structure of tremolite H₂Ca₂Mg₅(SiO₃)₈. *Zeit. Krist.* 72, 42-57.
- (1930) The crystal structure and chemical composition of the monoclinic amphiboles. *Zeit. Krist.* 72, 493-517.
- Watanabe T. (1975) Aegirine-augite and sodic augite from the Sambagawa and the Chichibu belts in the Oshika district, central Japan, with special reference to Na-metasomatism. *J. Fac. Sci. Hokkaido Univ. Ser. 4*, 16, 519-32.
- Watson E.B. (1979) Zircon saturation in felsic liquids: experimental results and application to trace element geochemistry. *Contrib. Mineral. Petrol.* 70, 407-19.

- Weaver S.D., Sceal J.S.C. and Gibson I.L. (1972) Trace-element data relevant to the origin of trachytic and pantelleritic lavas in the East African rift system. *Contrib. Mineral. Petrol.* 36, 181-94.
- Whittaker E.J.W. (1949) The structure of Bolivian crocidolite. *Acta Cryst.* 2, 312-7.
- (1960) Relationships between the crystal chemistry of pyroxenes and amphiboles. *Acta Cryst.* 13, 741-2.
- and Muntus R. (1970) Ionic radii for use in geochemistry. *Geochim. Cosmochim. Acta* 34, 945-56.
- Wilkinson J.F.G. (1966) Residual glasses from some alkali basaltic glasses from New South Wales. *Mineral. Mag.* 35, 847-60.
- Williams F.A., Meehan J.A., Paulo K.L., John T.U. and Rushton H.G. (1956) Economic geology of the decomposed columbite bearing granites, Jos Plateau, Nigeria. *Econ. Geol.* 51, 303-32.
- Wilshire H.G. (1968) Mineral layering in the Twin Lakes granodiorite, Colorado. *Geol. Soc. Am. Mem.* 115, 235-62.
- Wilson J-T. (1965) Evidence from oceanic islands suggesting movement in the earth. *Phil. Trans. Roy. Soc. Lond.* 258A, 145-67.
- (1973) Mantle plumes and plate motions. *Tectonophys.* 19, 149-64.
- and Burke K. (1975) Significance and consequences of the African plate becoming stationary over the deep mantle at the beginning of the Neogene. (Abs.) 7th Int. Colloq. Afr. Geol., Florence, 1973. *Trav. Lab. Sci. Terr., Marseille*, 11, p.157.
- von Wolf F. (1904) Ueber eine pantelleritartige Liparitlava von Major Island in der Bay of Plenty, Neu-Seeland. *Zentralblatt Mineralogie* 1904, 208-15. (In German)
- Wones D.R. and Eugster H.P. (1965) Stability of biotite : experiment, theory and application. *Am. Mineral.* 50, 1228-72.
- and Gilbert M.C. (1968) The stability of fayalite. *Carnegie Inst. Wash. Yearbk.* 66, 402-3.
- Wood D.A. (1978) Major an trace element variations in the Tertiary lavas of eastern Iceland and their significance with respect to the Iceland geochemical anomaly. *J. Petrol.* 19, 393-436.
- Woodrow P.J. (1967) The crystal structure of astrophyllite. *Acta Cryst.* 22, 673-8.
- Wright J.B. (1968) South Atlantic continental drift and the Benue trough. *Tectonophys.* 6, 301-10.
- (1975) Anorthosite - first occurrence in Nigeria and relevance to Younger Granite genesis. *Mineral. Mag.* 40, 193-6.
- Wright T.L. (1968) X-ray and optical study of alkali feldspar : II. An X-ray method for determining the composition and structural state from measurement of 2θ values for three reflections. *Am. Mineral.* 53, 88-104.
- (1974) Presentation and interpretation of chemical data for igneous rocks. *Contrib. Mineral. Petrol.* 48, 233-48.
- Wyllie P.J., Cox K.G. and Biggar G.M. (1962) The habit of apatite in synthetic systems and igneous rocks. *J. Petrol.* 3, 238-43.
- Yagi K. (1966) The system acmite-diopside and its bearing on the stability relations of natural pyroxenes of the acmite-hedenbergite-diopside series. *Am. Mineral.* 51, 976-1000.
- and Souther J.G. (1974) Aenigmatite from Mt. Edziza, British Columbia, Canada. *Am. Mineral.* 59, 820-9.
- Young E.J. and Powers H.A. (1960) Chevkinite in volcanic ash. *Am. Mineral.* 45, 875-81.
- Zielinski R.A. and Frey M.A. (1970) Gough Island : evaluation of a fractional crystallisation model. *Contrib. Mineral. Petrol.*

29, 242-54.
 Zies E.G. (1966) A new analysis of cossyrite from Pantelleria. Am. Mineral. 51, 200-5.

The fieldwork for this thesis was carried out while I was a Research Assistant at the University of St. Andrews, and I am deeply grateful to the Overseas Development Ministry (Research Scheme R0679) and to Dr. P. Brown and Professor G. J. Zinner for the opportunity to work in Nigeria and Niger. In Nigeria, Alhaji Babatundé Tobi, Head of State district, generously provided me with a compound in the town of Agba, my wife, gave encouraging encouragement and assistance which my fieldwork during the hot months of April would have been impossible. Many members of the mining community on the Jos Plateau were most helpful, particularly B. and J. Jambogo, T. and S. Funtayo and B. Sam-Dang O.S.S.

Subsequently Professor R. E. Maitland supervised my registration as a research student, and I thank him for his continued encouragement.

For expert sketches and photographic assistance I am grateful to J. Mackie, A. Hanson and J. Allan. S. A. Batchelor provided me with X-ray element and spectrochemical analyses, and J. A. Leitch conducted a gravimetric analysis. The major mineralogical rock analysis was done by L. A. F. at the University of Edinburgh Geology Department under the direction of Dr. G. Fitton. For microprobe analysis, G. Long and Dr. P. G. Mill, University of Edinburgh, assisted me on all stages of the day and night, and the University Library furnished me with almost every obscure inter-library loan. Dr. V. E. Stephens has provided me with his own computer program and assistance without which work of Chapter 3 would not have been possible.

I am particularly grateful to G. A. Altham, Professor

ACKNOWLEDGEMENTS

The fieldwork for this thesis was carried out while I was a Research Assistant at the University of St. Andrews, and I am deeply grateful to the Overseas Development Ministry (Research Scheme R2679) and to Dr. P. Bowden and Professor D. C. Turner for the opportunity to work in Nigeria and Niger. In Nigeria, Alhaji Mohammed Kebir, Head of Shira district, generously provided me with a compound in the town and Anne, my wife, gave unceasing encouragement and assistance without which fieldwork during the intense heat of April would have been impossible. Many members of the mining community on the Jos Plateau were kind and helpful, particularly H. and J. Jamieson, T. and B. Penhale and D. Dent-Young O.B.E.

Subsequently Professor E. K. Walton supported my registration as a research student, and I thank him for his continued encouragement.

For expert workshop and photographic assistance I am grateful to A. Mackie, A. Barman and J. Allan. R. A. Batchelor provided me with trace element and wet-chemical analyses and J. A. Baldwin undertook a gravimetric analysis. The major element whole rock analyses were made by X.R.F. at the University of Edinburgh Geology Department under the direction of Dr. G. Fitton. For microprobe analyses, C. Begg and Dr. P. G. Hill, University of Edinburgh, assisted me at all times of the day and night, and the University Library furnished me with often very obscure inter-library loans. Dr. W. E. Stephens has provided me with his own computer programs and assistance without which much of Chapter 5 would not have been possible.

I am particularly grateful to C. A. Abernethy, Professor

M.Barriere, Dr.P.Bowden, Dr.G. Fitton, A.B.Moyes, Dr.W.E. Stephens and Prof.D.C.Turner for many discussions, and for their critical comments on the thesis, and also to Dr.J.F.Brown, Dr.C.H.Donaldson, Dr.E.Ike and Prof.R.F.Martin. In addition, Professor M.Barriere has visited the Shira complex and has freely given of his time and experience, and as a result substantial improvements to this thesis have been made. Finally, Anne has been an unpaid typist and general assistant throughout, and despite that, maintained a much needed sense of humour.

In this work glass (1) had an area of between 20 and 25 μm^2 , was photographed in parallel light and mounted on a 10000 mesh grid. The total area was covered by a sheet of transparent epoxy resin and the surface of quartz and sapphire (if necessary) etched with hydrofluoric acid. However, a slight disadvantage is that sapphire and quartz are not distinguishable without the use of etching on the photomicrograph by showing the (10) surface with a microbeam under low voltage. The total area was divided on the grid paper into, for example, squares, which were numbered and assigned. In this way, the use of different coloured inks and each mineral is given its respective of labelling and possible confusion. Thus, by counting the number of full squares occupied by each mineral species and dividing this number by the total area of the thin section to obtain the area of alkali feldspar by difference, a total analysis was obtained, on an analogous manner to normal point counting. By using a large photomicrograph and fine grid paper, the final drawing can be very accurate.

An additional advantage of the method is that the photomicrographs themselves can be used as illustrations of the features of mineral grains in a way a normal photomicrograph cannot match.

(1) At this stage the rock slice had a thickness of 100 microns, rather than the final thickness of 20 microns, because the resulting photomicrograph had greater contrast between quartz and alkali feldspar.

APPENDIX 1Modal analysesa) Modal analyses from the Shira complex

In the case of coarse grained rocks from the Shira complex, modal analyses based on point counting of normal (20x40mm) thin sections could yield unrepresentative results. Accordingly, large thin sections in which the rock slice (1) had an area of between 20 and 80sq.cm., were photographed in parallel light and enlarged to a 30x40cm print. The print was then covered by a sheet of transparent graph paper and the outlines of quartz and mafic (+/- accessory) minerals were drawn in. However, a slight disadvantage is that aegirine and amphibole are not distinguishable within the mafic clusters on the photograph, but by viewing the (30 micron) thin section on a microscope under low power, the mafic areas could be subdivided on the graph paper into, for example, aegirine, alkali amphibole and aenigmatite. It was convenient to use different coloured inks for each mineral to avoid the necessity of labelling and possible confusion. Thus, by counting the number of 0.1 inch squares occupied by each mineral species and deducting this sub-total from the total area of the thin section to obtain the area of alkali feldspar by difference, a modal analysis was obtained in an analogous manner to normal point counting. By using a large photographic print and fine tipped pens, the final drawing can be very accurate.

An additional advantage of the method is that the photographs themselves may be used as illustrations of the textures of selected rocks in a way a normal photomicrograph cannot match.

(1) At this stage the rock slice had a thickness of 100 microns, rather than the final thickness of 30 microns, because the resulting photograph had greater contrast between quartz and alkali feldspar.

Without staining the feldspars however, this method is probably limited to hypersolvus rocks since plagioclase and alkali feldspar would probably not be sufficiently distinguishable. Also, in the Shira biotite granite, it was not possible to distinguish accessory iron-ore, fluorite and zircon which occur intergrown with biotite. Modifications to originally lamellar perthitic alkali feldspar such as enlargements of albite domains, were also indistinguishable, but in any case would normally be counted as 'alkali feldspar'.

b) Modal analyses from the Niger-Nigeria province

In order to compare modal analyses of rocks from the Shira complex with those from the province as a whole, 162 modal analyses from the literature (Table 30) were collated and plotted in Figure 35a. However, during the course of this literature survey, a number of difficulties were encountered in the interpretation of this data, which will be discussed.

In the Memoir (Jacobson et al., 1958) plagioclase is reported in the modal analyses as albite-oligoclase, but in subsequent Geological Survey Bulletins (Macleod et al., 1971; Jacobson and Macleod, 1977) and in other work, plagioclase is reported as albite only. Since plagioclase composition is of critical importance in modern classification (Streckeisen, 1976), this change is particularly notable, and it is believed by the present writer to be an unfortunate simplification since in many thin sections of rocks where albite has been reported in the mode, a more calcic plagioclase is in fact often present. This problem was mentioned in Chapter 1 and has been highlighted recently by Abernethy (in prep.) who provides textural criteria to distinguish magmatic plagioclase (i.e. probably $>An_5$) from postmagmatic albite, which in a number of instances has been shown by microprobe analysis to be almost pure albite.

Source of data in Table 30.

1 - 12	Jacobson et al. (1958)
13 - 31	Macleod et al. (1971)
32 - 49	Jacobson and Macleod (1977)
50 - 56	Macleod (1957)
57 - 60	Beer (1952)
61 - 65	Turner (1974a)
66 - 71	Turner (1974b)
72 - 89	Borley (1963a)
90 - 91	Jacobson (1947)
92 - 96	Karche and Moreau (1977)
97 - 104	Reay (1976)
105 - 115	Abaa (1976)
116 - 139	Badejoko (1977)
140 - 145	Moreau et al. (1978)
146 - 162	Mai Manga (1979)

Table 30. Modal analyses of rocks from the Niger-Nigeria province.¹

	1 ⁺ Bargesh biot.gnt. L 796	2 ⁺ Liruei biot.gnt. X 568	3 Amo ab.rieb. gnt. L 994	4 Liruei rieb.aeg. gnt. X 575	5 Kaffo ab.rieb. gnt.(Beer 1952)	6 Amo albite biot.gnt. L 946	7 Amo rieb. biot.gnt. L 1816	8 Hotum arfved. gnt. L 680	9 ⁺ Monguna hbl.biot. gnt. L 1657	10 ⁺ Mbul hbl.biot. gnt. L 1652	11 Kudaru qtz.pyx. fay. porph. syen. KD 46	12 ⁺ Kila- Warji porph. syen.	13 ⁺ Sara-Fier pyx.hbl. gnt. DT 61	14 ⁺ Sara-Fier hbl.pyx. μ gnt. DT 192
Quartz	35.6	37.0	31.4	30.0	35.5	33.2	24.2	23.4	28.0	16.5	19.2	0.2	25.0	15.0
Perthite	55.9	54.8	22.0	52.9	33.8	30.3	54.5	63.0	41.5	54.6	72.6	52.6	66.0	71.0
Albite	-	-	35.2	8.3	24.6	32.1	15.2	3.8	-	-	-	-	-	-
Plag.	4.9	6.3	-	-	-	-	-	-	16.0	15.5	-	22.5	2.5	5.2
Fayalite	-	-	-	-	-	-	-	0.7	-	-	1.0	-	0.7	1.3
Aug./Hed.	-	-	-	-	-	-	-	-	-	-	5.4	9.4	2.9	3.0
Ca-amph.	-	-	-	-	-	-	-	-	4.3	11.7	1.6	10.6	1.1	2.9
Alk.amph.	-	-	}3.9	}8.7	}4.3	-	}4.2	8.6	-	-	-	-	-	-
Aegirine	-	-	-	-	-	-	-	-	-	-	-	-	-	-
Aenigm.	-	-	-	-	-	-	-	-	-	-	-	-	-	-
Biotite	3.2	1.4	-	-	-	4.2	1.7	-	2.7	1.3	-	-	tr	tr
Access.	0.2	0.5	9.5	0.1	1.8	0.2	tr	0.5	0.2	0.3	-	-	0.8	0.8

	15 ⁺ Mbul hbl.fay. gnt. PB 38	16 ⁺ Vom hbl.biot. gnt. PB 96	17 ⁺ Ganawuri hbl.biot. gnt. PB 45	18 ⁺ Kumbul hbl.biot. gnt. DT 172	19 ⁺ Rough Range biot.gnt. L 1822	20 ⁺ Jos biot.gnt. L 34	21 ⁺ Gonzl biot.gnt. DT 53	22 Kadun biot.gnt. DT 101	23 Kigom rieb.aeg. gnt. PB 83	24 Sara-Fier rieb. μ gnt. DT 104	25 Hotum arfved. gnt. PB 37	26 ⁺ Limoro syen. L 1363	27 ⁺ Pankshin syen. PB 48	28 ⁺ Jivir Valley dolerite DT 255
Quartz	23.0	18.5	27.8	28.0	31.8	28.3	33.9	35.0	32.6	34.0	20.1	3.2	1.2	-
Perthite	65.1	68.7	49.8	51.0	56.5	46.9	41.8	37.0	55.9	59.0	67.2	43.2	79.6	-
Albite	-	-	-	-	-	-	-	-	7.4	2.6	1.9	-	-	-
Plag.	3.5	3.6	16.2	16.0	7.1	17.8	18.8	25.0	-	-	-	41.2	11.4	49.0
Fayalite	tr	tr	-	-	-	-	-	-	-	-	}2.9	0.2	tr	0.3
Aug./Hed.	-	-	-	-	-	-	-	-	-	-	-	1.4	2.2	12.0
Ca-amph.	3.5	4.7	2.9	2.0	-	-	-	-	-	-	-	9.2	4.5	20.0
Alk.amph.	-	-	-	-	-	-	-	-	2.1	4.4	7.9	-	-	-
Aegirine	-	-	-	-	-	-	-	-	0.7	0.2	-	-	-	-
Aenigm.	-	-	-	-	-	-	-	-	-	-	-	-	-	-
Biotite	1.4	3.3	3.3	3.3	4.6	5.7	5.2	2.2	-	-	-	-	-	6.5
Access.	-	0.5	0.2	0.3	-	1.2	0.2	0.4	1.2	0.1	-	1.7	1.3	12.5

¹ See opposite page for source of data.

Table 30 continued

	29 ⁺ Jivir porph. diorite DT 268	30 ⁺ Jivir qtz. diorite hybrid DT 145	31 ⁺ Mbul μ gabbro L 1642	32 Zuku aeg.gnt. X 2302	33 Zuku aeg.amph. gnt. X 2306	34 Zuku aeg.amph. gnt. X 2307	35 Zuku aeg.amph. gnt. X 2310	36 Gamawa aeg.amph. gnt. X 2111	37 Guraka outer syen. X 2206	38 Guraka inner syen. X 2205	39 Gamawa pyx.fay. qtz.syen. X 2127	40 Gamawa pyx.amph. qtz.syen. X 2108	41 Zuku pyx.qtz. syen. porph. X 2308	42 Liruei rieb.aeg. gnt. PB 7
Quartz.	1.3	16.0	-	27.7	11.1	10.4	24.3	30.0	-	-	5.9	6.9	2.7	27.0
Perthite	3.6	16.0	-	64.8	}73.8	}74.0	}65.5	}62.9	86.9	90.7	85.5	85.1	84.2	58.2
Albite	-	-	-	3.8					-	-	-	-	-	-
Plag.	57.0	46.0	60.0	-	-	-	-	-	-	-	-	-	-	-
Fayalite	-	-	-	tr	tr	tr	-	-	-	1.8	2.6	-	-	-
Aug./Hed.	-	-	3.0	-	-	-	-	-	5.4	5.2	5.8	1.7	9.8	-
Ca-amph.	32.0	13.0	27.7	-	-	-	-	1.2	1.4	1.3	-	5.1	-	-
Alk.amph.	-	-	-	0.6	9.0	8.5	4.8	-	-	-	-	-	-	2.4
Aegirine	-	-	-	2.8	6.0	7.0	5.4	4.5	-	-	-	-	-	2.9
Aenigm.	-	-	-	-	-	-	-	0.9	-	-	0.2	1.7	-	-
Biotite	0.6	7.0	7.3	-	-	-	-	-	3.1	0.4	-	-	-	} 0.6
Access.	5.1	1.7	2.0	-	-	-	-	0.3	2.3	1.2	0.4	0.3	3.1	
	43 Liruei rieb.aeg. gnt. PB 20	44 Kudaru rieb.gnt. PB 285	45 Liruei ab.rieb. gnt. PB 3	46 Dutsen Wal ab.rieb. gnt. X 2409	47 ⁺ Banke biot.gnt. X 2072	48 Dutsen Wal biot.gnt. X 2403	49 Kudaru biot.gnt. KD 165	50 Amo rieb.gnt. L 861	51 ⁺ Amo hbl.biot. gnt. L 1813	52 ⁺ Mbar gnt. porph. L 792	53 ⁺ Richa gnt. porph. L 1634	54 ⁺ Mbul biot. μ gnt. L 1651	55 ⁺ Mbul hbl.biot. gnt. L 1619	56 ⁺ Mbul hbl.biot. gnt. L 1623
Quartz	34.9	36.7	29.9	33.7	37.0	33.5	32.9	32.1	30.0	30.0	28.5	28.3	32.5	22.5
Perthite	62.1	52.8	42.7	8.5	40.4	56.8	64.0	61.4	61.7	61.8	52.9	49.7	53.3	42.9
Albite	1.2	3.8	13.3	48.5	-	5.6	-	2.0	-	-	-	-	-	-
Plag.	-	-	-	-	18.5	-	-	-	4.2	4.4	15.5	15.4	9.9	19.3
Fayalite	-	-	-	-	-	-	-	-	-	-	-	-	-	-
Aug./Hed.	-	-	-	-	-	-	-	-	-	-	-	-	-	-
Ca-amph.	-	-	-	-	-	-	-	-	1.6	0.7	-	-	3.2	9.6
Alk.amph.	1.8	6.2	8.1	7.7	-	-	-	5.5	-	-	-	-	-	-
Aegirine	-	-	1.0	0.3	-	-	-	-	-	-	-	-	-	-
Aenigm.	-	-	-	-	-	-	-	-	-	-	-	-	-	-
Biotite	-	} 0.5	} 4.8	} 2.0	3.3	3.9	2.5	tr	0.7	3.1	3.1	6.2	1.1	1.5
Access.	-				-	-	-	0.7	0.3	0.3	-	1.8	-	-

Table 30 continued

	57 ⁺	58 ⁺	59	60	61	62	63	64	65	66 ⁺	67 ⁺	68	69	70
	Ningi syen. (Beer 1952)	Liruei biot.gnt. (Beer 1952)	Liruei rieb.aeg. gnt. (Beer 1952)	Liruei ab.rieb. gnt. (Beer 1952)	Matsena arfved. gnt. DT 593	Matsena arfved. gnt. DT 609	Matsena arfved. gnt. DT 591	Matsena arfved. gnt. DT 617	Matsena arfved. gnt. DT 619	Warji augite rich porph.syen. DT 808	Warji hbl.rich porph. syen. DT 841	Kila syen. DT 724	Kila qtz.syen. porph. DT 731	Kila gnt. porph. DT 1
Quartz	7.4	38.4	34.7	27.9	24.9	31.8	31.7	38.5	30.4	2.3	3.1	3.3	10.9	21.4
Perthite	54.2	58.1	57.8	31.7	66.1	57.0	52.6	24.0	31.3	67.9	63.0	80.1	80.8	70.5
Albite	1.1	0.9	3.1	28.9	4.0	4.4	8.5	28.4	31.1	G'phy 8.2	G'phy 3.3	-	-	-
Plag.	14.6	1.0	-	-	-	-	-	-	-	1.4	8.8	-	-	-
Fayalite					-	-	-	-	-	0.4	-	-	-	-
Aug./Hed.	19.9	1.6	4.4	11.5	-	-	-	-	-	6.8	0.6	5.5	2.5	5.8
Ca-amph.					-	-	-	-	-	0.7	14.5	5.9	3.5	-
Alk.amph.	-	-	-	-	2.7	3.9	6.2	8.6	4.8	-	-	-	-	0.4
Aegirine	-	-	-	-	1.6	2.6	-	0.1	-	-	-	-	-	-
Aenigm.	-	-	-	-	0.3	-	-	-	-	-	-	-	-	-
Biotite	-	-	-	-	-	-	-	-	-	-	3.2	1.7	-	-
Access.	2.8	-	-	-	0.4	0.3	0.3	0.6	2.4	12.2	3.5	3.5	2.3	1.9

	71	72	73 ⁺	74 ⁺	75 ⁺	76	77 ⁺	78	79 ⁺	80 ⁺	81	82	83	84
	Kila aeg. arfved. gnt. DT 2	Liruei qtz.fay. porph. PB 13	Shere hbl.fay. porph. PB 71	Pankshin hbl.fay. gnt. PB 47	Jos- Bukuru hbl.fay. gnt. PB 94	Kaleri amph. biot.gnt. PB 36	Sara-Fier amph. biot.gnt. PB 24	Amo amph. biot.gnt. PB 87	Pankshin fine-gr. amph. biot.gnt. PB 51	Jos- Bukuru amph. biot.gnt. PB 97	Sara-Fier rieb.gnt. PB 50	Sara-Fier fine-gr. rieb.gnt. PB 57	Sara-Fier coarse- gr. rieb. gnt. PB 58	Shere ab.rieb. gnt. PB 63
Quartz	28.8	21.8	25.7	27.3	32.6	42.0	26.6	31.3	33.5	27.8	36.4	33.6	31.2	34.7
Perthite	55.4	62.3	63.4	56.6	60.5	55.4	69.7	66.8	57.7	66.1	60.1	64.9	62.7	49.9
Albite	8.7	-	-	-	-	tr	-	tr	-	-	2.6	tr	0.8	7.4
Plag.	-	-	1.4	11.9	1.1	-	1.7	-	2.0	2.8	-	-	-	-
Fayalite	-	3.3	2.8	0.8	0.7	-	-	-	-	-	-	-	-	-
Aug./Hed.	-	-	-	-	-	-	-	-	-	-	-	-	-	-
Ca-amph.	-	6.2	5.1	2.6	2.1	1.7	1.2	1.2	3.1	1.9	-	-	-	-
Alk.amph.	1.3	-	-	-	-	(incl. biot.)	-	(incl. biot.)	-	-	0.5	1.3	4.6	5.3
Aegirine	5.3	-	-	-	-	-	-	-	-	-	-	-	-	2.2
Aenigm.	-	-	-	-	-	-	-	-	-	-	-	-	-	-
Biotite	-	-	0.3	tr	2.6	-	tr	-	2.0	1.6	-	-	-	-
Access.	0.5	0.5	1.1	0.7	0.4	-	0.3	0.4	1.4	0.1	0.4	tr	tr	-

Table 30 continued

Table 30 continued

	85 Shere rieb. biot.gnt.	86 Amo rieb.gnt.	87 Kigom ab.rieb. gnt.	88 Kigom ab.rieb. gnt.	89 Buji ab.rieb. gnt.	90 Liruei biot.gnt.	91 Kudaru rieb.gnt.	92 Abontorok int. anorth.	93 Abontorok ext. anorth.	94 Abontorok gnt.amph.	95 Abontorok gnt.	96 Abontorok syen.	97 Adrar Bous oliv. gabbro	98 Adrar Bous oliv. gabbro
	PB 64	PB 30	PB 84	PB 85	PB 92	JAC 1	JAC 5	K-M1	K-M2	K-M3	K-M4	K-M5	SA 55X	SA 56
Quartz	32.8	23.7	28.1	36.4	28.0	37.9	37.8	1.5	-	25.3	30.3	5.1	-	-
Perthite	52.9	66.2	58.1	53.3	59.6	60.0	57.9	-	-	48.7	59.3	67.7	-	-
Albite	8.7	4.4	5.7	7.8	5.2	-	-	2.1	-	-	-	-	-	-
Plag.	-	-	-	-	-	-	-	92.8	78.1	8.7	7.0	3.0	61.0	63.0
Olivine	-	-	-	-	-	-	-	0.1	6.0	-	-	-	-	9.0
Aug./Hed.	-	-	-	-	-	-	-	0.1	3.8	-	-	8.0	15.0	26.5
Ca-amph.	-	-	-	-	-	-	-	0.8	-	11.4	-	7.8	19.0	-
Alk.amph.	4.0	6.7	5.8	0.4	4.2	-	-	-	-	-	-	-	(incl.	-
Aegirine	1.3	-	1.5	-	2.8	-	-	-	-	-	-	-	biot.)	-
Aenigm.	-	-	-	-	-	-	-	-	-	-	-	-	-	-
Biotite	-	-	-	-	-	1.7	-	-	4.6	-	-	-	-	-
Access.	-	tr	0.6	2.1	tr	0.4	-	2.7	7.5	5.9	3.4	8.4	5.0	1.5

	99 Adrar Bous oliv. gabbro	100 Adrar Bous trocto- lite	101 Adrar Bous anorth. (base)	102 Adrar Bous anorth. (top)	103 Ag. ara- guer anorth.	104 Aguera- guer anorth.	105 Ririwai biot.gnt.	106 Ririwai biot.gnt.	107 Ririwai biot.gnt.	108 Ririwai biot.gnt.	109 Ririwai biot.gnt.	110 Dutsen Wai biot.gnt.	111 Dutsen Wai biot.gnt.	112 Dutsen Wai biot.gnt.
	SA 60	SA 61	SA 62	SA 62	SA 82	SA 87	L 13-10	L13-190	L13-315	L13-411	L13-440	DW 7	DW 8	DW 16
Quartz	-	-	-	-	-	-	35.5	35.6	36.9	33.7	34.8	35.9	34.8	36.3
Perthite	-	-	-	-	-	-	54.7	55.8	54.1	52.3	52.4	54.1	55.9	54.8
Albite	-	-	-	-	-	-	-	-	-	-	-	-	-	-
Plag.	66.0	80.5	84.0	90.0	90-93	94-96	4.9	4.3	7.4	12.3	10.8	5.1	4.8	5.6
Olivine	14.5	19.0	14.5	9.5	6-9	3-4	-	-	-	-	-	-	-	-
Aug./Hed.	17.5	-	-	-	0-0.2	-	-	-	-	-	-	-	-	-
Ca-amph.	-	-	-	-	-	-	-	-	-	-	-	-	-	-
Alk.amph.	-	-	-	-	-	-	-	-	-	-	-	-	-	-
Aegirine	-	-	-	-	-	-	-	-	-	-	-	-	-	-
Aenigm.	-	-	-	-	-	-	-	-	-	-	-	-	-	-
Biotite	-	-	-	-	-	-	2.3	2.8	1.7	1.1	1.2	1.7	3.5	2.3
Access.	2.0	0.5	1.5	0.5	0.5-1.5	1.0-1.5	1.4	0.3	1.2	1.5	1.1	2.6	0.6	0.6

Table 30 continued

	113	114	115	116	117 ⁺	118 ⁺	119	120	121 ⁺	122 ⁺	123 ⁺	124	125	126	
	Dutsen Wai alb.arf. gnt.	Dutsen Wai alb.arf. gnt.	Dutsen Wai alb.arf. gnt.	Neils Valley gnt. porph.	Naraguta gnt. porph.	Jos biot.gnt.	Ngell biot.gnt.	Kuru biot.gnt.	Shen qtz.fay. gnt. porph.	Shen-Kuru qtz.fay. gnt. porph.	Vom hbl.biot. gnt.	Rayfield Gona biot.gnt.	Bukuru biot.gnt.	Sabon Gida biot.gnt.	
	DW 11	DW 12	DW 13	YB 1	YB 2	YB 3	YB 4	YB 5	YB 6	YB 7	YB 8	YB 9	YB 10	YB 11	
Quartz	32.4	35.3	28.5	23.2	30.3	34.2	33.6	36.4	28.3	27.9	33.4	33.2	33.2	37.5	
Perthite	37.9	43.3	52.6	68.3	56.3	54.9	56.6	54.8	62.6	61.9	51.2	49.6	56.1	54.9	
Albite	23.6	15.3	9.7	-	-	-	6.2	6.3	-	-	-	12.8	5.2	4.3	
Plag.	-	-	-	-	8.3	6.4	-	-	1.5	1.7	10.4	-	-	-	
Payalite	-	-	-	2.7	-	-	-	-	3.4	2.6	-	-	-	-	
Aug./Hed.	-	-	-	1.5	-	-	-	-	-	4.1	-	-	-	-	
Ca-amph.	-	-	-	2.7	2.6	-	-	-	2.9	2.6	1.6	-	-	-	
Alk.amph.	3.2	2.4	3.9	-	-	-	-	-	-	-	-	-	-	-	
Aegirine	-	0.1	3.8	-	-	-	-	-	-	-	-	-	-	-	
Aenigm.	-	-	-	-	-	-	-	-	-	-	-	-	-	-	
Biotite	-	-	-	-	1.4	3.7	3.3	2.9	-	-	3.0	3.5	3.3	3.9	
Access.	1.9	2.5	0.8	1.4	1.2	0.5	0.4	0.7	0.2	0.3	0.4	1.5	0.3	0.3	
	127	128	129 ⁺	130	131 ⁺	132 ⁺	133 ⁺	134 ⁺	135	136	137	138	139		
	Vom Road biot. μ gnt.	Delimi biot.gnt.	Fier hast. biot.gnt.	Tembis Hill hast. fay.gnt.	Wulmi biot.gnt.	Kula hast.fay. biot.gnt.	Gate hast.fay. gnt.	Mbai hast.hed. gnt.	Pankshin syen.	Pankshin syen.	Pankshin syen.	Pankshin syen.	Pankshin syen.		
	YB 12	YB 13	YB 14	YB 15	YB 16	YB 17	YB 18	YB 19	YB 20	YB 21	YB 22	YB 23	YB 24		
Quartz	30.8	30.6	24.3	19.6	26.4	28.0	20.8	13.5	8.5	7.8	8.2	9.3	8.5		
Perthite	49.3	54.8	56.6	72.6	55.6	54.9	67.9	72.7	50.2	51.6	49.8	49.4	50.3		
Albite	12.9	10.6	-	-	-	-	-	-	28.3	26.3	29.6	27.6	28.0		
Plag.	-	-	6.7	-	13.6	12.0	3.1	1.9	-	-	-	-	-		
Payalite	-	-	-	5.3	-	-	4.2	3.2	0.2	0.3	0.3	0.2	0.3		
Aug./Hed.	-	-	-	0.3	-	-	0.3	4.6	3.2	4.4	3.8	3.6	3.8		
Ca-amph.	0.6	-	6.5	1.6	-	1.9	-	3.7	6.3	7.5	6.1	7.2	6.8		
Alk.amph.	-	-	-	-	-	-	-	-	-	-	-	-	-		
Aegirine	-	-	-	-	-	-	-	-	-	-	-	-	-		
Aenigm.	-	-	-	-	-	-	-	-	-	-	-	-	-		
Biotite	4.4	4.0	3.8	-	4.3	2.2	-	-	0.9	0.6	0.8	0.7	0.8		
Access.	1.3	0.4	1.5	0.5	0.2	0.1	0.9	0.2	2.4	2.6	2.2	1.5	2.5		

Table 30 continued

	140	141	142	143	144	145	146	147	148	149	150	151
	Taguei monzo- anorth.	Ofoud anorth.	Abontorok external leuco- gabbro	Taguei external leuco- gabbro	Agaraguer olivine gabbro	Ofoud (Tarenat) pyx. gabbro	Iskou pyx. syen.	Iskou pyx. syen.	Iskou pyx. syen.	Iskou Na-amph. gnt.	Iskou Na-amph. gnt.	Iskou Na-amph. gnt.
	(1)	(3)	(4)	(5)	(6)	(7)	m.02	m.09	m.19	m.07	m.06	m.61
Quartz	4.0	-	-	-	-	-	1.0	0.5	0.5	28.0	33.0	35.5
Perthite	14.2	0.7	-	-	-	-	79.0	80.0	84.0	58.0	57.0	43.0
Albite	-	-	-	-	-	-	-	-	-	8.0	6.5	12.0
Plag.	74.9	94.4	78.1	73.7	61.4	47.5	8.0	3.0	7.0	-	-	-
Olivine	-	-	6.0	11.3	12.0	3.8	-	-	-	-	-	-
Aug./Hed.	-	0.4	3.8	7.7	6.0	32.2	9.0	10.0	6.5	tr	tr	9.5
Ca-Amph.	2.7	3.1	-	-	-	-	-	-	-	-	-	-
Alk. amph.	-	-	-	-	-	-	tr	tr	tr	5.0	2.0	tr
Aegirine	-	-	-	-	-	-	-	-	-	-	-	-
Aenigm.	-	-	-	-	-	-	-	-	-	-	-	-
Biotite	0.1	-	4.6	5.2	7.8	4.5	tr	tr	tr	tr	tr	tr
Access.	4.1	1.4	7.5	2.1	12.8	12.0	3.0	6.5	2.0	1.0	1.0	tr
	152	153	154	155	156	157	158	159	160	161	162	
	Iskou c.gr. syen.	Iskou c.gr. syen.	Iskou c.gr. syen.	Iskou c.gr. syen.	Iskou med.gr. qtz. syen.	Iskou med.gr. qtz. syen.	Iskou med.gr. qtz. syen.	Iskou hbl. biot. gnt.	Iskou hbl. biot. gnt.	Iskou hbl. biot. gnt.	Iskou hbl. biot. gnt.	
	m.10	m.60	m.36	m.08	m.56	m.01	m.03	m.57	m.49	m.55	m.12	
Quartz	1.5	2.0	2.5	5.0	12.5	14.0	17.0	18.5	19.0	20.0	24.0	
Perthite	55.0	73.0	65.5	73.0	57.0	50.0	60.0	52.0	50.5	42.0	48.0	
Albite	-	-	-	-	-	-	-	-	-	-	-	
Plag.	26.0	16.0	19.5	14.0	13.0	16.0	12.0	17.0	16.5	24.0	18.0	
Olivine	-	-	-	-	-	-	-	-	-	-	-	
Aug./Hed.	tr	tr	tr	tr	tr	-	-	-	-	-	-	
Ca-amph.	14.0	6.5	9.0	7.0	15.5	11.6	9.0	7.5	4.0	6.0	5.0	
Alk. amph.	-	-	-	-	-	-	-	-	-	-	-	
Aegirine	-	-	-	-	-	-	-	-	-	-	-	
Aenigm.	-	-	-	-	-	-	-	-	-	-	-	
Biotite	2.0	0.5	2.0	1.0	1.0	7.5	0.5	4.0	9.0	6.0	4.0	
Access.	1.5	1.7	1.5	0.6	1.0	0.9	1.0	1.0	1.0	2.0	0.5	

Thus, relatively early crystallising plagioclase, which may be rimmed by alkali feldspar and sericitised, is believed to have a composition which is more calcic than An₅. Such plagioclase commonly occurs in syenites and coarse grained hornblende and biotite bearing granites and syenogranites, and so the presence of a calcic pyroxene or amphibole for example may be used as indirect evidence that the 'albite' described in the mode is magmatic plagioclase. Therefore, reference has been made to the accompanying petrographic description (and/or thin section in this Department), and of 162 modal analyses, there are 47 cases where 'albite' appears in the mode but has been assumed to be plagioclase (i.e. An_{>5}). The changes mostly concern fayalite, hedenbergite and Ca-amphibole bearing granites and porphyries and some (early, coarse grained) biotite granites (i.e. granitic rocks only).

Since the distribution of rock types within the province is heavily in favour of granites, around 30% of the modes available have been adjusted in the manner described. However, because the amount of plagioclase is often less than 6-8%, many samples plot in the same (alkali feldspar granite) field in Figure 35a, in any case. Thus, only about 17% of the available modes now appear in the syenogranite field on the basis of this change.

The assumption that in some cases, what has been described as albite (assumed to be An_{<5}) is in fact plagioclase (An_{>5}) does of course ignore the possibility that a petrographer may have included what would now be termed both magmatic plagioclase and postmagmatic (or intergranular) albite within the same term, in a modal analysis. No correction is possible in this case, but this error is likely to be small because the amount of intergranular albite in a plagioclase bearing alkali feldspar, is known to be less than in plagioclase-free granites.

Since Figure 35a contains a large amount of data in simplified

form, the following points concern a more detailed breakdown of that data, which may be of interest to subsequent researchers:

1. Plagioclase does not occur (in measurable quantities) in peralkaline granites and related rocks.
2. Modal compositions of biotite granites have a relatively narrow spread along the modal quartz-alkali feldspar join, and contain 30-40% quartz.
3. A modal plot of the albite 'biotite' granites exactly superimposes the albite arfvedsonite granites and both have a narrow range of 34-40% quartz.
4. By contrast, alkali amphibole 'granites' plot over the same range but also extend into the alkali feldspar quartz syenite field (e.g. Shira and also the Zuku aegirine 'riebeckite granites'; Jacobson and Macleod, 1977).
5. Fayalite, hedenbergite and Ca-amphibole granites have a greater range of quartz-alkali feldspar ratios than the biotite granites and some (just) plot in the alkali feldspar quartz syenite field.
6. The isolated sample which lies just inside the granodiorite field in Figure 35a (sample DT145, Macleod et al., 1971) is a gabbroic rock from Sara-Fier which has been modified by the later intrusion of granites. In its original condition it would therefore be expected to plot in the monzodiorite/monzogabbro field.
7. From the relative dearth of modal analyses of basic and intermediate rocks in the province, it would appear that, compared to the available geochemical data, these rocks have been inadequately studied petrographically. This aspect of research would therefore be worth pursuing further.

Table 32 XRD reflections of microperthite from the Shira ferrorichterite alkali feldspar quartz syenite, indexed after Borg & Smith (1969).

2θ	d	hkl Potassic phase	hkl Sodic phase	2θ	d	hkl Potassic phase	hkl Sodic phase
13.13	6.737	110		36.51	2.459		222
13.63	6.491	001		36.92	2.433	$\bar{1}\bar{3}1, \bar{2}40$	$\bar{1}\bar{3}1$
13.83	6.398		001	37.32	2.408		240
21.01	4.225	$\bar{2}01$		37.59	2.391	$\bar{1}\bar{5}1$	
22.04	4.030		$\bar{2}01$	38.56	2.333	$\bar{3}\bar{3}1, \bar{1}\bar{1}\bar{3}$	
22.29	3.985	111		39.48	2.281		$\bar{1}\bar{1}\bar{3}$
22.63	3.926	$\bar{1}\bar{1}\bar{1}$		40.12	2.246	$\bar{2}\bar{2}\bar{3}$	$\bar{3}\bar{3}1$
23.21	3.829	130		41.78	2.160	060	
23.53	3.778		111	42.50	2.125		060
24.03	3.700	$\bar{1}\bar{3}0$		43.58	2.075	$\bar{1}\bar{3}\bar{3}$	
24.30	3.660		$\bar{1}\bar{3}1$	46.24	1.962	$\bar{2}\bar{2}\bar{2}$	
24.70	3.601	$\bar{2}\bar{2}\bar{1}$		47.17	1.925	400	
24.91	3.572	$\bar{1}\bar{3}1$		48.13	1.889	$\bar{3}\bar{3}\bar{2}$	$\bar{3}\bar{3}1$
25.54	3.485	$\bar{1}\bar{1}\bar{2}$	$\bar{2}\bar{2}\bar{1}$	49.00	1.857	152	
26.43	3.370	220	$\bar{1}\bar{1}\bar{2}$	49.97	1.824		062
27.46	3.245	002		50.54	1.804	$\bar{2}04$	
27.89	3.196		002	51.11	1.785		$\bar{2}04$
28.31	3.150		$\bar{2}\bar{2}0$	52.14	1.753		420, $\bar{2}\bar{2}4$
29.47	3.028	131		53.31	1.717		$\bar{4}\bar{4}1, \bar{2}\bar{6}2$
30.19	2.958	$\bar{1}\bar{3}1$		53.94	1.698		$\bar{1}\bar{1}4$
30.49	2.929		040, 0 $\bar{2}$ 2	55.02	1.668		242
30.76	2.904	022		55.05	1.653	$\bar{1}\bar{7}2$	
32.42	2.759	$\bar{3}\bar{1}\bar{1}$		58.64	1.573	0 $\bar{2}$ 4	0 $\bar{2}$ 4, $\bar{3}\bar{1}\bar{1}$
33.90	2.642		$\bar{1}\bar{3}2$	61.22	1.513	280	
34.22	2.618	$\bar{3}\bar{1}\bar{2}$		63.12	1.472	$\bar{2}\bar{8}0$	
34.93	2.566		$\bar{2}\bar{4}1$	63.88	1.456	$\bar{1}\bar{7}\bar{3}$	
35.51	2.526	240		65.26	1.429	262	$\bar{2}\bar{4}\bar{3}$
35.92	2.498	$\bar{3}\bar{1}0$		68.10	1.376	$\bar{1}\bar{1}\bar{5}$	

LiF CRYSTAL	Ca K2 2 θ 13 $^{\circ}$ 00'	Si K4 2 θ 31 $^{\circ}$ 55'	RAP CRYSTAL
	E 3.7 kev MPH 2.5 v Thr 1.0 v Win 5.0 v Bk \pm 2 $^{\circ}$ c.p.s. \approx 1,400	E 1.7 kev MPH 3.5 v Thr 1.25 v Win 5.0 v Bk + 1.5 $^{\circ}$ c.p.s. \approx 3,800	
	Fe K1 2 θ 57 $^{\circ}$ 23'	Mg K2 2 θ 44 $^{\circ}$ 39'	
	E 6.4 kev MPH 3.75 v Thr 1.25 v Win 5.0 v Bk \pm 2 $^{\circ}$ c.p.s. \approx 6,100	E 1.2 kev MPH 2.5 v Thr 0.5 v Win 5.0 v Bk + 1.5 $^{\circ}$ c.p.s. \approx 11,000	

GROUP 2

PET CRYSTAL	K K2 2 θ 50 $^{\circ}$ 40'	Na K2 2 θ 54 $^{\circ}$ 24'	RAP CRYSTAL
	E 3.3 kev MPH 4.0 v Thr 1.5 v Win 5.0 v Bk -1.75 $^{\circ}$ c.p.s. \approx 2,100	E 1.0 kev MPH 3.5 v Thr 1.25 v Win 5.0 v Bk +1.5 $^{\circ}$ c.p.s. \approx 850	
	Cl K2 2 θ 65 $^{\circ}$ 29'	F K2 2 θ 89 $^{\circ}$ 12'	
	E 2.6 kev MPH 3.0 v Thr 0.5 v Win 5.0 v Bk \pm 2 $^{\circ}$ c.p.s. \approx 5,000	E 0.7 kev MPH 2.0 v Thr 0.5 v Win 5.0 v Bk + 1.5 $^{\circ}$ c.p.s. \approx 180	

GROUP 3

LiF CRYSTAL	Ti K1 2 θ 86 $^{\circ}$ 45'	Al K2 2 θ 37 $^{\circ}$ 26'	RAP CRYSTAL
	E 4.5 kev MPH 3.0 v Thr 0.5 v Win 5.0 v Bk \pm 2 $^{\circ}$ c.p.s. \approx 5,000	E 1.5 kev MPH 4.0 v Thr 1.25 v Win 5.0 v Bk + 1.5 $^{\circ}$ c.p.s. \approx 12,000	
	Mn K1 2 θ 62 $^{\circ}$ 51'	Zn L1 2 θ 56 $^{\circ}$ 04'	
	E 5.9 kev MPH 3.7 v Thr 1.2 v Win 5.0 v Bk \pm 2 $^{\circ}$ c.p.s. \approx 6,200	E 1.0 kev MPH 2.5 v Thr 0.5 v Win 5.0 v Bk + 2 $^{\circ}$ c.p.s. \approx 4,300	

Zr L1 2 θ 87 $^{\circ}$ 55'
E 2.0 kev
MPH 3.5 v
Thr 1.0 v
Win 5.0 v
Bk \pm 2 $^{\circ}$
c.p.s. \approx 3000

Table 33. Analytical conditions for elements determined by W.D.S. on the electron microprobe. E = energy in thousands of electron volts; MPH = mean pulse height in volts; Thr = threshold; Win = window; Bk = background position relative to the peak; c.p.s. = expected counts per second. LiF = lithium fluoride; RAP = rubidium acid phthalate; PET = pentaerythritol. Qz = quartz.

b) Calculation of amphibole structural formulae from electron microprobe analyses

In the case of wet chemical analysis it is possible to calculate the formula of a monoclinic amphibole on the basis of 22 oxygens and $2(\text{OH}+\text{F}+\text{Cl})$, being the total number of anions in half the unit cell (e.g. Leake, 1978). In mineral analyses obtained by microprobe however, iron can only be determined as total Fe and because OH cannot be analysed for, the structural formula has to be expressed on the anhydrous basis of 23 oxygens. Since alkali amphiboles from the Nigerian Younger Granites are iron rich and have varying $\text{Fe}^{3+}/\text{Fe}^{2+}$ ratios (Borley, 1963a) a means of recalculating microprobe analyses to give an estimate of the $\text{Fe}^{3+}/\text{Fe}^{2+}$ ratio is desirable. Estimates of the ferric iron content were calculated using a computer program kindly provided by J.J.Papike, Department of Earth and Space Sciences, State University of New York (see Papike et al., 1974). The ferric iron calculation is based on the following charge balance equation:

$$\text{Fe}^3 = (\text{IV})\text{Al} + (\text{B})\text{Na} - [((\text{A})\text{Na},\text{K}) + (\text{VI})\text{Al} + 2(\text{VI})\text{Ti}]$$

The Papike program does not include the cations Zn and Zr, so these cation proportions have been determined separately, using the structural formula program NLSTFR (written by N.Lock).

Since, in a magma, the cations may be said to compete with one another for a given crystallographic site largely on the basis of their ionic radii (Onuma et al., 1968; Higuchi and Nagasawa, 1969; Philpotts, 1978), structural formulae in Tables 3 to 8 have cations listed in order of increasing ionic radii, using data from Whittaker and Muntus (1970). This order follows that of the I.M.A. (Leake, 1978) except for one important difference - it appears that Ca may enter the C sites of alkali amphiboles, but only as the least favoured element. Usually, Ca is considered too large to compete for the octahedral sites (Leake, 1978; Higuchi and Nagasawa, 1969), but in certain alkali amphiboles the

abundance of the usual octahedral cations (except Fe) is so low that Ca may be required to fill the octahedral positions. This approach is supported by the observation that the magnitude of excess cations in the B and A sites is almost exactly equal to the size of the depletion in the octahedral (C) sites. In a study of the structure and chemistry of arfvedsonite, Hawthorne (1976) similarly concluded that Ca could substitute in the octahedral positions in alkali amphiboles.

Papike's program incorporates a series of tests (applied to the structural formula) for a 'superior' analysis. Most commonly, alkali amphiboles, whether analysed by wet methods or by electron microprobe, fail these tests because Si is in excess of 8.02 atoms, total alkalis exceed 3 atoms and the C-site cations sum to less than 4.98. The quality of the microprobe analyses, as a possible source of error, can be ruled out because analyses for other minerals are perfectly satisfactory and the alkali pyroxenes practically always pass an equivalent set of tests. Whilst the apparently depleted C-sites can be explained by entry of Ca, excess Si and alkalis are not encountered in formulae from wet chemical analyses of similar amphiboles from Nigeria (Borley, 1963b). In addition, the amount of ferric iron calculated by the Papike program using the charge balance equation given above, is much less than that determined by bulk analysis on equivalent material. These two sets of observations are probably linked, because, for a given anion content, a higher Fe³⁺ value results in lower proportions for the other cations. Thus structural formulae of wet analyses with Fe recalculated as total Fe³⁺, when calculated by the Papike program contain much less Fe³⁺ than is known to be present. Also, of course, the proportions of all the other cations are higher. A comparison of the structural formulae of two bulk analyses calculated on the basis of 24(O+OH+F+Cl) and also on the anhydrous basis of 23 oxygens with Fe as total FeO are shown in Table 34.

Table 34 Analyses and structural formulae of arfvedsonite

Analysis	(1)	(2)	(3)	(4)
SiO ₂	48.44	48.44	49.61	49.89
TiO ₂	1.15	1.15	0.89	0.94
Al ₂ O ₃	0.10	0.10	0.53	0.28
Fe ₂ O ₃	12.42	-	10.04	-
FeO	21.12	32.30	25.41	34.77
MnO	0.52	0.52	0.67	0.59
MgO	0.42	0.42	tr.	0.03
CaO	1.95	1.95	1.30	1.19
Na ₂ O	7.92	7.92	7.87	8.06
K ₂ O	1.68	1.68	1.90	1.80
P ₂ O ₅	0.04	0.04	n.d.	-
Li ₂ O	0.97	0.97	0.08	-
ZnO	0.62	0.62	0.14	0.04
ZrO ₂	0.15	0.15	0.06	0.03
F	2.33		1.40	0.63
H ₂ O ⁺	1.10		0.72	-
less O=F	0.96		0.59	0.26
	<u>99.93</u>		<u>100.03</u>	<u>97.99</u>
Σ Fe as FeO	32.30	-	34.45	34.77
H ₂ O ⁻	0.03	-	0.00	-
Si	7.633	8.077	7.947	8.032
Al ^{IV}	0.019	-	0.053	-
Fe ³	0.348	-	-	-
Σ T	<u>8.000</u>	<u>8.077</u>	<u>8.000</u>	<u>8.032</u>
Al ^{VI}	-	0.020	0.047	0.053
Fe ³	1.125	0.077	1.210	0.423
Ti	0.136	0.144	0.107	0.114
Zr	0.012	0.012	0.005	0.002
Mg	0.099	0.104	-	0.007
Li	0.615	-	0.052	-
Zn	0.072	0.074	0.017	0.005
Fe ²	2.783	4.427	3.404	4.259
Mn	0.069	0.073	0.091	0.081
Ca	0.089	0.069	0.067	0.056
Σ M1-3	<u>5.000</u>	<u>5.000</u>	<u>5.000</u>	<u>5.000</u>
Ca	0.240	0.279	0.156	0.149
Na	1.760	1.721	1.844	1.851
Σ M4	<u>2.000</u>	<u>2.000</u>	<u>2.000</u>	<u>2.000</u>
Na	0.660	0.840	0.601	0.665
K	0.338	0.357	0.388	0.370
Σ A	<u>0.998</u>	<u>1.197</u>	<u>0.989</u>	<u>1.035</u>
Σ Na + K	2.758	2.918	2.833	2.886
Class.	Arf	Arf	Arf	Arf

Analysis (1) is sample R64 from Borley (1963a). Analysis (2) is identical to (1) except that Fe is expressed as LFeO. Analysis (3) is a 2g hand picked separate from a Shira pegmatite, analysed by J.R. Baldwin, University of St. Andrews. Analysis (4) is an average of 5 microprobe analyses of arfvedsonite from the same pegmatite and Fe is expressed as total FeO. Formulae for (1) and (3) are calculated on the basis of 24 (O+OH+F), while formulae for (2) and (4) are calculated on the basis of 23 oxygens using the Papike program.

Table 34 shows that whilst the Papike method of Fe^{3+} calculation may be quite satisfactory for calcic amphiboles, in the case of alkali amphiboles it does not calculate sufficient Fe^{3+} . In the case of sample SH101 for example, the Li content is low and is unlikely to make any real difference to the structural formula obtained.

In view of the fact that the Fe^{3+} estimation for alkali pyroxenes using an analogous method appears perfectly satisfactory, it is necessary to look at the assumptions inherent in any structural formula calculation. These assumptions, as given by Edwards (1976), are that:

1. the analysis is complete and accurate,
2. the mineral is stoichiometric,
3. Fe is the only element present with a variable valency,
4. oxygen is the only anion, and
5. charge balance is maintained.

With regard to (1), Li and OH are the major species not analysed for in this study. However Borley's data shows that except for arfvedsonite from albite rich granites, the Li content is less than 1% Li_2O , but H_2O^+ usually exceeds 1%. Zn and Zr have been analysed for in many cases and the totals of all analyses are quite reasonable in view of the absence of H_2O and Fe^{3+} determinations. Thus to a good approximation, assumption (1) is met. Since Mn contents are low anyway, assumption (3) is probably also correct. Although these amphiboles are F rich, the formulae are calculated on the basis of 23 oxygens, so point (4) is not strictly valid here. A charge balance equation is incorporated into the recalculation procedure, and so assumption (5) is met.

The assumption that the mineral is stoichiometric remains untested but is regarded by the writer as being of some possible significance, since slight non-stoichiometry might account for entry of Ca into octahedral positions and provide a means for inadequate Fe^{3+}

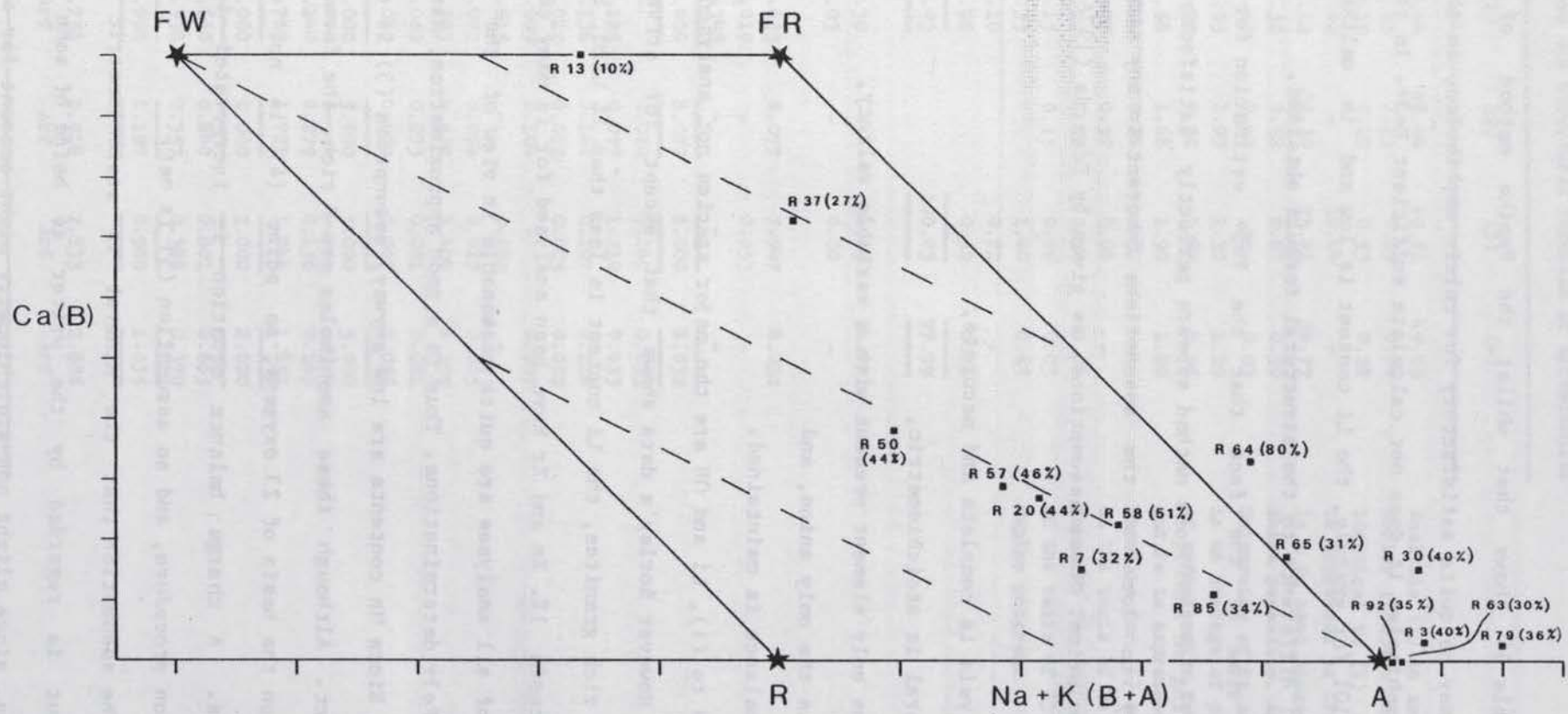


Figure 38. Ca v alkalis diagram for wet analyses of amphiboles from Nigeria (Borley, 1963b)

recalculation. In any case, in a trend from ferrowinchite or ferrorichterite to arfvedsonite for example, the cation total can be expected to vary from 15 to 16 (A site 0-1 respectively), so that stoichiometry does vary over the range of compositions encountered in this study.

Thus, in the structural formulae of alkali amphiboles analysed by electron microprobe, there would appear to be a slight but persistent error in that the calculated Fe³ content is probably lower than would be expected from wet chemically determined values. The magnitude of this error cannot be realistically assessed however, because of the discrepancy between the Fe³ content of the wet analyses and the Fe³⁺ content of ideal alkali amphiboles. This discrepancy is expressed on a Ca v alkalis plot in Figure 38. In Figure 38, the end-member compositions are linked by theoretical lines of equal oxidation state, beside which are plotted Borley's (1963b) analyses with Fe³⁺/(Fe²⁺+Fe³⁺) values in brackets. It is apparent that the natural amphiboles have Fe³ contents approximately double that expected, except for R13 which is in reasonable agreement. This is the principle reason why no attempt has been made at using an assumed Fe³⁺/(Fe²⁺+Fe³⁺) ratio and applying it to the probe analyses, even though the average ratio of alkali amphiboles from Borley (1963b) at 36.5%, is very close to the 37.5% value obtained from 13 samples in Deer et al. (1963).

In conclusion therefore, calculation of structural formulae from alkali amphibole analyses is not straightforward due possibly to the presence of ferric iron, water and halogens and some degree of non-stoichiometry. An attempt has been made to minimise the errors by estimating the ferric iron content, but this has only been partially successful.

The calculation of structural formulae of other mineral analyses has not presented comparable problems.

APPENDIX 4Whole rock analyses

All major elements have been analysed by X-ray fluorescence (X.R.F.) at the Grant Institute of Geology, University of Edinburgh. Glass beads have been used on an automatic Phillips PW1410 instrument under the direction of Dr.G.Fitton, who has kindly supplied the experimental conditions given in Table 35, and the analysis of international sample GS-N. Trace elements have been determined by X.R.F. and by atomic absorption spectrophotometry (A.A.S.).

Major elements

Dry powder samples are fused in a flux (Johnson Matthey Spectroflux 105) consisting of lithium tetraborate, lithium carbonate and lanthanum oxide, to produce a glass bead. This procedure is used in order to overcome correction procedures as a result of absorption, enhancement, surface and particle size effects inherent in the use of pressed powder mounts (Jenkins and de Vries, 1970).

The preparation technique is as follows:

1. 1g of sample is weighed into a Pt/5% Au crucible and 5.3333g of spectroflux added.
2. In batches of 3, the crucibles are heated (with lids) over Meker burners (or in a muffle furnace) for 20 minutes, and swirled occasionally. (With peralkaline granites and syenites, dissolution usually takes place in 5 minutes.)
3. When cool, the crucibles are reweighed and the sample made up to its original weight with flux, then returned to the Meker burners for a few minutes.
4. The molten sample is poured into a graphite mould surrounded by a

Table 35. X.R.F. analytical conditions

Line	Crystal	kv	mA	Colli- mator	Counter	2 θ B/g offset	L.L.	W.
SiK α	PE	50	45	C	F	+4.40	25%	60%
TiK α	LiF200	50	45	F	F	+4.74	30%	50%
AlK α	PE	60	45	C	F	-5.75	25%	60%
FeK α	LiF200	50	45	F	F	-1.63	20%	60%
MnK α	LiF200	60	45	F	F	-1.00	15%	70%
MgK α	TlAP	60	45	C	F	+2.70	25%	50%
CaK α	LiF200	50	30	F	F	-3.00	25%	60%
NaK α	TlAP	60	45	C	F	-2.25	30%	50%
KK α	LiF200	50	45	F	F	-4.55	25%	60%
PK α	Ge	50	45	C	F	+3.14	35%	40%

PE = Pentaerythritol. LiF = Lithium fluoride. TlAP = Thallium acid phthalate. Ge = Germanium.

Collimators: C = coarse, F = fine.

Counter: F = gas flow proportional counter.

Pulse height analysis: L.L. = lower level, W. = window.

A Cr X-ray tube is used throughout.

stainless steel jacket on a hotplate at 220 degrees C, and pressed into a flat disc with an aluminium plunger. The bead is allowed to anneal on the hotplate for about 30 minutes and then cooled slowly to room temperature, covered by a fused silica dish.

Analytical accuracy is checked against international rock standards such as GS-N (Abbey, 1977). Dr. Fitton reports (pers. comm.) the following comparison for GS-N:

	SiO ₂	TiO ₂	Al ₂ O ₃	Fe ₂ O ₃	MnO
	66.09	0.66	14.81	3.82	0.06
Abbey(1972)	65.98	0.68	14.71	3.75	0.06

	MgO	CaO	Na ₂ O	K ₂ O	P ₂ O ₅
	2.30	2.45	3.60	4.69	0.27
Abbey(1972)	2.31	2.51	3.78	4.64	0.28

Ferrous iron (and H₂O⁺ and H₂O⁻) has been determined by R.A. Batchelor using solution 'B' derived from an acid digestion of rock powder, as described below.

Trace elements

Trace elements Y and Zr have been determined by X.R.F. using a manual Phillips PW1540/10 instrument employing a W tube operating at 36 kv and 18 ma. The experimental conditions are listed below:-

Element	Line	2θ Peak	20 B/g's	L.L.	W. E.H.T.
Y	K	23.79	23.25 , 24.40	245	250 150v
Zr	K	22.50	22.00 , 23.25	241	238 145v

The detection limit for Zn is about 10 ppm, and for Rb, Sr, Y

and Zr, about 5 ppm or less. Possible interference of the Zr k_{α_1} line by Sr k_{β_1} is not a problem in granitic rocks from this province, because of the extremely low Sr contents. Another possible interference, of the Y k_{α} line by the Rb k_{β_1} line, is however more serious for the majority of the Younger Granites. In both instances, a correction procedure has been applied as follows:-

$$\text{Zr corr.} = \text{Zr uncorr.} - (\text{Sr} \times 0.055)$$

$$\text{and Y corr.} = \text{Y uncorr.} - (\text{Rb} \times 0.05)$$

(all values in ppm)

This procedure had to be adopted as the interferences were not known at the time the analyses were made.

Sample and standard count rates are fed into a computer program (XRF7) from which the elemental concentration in ppm is calculated from the equation:-

Conc.(sample, S) =

$$\text{Conc. (standard)} \times \frac{\text{Counts (S)}}{\text{Counts (std)}} \times \frac{\text{T.M.A.C. (S)}}{\text{T.M.A.C. (std)}}$$

The total mass absorption coefficient (T.M.A.C.) for the sample is estimated by assuming that the ratio of the background counts of the sample to the standard is equal to the ratio of the T.M.A.C. in the sample to that in the standard. A possible shortcoming of this method, is that an accurate T.M.A.C. is not calculated from the major element chemistry but is estimated from the ratio of backgrounds.

Li, Zn, Rb and Sr have been determined by a Varian Techtron AA4 atomic absorption spectrophotometer. The rock powder is dissolved in mixed hydrofluoric/perchloric acid to produce solution 'B'. This solution is aspirated directly for the determination of Li and Zn, but for Rb and Sr, the solution is acidified, evaporated to dryness and then redissolved with the addition of potassium chloride and lanthanum chloride solutions.



Geological map of the Shira Younger Granite Ring Complex

TR QE463. N5B

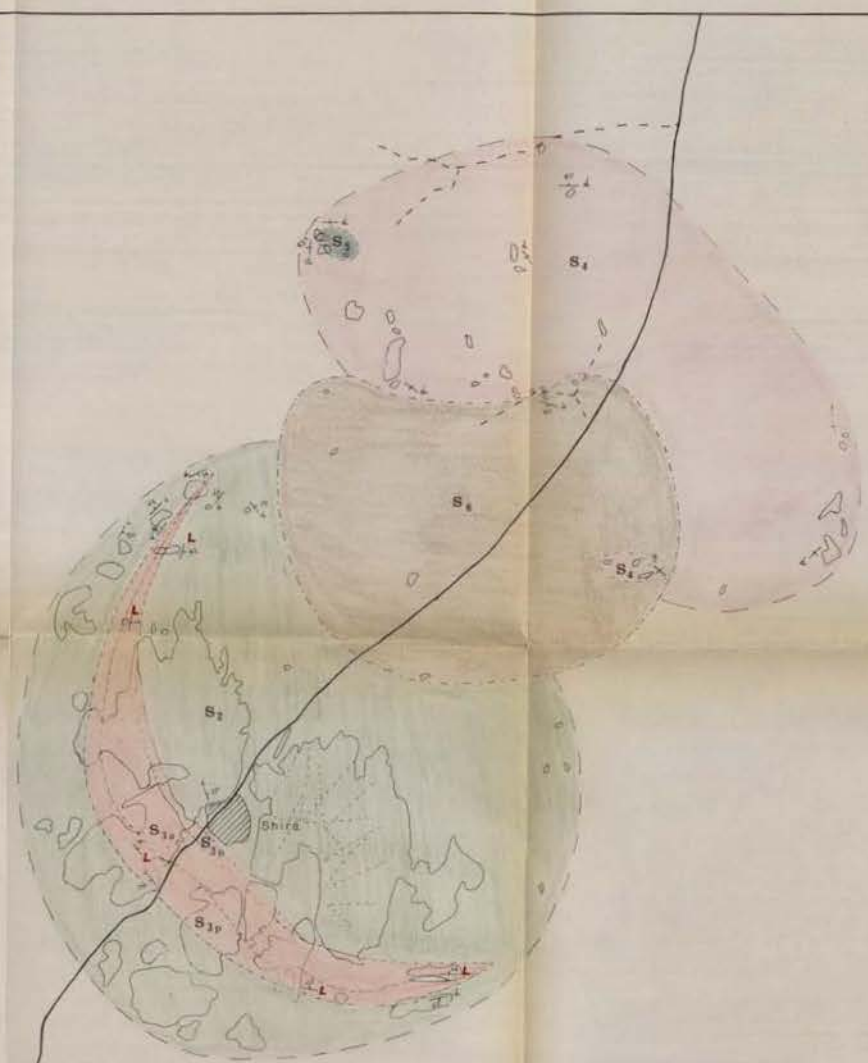
Scale = 1 : 50,000

11°35'

11°30'

11°25'

	S ₁ Zigau fayalite ferrohedenbergite granite porphyry
	S ₂ Shira ferrichterite-arfvedsonite senigmatite alkali feldspar quartz syenite
	S _{3a} Birji aegirine arfvedsonite alkali feldspar granite - acicular facies dominant
	S _{3p} Birji aegirine arfvedsonite alkali feldspar granite - poikilitic facies dominant
	S ₄ Andaburi ferrichterite-arfvedsonite alkali feldspar granite
	S ₅ Andulayi ferrowinchite/ferrichterite-arfvedsonite senigmatite alkali feldspar syenite/quartz syenite
	S ₆ Eldevo annite-biotite alkali feldspar granite
	Y Yana agglomerate
	C Chida porphyritic granophyre
	Basement
	Orientation of layering (L) in Birji granite or of dykes (d) or greisen (g)
	Postulated ring fault
	Geological boundary - definite/indefinite
	Joint
	Outcrop
	Road
	Track
	Village



10°00'

10°10'

